AGARD-CP-442

AGARD-CP-442

AGARD

ADVISORY GROUP FOR AEROSPACE RESEARCH & DEVELOPMENT

7 RUE ANCELLE 92200 NEUILLY SUR SEINE FRANCE

AGARD CONFERENCE PROCEEDINGS No.442

Propagation Effects and Circuit Performance of Modern Military Radio Systems with Particular Emphasis on those Employing Bandspreading

NORTH ATLANTIC TREATY ORGANIZATION

DISTRIBUTION AND AVAILABILITY
ON BACK COVER

NORTH ATLANTIC TREATY ORGANIZATION

ADVISORY GROUP FOR AEROSPACE RESEARCH AND DEVELOPMENT

(ORGANISATION DU TRAITE DE L'ATLANTIQUE NORD)

AGARD Conference Proceedings No.442

PROPAGATION EFFECTS AND CIRCUIT PERFORMANCE OF MODERN MILITARY RADIO SYSTEMS WITH PARTICULAR EMPHASIS ON THOSE EMPLOYING BANDSPREADING

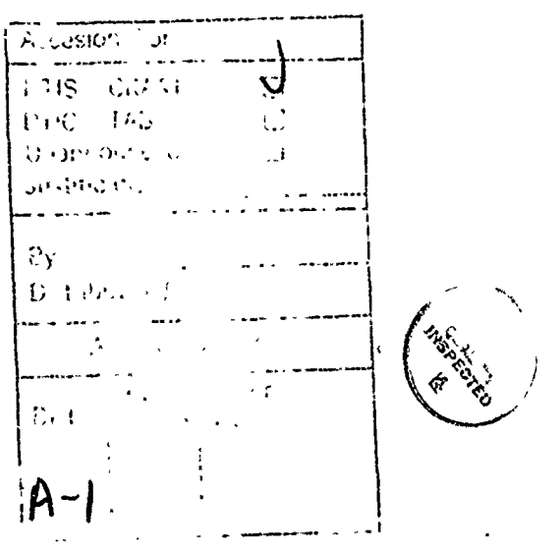

Papers presented at the Electromagnetic Wave Propagation Panel Symposium
held in Arcueil (Paris), France, 17—21 October 1988

THE MISSION OF AGARD

According to its Charter, the mission of AGARD is to bring together the leading personalities of the NATO nations in the fields of science and technology relating to aerospace for the following purposes:

- Recommending effective ways for the member nations to use their research and development capabilities for the common benefit of the NATO community;
- Providing scientific and technical advice and assistance to the Military Committee in the field of aerospace research and development (with particular regard to its military application);
- Continuously stimulating advances in the aerospace sciences relevant to strengthening the common defence posture;
- Improving the co-operation among member nations in aerospace research and development;
- Exchange of scientific and technical information;
- Providing assistance to member nations for the purpose of increasing their scientific and technical potential;
- Rendering scientific and technical assistance, as requested, to other NATO bodies and to member nations in connection with research and development problems in the aerospace field.

The highest authority within AGARD is the National Delegates Board consisting of officially appointed senior representatives from each member nation. The mission of AGARD is carried out through the Panels which are composed of experts appointed by the National Delegates, the Consultant and Exchange Programme and the Aerospace Applications Studies Programme. The results of AGARD work are reported to the member nations and the NATO Authorities through the AGARD series of publications of which this is one.

Participation in AGARD activities is by invitation only and is normally limited to citizens of the NATO nations.

Published December 1989

ISBN 92-835-0511-5

Printed by Specialised Printing Services Limited
40 Chigwell Lane, Loughton, Essex IG10 3TZ

THEME

The importance of understanding radio wave propagation increases as radar and communication systems become more complex, i.e. digital systems, frequency adaptive systems, spread spectrum systems, etc. Increasingly wider frequency bandwidths are used in modern military systems. for telecommunication applications to increase the rate or the safety of the transmissions; for radar or navigation, to more precise location or target definition.

In contrast with traditional systems, signal processing for modern systems can be realized in software, employing digital signal processing chips to perform the required modulation and demodulation processes. The recent development of such signal processors is radically changing the engineering approach to designing communications equipment. The flexibility offered by software implementations makes them ideal vehicles to realize and optimize new approaches, but these realizations can only be achieved by the communications engineer if those conducting propagation research keep pace with the increasingly more detailed knowledge needed to specify/quantify the channel characteristics.

Advanced realizations for tactical communications in modern armies, as they are operational or in introduction, now include digital transmission, voice and data capability and ECM resistant systems. Various techniques such as coding encryption, spread spectrum, are needed to enhance security of communications and to improve resistance to jamming. The adaptability to the varying channel conditions, such as mobile radio communications or real time channel evaluation, requires a better knowledge of the propagation medium; particularly in respect of ECM resistance methods, and the use of sophisticated methodologies, such as computer or microprocessor technologies, is needed. Microprocessor technology is changing the way systems operate and the requirements for radio operators to control and operate the systems.

Therefore it is appropriate to examine the state of the art in development of present-day radio communication systems, to examine the rôle and the need for radio propagation research, to assess the effects of propagation on existing military systems; and to propose how new systems can be improved to meet operational requirements.

* * *

L'importance d'une bonne compréhension de la propagation des ondes radio électriques augmente à mesure que les systèmes radar et de communication deviennent plus complexes, à savoir les systèmes numériques, les systèmes à adaptation de fréquence, les systèmes à spectre étalé, etc. Des largeurs de bande de fréquence sans cesse plus grandes sont utilisées dans les systèmes militaires modernes. pour des applications aux télécommunications, pour accroître la vitesse ou la sûrete des transmissions: pour les radars ou la navigation pour une localisation ou une définition plus précise des cibles.

Contrairement aux systèmes traditionnels, le traitement des signaux destinés aux systèmes modernes peut être realise dans le logiciel, en utilisant des microplaquettes de traitement des signaux numériques pour effectuer les processus de modulation et de démodulation nécessaires. Le récent développment de tels processeurs de signaux est en train de modifier radicalement l'approche technique de la conception des équipements de communications. La souplesse offerte par les différentes utilisations des logiciels en fait de véhicules idéaux pour réaliser et optimiser de nouvelles approches. Mais ces réalisations ne peuvent être menées à bien par l'ingénieur spécialiste des communications que si ceux qui sont charges de la recherche sur la propagation progressent au même rythme que l'acquisition des connaissances sans cesse plus detaillees qui sont nécessaires pour spécifier ou quantifier les caractéristiques des voies de transmission.

Les réalisations avancées en matière de communications tactiques dans les armées modernes, qu'elles soient opérationnelles ou en cours de mise en service, comprennent la transmission de signaux numériques, la capacité de transmission de signaux vocaux et de données et les systèmes résistant aux contre-mesures électroniques. Diverses techniques, telles que le chiffrement par code, le spectre dispersé, sont nécessaires pour augmenter la sécurité des communications et pour améliorer la résistance au brouillage. La capacité d'adaptation aux conditions changeantes des voies de transmission, telles que les communications radio mobiles ou l'evaluation des voies de transmission en temps réel nécessite une meilleur connaissance du milieu dans lequel se propagent les ondes radio-électriques, en particulier en ce qui concerne les méthodes de résistance aux contre-mesures électroniques, et l'utilisation de méthodologies sophistiquees telles que celles des ordinateurs et des micro-processeurs est nécessaire. La technologie des microprocesseurs est en train de modifier la façon dont fonctionnent les systèmes ainsi que les besoins en opérateurs radio pour exploiter et mettre en œuvre les systèmes.

C'est pourquoi il convient de faire le point des connaissances actuelles en matière de développement de systèmes de radiocommunication modernes, de se faire une opinion sur le rôle et la nécessité de la recherche sur la propagation des ondes radio-électriques, d'évaluer les effets de cette propagation sur les systèmes militaires existants et de proposer de nouveaux systèmes améliorés pour répondre aux exigences opérationnelles.

ELECTROMAGNETIC WAVE PROPAGATION PANEL

Chairman: Prof. C.Goutelard
Laboratoire d'Etude de Transmissons
Ionosphériques
9, Avenue de la Division Leclerc
94230 Cachan
France

Deputy Chairman: Ir. H.Vissinga
Physics and Electronics Lab. TNO
PO.Box 96864
2509 JG The Hague
Netherlands

TECHNICAL PROGRAMME COMMITTEE

Co-Chairman: Prof.C.Goutelard (Fr)
Dr J.Belrose (Ca)

Committee: Dr D.Rother (Ge)
Ir. H.Vissinga (Ne)
Dr J.H.Blythe (UK)
Eng. J.F.Patricio (Po)
Prof. Dr A.N.Ince (Tu)
Mr D.Fang (US)

HOST NATION COORDINATOR

ICA P.Fuerxer
Chef du Groupe 2
Télécommunications et Détections
DRET
26, Bd Victor
75996 Paris Armées

PANEL EXECUTIVE

Lt. Col. P.A.Brunelli

From Europe
AGARD-OTAN
7, Rue Ancelle
92200 Neuilly-sur-Seine
France

From US and Canada
AGARD-NATO
APO New York 09777

Tel: (1) 47 38 57 68 — Telex 610176 F
Telefax: (1) 47 38 57 99

AVANT-PROPOS

Les systèmes modernes de communication et de détection bénéficient des avances technologiques en matière de traitement du signal et des théories puissantes peuvent désormais être appliquées pour accroître l'efficacité des systèmes. Dans les recherches actuelles, elles sont utilisées pour obtenir une caractérisation plus precise des canaux et elaborer des methodes plus complexes mais plus puissantes, de systèmes qui, des traitements analogiques, s'orientent plus maintenant vers les systèmes numeriques.

De nouvelles méthodes, telles que le traitement numérique du signal, les méthodes adaptatives, l'étalement de spectre, le codage... conduisent à utiliser des bandes de fréquence sans cesse croissantes en vue d'accroître la sûreté et la vitesse des communications, la précision de localisation dans les systèmes radar ou en radiolocalisation.

Les opérations qui doivent être effectuées dans le traitement du signal, pour mettre en oeuvre de telles méthodes, sont, désormais, exécutables par des composants spécialisés rapides, les processeurs de signal, et les systèmes programmables, des microprocesseurs aux ordinateurs. si bien que les aproches techniques et la conception des équipements s'en trouvent modifiées.

L'objectif final de ces techniques est l'adaption optimale des systèmes au milieu de propagation qui impose ses caractéristiques.

Dans les communications ou les systèmes de détection militaires, cette adaption est primordiale compte tenu notamment, des contraintes particulières imposées par l'environnement et des exigences dem. adées.

Cette adaption repose d'abord sur une bonne connaissance des canaux de propagation dont la diversité des caractéristiques est due, à la fois aux gammes de fréquences utilisées, à l'étendue spectrale des signaux, a l'environnement — urbain, rural ou battlefield — aux conditions climatiques et, pour la haute atmosphère, à l'activité solaire.

L'objectif de ce s. mposium a été de réunir les meilleurs spécialistes de ces domaines pour faire le point sur l'etat de l'art en ce qui concerne la connaissance des milieux de propagation, la caractérisation des canaux de transmission, plus spécialement ceux utilisés en large bande, et les solutions apportées dans les systèmes modernes.

Ces sujets ont été couverts par quatre sessions qui ont réuni une quarantaine de communications. La première a été consacrée à la caractérisation des canaux, la seconde aux nouvelles approches dans la conception des systemes, la troisième aux performances des systèmes modernes et enfin, une session classifiée, a été consacrée aux sujets plus particuliers.

Cette édition reproduit les textes des conférences données par chaque auteur et des discussions qui les ont accompagnées. Chaque président de session présente un sommaire des thèmes abordés. Une table ronde, où chaque président de session a fait une synthèse des questions débattues et des perspectives qui sont apparues, a donne lieu à une large dicussion.

J'ai beaucoup de plaisir à remercier les présidents de sessions et les membres du comité technique pour l'important travail qu'ils ont accompli.

je voudrais plus particulièrement remercier l'administrateur de l'EPP et son secretaire pour l'aide precieuse qu'ils ont apportée avant, pendant et après la réunion de ce symposium, ainsi que le délégué national français, le coordonnateur local et son équipe pour l'excellente organisation de cette réunion à Paris.

Comment pourrais-je enfin oublier le docteur J.Belrose, coprésident et coéditeur de ce sympostum pour son action, qui, dans un travail commun, a contribué à la bonne réussite de cette manifestation.

C.Goutelard
Co-éditeur.

PREFACE

Today's communications and detection systems feature sophisticated signal processing techniques, and advanced theories can now be applied in order to improve system efficiency. In current research work these theories are used to achieve more accurate channel characterisation and to produce more complex and more powerful system methods, which are tending now away from analog processing towards digital systems.

New methods, such as digital signal processing, matching methods, spread spectrum and encoding are leading to the use of an increasing number of frequency bands in order to improve the security and speed of communications and to enhance location accuracy in radar and radiolocation systems.

The signal processing operations required in order to use such systems can now be carried out by dedicated high-speed components, signal processors and programmable systems, from microprocessores to computers, and this has modified equipment design and the technical approaches adopted.

The final aim of these techniques is to achieve optimum matching of systems to the propagation environment, which imposes its own characteristics.

In military communications or detection systems, this matching is vital, given in particular the constraints imposed by the environment and the operational requirements.

Successful matching depends primarily on a thorough knowledge of the propagation channels, the diversity of whose characteristics is explained by both the frequency ranges used, the spectral spread of the signals, the environment — urban or battlefield — the climatic conditions, and, in the upper atmosphere, solar activity.

The object of this Symposium was to bring together the foremost specialists in these fields in order to provide a state of the art overview of propagation environments, the characterisation of transmission channels, and in particular broadband transmission channels, and of the solutions offered by today's systems. KEYWORDS: NATO FURNISHED. (ER)

These subjects were covered in four sessions, representing a total of 40 papers. The opening session was devoted to channel characterisation, the second session to new approaches to system design, the third to system performance and the final, classified session to subjects of more specific interest.

This edition presents the full text of the papers given by each author and the discussions which ensued. Each session chairman provides a summary of the topics discussed. The final round table session, in which each session chairman reviewed the topics discussed and the answers which emerged, led to a broad-ranging discussion.

I have much pleasure in thanking the session chairmen and the members of the technical committee for the important work which they accomplished during the symposium.

In particular, I should like to thank the EPP Executive and his secretary for their precious help, both prior to, at the time of, and following this symposium, as well as the French National Delegate and the local Coordinator and his team for the excellent organisation of this meeting in Paris.

Finally, how could I forget Dr J Belrose, co-chairman and co-editor of this symposium, whose efforts combined to ensure the success of the meeting.

C.Goutelard
Co-editor

CONTENTS

* Printed in classified publication CP442 (Supplement)

* Printed in classified publication CP442 (Supplement)

* Printed in classified publication CP442 (Supplement)

An Overview of Canadian Radio Propagation/Communications Technologies Research

J.S. Belrose, R. Bultitude, D. Clark,
R.W. Jenkins, W. Lauber, G. Nourry,
N.M. Serinken, and G. Venier
Communications Research Centre
Ottawa, Ontario, Canada K2H 8S2

The Communications Research Centre (CRC) has and is carrying out research in radio propagation and radio communications technologies in areas relevant to the theme of this meeting. This paper briefly overviews some of this research. The overview will begin with a brief tutorial on the characteristics of fading channels. Topics to be addressed include characterization and simulation of the channel (HF and land mobile channels), simulation of the HF spread spectrum channel, broad band adaptive antennas; and coding and packet switching technologies (particularly for the HF channel). The subject of microprocessors and radio will be briefly mentioned. While the review is concerned with Canadian (CRC) research, since a number of topics areas will be addressed, some of which will disserted by others during the course of this meeting, this paper is in effect a sort of subject introduction.

1. Characterization of Fading Dispersive Channels

1.1 Mathematical Representation of Fading Channels
1.2 Classification of Fading Channels
1.3 Propagation Measurements and Analysis Techniques
1.4 Application of Measurement Results

2. Channel Simulators

2.1 Mobile Radio Channel Simulator
2.2 A Recorder-Type HF Channel Simulator
2.3 A Spread-Spectrum Simulation Facility (Implemented in Software)

3. Some New Approaches to Communications System Design

3.1 Use of Coding Diversity on HF Data Channels
3.2 HF Radio Communication Equipment for Digital Facsimile and Hard Copy Messages
3.3 Adaptive HF Communications
3.4 Broadband Adaptive Antennas

4. Closing Remarks

References

1. Characterization of Fading Dispersive Radio Channels

Ionospheric HF as well as tropospheric mobile radio channels are fading channels as a result of dispersive phenomena that take place in both the time and frequency domains. Frequency dispersion is caused by Doppler phenomena, whereas, in most cases, time dispersion is caused by multipath propagation. Such channels can often be modelled [Bello, 1963a] as time-variant linear filters, the inputs and outputs of which are effectively the transmit and receive antennas. The statistical properties of their complex envelope low pass equivalent impulse response are described by a number of different time and frequency correlation functions that are used in channel classification and modelling for the prediction of proposed communication system performance. This section of the paper discusses the mathematical representation of fading radio channels, their classification and modelling, and propagation measurement and analysis techniques by which the information for classification and modelling can be obtained. As well, comments are given throughout the text with regard to the application of various channel functions and analysis techniques in digital system performance predictions.

1.1 Mathematical Representation of Fading Channels

Consider a bandpass signal

$$\mathrm{A}(t) = |a(t)| \cos[\omega_c t + \theta(t)].$$

$$= |a(t)| \cos\theta(t) \cos\omega_c t - |a(t)| \sin\theta(t) \sin\omega_c t.$$

If one represents $a(t)$ as

$$a(t) = |a(t)| e^{j\theta(t)},$$

then it is easy to show that

$$\mathrm{A}(t) = Re\{a(t) e^{j\omega_c t}\}.$$

The signal $a(t)$ is referred to as the complex envelope low pass equivalent for the bandpass signal $\mathrm{A}(t)$. The term "complex envelope" [Bello, 1963b] is used because $a(t)$ has the conventional envelope of $\mathrm{A}(t)$, but also has a phase $\theta(t)$ (with respect to the carrier frequency) associated with it. Hence it is a complex envelope.

An expression for the complex envelope low pass equivalent for a radio channel impulse response can be developed through considering the transmission of the bandpass signal $\mathrm{A}(t)$ over the channel. The multipath phenomenon can be represented by a continuum of distorted replicas of the transmitted signal which arrive at the receiver with random delays and amplitudes, both of which are functions of time. Then the received bandpass signal can be written as

$$\mathrm{R}(t) = \int_{-\infty}^{\infty} \alpha(\tau; t) \mathrm{A}(t - \tau) d\tau,$$

where α represents the attenuation of the signal components at delay τ, and time t.

Now, by substitution for $\mathrm{A}(t)$ and rearrangement, one can write

$$\mathrm{R}(t) = Re\{\int_{-\infty}^{\infty} \alpha(\tau; t) a(t - \tau) e^{-j\omega_c \tau} d\tau \times e^{j\omega_c t}\},$$

from which it is clear that the complex envelope low pass equivalent for the channel impulse response is

$$h(\tau;t) = \alpha(\tau;t)e^{-j\omega_c\tau}.$$

Various covariance functions for $h(\tau;t)$ can be derived that are often used in characterization of the channel. To begin, assume that $h(\tau;t)$ is wide-sense stationary, and that it has been divided into descrete intervals (ex. measurement resolution windows) in the time and frequency domains , ordered by the indicies i, and j. Its time autocovariance function can then be written as

$$R_h(\tau_i,\tau_j;t_i,t_j) = R_h(\tau_i,\tau_j;\Delta t) = \frac{1}{2}E\{h^*(\tau_i,t)h(\tau_j;t+\Delta t)\},$$

where the factor of one half is due to the complex envelope notation.

If the attenuation and phase shift of the propagation path "i" is uncorrelated with those parameters of the path "j", the channel is referred to as having uncorrelated scattering, and its WSS property makes it a wide-sense-stationary-uncorrelated-scattering (WSSUS) channel. For uncorrelated scattering

$$R_h(\tau_i,\tau_j;\Delta t) = 0, i \neq j,$$

and,

$$R_h(\tau;\Delta t) = \frac{1}{2}E\{h^*(\tau;t)h(\tau;t+\Delta t)\}.$$

The correlation among simultaneous variations of the channel impulse response at different delay times is given when Δt is set to zero by

$$R_h(\tau) = \frac{1}{2}E\{|h(\tau;t)|^2\}.$$

This function is the delay power density spectrum [Bello, 1963a] for the channel. The range of τ over which it is nonzero is called the multipath spread (S_M) of the channel. Since $R_h(\tau)$ can be computed directly from measured impulse response estimates by sample averaging, the assumptions of uncorrelated scattering and WSS channel behavior are often forgotten in its application in the derivation of other channel characteristics and in its use in digital system performance predictions. This can lead to misapplications of channel statistics and erroneous system performance predictions.

A Fourier transform can be applied to $h(\tau,t)$ to obtain the complex envelope equivalent low pass transfer function for the channel

$$H(f;t) = \int_{-\infty}^{\infty} h(\tau;t)e^{-j2\pi f\tau}d\tau.$$

Its autocorrelation function is then given by

$$R_H(f_i,f_j;t_i,t_j) = \frac{1}{2}E\{H^*(f_i;t_i)H(f_j;t_j)\},$$

and if the WSS property is carried through the transformation, R_H is independent of t. Further, if there is uncorrelated scattering [Proakis, 1983; Bultitude, 1983], the function is independent of f and one can write

$$R_H(\Delta f;\Delta t) = \frac{1}{2}E\{H^*(f;t)H(f+\Delta f;t+\Delta t)\}.$$

It can be shown [Proakis, 1983; Bultitude, 1983] that, given the WSSUS conditions,

$$R_H(\Delta f;\Delta t) = \int_{-\infty}^{\infty} R_h(\tau;\Delta t)e^{j2\pi\Delta f\tau}d\tau.$$

If Δt is set equal to zero, the autocorrelation function for simultaneous variations in the channel transfer function at different frequencies is given by

$$R_H(\Delta f) = \int_{-\infty}^{\infty} R_h(\tau)e^{-j2\pi\Delta f\tau}d\tau.$$

This function is called the spaced frequency correlation function. As a result of the Fourier transform, $R_H(\Delta f)$ vanishes at $\Delta f = \frac{1}{S_M}$. This frequency separation is called the coherence bandwidth, B_C of the channel. Again, the assumptions involved are often neglected in applying the Fourier transform relationship leading to erroneous results for $R_H(\Delta f)$, as discussed in [Bultitude, 1983] It is noteworthy also that the coherence bandwidth is often taken as the reciprocal of the rms delay spread (discussed later), rather than the reciprocal S_M in the calculation of a bandwidth in which digital data can be transitted on the channel without intersymbol interference (ISI). The careless estimation of ISI-free bandwidths based on reciprocal delay-spread results from channel measurements is prevalent in the literature and is a subject of great concern [Bultitude and Bedal, 1989] at CRC.

It is useful to note that if there are correlations among scattered signals, the dependence of R_H upon f results in asymmetries in the spaced frequency correlation function. Such asymmetries can readily be seen in the results of time series analyses as outlined in [Bultitude, 1983] which avoid the assumptions in the derivation discussed above.

Time variations on a radio channel result in Doppler broadening and perhaps a Doppler shift of transmitted spectral components. In order to relate Doppler effects on the transmitted signal to time variations on the channel, it is convenient to employ the Fourier Transform of $R_H(\Delta f;\Delta t)$ with respect to Δt, given by

$$S_H(\Delta f;\nu) = \int_{-\infty}^{\infty} R_H(\Delta f;\Delta t)e^{-j2\pi\nu\Delta t}d\Delta t,$$

where ν represents Doppler frequency.

For a single spectral position in the channel transfer function, $\Delta f = 0$, and one can write

$$S_H(\nu) = \int_{-\infty}^{\infty} R_H(\Delta t)e^{-j2\pi\nu\Delta t}d\Delta t.$$

$S_H(\nu)$ is a power spectrum, and for a single frequency component, gives the received signal intensity as a function of Doppler frequency. The range over which $S_H(\nu)$ is nonzero is called the Doppler spread (S_D), or fading bandwidth of the channel. This function characterizes the rapidity of fading.

The spaced time correlation function for the channel can be obtained from $R_H(\Delta f;\Delta t)$ if Δf is set equal to zero. This is the correlation of temporal variations on the channel at a particular frequency, given by

$$R_H(\Delta t) = \frac{1}{2}E\{H^*(t)H(t+\Delta t)\}.$$

The range Δt over which it is nonzero is the coherence time T_C for the channel. From the Fourier relationship between $S_H(\nu)$ and $R_H(\Delta t)$, it is clear that T_C is the reciprocal of S_D.

One other function, the channel scattering function, which is used in the analysis of doubly dispersive channels, can be derived through a double Fourier transform [Proakis, 1983] of $R_H(\Delta f; \Delta t)$ with respect to Δt and Δf. It is written as

$$S(\tau;\nu) = \int_{-\infty}^{\infty} R_H(\Delta f;\Delta t) e^{-j2\pi\nu\Delta t} e^{j2\pi\Delta f\tau} d\Delta\tau d\Delta f.$$

This function provides a measure of the average power of random processes which perturb the channel as a function of multipath delay (τ) and Doppler frequency (ν).

Finally, a short discussion of the rms delay spread of the channel and its application in system performance predictions is warranted. This parameter can be calculated from the delay power density spectrum for the channel, and is a useful parameter in the comparison of different channels with regard to their suitability for digital communications. A channel with a large rms delay spread has significant multipath components at large delays. Therefore there is a greater probability of frequency selectivity (and intersymbol interference) on such a channel than on a channel with a smaller rms delay spread.

Use of the rms delay value in channel characterization work originated with Bello [1963a]. In the referenced paper it is shown to be the ratio of the power of the second term to that of the first in a Taylor series expansion for the transfer function of the channel. Since more terms are required in Taylor series representations for channels with higher degrees of frequency selectivity, the rms delay is an indicator of the degree of selectivity that can be expected on the channel.

The average multipath component delay is given by

$$\tau_{ave} = \frac{\int \tau R_h(\tau) d\tau}{\int R_h(\tau) d\tau},$$

where τ is the delay parameter. For impulse response estimates sampled at the outputs of a measurement system, this equation transforms [Cox, 1972] to

$$\tau_{ave} = \frac{\sum_{k=1}^{N} \tau_k \tilde{R}_h(\tau_k)}{\sum_{k=1}^{N} \tilde{R}_h(\tau_k)} - \tau_0,$$

where k orders the N sampled delay intervals in each estimate of the sum, $\tilde{R}_h(\tau_k)$ is the sampled estimate of $R_h(\tau)$ at delay τ_k, and τ_0 is the earliest delay at which there is power in $\tilde{R}_h(\tau)$ above the noise floor of the measurement system.

If the time required by a measurement system to form an impulse response estimate is considered as a time window during which multipath components are received and their powers and delay times recorded, it becomes clear that if the total integrated power defined by the function $\tilde{R}_h(\tau)$ is normalized, the result is the relative frequency function $\tilde{f}(\tau)$, or experimental estimate for the density function $f_\tau(\tau)$ for multipath delays [Devasirvatham, 1987]. That is,

$$\tilde{f}(\tau_k) = \frac{\tilde{R}_h(\tau_k)}{\sum_{k=1}^{N} \tilde{R}_h(\tau_k)}.$$

The second central moment of multipath component delays is then given by

$$\sigma_\tau^2 = \sum_{k=1}^{N} \tilde{f}(\tau_k)[\tau_k - \tau_0) - (\tau_{ave} - \tau_0)]^2.$$

The parameter σ_τ is known as the rms delay spread for the channel.

If care is taken, rms delay spread values can be useful in the comparison of multipath radio characteristics on different channels. Their use in the prediction of flat fading boundaries and error performance, however, requires careful consideration. In connection with work on mobile radio channels, Jakes [1974] has shown that on a Rayleigh fading channel having an assumed Gaussian shaped delay power density spectrum, the irreducible error rate for DPSK increases with increasing rms delay spread. Further, B_C is often assumed to bear an inverse relationship to the rms delay spread. It has been reported [Bajwa and Parson, 1985] for mobile radio channels, however, that the sensitivity of this relationship varies considerably with environment. This variation is conjectured to be a result of variations in the channel fading distributions and violation of the uncorrelated scattering conditions. The reciprocal delay spread relationship is therefore considered to be a potentially misleading rule of thumb for application in channel performance predictions.

1.2 Classification of Fading Radio Channels for Digital Communications

If receiver front-end noise is neglected, the complex equivalent low pass signal at the input to the receiver after transmission over a fading channel can be represented [Proakis, 1983] as

$$r'(t) = \int_{-\infty}^{\infty} H(f;t)S(f)e^{j2\pi ft}df,$$

where $S(f)$ is the spectrum of a low pass modulating signal $s(t)$.

If $s(t)$ is a series of pulses which modulate f_c at a rate $1/T$, two types of distortion can be introduced by the random channel. These include: intersymbol interference caused by spreading of the signal in the time domain due to multipath propagation, and variations in received signal characteristics during one signalling interval caused by shadowing and spreading of the signal in the frequency domain due to Doppler phenomena. Temporal dispersion is manifested in the frequency domain as frequency selectivity the characteristics of which are dependent upon S_M and B_C. Frequency dispersion is manifested in the time domain as time selectivity, the characteristics of which are dependent upon S_D and T_C.

The influence of a propagation channel on a digital signal transmitted over it is a function of the relationship between the time-bandwidth product of transmitted symbols, and the correlation properties of the channel. For instance, if B_C is significantly greater than the transmission bandwidth (W), negligible inter-symbol interference will be introduced by the channel.

Classification and modelling of fading digital radio channels is in accordance with their effect on transmitted signals. The following paragraphs outline common classifications [Bello, 1963a, 1963b] that apply to digital radio channels the statistictics of which are nonstationary, but which may be regarded as wide-sense-stationary (WSS) for time and frequency intervals which are short, but which are greater than the durations (T) and bandwidths respectively of transmitted signals. This allows the application of the large body of theory available for WSS random processes to problems that would otherwise be intractible. Because of their quasi-stationary nature, such channels are referred to as quasi-wide-sense-stationary (QWSS) channels. Quantitatively, for a QWSS channel,

$$W << \frac{1}{\delta_{max}} \text{ and } (T + S_M) << \frac{1}{\sigma_{max}},$$

where δ_{max} and σ_{max} are the maximum rates at which $R_H(f_i, f_j; t_i, t_j)$ fluctuates in the f and t domains. These criteria can be verified through the analysis of measured data as discussed in a later paragraph.

If the bandwidth of transmitted digital symbols is much less than B_C, and T is much less than T_C, the channel falls into the category of a flat/flat fading channel [Bello, 1963a] or a slowly varying nonselective channel [Proakis, 1983]. If the flat fading criteria are satisfied all spectral components of the transmitted signal fade in unison. Therefore within the bandwidth of $S(f)$, the fading statistics of the channel are independent of frequency. Additionally, if the bandwidth of $S(f)$ is small compared with f_c, $H(f,t)$ can be assumed to be constant. Under these conditions the channel transfer function can be removed from the integral in the expression for $r'(t)$. Also, since $s(t)$ is a low pass signal, $H(f;t)$ can be assumed to be constant at its value for $f = 0$, and on completion of the integration one can write

$$r'(t) = H(0;t)s(t).$$

Then by writing the channel transfer function as the Fourier inverse of its impulse response

$$r'(t) = \int_{-\infty}^{\infty} \alpha(\tau;t)e^{-j2\pi f_c\tau}d\tau \times s(t).$$

If the transmitted signal characteristics are such that $WT = 1$, in the frequency nonselective case $T >> S_M$ and for a practical receiver the multipath signal components are nonresolvable. The integral with respect to τ then disappears and the phase term becomes a function of time due to the vector addition of multipath components with delay separations smaller than the receiver resolution so that one can write

$$r'(t) = \alpha(t)e^{-j\phi(t)}s(t).$$

Thus, the random channel is modelled as a multiplicative process in the time domain which randomly affects the amplitude and phase of the received signal. If the flat fading criteria are considered further it is evident that the amplitude and phase of the received signal are constant over at least one symbol interval and the time dependence can be dropped from the channel gain and phase representations for the purpose of calculating probability of symbol error. Then the average probability of error on the channel can be calcuated by averaging the error rate for the mean signal to noise ratio based on link budget calculations over the distribution of slow variations in α.

Flat/flat fading channels are the easiest to model and lead to the most simple of error rate computations for digital transmission. The upper UHF (900 MHz) mobile radio bands, for urban communications (tall buildings and moderately low vehicle speeds) afford flat/flat fading channels for transmission bandwidths [Bultitude, 1987a] up to about 25 kHz.

Digital radio channels which carry signals for which the duration of transmitted symbols is comparible with or greater than T_C, but which have bandwidths which are much smaller than B_C are classified as time-selective/frequency-flat channels. On such channels the amplitudes and phase relationships of the received signal can be expected to change over a single symbol duration, but inter-symbol inteference is negligible. An example is the channel between a base station and a vehicle moving rapidly in an open environment.

Since this type of channel exhibits no frequency selectivity, the same derivation applies as for the channel model in the flat fading case and the multiplicative model remains valid. If the temporal variations of $\alpha(t)e^{-j\phi(t)}$ form a complex Gaussian process, closed form error probability equations can be derived [Bello and Nelin, 1962]. For most of the common digital modulation types the derivation follows the general routine of first reducing the expression for the decision variable to a Hermitian quadratic form. Its probability density function (pdf) can then be derived using the channel and transmitted signal correlation functions and a decision rule can be established. If the channel process is not Gaussian the mathematics involved in the derivation of a closed form pdf appear to be intractible, and simulations are necessary in order to arrive at digital system performance predictions. Radio propagation measurements are still required, however, to obtain parameters or storred channel inputs for the channel simulations.

If the transmit signal bandwidth is much greater than B_C, but the total duration of transmitted symbols, plus multipath interference is less than T_C, the channel is classified as frequency-selective/time-flat. A good example [Bultitude, 1987a] is the UHF urban mobile channel which exhibits time dispersion due to multipath propagation, but frequency dispersion is low, as vehicle speeds are not fast enough to create Doppler effects of any significance.

For this type of channel propagation conditions are independent of time over at least one symbol duration, but the channel transfer function is dependent on frequency over the transmit bandwidth. The time dependence can therefore be dropped from the channel transfer function representation and, neglecting noise at the receiver front end, the received signal can be written as

$$r'(t) = \int_{-\infty}^{\infty} H(f)S(f)e^{j2\pi ft}df.$$

As in the time-selective/frequency flat case, error probabilities can then be computed from a Hermitian quadratic representation for the decision variable provided the channel can be represented as a complex Gaussian process.

The final channel classification, that of Doubly Selective, applies to channels the correlation times and correlation bandwidths of which cannot be considered as being much greater than transmitted symbol durations or bandwidths. Again if fading is characterised by Gaussian statistics a closed form solution for the symbol-by-symbol probability of error can be derived [Bello and Nelin, 1964]. In this case, however, the derivation of the pdf for the decision variable involves the channel scattering function rather than one dimensional correlation functions, and a cross ambiguity function between the received mark and space waveforms. It is interesting to note that on doubly selective channels there is an optimum signalling rate at which the probability of error is minimum. This signalling rate is dependent upon the spread factor ($S_M \times S_D$) of the channel and is given by

$$R_{min} = \frac{1}{2T(S_D/S_M)^{1/2}}.$$

For signalling rates near this optimum, the channel behaves as if it were a flat fading channel. For lower rates, the channel behaves as if it were purely time selective and for higher signalling rates it behaves as if it were purely frequency selective.

1.3 Propagation Measurement and Analysis Techniques

From a consideration of the channel models and classifications discussed in the foregoing paragraphs it is clear that if predictions for digital system performance are to be made based on propagation measurements, the measurements must be designed to yield enough information to classify the channels and to derive the necessary parameters for use in the varied prediction methods that must be used for different channel classifications. For flat fading channels (narrowband channels on which Doppler phenomena are not significant) it is sufficient to be able to derive the statistics of the received signal envelope from a CW transmission (those of $\alpha(t)$) in order to predict digital system performance. As selectivity becomes more probable, however, usually due to the desire for wider transmission bandwidths or higher speeds in a mobile system, more sophisticated measurement and analysis techniques are required. In addition, regardless of the degree of selectivity on the channel, it must be proven that the channel can be classified as QWSS before any of the closed form prediction techniques based on the application of mathematics for WSS random processes can be applied. The following section explains one of the more complicated measurement techniques and analyses that can be applied to the measured data in order to correctly classify and model fading radio channels. A concerted effort has been put forward toward this end over the past five years at CRC in connection with investigations [Bultitude, 1987a] on mobile radio channels in the 900 MHz band.

It is clear that modelling and classification of radio channels depends on a knowledge of the equivalent impulse response or transfer function of the channel. Kailath [1962] proposed a cross correlation technigue for estimating channel impulse response functions from propagation measurements. This technique has been used for measurements on a variety of channels by different researchers [Cox, 1972; Linfield et al, 1976; Bultitude, 1983; Bajwa and Parsons, 1985; 1962; Devasirvatham, 1987] and is well explained in simplistic terms by Linfield et al [1976], in a similar development to that outlined below

Consider a fixed linear filter with impulse response $g(t)$. An arbitrary input, $x(t)$ to the filter would produce an output $y(t)$ given by

$$y(t) = \int_{-\infty}^{\infty} x(t-u)g(u)du.$$

If both sides of this equation are multiplied by $x^*(t-\tau)$, one can write

$$y(t)x^*(t-\tau) = \int_{-\infty}^{\infty} x(t-u)x^*(t-\tau)g(u)du.$$

Now, if $x(t)$ is a WSS random process, expected values can be taken on both sides of this equation to give

$$\begin{aligned} R_{xy}(\tau) &= \int_{-\infty}^{\infty} R_{xx}(\tau-u)g(u)du \\ &= R_{xx}(\tau) * g(\tau), \end{aligned}$$

where R_{xx} and R_{xy} represent autocorrelation and cross correlation functions for the random processes $x(t)$ and $y(t)$.

It is clear that if $x(t)$ is white noise

$$R_{xy}(\tau) = \delta(\tau) * g(\tau) = g(\tau),$$

where $\delta(\tau)$ is the unit impulse function. That is, the cross correlation function $R_{xy}(\tau)$ is identical to the response of the filter at time t to an impulse applied at its input at time $(t-\tau)$.

In most channel probes reported in recent literature, and almost white (flat spectrum over a large part of the measurement bandwidth) stationary pseudo-random process $y'(t)$ is transmitted over a radio channel and is cross-correlated at the receive terminal in a complex base-band correlator with a second pseudo-random process $x'(t)$ which is identical to the random process transmitted at time $(t-\tau)$, where τ is the propagation delay of the channel. If it is assumed that the channel is linear, this cross correlation product can be taken [Benvenuto, 1984] as a good estimate of the complex envelope low pass equivalent for the impulse response of the channel. The phase characteristics of the channel are normally preserved during this type of measurement through the use of coherent atomic frequency standards to which all oscillators are slaved at both receive and transmit terminals.

For time variant channels, the time variant impulse response $h(\tau;t)$ can be measured by recording samples of $h(\tau)$ measured over repetitive, evenly spaced time intervals.

1.4 Application of Measurement Results

With a knowledge of the channel impulse response estimates, all of the information required for channel classification and modelling can be obtained. It appears, however, that it is easiest to work with the channel transfer function, rather than the impulse response. Therefore in analysis done at CRC a complex fast Fourier transform is taken of each impulse response estimate after it is recorded. This yields complex time series information for a number of spectral positions across the measurement bandwidth. Time series analysis techniques can then be applied to investigate various channel characteristics and thereby avoid the necessity for assumptions regarding channel statistics, including statistical stationarity, applicable distribution functions, and space and time correlation intervals.

First it must be determined if the measured channels can be considered quasi-wide-sense stationary for intended signal transmissions. The mathematical definition given earlier for QWSS behavior can be interpreted as defining a channel to be QWSS if symbol durations and transmission bandwidths are limited to time and frequency intervals over which there is negligible change in the channel autocorrelation function $R_H(f_i, f_j; t_i, t_j)$. The range of symbol rates for which a channel can be considered to be QWSS can be ascertained from propagation measurements through independent examinations of the characteristics of $R_H(t_i, t_j)$ and $R_H(f_i, f_j)$. A random process [Lee, 1976] is said to be stationary if its statistical properties are invariant to translation of the index paramenter for the process. It is said to be stationary in the wide sense if it has finite variance and its autocorrelation function is independent of the index parameter. Therefore the QWSS ranges can be determined by comparing correlation functions for the channel computed for contiguous reference values until significant dissimilarities can be identified among the functions. So long as the correlation functions remain approximately constant, the channels can be considered WSS for the purpose of mathematical error performance calculations. This procedure is outlined in more detail by Bultitude [1987a], where it is shown that for urban vehicle speeds up to 100 Km/hr, urban mobile radio channels can be considered QWSS for transmission rates over the range

$$232\ b/s \leq R \leq 325\ Kb/s,$$

with rectangular signalling elements.

The next step is to chose the appropriate model for the channel, depending upon the degree of selectivity. This also can be effected by an examination of correlation functions computed from measurement data.

The spaced frequency correlation function $R_H(f_i, f_j)$ can be calculated through a complex cross-correlation of time series data at different spectral positions in channel transfer functions derived from fast Fourier transforms of measured impulse response estimates as outlined in [Bultitude, 1983]. The channel can be classified as frequency selective or frequency flat by comparison of the intended transmit bandwidth with the bandwidth B_C over which the envelope of the correlation function (the complex parts have shapes depending on the phase defined by t_0 in the FFT input) drops to zero The channel can then be considered as frequency-flat if the transmission bandwidth is "much much less" than B_C. The qualitative description of "much much less" has been a subject of research at CRC on mobile channels over the past several years. It appears [Bultitude and Bedal, 1989; Bultitude, 1987a] that this is dependent upon the CW envelope fading distribution on the channel (ex Rayleigh or Rician) and current analyses indicate that W should be about 1/10th of B_c for flat fading on Rayleigh channels.

Determination of the time selectivity can be made in an analogous manner. The function $R_H(t_i, t_j)$ can be computed from a time series of values at a single spectral line in estimated channel transfer functions. The time lag required for the envelope of this function to decrease to zero then defines correlation time on the channel. This must then be compared to

the sum of the measured multipath spread and intended symbol durations for classification of the channel with regard to its time selectivity.

Once the selectivity of the channel under study has been determined an appropriate model can be chosen. Error probabilities can then be computed based on the channel model using techniques specific to the distribution of CW envelope fading. This distribution is that of the envelope of a single spectral line in transfer functions computed from the impulse response measurements. In the nonselective cases a simple averaging of the nonfading probability of error can be done either numerically or analytically depending on the availability of an integrable closed form expression for the fading distribution. If the channel has been determined to be selective, analyses become more difficult. For the Rician and Rayleigh CW distribution cases, the channel has Gaussian statistics and closed form equations can be developed following Bello's [Bello, 1963b; Bello and Nelin, 1962; Bello and Nelin, 1964; Bultitude, 1987a] methods. In other cases simulations are required.

Other information such as the burstiness of fading, and the fading bandwidth [Bultitude, 1987b] can also be determined directly from the measured data. This information is of use in the determination of suitable methods for use of the channel models in the prediction of system performance. For instance, a channel with continuous fading would lend itself to direct application of Bello's methods. Performance calculations for a bursty channel might be made differently, depending on the rapidity of fading and the lengths of the bursts.

In summary, given the availability of equipment to make propagation measurements which allow estimation of the channel impulse response, there is no need for assumptions regarding statistical stationarity, uncorrelated scattering, Gaussian characteristics, or the channel selectivity. Additionally, either through similations which use the measured channel data as inputs, or through analytical methods, error performance can be calculated explicitly for the exact or most probable channel conditions. There is no need to blindly apply rules of thumb, such as the reciprocal rms delay spread flat fading critereon, to all channels regardless of their statistical stationarity or envelope fading characteristics in order to guess what implemented system performance might be. This is done too often in current literature. Modern measurement and analysis techniques afford the opportunity for better founded prediction results. The information obtained from propagation measurements can be used to verify conditions in every step of performance prediction procedures to make results fit exactly the conditions of the measured channel.

2. Channel Simulators

2.1 VHF/UHF Mobile Radio Channel Simulator

2.1.1 Fading Simulator

Several years ago CRC started a project to build a test facility for land mobile radio communications equipment, Fig. 1. A major part of this test facility was a channel simulator built under contract by Miller Communications Systems Ltd, Fig. 2. The channel simulator simulated the following propagation characteristics: Rayleigh fading, Lognormal shadowing, delay, and external broad band Gaussian noise.

A channel simulator, circumvents the need for performing on-site operational tests and offers the following important advantages over on-site testing: 1) AVAILABILITY: A simulator provides immediate access to the desired conditions without having to move to a suitable location and to wait for the specific conditions. 2) STATIONARITY: A simulator provides stationary statistics which allows one to perform tests involving a number of hours, whereas the statistics of true conditions generally change rapidly enough to render such tests impractical and the results useless. 3) REPEATIBILITY: A simulator offers accurately defined and controlled conditions for comparison testing of one system at one time and place against other systems at other times or places, or for repeated testing of the same system after adjustments or modifications are made. 4) RANGE: A simulator provides test conditions that extend to or beyond those found rarely in nature. 5) COST: A simulator allows measurements to be made in a laboratory more quickly and economically than similar on-site measurements.

A number of hardware fading simulators [Arredondo et. al., 1973; Jakes, 1974; Ball, 1982; Lorenz and Gelbrich, 1984] and channel simulators [Caples et. al., 1980; Hagenauer and Papke, 1984; Davarian, 1987] have appeared in the literature. In our channel simulator, as shown in Fig. 2, the signal may go through any combination of three paths, DIRECT, FADING and FADING DELAY. The simulator can be operated at 70 MHz for modems as well as at the 3 Land mobile bands (ie 138 to 174 MHz, 406 to 470 MHz and 806 to 890 MHz). Operational Parameters for the channel simulator include: an instantaneous bandwidth of 10 MHz, fading bandwidths from 3.6 to 1844 Hz, a maximum fade depth >25dB, Rice parameters from 0 to -25 dB (the value of the Rice parameter is the ratio of FADING power to the DIRECT power in dB), Lognormal shadowing bandwidths from .036 to 18.44 Hz, Lognormal shadowing sigma from 0 to 6 dB, a shadowing depth of 2.5 sigma, fixed delays of 0,1,2,5 usec, signal to noise ratios of 40 to 99 dBHz and remote control via an IEEE 488 bus. To-date we have not compared the channel simulator to any real data, however, we have exercised it and present three examples below.

Fig.3 shows a typical output from the fading channel. The Rayleigh fading bandwidth, FD, is a function of vehicle speed and operating frequency, i.e. FD = V/LAMDA. For a vehicle travelling at 100 km/hr and operating at 150 MHz FD= 13.9Hz. This rapid fluctuation of the signal envelope is caused by multipath propagation leading to wave interference as the waves add and cancel.

For many urban situations the channel can be characterized by a combination of DIRECT and FADING paths. The effect of varying the Rice parameter from 0 dB (equal powers) to -10 dB (mostly direct path) is to reduce the dynamic range of the envelope of the received signal level. This is shown in Fig. 4 which is a family of Amplitude Probability Distributions (APD) for varying values of the Rice parameter for 860 MHz and a vehicle travelling at 100 km/hr (FD = 79.52 Hz). The APDs are plotted on Rayleigh graph paper where a Rayleigh distribution plots as a straight line with slope of -1/2. Values of -6 to -8 dB are typically found in the literature for the Rice parameter [ITU, 1978; Norton et. al., 1985; Bajwa, 1985; Davis and Bogner, 1985].

A second aspect of mobile radio propagation, shadowing of the received signal by buildings and hills, leads to slow changes in the local mean signal level as a vehicle moves through an area. This slow variation has been modelled by a lognormal distribution in the literature [Jakes, 1974; French, 1978; Parsons and Ibrahim, 1983]. Results of varying the Lognormal shadowing parameter are presented as a family of APDs in Fig.5. This example is for 450 MHz and a vehicle travelling at 80 km/hr (FD = 33.42 Hz). There is a significant change in the shape of the APD as sigma varies from 0 to 6 dB. French [1978] has noted that values of 6 dB for sigma are typical in London and suburban locations, however, in urban cores with many high rise buildings sigma may be typically 8 to 12 dB.

Table 1

Average Fade Durations

Fading Channel at 150 MHz, FD = 13.9 Hz

Threshold (dB)	Measured T (MSEC)	*Theoretical T (MSEC)
- 2	31.8	31.7
- 4	21.5	22.2
- 6	17.1	16.3
- 8	11.9	12.4

Fading Channel at 860 MHz, FD = 64Hz

Threshold (dB)	Measured T (MSEC)	*Theoretical T (MSEC)
- 2	6.88	6.86
- 4	5.55	4.81
- 6	3.74	3.53
- 8	2.68	2.67

* Using Jakes' Formula for T

The third study that we carried out relates to fade durations. Jakes [1971] presents a formula for the average fade duration at a specified threshold. Table 1 shows good agreement for the two cases shown. In calculating the average fade duration we had to compute the distribution of fades. On plotting these we find, for example, that although the average fade duration is 33 msec there is a wide spread which may be modelled by an exponential distribution (see Fig. 6).

2.1.2 Non-Gaussian Noise Simulator

The external noise used in the simulator was broad band Gaussian noise, whereas, the urban land mobile channel environment is characterized by impulsive noise which in many instantances can be characterized by a Lognormal amplitude distribution. We have been able to modify the channel simulator to implement an impulsive noise generator which will be interfaced to it. Over the years several noise simulators have appeared in the literature. An atmospheric noise simulator was built at the ITS laboratory in 1969 for LF and HF noise [Coon et. al., 1969; Bolton, 1971]. In 1975 workers at Cornell University developed a Pseudorandom Gaussian and impulsive noise source with a Lognormal amplitude distribution [Neuvo and Ku, 1975]. In 1984 workers at the University of Liverpool UK developed an impulsive noise simulator especially designed for the VHF UHF land mobile environment [Parsons, 1984].

The design of this simulator followed the basic concept of Neuvo and Ku [1975]. This consists of a three step process. 1) generating pseudorandom noise with a uniform amplitude distribution, 2) generating Gaussian noise by summing a finite number of values of the uniformly distributed sequence, and 3) forming a lognormal process by taking the exponential function of each gaussian sample.

To obtain a useful prototype we had to reach a compromise of three conflicting design criteria. First, the speed of sample generation is proportional to 1/2B, where B is the bandwidth; second, the noise must have an accurate estimate of the design distribution and third flexibility, ie being able to adjust the shape of the distribution. The first criterion is of prime importance as we must have a noise source with at least a 10KHz bandwidth. The second is also of prime but slightly lessor importance. Flexibility has the lowest importance at this time, however, it must be added to the final design. Generating noise samples and then outputting them one at a time did not meet the first criterion. The only way of meeting this criterion was by having two parts to the program; one to generate and store noise samples in memory and a second part to read the stored values from memory and output them. In the prototype hardware restrictions allowed us to store a maximum of 15,000 noise samples, however, we could output values at a 50 KHz rate

ie. a bandwidth of 25 KHz. The program produced values with the correct amplitude distributions as tested by the Kolmogorov-Smirnov goodness of fit test.

The prototype noise generator utilizes an 8088 microprocessor with a 16 bit word. The uniform number routine uses a 16 bit Pseudo-Random Binary Sequence (PRBS) requiring 4 feedback taps. This produces a PRBS of lengtht 2^{16} - 1 which is a maximal length shift register sequence. This method was used by Hurd [1974] and Ball [1982] to produce statistically accurate uniformly distributed random numbers. The Gaussian numbers are found by averaging 16 uniform numbers and the lognormal values are found by use of a lookup table.

2.2 A Recorder-Reproducer Type HF Channel Simulator

2.2.1 Introduction

A channel simulator for HF has been designed that allows comparison of system under repeatable and realistic conditions. Tests conducted over actual HF circuits can be costly due to large number of trials required to achieve statistical validity. The use of simulator is beneficial only if a realistic channel is simulated.

This report describes a technique where the characteristics of the ionosphere are first recorded on magnetic tape then simulator is controlled by the recorded information on the tape to accurately model the channel. This simulator can provide a means of checking the results obtained using other simulators such as the ones described in [Prel, 1984].

2.2.2 Equipment Description

The simulator consists of three sub-systems as shown in figure 7 and 8.

2.2.2.1 Probe

The function of the probe is to enable a tape recording to be produced from which the instantaneous characteristic of the ionosphere can be extracted by the analyzer. The probe generates a signal called Frank code [Heimiller, 1961] repeated at intervals of 12.25 ms. The probe signal is generated at audio baseband level and transmitted by an HF SSB transmitter. After traversing the ionospheric path, the signal appearing at the receiver audio output is recorded on an analogue tape recorder.

2.2.2.2 Analyzer

The function of the analyzer is to produce channel characteristics in the form of the channel impulse response. A matched filter for the Frank code implemented in digital form is used to extract the channel impulse response. The impulse response as function of time is then passed to the simulator. The analyzer generates a timing signal synchronized to the Frank code repetition rate. The analyzer also filters the probe signal from the recorded information and residual noise is transferred to the simulator section.

2.2.2.3 The Simulator

The simulator consists of a tapped delay line whose impulse response can be controlled by adjusting the tap weights. The output of the system under test is connected to the input of the variable delay line. The output of the delay line is the simulator output, representing the signal distorted by the process of propagation through the ionosphere. The simulator receives the channel impulse response from the analyzer every 12.25 ms and the tapped delay line is updated with the channel information. The channel information can be time averaged and updates can be made at a reduced rate. The simulator can also add the noise information supplied by the analyzer to the transversal filter output.

2.2.3 System Parameters

System bandwidth:	300 to 3000 Hz
Input impedance:	600 Ohm balanced
Input level:	$\pm$6 V into 600 Ohm analog
Tape recorder:	Analog audio recorder with jitter < 50 parts per million
Dynamic range:	50 dB.

2.3 A Spread-Spectrum HF Simulation Facility (Implemented in Software)

The CRC spread-spectrum simulation facility is intended as a tool for the investigation and comparison of both existing and proposed spread-spectrum systems. It was designed to simulate the operation of a complete spread-spectrum communication system including transmitter, HF propagation path, interference, and receiver, and to provide all the data and signal generation and analysis capabilities necessary to determine the performance of the simulated systems. Direct-sequence and frequency-hopping systems as well as conventional communication systems may be simulated. The simulation is performed in software on a Digital Equipment Corporation VAX 11/750 computer. The following is a very brief description of the facility. Much greater detail can be found in Venier [1986].

Figure 9 indicates the general structure of the simulator and some of the processes implemented. The solid arrows show the normal flow of data and signals, while the dashed ones indicate alternative routes which can be used for testing of particular parts. The user decides which of the processes he wishes to include in the simulation and selects them and their parameters in an interactive process in which the program questions him on the desired values. A batch mode of operation under control of a command file is offered as an alternative for long runs of complex systems. The simulator was made as flexible as possible, providing a good selection of subsystems that should cover a wide range of actual and proposed systems.

Waveforms in the simulation are represented by complex floating point samples. This allows both positive and negative frequencies to be independently specified, and therefore carrier frequencies can be set at or near zero Hz in order to minimize the required sample rate.

In a frequency-hopping system a new carrier frequency is selected periodically in a pseudo-random manner from a pre-determined set of frequencies. Since the simulation is carried out entirely at baseband the simulated signal is not actually hopped in frequency, but the samples at a given frequency are grouped into a block with the first two words of the block used to indicate the frequency of that block and the number of samples in the block. The propagation medium routines make use of the frequency words to determine which propagation characteristics to apply to the samples in that block. The front end of the receiver also looks at the frequency words to determine whether to accept the samples (a frequency hop generator in the receiver determines receiver tuning).

The simulator attempts to model HF propagation conditions. Many discrete paths with user-selected attenuation, delay, and doppler frequency can be simulated. The paths may be either fixed or have Rayleigh fading. In the case of Rayleigh fading, the amplitude and phase of each component are derived from a filtered pseudo-random Gaussian noise generator, with mean amplitude and Doppler frequency selected by the user. The filter characteristics are selected by the user to determine the fading rate. Rician fading may be simulated by combining fixed and Rayleigh paths. Delay-spread conditions are simulated by a providing a number of paths with delays spaced only one sample interval apart and therefore unresolvable by the simulated signal. Different propagation conditions may be specified at different transmission frequencies to allow realistic simulation of frequency-hop systems.

The noise and interference, like the propagation characteristics, are functions of frequency, but in this case it is the frequency to which the receiver is tuned, rather than the the transmission frequency. Since these two may not always be the the same, the simulated noise and interference are added in the receiver and controlled by the dehopping frequency generator. Their characteristics are specified by the user for the different frequency ranges.

Types of noise and interference provided in the simulator are: Gaussian noise; pure impulse noise with random intervals and, if desired, random energy; pulse interference with random intervals; tone interference; swept-frequency interference; and impulsive noise modeled on the CCIR HF noise probability distribution curves [2]. The different types of noise and interference may be combined.

Other functions available in the simulator include: direct-sequence modulation, various types of data modulation and demodulation, filtering, automatic gain control, amplitude limiting, error-correction coding using cyclic block codes, interleaving, synchronization of data symbols and spreading codes, and various routines for the analysis of signals and data.

3. Some New Approaches to Communications System Design

It was noted in the theme for this meeting that microprocessor technology is radically changing the engineering approach to designing and operating communication systems. The flexibility offered by software implementation makes them ideal vehicles to realize and optimize new approaches. In contrast with traditional systems, signal processing for modern systems can be realized in software, employing digital signal processing chips to perform the required modulation and demodulation processes. For example, the input voice signal can be digitized, transformed to the frequency domain by an FFT, where block filtering and frequency translation are easy. An inverse FFT returns the signal to the time domain, but at a low IF frequency. The signal is then translated to RF. On receive the reverse takes place. The received signal is translated to low IF, digitized, and transformed to the frequency domain by an FFT. In this domain the signal is translated back to base-band, and the return to an analogue signal is achieved by application of an inverse FFT. One can then put on a pair of earphones and listen to the signal. The paper by Boucher et. al. to be presented at this meeting describes CRC research in this area.

The use of microprocessors for coding and decoding, for code diversity, for transmission of digital facsimile, for adaptive HF systems employing real-time-channel evaluation and adaptive networking, and for adaptive antenna arrays for cancelling interference or jamming are described below.

3.1 Use of Coding Diversity on HF Data Circuits

3.1.1 Introduction

There is a need for HF data transmission systems to provide reliable service in an efficient manner with multi-tone FSK or PSK modems (see CCIR Recommendation 436-2 and Report 864-1 Dubrovnik, 1986). To compensate for the unfavourable nature of the selective fading phenomenon of the transmission medium, in-band or other frequency diversity techniques are widely utilized.

This report describes a coding technique that improves the in-band frequency diversity system.

3.1.2 System Description

The transmission scheme described in this report is shown in Fig. 10. The output m(t) from a binary information source is fed into an encoder shift register of length K. After each shift of the register at the source data rate, the encoder generates two code bits, $c_1(t)$ and $c_2(t)$, which in turn drive corresponding conventional data modulators. In practice the centre frequency separation of these data modulators is usually about 1 kHz. The combined output of the modulators is then fed into a HF SSB transmission system.

In frequency diversity operation, the system of Fig. 10. assumes its simplest form. The code bits are simply replicas of the information bit, i.e. $c_1(t)=c_2(t)=m(t)$. The decision on the value of a given information bit is based on the combined value of the outputs of the two demodulators. From an information theory context, frequency diversity can be described as a rate 1/2 repetition coding scheme that uses soft decisions.

In frequency diversity transmission, only two code bits contain information about any given information bit. With nonzero probability, both of these bits can be simultaneously corrupted by fading, interference or noise so that an incorrect decision is made on the information bit. When this occurs, there is no possibility of correcting the error by using the values of the other code bits. It therefore appears desirable to encode the information sequence such that more than a single pair of code bits is related to any given information bit. The system of Fig. 1 does this by mapping the information sequence prior to transmission.

Any type of rate 1/2 error correcting code could be used in coded frequency diversity transmission, but convolutional codes are particularly suitable because their encoder structure fits with the structure of frequency diversity transmission systems, and the Viterbi algorithm can be used to efficiently carry out soft-decision decoding [Clark and Cain, 1981]. The outputs of the demodulators are fed to A/D converters in a Viterbi decoder which replace the combining operation of the conventional frequency diversity system.

3.1.3 Experimental Results

On the air performance comparison of frequency diversity and coding diversity has been made. Convolutional codes of constraint length K=5, and 7 were chosen, and the output of the encoder is fed into a multi tone FSK modulator centre frequencies 1105 and 2125 Hz and $\pm$ 42.5 Hz shift. The data rate of each synchronous channel was 75 bps. The eye signal from each demodulator was digitized by a sample taken from the centre of the eye period. The HF radio equipment used were a 100 watt transmitter, broadband antennas, and a synthesized communications receiver. Maximal ratio combining was used for the diversity reception experiments. A real time Viterbi decoder, implemented in software with an 8 bit general purpose micro processor, was used for the coding experiments. Details of this system have been published [McLarnon, 1985; Garcia et al., 1985].

Three series of on-the air tests were conducted from Ottawa. short range test over a distance of 60 km, which has a weak groundwave component; medium range distance of 400 km to Toronto; and a third test from a ship operating off the east coast of Canada. Her voyage took it from Quebec City to The High Arctic, allowing tests to carried cut over distances ranging from about 400 to 2500 km. During the latter part of this test period, the HF link traversed the auroral belt and rapid fading was often present.

The error patterns of frequency diversity and coding diversity were analyzed. It was observed that both sets of data exhibited the burstiness characteristic of the HF channel; however, in the case of diversity, transition between bursts and the periods of lower error rates were gradual. The errors were random much of the time, with frequent isolated single errors. The data from the coding diversity system had dense bursts with relatively abrupt beginning and end, longer error free gaps, and an absence of single and double errors. The bursts tended to be longer than those in the diversity system. After a long burst the decoder requires some time to recover. Thus the bit error rate in the decoded sequence may actually be higher than that in a conventional diversity system. This is not the case for the block error rate performance.

This system is intended to be used in an ARQ protocol environment which precludes the use of interleaving or time diversity. These schemes have been shown to result in improvements in the bit error rate, but they require delays of the order of several hundred bits. In block transmissions blocks are rejected due to single or more errors which is the case for frequency diversity combining. But in coding diversity the block rejection is reduced by reduction of isolated errors. The tests were done for block sizes of 128 and 512 bits, which is typical for the system that is going to utilize the coding diversity.

The block error rates of the two techniques were compared and are shown in Table 2. The table includes the percentage increase in probability of receiving an error free block for the coding technique versus frequency diversity. The improvement obtained varied from good to insignificant, and a larger improvement for 512 bit blocks are observed In some instances the diversity transmission was virtually error-free itself, and thus there was little room for improvement; in other cases, the channel was so poor that neither system provided a useable error rate. It was observed that in no instance was the performance of the coding scheme significantly worse than that of the standard diversity system.

Table 2
Experimental Block Error Rate (BER) results

Test Number	Constraint Length	Diversity BER	Coding BER	Total Bits	Throughput Improvement %
Block Size = 128 (bits)					
1	K=7	293	201	1,430,000	13.0
2	K=7	217	127	506.000	11.5
3	K=5	321	227	352,000	13.8
4	K=7	084	015	217,000	7.5
5	K=7	083	019	217,000	6.5
Block Size = 512 (bits)					
6	K=7	548	406	1,430,000	31.4
7	K=7	378	223	506,000	24.9
8	K=5	570	420	352,000	34.9

3.1.4 Implementation Considerations

The coding technique described in this report has a number of practical limitations and it will not replace a general purpose diversity combiner in all applications. It is incompatible with asynchronous data transmissions systems. It is potentially useful with ARQ systems using synchronous transmissions provided that the transmissions are not so short that the improvement in throughput is nullified by the increase in overhead bits required for proper operation of the Viterbi decoder. The overhead is 4 times K bits (where K is the constraint length) needed at the beginning of the transmission, plus there is a postamble of K-1 bits at the end of the transmission.

3.1.5 Conclusions

An error control scheme based on convolutionally coded frequency diversity transmission has been tested. Experimental results show that this system has better block error rate performance than ordinary frequency diversity systems. The scheme is suitable for systems that presently use ordinary frequency diversity in combination with a synchronous ARQ protocol.

3.2 HF Radio Communication Equipment for Digital Facsimile and Hard Copy Messages

3.2.1 Introduction

An automatic HF digital facsimile and hard copy terminal developed in Canada described in this report [Scrinken 1988]. The system has the following general characteristics:

- HF frequency evaluation and selection;
- access from the switched network for remote terminal operations;
- storage, editing and transmission of messages from disk media;
- high quality Group 3 facsimile image with (7.7 x 3.85 line/mm) resolution;
- enhanced throughput through hybrid ARQ with forward error correction;
- hardware built to fit into one slot of a 8088 based personal computer;
- interfaced to HF SSB transceivers via baseband audio ports.

3.2.2 System Description

The terminal is built around an 8088 microprocessor based personal computer that has a real time multitasking disk operating system environment. The resources of the computer are utilized by the terminal software and the user has access to the file management utilities for entry or retrieval of information from the terminal. The information that is transmitted and received by the terminal is stored in the disk storage of the computer.

The HF modem is a 12 channel (see CCIR Recommendation 436-2 Dubrovnik, 1986) FSK modem with $\pm$42.5 Hz and 170 Hz channel separations. The modulator and demodulator are implemented in Digital Signal Processing (DSP) devices and interfaced to the computer bus. The modem and interface hardware is contained on a plug-in card for the computer expansion bus. Data are fed to the modulators as 12 bit binary words at 10 ms intervals through a parallel data output port. The modem outputs are combined and applied to the audio input of an HF SSB communication transmitter.

The HF SSB receiver audio output is digitized and fed to the 12 modem inputs. The demodulator generates a 100 Hz clock synchronized to the received data signal. Each demodulator output "eye signal" is sampled in the middle of the bit timing interval. and the sample is converted into a 5 bit digital word. At every 10 ms interval 12 demodulator samples are transferred to the computer memory for processing. Although the signalling rate is 100 Bauds, the presence of 12 channels result in a raw data rate of 1200 bit/s.

The terminal is designed to operate with a packet radio protocol which provides the system with a framework for exchange of control information such as station identification, message types and options In particular, the protocol permits the implementation of a selective repeat ARQ algorithm, which ensures the

message integrity. Every packet starts with a bit synchronization sequence followed by a packet framing word transmitted on all the channels. The computer combines all the sampled data from 12 channels and performs a matched filter detection for the packet framing word. The information following the framing word is called the packet header. The data bytes of the packet header are coded with block code of (12,8) minimum distance 3, which is transmitted in parallel from the 12 modulators. The block code is decoded with a soft decision decoding algorithm by the receiver. The validity of the packet header is verified with a high rate error detection code which is transmitted as part of the header packet. In the packet header coding diversity is utilized instead of conventional inband frequency diversity.

The information is assembled into 96 small packets and transmitted after the packet header. Each information packet contains data bytes plus a sequence number and error detection code. The information packets are then coded with a rate one half error correction code. The error correction code is chosen such that the information can be recovered for either half of the coded packet. The transmitter does not transmit the parity portion of the coded packets initially but saves them for future repetition requests. Each of the 12 modulators are fed with 8 information packets sequentially without any duplication. In addition to information packets a packet sent containing the sequence numbers of packets that are contained in that transmission. The receiving terminal checks the information packets for presence of errors, if the packet is error free the information is stored in its proper location as indicated by the sequence number. If the information packet has one or more errors the sampled analog values of the packet from the demodulator output are saved for future processing. The message receiving terminal requests repeat of the outstanding information packets in the acknowledgment packet. Whenever the transmitter has to repeat an information packet the parity part of the error detection code version of the packet is sent. The transmitter alternates the repetition of the same packet between the information and parity part of the coded packet. If the parity part of the error detection code of the packet is received error free then the information is recovered by an inversion process. If the second transmission also contains errors a soft decision error correction process is activated using the stored samples of the same packet from first and second receptions. The output of the error correction process is verified with error detection code of the packet before accepting the data. The receiver linearly combines the stored sampled analog values of the same packet whenever the received packet fails the error detection process in order to build signal strength and utilize time diversity [Lin et al., 1984]. When the transmitter has to repeat an information packet the repetition of that packet is made through a different channel to avoid persistent channel disturbance that

The terminal scans the assigned radio frequencies continually and when a message transmission is initiated, the message originating terminal calls the destination terminal sequentially on all the assigned radio channels. The message session is established on a frequency that is suitable for data transmission. In this way, the reliability of the network is maintained even when experienced operators are not available.

Interface to CCITT Group 3 facsimile apparatus is provided through a special port built into the computer interface card of the terminal. The document is scanned in 7.7 by 3.85 line/mm resolution and the image data is compressed with an error free algorithm described in [Rissanen and Langdon, 1981]. This algorithm has been found to be 65% more efficient then the CCITT Group 4 facsimile apparatus data compression technique. The image compression algorithm when applied to eight CCITT test images results in an average image size of 12 kilobytes. The compressed image is transmitted from the disk file and the receiving terminal places the image into disk storage. The image can be expanded with the inverse of the data compression algorithm and viewed by the video display unit of the computer or printed by the facsimile machine.

3.2.3 Experimental Results

The system tested on a link from Ottawa to a location near Vancouver a distance of 3500 km. A 4096 byte test message was transmitted periodically over a 15 day trial period. The terminals were programmed to scan 3 assigned radio channels and no operator was utilized for channel selection. Fig. 11 shows the distribution of transmission times for 344 experiments that were conducted during this trial. Tests were also made over a 100 km link near Ottawa, the results obtained were substantially the same as those obtained in the long range trial. The received files from the trials were checked for undetected errors and none were found in 6000 kilobytes of data.

3.2.4 Conclusions

The HF system design achieved reliable data and message transmission over HF radio channels. The memory ARQ performs as a diversity on demand technique adapting the system to changing channel conditions, thus achieving higher throughput when compared to systems utilizing inband frequency diversity and simple ARQ protocols where the received data is discarded in the presence of errors. The parallel modems are used in a flexible mode where the data can be coded and spread over all the channels,

and the error correcting capability of soft decision decoding enhances the performance when extra protection is required for packet headers. The built-in facility for monitoring different radio frequencies improves the success for establishing a link under changing propagation conditions. The data compression algorithm incorporated into the terminal software performs efficient data compression thereby reducing the size of the file and time to transmit. The images are reproduced by the receiving terminal with the same fidelity as the scanned image in the transmitting terminal due to error protection provided by the data transmission protocol.

The system has been tested through HF skywave paths for a period of 3 months and the performance met all the design goals. The HF facsimile and data terminal provides reliable data service with a modest combination of equipment.

3.3 Adaptive HF Communications

Adaptive techniques form a useful set of tools for combatting the time and space variability of HF channels and the other factors adversely affecting HF communications. When combined with packet-switching techniques, adaptive techniques are probably the most serious contender for improving HF communications performance as expressed by connectivity, speed, throughput, reliability and survivability. A system, the adaptive, packet-switched HF data terminal, based upon such techniques has been built and tested at CRC. Its design and performance have been described by Nourry and Mackie [1988].

Current R&D on adaptive HF communications at CRC follows the adaptive-system approach used for the terminal and consists mainly of three projects: the packet-switched HF data terminal project, the A/G/A data/voice HF terminal project and the adaptive serial modem project. The highlights of each of these projects are briefly described below.

The adaptive, packet-switched HF data terminal is currently being enhanced to provide FDMA network operation, secure data transfer and enhanced throughput. FDMA network operation and secure data transfer are operational requirements dictated by the environment in which this system is to evolve. Enhanced throughput will be achieved through refinements in the system algorithms (especially at the physical and link levels), a new channel access strategy and by the use of a multi-microprocessor design where microprocessors are specialized to functions characteristic of specified levels in the ISO/OSI reference model. As shown in Figure 12, the new architecture includes one processor for the transport and network levels functions, one physical/link processor per link supported by this network node, and one or more I/O processor as dictated by the equipment configuration.

The new throughput figures resulting from these changes and the additional processing power will be available in early fall 1988. It is planned to test this version of the terminal in 1989 over a four-node network across Canada. This would be followed by an evaluation of this system over a similar network but including trans-auroral and polar cap paths.

The adaptive air-ground-air (A/G/A) data/voice HF terminal will include both data and voice components. The emphasis in this system is placed upon throughput and upon a controlled error level as opposed to the error-free transmission provided by the previous system. The A/G/A terminal includes Link-11 type formatting of the transmitted data. The voice component makes use of an LPC-10 vocoder developed at CRC. Due to limitations in the RF equipment and antenna in aircraft, the communication links are half-duplex and thus voice communications temporarily interrupt the normal flow of data on the link.

The A/G/A system will be evaluated over a one year period, starting in summer 1989, in the Canadian Arctic. Following an extensive site survey in January 1988, four sites have initially been selected for this experiment. Yellowknife, Inuvik, Cambridge Bay and Resolute Bay. This selection of sites allows for the testing of the system over polar cap circuits. The experimental plan will include provisions for the evaluation of the importance of path and frequency diversity in this environment as well as the impact of such factors as sporadic E [c.f. BR Communications, 1986] and polar cap absorption events on HF propagation in the Arctic.

Both of the above systems will make use of the adaptive serial modem being developed at CRC. This modem utilizes a decision feedback equalizer (DFE), the tap weights of which are adapted by a stochastic descent or LMS algorithm iterated several times per baud. The adaptation capability of the LMS algorithm has been observed to be roughly proportional to the number of iterations of the algorithm completed per baud. Even with a reasonable number of iterations (7-8), however, the modem has been found to be adaptation-rate limited for (equal strength, two-path, Rayleigh) fading rates exceeding about 0.5 Hz. To overcome this limitation, the received modem signal will first be passed through an adaptive lattice decorrelation (whitening) filter [Frienlander, 1982] before entering the input to the equalizer.

Experimental evaluation of the lattice filter/multiple-iterated LMS algorithm should be completed in the late summer of 1988.

In selecting the particular approach described above, cost, consistentwith a reasonable performance, was an important consideration. The use of algorithms having low to moderate computational requirements reduces system cost since the need for bit-sliced or custom-designed array processors is avoided. Two characteristics of the algorithms selected, namely, the absence of feedback between the DFE and the lattice filter, and the proportional increase in required computation with the number of iterations performed per baud in updating the equalizer tap weights, make these algorithms well suited for implementation on a multiprocessor system and for parallel processing.

The modem will provide various operating modes including that specified in STANAG 4285. These modes differ primarily in the details of the coding and interleaving subsystems. Convolutional and Reed-Solomon (block) forward error correction coding will be implemented. Various interleaving strategies are being tested to maximize performance for a specified maximum interleaving depth. The modem provides estimates of the channels S/N ratio, delay and Doppler spreads. The HF terminal makes use of these parameters along with pseudo-bit error rate measurements and other factors, to rank the available communication channels.

3.4 Broadband Adaptive Antennas

Adaptive antenna arrays have been shown to be highly effective in cancelling interference or jamming, in a wide range of communications receiving applications. One factor limiting the performance of such arrays is the bandwidth of the signals they are required to receive (and thus the interference they must reject). Individual components in the individual element receive channels will not be completely identical in frequency response, to components in the other channels. Also, the spatial separation of array elements gives rise to a frequency-dependent difference in phase response, between channels. As a result of these frequency-dispersive effects, array weights which cancel one frequency component of an interfering signal may not be able to cancel other frequency components.

Work at CRC up to the present time, has been restricted to adaptive arrays working with conventional narrowband signals, mainly HF. The weighting and combining of signals from the array elements has been performed digitally, at baseband, using as input the signals from a set of commonly-tunded receivers attached to the individual array elements (Figure 13). The frequency-dispersive effect of spatially separate antenna elements are not significant in limiting array performance for these applications. However, channel component mismatches in frequency response do play a major role here, as well as in broadband systems.

3.4.1 Channel Mismatches

Channel mismatches in arrangements similar to that of Figure 13 arise mainly in the later stages of the receivers, and in the bandwidth-limiting filters. We have used matched filters to provide the final band-limiting in order to minimize this problem. An analysis of the effect of frequency-dependent mismatches on array performance [Robinson and Jenkins, 1982] show that the achievable null depth of an array operating against spectrally-flat interference is given in terms of the fraction of interference power passing through the adapted array, by

$$\delta P/P = \sigma_\phi^2 + \sigma^2_A$$

where σ_ϕ is the rms variation in relative phase response remaining once the average frequency dependence and mean phase difference between channels have been removed, as measured in radians, and σ_A is the corresponding rms variation in relative amplitude response, expressed as a fraction of the mean. Measurements on a set of HF receivers, I and Q downconvertors, and matched low-pass filters similar to those shown in Figure 13 reveal the major portion of the limit to null depth arises from phase mismatches, and these are largely a linear function of frequency across the signal bandwidth. As such, they are equivalent to differences in time delays introduced by the equipment. In the digital systems developed at CRC, they have been corrected for by staggering the input sampling times by appropriate amounts. In this way, a measured limit to null depth of approximately 23 db over the conventional 3 kHz HF bandwidth was increased to 35 dB [Robinson and Jenkins, 1982].

3.4.2 Compact Adaptive Arrays

Another CRC development, of interest in broadband systems, is that of a compact HF adaptive array configuration [Jenkins, 1986].

The frequency dispersion between channels introduced by the spatial extent of the array is a major consideration in implementing a broadband adaptive array. For instance, a linear array of say, one wavelength aperture, would, without any means of compensation, be limited to null depths as low as 13 dB in some directions, for a bandwidth of 0.1 times the central frequency. Thus, it is useful to consider small-aperture arrays.

The phase differences between elements are what enable arrays with omnidirectional elements to distinguish between signals from different directions. As these become very small in a compact array, the array elements are required to be directional in their response, and differently directed. An example of of a compact 3-element system which lends itself to broadband signal reception is that of two crossed loop antennas and a whip antenna. Such a system has been presented in the literature [Flan et. al., 1986].

The CRC system [Jenkins, 1986], shown in Figure B, consists of a square arrangement of four short active receiving whip antennas, separated by grounded reflectors. This array, which is 2 meters on edge, is capable of achieving null depths of 34 dB against 2 MHz wide signals. At the same time, its directional discrimination is such that it has been demonstrated to achieve processing gains of 20 dB, at angular separations (between wanted communications and jamming) of 10 degrees, at an operating frequency near 5 MHz. At larger angular separations, the processing gain reached 30 dB, a limit which was set in part by the limited digital accuracy (8 bits) of the adaptive antenna processor used.

3.4.3 Frequency-hopped Signals

One class of broadband signals, with which we are concerned at CRC, are frequency-hopped signals. At the HF or VHF ranges of interest to us, these signals might be hopped over a band comparable to the center frequency. In any one hop, the bandwidth is narrow. Therefore, provided that array adaptation is completed within a fraction of a hop, the adaptive array can be implemented in narrow band form. Digital techniques studied at CRC include direct matrix inversion [Jenkins, 1984], in which weights derived from a time sequence of samples are applied to the same samples. This form of adaptation is effectively instanteous, apart from a delay introduced by the processing, and can be used with frequency-hopped signals to advantage.

If the hop rate is too fast to adapt within a single hop, problems arise in the use of conventional adaptive array techniques [Acar and Compton, 1985], and changes are required. Torrieri and Bakhru [1987] discuss several approaches for an array using the Minimax algorithm, hopping over a band 0.1 times the center frequency. Approaches considered include the use of tapped delay lines, dividing the hop band into several 'bins' for which weights are adapted and stored separately, and anticipating or developing weights one hop ahead of the actual transmissions. Each approach is found to have merit, the most appropriate depending on the specific application.

3.4.4 Use of Tapped Delay Lines

The remaining class of more general broadband signals, for which the instantaneous bandwidth is wide, have not so far been considered at CRC for adaptive array implementations. Widrow et al. [1967], first suggested the use of tapped delay lines behind the array elements to compensate for the frequency-dispersive effects of finite array dimensions. Rodgers and Compton [1979], and Compton [1988] have simulated adaptive arrays with tapped-delay lines working with broadband signals in order to determine the appropriate number of taps and tap spacing, and the resultant improvement in performance. Significant benefits result from only several taps per channel. More work in this area is indicated.

4. Closing Remarks

Characterization of fading dispersive channels and development of channel simulations, which simulate the propagation characteristics of ionospheric HF and land mobile VHF/UHF channels, permitting non-gaussian realistic radio noise and interference to be added to the signal are essential tools for developing new/and for improving the performance of modern military and civilian radio systems. It is clear from this overview that a considerable effort has been and is being expended, at the Communications Research Centre toward these endeavours. The group concerned with land mobile propagation research have as well recently gone indoors, and they are carrying out indoor propagation/and EMC research in support of anticipated development of wireless local-area-network systems [Bultitude, 1987; 1989]

At the CRC radio communications technologies research is being conducted in the areas of rural and remote communications, satellite communication, particularly in support of the MSAT (mobile

satellite) program; in the (terrestrial) tactical/land mobile communications area; and in the area of HF communications. In recent years there has been a renaissance in the need/requirement for HF communications, for both military and civilian requirements [Belrose, 1988]. The increasing need to provide more reliable HF communications has stimulated renewed research into a better understanding of the high latitude ionosphere (Canada is a northern nation), on which HF communications depends, and on the development of adaptive HF systems, particularly those that depend on real time channel evaluation (RTCE) and adaptive networking for improved performance.

The new interest in HF communications has also stimulated the development of new systems, such as digital facsimile, digital data transmission, and for connectivity to the public telephone system [Belrose, 1986]. Interference is a major problem at HF, whether intentional (jamming) or unintentional, and this has stimulated research into adaptive HF antenna systems. Some of these research/and developments have been briefly described in this overview.

References

Acar, L. and Compton Jr., R.T. [1985] The Performance of an LMS Adaptive Array with Frequency Hopped Signals, IEEE Trans. Aerospace Electron. Syst., Vol. AES-21, pp. 360-371.

Arrendondo, G.A., Chriss, W.H. and Walker, E.H. [1973] A Multipath Fading Simulator for Mobile Radio, IEEE Trans on Comunications, Vol. COM-21, No. 11, pp. 1325 - 1328.

Bajwa, A.S. [1985] WHF Wideband Statistical Model and Simulation of Mobile Radio Multipath Propagation Effects, Proceedings of the IEE, Vol. 132, pt F, No. 5, pp. 327 - 333.

Bajwa, A.S., and Parsons, J.D. [1985] Large area characterisation of urban UHF multipath propagation and its relevance to the performance bounds of mobile radio systems, IEE Proc., Vol. 132, Pt. F, No. 2.

Ball, J.R. [1982] A Real Time Fading Simulator for Mobile Radio, The Radio and Electronic Engineer, Vol. 52, No. 10, pp. 475 - 478.

Bello, P.A. and Nelin, B.D. [1962] The influence of fading spectrum on the binary error probabilities of incoherent and differentially coherent matched filter receivers, IRE Trans. Com. Sys., Vol. CS-10.

Bello, P.A. [1963a] Characterization of time-variant linear channels, IEEE Trans. Com. Sys., Vol. CS-11.

Bello, P.A. and Nelin, B.D. [1963b] The effect of frequency selective fading on the binary error probabilities of incoherent and differentially coherent matched filter receivers, IEEE Trans. Com. Sys., Vol. CS-11.

Bello, P.A. and Nelin, B.D. [1964] Optimization of subchannel data rate in FDMA-SSB transmission over selectively fading channels, IEEE Trans. Com. Sys., Vol. CS-12.

Belrose, J.S. [1988] HF Communications and Remote Sensing in the High Latitude Region, AGARD LS 162.

Belrose, J.S. [1986] Canadian Technologies for Rural and Remote Communications: An Overview, World Telecommunications Forum, 16 - 19 September, Nairobi, Kenya pp. 129 - 139, published by the ITU, Geneva, Switzerland.

Benvenuto, N. [1984] Distortion analysis on measuring the impulse response of a system using a crosscorrelation method, AT&T Bell Laboratories Technical Journal, Vol. 63, No. 10.

Bolton, E.C. [1971] Simulating Atmospheric Radio Noise from Low Frequency through High Frequency, The Review of Scientific Instruments, Vol. 42, No. 5, pp. 574 - 577.

Boucher, L., Jolly, Y. and Lodge, J.H. [1989] Increased Communication Channels for the VHF and UHF Frequency Spectrum, to be published in this AGARD CP, paper No. 16.

Bultitude, R.J.C. [1983] A study of coherence bandwidth measurements for frequency selective radio channels, Proc. IEEE Veh. Tech. Conference, Toronto.

Bultitude, R.J.C. [1987] Measurement, characterization and Modelling of indoor 800/900 MHz radio channels for digital communications, IEEE Com. Mag. 25, No. 6, 5 - 12.

Bultitude, R.J.C. [1987a] Measurement, characterization and modelling of 800/900 MHz mobile radio channels for digital communications, PhD. Thesis, Electronics Engineering Dept., Carleton University, Ottawa.

Bultitude, R.J.C. [1987b] Measurement, characterization and modelling of indoor 800/900 MHz radio channels for digital communications, IEEE Communications Magazine, Vol. 25, No. 6.

Bultitude, R.J.C. and Bedal, G.K. [1989] Propagation characteristics on microcellular urban mobile radio channels at 900 MHz, IEEE Journal on Selected Areas in Communications, Special issue on mobile/portable radio systems (to be published).

Bultitude, R.J., Mahmoud and Sullivan, W. [1989] A comparison of indoor radio propagation characteristics of 910 MHz and 1.75 GHz, IEEE J. on Selected Areas in Communications (to be published).

Caples. E.L., Massad, K.E. and Minor, T.R.[1980] A UHF Channel Simulkator for Digital Mobile Radio, IEEE Trans on Vehicular Technology, Vol. VT™29, No. 2, pp. 281 - 289.

Clark, G.C. and Cain, J.B. [1981] Error-correction Coding for digital Communications. Plenum Press, New York.

Compton Jr., R.T. [1988] The Bandwidth Performance of a Two-Element Adaptive Array with Tapped Delay-Line Processing, IEEE Trans. Ant. Propagation, Vol. AP-36, pp. 5 - 14.

Coon, R.M., Bolton, E.C. and Eensema, W.E. [1969] A Simulator for HF Atmospheric Radio Noise, ESSA Technical Report ERL 128-ITS 90, Boulder Colorado.

Cox, D.C. [1972] Delay doppler characterisitcs of multipath propagation at 910 MHz in a suburban mobile radio environment, IEEE Trans. Ant. and Prop., Vol. AP-20, No. 5.

Davarian, F. [1987] Channel Simulation to Facilitate Mobile-Satellite Communications Research, IEEE Trans on Communications, Vol. COM-35, No. 1, pp. 47 - 56.

Davis, B.R. and Bogner, R.E. [1985] Propagation at 500 MHz for Mobile Radio, Proceedings of the IEE, Vol. 132, pt F, No. 5, pp. 307 - 320.

Devasirvatham [1987] Multipath time delay spread in the digital portable radio environment, IEEE Communications Magazine, Vol. 25, No. 6.

Flam, R.P., Bull, J.F. and Burgess, L.R. [1986] A Null-Forming Array for Frequency Hopping HF Communications IEEE ICC Conf. Proc., CH2314-3/86, pp. 1913 1916.

French, R.C. [1978] Error Rate Predictions and Measurements in the Mobile Radio Data Channel, IEEE Trans on Vehicular Technology, Vol. VT-27, No. 3, pp. 110 - 116.

Frienlander, B. [1982] Lattice filters for adaptive processing. Proceedings of the IEEE, Vol. 70, 829 - 867.

Garcia, A.L., Chow, S. and Serinken, N. [1985] A Coded frequency diversity System for HF Data Transmission. Canadian Electrical Eng. Journal, Vol. 10 No. 4 pp. 173-9.

Hagenauer, J. and Papke, W. [1984] Data Transmission for Maritime and Land Mobiles Using Stored Channel Simulation, 32nd IEEE Vehicular Technology Conference, IEEE Catalog No CH82-1720-2, San Diego California.

Heimiller, R.C. [1961] Phase shift pulse code with good correlation properties, IRE Trans. Inform. Theory, Vol. IT-7, 4, 254-257.

Hurd, W.J. [1974] Efficient Generation of Statistically Good Pseudonoise by Linearly Interconnected Shift Registers, IEEE Trans on Computers, Vol. C-23, No. 2 pp. 146 - 152.

Jakes Jr., W.C. [1971] A Comparison of Specific Space Diversity Techniques for Reduction of Fast Fading in UHF Mobile Radio Systems, IEEE Trans on Vehicular Technology, Vol. VT-20, No. 4, pp. 81 - 92.

Jakes Jr. W.C. [1974] Microwave Mobile Communications, John Wiley and Sons, New York.

Jenkins, R.W. [1984] Implementing a Matrix-Inversion Algorithm in a Limited-Precision Adaptive Antenna Array Processor, CRC Tech. Note 725.

Jenkins, R.W. [1986] Compact Antenna Array for Interference Cancellation, Canadian Patent 1,204,205.

Kailath, T. [1962] Measurements on time-variant communication channels, IRE Trans. on Information Theory, PGIT IT-8.

Lee, Y.W. [1976] Statistical Theory of Communications, John Wiley & Sons., Inc., New York.

Lin, S., Costello, D.J. and Miller, M.J. [1984] Automatic-Repeat-Request Error Control Schemes. IEEE Com. Magazine December Vol. 22, No. 12, pp. 5 - 17.

Linfield, R.F., Hubbard, R.W. and Pratt, L.E. [1976] Transmission channel characterization by impulse response measurements, OT REPORT 76-96, U.S. Dept. of Commerce.

Lorenz, R.W. and Gelbrich, H.J. [1984] Bit-Error Distribution in Digital Mobile Radio Communication - Comparison Between Field Measurements and Fading Simulation, IEE International Conference on Mobile Radio Systems and Techniques, University of York UK.

McLarnon, B.D. [1985] Experimental Results on the Application of Convolutional Coding and Viterbi Decoding as a Frequency Diversity Technique in HF Data Transmission. CRC report No. 1377 Department of Communications Government of Canada.

Neuvo, Y. and Ku, W.H. [1975] Analysis and Digital Realization of a Pseudorandom Gaussian and Impulsive Noise Source, IEEE Trans on Communications Vol. COM-23, No. 9, pp. 849 - 858.

Norton, K.A., Vogler, L.E., Mansfield, W.V. and Short, P.J. [1955] The Probability Distribution of the Amplitude of a Constant Vector Plus a Rayleigh-Distributed Vector, Proceedings of the IRE, pp. 1354-1361.

Nourry, G.R. and Mackie, A.J. [1987] The design and performance of an adaptive, packet-switched HF data terminal. AGARD Conference Preprint No. 420, AGARD-CPP-420.

Parsons, J.D. and Ibrahim, M.F. [1983] Signal Strength Predictions in Built-Up Areas Part 2: Signal Variability, Proceedings of the IEE, Vol. 130, pt F, No. 5, pp. 385-391

Parsons, J.D. [1984] An Impulsive Noise Simulator for the Laboratory Testing of Radio Communication Systems, 1984 IEEE National Symposium on EMC, San Antonio Tx, IEEE CAT No. 84CH2035-4.

Perl, J. M. [August, 1984] Simulator simplifies real time testing of HF channels. Defense Electronics, Vol. 16, 8, 103 - 108.

Proakis, J.G. [1983], Digital Communications, McGraw Hill Co., New York,

Rissanen, J. and Langdon, G.G. [1981] Compression of Black-White Images with Arithmetic Coding. IEEE Trans. on Com., June Vol. Com-29, No. 6.

Robinson, J.L., and Jenkins, R.W. [1982] Corrections for Frequency Response Differences in Multiple Receiver Arraysand R. W., CRC Tech. Note 711.

Rodgers, W.E. and Compton, Jr., R.T. [1979] Adaptive Array Bandwidth with Tapped Delay-Line Processing, IEEE Trans. Aerospace Electron. Syst., Vol. AES-15, pp. 21 - 27.

Serinken, N. [1988] HF Data and Facsimile Terminal System.Fourth International Conference on HF Radio Systems and Techniques London, UK, 11 - 14 April. pp. 29 - 32.

Torrieri, D. and Bakhru, K. [1987] Frequency Compensation in an Adaptive Antenna System for Frequency-Hopping Communications, IEEE Trans. Aerospace Electron. Syst., Vol. AES-23, pp. 448-467.

Venier, G.O. [1986] User's Guide for the DRL Spread-Spectrum Simulation Facility, CRC Report No. 1403, Communications Research Centre, Ottawa.

Widrow, B., Mantey, P.E., Griffiths, L.J., and Goode, B.B. [1967] Adaptive Antenna Systems, Proc. IEEE, Vol. 55, pp. 2143 - 2159.

ITU, Models of Phase-Interference Fading For Use in Connection With Studies of the Efficient Use of the Radio-Frequency Spectrum, CCIR Report 415, Geneva, 1978.

BR COMMUNICATIONS [1986] HF propagation in the arctic. High performance communication channels are available if you know where to look. Presentation at the AFCEA show (Canada), April 1986.

CCIR (International Radio Consultative Commi·ee) [1964] World Distribution and Characteristics of Atmospheric Radio Noise, CCIR Report 322, Figure 27, International Telecommunications Union, Geneva, Switzerland.

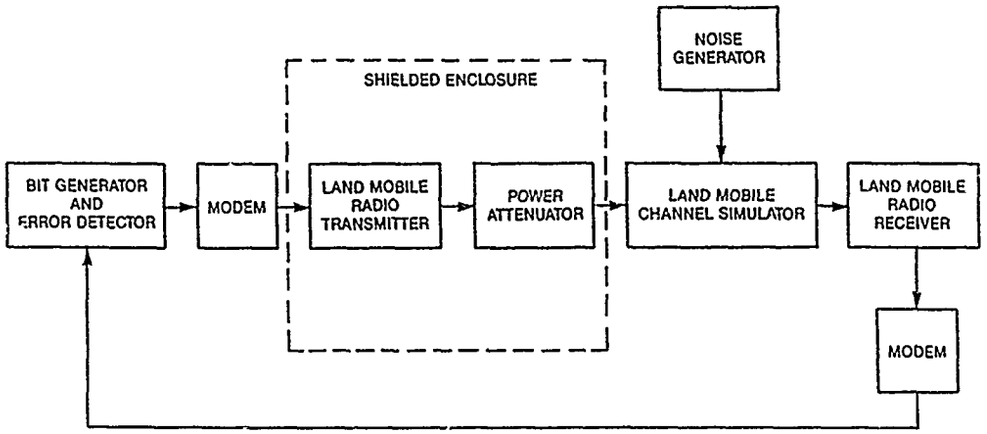

Fig. 1 Test facility for evaluating operational performance of digital/analogue land mobile radio communications equipments.

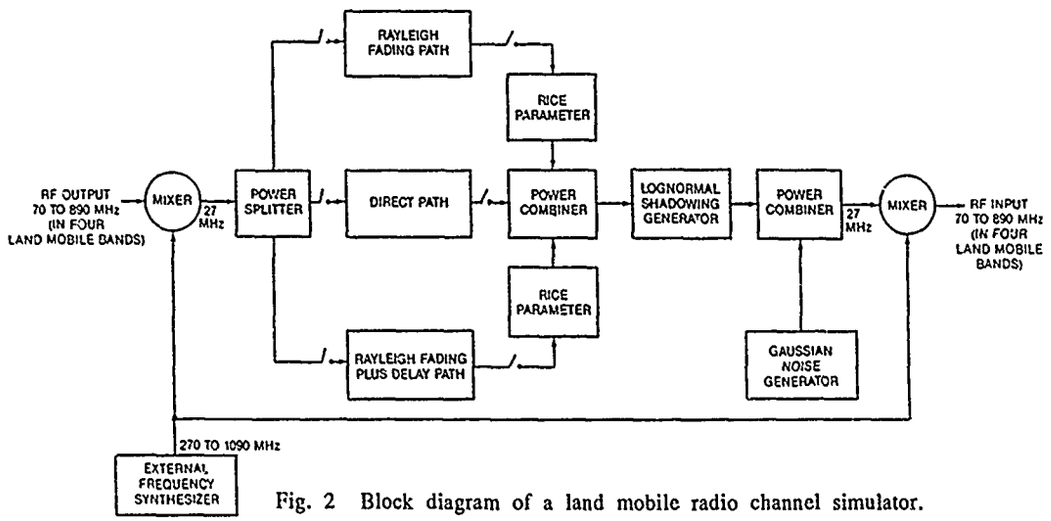

Fig. 2 Block diagram of a land mobile radio channel simulator.

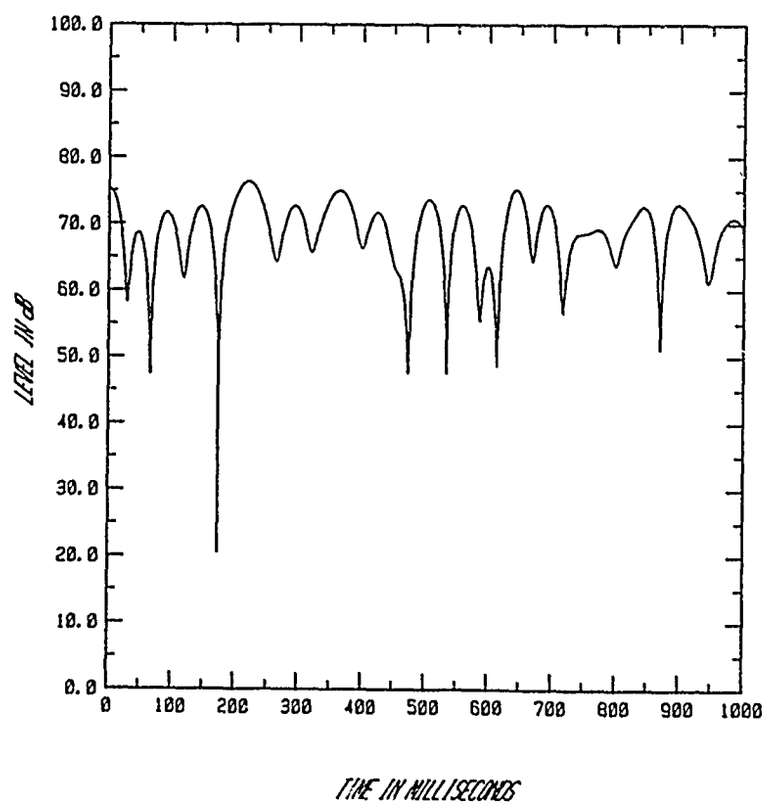

Fig. 3 Typical signal output from the fading channel simulator for a vehicle travelling at 100 km/hr. and operating at 150 MHz (F_D = 13.9 Hz).

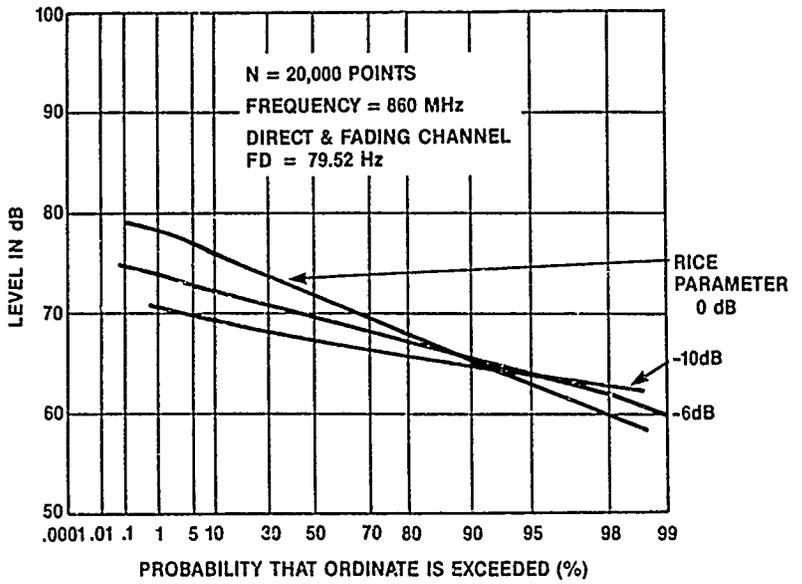

Fig. 4 Amplitude probability distribution for a direct and a fading channel as simulated by the land mobile channel simulator, to show effect of varying the Rice parameter. The simulation is for a vehicle travelling at 100 km/hr. and operating at a frequency of 860 MHz (F_D = 79.52 Hz).

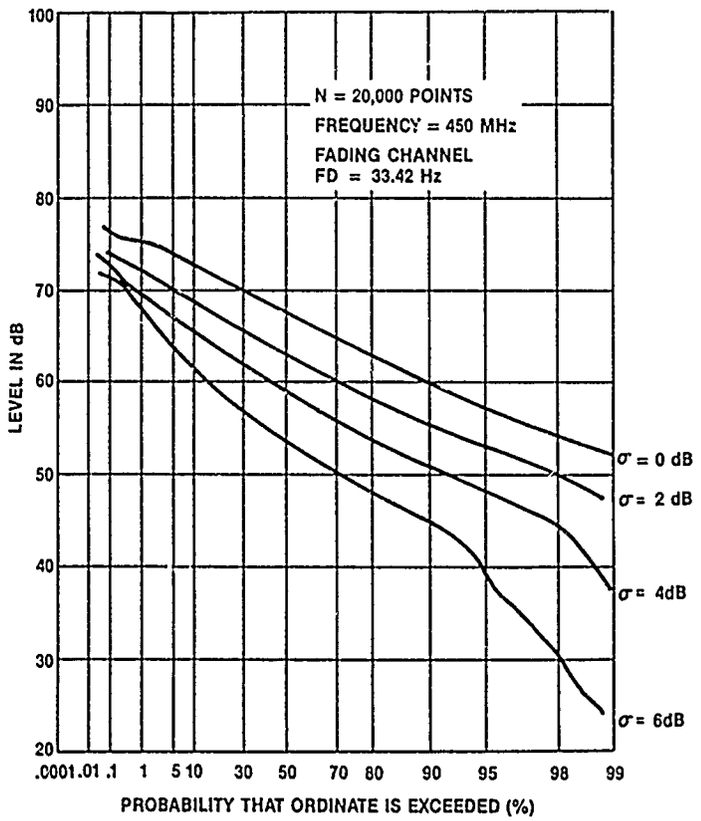

Fig. 5 Simulation of effect of shadowing by buildings and hills. The APD corresponds to a vehicle travelling at 80 km/hr. and operating on a frequency of 450 MHz (F_D = 33.42 Hz). The figure shows the effect on the shape of the APD as the shadowing parameter σ is varied from 0 to 6 dB.

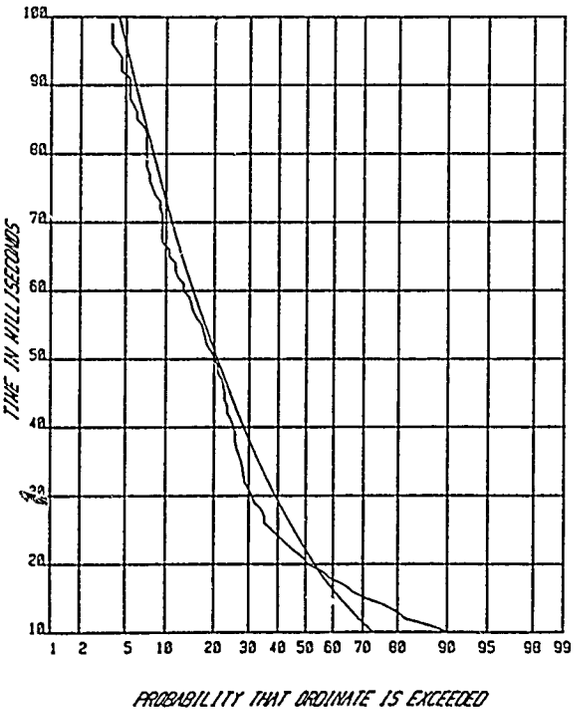

Fig. 6 APD of fade duration as measured (wiggly line) for a vehicle travelling at 100 km/hr. and operating on a frequency of 150 MHz (F_D = 13.9 Hz).

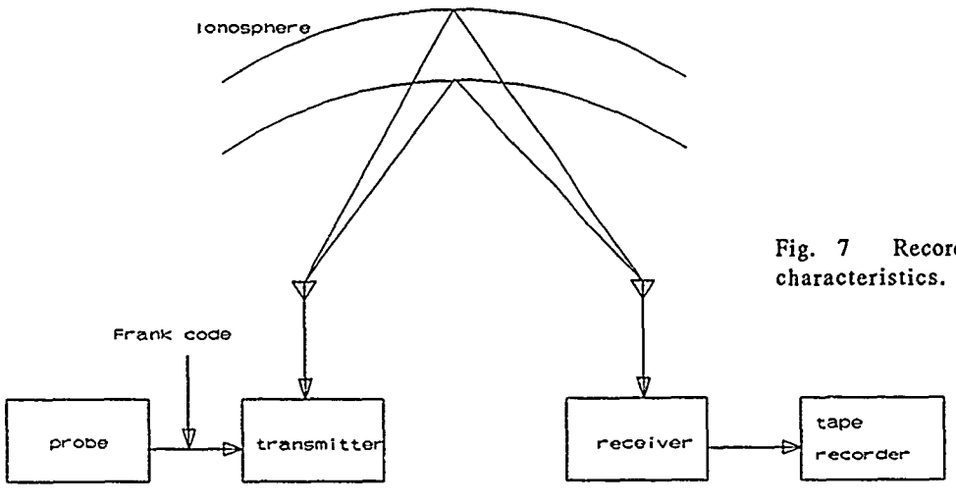

Fig. 7 Recording of the HF channel characteristics.

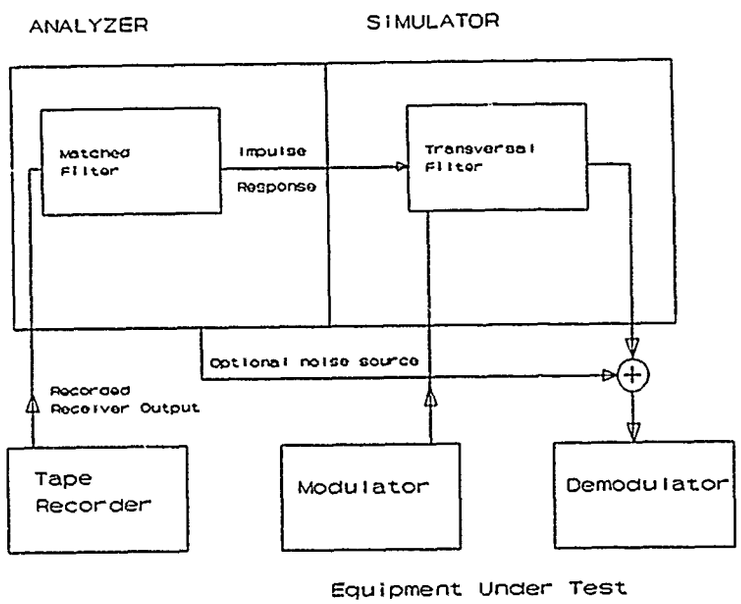

Fig. 8 Simulation of the HF channel using the recorded characteristics.

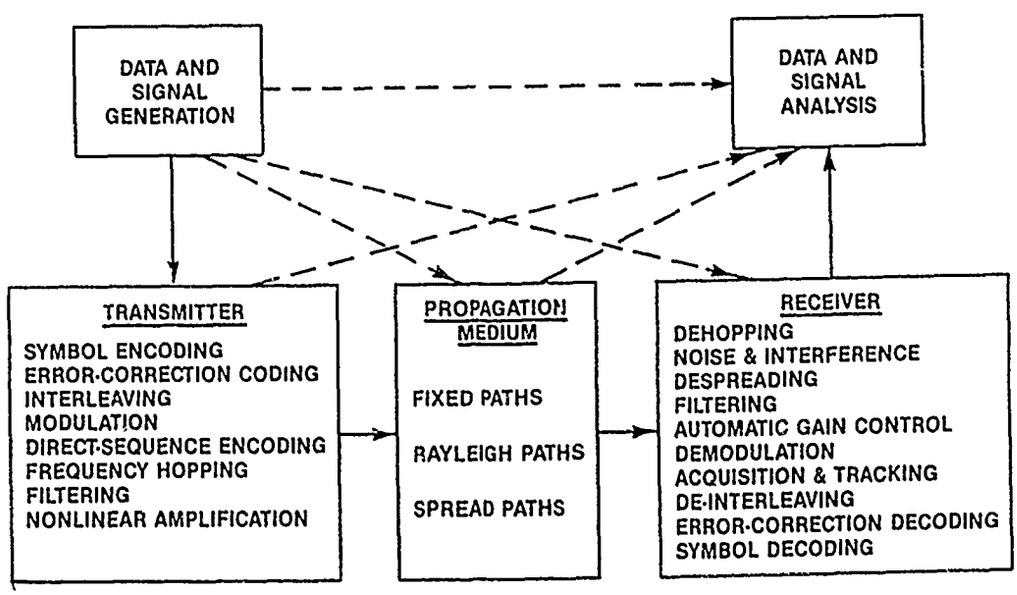

Fig. 9 Simulator structure and processes for an HF spread-spectrum channel simulator. The simulation is performed in software on a VAX 11/750 computer.

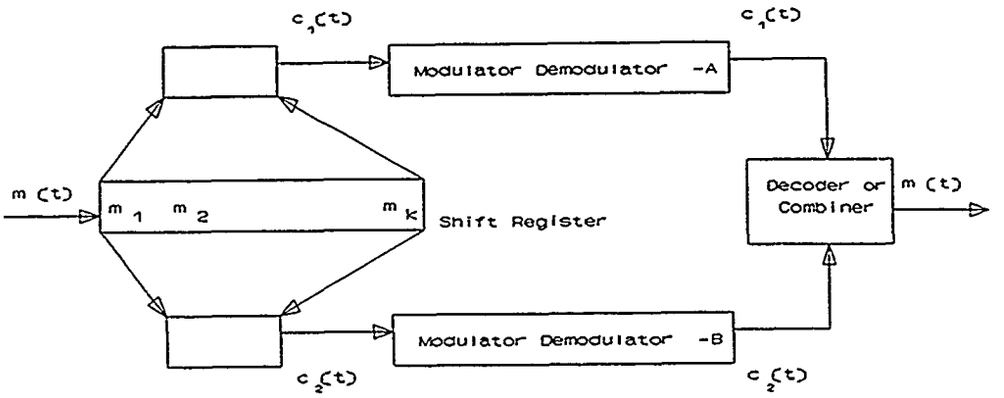

Fig. 10 General diversity structure.

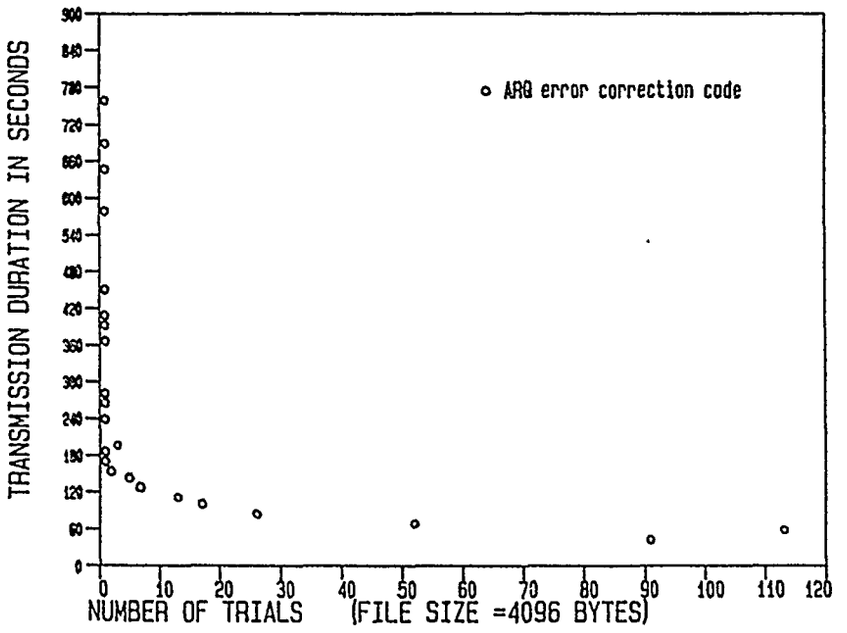

Fig. 11 Distribution of transmission lines.

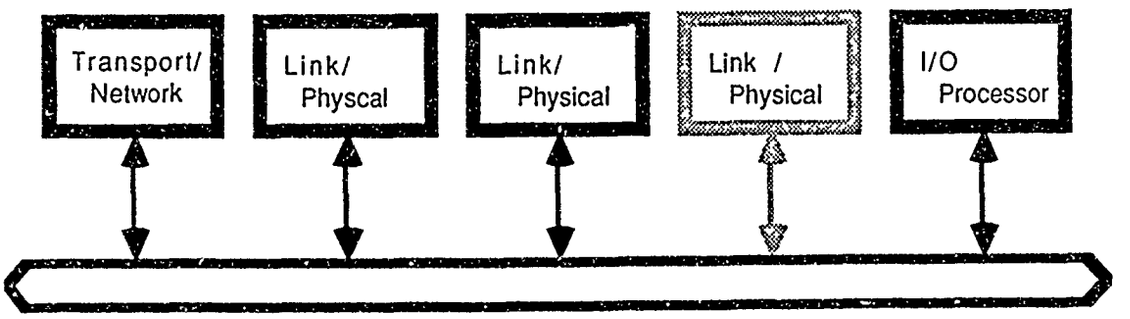

Fig. 12 Multi-microprocessor architecture of the packet-switched IIF data terminal.

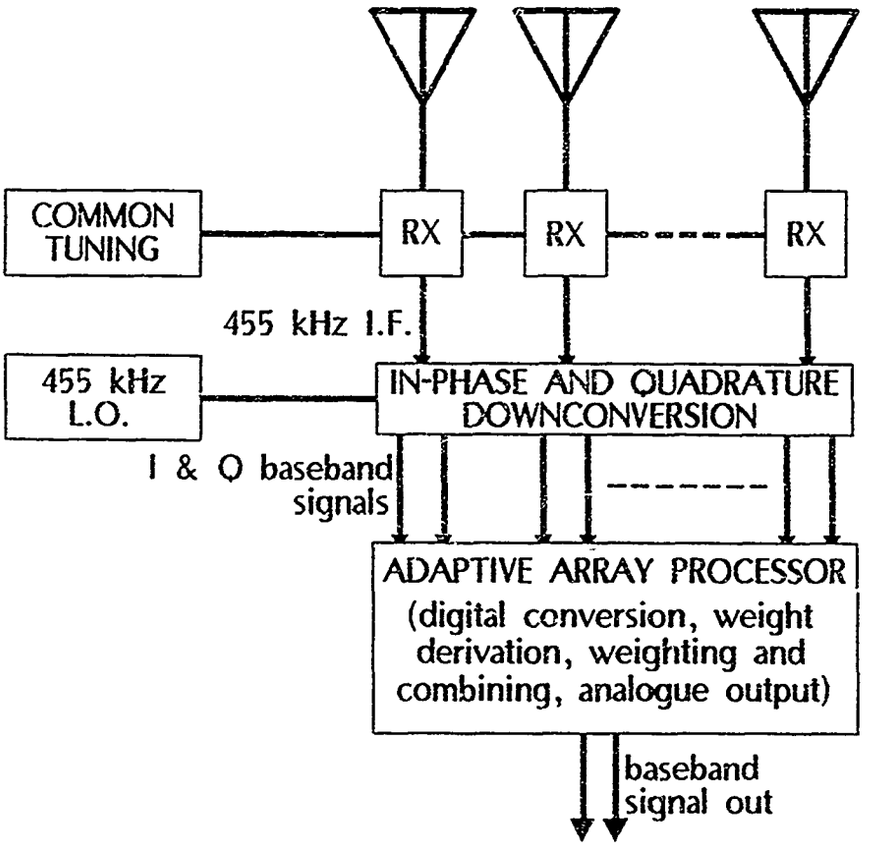

Fig. 13 Base band adaptive antenna array implementation.

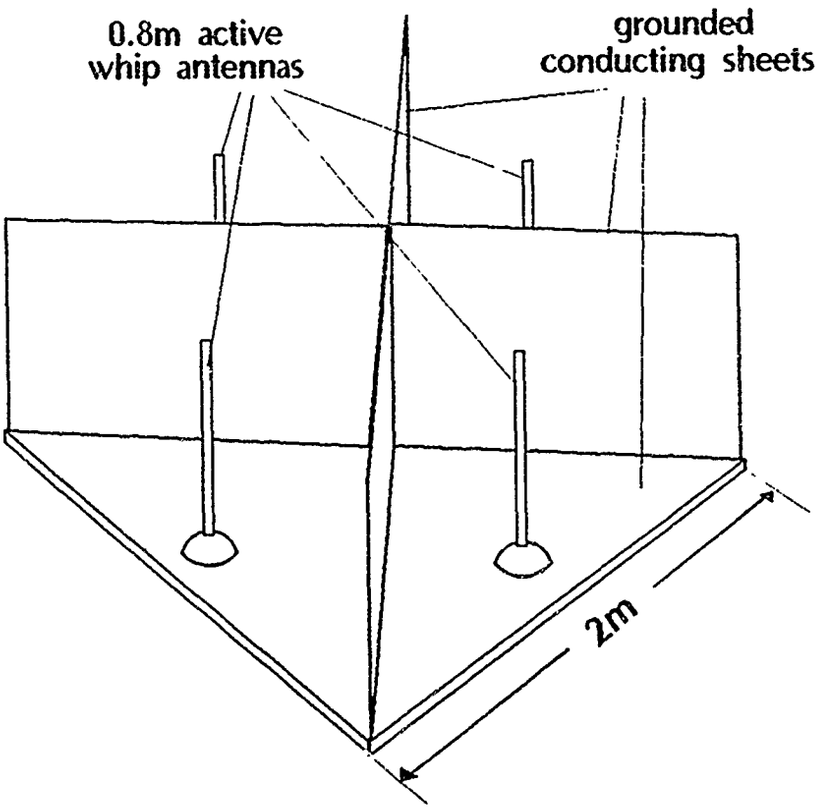

Fig. 14 Compact HF adaptive antenna array.

SUMMARY OF SESSION I

CHARACTERIZATION OF THE CHANNEL

par

C. GOUTELARD, Président de Session

Quatorze communications ont été présentées lors de la première session consacrée à la caractérisation des canaux.
Deux communications à caractère général ont été faites par le Colonel F.H. EVANGELIST et le Docteur J. BELROSE.
Les autres communications ont couvert les gammes de fréquences et les types de canaux les plus utilisés actuellement.
Le canal décamétrique par voie ionosphérique a fait l'objet de trois communications. La complexité de ce canal, dont les caractéristiques varient considérablement en fonction de la longueur de la liaison, de l'état du plasma ionosphérique, anisotrope, et en relation avec l'activité et la position du soleil, rend sa modélisation des plus complexes. Le Professeur M. DARNELL a présenté un projet de système de mesure des caractéristiques du canal et le Docteur Y. LE ROUX a proposé un système de mesure opérationnel dont les résultats sont utilisés en vue d'améliorer le modèle de WATSON. Le Docteur J.E. OFFMEYER enfin, a présenté une modélisation sophistiquée du canal utilisé avec de grandes largeurs de bande.
Ces communications ont montré le souci de modélisations nouvelles vers lesquelles le monde scientifique s'oriente par l'utilisation de mesures plus précises et de calculateurs plus puissants, mais également les difficultés que l'on rencontre face à la complexité du problème.

Les liaisons mobiles sont une préoccupation grandissante dans le monde des applications. Elles sont une plateforme de l'ingénérie de pointe et si de nombreuses mesures ont déjà été faites, elles n'étaient malheureusement pas toujours comparables. Les six communications présentées, bien que s'appliquant à des gammes de fréquence différentes, ont mis en évidence une tendance vers des types de mesures unifiés qui permettent d'effectuer de meilleures comparaisons. Deux communications ont été consacrées à la bande des 900MHz, l'une en milieu urbain présentée par le Professeur J. CITERNE, l'autre en milieu urbain et rural présentée par le Docteur R.W. LORENZ. Trois communications étaient orientées vers les tests et caractérisation d'une même liaison à des fréquences différentes. Le Docteur D. SORAIS a présenté une étude sur une liaison à 150-250 et 400MHz en milieu rural, le Docteur ALTMARY une étude à 400 et 900MHz sur la propagation à travers les forêts et le Docteur E. GURDENLI une étude comparative sur les propagations à 160, 900 et 2000MHz. Enfin, le Docteur M. SYLVAIN a présenté une étude à 11GHz en milieu rural.
Ces communications ont montré la grande diversité des problèmes, diversité due aux fréquences utilisables mais aussi aux milieux, ainsi que la complexité apportée par la non stationarité inévitable du canal. D'ardentes discussions, liées notamment aux méthodes employées, ont accompagné ces communications.

Les liaisons par traînées météoritiques ont été abordées par le Docteur K. WATSON qui a évoqué la possibilité d'adaptation en bilan de liaison variable et une seule communication consacrée au bruit des canaux a été présentée par le Docteur K.S. KHO. Enfin, une communication consacrée à l'étude de séquences de synchronisation réduisant la complexité des systèmes a été présentée par le Professeur C. GOUTELARD.

Il est singulier de constater qu'aucune communication sur les canaux terre-satellites ou satellite-satellite n'a été présentée.

Les quatorze communications conduisent à poser trois questions :

- Est-il possible et souhaitable de normaliser et de coordonner les mesures pour les rendre plus comparables, donc en extraire davantage d'informations ? Ne serait-ce pas aussi une limitation à la créativité ?

- Jusqu'à quel point peut-on sophistiquer les modèles ? Le meilleur modèle est le canal lui-même. Ces perfectionnements, possibles grâce à l'informatique, dépassent souvent la précision de mesure des paramètres mesurés sur le canal.

- Quels seront les paramètres nouveaux qui devront être pris en compte dans les systèmes futurs : modélisation large bande, insertion de la polarisation... ?

Cette première session a donc montré les progrès récents et les étapes atteintes. Elle a également permis de poser un certain nombre de questions dont les réponses, on peut l'espérer, surgiront dans de futurs symposia.

A GLOBAL COMMON-USER SYSTEM FOR THE PROVISION OF HF PROPAGATION DATA

M. Darnell, J. Hague & A. Chan

Hull-Warwick Communications Research Group
Department of Electronic Engineering
University of Hull
HULL HU6 7RX
UK

SUMMARY

The system design described in the paper comprises a world-wide network of HF (2 - 30 MHz) transmitters and receivers designed to allow the collection of field strength and other propagation data. The primary objective of the system is to enable the effectiveness of HF propagation/noise prediction methods to be enhanced by means of real-time measurement data.

Historically, control of HF broadcasts and communications has been heavily dependant on off-line path predictions: however, the degree of precision associated with such propagation analysis is somewhat limited. Some use has also been made of passive monitoring of known transmitters to update off-line models, but problems of transmitter identification and inappropriate signal formats limit the efficiency of this approach.

For these reasons, a system has been designed comprising a number of dedicated HF transmitters, sited in different parts of the world, and emitting signals with a defined format, unique to each site. Reception of the signals can take place at various levels of sophistication, depending upon the requirements and resources of the users. Information about transmitter identification, signal strength, phase stability, fading, multipath structure, signal-to-noise ratio, noise/interference and predicted error rates for digital traffic can all be extracted from the transmissions.

The signals can be received and exploited by a range of users, from those with simple manual receivers with S-meter monitoring to those with sophisticated automatic receivers interfaced with powerful processors. Facilities for system evolution in response to user requirements are incorporated.

The paper describes the detailed design philosophy of the system, the implementation of a prototype system and the results of trials carried out with the prototype system over a medium range skywave path. Problems of system deployment and global data collection and analysis are also discussed.

1. INTRODUCTION

The system described in this paper comprises a global network of HF (2 - 30 MHz) transmitters and receivers which will enable users of many types to be able to monitor and collect a variety of real-time data on propagation and noise/interference conditions in the HF band on a world-wide basis. The intention is that the system should be accessible by anyone with a requirement for such data, whether they belong to professional or amateur radio communication communities. Any individual user of the system will be limited in the nature of the information he can extract only by the sophistication of the radio receiving and signal processing equipment at his disposal. However, the system design enables users with even the most simple manually-controlled receiving systems to have access to basic real-time propagation data.

The major initial objective of the system is to provide information to enable the effectiveness and accuracy of off-line HF propagation and noise prediction methods to be enhanced; in the first instance, emphasis is placed upon the improvement of HF broadcast planning and operational procedures - although, as will be indicated later, the system described here can be expected to have a much wider application to general HF communications.

At present, off-line prediction methods, for example (CCIR, 1978), are applied to a variety of operational scenarios, involving skywave propagation over ranges from vertical-incidence to world-wide. The database, although extensive, and the analysis algorithms do not provide the required degree of precision in the prediction process. It seems improbable that this level of precision can be improved substantially by further refinement of analysis algorithms in the absence of an additional body of data collected in an efficient, systematic and directed manner, with user requirements being borne in mind. Alternatively, broadcast planning based more on real-time monitoring of the propagation medium characteristics is an option. The system described in this paper can fulfil either, or both, of these roles.

In the past, attempts have been made to exploit passive monitoring of "transmissions of opportunity", such as broadcasts, standard time transmissions, etc., in order to obtain data that can be used to updata off-line analysis procedures via an indication of real-time conditions on certain paths. However, the effectiveness of such procedures is limited because of:

(a) the difficulty of positive transmitter identification in many cases;

(b) co-channel interference from other HF transmissions;

(c) the difficulty of extracting the required propagation data from broadcast and other transmissions with a variety of formats;

(d) insufficient knowledge of the nature of the transmitters and transmitting antennas, in terms of effective radiated power and directional characteristics.

The following sections of the paper outline the overall system design concept, the detailed design of a prototype single-transmitter/single-receiver system, examples of the performance of the prototype system over a medium-range skywave path and the problems of data collection, analysis and dissemination on a global basis; finally, the applications and wider development of the system are considered.

2. SYSTEM DESIGN CONCEPT

Because of the problems with both off-line forecasting and passive monitoring procedures outlined in the previous section, the system design incorporates a number of dedicated transmitters sited in various parts of the world. These transmitters radiate signals with a defined format, unique to each site. Reception of the signals can take place at various levels of sophistication, depending upon the requirements and resources of the users, ie

(a) simple audio identification and monitoring via a CW code sequence unique to each transmitter;

(b) visual monitoring of signal strength via S-meter readings;

(c) automatic signal strength measurements via analysis of digitised received signal samples by an appropriate processor;

(d) automatic identification of multipath structure via analysis of digitised signal samples by an appropriate processor;

(e) automatic estimation of signal-to-noise ratio (SNR) via analysis of digitised samples by an appropriate processor;

(f) automatic characterisation of noise/interference via analysis of digitised samples by an appropriate processor;

(g) automatic estimation of predicted error rates for various forms of digital transmission via analysis of digitised samples by an appropriate processor;

(h) automatic characterisation of flat- and frequency-selective fading effects via analysis of digitised signal samples by an appropriate processor;

(i) automatic characterisation of phase stability and Doppler effects via analysis of digitised signal samples by an appropriate processor.

In general, any given user will be able to select a subset of the above analysis options appropriate to his operational and/or technical requirements.

Clearly, the system depends heavily upon digital signal processing procedures for all but the simplest analysis functions. For this purpose, specialised signal processing architectures and devices have been employed; these have the great practical advantage of being software-variable and hence flexible. It has therefore been possible to ensure that the system design is evolutionary, ie other processing functions can be incorporated into the software as new user requirements arise. Thus, the list of analysis options given above should not be regarded as exhaustive.

Facilities have also been incorporated into the prototype system for data collection on disc; the disc can then be processed on-site to obtain the desired parameters in reduced form or, alternatively, the discs can physically be sent to a central data reduction site. One possible objective for the system is to provide comprehensive measurement data that can be made generally available to all interested parties via a suitable co-ordinating organisation.

It is not the purpose of this paper to identify appropriate locations for the system transmitters, to suggest frequency complements or to specify antenna types in anything other than the broadest terms.

The system design also flexible enough to allow the basic architecture to be used in a "stand-alone" mode, as a real-time channel evaluation (RTCE) sub-system supporting say a point-to-point HF communication link. In this case, the additional cost of the elements required would be small compared with the overall communication system cost.

The following section will describe the main features of the system design in greater detail.

3. ELEMENTS OF THE PROTOTYPE SYSTEM DESIGN

3.1 Transmission Uniqueness

The basis of the system design is

(i) that each transmitted component should be uniquely identifiable, both manually and automatically;

(ii) that the required path analysis data can be extracted from each transmitted component.

This may be achieved reliably by employing appropriate combinations of

- transmission time interval
- frequency of operation
- signal format.

Figure 1 illustrates this concept by means of a quasi 3-dimensional representation; here, for transmission identification to be unambiguous, the signal "volumes" in signal-time-frequency space must not intersect.

3.2 Transmission Time Schedule

In dimensioning the system design, a basic analysis time slot of 12 seconds was chosen, representing the interval spent by a receiver in analysing any transmitted component from any transmitter site. The total number of transmitters required for a world-wide network, and the number of frequency components per transmitter, are variable within the system architecture; the prototype system is configured for any number of transmitters, n, each radiating 5 frequency components in sequence, with a dwell time of 4 minutes on any one component.

For broadcast applications, it is desirable that each of the n transmitters should radiate one frequency component in each of the five fixed service bands near to 5.5, 8, 11, 15 and 20 MHz (CCIR, 1988). The transmissions in each band should commence at 0, 4, 8, 12 ... minutes past each hour sequentially, thus yielding a cycle time of 20 minutes for any given transmitter. When the number of transmitters, n, is greater than 5, more than one frequency will be required in each of the broadcast bands if mutual interference is to be avoided. In general, the maximum number of separate frequencies necessary for each of the n transmitter sites, N, will be given by

$$N = n/5 \qquad (1)$$

if n is exactly divisible by 5, and

$$N = [\lfloor (n/5) \rfloor + 1] \qquad (2)$$

otherwise ($\lfloor\ \rfloor$ denotes "the integer part of").
Figure 2 shows an example of a possible schedule for a system comprising 9 transmitter sites, with two frequencies being assigned in each of the 5 bands.

3.3 Receiver Time Schedule

A given receiver terminal, in which retuning time is small, can monitor 5 separate transmitted components per minute, or take 4 samples of each of 5 transmitted components in 4 minutes. In a 20-minute interval, a total of 25 components will be radiated by a 5-transmitter system; these can all be monitored 4 times by one receiver. Clearly, in the 9-transmitter system of Figure 2, there will be a total of 45 transmitted components radiated in 20 minutes; therefore, 2 receivers operating in parallel will be required in order to monitor all components 4 times.

When n exceeds 5, and a given user has a single receiver available, only a subset of the radiated components can be monitored; the nature of this subset monitoring will be dictated by the requirements of individual users.

3.4 Overall Operational Sequence

Figure 3 illustrates the overall sequence of operations diagramatically. It is apparent from the timing shown in Figure 3 that in one hour, twelve 12 second samples of each of 25 frequency components can be taken by any given receiver - a level of sampling considered adequate to allow meaningful statistical characterisation of the relevant path parameters - as will be discussed in Section 5 of this paper.

For demonstration purposes, a prototype single-transmitter/single-receiver system has been designed, constructed and tested. The system is compatible in all respects with the requirements of the operational scheduling described above. The major elements of this prototype system design will now be discussed in some detail.

3.5 Synchronisation Considerations

As indicated in Fig. 1, the transmission time schedule simply provides a unique time slot in which a receiver can attempt to detect the presence of any transmitted component from any transmitter site. Although a specific timing schedule was chosen for the prototype system, it can be varied under software control to meet different or evolving user requirements.

The basic 12 second time slot was selected to be compatible with a readily achievable degree of time synchronisation between transmitting and receiving terminals of different types. To cater for the worst-case of a simple manually-controlled receiving installation, a required timing accuracy between transmitter and receiver to within 1 second or better is assumed. This allows the use of timing control based upon a simple quartz oscillator or timing derived from a standard transmission such as MSF (Rugby) or WWV. For a processor-based receiving terminal, timing would typically be obtained via the use of a real-time clock module within the processor architecture.

3.6 Transmitter Terminal Architecture

Figure 4 shows a schematic diagram of a transmitter terminal for use within the system. The signal generation process is software-based, with the signal format being adaptable in response to user requirements; similarly, transmission sequencing is also software controlled and modifiable. The control interface unit would not be used in normal operation: it is provided specifically for the purposes of system initialisation after switch-on and to allow any desired modifications to be made to the signal format and/or timing sequence as user requirements evolve.

The SSB transmitter should have a rating of between 5 and 10 kW. Transmitting antennas should have an omnidirectional azimuthal radiation pattern and a broad elevation pattern. To avoid the process of frequent high RF power switching, a single wideband monopole or conical structure would appear to be appropriate.

3.7 Receiver Terminal Architecture

The architecture of a fully automatic and flexible receiving terminal, as implemented for the prototype system, is shown in Figure 5. It should be noted that this design is representative of the more sophisticated user terminals to be expected within the network. For the purposes of demonstration, an amateur grade receiver was interfaced to a cheap processor system, a frequency-agile frequency-shift keying (FSK) demodulator (based upon switched-capacitor filters), a real-time clock module and a special-purpose signal processing system. All elements, with the exception of the receiver itself and the control interface unit, are housed in a standard STE bus system rack.

Again, the control interface unit is provided for the purposes of system initialisation after switch-on and to allow modifications to the control and/or signal processing procedures if user requirements change. It is also instrumental in the data collection and logging functions described in Section 5.

The receiving antenna used should be a short, vertical, active type, capable of being precisely calibrated for field strength measurements. Any receiver used in an automatic terminal should have a specification at least equivalent to that of the receiver employed for the prototype system, both in terms of its RF performance and control facilities. Simpler forms of receiver can however be used in manually-controlled terminals.

4. SIGNAL DESIGN & PROCESSING

Figure 6 shows the overall format of the signal transmitted on the assigned frequencies in each 12 second slot. The emission should be of class F1B with a frequency shift of 850 Hz where appropriate. All elements of the signal have specific purposes - as will be discussed below.

4.1 FSK Preamble

The binary FSK preamble, keyed at 100 bits/s and commencing on the lower of the two FSK tone frequencies, is of 1 second duration and is intended to allow initialisation of receiver AGC (if required). This preamble also provides a degree of "slack" in the system so that any synchronisation differences between transmitters and receivers are not detrimental to the system performance.

The preamble if then followed by a pause of duration 50 ms.

4.2 CW Identification Sequence

Within a period of 3.3 seconds, a transmitter identification sequence is transmitted using the higher of the two FSK tone frequencies. The identification signal used could be in morse code format, with specified "dot" and "dash" intervals; alternatively, it could employ any other format convenient for the system users, eg one based on the international locator code as used by radio amateurs. It is

essential that the sequence code keying rate should be compatible with audio identification by simple manually-operated receiving terminals.

This CW sequence is then followed by a pause of 50 ms.

4.3 Complementary Sequences

To provide a means of identifying the multipath structure efficiently, two 256-bit binary complementary sequences are then transmitted in succession at a rate of 1.2 kbits/s, with an interval of 50 ms after each sequence to allow for the presence of any multipath returns. The upper of the two FSK tones is used for this purpose. The keying rate of the sequences is dictated by the need for transmitted signal energy to be confined effectively within a nominal 3 kHz bandwidth.

In the prototype system, the formats of the complementary sequences are as follows:

Sequence 1

1110010000101000000101001101100000011011001010001110101111011000
0001101111010111000101001101100011100100111010111111010111111011000
0001101111010111111101011001001110001101100101000111010111111011000
1110010000101000111010110010011111110010011010111111010111111011000

Sequence 2

0001101111010111111101011001001111111001001101011110001010000100111
0001101111010111000101001101100011100100111010111111010111111011000
1110010000101000000101001101100011100100111010111000101000010011 1
1110010000101000111010110010011111110010011010111111010111111011000

The important property of complementary sequences which makes them an appropriate test signal for evaluating the channel impulse response, and hence its multipath profile, is the form of their individual and summed autocorrelation functions (acf's). Typical formats for these are illustrated in Figure 7; it is seen that if the two component acf's can be processed in synchronism and summed, then their side-lobes cancel out and only an impulsive central peak is left in the summed acf. In this case, the acf of the complementary sequence test signal x(t), which is now denoted by $\phi_{xx}(\tau)$, is given by

$$\phi_{xx}(\tau) \propto \delta(\tau) \qquad (3)$$

where τ is a delay variable and $\delta(\tau)$ is a unit impulse function centred on $\tau = 0$. It can be simply shown (Lee, 1960) that the input-output crosscorrelation function (ccf) for any linear time-invariant system, $\phi_{xy}(\tau)$, is given by

$$\phi_{xy}(\tau) = 1/T \int_{-T/2}^{T/2} x(t)\, y(t + \tau)\, dt \qquad (4)$$

where y(t) is the system output and T is the effective duration of the syste- input x(t); equation (4) can also be expressed in the form of a convolution

$$\phi_{xy}(\tau) = \int_{-\infty}^{\infty} h(u)\, \phi_{xx}(\tau - u)\, du \qquad (5)$$

where u is a dummy time variable and h(t) is the system unit impulse response function. Clearly, if the input acf is impulsive, then the input-output ccf will be proportional to the system unit impulse response function, ie

$$\phi_{xy}(\tau) \propto h(\tau) \qquad (6)$$

Figure 8 illustrates the principle of this method of response identification where the cross-correlator can be realised as a matched filter. Here, the system to be identified is the HF channel and the resulting impulse response indicates the multipath profile.

4.4 FSK Reversals

Following the 50 ms pause after the second complementary sequence, a series of FSK reversals comprising 400 bits at 100 bits/s is transmitted, with the first bit of the series commencing on the lowest of the two FSK tones. These section of the transmission allows the following information to be extracted at the receiver:

(a) the characterisation of the short-term fading, ie flat or frequency-selective, if a Law-assessor FSK demodulator is used (Alnatt, Jones & Law, 1957);

(b) estimation of SNR in each FSK sub-channel, as illustrated in Figure 6, by

comparing levels in "mark" and "space" intervals;

(c) characterisation of noise/interference by, for example, carrying out FFT analysis in the "space" intervals in each of the two FSK sub-channels.

For (b), the composite level in each "mark" interval is the sum of signal power S and noise/interference power N whereas, in the "space" interval, only noise/interference power N is present. Taking the ratio of "mark" level to "space" level gives

$$(S + N)/N = 1 + S/N \qquad (7)$$

hence the SNR S/N. Averaging over the entire 4-second (400 bit) interval will enable a more reliable value of SNR to be obtained. Once an SNR estimate is available, the bit error rate (BER) for various forms of digital traffic can also be estimated using the relevant relationship between BER and SNR.

Immediately following the FSK reversals, a CW signal on the higher of the two FSK tones is transmitted for a duration of at least 3 seconds in order to bring the total transmission time to 12 seconds, at which time a frequency change occurs.

4.5 Other Measurement Possibilities

If phase coherence is maintained over the complete 12 second duration of the signal for both "mark" and "space" tones, the nature of the received zero-crossings can be analysed to yield data on the phase stability and Doppler characteristics of the propagation medium. The preamble, identification code and FSK reversals can all contribute to this assessment, giving a total maximum analysis duration of about 9 seconds for this purpose.

Using a processor-based receiving terminal, all parameters analysed can be output in terms of raw data, spot values, median values, etc.

5. DATA COLLECTION, ANALYSIS & DISSEMINATION

5.1 Collection

In the first instance, the most important data collected by the system will be associated with field strengths, ie from the 4s element of the test signal discussed in Section 4.4. It is proposed that a standardised active receiving antenna be used by all receiving stations so that measured signal voltages can be converted to field strength values. Local calibration and checking of the receiving terminal will be achieved via the injection of a calibration signal at appropriate intervals. As indicated previously, the test signal format also allows the extraction of other propagation data should users require this.

Data will be stored on double-sided/double-density 5.25 inch diskettes with 360 kbytes capacity. A single disk will be sufficient to store all data relating to one week's monitoring as detailed below. For signal strengths, actual individual 4s signal and noise/interference level values will be recorded on disk. This will require considerably more off-line processing at a central analysis site than if some data reduction were to be carried out at the receiving location; however, it will simplify any changes in analysis procedures which may be introduced in the future. The following information will be stored on each disk:

(a) Descriptive file;

(b) Calibration file;

(c) Measurements file (168 hourly values of signal and noise/interference.

5.2 Analysis & Dissemination

For every circuit monitored, ie transmitter/receiver/frequency combination, the receiving terminal must take sufficient samples of both wanted signal and noise to allow meaningful statistical parameters to be derived for both, bearing in mind the likely time variability of the received signals; typically, hourly median values will be required. For this purpose, it has been estimated that the 12 4-second samples per hour taken by the system described in this paper will be adequate.

Monthly median values, together with upper and lower decile values, of signal amplitude can be derived from the hourly median values taken for corresponding hourly intervals on different days. The noise samples can be analysed using the methods already specified in CCIR Report 253 (1978).

It is intended that data received in sample form from the various sites should be normalised by making use of the antenna and receiver calibration information from each site. It is intended that the reduced statistical data will first be validated by an appropriate international group of experts and then be incorporated into a world data bank; the data held in this bank will be continuously refined and updated,

being available on request to appropriate users of the HF band.

Any individual user, or group of users, can of course carry out their own processing and data reduction. As indicated previously in Section 4, propagation parameters other than signal strengths can also be derived from the received signals if required.

6. TYPICAL RESULTS FROM THE PROTOTYPE SYSTEM

In May 1988, the prototype system was demonstrated over a skywave path between the UK and Geneva. Only two frequencies were available for these tests, ie 9.915 MHz and 12.040 MHz. Records of signal stength were accumulated over two days and representative examples of the output in graphical form are given as Figures 10 (a) - (d); the vertical scale in these records is uncalibrated.

Following these tests, some of the recorded data was processed off-line to validate the procedures for estimating the multipath structure using the complementary sequence section of the test transmission, described in Section 4.3, in conjunction with correlation processing. Figures 11 (a) and (b) are two examples of diagramatic output of multipath profiles, showing the level of delay definition to be expected for a 3 kHz bandwidth measurement. Such an output can be computed for each 12s test transmission.

The computational procedures for calculating SNR's and for automatically identifying test transmission identification codes have also been developed.

7. CONCLUDING REMARKS

This paper has described the principles of operation of a global common-user system designed to enhance the quality and reliability of HF skywave propagation models. Examples of system performance are presented. The system can be accessed by a wide range of potential users, from those with simple manually-controlled receivers with audio and S-meter monitoring, to those with fully automatic receivers interfaced with powerful data processors. In its more sophisticated form, the system employs special-purpose, programmable, signal processing devices for signal analysis, ie TMS 320-C25; it is therefore compatible with evolutionary changes in user analysis requirements.

The system design is such that it can also be used as a dedicated real-time channel evaluation system to support specific communications links. If necessary, the signal format can be modified to meet particular requirements for data output or transmission timing.

8. ACKNOWLEDGEMENTS

The authors wish to acknowledge with thanks the support of the Department of Trade & Industry for the work described in this paper; in particular, the guidance and help provided by Mr L.W. Barclay has been especially valuable. The British Broadcasting Corporation made transmission facilities available for trials purposes, and that help is also acknowledged with gratitude. In addition, the input and comments provided by CCIR Interim Working Party 6/14 have been most helpful.

9. REFERENCES

1. CCIR: "Second CCIR computer-based interim method for estimating sky-wave field strength and transmission loss at frequencies between 2 and 30 MHz", Supplement to Report 252-2, Doc. of the XIVth Plenary Assy, ITU, Geneva, 1978.

2. CCIR: ""HF field strength measurements", Draft New Report produced by IWP 6/14, Document 6/32 (Rev. 1) - E, 27 April, 1988.

3. Darnell, M.: "Principles and applications of binary complementary sequences", Proc. of Int. Symp. on "Walsh and other non-sinusoidal functions", Hatfield Polytechnic, 1975.

4. Lee, Y.W.: "Statistical theory of communication", Wiley, 1960.

5. Alnatt, J.W., Jones, E.D.J. & Law, H.B.: "Frequency diversity in the reception of selectively fading binary frequency-modulated signals", Proc. IEE, Vol 104, Part B, pp 98 -110, 1957.

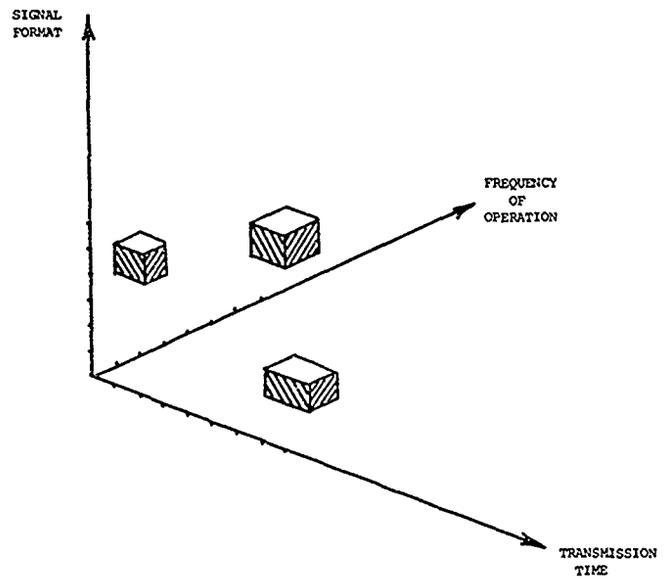

Figure 1: Unambiguous Signal "Volumes"

MINUTES

TRANSMITTER	0	4	8	12	16	20
1	A1	B1	C1	D1	E1	
2	B1	C1	D1	E1	A2	
3	C1	D1	E1	A2	B2	
4	D1	E1	A2	B2	C2	
5	E1	A2	B2	C2	D2	
6	A2	B2	C2	D2	E2	
7	B2	C2	D2	E2	A1	
8	C2	D2	E2	A1	B1	
9	D2	E2	A1	B1	C1	

Figure 2: Possible Transmission Schedule for a 9-Transmitter System

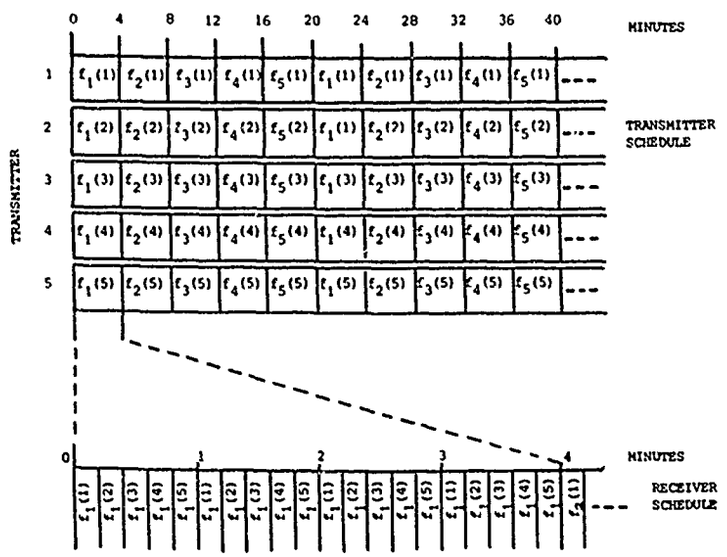

Figure 3: Overall Transmitter & Receiver Timing

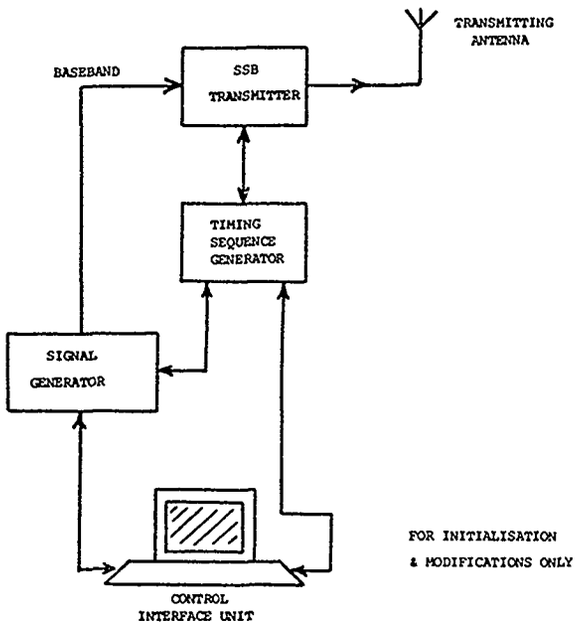

Figure 4: Transmitter Terminal Architecture

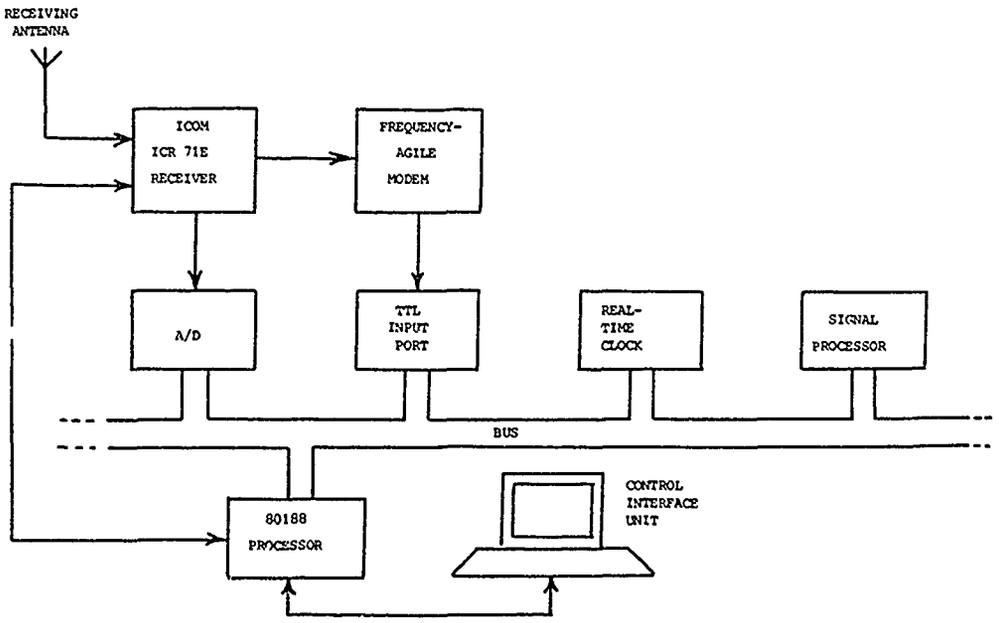

Figure 5: Receiver Terminal Architecture

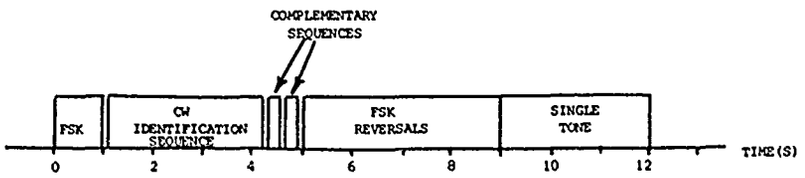

Figure 6: Overall Format of Transmitted Signal

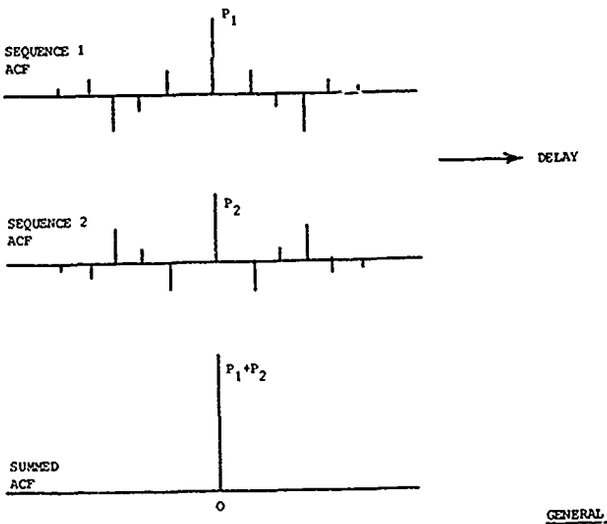

Figure 7: Typical Complementary Sequence ACF's

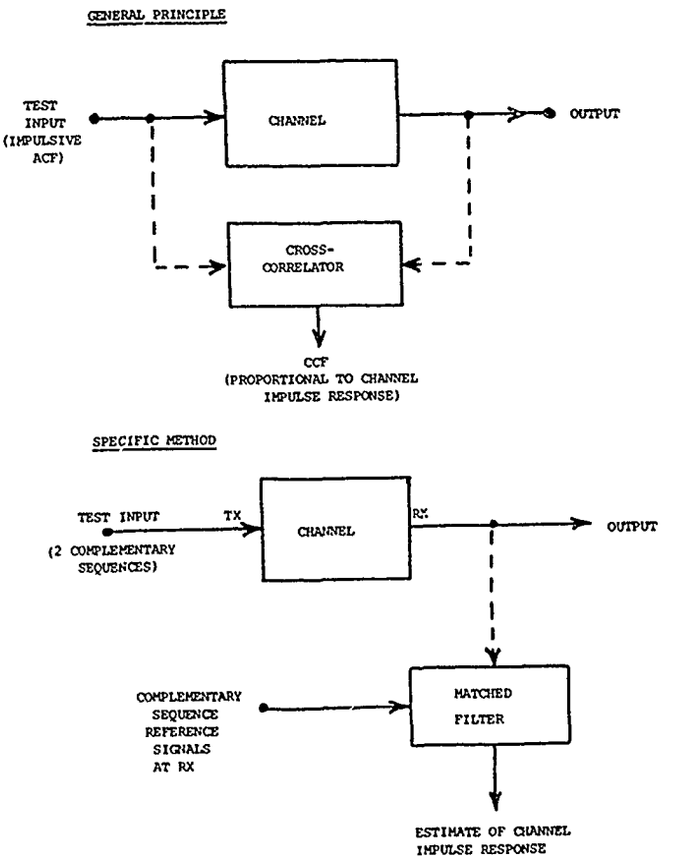

Figure 8: Channel Impulse Response Identification

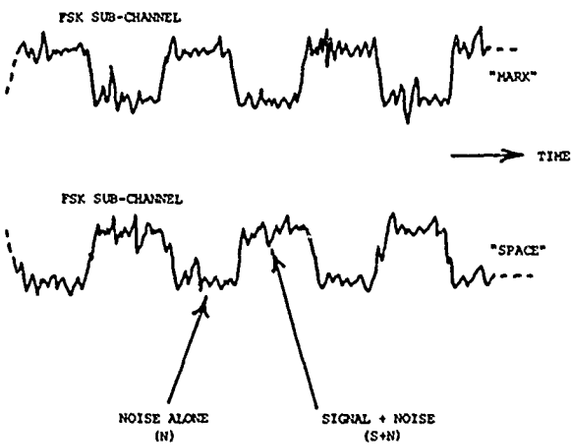

Figure 9: Estimation of SNR from FSK Reversals

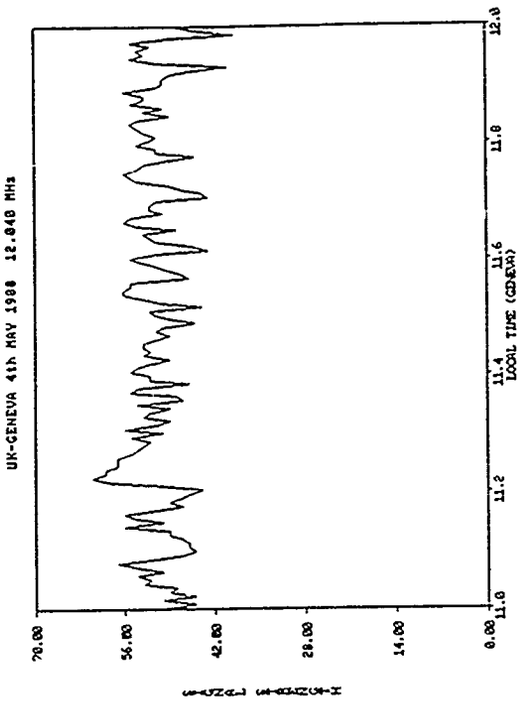

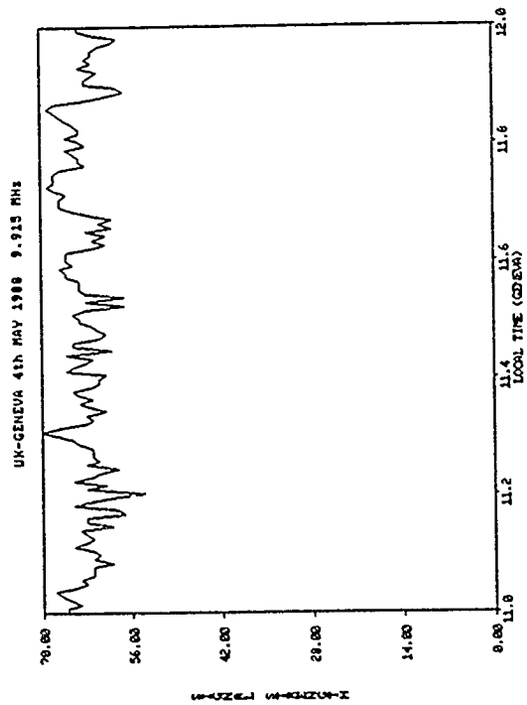

Figure 10(a)

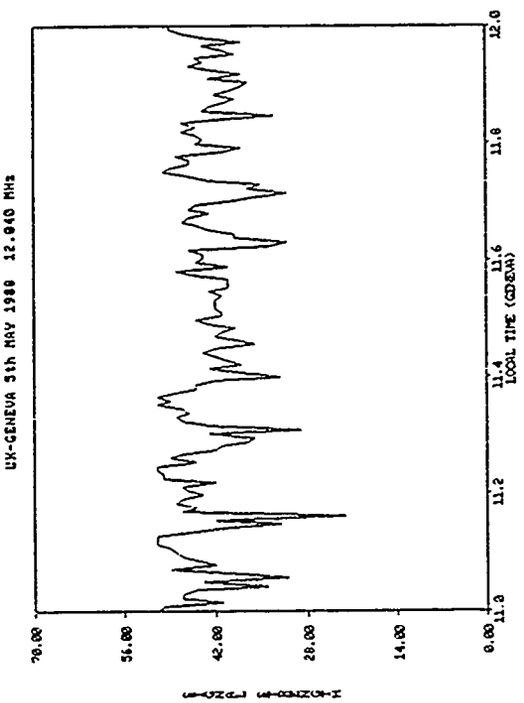

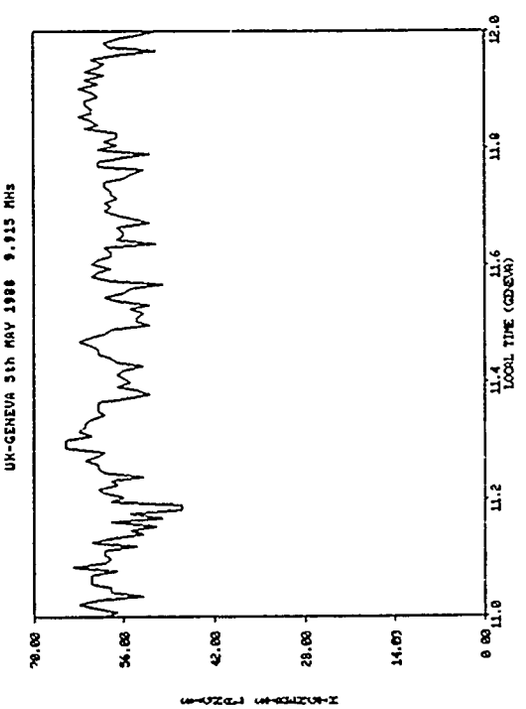

Figure 10(b)

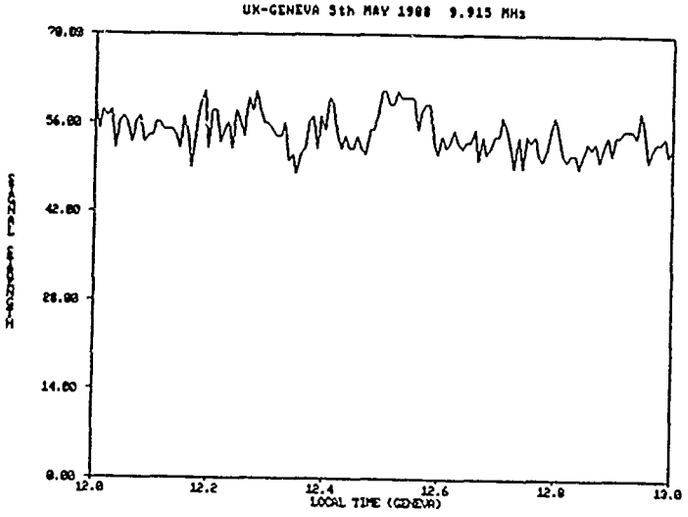

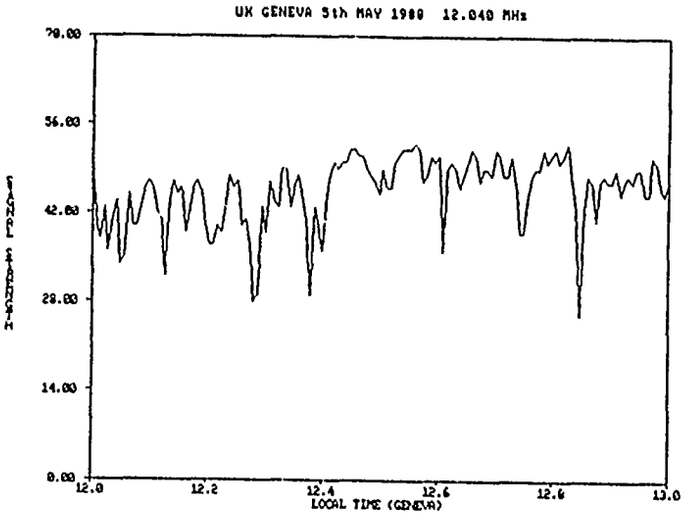

Figure 10(c)

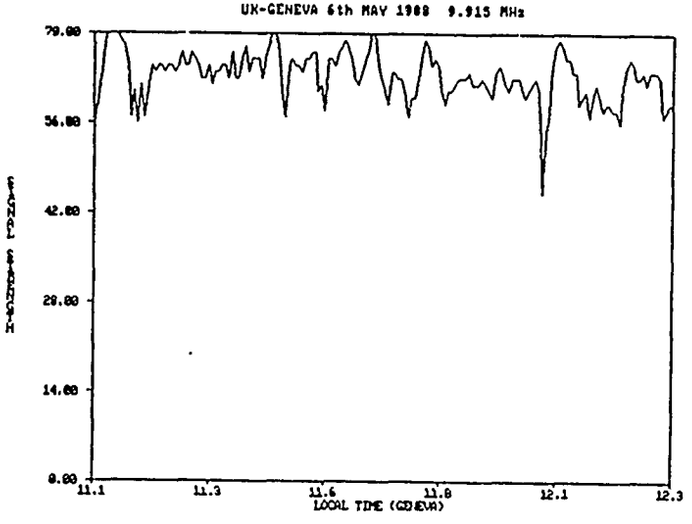

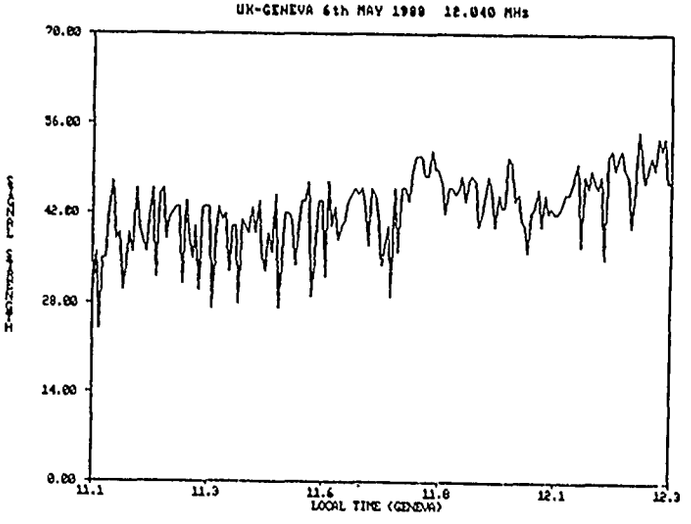

Figure 10(d)

Representative Records of Signal Strength
from UK-Geneva Trial

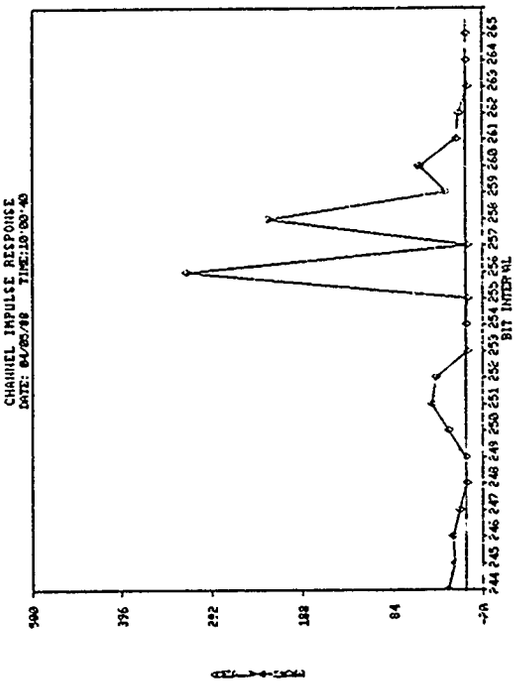

Figure 11(b)
Typical Channel Impulse Response Estimates
from UK-Geneva trial

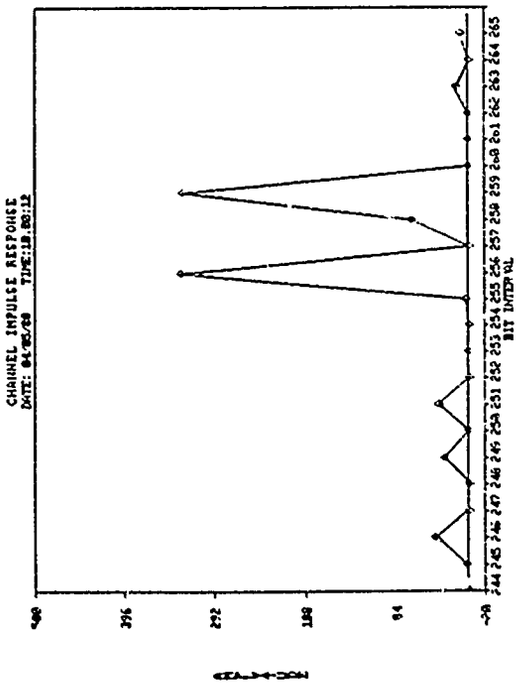

Figure 11(a)

DISCUSSION

T. CROFT

The Entire World is a very large place. How many transmitters will be needed to provide "world-wide coverage".

AUTHOR'S REPLY

About 9-10 are envisaged. It is appreciated that this is a somewhat coarse sampling of the environment, but this number is considered to be the maximum that can be economically supported.

C. GOUTELARD

Je ne suis pas convaincu par le choix de vos signaux : vous utilisez 4 signaux, 2 à large bande, 2 à bande étroite. Je vois 2 inconvénients :

- Vous multipliez le nombre de signaux, ce qui complique le récepteur et l'émetteur.
- Vous avez un système séquentiel qui fait un échantillonnage assez pauvre pour chaque mesure.

L'utilisation de 2 signaux orthogonaux, l'un large bande, l'autre à bande étroite, permettrait de faire les mêmes mesures de façon continue sans qu'il y ait, me semble-t-il, une complexité plus grande du récepteur.

AUTHOR'S REPLY

Thank you for those comments. In response, may I make the following points :

1 - That the receiving system is software - based and implemented using TMS320C25 technology : therefore, the nature of the processing used can be simply changed depending on which section of the transmission is being received at any time.

2 - That certain specifications for the transmitted signal were provided by the potential users of the system : these included access by the most simple manually operated receiving terminals.

In fact, only 2 basic demodulators are required - one for the FSK sections of the transmission - one for the complementary sequence section.

In terms of frequency of environmental sampling by the system, 12 samples of each component per hour were specified by the potential users as being sufficient for their characterisation purposes.

ANALYSE EXPERIMENTALE DE LIAISONS HF

Y.M. LE ROUX, R. FLEURY, J. MENARD, J.P. JOLIVET
CENTRE NATIONAL D'ETUDES DES TELECOMMUNICATIONS
Route de Trégastel
22300 LANNION
FRANCE

L'amélioration de la qualité et de la fiabilité des transmissions dans la gamme décamétrique passe par une meilleure connaissance des mécanismes de la propagation ionosphérique. Selon cet objectif, un outil de caractérisation expérimentale du canal HF sur des liaisons test a été élaboré au CNET. Ce système est actuellement opérationnel sur une liaison d'environ 650 km, située aux moyennes latitudes. Il permet de mesurer simultanément, d'une part la réponse impulsionnelle du canal, dans une bande utile de 10 KHz, avec une période de réactualisation de 10 ms, et d'autre part, les paramètres principaux de la propagation dans une bande de 50 KHz : temps de groupe, atténuations et phases instantanées relatifs à chaque mode ou trajet propagé. Des analyses des caractéristiques de bruits et brouillages sont également possibles. Le système, ainsi que ses principaux modes de fonctionnement sont décrits dans le présent article. Ils sont illustrés par des résultats expérimentaux. Une des conclusions importantes est que, de par ses performances, l'analyseur de liaisons met en évidence l'insuffisance des modèles de canal actuellement existants (type Watterson), à expliquer dans sa totalité le comportement de la propagation ionosphérique. Un modèle général de canal, basé sur une représentation de système linéaire variant dans le temps, est par ailleurs en cours de validation.

I. INTRODUCTION

L'ionosphère permet d'établir des liaisons de communication transhorizons dans la gamme des hautes fréquences 2-30 MHz. Elle constitue ainsi un support naturel de transmission, ne nécessitant pas de relais radio. Cependant, l'ionosphère est un milieu dispersif en temps et en fréquence. Les signaux qui y transitent sont donc soumis à des mécanismes de fluctuations rapides de leur phase et de leur amplitude. Ceci a pour conséquence de limiter, parfois sévèrement, la fiabilité et la qualité des communications, via le canal ionosphérique. Divers types de bruits et de brouillage encombrent tout le spectre HF de façon plus ou moins importante selon les zones géographiques. Ils sont une source supplémentaire de dégradation de ces communications.

Ainsi, pour pouvoir assurer dans les meilleures conditions possibles, des débits de plusieurs kb/s, il est indispensable que la conception des appareils de transmission soit effectuée dans le sens de leur adaptation aux réalités de comportement du canal. Pour y parvenir et acquérir une meilleure connaissance des caractéristiques de la propagation dans la gamme décamétrique, des campagnes d'expérimentation doivent être menées. Un bon moyen de synthétiser cette connaissance physique et expérimentale du milieu est alors de la traduire sous forme de modèle. L'intérêt de disposer d'une modélisation réaliste du canal est en effet double :

- contribuer à la définition de techniques de modulation-démodulation

- permettre de simuler en laboratoire le canal, afin de tester les équipements de transmission.

De nombreux modèles du canal HF ont ainsi été établis jusqu'à présent. Parmi ceux-ci, le modèle de Watterson (1970), faisant l'objet d'une recommandation du CCIR (R.549-1, 1974, 1978), est certainement celui dont l'utilisation est la plus répandue. Il s'agit d'un modèle décrivant le canal de façon purement statistique et dont le principe est désormais bien connu : lignes à retard et gains complexes qui ont pour effet de moduler en phase et en amplitude le signal entrant, afin de le soumettre à des évanouissements de type Rayleigh. Il faut cependant insister sur le fait que la validité de ce modèle est assujettie à plusieurs hypothèses et notamment :

- la stationnarité statistique au second ordre du comportement du canal

- l'indépendance statistique des caractéristiques de propagation relatives à chaque mode ou trajet.

Lorsque ces hypothèses sont vérifiées, le modèle est certainement représentatif du canal, du moins dans une bande étroite, et son grand intérêt réside alors dans sa simplicité de mise en oeuvre. Il apparaît malheureusement, que de nombreux cas d'expérimentation viennent invalider les hypothèses de base du modèle. En outre, des caractéristiques de propagation telles que les effets de diffusion et de dispersivité en fréquence ne sont pas prises en compte par ce modèle. Sa bande fréquentielle de validité s'en trouve donc limitée.

Pour éviter les restrictions qui viennent d'être citées, il convient d'envisager une modélisation plus générale du canal de transmission ionosphérique. Il faut toutefois noter qu'un souci majeur doit être de s'assurer qu'un tel modèle reste pratiquement utilisable. Dans cette optique, après avoir brièvement rappelé les caractéristiques principales de la propagation, nous proposons un modèle susceptible de les prendre en compte. Sa validation expérimentale est en cours, à l'aide d'un système d'analyse de liaisons HF dont le principe sera décrit et les performances illustrées par quelques résultats de mesure.

II. MODELISATION DU CANAL IONOSPHERIQUE

Les caractéristiques de la propagation ionosphérique qui ont une influence prépondérante sur la qualité et la fiabilité des transmissions dans la gamme décamétrique sont rappelées au tableau 1. Des valeurs numériques ont été affectées à la plupart des paramètres. Elles correspondent à des ordres de grandeur convenant à des liaisons aux moyennes latitudes. Lors de conditions "extrêmes" de propagation et notamment dans les zones géographiques aurorales et équatoriales, ces valeurs peuvent être largement dépassées (WAGNER et al., 1987).

Les caractéristiques de propagation qui viennent d'être mentionnées induisent des évanouissements et des distorsions de toutes natures aux signaux qui transitent par le canal ionosphérique. Il faut également remarquer que le comportement de ce canal est extrêmement variable en temps et en espace. Il est donc difficilement prévisible. La dégradation des transmissions est d'autre part accentuée par la présence de bruits et de brouilleurs que l'on rencontre dans tout le spectre HF.

Malgré la complexité de l'influence du canal sur les signaux qui y transitent, deux propriétés intéressantes permettent de simplifier sa modélisation :

- Le canal ionosphérique peut, en bonne approximation, être assimilé à un système linéaire (au moins aux puissances d'émission couramment utilisées pour l'établissement de liaisons de communication).

- Bien que pouvant souvent paraitre quelque peu erratique, l'évolution dans le temps des paramètres de la propagation comporte parfois un caractère quasi-déterministe. C'est par exemple le cas des phénomènes ondulatoires se propageant dans le milieu ionosphérique et influençant son comportement (ondes de gravité par ex.).

PARAMETRE DE PROPAGATION	NOTATION	ORDRE DE GRANDEUR
Variable liée à l'évolution temporelle des caractéristiques du canal	t	$t \simeq f_d$
Nombre de trajets principaux Chaque trajet principal peut être la résultante d'un nombre important de sous-trajets par effet de diffusion par exemple	n	8
Variable liée à la mémoire du canal. Représente les retards de groupe	τ	0 à 8 ms
Etalement du retard de groupe	$\Delta\tau$	0 à quelques centaines de μs
Décalage fréquence Doppler moyen	f_d	2.5 Hz
Etalement fréquence Doppler	Δf_d	2 Hz, à -3 dB sur le spectre d'étalement
Amplitude relative	A	dynamique significative retenue = 40 dB
Phase relative	φ	
Dispersion en fréquence du canal	V	200 μs/MHz
Anisotropie du milieu - Polarisation Existence de deux modes magnétoioniques notés "o" et "x" et polarisés inversement.	-	Pris en compte par les autres paramètres de phase et d'amplitude.

Tableau 1

Compte tenu de ce qui vient d'être dit, il peut être fait appel à la théorie des systèmes variant dans le temps pour représenter le comportement du canal ionosphérique. Parmi les différentes fonctions permettant de décrire un tel système (KAILATH, 1961), nous retiendrons ici $h(\tau,t)$ défini comme suit :

$h(\tau,t)$ = réponse mesurée à l'instant $t + \tau$ à une impulsion de type Dirac émise à l'instant t.

Par convention, nous considérons $h(\tau,t)$ comme étant la réponse impulsionnelle du canal. La raison du choix de cette fonction est, d'une part son accessibilité relativement aisée à la mesure, comme nous le verrons par la suite, et d'autre part, sa bonne adaptation à des fins de simulation du canal.

Un modèle mathématique du canal ionosphérique peut alors être établi en formulant une expression analytique qui prenne en compte les caractéristiques de propagation énoncées plus haut (cf tableau 1). Cette formulation doit de toute évidence s'appuyer sur la connaissance physique et expérimentale du milieu. Nous n'en fournissons ici qu'une expression générale (LE ROUX et al. 1987) :

$$h(\tau,t) = \Sigma_{i=1}^{n} f_i \left(t, \tau_i, \Delta\tau_i, f_{d_i}, \Delta f_{d_i}, A_i, \varphi_i, \nabla_i \right) \qquad (1)$$

où toutes les grandeurs qui figurent sont définies au tableau 1. De plus, nous exprimons la variabilité du canal dans le temps sous la forme de deux composantes : l'une à caractère déterministe, l'autre à caractère statistique. Chaque paramètre p_i du modèle est donc de la forme :

$$p_i(t) = dp_i(t) + ap_i(t) \qquad (2)$$

La raison de l'introduction d'une composante déterministe $dp_i(t)$ a déjà été indiquée : elle résulte de l'analyse de mesures expérimentales pouvant par ailleurs être interprétées physiquement. Une idée sous-jacente au formalisme (2) est également d'imputer la majeure partie des causes de non stationnarité statistique du canal à la présence de composantes déterministes. La composante aléatoire $ap_i(t)$ est alors susceptible de pouvoir être considérée comme stationnaire au deuxième ordre et se trouver ainsi sous une des hypothèses de validité du modèle de Watterson. On peut en outre noter que le modèle de Watterson est un cas particulier du modèle exprimé par (1) et (2). Il en constitue en fait la partie purement statistique, en y otant toutefois un certain nombre de paramètres et en y supposant une indépendance de comportement entre trajets.

La mise en oeuvre pratique du modèle (1) peut s'effectuer en exploitant la relation d'entrée sortie suivante :

$$s(t) = \int h(\tau,t-\tau).e(t-\tau)\, d\tau$$

Il convient enfin de remarquer qu'il n'y a pas de relation directe par transformation de Fourier entre $h(\tau,t)$ et la fonction de transfert du canal $F(\upsilon,t)$; cette dernière étant définie de façon naturelle par :

$$F(\upsilon,t) = \frac{\text{Réponse du système à } e^{2\pi j \upsilon t}}{e^{2\pi j \upsilon t}}$$

III. L'ANALYSEUR DE LIAISONS

1. Principe général des mesures :

Un moyen de disposer d'une représentation réaliste du canal ionosphérique est de procéder à la mesure de sa réponse impulsionnelle. Cependant, les séquences de réponses impulsionnelles contiennent une grande quantité d'informations qu'il est parfois difficile d'interpréter directement. Il est donc souhaitable de pouvoir mesurer simultanément quelques paramètres essentiels de la propagation. Il s'agit par exemple de (cf tableau 1) : n, τ, A et f_d (ou mieux, la phase instantanée des signaux reçus).

Les techniques de mesure de la réponse impulsionnelle et des paramètres principaux de la propagation doivent être adaptées, d'une part à la dispersion temporelle du canal, et d'autre part à sa variabilité en temps. Ainsi une méthode de réception par intercorrélation du signal reçu avec une copie du signal émis ne peut en toute rigueur convenir. Elle pourra cependant être considérée comme satisfaisante lorsque le rythme de variation du canal est suffisamment faible devant la durée de corrélation. C'est l'hypothèse qui a été faite pour des liaisons situées aux moyennes latitudes. Une technique de mesure adaptée à une grande variabilité du canal a toutefois été mise au point pour une utilisation future sous d'autres latitudes. De même, la non stationnarité du canal sur de courtes durées doit conduire à éliminer dans la majeure partie des cas, une analyse spectrale par transformation de Fourier. Il apparait en effet que des durées d'intégration de 10 à 20 s ne doivent pas être dépassées lors d'une mesure fréquentielle portant sur les évolutions du canal ; ceci sous peine d'une interprétation erronée des résultats..! Des techniques d'analyse spectrale non linéaire, du type "Maximum d'entropie" ont donc été retenues pour l'analyseur de liaisons. Elles préservent en effet une bonne résolution en fréquence pour de faibles temps d'intégration.

2. Le système de mesure

L'analyseur de liaisons est composé de deux parties distinctes :

- l'ensemble d'émission comportant l'amplificateur de puissance (600 W), la gestion et la génération des signaux transmis, ainsi que les aériens d'émission (antenne large bande type V inversé et antennes accordées)

- l'ensemble de réception comportant les aériens de réception (types Delta et fouets actifs), le récepteur HF et toutes les tâches de traitement en temps réel de l'information.

Les caractéristiques d'émission et celles leur correspondant en réception sont totalement programmables à l'aide de terminaux alphanumériques. Ainsi, le choix de la fréquence d'émission, l'heure de début et la durée d'une analyse, le type de modulation et la séquence de codage transmis, de même que tous les paramètres des traitements de réception peuvent être présélectionnés pour un fonctionnement

totalement automatique du système. La synchronisation des deux sous ensembles d'émission-réception est assurée par des étalons de fréquence au Rubidium.

Le schéma bloc de la partie réception de l'analyseur de liaisons est fourni par la figure 1. La période minimale de réactualisation des mesures de réponses impulsionnelles est de 10.2 ms. Elles sont obtenues dans une bande de 10 KHz. Les autres paramètres de propagation sont mesurés dans une bande d'environ 50 KHz avec une période minimale de réactualisation de 160 ms pour les temps de groupe, les atténuations, les phases instantanées,et les niveaux moyens de bruit. Pour les analyses spectrales de type non linéaire, la durée d'intégration minimale est de 10 s. La dynamique utile des mesures est d'environ 30 dB.

La durée d'une analyse est fonction de la quantité d'information enregistrée, compte tenu de la mémoire de masse utilisée : bande magnétique de 180 Mbytes. Ainsi, lorsque les périodes de réactualisation minimales sont choisies et que toute l'information disponible est enregistrée, cette durée est de 24 mn environ. A l'opposé, si aucune réponse impulsionnelle n'est enregistrée et que l'on ne conserve que les divers paramètres de propagation, l'analyse du canal peut se poursuivre durant 48 h environ. Tous les choix intermédiaires sont possibles : enregistrement d'une réponse impulsionnelle parmi N par exemple.

Un autre mode de fonctionnement de l'analyseur de liaisons est actuellement opérationnel. Il offre la possibilité d'une réception au choix sur 1, 2, 3 ou 4 antennes. Dans ce mode de fonctionnement, la réception s'effectue par scrutation cyclique des antennes retenues. La durée minimale de scrutation d'une antenne est d'environ 30 ms.

Enfin, sur le site de réception un controle permanent de l'état du canal peut être effectué par l'opérateur. Il dispose pour cela de la visualisation en temps réel sur une console graphique de la réponse impulsionnelle complexe du canal et de l'affichage sur terminal alphanumérique de tous les paramètres de propagation mesurés.

IV. RESULTATS EXPERIMENTAUX

Parmi les nombreux résultats obtenus avec l'analyseur de liaisons entre St Santin et Lannion, nous proposons trois échantillons illustrant les performances du système de mesure et le caractère fortement non stationnaire du canal ionosphérique. L'interprétation géophysique des mesures portant sur les temps de groupe résulte de l'exploitation des ionogrammes verticaux de Poitiers (point milieu de la liaison) et de ceux de Lannion. Leur transformation en ionogrammes obliques s'effectue selon le théorème de Martyn, en supposant une terre sphérique et une ionosphère courbe (Davies, 1965). Un exemple de transformation est fourni par la figure 5. L'opération consiste en une saisie de l'ionogramme vertical sur une tablette à digitaliser (caractère *) puis en une représentation en trait continu des modes "o" et "x" de la propagation oblique équivalente. La fréquence d'utilisation de la liaison est visualisée par un trait pointillé vertical.

Les figures concernant les trois premiers échantillons de mesure présentent l'évolution au cours du temps des paramètres suivants :

- temps de groupes (sans notion d'amplitude pour éviter un masquage d'information par effet de perspective), fig. 2a, 3a et 4a.

- amplitudes et temps de groupe, fig. 2b et 3b.

- décalages fréquence Doppler (obtenus chacun sur 20 s d'intégration) et temps de groupe, fig 2c et 3c.

1. Premier échantillon

La période d'observation est située bien après le lever du soleil, le 16.06.1988 et la fréquence de transmission est de 7.83 MHz. Les trajets qui peuvent être identifiés sur la figure 2a sont :

- A 2.22 ms, le mode extraordinaire par la couche E (1Ex).

- A 2.31 ms - 2.36 ms, nature des trajets plus délicate à déterminer. Il s'agit probablement du mode 1 E_o, et du bond par la couche E sporadique.

- Vers 2.60 ms, le mode extraordinaire par la couche F_1.

- Au dessus de 3.00 ms, le mode extraordinaire par la couche F_2 et une réflexion du même type mais selon le rayon haut ou rayon de Pedersen. Vers 8 h 05, les deux rayons se confondent en un point correspondant à la fréquence maximale utilisable (MUF) sur le trajet.

L'observation de la figure 2b indique un fort niveau d'amplitude moyenne pour la réflexion $1E_x$ avec des évanouissements peu profonds. Le niveau reçu via le mode $1F_{1x}$ est par contre plus faible, allant jusqu'à une extinction totale du mode. On peut également remarquer une certaine corrélation entre les niveaux reçus par les modes $1F_{2x}$ haut et bas, du moins jusqu'à 8 h 05. Un accroissement maximal de l'ionisation est visible vers 8 h 30 sur la couche F2. Plusieurs minutes après son établissement, l'amplitude du rayon haut devient de plus en plus faible permettant de confirmer l'idée généralement admise que les rayons hauts sont plus atténués que les rayons bas.

La figure 2c confirme la stabilité dans le temps des modes propagés par E et F_1, puisque les décalages doppler qui leurs sont associés sont très faibles. La grande dynamique constatée sur les rayons bas et hauts propagés par la couche F_2 est également traduite par la présence de décalages fréquence Doppler importants (jusqu'à -1 Hz) et évoluant rapidement au cours du temps. On peut ici encore noter une certaine dépendance d'évolution entre les trajets haut et bas.

2. Deuxième échantillon

Recueilli le 10.06.1988, cet échantillon fait suite à une légère agitation magnétique ($K \approx 5$). La fréquence de transmission est de 8.24 MHz. De même que pour le premier échantillon, les divers trajets de propagation identifiés sont indiqués sur la figure 3a. L'interprétation de cet échantillon est toutefois rendue plus délicate par l'absence d'écho signalant la naissance des rayons hauts des modes "o" et "x" de la couche F_2 alors que l'on observe très bien leur disparition. Cet échantillon met, lui aussi, en évidence la grande variabilité en temps des retards de groupe, et des amplitudes des divers trajets détectés. Les décalages en fréquence Doppler (cf fig 3c) présentent des fluctuations importantes au cours du temps et des évolutions de type quasi-périodique peuvent être discernées.

3. Troisième échantillon

Cette période d'observation fait suite à celle du 2ième échantillon. Elle couvre 25 heures d'analyse continue du canal. Les trajets identifiés sont indiqués sur la figure 4. Cet échantillon est présenté pour situer les différents modes de propagation en fonction de l'heure de la journée (nuit/jour) et pour illustrer la variabilité du retard de groupe par la région F_2, une fois que ce mode établi. Dans la première période entre 18 h et 22 h 30, on peut facilement isoler les échos $1F_x$ et $1F_o$ et conclure que cette transition horaire n'est pas brutale. Vers 23 h, l'ionisation de la région F_2 diminue rapidement et n'est plus suffisante pour assurer la propagation. Les nombreux échos retenus vers 3 h-4h peuvent provenir de l'algorithme de traitement et non de mécanismes de diffusion. Il faut attendre 5 h, soit quelques heures après le lever du Soleil, pour voir réapparaitre la réflexion $1F_x$ et 6 h 15 pour la réflexion $1F_o$. La forme d'évolution alors obtenue est différente et plus simple que celle observée lors de la journée précédente (cf. fig.3 a). A partir de 09 h 00, la densité de la couche F_2 se stabilise et l'observation de ses évolutions temporelles au cours de la journée suggère deux remarques. La première concerne la séparation entre les modes o et x qui est comprise entre 0 et 0.1 ms. Cette plage de variation est confirmée par les ionogrammes verticaux de Poitiers qui situent la zone de réflexion proche de la base de la région F_2, c'est à dire vers 300-320 km de hauteur virtuelle. La deuxième observation concerne la variabilité du retard qui présente plusieurs oscillations de 0.1 à 0.3 ms avec une période inférieure à une heure. Cette fluctuation est liée au mouvement de la couche F_2 ainsi que le montre la figure 6 où l'on a reproduit le retard mesuré avec les deux paramètres foF_2 et $h'F_2$ à Poitiers.

L'élévation importante de la couche F_2 à 12 h est fortement corrélée avec un saut sur le retard de groupe de 0.5 ms environ. Les bonds multiples sont présents, en particulier $2F_x$ avec un retard supérieur à 5 ms et une plus grande variabilité (≈ 1 ms) que le 1F. Ceci peut être attribué à l'altitude de réflexion, plus élevée et donc moins stable qu'à la base de la couche. La séparation o,x est moins nette car le mode o n'est pas systématiquement assuré en raison du niveau d'ionisation.

Enfin, après 17 heures, tandis que la densité de la couche F_2 augmente, et que la hauteur virtuelle diminue (cf. figure 6), on observe simultanément les trois premiers bonds de la région F_2. Les modes o et x sont alors distincts pour $2F_2$ et $3F_2$. On constate donc que 6 à 7 rayons séparables en temps par l'analyseur de liaisons déterminent le niveau de champ reçu à Lannion, chacun avec un angle d'arrivée différent.

V - CONCLUSION

L'amélioration de la qualité et de la fiabilité des communications dans la gamme décamétrique passe par une bonne caractérisation expérimentale du canal de transmission ionosphérique. Cette caractérisation peut être présentée soit sous forme de modèles, soit sous forme de séquences de réponses impulsionnelles du canal. Pour y parvenir, un analyseur de liaisons HF a été développé au CNET. Les techniques qu'il utilise pour le traitement de l'information doivent être adaptées au comportement non stationnaire de la propagation ionosphérique. Cette grande variabilité en temps du canal est clairement mise en évidence par les quelques résultats qui ont été présentés. En conséquence, un modèle de canal mieux représentatif que les modèles existants a été décrit. Il est actuellement en cours de validation expérimentale. Pour contribuer a la construction de ce modèle, une interprétation géophysique des résultats est nécessaire. Elle est effectuée à l'aide d'ionogrammes verticaux obtenus au point milieu de la liaison. Cependant, la méthode de tracé de rayons utilisée dans le cas présent est un peu sommaire du fait d'approximations. L'utilisation d'un seul profil ionosphérique tous les quarts d'heures, en un seul point du trajet est également insuffisante du fait de la variabilité temporelle du canal. De plus, la présence de gradients fait apparaître ou disparaître des modes de propagation. Elle modifie ceux déjà existants et rend ainsi l'interprétation géophysique parfois difficile. Il faut rappeler que la trajectoire est relativement courte et que des mesures sur des distances plus longues voire des latitudes différentes ne feront certainement qu'augmenter le degré de complexité de l'interprétation. En conclusion, nous mettons l'accent sur le caractère performant de l'analyseur de liaisons dont les mesures doivent permettre une meilleure représentation du canal de transmission ionosphérique mais aussi un approfondissement des connaissances géophysiques sur le milieu.

REMERCIEMENTS

Nous remercions les responsables des stations ionosphériques de Poitiers et Lannion pour la fourniture des ionogrammes verticaux.

BIBLIOGRAPHIE

C.C.I.R., 1978, Simulateurs de voies ionosphériques en ondes décamétriques, rapport 549-1.

DAVIES, K., 1965, "Ionospheric Radio Propagation", National Bureau of Standards Monograph 80.

KAILATH, T., 1961, "Channel characterization : time-variant dispersive channels", Communication System Theory edited by Baghdady, Chap.6, Mc graw-Hill Book Company.

LE ROUX, Y.M., G. SAVIDAN, G. DU CHAFFAUT, P. GOURVEZ, J.P. JOLIVET, 1987, "A combined evaluation and simulation system of the HF channel", ICAP87, 171-175.

WAGNER, L.S., J.A. GOLDSTEIN, W.D. MEYERS, 1987, "Wideband probing of the trans-auroral HF channel", IEEE MILCOM87, article 43.

WATTERSON, C.C., J.R. JUROSHEK, W.D. BENSEMA, 1970, "Experimental confirmation of an ionospheric HF channel model", IEEE Trans. on Commun Technol., COM-18, 792-803.

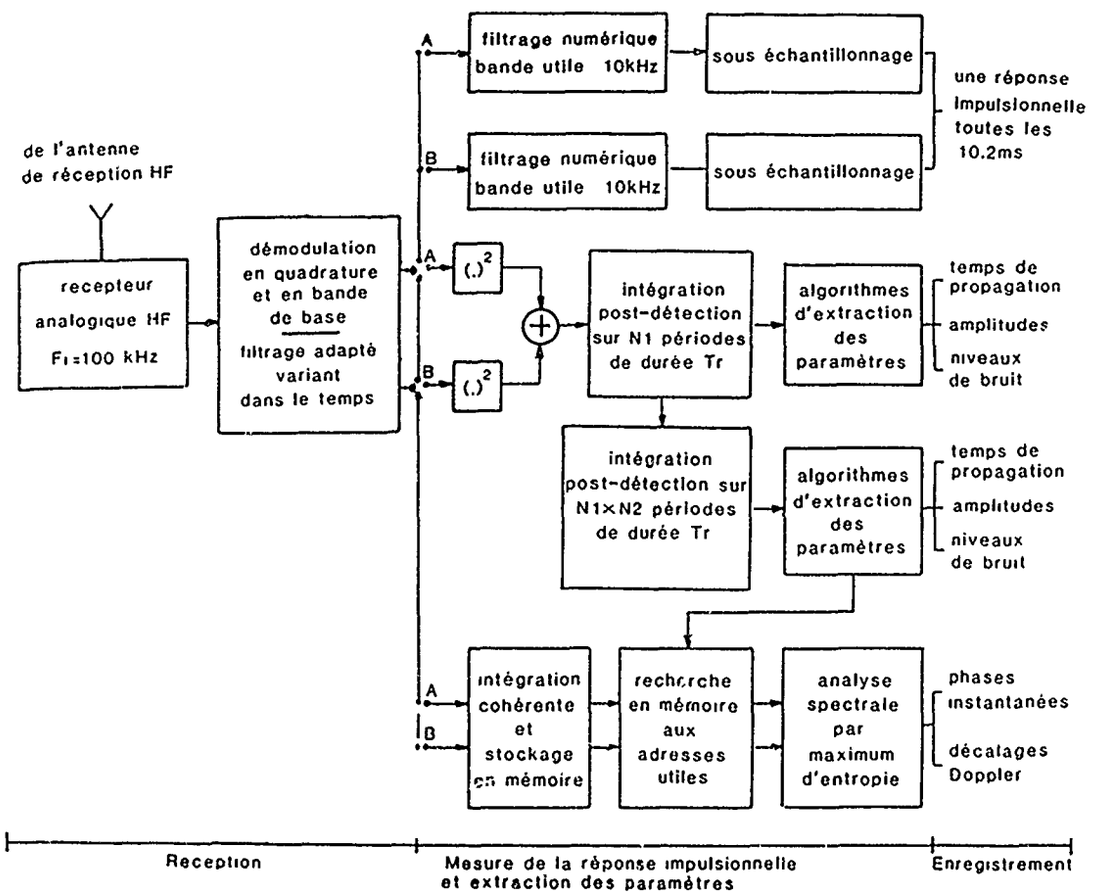

Figure 1. Schéma bloc de la partie réception de l'analyseur de liaisons.

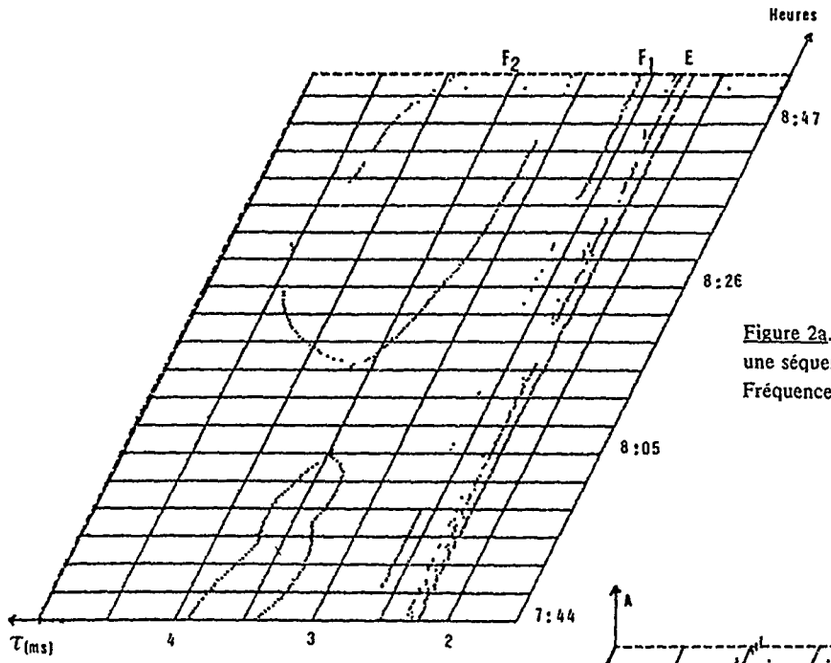

Figure 2a. Evolution du temps de groupe pour une séquence d'observation le 16 Juin 1988. Fréquence = 7.83 MHz.

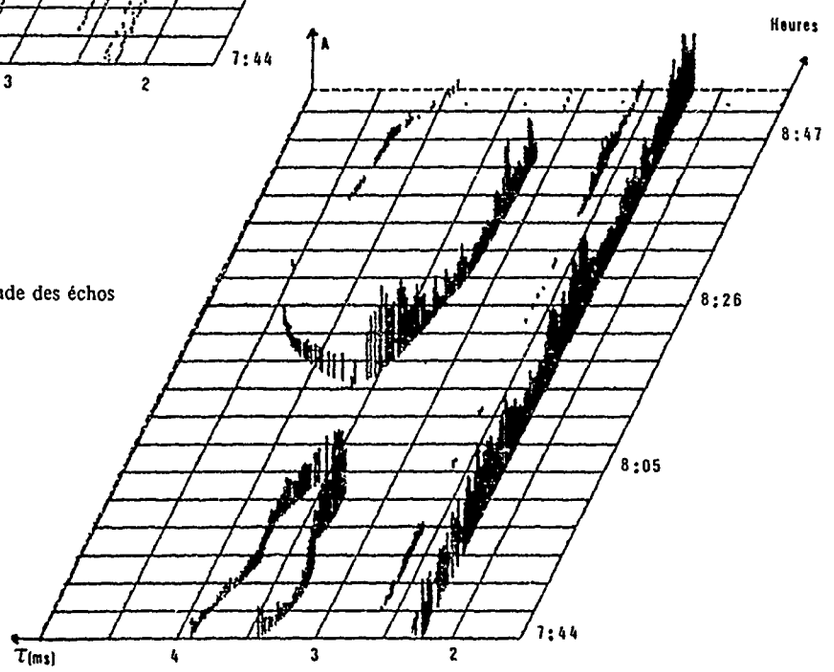

Figure 2b. Evolution de l'amplitude des échos pour la même séquence.

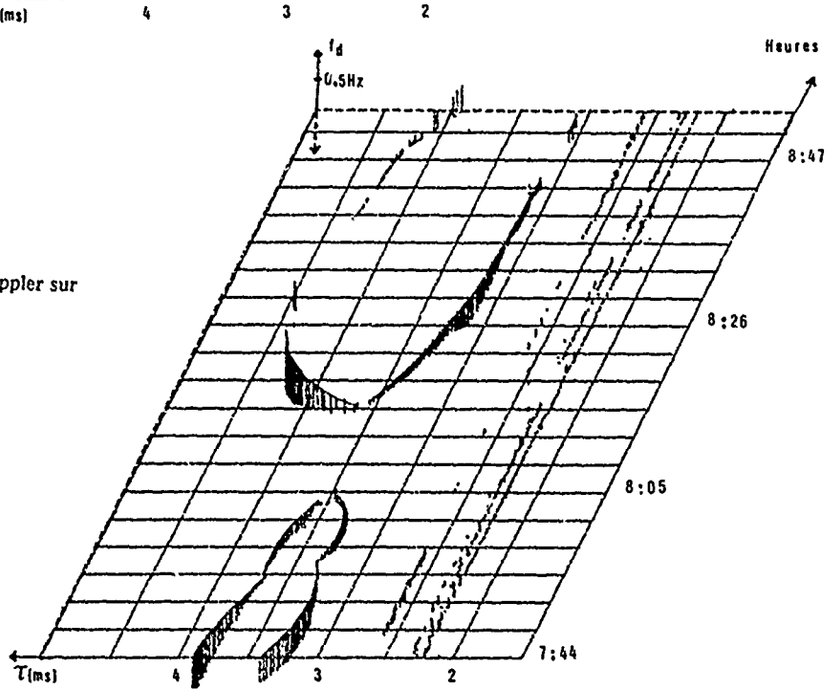

Figure 2c. Evolution du décalage Doppler sur la même période.

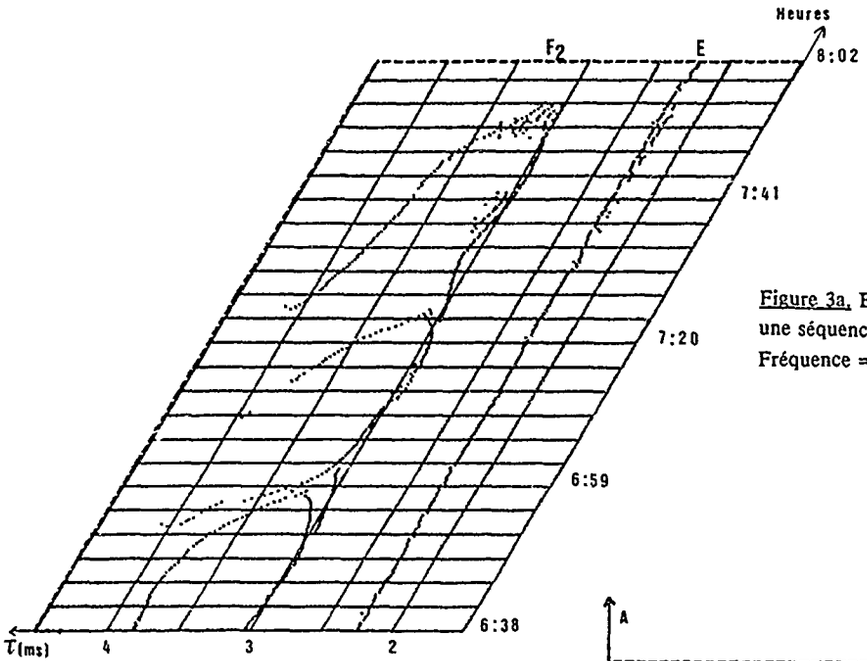

Figure 3a. Evolution du temps de groupe pour une séquence d'observation le 10 Juin 1988. Fréquence = 8.24 MHz.

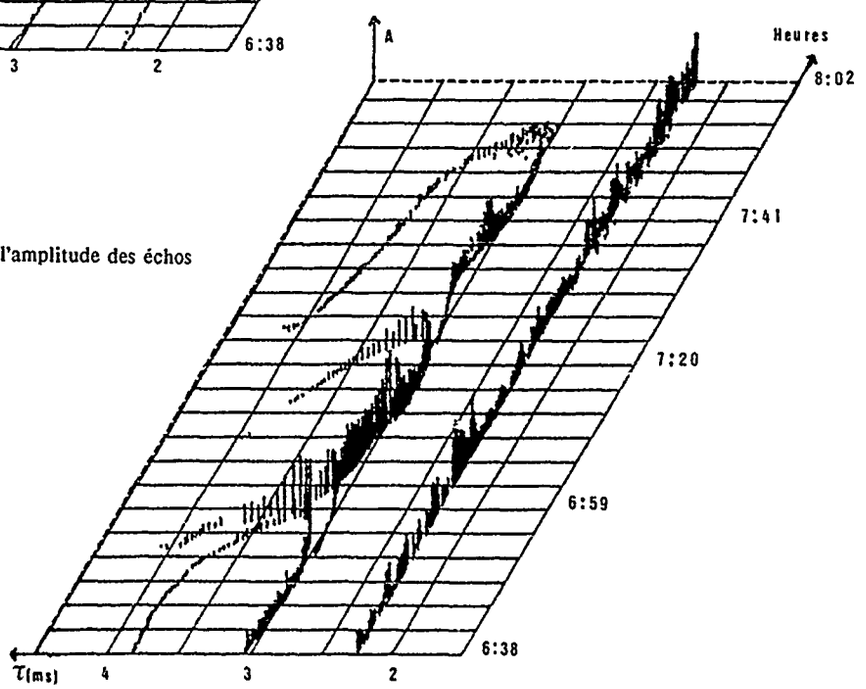

Figure 3b. Evolution de l'amplitude des échos pour la même séquence.

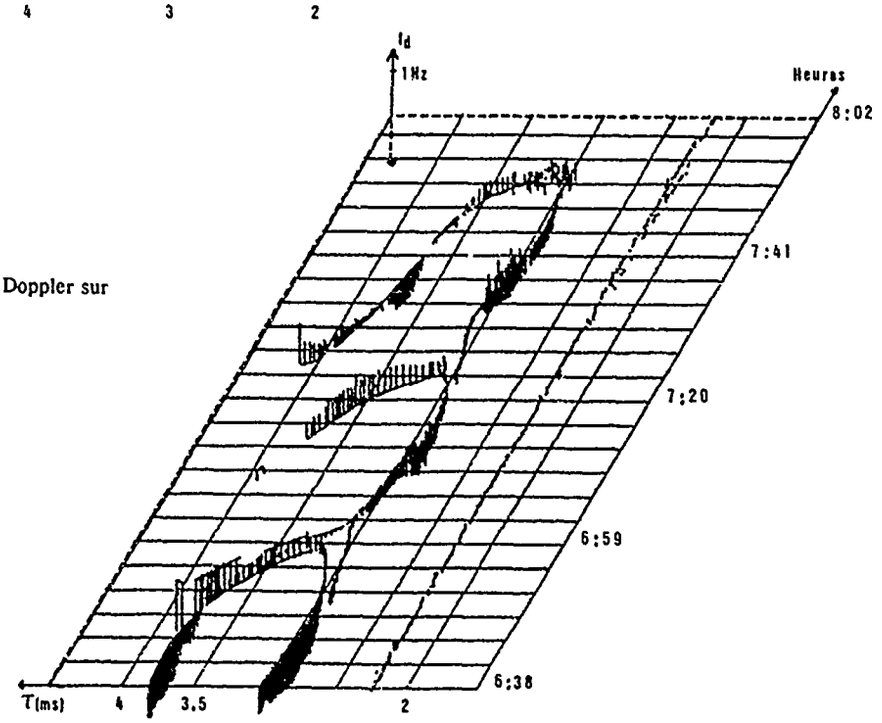

Figure 3c. Evolution du décalage Doppler sur la même période.

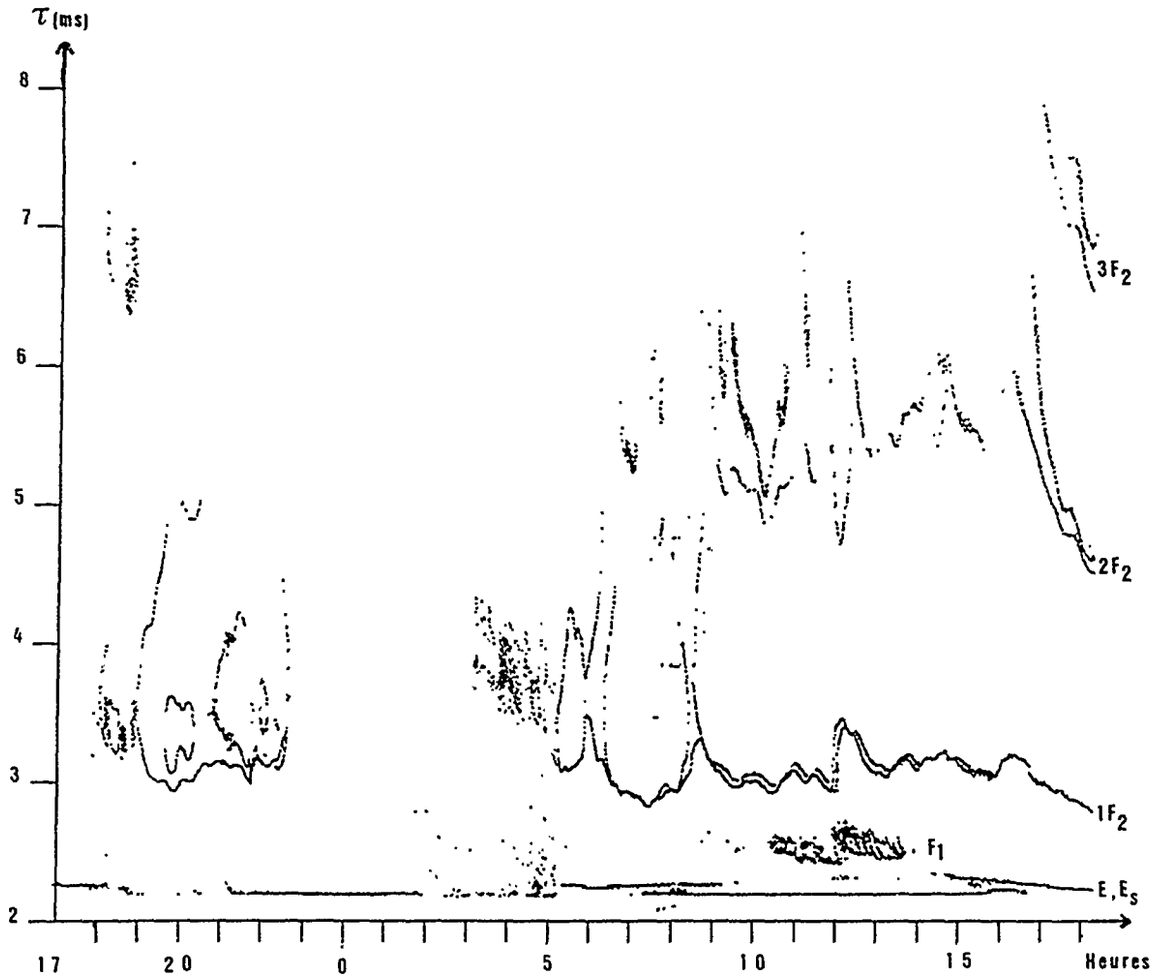

Figure 4. Evolution du temps de groupe sur une période du 10 au 11 Juin 1988. f=8.23 MHz.

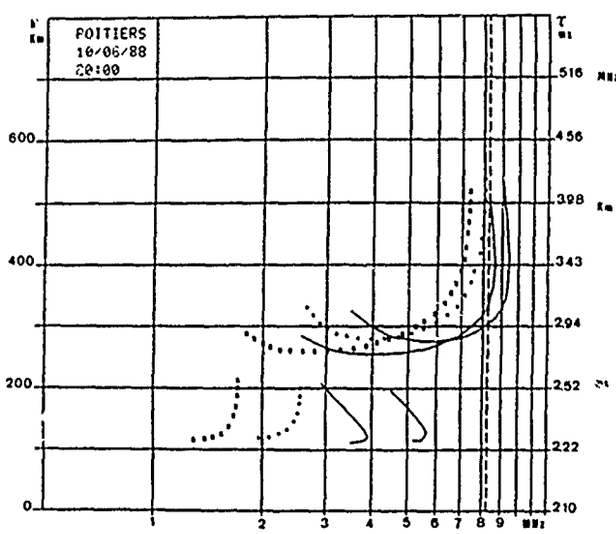

Figure 5. Ionogramme vertical de Poitiers (* et +) et ionogramme oblique équivalent (trait continu) entre St. Santin et Lannion.

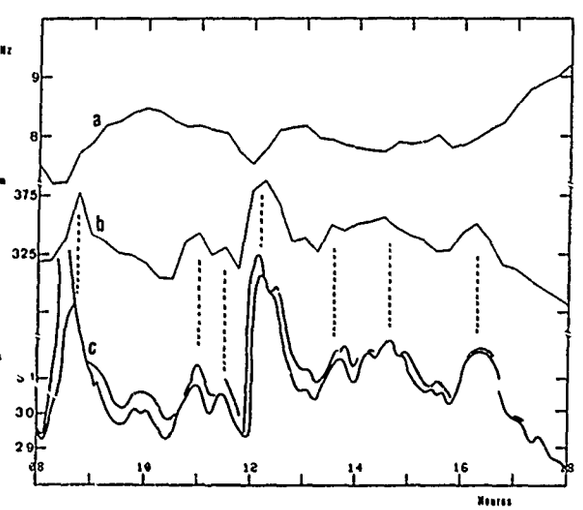

Figure 6. Lors de la journée du 11 Juin 1988 :
(a) foF2 quadri-horaires à Poitiers,
(b) h'F2 quadri-horaires à Poitiers,
(c) temps de groupe en ms pour le bond 1F2 entre St. Santin et Lannion.

PROGRESS AND REMAINING ISSUES IN THE DEVELOPMENT OF A WIDEBAND HF CHANNEL MODEL AND SIMULATOR

L. Vogler, J. Hoffmeyer, J. Lemmon, and M. Nesenbergs

U.S. Department of Commerce
National Telecommunications and Information Administration
Institute for Telecommunication Sciences
Boulder, CO 80303
US

SUMMARY

Although high frequency (HF) communication systems have been used for many decades, these systems are currently the subject of renewed interest, particularly in assessing the capabilities of the HF channel with regard to wideband (of the order of 12-1000 kHz) signals. This interest has generated a need for wideband HF channel propagation measurements and the development of wideband channel models and simulators.

This paper provides a brief review of recent work in wideband HF, discusses some limitations of existing HF channel models, describes on-going work at the Institute for Telecommunication Sciences in the development of a validated wideband HF channel model, and concludes with a discussion of key technical issues remaining in the development of this model.

1. INTRODUCTION

Most high frequency (HF) ionospheric systems have traditionally had bandwidths of a few kilohertz or less. The feasibility of HF systems with bandwidths of the order of 100 kHz to 1 MHz has been investigated in a number of recent studies [1-14]. The HF Azimuth Diversity Propagation Experiment conducted by the U.S. Air Force Rome Air Development Center has resulted in a large data base of propagation data for polar ionospheric paths [15]. Experimental data are also reported by Basler [16] on disturbed skywave HF paths including polar, auroral, and equatorial regions. As can be seen from these references, several different NATO countries are currently conducting research in the field of wideband HF. The application of state-of-the-art digital technology to HF communications systems makes new capabilities feasible, and in particular, the use of spread-spectrum technology for both HF communications and over-the-horizon radar systems is of interest.

For communication systems, the advantages of spread-spectrum technology are well known. These advantages include low-probability-of-intercept (LPI) communications, interference rejection, simultaneous operation of several transmitters in the same frequency band, and resolution of multipath skywave returns. For HF radar systems, the use of wideband spread-spectrum signals results in improved range resolution. Thus, both applications require the use of the widest possible bandwidth for a given path, time of day, season, sunspot number, etc.

We need to be able to evaluate the performance of prototype wideband HF systems. Such performance evaluation can best be attained through the use of channel simulation. The advantages of channel simulators for the testing of communication systems are well known [17, 18]. The advantages include accuracy, repeatability, stationarity, availability, parameter variation, and cost. Thus, a wideband HF channel model that has been validated by wideband channel measurements is needed.

Figure 1 depicts the interrelationship between the required measurements, the wideband high frequency (WBHF) models, and both hardware and software implementations of those models. The parts of the WBHF modeling process are: the propagation model or channel transfer function, and the noise and interference models. All parts of the WBHF modeling process will be discussed in this paper. The models can be implemented in either software or hardware. Software implementations of the models are useful during the system design phase of, for example, a wideband HF modem. If the HF system as well as the WBHF models are implemented in a software simulator, the theoretical performance of various modem designs can be evaluated. Hardware implementations of the models are useful in the performance testing of the complete HF system hardware. A logical sequence of events would be the use of a software simulator during the design phase of a wideband HF system and a hardware simulator to evaluate the performance after the chosen design had been implemented into hardware.

2. BACKGROUND

Research programs in wideband HF have followed four parallel but strongly interconnected paths:

- development and field testing of experimental wideband communication systems
- channel noise and interference measurement and modeling programs
- wideband channel propagation measurement programs
- channel modeling programs

Clearly, the channel modeling programs depend on the availability of wideband channel propagation measurements to ensure the validity of the model. However, they are treated in this section as

independent programs, because often the propagation measurement programs may not have the development of a validated channel model as their primary objective. Rather, the channel propagation measurement programs tend to be oriented toward an enhanced understanding of the ionosphere. The tight coupling of the wideband channel measurement and modeling efforts will be discussed in Section 6.

2.1 Wideband Communication System Experimentation

Early interest in the feasibility of wideband HF was reported by Belknap et al., in 1968 [19]. This early work addressed the problem of automatic compensation for ionospheric distortions that result from dispersion, multipath, and Faraday rotation. Analysis of data collected on an HF link from Lubbock, TX to Stanford, CA showed the feasibility of equalization of the channel. However, real-time channel equalization awaited the advent of LSI technology more than a decade later [2].

The status of wideband communication programs being conducted by the Mitre Corporation is summarized by Perry et al. [1]. Important questions being investigated include adaptive equalization for wideband HF and the effect of interference excision on system performance [1-4]. The programs described in these papers do not appear to have the level of data collection needed for wideband propagation modeling as their primary objective and will therefore not be addressed further in this paper.

2.2 Channel Noise and Interference Measurement and Modeling Programs

The modeling and simulation of wideband HF noise and interference is an important part of the process of performance evaluation of wideband HF systems. A number of HF interference measurement and modeling programs in several NATO countries have been reported in the recent literature [20-27]. The measurements have resulted in the development of channel occupancy models. The applicability of these models to wideband HF simulation will be discussed in Section 7.

2.3 Wideband Channel Propagation Measurement Programs

Numerous wideband HF channel propagation measurement programs are being conducted in the United States, Norway, and the United Kingdom [5-13]. The apparent objectives of these programs are to provide data useful for the understanding of the HF channel and for the eventual development of spread-spectrum HF systems. These data are also critically needed for the development of a validated wideband HF channel model. The channel probe described by Wagner et al. [5] has the highest resolution of any of the systems described in references [5-13]. The Institute for Telecommunication Sciences has been provided with wideband HF channel probe data through the courtesy of Dr. Wagner and the U.S. Naval Research Laboratory. The use of these data in the development of a wideband channel model will be described in Section 6.

2.4 Channel Modeling and Simulation Programs

Watterson developed a model of a narrowband channel in the late 1960's [28, 29]. The structure of this model is provided in Figure 2. The mathematical formulation of the model is:

$$H(f,t) = \sum_i c_i(t) \exp(-j2\pi\tau_i f) \qquad (1)$$

where for path i: c_i is a bivariate, complex Gaussian function
τ_i is the constant path delay

The summation in (1) is for a finite number of paths, each of which is assumed to have independent statistics.

The Watterson model has been given by the CCIR [30]. It has been implemented in several different hardware and software simulators [18, 31, 33, 34], and has been used for HF modem testing [18, 32, 33, and 36]. Girault et al. [35] report an extension of the model for software testing of frequency hopping systems.

Although the Watterson model was developed almost 20 years ago, it is still widely used and recognized as being the best model for simulation of the narrowband HF skywave channel. Unfortunately, it appears that with the passage of time limitations on the use of the model are sometimes forgotten. Watterson [28, 29] very clearly explained the procedures he used in the validation of the model and its limitations. Table 1 provides a summary of the data used in the validation of the model. Note that the model has not been proven valid all of the time for channel bandwidths in excess of 2.5 kHz. Furthermore, the model is limited to

- channels having time and frequency stationarity
- channels having negligible delay dispersion (e.g., no spread-F)
- channels having only a low-ray path

LeRoux et al. [37] question the adequacy of the model for a number of important cases (e.g., when the path is nonstationary in time).

The limitations of the Watterson model, particularly in regard to its validated bandwidth, and the recent interest in wide bandwidth HF have provided motivation for researchers in a number of organizations to investigate either extensions to the model or entirely new models [38-41]. Serrat-Fernandez et al. [38] propose a slight modification of the Watterson model in which the Gaussian shape of the Doppler spectrum is replaced by a Butterworth shape. The assumption, valid for narrowband models, that the group delay (τ_i) is not a function of frequency is one area of current interest. Clearly, this assumption does not hold for wideband HF. The methodology for modeling this and other parameters for the wideband case is the target of research [39-41], and the subject of the remainder of this paper.

3. ALTERNATIVE APPROACHES TO WIDEBAND CHANNEL MODELING

The Institute for Telecommunication Sciences has investigated three alternative approaches to the development of a wideband channel model:

- model based on scintillation theory
- Tap Delay Line or Extended Watterson Model (EWM)
- Ionospheric Parameters Model (IPM)

Each of these three approaches will be briefly described in Sections 3.1 through 3.3. The Ionospheric Parameters Model will be discussed in detail in Sections 4 through 6.

3.1 Scintillation Theory

Theoretical understanding of radio-wave propagation in the HF band has been based on a number of models for the ionosphere. Ionospheric models that depict the spatial and temporal variations of the refractive index have evolved through many stages. They include the earliest smooth, unperturbed, stationary, and layered models [42, 43] as well as the more recent irregular, disturbed, turbulent, time variant models [44, 45].

The latest characterization of scintillation theory as applied to HF radio-wave propagation is found in [46-48]. These papers combine lengthy mathematics with many justified and simplifying physical approximations.

To summarize the application of scintillation theory to radio waves in a turbulent ionosphere, the theory starts with assumed properties for an irregular ionosphere mode (i.e., a layer with a given mean square of refractivity index fluctuations and its wavenumber spectrum). For a CW signal, the application of scintillation theory leads to the following quantities:

- the second order characteristics of the received phase fluctuations in time
- estimates of the nominal HF channel correlation bandwidth
- the angle of divergence of the received rays with respect to the direction of arrival
- fading correlation distance at the receiver
- twinkling correlation distance at the receiver
- quasi-period of fading
- quasi-period of twinkling

In the above list, the term "twinkling" deserves a comment. Following the terminology of Booker et al. [46, 48], fading and twinkling can be viewed as two separate facets of signal scintillation. Twinkling is a slow modulation of the typically much faster fading of the signal. Theoretically estimated twinkling periods range from a few minutes to an hour, while those of fading range from a fraction of a second to several minutes.

Real data are needed for the wideband HF channel modeling and simulation program. The data confirm how the ionosphere affects wideband signals, while the theory strives to explain and to define a physically and logically acceptable framework. The central role of experimental measurements is depicted in Figure 3. Data resulting from these measurements are needed both for the confirmation of scintillation theory and for the validation of a wideband HF channel model. The direct application of measured wideband HF propagation data to the development of a validated wideband channel model is emphasized by the solid lines. The role of scintillation (as shown by the dashed lines) theory should be to more fully characterize the turbulent ionospheric medium rather than to form the basis for a channel propagation model.

3.2 Tapped Delay Line Model

Let $H(f,t)$ be the time-varying channel transfer function. The customary models for $H(f,t)$, at least for its narrowband version, are those of a tapped delay line. An example is

$$H(f,t) = \sum_i H_i(f,t), \tag{2}$$

where

$$H_i(f,t) = A_i(f)u_i(f,t)\exp[-j2\pi\tau_i(f)f]. \tag{3}$$

Here one assumes

- index i identifies individual multipath modes.
- $A_i(f)$ is a real, nonnegative, amplitude of the i-th mode. It depends on frequency, but not on time.
- $u_i(f,t)$ is a complex, bivariate Caussian, random process with zero mean and statistically independent real and imaginary parts. It depends both on time and frequency.
- $\tau_i(f)$ is the path delay for the i-th mode. It depends on frequency and has been called the dispersion slope.

For narrowband HF, where bandwidths usually do not exceed 3 kHz, it has been justified [29] to replace $A_i(f)$, $u_i(f,t)$, and $\tau_i(f)$ with their constant (frequency insensitive) versions c_i and τ_i, respectively. Since the constant parameter model for narrowband HF has been referred to as the Watterson model, the wideband manifestation of (3) may be viewed as an "extended Watterson model."

A wideband variation of the Watterson model has been used by Malaga [39]. Other variations, also suitable to the wideband case, include the representation

$$H_i(f,t) = A_i(f,t)\exp[-j2\pi\tau_i(f,t)f], \tag{4}$$

as proposed by Barratt and Walton [40]. Note that if $\tau_i(f)$ is identified with the time-average of $\tau_i(f,t)$, and the deviation $\tau_i(f,t)-\tau_i(f)$ is made a separate factor, then this form agrees for all practical purposes with the model defined by (3).

A complete channel model requires numerical values, parameter ranges, and functional dependencies. These can be obtained mainly through channel propagation measurements such as those reported by Wagner [6-9].

One approach to the development of a wideband channel model would be to attempt to fit wideband channel probe data to the proposed wideband channel transfer functions given by (3) or (4). This would result in a channel simulator having the functional structure of a tap delay line as shown in Figure 2. Although this approach is appealing and could possibly be achievable, some difficulties are expected. As noted in Section 2.4, the Watterson model was validated for only a limited set of propagation conditions. One problem is finding a representation for the tap gain multipliers, $c_i(t)$, of (1). Even for a narrowband HF channel, measured propagation data could be fit to a Gaussian distribution only under very limited conditions. At times an adequate fit could be obtained only for a 2.5-kHz bandwidth (see Table 1). Therefore, the likelihood of finding a distribution that would fit the measured data for much wider bandwidths (100 - 1000 kHz) is low. Additionally, the Watterson model was validated only for stationary, stable conditions.

The above limitations provided motivation to seek an entirely new approach to the HF channel model development process. It is desirable that the model be capable of adequately representing the channel for a wide variety of propagation conditions, not just stationary, stable conditions. The modeling approach we have taken is outlined in Section 3.3 and discussed in detail in Sections 4 through 6.

3.3 Ionospheric Parameters Model (IPM)

The Ionospheric Parameters Model, which will be described in more detail in Section 4, is a model that relates the quantities of the transfer function to actual physical parameters of the ionosphere.

In any wideband HF simulation model, the relationship between delay time and frequency is of major importance. The frequency components of a pulse reflected from the ionosphere arrive at the receiver with different delay times, thus causing a distortion of the original pulse shape. For narrow bandwidths (e.g., 3 kHz), the effect of the delays (caused by frequency dispersion) on the shape is negligible. However, there can be considerable effect on signals having bandwidths of the order of 100 kHz or more [6]. If a true impulse could be transmitted, the impulse response would have a very broad shape because of the delays encountered by all the frequencies in the "infinite" bandwidth. An indication of the broadening of the impulse response can be obtained from the examination of a typical ionogram (see figure 5a).

A disadvantage of the Extended Watterson Model approach is the difficulty of getting quantitative estimates for the delay time/frequency relationship. A suggested procedure is to measure the slope of an ionogram trace over the bandwidth of interest. This works as long as there are stable conditions and the noise threshold is fairly constant.

The Ionospheric Parameters Model approach provides an analytic expression for the delay-frequency relation that serves as a long-term median or deterministic base around which statistical variations can be added. The analysis is based on a well-known electron density model and can be related to the physical parameters for each of several ionospheric layers. Thus, it is a variable base applicable to many different seasons and locations and can utilize the extensive information fund already available concerning the deterministic and statistical characterizations of ionospheric parameters.

The use of an analytic expression for the phase was suggested many years ago in a paper by Wetzel [50] in which he assumed a parabolic layer model for the electron density profile. As is well known, the parabolic model provides a fairly realistic description of a stable ionospheric layer; however, the equation relating delay time and frequency requires iterative procedures to evaluate. On the other hand, the corresponding equation derived for the IPM is an explicit expression for the frequency in terms of the delay time. The following section describes the mathematical derivation of the channel transfer function for the IPM.

4. TRANSFER FUNCTION FOR THE IPM

In this section, we show how the IPM transfer function for a single mode is developed to obtain the phase ϕ and delay time ϕ' for vertical incidence. The extension to oblique incidence is then discussed, and the key relationship between frequency and equivalent height $\overline{h}$ is derived.

A symbolic representation of the transfer function $H(\omega,t)$ of an ionospheric reflection channel can be expressed as

$$H(\omega,t) = \sum_i H_i(\omega,t), \tag{5}$$

where $H_i(\omega,t)$ denotes the transfer function of a particular path or mode in the channel, and $\omega = 2\pi f$ is the (angular) frequency. Variation of the ionosphere's physical constituents over time is represented by the symbol t. In most of the following discussion, the derivations refer to a single path or mode, and the subscript i is suppressed.

In the present case, the transfer function is formulated as the summation of reflection coefficients $R(\omega) = H_i(\omega)$, t constant, associated with the different layers of the ionosphere. In general the coefficients depend on electron density, collision frequency, geomagnetic field, and the geometry of the propagation path. If all of these quantities were constant over time for a given channel, then the transfer function and, thus, signal response could be evaluated deterministically because of the stable conditions. However, a model applicable to actual channels requires a statistical description due to time variations of the physical processes. The utility of the model will be enhanced if the deterministic base, around which the statistical variations are applied, can provide "long term" or median values appropriate to a wide variety of propagation conditions. A deterministic base for the wideband model that provides a fairly realistic description of the ionospheric reflection process can be obtained from the following considerations.

For the case of no magnetic field and negligible electron collision frequency, the W.K.B. solutions to Maxwell's equations for the electric field E can be expressed as [43, pp. 133-136]

$$E(z) = A \exp\{\mp jk\textstyle\int_0^z \mu dz\}, \tag{6}$$

where A is a constant, $k = 2\pi f/c$ is the wave number, z is height above ground, and μ denotes the index of refraction of the ionosphere. Under the present assumptions, μ may be given the form

$$\mu = \{1-(f_N/f)^2\}^{1/2}, \tag{7}$$

where f_N, the plasma frequency, is a function of height and ionospheric layer parameters.

The minus and plus signs in (6) correspond to upgoing and downgoing waves, respectively, and if reflection occurs where $\mu = 0$ at the height z_o, then the reflection coefficient R is

$$R(\omega) = \exp\{-j2k\textstyle\int_0^{z_o}\mu dz\} \triangleq e^{-j\phi(\omega)}, \quad \omega = 2\pi f. \tag{8}$$

Thus, by choosing an appropriate function for the plasma frequency, we can obtain a deterministic base for the transfer function of (5) through the relation

$$H_i(\omega, t: \text{constant}) = R_i(\omega). \tag{9}$$

A model that has been used to approximate the electron density profile of a single ionospheric layer is the sech^2 model [43, p. 156]:

$$f_N^2 = f_p^2 \operatorname{sech}^2\{(z_m-z)/2\sigma\}, \tag{10}$$

where f_N^2 is proportional to the electron density and σ is related to the thickness of the layer. The maximum electron density occurs at the height z_m and, thus, f_p denotes the penetration frequency for vertical incidence. By varying the layer height, thickness, and maximum electron density parameters of the sech^2 model, one can approximate a wide variety of single layer configurations. In terms of the refractive index μ, $\phi(\omega)$ and its derivative, $\phi' \triangleq d\phi/d\omega$, become

$$\phi = (2/c)\omega\textstyle\int_0^{z_o}[1-(f_p/f)^2\operatorname{sech}^2\{(z_m-z)/2\sigma\}]^{1/2}dz. \tag{11a}$$

$$\phi' = (2/c)\textstyle\int_0^{z_o}[1-(f_p/f)^2\operatorname{sech}^2\{(z_m-z)/2\sigma\}]^{-1/2}dz. \tag{11b}$$

The integrals in (11a, b) are known respectively as the phase height h(f) and equivalent (or virtual) height $\bar{h}(f)$ of reflection. (The usual notation for equivalent height is h', but we here reserve the prime to denote differentiation). Both integrals are expressible in closed form through the change of variable

$$\sinh\{(z_m-z)/2\sigma\} = C_o \cosh x, \quad C_o^2 \triangleq (f_p/f)^2-1, \tag{12}$$

resulting in

$$\bar{h}(f) = 2\sigma x_1, \quad x_1 = \cosh^{-1}\{\sinh(z_m/2\sigma)/C_o\}, \tag{13a}$$

$$h(f) = 2\sigma[x_1-(f_p/f)\tanh^{-1}\{(f/f_p)\tanh x_1\}]. \tag{13b}$$

If we impose the conditions $h_o \triangleq z_m >> 2\sigma$ and $\bar{h}(f) >> 2\sigma$, then the heights of (13) approximate to

$$\bar{h}(f) = h_o-\sigma\ln\{(f_p/f)^2-1\}, \tag{14a}$$

$$h(f) = \bar{h}(f)-\sigma(f_p/f)\ln\{(f_p+f)/(f_p-f)\}, \tag{14b}$$

where use has been made of the relationships between inverse hyperbolic functions and the logarithm. Thus, explicit expressions for (11) are given by:

$$\phi(\omega) = \omega t_o-\alpha[\omega\ln\{(\omega_p/\omega)^2-1\}+\omega_p\ln\{(\omega_p+\omega)/(\omega_p-\omega)\}], \tag{15a}$$
(vertical incidence)

$$\phi'(\omega) \triangleq d\phi/d\omega = t_o-\alpha\ln\{(\omega_p/\omega)^2-1\}, \tag{15b}$$

$$t_o = 2h_o/c, \quad \alpha = 2\sigma/c. \tag{15c}$$

The above discussion has assumed vertical incidence, with the signal being transmitted and received at the same site. The problem of timing the frequency components of a pulse over an oblique path of distance D between terminals is resolved by applying the theorems of Breit and Tuve and of Martyn [51, pp. 220-226]:

$$\bar{P}(\omega) = D/\sin\theta_I, \text{ (Breit and Tuve)} \tag{16a}$$

$$\bar{h}(\omega) = \bar{h}(\omega_v) = \bar{h}, \text{ (Martyn)} \tag{16b}$$

$$\omega = \omega_v \sec\theta_I = \omega_v\{1+(D/2\bar{h})^2\}^{1/2}, \tag{16c}$$

where θ_I is the incidence angle of the ray (for vertical incidence, $\theta_I = 0$), and $\bar{P}(\omega)$ is the equivalent path for the ω component, i.e., the distance from the transmitter to the reflection height $\bar{h}$ and back to the receiver. The notation ω_v refers to the frequency associated with vertical incidence.

From (14a) the relationship between ω_v and $\bar{h}$ is seen to be

$$\omega_v = \omega_p[1+\exp\{(h_o-\bar{h})/\sigma\}]^{-1/2}, \tag{17}$$

and from (16c) it follows that

$$\omega = \omega_p\{1+(D/2\bar{h})^2\}^{1/2}[1+\exp\{(h_o-\bar{h})/\sigma\}]^{-1/2}. \tag{18}$$

Thus, if for notational convenience, we introduce the functions

$$\nu = \nu(\bar{h}) = 1+(D/2\bar{h})^2, \quad \delta = \delta(\bar{h}) = 1+\exp\{(h_o-\bar{h})/\sigma\}, \tag{19}$$

then the travel time over the oblique path of that component of the signal with angular frequency ω is given by:

$$\bar{P}(\omega)/c = (2/c)\bar{h}\sec\theta_I = (2\bar{h}/c)(\nu)^{1/2}, \tag{20}$$

and the relationship between ω and the equivalent height $\bar{h}$ is

$$\omega = \omega_p\{\nu/\delta\}^{1/2}. \tag{21}$$

The reflected travel time is associated with the first derivative of the phase in the reflection coefficient (8):

$$\phi'(\omega) = d\phi/d\omega = \bar{P}(\omega)/c = (2\bar{h}/c)(\nu)^{1/2}, \tag{22}$$

and, in fact, (22) reduces correctly to (15b) in the case of vertical incidence (D = 0). In the general case of oblique incidence, the phase function,

$$\phi(\omega) = \int\phi'(\omega)d\omega, \tag{23}$$

must either be evaluated numerically or approximated by simpler functions, the latter alternative being used in the present computer implementation of the simulation model. Because of space limitations, the specific equations cannot be given here but can be found in [52].

Equations (21) - (23) for ω, ϕ', and ϕ can be used to compute a deterministic base for each term of the transfer function (5) by setting $H_i(\omega) = R_i(\omega)$ as in (9). It is important to notice that the statistical variations with time of the physical parameters h_o, σ, and f_p provide the t dependence of the channel transfer function.

5. PULSE RESPONSE FOR THE IPM

For a received signal $E_r(\tau)$ normalized by a constant amplitude E_o, the pulse response for the attenuation $A(\tau)$ may be written as

$$E_r(\tau)/E_o = A(\tau) = (1/2\pi)\int_{-\infty}^{+\infty}S_T(\omega)H(\omega)S_R(\omega)e^{j\omega\tau}d\omega, \tag{24}$$

where $S_T(\omega)$, $S_R(\omega)$ denote the source and receiver frequency responses and $H(\omega)$ is the channel transfer function. In order to test the adequacy of a model for the transfer function, it is desirable to compare the predicted pulse response from (24) with actual measurements. Most pulse sounders measure only the group delay of a propagating mode, resulting in the usual ionogram trace of time delay versus frequency. The recently developed NRL Channel Prober [5-9] measures group delay, amplitude, and delay dispersion for wideband or narrow-band pulses and for either vertical or oblique incidence. Thus, results from this instrument can be used to investigate the usefulness of a proposed model.

It is not possible in general to represent the integral of (24) in closed form, and some type of approximation is necessary. Numerical integration, using a Fast Fourier Transform, is usually adequate if one is restricted to lower frequency components, but this becomes unwieldy at higher frequencies. The most satisfactory solution, at least for a model based on a sech^2 electron density profile [53] is the method of stationary phase. This approach takes advantage of the fact that the major contribution to the integral occurs near those frequencies where the first derivative of the phase of the integral equals zero [54, pp. 139-141]. When applied to (24), the result is

$$A(\tau) = \sum_{\omega_o}F(\omega_o)\left|2\pi\phi''(\omega_o)\right|^{-1/2}e^{j\{\phi(\omega_o)-\omega_o\phi'(\omega_o)\pm\pi/4\}}, \tag{25}$$

$$\text{where } F(\omega) = \left|S_T(\omega)H(\omega)S_R(\omega)\right|, \tag{26a}$$

$$\Phi(\omega) = \arg S_T(\omega)+\arg H(\omega)+\arg S_R(\omega), \tag{26b}$$

$$\Phi'(\omega_o)+\tau = 0, \tag{26c}$$

and the primes denote differentiation with respect to ω. The summation is over all values of ω_o that satisfy (26c).

The stationary phase method yields a good approximation to the pulse response as long as $F(\omega)$ is not oscillatory near the roots $\omega = \omega_o$. For the comparison examples presented here, $|H(\omega)|$ is nearly constant over the whole frequency range of interest. The receiver frequency response is assumed to be ideal in the sense that its only effect is to place a constant valued "ceiling" and "floor" on the received signal amplitude. The source pulse is taken to be Gaussian shaped with an arbitrarily chosen pulse width and center frequency. Other source and receiver responses may be assumed, of course, but their numerical behavior must follow the above qualifications if (25) is to be used.

A display of the pulse response can be shown in a three-dimensional format equivalent to the NRL Channel Prober outputs in Wagner and Goldstein [6]. The amplitude is plotted versus time delay and center frequency of the source pulse resulting in a three-dimensional ionogram. The receiver threshold and AGC are simulated by the receiver "floor" and "ceiling" mentioned above, and the threshold level that is chosen can affect the width of the received dispersed pulse.

In the present comparisons, we set arg $S_T(\omega)$ and arg $S_R(\omega)$ to zero and assume $H(\omega) = \exp\{-j\Phi(\omega)\}$. The expressions used in computing an impulse response then depend on the input parameters representing the layer height and thickness (h_o and σ), the penetration frequency f_p, and the path distance D. A key relationship that describes the trace of a delay time versus frequency (τ vs f) record can be derived from (21), (22), and (26c):

$$\bar{h}_\tau = \{(c\tau/2)^2-(D/2)^2\}^{1/2}, \tag{27}$$

$$\omega_\tau = \omega_p\{\nu_\tau/\delta_\tau\}^{1/2}, \tag{28}$$

$$\nu_\tau = \nu(\bar{h}_\tau),\ \delta_\tau = \delta(\bar{h}_\tau), \tag{29}$$

with ν and δ given by (19). For a given value of τ, ω_τ can be found from (28). Alternatively, one could choose ω_τ and then compute the corresponding delay time τ, although in this case, a root-finding procedure is necessary to calculate the equivalent height $\bar{h}_\tau$. Note that the minimum τ must be greater than D/c, the time taken to transverse the straight line distance between terminals.

A maximum frequency ω_M occurs as $\bar{h}_\tau$ in (28) increases. This maximum, called the MUF, is given by

$$\omega_M = \omega_p\{\nu_M/\delta_M\}^{1/2}, \tag{30a}$$

$$\nu_M = \nu(\bar{h}_M),\delta_M = \delta(\bar{h}_M), \tag{30b}$$

$$\bar{h}_M = \bar{h}_{n+1} = h_o+\sigma\ln[(\bar{h}_n/2\sigma)\{1+(2\bar{h}_n/D)^2\}-1], \tag{31}$$

$$\bar{h}_1 = h_o,\ n = 1, 2, \ldots$$

This procedure works reasonably well as long as D is not too near zero and $h_o > 2\sigma\{1+\ln(D/4\sigma)\}$. At vertical incidence, ω_M approaches ω_p as $\bar{h}_\tau$ goes to infinity. At oblique incidence, signal components are reflected back to the receiver from two different heights, giving rise to the so-called low ($\bar{h}_\tau \leq \bar{h}_M$) and high ($\bar{h}_\tau > \bar{h}_M$) rays. Components at frequencies greater than ω_M usually pass on through the ionosphere, although returns caused by scattering processes are sometimes received at higher frequencies.

The (deterministic) pulse response for a single ionospheric layer, assuming the IPM, can be put in the form

$$A(\tau) = \left|S_T(\omega_\tau)\hat{H}(\omega_\tau)S_R(\omega_\tau)S_R(\omega_\tau)\right|e^{j\theta(\omega_\tau)}, \tag{32}$$

where S_T and S_R are determined by the source and receiver, and $\hat{H}$ and θ are explicit functions of ω_τ, which in turn depend on ionospheric physical parameters. (The derivations of $\hat{H}$ and θ are described in a forthcoming report [52].) Statistical variations of the pulse response are the result of variations over time of these physical parameters. Some examples in the comparisons later show how the IPM can simulate time variations.

Equation (32) provides a deterministic base or statistical mean of the response for a given ionospheric layer configuration and propagation path distance. As the path distance goes to zero, the response reduces to the values expected for vertical incidence, and the high ray disappears. In addition to the pulse response, (27)-(29) can be used to plot delay/frequency traces similar to the displays of ionograms.

The total response at the receiver is, of course, the sum of pulse responses from all reflections. These may be caused by multiple layers in the ionosphere or by multihops from one layer. Modifications to the single-mode amplitude may be introduced to account for the effects of ground reflections or absorption by intervening layers, although no explicit factor has been used in the comparisons that follow.

The influence of an intervening layer on the trace of an ionogram can also be simulated in the present model, but this is not yet included in the current pulse response computer program. For instance, if an E layer is present, frequency components that pass through and then are reflected back from the F layer show a characteristic retardation near the E layer critical frequency f_{pE}. This can be accounted for in the model by adding an E layer term to (14a):

$$\bar{h} = h_o - \sigma \ln\{(f_p/f)^2-1\} - \sigma_E \ln\left|(f_{pE}/f)^2-1\right|, \quad f_{pE} < f < f_p. \tag{33}$$

An indication of the merit of (33) is shown in Figure 4, which compares the equation with an actual data sample. The measured points (denoted by X) are taken from Figure 4(a) of CCIR [55] and represent measurements from an ionogram recorded at Argentine Islands in the fall of 1958. The penetration frequencies, σ's, and h_o were found by a simple fitting procedure to the measured ionogram:

h_o	σ	f_p	σ_E	f_{pE}
260	34.0	8.2	39.3	2.4

The model appears to provide a reasonable fit to the actual ionogram.

In summary, we have that the required inputs to the IPM are the path distance and the ionospheric parameters of layer height, thickness, and penetration frequency. If one desires to simulate a particular ionogram, these values can be obtained by a fit of the analytic functions to the measured data. Also required are source and receiver characteristics as expressed by their frequency responses or appropriate approximations. The output is the amplitude and phase of the pulse response.

6. COMPARISONS OF MEASUREMENTS WITH IPM

Figure 5 reproduces an ionogram from the NRL Channel Prober taken over a 126-km path in southern California [6]. At the time this ionogram was recorded, the instrument was operating as a narrowband (125 kHz) sounder with the amplitude limited to eliminate most of the noise. A simulation of the one-hop F_2 layer return is presented in Figure 5b showing the O- and X-modes and the crossover that occurs before the critical frequencies are reached. No knowledge of the actual layer conditions was available, so the simulation inputs were obtained by fitting the analytic functions to the measurement traces. For the ordinary mode, the results were: $f_p = 12$ MHz, $\sigma = 30$ km, $h_o = 260$ km; for the extraordinary mode: $f_p = 13$ MHz, $\sigma = 28$ km, $h_o = 275$ km. The model appears to provide a reasonable simulation of the return, at least as a reference base. Because of stable conditions during the measurement period (a fall morning), statistical effects are of minor importance.

Figure 6 reproduces the wideband (1 MHz) response at a center frequency of 5.5 MHz. A slow variation of ionospheric conditions occurred over a 10-minute interval of the measurement. This time variation could be interpreted as either a variation of the layer height with time or, perhaps more likely, the result of gravity waves. In any event, the effect of the time variation of the ionosphere can be simulated by the IPM by a time variation of the IPM parameters. Both the O- and X-modes show a slight variation of delay time, and this is achieved in the model by varying the height input h_o. The different delay widths of the two modes are obtained by fitting to the measured data. The cause of the differences in the O-mode and X-mode delay widths in the measured data is unknown, but is thought to be due to X-mode attenuation of the leading edge of the X-mode return. The cause of the null near the beginning of the ordinary mode response is unknown, and no attempt has been made to duplicate this in the simulation.

The applicability of the model to multiple returns is investigated in Figure 7, which shows a simulation of an ionogram taken over a 2600 km path from Colorado to New York. Three modes were assumed in the simulation with h_o values of 300, 400, and 520 km. Since there was no indication of what the layer thickness might be, $\sigma = 30$ km was used in all three modes. Junction frequencies were estimated from the measured ionogram, and from these were obtained approximate values for f_p: 7, 6.8, and 7.3 MHz. X modes were assumed in the high rays of both the first and third returns, so these inputs varied slightly from the O-mode inputs. A simple random function was introduced into the pulse width parameters of the second return and the X-mode of the third return, the purpose being only to see what effect this would have on the delay dispersion.

Simulation of Z-mode propagation, along with the O- and X-modes, is shown in Figure 8. The measured ionogram is from Reber [56], and the simulation (of the lower traces) is achieved by assuming three different values for the penetration frequencies and layer heights. The values used in the simulation of the lower trace are f_p(MHz) = 4.5, 5.3, 5.8, and h_o(km) = 284, 300, 308. The comparison displayed here emphasizes the importance of having a realistic frequency-delay time relationship in any model purporting to simulate wideband communication. Whether evaluating modems, protocols, or systems, a model restricted to stable configurations and slowly varying frequency ranges will not allow an adequate testing of performance under the wide variety of conditions encountered in actual practice.

The so-called "pulse prints" of the NRL Channel Prober can be simulated by the IPM if the phase term in (32) is modified to include the Prober signal detection process. The phase of the received signal is mixed with a local oscillator signal at the appropriate carrier frequency f_c and, after filtering and further processing, a translated and modified phase $\hat{\theta}$ is obtained. An analytic expression that simulates the pulse print pattern is

$$\begin{aligned}\theta(f,t) &= \hat{\theta}(f,t_o)+(d\theta/dt)t \\ &= 2\pi\kappa(f-f_c)(\tau-\tau_c)+2\pi f_D t,\end{aligned} \tag{34}$$

where τ_c is the delay time associated with f_c and κ is a constant dependent on the response width for a

given mode. The Doppler frequency, $\omega_D = d\theta/dt$, is a function of the time variations of layer height and penetration frequency.

Figure 9 presents the simulation of a pulse print obtained by the NRL Prober [6] over the same path as in Figure 5. Both the O- and X-modes are shown, but the simulation extends only over the first 30 seconds of time. The print represents the positive portion of the in-phase component of a signal received on a winter afternoon, and the mode Doppler frequency is constant over the time interval shown.

7. APPROACHES TO MODELING AND SIMULATION OF NOISE AND INTERFERENCE

Taking into account the effects of noise and interference is an important part of assessing the performance of any radio system. In this section, we begin by briefly reviewing the noise and interference models currently in general use. Then we propose a noise and interference model for the wideband HF channel and discuss approaches for the inclusion of noise and interference in a wideband HF channel simulator.

7.1 Noise Models

Noise and interference processes can be categorized into two general types: Class A and Class B. Class A processes are those for which the bandwidth of the noise is comparable to, or less than, the bandwidth of the receiving system, i.e., noise pulses that do not produce transients in the front end of the receiver. Examples of Class A noise are narrowband processes composed of intentionally radiated narrowband signals and various kinds of unintentionally radiated man-made noise. Class B processes are defined to be those for which the bandwidth of the noise is greater than the bandwidth of the receiving system, i.e., noise pulses that produce transients in the receiver. Class B noise is composed of broadband processes such as atmospheric noise from lightning and various forms of man-made noise such as automotive ignition noise.

The theoretical determination of communication system performance in the presence of noise and interference requires a mathematical model of the noise and interference. The main problem has been to develop a model that is consistent with all of the available measurements and that is physically meaningful; that is, it can be directly related to the physical mechanisms giving rise to the noise. With a few exceptions, none of the models developed to date satisfy both these criteria. Noise models can be grouped into two general categories: empirical models, which are designed to fit certain measured statistics of the noise, and physical models, which represent the entire noise process itself.

Nearly all of the existing noise models are for Class B noise (atmospheric noise and certain forms of manmade noise), an historical summary of which has been provided by Spaulding [57, 58]. Probably the most widely recognized empirical model for atmospheric and certain forms of man-made noise is that specified by the CCIR [59, 60]. This model provides the exceedence probability of the received noise envelope as a function of the "voltage deviation" parameter V_d, which is the dB difference between the average and rms voltages of the envelope. Since atmospheric noise is impulsive in nature, its statistical properties, unlike Gaussian noise, depend upon the receiver bandwidth. However, results on the effects of bandwidth on received atmospheric noise have been given by Herman and DeAngelis [61].

Another well-known model for atmospheric noise, which is mathematically simple, is a model developed by Hall [62]. The Hall model has two parameters, θ and γ, and is given by

$$p_Z(z) = \frac{\Gamma\left(\frac{\theta}{2}\right)\gamma^{\theta-1}}{\Gamma\left(\frac{\theta-1}{2}\right)\sqrt{\pi}\left[z^2+\gamma^2\right]^{\theta/2}} \tag{35}$$

and

$$P[E>E_0] = \frac{\gamma^{\theta-1}}{\left(E_0^2+\gamma^2\right)^{(\theta-1)/2}} \tag{36}$$

where $p_Z(z)$ is the probability density function (pdf) of the received instantaneous amplitude z corresponding to the noise process Z(t), and $P(E>E_0)$ is the cumulative distribution of the noise envelope, or amplitude probability distribution (APD).

In a series of papers, Middleton [63-65] has developed physical-statistical models of the entire noise process for both Class A and Class B noise. These models are based upon the physical processes responsible for the noise, are canonical (the mathematical form of the models does not change for different physical situations), and are mathematically difficult to derive. The pdf for the Middleton model for Class B noise is

$$p_Z(z) = \frac{e^{-z^2/\Omega}}{\pi\sqrt{\Omega}} \sum_{m=0}^{\infty} \frac{(-1)^m}{m!} A_\alpha^m \Gamma\left(\frac{m\alpha+1}{2}\right) {}_1F_1\left(-\frac{m\alpha}{2};\ 1/2;\ \frac{z^2}{\Omega}\right), \quad -\infty \le z \le \infty \tag{37}$$

where ${}_1F_1$ is a confluent hypergeometric function. The parameters α and A_α are related to the physical processes causing the noise and Ω is a normalization parameter. The corresponding expression for the APD is

$$P(E > E_0) = e^{-E_0^2/\Omega}\left[1-\frac{E_0^2}{\Omega}\sum_{m=1}^{\infty}\frac{(-1)^m}{m!}A_\alpha^m\,\Gamma\left(1+\frac{m\alpha}{2}\right){}_1F_1\left(1-\frac{m\alpha}{2};\ 2;\ \frac{E_0^2}{\Omega}\right)\right] \tag{38}$$
$$0 \le E \le \infty.$$

Middleton has shown [64] that this Class B model approximately reduces to the Hall model for certain values of the parameters.

For Class A noise the only model developed to date is the Middleton Class A model. This model is given by

$$P_Z(z) = e^{-A} \sum_{m=0}^{\infty} \frac{A^m}{m!\sqrt{2\pi\sigma_m^2}} e^{-z^2/2\sigma_m^2}, \tag{39}$$

where

$$\sigma_m^2 = \frac{m/A+\Gamma'}{1+\Gamma'}, \tag{40}$$

and

$$P(E>E_0) = e^{-A} \sum_{m=0}^{\infty} \frac{A^m}{m!} e^{-E_0^2/\sigma_m^2} . \tag{41}$$

The model has two parameters, A and Γ'. A is related to the impulsiveness of the noise, and as A becomes large (>10) the noise approaches narrowband Gaussian noise; Γ' is the ratio of the energy in the Gaussian component of the noise to the energy in the non-Gaussian components.

To date the Middleton models are the only noise models which have been physically derived and show agreement with a wide variety of measurements. For a large number of comparisons of the models with measurements and for a review of other noise models, see Spaulding and Middleton [66].

7.2 Wideband Noise and Interference Modeling and Simulation

As discussed above, noise and interference models fall into two general classes: empirical models and physical-theoretical models. However, from the point of view of predicting system performance and designing optimum detectors, a model based upon the physics of the noise process is preferable to an empirical model because of its greater flexibility. For Class A noise, the only model is the Middleton model, which is analytically quite complicated. However, over bandwidths on the order of 1 MHz, one expects to encounter many (perhaps hundreds) narrowband HF interferers. In the limit of large bandwidth, it can therefore be argued that one expects the Class A noise to be approximately described by a Gaussian process as a result of the central limit theorem, assuming the noise is not dominated by a few noise sources. This approximation corresponds to truncating the Middleton Class A model after one term.

In the case of Class B noise, it is not so clear that the above argument can be applied, particularly if the noise is dominated by a few impulsive processes, for example, noise pulses from lightning in a local thunderstorm. However, as pointed out above, the Middleton Class B model approximately reduces to the Hall model for atmospheric noise for certain values of the model parameters. We therefore propose describing wideband noise and interference as a combination of a Gaussian process and the Hall model.

Since a zero-mean Gaussian process is described by one parameter (the variance or rms deviation) and the Hall model is described by two parameters, the proposed wideband model contains a total of three parameters. If one fixes the Hall model parameters with those values for which it approximates the Middleton Class B model [63], the total number of parameters is reduced to one.

The verification of this proposed model by comparisons with measurements is currently under investigation. In this connection, an empirical wideband HF noise and interference model based on measured data has recently been proposed [26]. This model is a spectral occupancy model that describes the fraction of spectral resolution cells in which the power exceeds a given threshold as a function of that threshold. It can also be viewed as the probability that a given power level is exceeded as a function of power level. Figure 10 is a schematic illustration of this model, in which the logarithm of the exceedence probability is plotted as a function of power level on a log-log plot. The point we wish to make is that between a minimum power level (corresponding to the noise floor) and the maximum observed power level the plot is linear, as suggested by the data. Moreover, it can be shown that, for sufficiently high power levels, "Hall noise" leads to an approximately linear relationship between exceedence probability and power, when plotted on a log-log scale. On the other hand, Gaussian noise leads to a logarithmic relationship on a log-log scale. In Figure 10 the occupancy models arising from pure Gaussian noise and pure "Hall noise" are also shown. Current studies are directed toward obtaining an expression for the spectral occupancy of combined Hall plus Gaussian noise.

In order to simulate the noise and interference, one needs a model for the time statistics as well as amplitude statistics. For his model Hall also developed expressions for the average rate of envelope crossings and distributions of pulse width and pulse spacing. For LF atmospheric noise the model showed good agreement with data for the envelope crossing rate but poor agreement for pulse width and spacing. In the case of HF noise, the predictions should be checked with wideband HF measurements, similar to those performed by Coon et al. [66] in the case of narrowband HF noise. Measurements of the time statistics are important not only for model verification, but for system planning as well. For example, both amplitude and time statistics are needed to obtain distributions of the duration of unoccupied channels, which is of practical interest.

8. CONCLUSIONS AND FUTURE WORK

The initial motivation for the investigation of a new HF channel model was the interest in wideband HF systems for both communications and over-the-horizon radar applications. The Watterson model was validated only for narrowband (less than 3 kHz) channels and is, therefore, not applicable to the modeling of the wideband HF channel. Further motivation for the development of a new HF channel model is due to the limitations of the Watterson model, which are

- channels having time and frequency stationarity

•channels having negligible delay dispersion (e.g., no spread-F)

•channels having only a low-ray path

As noted by LeRoux et al. [37], the CCIR HF channel model [30] is representative of the HF medium in only a limited number of cases. The Watterson model, and simulators based on this model, have provided a powerful means for the laboratory evaluation of narrowband HF communication systems. However, the limitations on the model restrict the generality of the test results obtained from such laboratory testing.

A new approach to HF channel propagation modeling is reported in this paper. The objective of the Ionospheric Parameters Model (IPM) project is to develop a model that can be used for the wideband HF channel. The model can also be used for modeling the narrowband HF channel but is less restrictive than the Watterson model. The deterministic portion of the model is complete. Good results have been obtained in the comparison of the model output with measured wideband channel probe data for a variety of propagation conditions.

The next step in the model development methodology is to add the time-varying statistics to the deterministic base reported in this paper. After the time variations are added to the model, it must be subjected to the same statistical validation techniques used by Watterson [28, 29] in the validation of the narrowband model.

The software implementation of the IPM model is straightforward. Less clear is the functional structure of the model that can be readily implemented in a hardware wideband HF channel simulator. This issue is under investigation.

Modeling of the noise and interference for a wideband HF channel is equally important. An approach for this part of the wideband model was outlined in Section 7. Work remains in validation of the noise/interference model through the use of wideband noise and interference measurements.

REFERENCES

[1] Perry, B.D., E.A. Palo, R.D. Haggarty, and E.L. Key, "Trade-Off Considerations in the Use of Wideband HF Communications," IEEE 1987 Intl. Conf. Commun., Seattle, WA, Paper No. 26.2.

[2] Perry, B.D., "A New Wideband HF Technique for MHz-Bandwidth Spread-Spectrum Radio Communications," IEEE Commun. Mag. 21, No. 9., Sept. 1983, pp. 28-36.

[3] Dhar, S., and B.D. Perry, "Equalized Megahertz-Bandwidth HF Channels for Spread Spectrum Communications," IEEE 1982 Military Commun. Conf., Boston, MA, Paper No. 29.5.

[4] Low, J., and S.M. Waldstein, "A Direct Sequence Spread-Spectrum Modem for Wideband HF Channels," IEEE 1982 Military Commun. Conf., Boston, MA, Paper No. 29.6.

[5] Wagner, L.S., J.A. Goldstein, and E.A. Chapman, "Wideband HF Channel Prober: System Description," Tech. Report 8622, Mar. 1983, Naval Research Laboratory, Washington, DC.

[6] Wagner, L.S., and J.A. Goldstein, "High-Resolution Probing of the HF Ionospheric Skywave Channel: F_2 Layer Results," Radio Sci. 20, No. 3, May-June 1985, pp. 287-302.

[7] Wagner, L.S., J.A. Goldstein, and W.D. Meyers, "Wideband Probing of the Trans-Auroral HF Channel," IEEE 1987 Military Commun. Conf., Washington, DC, Paper No. 43.2.

[8] Wagner, L.S., J.A. Goldstein, and W.D. Meyers, "Wideband Probing of the Trans-Auroral HF Channel: Solar Minimum," 1987 Ionospheric Effects Symp., Naval Research Laboratory, Washington, DC, pp. 31-43.

[9] Wagner, L.S., "Characteristics of Mid-Latitude Sporadic E Observed with a Wideband HF Channel Probe, Radio Sci. 22, No. 5, Sept.-Oct. 1987, pp. 728-744.

[10] Haines, D.M. and B. Weijers, "Embedded HF Channel Probes/Sounders," IEEE 1985 Military Commun. Conf., Boston, MA, Paper No. 12.1.

[11] Salous, S., and E.D. Shearman, "Wideband Measurements of Coherence Over an HF Skywave Link and Implication for Spread-Spectrum Communication," Radio Sci. 21, No. 3, May-June 1986, pp. 463-472.

[12] Skaug, R., "Experiment with Spread Spectrum Modulation on an HF Channel," IEE Proc. 131, Part F, No. 1, Feb. 1984, pp. 87-91.

[13] Skaug, R., "An Experiment with Spread Spectrum Modulation on an HF Channel," IEE Second Conf. on HF Commmun. Systems and Techniques, London, UK, 1982, IEE Pub. 206, pp. 76-80.

[14] Milsom, J.D., and T. Slator, "Consideration of Factors Influencing the Use of Spread Spectrum on HF Sky-Wave Paths," IEE Second Conf. on Commun. Systems and Techniques, London, UK, 1982, IEE Pub. 206, pp. 71-74.

[15] Baker, K.A., D.M. Haines, and B. Weijers, "Polar Azimuth Diversity HF Propagation Experiment," Rome Air Development Technical Center TR 86-11, Rome, NY 13441, 1986.

[16] Basler, R.P., P.B. Bently, G.H. Price, R.T. Tsunoda, and T.L. Wong, "Ionospheric Distortion of HF Signals," Defense Nuclear Agency Report DNA-TR-87-246, Defense Nuclear Agency, Washington, DC 20305, 1987.

[17] Hoffmeyer, J.A., and L.E. Vogler, "Measurement, Modeling, and Simulation of LOS Microwave Channels," NATO AGARD Conf. Proc., No. 419, Scattering and Propagation in Random Media; Rome, Italy, May 1987, Paper No. 31.

[18] Watterson, C.C., "HF Channel-Simulator Measurements on the KY-870/P FSK Burst-Communication Modem-Set 1," NTIA Report CR-81-13, (NTIS* Order No. PB 82-118944).

[19] Belknap, D.J., R.D. Haggarty, and B.D. Perry, "Adaptive Signal Processing for Ionospheric Distortion Correction," MITRE Tech. Report MTR-746, Aug. 1968, MITRE Corp., Bedford, MA.

[20] Eley, A.S., And B.S. Abrams, "Receiving Subsystem Adaptive Interference Cancellation," IEE Third Intl. Conf. on HF Commun. Systems and Techniques, London, UK, 1985, IEE Pub. 245, pp. 126-130.

[21] Mousley, T.J., "HF Data Transmission in the Presence of Interference," IEE Third Intl. Conf. on HF Commun. Systems and Techniques, London, UK, 1985, IEE Pub. 245, pp. 67-70.

[22] Gibson, A.J., and L. Arnett, "New HF Spectrum Occupancy Measurements in Southern England," IEE Fourth Intl. Conf. on HF Radio Systems and Techniques, London, UK, 1988, IEE Pub. 284, pp. 159-164.

[23] Gibson, A.J., P.A. Bradley, and J.C. Schlobohm, "HF Spectrum Occupancy Measurements in Southern England," IEE Third Intl. Conf. on HF Commun. Systems and Techniques, London, UK, 1985, IEE Pub. 245, pp. 71-75.

[24] Wilkinson, R.G., "A Statistical Analysis of HF Radio Interference and its Application to Communication Systems," IEE Second Intl. Conf. on HF Commun. Systems and Techniques, London, UK, 1982, IEE Pub. 206, pp. 101-105.

[25] Laycock, P.J., M. Morrell, G.F. Gott, and A.R. Ray, "A Model for HF Spectral Occupancy," IEE Fourth Intl. Conf. on HF Radio Systems and Techniques, London, UK, 1988, IEE Pub. 284, pp. 165-171.

[26] Perry, B.D., and L.G. Abraham, "Wideband HF Interference and Noise Model Based on Measured Data," Report M88-7, Mar. 1988, MITRE Corp., Bedford, MA.

[27] Pennington, J., "Interference Tests on HF Modems," IEE Fourth Intl. Conf. on HF Radio Systems and Techniques, London, UK, 1988, IEE Pub. 284, pp. 318-320.

[28] Watterson, C.C., J.R. Juroshek, and W.D. Bensema, "Experimental Verification of an Ionospheric Channel Model," ESSA Tech. Report ERL-112-ITS-80, 1969.

[29] Watterson, C.C., J.R. Juroshek, and W.D. Bensema, "Experimental Confirmation of an HF Channel Model", IEEE Trans. Commun. Technol. COM-18, 1970, pp. 792-803.

[30] CCIR, "HF Ionospheric Channel Simulators", Report 549, XIIIth Plenary Assembly, Vol. III, pp. 66-72, ITU, Geneva, Switzerland.

[31] Watterson, C.C. and R.M. Coon, "Recommended Specifications for Ionospheric Noise Simulators," ESSA Tech. Report ERL-127-ITS-89.

[32] Watterson, C.C., "HF Channel-Simulator Measurements on the KY-879/P FSK Burst-Communication Modem-Set 2," NTIA Contractor Report CR-82-20, Dec. 1982, (NTIS* Order No. PB 83-194738).

[33] Ehrman, L., L.B. Bates, J.F. Eschle, and J.M. Kates, "Real-Time Software Simulation of the HF Radio Channel," IEEE Trans. Commun. COM-30, No. 8, Aug. 1982, pp. 1809-1817.

[34] Mooney, O.J., "Implementation of an HF Ionospheric Channel Simulator, Using a Digital Signal Processor," IEE Third Intl. Conf. on HF Commun. Systems and Techniques, London, UK, 1985, pp. 27-31.

[35] Girault, R., J. Thibault, and B. Durand, "Software Ionospheric Channel Simulator," IEE Fourth Intl. Conf. on HF Radio Systems and Techniques, IEE Pub. 284, London, UK, 1988, pp. 321-325.

[36] McRae, D.D., and F.A. Perkins, "Digital HF Modem Performance Measurements Using HF Link Simulators," IEE Fourth Intl. Conf. on HF Radio Systems and Techniques, IEE Pub. 284, London, UK, 1988, pp. 314-317.

[37] LeRoux, Y.M., G. Savidan, G. DuChaffaut, P. Gourvez, and J.P. Jolivet, "A Combined Evaluation and Simulation System of the HF Channel," IEE Fifth Intl. Conf. on Ant. and Prop., York, UK, 1987, IEE Pub. 274, pp. 171-175.

[38] Serrat-Fernandez, J., J.A. Delgado-Penin, E. Munday, and P.G. Farrell, "Measurement and Verification of an HF Channel Model," IEE Third Intl. Conf. on HF Commun. Systems and Techniques, London, UK, 1985, IEE Pub. 245, pp. 52-56.

---

*National Technical Information Service, 5285 Port Royal Rd., Springfield, VA 22161.

[39] Malaga, A., "A Characterization and Prediction of Wideband HF Sky-Wave Propagation," IEEE Military Commun. Conf., Boston, MA, 1985, paper no. 12.5.

[40] Barratt, J.J., and T.L. Walton, "A Real-Time Wideband Propagation Simulator for the High Frequency Band," Ionospheric Effects Symp., Naval Research Laboratory, Washington, DC, 1987, pp. 9-20.

[41] Hoffmeyer, J.A., and M. Nesenbergs, "Wideband HF Modeling and Simulation," NTIA Report 87-221, July 1987, (NTIS* Order No. PB 88-116116/AS).

[42] NBS, "Ionospheric Radio Propagation," National Bureau of Standards Circular 462 , 1948, (Superceded by [47]).

[43] Budden, K.G., Radio Waves in the Ionosphere, Cambridge University Press, UK, 1961.

[44] Tatarskii, V.I., The Effects of the Turbulent Atmosphere on Wave Propagation, U.S. Dept. of Commerce, NTIS, Springfield, VA, 1971.

[45] Ishimaru, A., Wave Propagation and Scattering in Random Media, Academic Press, New York, NY, 1978.

[46] Booker, H.G., "Scintillation Theory--a Simplified Treatment," Indian J. of Radio and Space Physics, 1986.

[47] Booker, H.G., and J.W. Tao, "A Scintillation Theory of the Fading of HF Waves Returned from the F-Region: Receiver Near Transmitter," J. of Atmos. and Terr. Physics 49, 1987, pp. 915-938.

[48] Booker, H.G., J.W. Tao. and A.B. Behroozi-Toosi, "A Scintillation Theory of Fading in Long-Distance HF Ionospheric Communications," J. of Atmos. and Terr. Physics 49, 1987, pp. 939-958.

[49] Davies, K., "Ionospheric Radio Propagation," NBS Monograph No. 80, 1965 (NTIS* Order No. PB 257-342/6ST).

[50] Wetzel, L., "On the Theory of Signal Distortion Due to Ionospheric Dispersion," Pap. Inst. Def. Anal., P-317, 1967, pp. 15-31.

[51] Kelso, J. M., Radio Ray Propagation in the Ionosphere, McGraw-Hill, New York, NY, 1964.

[52] Vogler, L.E., "Wideband HF Ionospheric Parameters Model," (To be published. Preprint available from the author on request.)

[53] Vogler, L.E., "Impulse Response for Ionospheric Relection with a $Sech^2$ Profile," Radio Sci. 19(6), 1984, pp. 1543-1551.

[54] Papoulis, A., The Fourier Integral and its Applications, McGraw-Hill, New York, NY, 1962.

[55] CCIR, "Supplement to Report 252-2 (Green Book)," XIVth Plenary Assembly, Kyoto, 1978, ITU, Geneva, Switzerland, 1980.

[56] Reber, G., "World-Wide Spread F," J. Geophys. Res. 61, 1956, pp. 157-164.

[57] Spaulding, A.D., "Stochastic Modeling of the Electromagnetic Interference Environment," Conf. Record, Intl. Conf. on Commun., ICC '77, Chicago, IL, June 12-15, 1977, pp. 43.4-114-123 (IEEE Catalog No. 77CH-1209-GCSCB).

[58] Spaulding, A.D., "Atmospheric Noise and its Effects on Telecommunication System Performance," Chapter 7, Handbook of Atmospherics, Vol. 1, H. Volland, Ed., 1982 (CRC Press, 2000 N. W. 24th St., Boca Raton, FL, 33431).

[59] CCIR, "Characteristics and Applications of Atmospheric Radio Noise Data," CCIR Report 322-3, Intl. Radio Consultative Committee, Intl. Telecommun. Union, Geneva, Switzerland, 1986.

[60] Spaulding, A.D., and J.S. Washburn, "Atmospheric Radio Noise: Worldwide Levels and Other Characteristics," NTIA Report 85-173, April 1975 (NTIS* Order No. PB 85-21942).

[61] Herman, J.R., and X.A. DeAngelis, "Bandwidth Expansion Effects on the Voltage Deviation Parameter (V_d) of MF and HF Atmospheric Radio Noise," Radio Sci. 11, No. 1, Jan.-Feb. 1987, pp. 26-36.

[62] Hall, H.M., "A New Model of "Impulsive" Phenomena: Application to Atmospheric Noise Communications Channels," Electron. Lab., Stanford Univ., Stanford, CA, Tech. Rep. 3412-8 and 7050-7, SU-SEL-66, 052 Aug. 1966.

[63] Middleton, D., "Statistical-Physical Model of Urban Radio-Noise Environments--Part I: Foundations," IEEE Trans. Electromagn. Compat., EMC-14, May 1972, pp. 38-56.

[64] Middleton, D., "Statistical-Physical Models of Electromagnetic Interference," IEEE Trans. Electromagn. Compat., Vol EMC-19, Aug. 1977, pp. 106-127.

[65] Middleton, D., "Procedures for Determining the Parameters of the First-Order Cononical Models of Class A and Class B Electromagnetic Interference," IEEE Trans. Electromagn. Compat., Vol. EMC-21, Aug. 1979, pp. 190-208.

[66] Spaulding, A.D., and D. Middleton, "Optimum Reception in an Impulsive Interference Environment," 1975, OT Report 75-67 (NTIS* Order No. COM 75-11097/AS).

[67] Coon, R.M., E.C. Bolton, and W.E. Bensema, "A Simulator for HF Atmospheric Radio Noise," 1969, ESSA Tech. Report ERL 128-ITS 90.

ACKNOWLEDGMENTS

The authors would like to express their appreciation to Mr. J. McEvoy of the Rome Air Development Center who provided funding support for the wideband HF research at ITS. Mr. McEnvoy's foresight and constructive comments during the course of this project are gratefully acknowledged. We also appreciate the contributions of Mr. B. Weijers of the Rome Air Development Center.

Finally, the authors would like to express their appreciation to Dr. L. Wagner of the U.S. Naval Research Laboratory for permission to use the data plots provided in Figures 5a, 6a, 7a, and 9a.

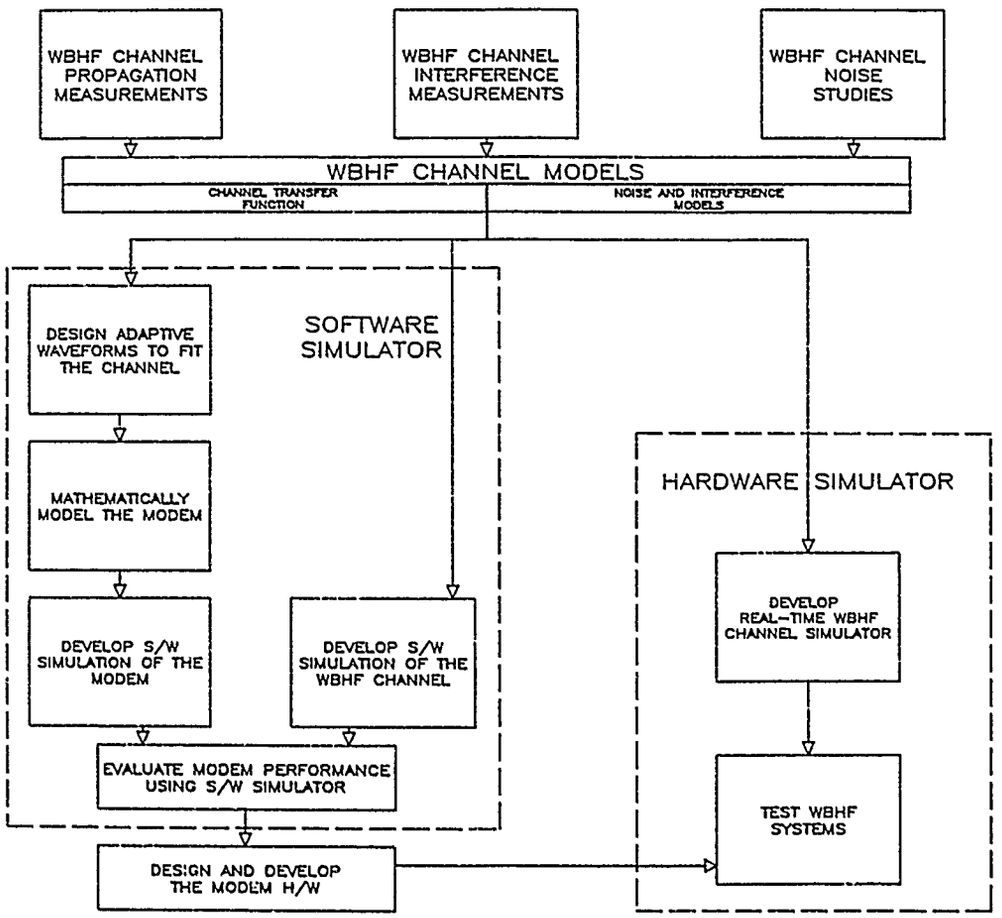

Figure 1. Interrelationship of wideband HF channel measurements, modeling, and simulation programs.

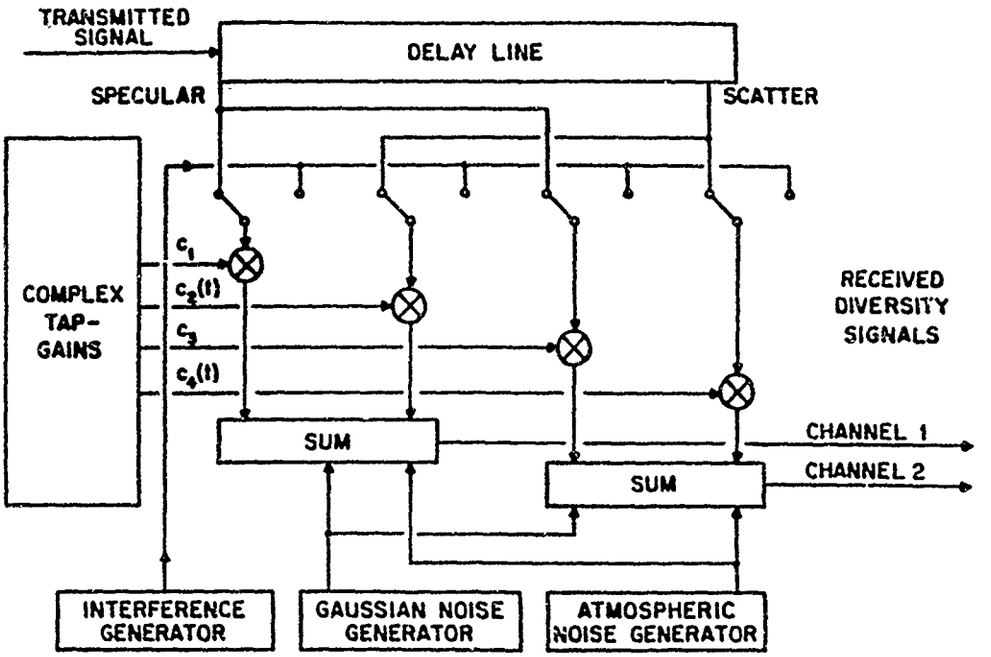

Figure 2. Tap delay line channel model structure.

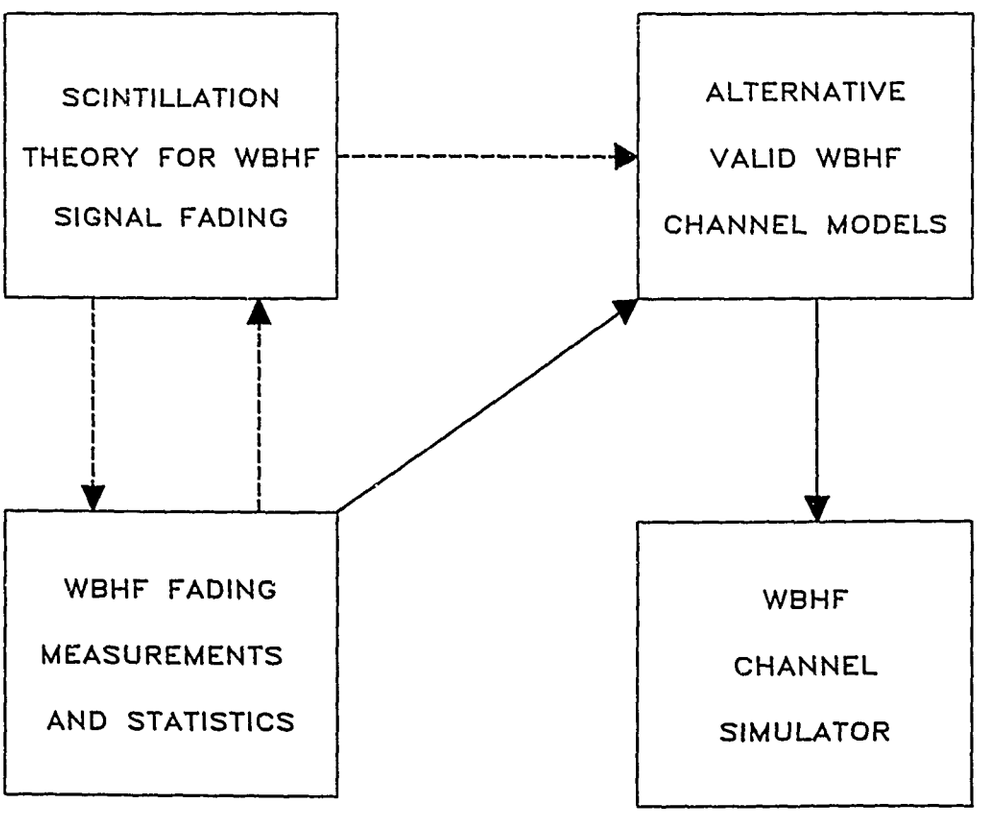

Figure 3. The role of channel theory and measurements in modeling and simulation.

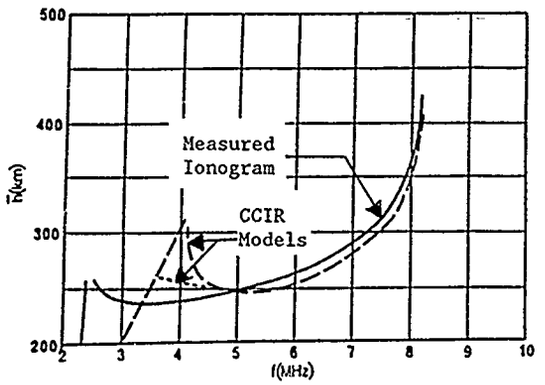

a) Synthesized ionograms from CCIR [55] models compared to measured ionograms.

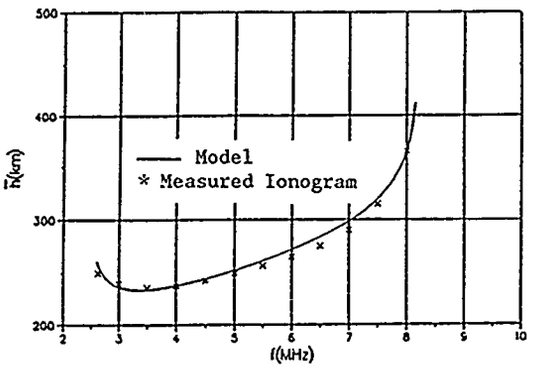

b) Synthesized ionograms from ITS ionospheric parameter model compared to measured ionograms.

Figure 4. Comparison of Ionospheric Parameters Model ionogram with ionograms produced by other models.

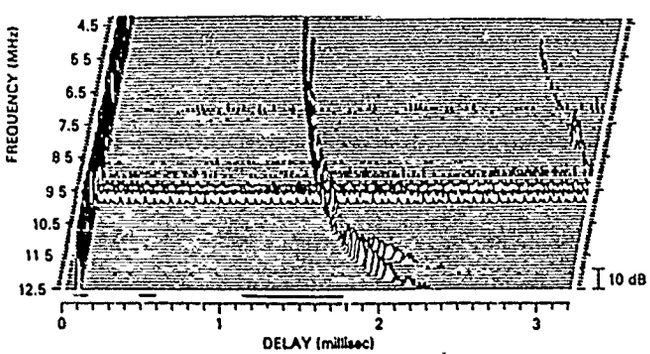

a) ionogram from NRL channel probe [6].

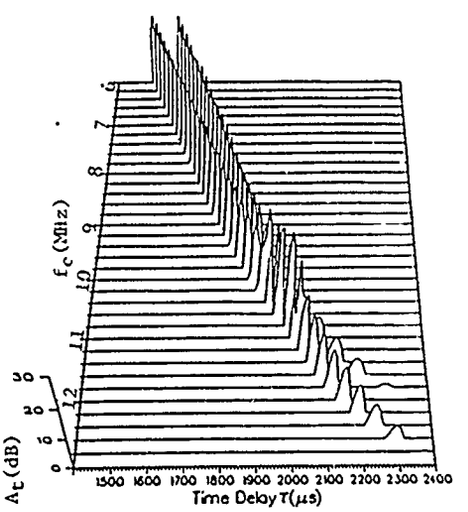

b) ionogram produced by IPM model.

Figure 5. Comparison of measured ionogram for a 126-km path (fall, morning) with an ionogram produced by Ionospheric Parameters Model.

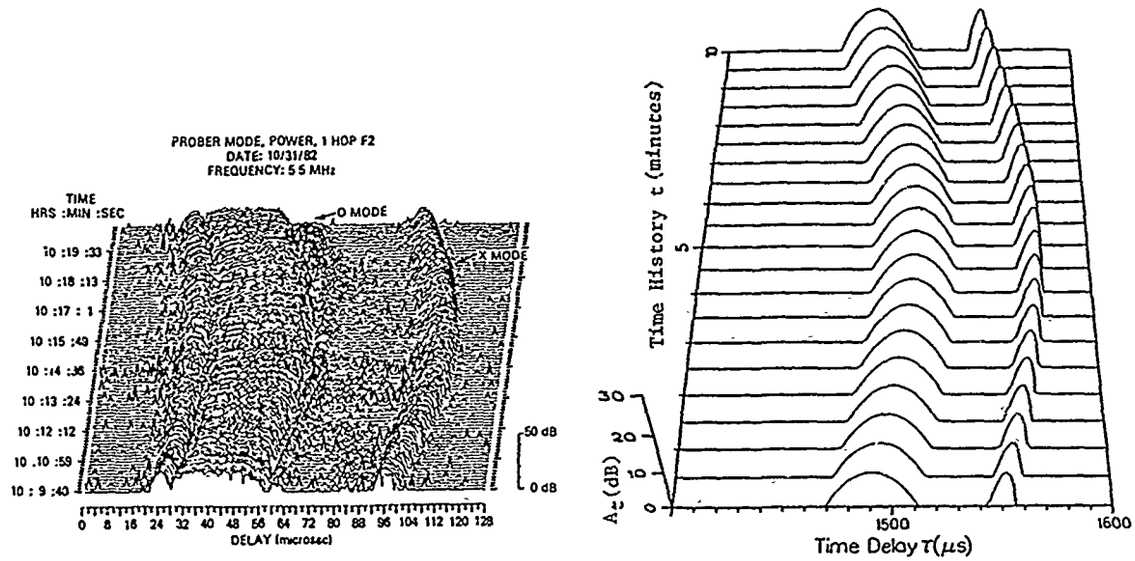

a) time history of data from NRL wideband channel probe [6].

b) time history from IPM model.

Figure 6. Comparison of measured pulse response time history with time history produced by IPM model.

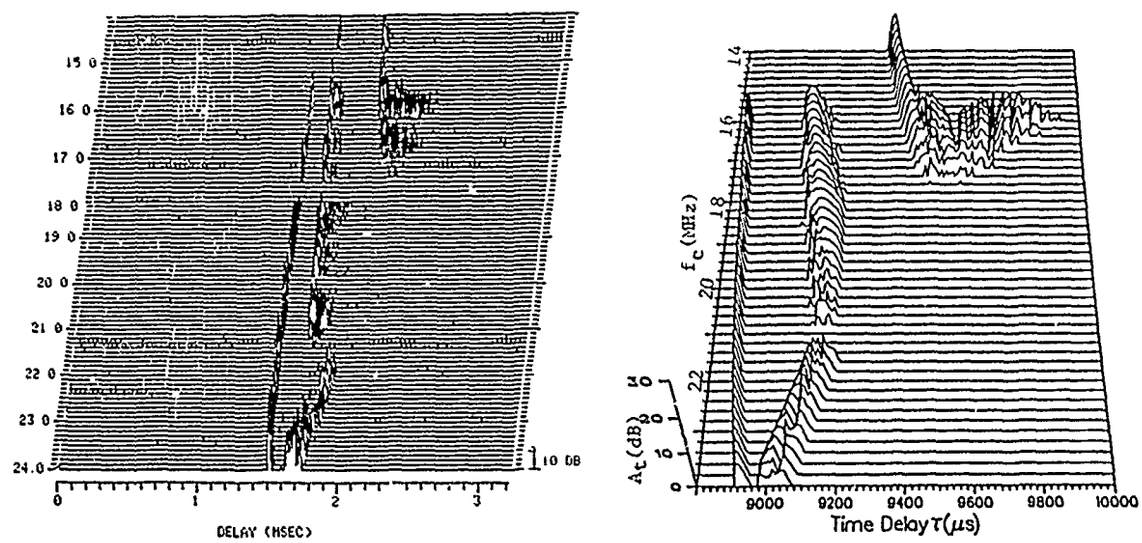

a) ionogram from NRL channel probe (provided courtesy of L. Wagner).

b) ionogram produced by IPM model.

Figure 7. Comparison of measured ionogram for 2600-km path (Boulder, CO, to Verona, NY) with an ionogram produced by the IPM model.

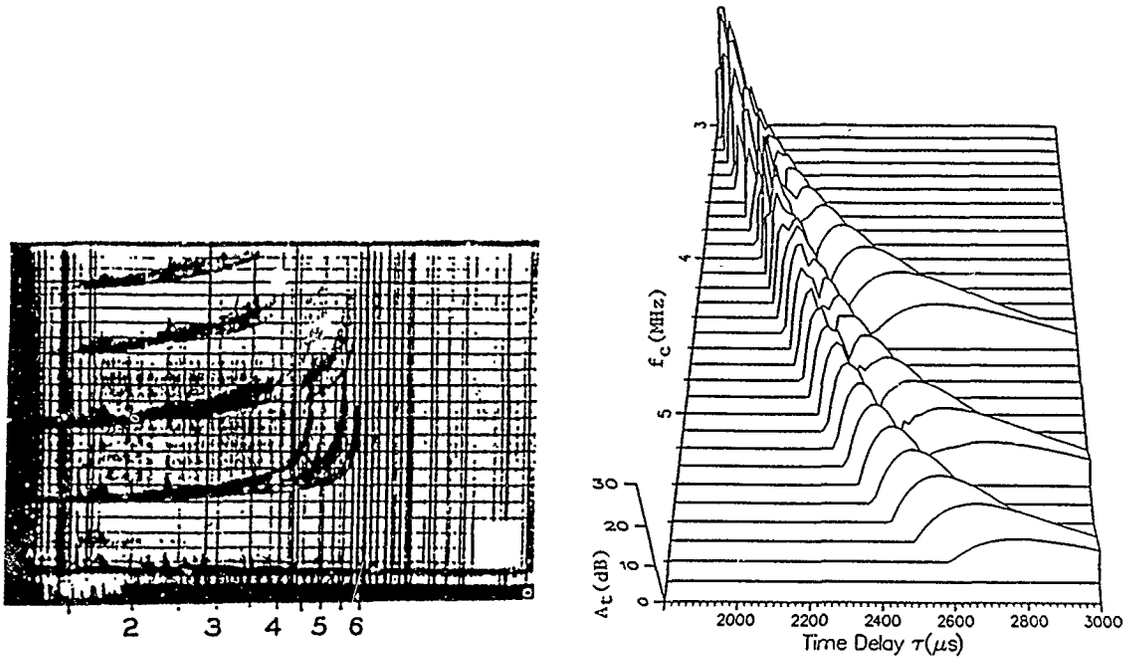

a) measured [55]. b) ionogram produced by IPM model.

Figure 8. Comparison of measured and model ionograms showing Z-, O-, and X-modes.

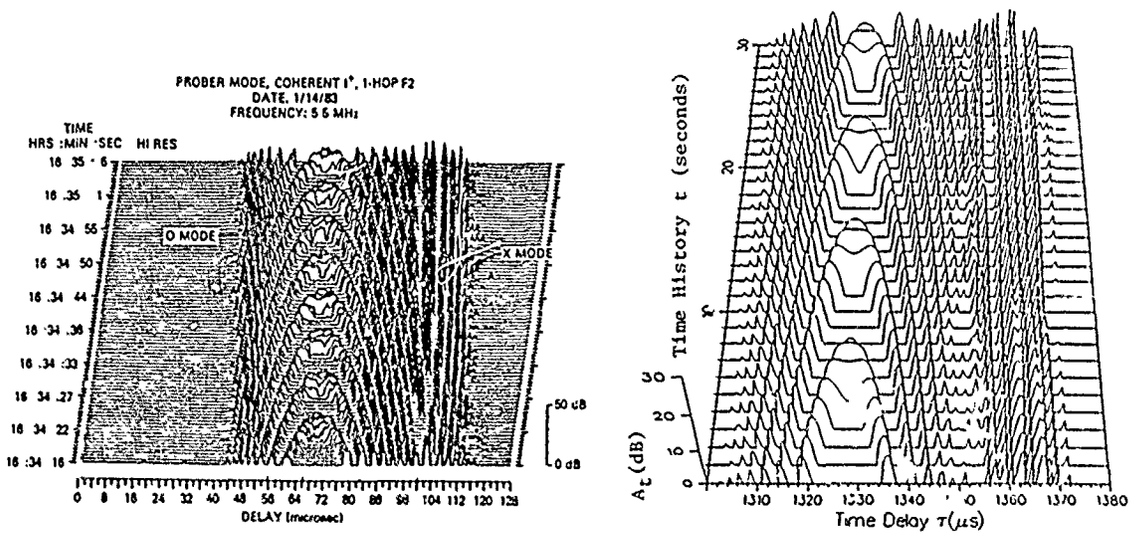

a) pulse print from NRL channel probe [6]. b) pulse print produced by IPM model.

Figure 9. Comparison of pulse prints from measured data and from the IPM model.

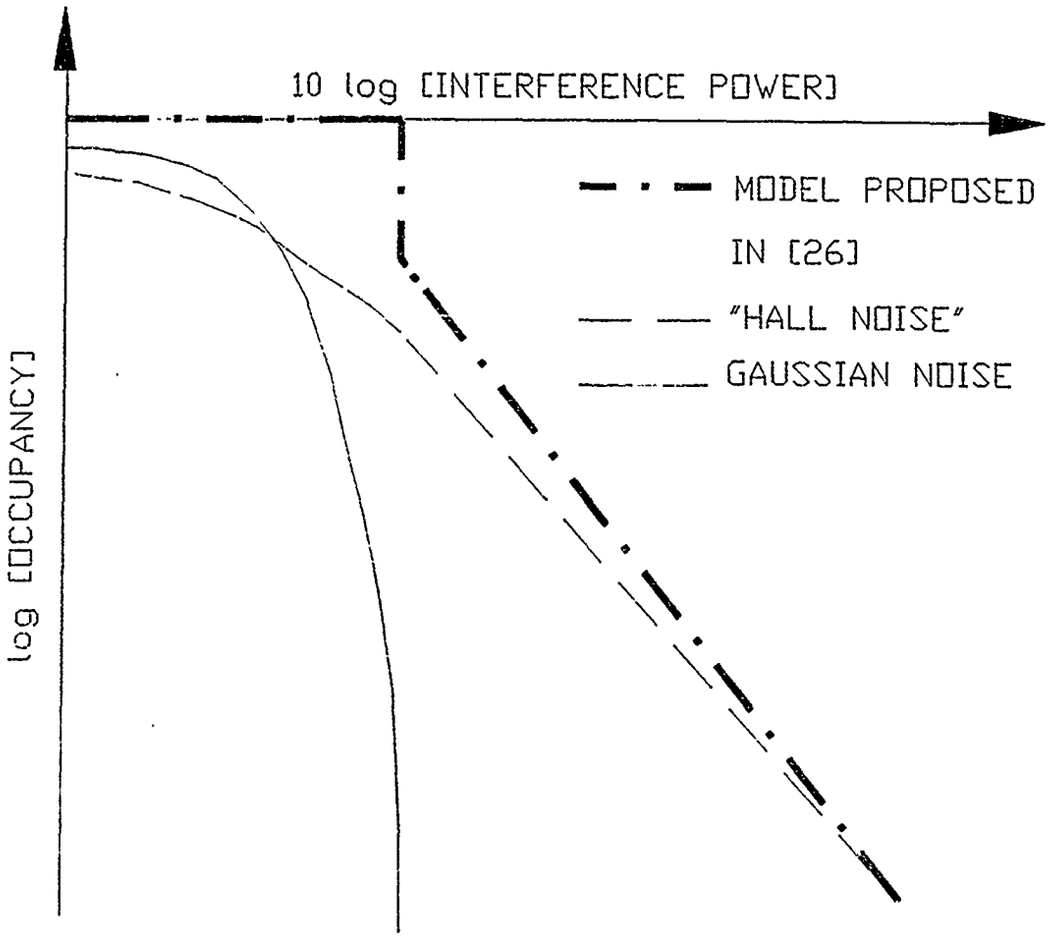

Figure 10. Schematic illustration of occupancy models.

Table 1. Validation of Watterson Model

Sample	Period	Tx. Frequency (MHZ)	Valid Bandwidth
1	13 minutes (daytime)	9.259 MHZ	12.0 kHZ
2	10 minutes (daytime)	9.259 MHZ	8.0 kHz
3	13 minutes (evening)	5.864 MHZ	2.5 khz

One path: Long Branch, IL, to Boulder, CO (1294 km)

One season: November, 1967

Data were chosen that "seemed most nearly stationary in terms of fading rates, model time delays, and average power in the modes" [28].

DISCUSSION

J.S. BELROSE

I am absolutely astonished by the assumptions you have made to model propagation, viz no magnetic field and no collisional damping of the wave. Polarization fading, magneto-ionic fading, deviative and non-deviative absorption are such fundamental parameters that they cannot be neglected in any realistic modelling. A further comment, an X-mode trace was modelled, but with no magnetic field there would be no X-mode. This is curious, and particularly since you seem to show a very detailed correlation between your model and sophisticated ionospheric probe data.
Could you clarify ?

AUTHOR'S REPLY

It must be remembered that the IPM is a simulation model and not a propagation prediction model. The IPM should be considered in the same manner as the narrowband Gaussian-based simulation models, i.e., such things as X-modes and collisional damping are described by model parameters that give the effect of the physical process. For instance in figure 5, the O-mode and X-mode are simulated by the two sets of layer parameters stated in the text ; however, the X-mode parameters are not obtained through any theoretical analysis of the geomagnetic field.

K.C. YEH

It is not clear how comparison between the experimental data of L. WAGNER and your model was made. As I recall your ionospheric model of sech ionospheric profile requires a few parameters such as layer height, thickness and critical frequency. How are these parameters obtained ?
Was there simultaneous vertical ionosonde data during oblique sounding ?
Of course, L. WAGNER's system does provide the oblique sounding data which can be used to get a model profile. Was it used ?

AUTHOR'S REPLY

The values for the model parameters were obtained by fitting the tau-frequency relation (Equation (28)) to the measured ionogram traces. For instance, the penetration frequency is usually easy to determine, and the layer height and thickness can then be solved for by a fit of the equation to the measured trace. No attempt was made to "fine-tune" the fit, and the rough approximations used appear to describe the returns quite adequately. If parameter values had been available from independent measurements, these, of course, would have been used.

C. GOUTELARD

Are you using the theorems of MARTYN and of BREIT and TUVE in your model, which seems so sophisticated ?

AUTHOR'S REPLY

The theorems of MARTYN and of BREIT and TUVE are necessary to derive the tau-frequency relation for oblique incidence. This allows the IPM to characterize the low- and high-ray returns near the junction frequency in a realistic manner. It is this frequency region that the usual Gaussian model approach is least able to simulate.

SEQUENCES D'ETALEMENT A SYNCHRONISATION OPTIMALE PAR COMMUTATION D'OPERATEURS INCOMMUTABLES

C. GOUTELARD
Laboratoire d'Etude des Transmissions Ionosphériques
94230 CACHAN - FRANCE

RESUME

L'un des principaux problèmes des transmissions par étalement de spectre réside dans la difficulté d'acquérir la synchronisation sur la séquence d'étalement. La procédure basée sur la corrélation pour les séquences longues nécessite un grand nombre d'opérations considérées dans les méthodes classiques comme incommutables.

Il existe cependant des séquences dans lesquelles la commutation des opérations est possible, ce qui réduit le nombre d'opérations, allège la complexité des décodeurs et surtout assure, avec le maximum de sécurité, une synchronisation en un temps minimum.

Les contraintes mathématiques que doivent respecter ces séquences pour obtenir la commutativité des opérateurs sont définies et des structures de séquences sont proposées.

Une famille de séquences est donnée en exemple.

I. - INTRODUCTION -

Les techniques d'étalement de spectre par des séquences numériques utilisent souvent des codes pseudo aléatoires. Leur utilisation est souvent dictée par la simplicité des systèmes générateurs, cependant la synchronisation de la réplique à la réception qui est nécessaire pour obtenir une bonne adaptation est une procédure souvent longue. Des procédures générales de synchronisation [1] [2] ont été étudiées et de nombreuses procédures spécifiques ont été proposées [3], [4], [5].

L'utilisation de filtres adaptés a permis d'effectuer, dans certains cas [6], les calculs avec rapidité.

L'emploi des fonctions de corrélation partielles [7] ou de combinaisons de séquences [8] a été proposé pour apporter des améliorations dans la discrétion ou dans la facilité de synchronisation.

Cependant, la synchronisation des séquences demeure particulièrement complexe dans le cas des forts taux d'étalement. La synchronisation se fait alors par l'intercorrélation entre le signal reçu et la réplique du signal d'étalement et sa recherche nécessite alors de nombreuses opérations. Ainsi, dans le cas d'étalements obtenus par séquences directes à L symboles, le nombre moyen de corrélations à effectuer est égal à $\frac{L}{2}$.

Lorsque la corrélation est effectuée sur la séquence complète, le nombre moyen de multiplications complexes à réaliser est égal à $\frac{L^2}{2}$.

La réalisation de corrélations effectuées sur une partie de la séquence, sur αL symboles, réduit le nombre moyen d'opérations à $\frac{\alpha L^2}{2}$ mais la détection est d'autant plus sous optimale que α est petit. En effet, le signal obtenu est d'énergie plus faible et le fonction de corrélation est altérée.

Une méthode d'acquisition de la synchronisation réduisant la complexité du calcul est proposée. Elle s'appuie sur l'utilisation de séquences décomposables en sous séquences soumises à des contraintes mathématiques particulières.

II. - METHODE ET RELATIONS GENERALES -

Soit deux suites S_k et S_h définies par une suite de N symboles.

$$S_k = [s_{ko}, s_{k1}, s_{k2} \cdots s_{k\,N-1}]$$

et $$S_h = [s_{ho}, s_{h1}, s_{h2} \cdots s_{h\,N-1}]$$

On forme

$$S_{pk} = [S_k, S_k, S_k] = [p_o \cdots p_i \cdots p_{3N-1}]$$

$$S_{oh} = [S_o, S_h, S_o] = [q_o \cdots q_i \cdots q_{3N-1}]$$

où S_o dénote la suite composée de N symboles nuls.
On définit alors la fonction de corrélation périodique par :

$$C_{kh}{}^n = \sum_{n=1}^{N-1} p_{(i+n)}\, q_i \quad \text{où} \quad n \in \left\{ -(N-1), (N-1) \right\}$$

Soient K suites $S_1, S_2, \ldots S_h, S_k \ldots S_K$ telles que

$$C_{kh}(n) \equiv 0 \qquad \forall\, k,\ h \neq k \in \left\{ 1,\ K \right\} \tag{1}$$

Théorème 1

Si on forme la suite

$$S_E = [\ldots \qquad S_{Ei} = [s_{1i}, s_{2i}, \ldots s_{Ki}] \ldots\ldots]$$

alors la fonction d'auto corrélation $C_{SE}(n)$ de la suite S_E prend les valeurs

$$C_e(n) \equiv 0 \quad \text{si } n \neq Km \in \left\{ -K(N-1) \ldots\ldots K(N-1) \right\}$$

$$m \in Z$$

$$C_E(Km) = \sum_{k}^{K} C_{kk}(m)$$

Théorème 2

Si on forme la suite

$$S_A = [\ldots \quad s_{Ai} = \sum_{k \in K} \alpha_k s_{ki} \ldots]$$

alors la fonction d'autocorrélation $S_A(n)$ de S_A prend la valeur :

$$C_A(n) = \sum_{k \in K} ||\alpha_k||^2 C_{kk}(n)$$

Une suite S_E, de longueur KN, a une fonction de corrélation à pointe unique si et seulement si :

$$\sum_{k \in K} C_{kk}(m) \equiv 0 \qquad \forall m \in \{1, N-1\} \qquad (2)$$

Ce type de fonction est celui recherché dans les systèmes à étalement de spectre. Il peut donc être obtenu à partir de suites élémentaires répondant aux conditions (1) et (2).

En choisissant $||\alpha_k||^2 = 1$, la fonction de corrélation $C_A(n)$ de la suite S_A prend alors les valeurs :

$$C_A(n=0) = C_E(n=0) = N^2$$

$$C_A(n\neq 0) = C_E(n\neq 0) = 0$$

Les deux suites formées ont même fonction de corrélation pour $n \in \{0, N-1\}$, cependant la séquence S_E est de longueur KN alors que la séquence S_A est de longueur N. Le calcul de la fonction $C_E(n)$ nécessite K^2N^2 opérations alors que $C_A(n)$ n'en impose que N^2.

L'existence de telles suites permet donc de réduire la complexité des calculs relatifs à la synchronisation par la transformation de la séquence émise S_E en une séquence S_A.

III. - CONSTRUCTION DES SUITES D'ETALEMENT -

Des suites optimales répondant aux conditions (1) et (2) sont constructibles.

Considérons la suite à q valeurs dans $F_q = 2^r$

$$s_{(k,b)} = [s_o, \ldots s_i \ldots s_{bNo-1}]$$

où

$$S_{(i=ko+lb)} \equiv l(k_l + k_o Ko) \mod q = 2^r$$

avec

$k_o \in \{0, \ldots b-1\}$

$l \in \{0, \ldots N_o-1\}$

$k \in \{0, \ldots K-1\}$ avec $bK = N_o$

On peut alors construire K suites de longueur bN_o auxquelles on peut faire correspondre K séquences à q valeurs complexes distinctes.

$$W_{k,b} = [W_o, \ldots W_i = W^{si} \ldots W_{bNo-1}]$$

en posant

$$W = e^{\frac{j2\pi p}{No}} \qquad p \text{ et } No \text{ premiers.}$$

Ces suites sont munies des propriétés suivantes :

Propriété 1.

$$C_{kk}(n) \equiv 0 \qquad \forall n \neq b^2B$$
$$\text{avec} \quad B \in \{0, \ldots K-1\}$$

$$C_{kk}(n=b^2B) = N_o b \quad [(kbB) \bmod q]$$

Propriété 2.

$$C_{kh}(n) \equiv 0 \qquad \forall n$$
$$\forall k \neq h$$

Propriété 3.

$$\sum_{k \in K} C_{kk}(n) = 0 \qquad \forall n$$

Les conditions (1) et (2) sont vérifiées et on obtient finalement une suite S_E de longueur $L = N_o^2$, telle que :

$$C_E(n) = N_o^2 \qquad \text{si } n = 0 \qquad n \in \{-(N_o^2-1), (N_o^2-1)\}$$

$$C_E(n) \equiv 0 \qquad \text{si } n \neq 0$$

IV. - ACQUISITION DE LA SYNCHRONISATION -

Si on effectue la synchronisation sur la longueur totale de la séquence, le nombre de multiplications moyen (figure 1) est égal à

$$N_E = \frac{N_o^2}{2} = \frac{L^2}{2}$$

La séquence est en fait composée de K suites de longueur bN_o avec lesquelles il est possible de former une séquence S_A selon le schéma de la figure 2 dans laquelle on effectue en premier l'opération donnant s_{Ai} :

$$s_{Ai} = \sum_{k \quad K} \alpha_k \, s_{ki}$$

Le nombre moyen de multiplications à effectuer pour rechercher le maximum de C_A est alors

$$N_{Al} = \frac{b^2 No^2}{2} = \frac{b^2 L}{2}$$

La détermination de la synchronisation nécessite ensuite de rechercher la synchronisation de la suite S_E parmi les K positions données par la suite S_A. Le nombre d'opérations moyen pour cette dernière étape est égal à $\frac{KNo^2}{2}$ si bien que le nombre moyen d'opérations devient :

$$N_A = \frac{b^2 L + KL}{2}$$

La valeur optimale de N_A est obtenue pour $b = (\frac{No}{2})^{1/3}$ qui donne alors

$$N_{Amin} = \frac{3}{2^{5/3}} L^{4/3} = 0,95\ L^{4/3}$$

La complexité du calcul varie dans ce cas en $L^{4/3}$ au lieu de L^2 dans le cas d'un calcul direct.
Ainsi, pour des séquences de longueur L = 1000, le volume de calcul est divisé par 50 et pour des longueurs L = 10000 le volume de calcul est divisé par 250.

V. - CONCLUSION -

La recherche de synchronisation dans les système à étalement de spectre requiert un volume de calcul qui croît rapidement avec le taux d'étalement.

En formant des séquences d'étalement à partir de sous séquences dotées de caractéristiques spécifiques, il devient posible de commuter les opérateurs additionneurs et multiplicateurs.
Cette commutation conduit à une réduction conséquente du volume de calcul qui permet d'envisager des procédures de synchronisation optimales rapides.

BIBLIOGRAPHIE

[1] R.C. DIXON - Spread Spectrum Systems. New York. Wiley 1976.

[2] J.K. HOLMES - Coherent spread Spectrum Systems. New York. Wiley 1982.

[3] J.K. HOLMES, C.C. CHEN - Acquisition time performance of PN spread spectrum systems. IEEE Trans. Commun. Vol. COM 25 August 1977.

[4] D.M. dicarlo, K.T. WEBER - Multiple dwell serial search : performance and application to direct sequence code acquisition. IEEE Trans. Commun.

[5] S. DAVIDOVICI, L.B. MILSTEIN, D.L. SCHILLING - A new rapid acquisition technique for direct sequence spread spectrum communications. IEEE Trans. Commun. Vol. COM 32 Nov. 1984.

[6] Y.T. SU - Rapid code acquisition algorithms employing PN matched filters. IEEE Trans. Commun. Vol. 36 N° 6 June 1988.

[7] D.V SARWATE, M.B. PURSLEY, T. BASAR - Partial correlation effects in direct sequence spread spectrum multiple access communication systems. IEEE Trans. Commun. Vol. COM 32 N° 5 May 1982.

[8] L.B. MILSTEIN, R.R. RAGONETTI - Combination sequences for spread spectrum communications. IEEE Trans. Commun Vol July 1977.

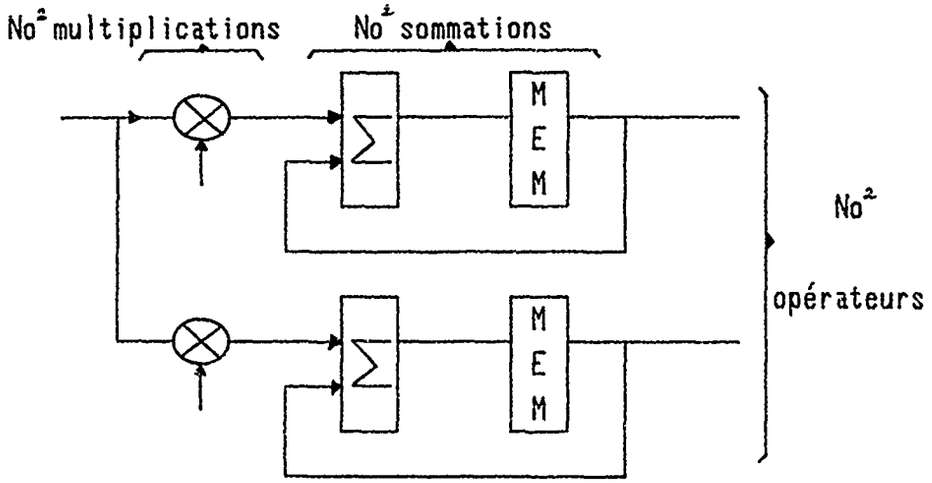

Figure 1

Schéma conventionnel des corrélateurs

No⁴ multiplications

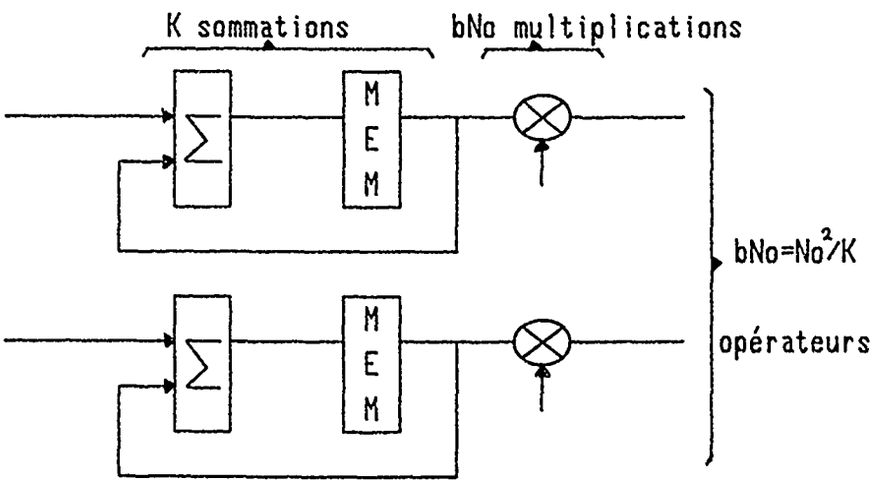

Figure 2

Schéma de corrélateur obtenu par commutation d'opérateurs : bNo² multiplications

DISCUSSION

D.J. FANG

Could you comment on the interleave requirement for implementing your scheme ? In particular, what is the buffersize capacity (or the total No. of bits to be interleaved). Is the capacity comparable to the state-of-the-art memory size ?

AUTHOR'S REPLY

L'implantation ne nécessite pas une mémoire de grande capacité. En effet, les calculs se font "on line" et il n'est pas nécessaire de stocker, comme dans un entrelacement classique, la totalité des symboles avant le traitement. Cette simplification vient justement de la commutation décrite des opérateurs.

RADIO CHANNEL MEASUREMENT AND MODELLING FOR FUTURE MOBILE RADIO SYSTEMS

E Gürdenli and P W Huish
British Telecom Research Laboratories
Martlesham Heath
Ipswich IP5 7RE
United Kingdom

SUMMARY

Digital mobile radio systems will require planning methods that provide accurate predictions of signal strength, distortion and interference for situations ranging from very small cells in dense urban locations to large rural cells. Topographic and land usage data bases will find increasing use to enhance the accuracy of prediction models.

The paper discusses the implications of these issues and reports on the work in progress at British Telecommunications Research Laboratories on land mobile radio propagation modelling and wide-band channel measurements.

1. INTRODUCTION

The growth of analogue private mobile radio (PMR) and cellular radiotelephone systems has emphasised the need for accurate means of predicting the coverage area and quality of service given by a particular base station and the system as a whole. This trend is likely to continue with the introduction of the Groupe Specíale Mobile (GSM) Pan-European digital cellular radio system and subsequent generations of systems, which will be capable of supporting a larger number of users, offer a greater variety of, perhaps, integrated services and achieve a much greater utilisation of the radio spectrum than their predecessors. In addition, with hand portable units becoming a significant part of the mobile population, coverage must be planned in a diverse range of environments including buildings and public transport.

The performance of an analogue radio system is mainly determined by an adequate signal to noise and signal to interference ratio. The planning of an analogue system is therefore often performed on the basis of achieving a sufficiently high probability of adequate signal strength and signal to interference power ratio within the service area. With appropriate software, embodying a reliable prediction method, radio coverage maps, such as that shown in Fig 1, can be produced to show the coverage provided by a particular transmitter.

Digital systems provide comparable quality at lower signal to noise or signal to interference ratios than current analogue systems. However the threshold effect associated with all digital systems may cause the edge of the service area to be sharply defined as are any 'holes' within that area. This will place a greater requirement for accuracy in the propagation prediction models used to plan these systems, and hasten the introduction of an environment dependent path loss correction.

The work of contributors to the EEC collaborative project COST 207 and the various working groups of the GSM have demonstrated the effect of multipath distortion on the performance of the radio system. Thus, account should be taken of the radio system equaliser's ability to counteract the environment dependent multipath distortion in the presence of interference and noise when planning a system. Since multipath propagation is generated principally by the mobile's local environment, the introduction of an algorithm that relates multipath phenomena to the local environment seems inevitable.

The major differences between current (analogue) and future (digital) systems can be summarised as these.

- much greater numbers of handheld units, with users located in buildings, open spaces and public transport,
- wider range of cell sizes, ranging from micro-cells in cities to large rural cells,
- a sharper definition of the coverage area due to the different variation of quality with signal to noise ratio of a digital system,
- a tendency to be interference limited in the areas of densest use.

These factors create the need for new prediction methods that will facilitate the planning and implementation of digital systems.

2. PATH LOSS PREDICTION

The various methods of predicting the power received in a mobile receiver from a fixed transmitter (and vice versa) can be broadly divided into two categories. One category might include the empirical prediction methods such as those of Okumura [1], and Ibrahim, Parsons [2], etc. These rely on a simple power law dependence of signal strength with distance, and some empirically derived factors which relate to, for example, the height-gain of the antenna system and the operating frequency. Since the path loss is related to the other parameters by a simple, linear, algebraic equation, it is possible to calculate the value of one parameter (e.g. antenna height), given a knowledge of all the other parameters, by a simple rearrangement of the equation. This is a particular advantage of these models.

The second category includes those models where an attempt is made to calculate the diffraction loss along the direct path between the transmitter and receiver. Typical methods include those used by the BBC [3], and Longley and Rice [4].

For areas where terrain features are not significant, empirical models, usually based on Okumura are used. However the presence of significant terrain features require diffraction effects to be considered, and the methods of the second category find favour. Figure 1 demonstrates the close relationship between the terrain features (heights in metres) above sea level and the path loss predictions (in dBs) for a hilly area of 20 x 20 km square.

The improved accuracy obtained with the diffraction based models in hilly terrain can still be compromised by the effect of buildings and other natural and man made features which obstruct or otherwise influence the propagation path between mobile and base station and are not included in the terrain database. A solution to this deficiency is the incorporation of an empirical correction factor, based on

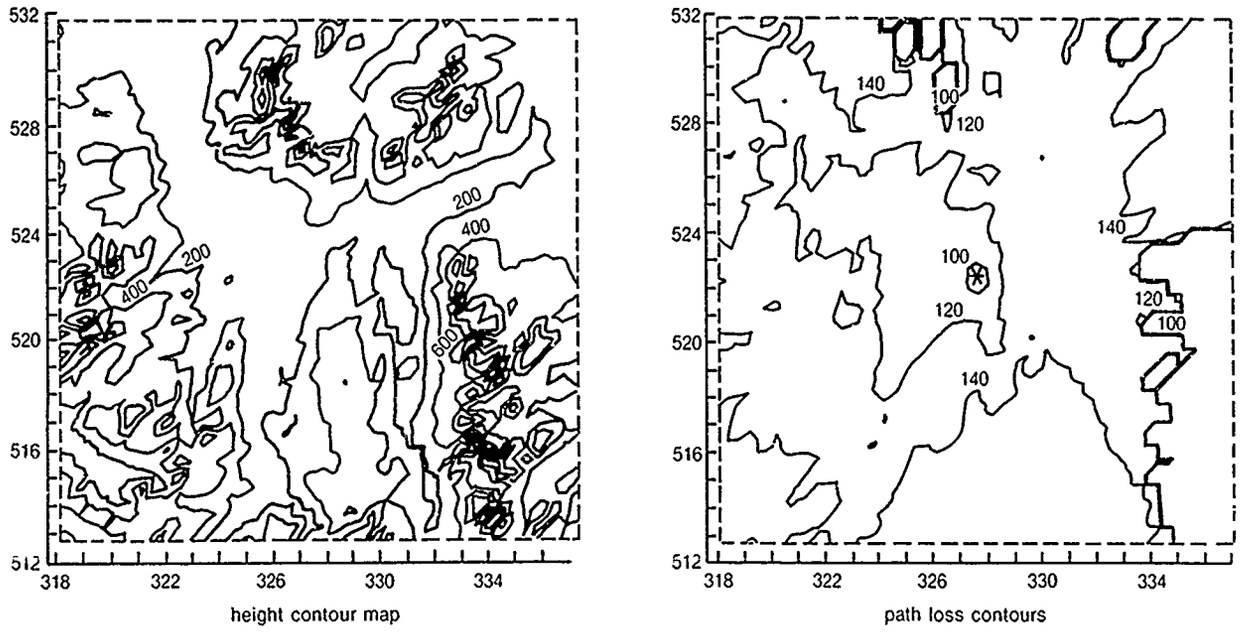

Fig 1 Height and path loss contours for a hilly area in NW England.

the mobile's local environment, into the path loss calculation. This correction factor can be derived by comparing measured and predicted path loss data for similar environments. A central feature of this is the classification of the environment according to its land cover or usage. The base station is assumed always to be sited clear of immediate obstructions, although in practice this might not be the case.

The derivation of this land usage data almost invariably involves manual, and therefore, costly procedures. With the emergence of geographic information systems (GIS) [5], which use digital database technology to enable the storage and retrieval of geographic (and other) information indexed to some co-ordinate system, it seems inevitable that land usage data will ultimately become available in machine readable form. This process would be enhanced by the adoption of some standard categories of land use, which relate to the standards employed in a GIS, and which are generally applicable throughout the world.

The number of categories can be decided from both statistical and intuitive viewpoints which, in this instance, yield a similar result. Okumura's correction factors cover a range of about 30 dB and a good prediction model might be expected to achieve an accuracy characterised by a standard deviation of about 3 dB. Different categories must be separated by an amount similar to this standard deviation, giving about ten categories.

On a more subjective basis, consideration of the known effects of vegetation and buildings on radio propagation suggests the following characteristics should be used to distinguish between land usage types:

- vegetation density, e.g. a few trees or a dense forest,
- building density — fraction of area covered by buildings,
- building height.

This also leads to a ten point scale, which is shown in Table 1. Table 2 shows how this corresponds with the various categories employed by other organisations [1,3,6,7].

In order to determine the correction factors for each category, the approach has been as follows. First any land usage corrections used in the prediction method are suppressed. Measured and predicted path loss data for a particular base station site are then grouped according to land usage and the correction factors found as the average difference between measured and predicted values. The standard deviation illustrates the spread in the results, which is due to several factors. These include the intrinsic accuracy of the prediction model on different terrain profiles, the accuracy of determining the land usage category (often a subjective process), and how well the measured data represents the areas being considered.

As an example, data measured in the Ipswich area was used to derive correction factors, at 160 MHz, 900 MHz and 2 GHz, for a diffraction based model. The transmitter was mounted on the radio tower, 55 m AGL, at the British Telecom Research Laboratories, located some 7 km to the east of the town centre. The data was gathered by recording, with position information, the mean value of a block of 1024 samples, taken at 3.3 cm intervals, of the received power level from a CW transmission. These mean values were converted to path loss and assembled into blocks corresponding to squares on a 500 × 500 m grid. The use of a high base station in a relatively flat environment means that the results should be relatively immune to any additional diffraction loss arising from buildings along the path.

The land usage data was derived manually using a mixture of large scale maps, local knowledge, and site visits. Whilst this effort is justified for experimental work, it is probably unacceptable for routine system planning work. To avoid problems due to small, and potentially unrepresentative data, 500 m squares containing less than ten values are discarded, as are land usage categories represented by less than 50 squares. Thus, for this particular set of data, correction factors could only be obtained for land usage categories 1, 5, and 6 giving the results in Table 3, showing the average correction factors and their standards deviations in dBs.

It is worth noting that the correction factor, predictably, increases with increasing level of urbanisation (from category 1 to 6). This effect becomes more pronounced with increasing frequency. The accuracy of the predictions, indicated by the standard deviation, is

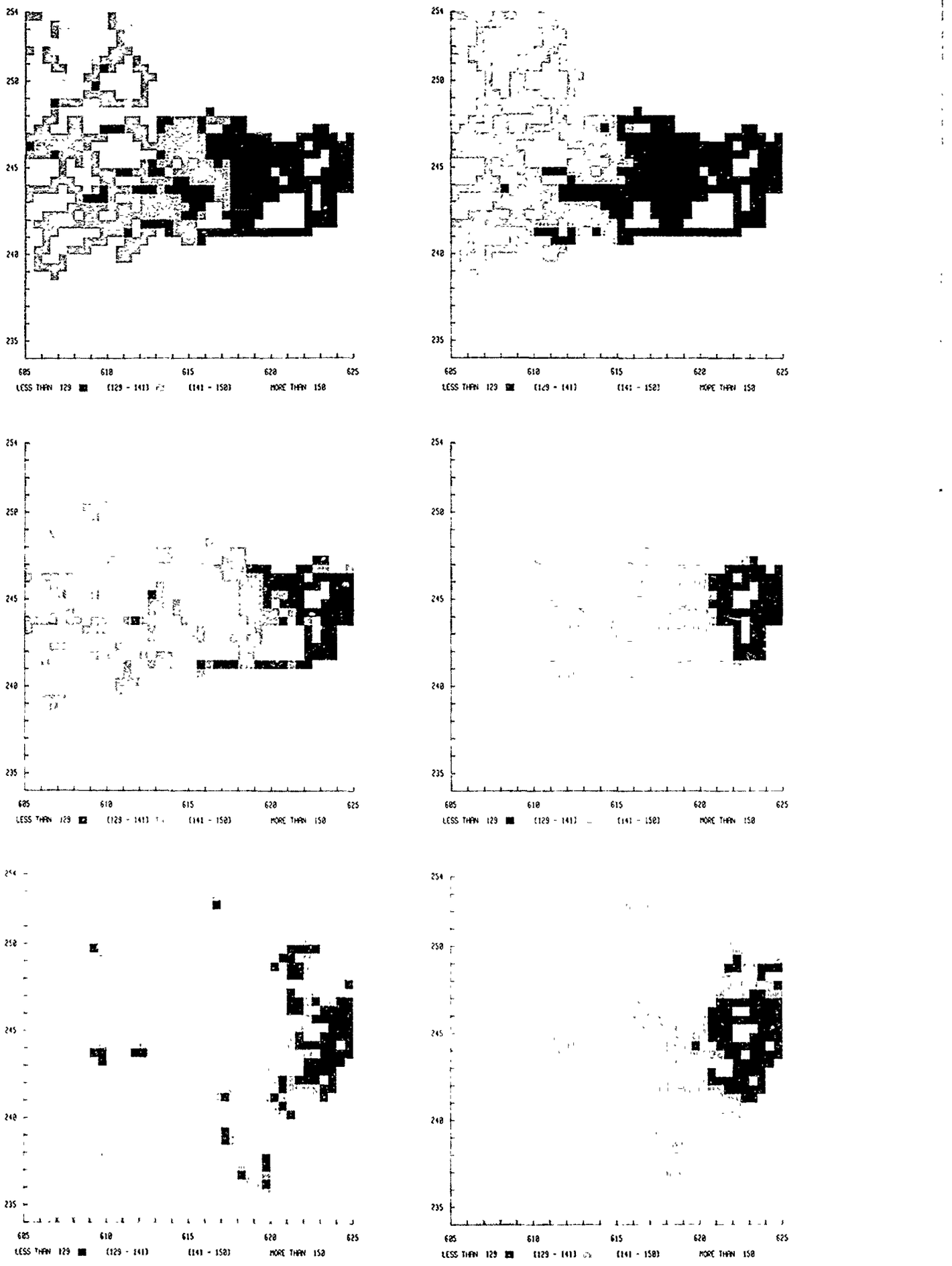

Fig 2 Comparison of measured (on the left) and predicted (right) path loss.

channel. The amplitudes of the direct signal and the echoes may undergo rapid fluctuations thereby altering the impulse response of the channel according to the speed of the mobile (and/or the scatterers). Therefore, a receiver has to be able to cope with the distortion arising from echoes in the channel as well as the rapid changes in the nature of this distortion. Such characteristics of the mobile radio channel are described by the 'power-delay profiles' and the 'Doppler spectra' which are obtained from wide-band channel sounding measurments.

From the works of Zadeh [8] Kailath [9], and Bello [10] it has been shown that a time-varying linear channel can be characterised in a systematic manner by a linear transversal filter. The output of this filter contains a sum of delayed and Doppler shifted versions of the input signal. The channel is then represented by what Bello calls the 'delay-Doppler-spread function'. This function (sometimes referred to as the 'scattering function') represents the multipath phenomenon in the three dimensions of time delay, Doppler frequency and power. It has been adopted in the more recent works of Cox [11] in the USA, and Parsons and Bajwa [12] in the UK. This formulation is particularly suitable for constructing a multipath simulator in the form of a dynamic transversal filter.

4. WIDE-BAND CHANNEL MEASUREMENT TECHNIQUES

4.1 Techniques

The various techniques used to measure the wide-band channel fall into three categories — unit impulse measurements, swept frequency measurements and cross-correlation techniques. The first of these requires high peak powers whilst swept frequency measurements can be time consuming, due to low sweep rates, and require the use of the Fourier transform to extract the impulse response. Correlation techniques offer increased sensitivity over the unit impulse methods as well as higher measurement rates and simpler data processing than the swept frequency measurements. Measurements using both pulse and correlation techniques are described in Berthoumieux et al [13], whilst results from the swept fequency technique are described in Matthews and Molkdar [14].

The correlation technique involves the transmission of a 'sounding' signal which consists of a carrier frequency modulated with a pseudo-random binary sequence. This is detected in the receiver which can use either a matched filter or a series of correlators to extract the impulse response. The use of a matched filter allows the impulse responses to be recorded in real time and places no practical limitation on the vehicle speed for collecting Doppler information. However, this requires fast sampling speeds and produces large amounts of data for storage before processing. The alternative to matched filter reception is to use PRBS correlators in the receiver. Early sounders using this technique employed multiple correlators working in parallel (one for each delay). A time-multiplexed correlator was developed by Bailey [15] to characterise the tropospheric channel at 2 GHz obviating the need for a number of correlators in the receiver. A similar type of sounder was used by Cox [11] to study multipath propagation at 910 MHz in a mobile radio environment. In this technique, the phase-keyed pseudo-random reference signal is swept by the incoming signal in the receiver producing a complex (in-phase and quadrature) analogue correlation output which is proportional to the true channel impulse response, but scaled in time. This is the type of sounder chosen by BTRL for the simplicity of its construction, lower transmitter power and recording bandwidth requirements and the relatively simple data logging and processing involved.

4.2 The BTRL sounder

The important parameters of the BTRL sounder are 911.25 MHz RF frequency, 5 Mbit/s chip rate, 255 bit PRBS sequency and 1 kHz clock offset giving a bandwidth reduction factor (time scaling) of 5000. Thus a complete record of the channel impulse response is obtained in its quadrature components in 255 ms. The resolution is 0.2 μs and the maximum delay measurable 51 μs. Time and frequency synchronisation between the transmitter and the receiver is provided by a pair of atomic frequency references capable of an accuracy of 1 part in 10^{11}. Quadrature components of the impulse response are recorded, along with timing and mobile receiver position information, on an analogue tape recorder. The recording is subsequently digitised in the laboratory and transferred to a microcomputer Figure 3 shows a schematic diagram of the sounder.

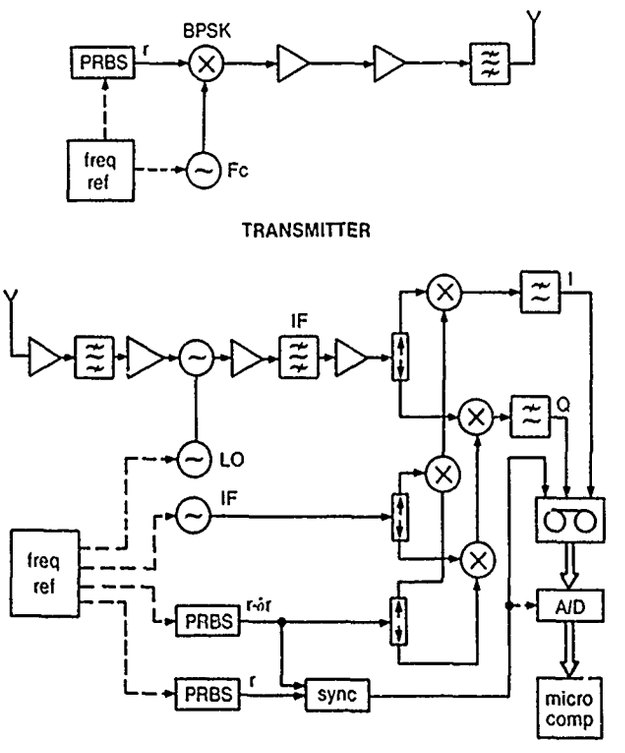

Fig 3 The sounder.

A knowledge of the receiver movement with respect to the position of the transmitter makes it possible to remove the line-of-sight propagation delay from the impulse responses during data processing. Although recorded in complex form (thus making it possible to calculate the Doppler spectra), only the amplitude of the channel impulse response has been processed in the form of 'power-delay profiles'.

4.3 Vehicle speed and averaging distance

It has been observed that the greatest change in the echo delay occurs when the mobile moves along the same or reciprocal bearing as the echo. Since the main concern is with echo delays that are greater than a few hundred nanoseconds (from a comparison of coherence bandwidths with the proposed GSM system bandwith and possible frequency hopping distances), changes in echo delays of a few tens of nanoseconds are of little importance. Therefore, it can be assumed that the channel impulse response is stationary over distances corresponding to such small variations in the delays as far as the macroscopic multipath structure is concerned. The resolution of the sounder represents a radial distance of 60 m. This has been used as the averaging distance to remove the Rayleigh fading leaving the slow fading or shadowing effects unchanged. Given that the sounder records four impulse responses per second a vehicle speed of up to 20-30 mph is possible with between 18 and 27 records averaged over a distance of 60 m.

On the other hand, to collect Doppler information accurately, a more severe restriction exists on the mobile speed. The measurement rate of four impulse responses per second, restricts the measurement of Doppler frequency to 2 Hz, and limits the vehicle speed to 2.4 km/h at 900 MHz. Clearly with such restrictions on the speed of the mobile, a practical measurement cannot be expected to collect the fast fading information required without risking the safety of the survey team in fast traffic conditions. For this reason the measurements reported here were taken at normal urban traffic speeds (20-30 mph) and the delay-Doppler information is not available.

5. ANALYSIS AND PRESENTATION OF THE MEASURED DATA

The aim of the measurements described here was to facilitate the specification, optimisation and planning of the GSM system. Thus care had to be taken to ensure they represented realistic conditions of use. The most important considerations were as follows.

- The transmitter power and the receiver sensitivity had to be compatible with the proposed system.
- The base station antennas had to be placed at realistic heights, i.e. not too low.
- The measurement locations would cover a range of terrain types and land usage variations.
- The size of the measurement area had to be appropriate for the location and land usage, e.g. smaller in urban areas than in rural ones.

Furthermore, the results must be presented in context of their geographical probability so that their significance from a system design and planning point of view is appreciated. For example, any performance criterion expressed in terms of a percentage of locations must be related to traffic density. Whilst this latter point is not addressed here, the results are presented in the form of cumulative distributions (CDs) providing an indication of the probability of occurrence in a given location.

The quantities 'mean delay' and the 'delay spread' as defined by Cox [11] had been used previously to present this type of data statistically However, these two parameters are not sufficient to describe some of the important characteristics of the channel. Recognising this fact, COST 207 has recommended [16,17] the use of two further parameters in the statistical analysis, to describe the length of the impulse response and the distribution of the energy within it. The first of these is the 'delay interval' defined as the length of the impulse response between two values of excess delay which mark the first time the amplitude of the impulse response exceeds a given threshold and the last time it falls below it. The other is the length of the middle portion of the power profile containing a certain percentage of the total energy found in that impulse response.

It is worth noting that the effects of noise and spurious signals in the system (from rf to data processing) can be very significant. Therefore, it is important to determine the noise/spurious threshold of the system accurately and to allow a safety margin on top of that.

In the analysis of the results reported here, minimum peak-to-spurious ratios of 15 dB for Keswick and 10 dB for London were used as acceptance criteria for a record to be included in the statistics. It should be pointed out that the highest-percentage delay window CDs and the lowest-threshold delay interval CDs should be interpreted with care, as these CDs contain entries closest to the spurious threshold of the system The lowest-threshold delay intervals are particularly sensitive in this respect because of the peak-to-spurious acceptance criterion mentioned above.

The measured impulse reponses were subjected to a qualitative evaluation by playing back the recorded components of the impulse responses through a quadrature modulator at a suitable IF to display the power-delay profiles on a network analyser (this also gave alogarithmic display). The use of a storage normaliser allowed the averaging to be implemented. This provided a quick, qualitative assessment of the location surveyed.

6. MEASUREMENTS IN AN URBAN AREA

The transmittter was located at a height of 58 m above ground, on the roof of a 15 storey building near Old Street station in north-east central London The ERP from the omni-directional antenna was 14 dBW (including an antenna gain of 8 dB). A 3 dB gain receiver aerial was mounted at around 1.2 m above ground, on the roof of a saloon car carrying the receiver. The route, lying in a dense urban area, varied between 1.6 and 3.2 km in distance from the transmitter.

Results for three sections of this route are presented. These sections were selected because they are appreciably different from each other in composition and yet sufficiently homogenous within each section. In each case, a sample impulse response is given together with CDs of the mean delay, delay spread, 50, 75 and 90% delay windows and -5, -7 and -12 dB delay intervals.

The first section runs along the Embankment between its junctions with Blackfriars Bridge and Waterloo Bridge and is just under 1 km long Most of this section is bordered on one side by the River Thames (200+ m wide) and on the other (transmitter) side by tall buildings and rising ground The majority of this section is characterised by a relatively high signal strength comprising an attenuated direct path due to shielding and a strong source of echoes from the far side of the river. A sample impulse response is shown in Fig 4. The CDs of the mean delay, delay spread, delay window and delay interval as defined above are also shown for this section of the route.

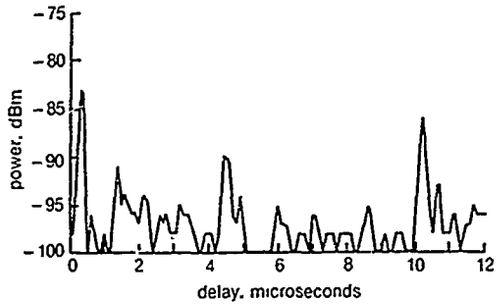

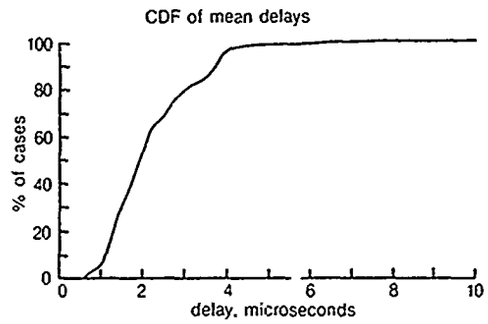

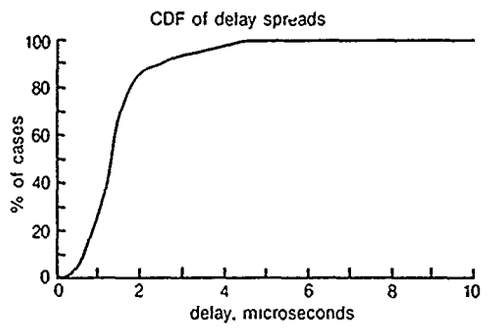

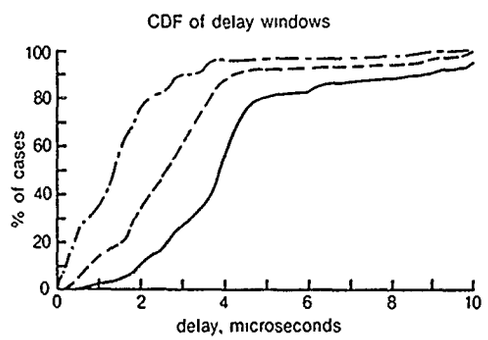

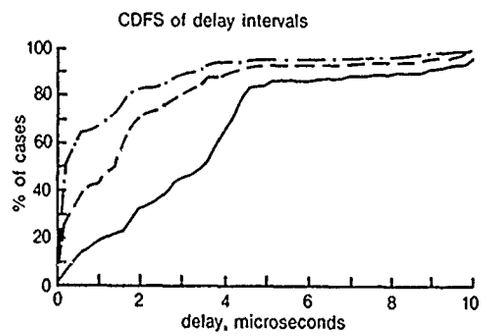

Fig 4 London: sample impulse response and cumulative distributions along the Embankment between Blackfriars and Waterloo Bridges.

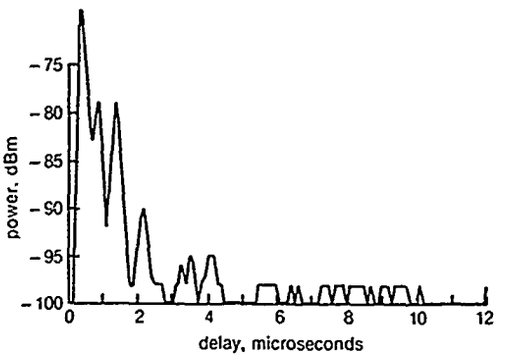

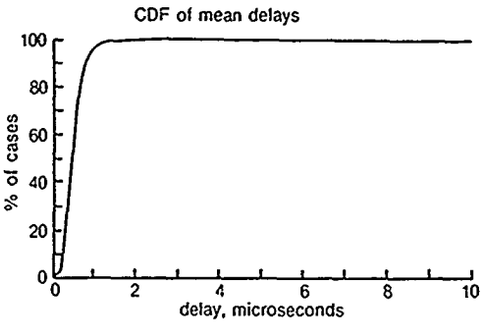

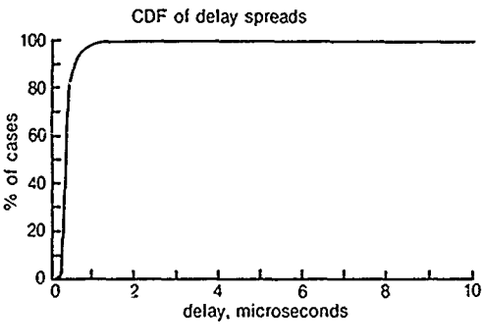

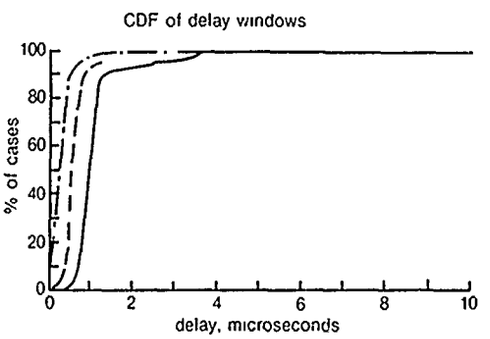

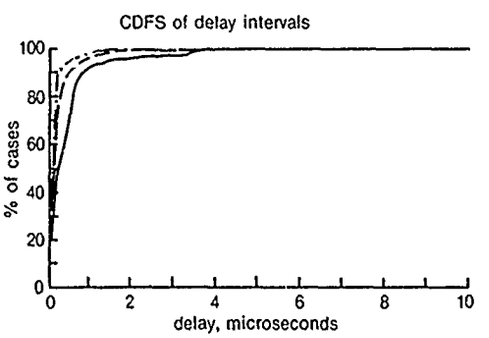

Fig 5 London: sample impulse response and cumulative distributions along the Embankment between Waterloo Bridge and the Houses of Parliament.

The second section of the route runs from Waterloo Bridge to the Houses of Parliament and is just over 1 km long. It is similar to the first section but lies almost radially to the transmitter. Consequently, a strong direct signal is observed and the delay spread reduces although a strong echo from the other side of the river is occasionally present. Figure 5 shows a sample impulse response from this section and the CDs of the four delay parameters.

The third section represents 'inland' parts of the route, lies along Long Acre near Covent Garden and is around 1 km long. This part of the route is substantially flat and heavily built up. Generally, the signal strength was low, often below the threshold of the sounder. Therefore, only a less detailed account is possible and this is represented by Fig 6.

7. MEASURMENTS IN A HILLY AREA

The area surrounding Keswick, in Cumbria, was chosen as the location for measurements in a hilly/mountainous ar . The transmitter was located just outside Keswick (about 1.5 km from the town centre) at the site of an IBA television transmitter. The height of the ground was 170 m above sea level (ASL), the antenna being mounted on a 10 m high mast. The ERP was 11 dBW including the 5 dB gain of the horizontally omni-directional antenna. The vertical beamwidth of the antenna was 18 ° with a 6 ° down-tilt. The surroundings were mainly farmland with partial blockage due west and north because of trees. The IBA mast, a 45 m lattice structure, was about 10 m away due south-west. During the measurements the weather was overcast, breezy but dry on the first day and wet with frequent rain showers on the second. The route, around 50 km long, lay in an area about 10 km by 15 km mostly within 5 km of the transmitter, the furthest point being around 12 km away. There were two lakes (70—80 m ASL) in the area surrounded by hills and mountains generally 200—500 m ASL with some peaks in the range 700—900 m ASL. The more gentle slopes were covered by farmland whereas the steeper hills were afforested. Most of the route lay on low ground, frequently along the edge of the lakes. Height contours for the area were used to check the path profiles for line-of-sight from the transmitter to the points along the route. A total of approximately 50% of the route was found not to have line-of-sight. However, it should be pointed out that some of the distant parts of the route which did not have line-of-sight to the transmitter did not yield useable data either.

Data from the whole route was analysed in 500 record blocks representing up to 2.2 km of road distance travelled (for a maximum vehicle speed of 40 mph). Three such blocks have been selected for presentation here representing 'better than typical', 'worse than typical' and 'typical' parts of the route. This categorisation is based on a subjective assessment made from a study of the impulse responses observed and the CDs obtained following the statistical analysis of the data and its correspondence with system performance may not be exact. The typical category represents approximately 50% of this route whilst 20% is better and 30% worse than typical. In each case, a sample impulse response is included to give a direct impression of the channel. This is accompanied by the usual four CDs of the mean delay, delay spread, 50, 75 and 90% delay windows and -10, -12 and -15 dB delay intervals.

Figure 7 shows results from a 'better than typical' part of the route when the channel is relatively 'quiet'. Few echoes are present and they are much smaller than the direct signal. The corresponding CDs reflect the absence of long excess delays. 75%-window and -12 dB interval CDs show that almost all excess delays are under 1 μs.

The channel can, at times, contain a large number of echoes, some ranging up to 30 μs although the amplitudes of such echoes are rarely large compared with the direct signal. Such 'worse than typical' parts of the route can be represented by the CDs of Fig 8 which shows 90% of 75%-windows to be under 18 μs and 90% of -12 dB intervals under 14 μs.

On average, this route may best be characterised by the CDs of Fig 9. The sample impulse response shows most of the energy to be concentrated around the direct signal, nominally within 10 μs. The mean and spread CDs show 90% of the mean delays to be under 2 μs and 90% of the delay spreads under 5 μs. The 75% delay windows as well as -12 dB delay intervals indicate values under 3 μs for 90% of the time.

8. CONCLUSIONS

Because of the increased operational requirements and the particular characteristics of digital systems, the system planner must adopt additional methods and a higher degree of precision when planning future mobile communications systems. The requirements may be summarised as follows:

- accurate prediction of signal strength in open areas, inside buildings and in public transport,
- accurate prediction of interference, particularly in small cell arrangements in urban areas,
- prediction of distortion that would degrade system performance even if the above two points were adequate.

The first two points above require advances in path loss prediction techniques such as the incorporation of correction factors based on land usage. To facilicate the widespread availability of land usage data a ten point scale has been proposed illustrating how empirical correction factors can be derived from measured data. The widespread application of this technique requires that reliable land usage information be available in machine readable form, perhaps from a geographic information system.

An additional requirement for digital systems is to relate the system's ability to cope with distortion and interference to the distortion and interference present at a particular location. This, in turn, requires a statistical knowledge of the variability and magnitude of the multipath propagation and a knowledge of the values of the parameters that define the limits of the system's performance. In this context, the concept of a signature as used for terrestrial microwave radio relay systems is a useful starting point although there is considerable need for enhancement both in providing realistic dynamic stress as well as additional echo paths.

Work is under way to gather the propagation data and develop the planning tools required. The results of measurements at two locations have been presented. Slow speed measurements are necessary to obtain Doppler information, but higher speed measurements can provide useful information on delay/power profiles that characterise different environments. There remains the need to develop a prediction model for the performance of digital systems based on topographic and land usage information using either empirical, or analytic methods.

From the results presented here it is possible to draw some comparative conclusions and to offer a subjective assessment of the mobile radio channel at 900 MHz. As expected, longer delays have been measured in the hilly environment of Keswick than in dense-urban central London. Although excess delays reaching 10 μs have been seen in London, in the majority of cases the delays are of the order of

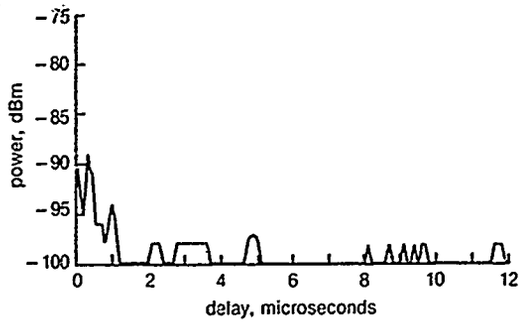

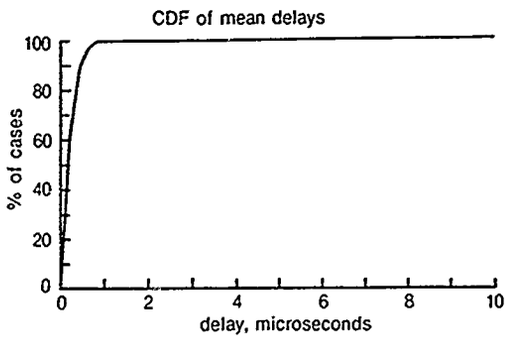

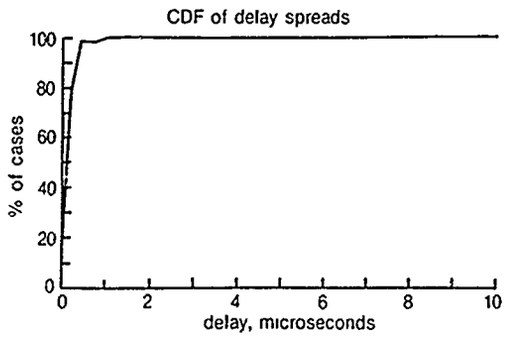

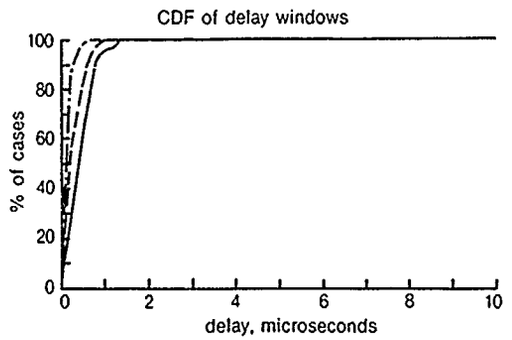

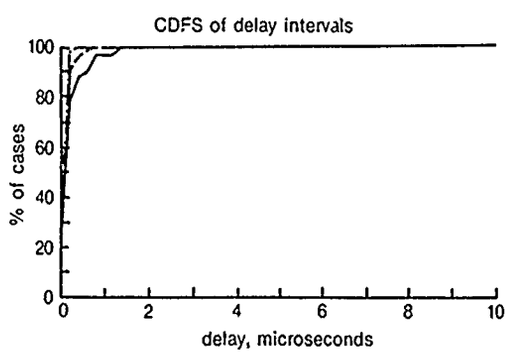

Fig 6 London. sample impulse response and cumulative distributions along Long Acre near Covent Garden.

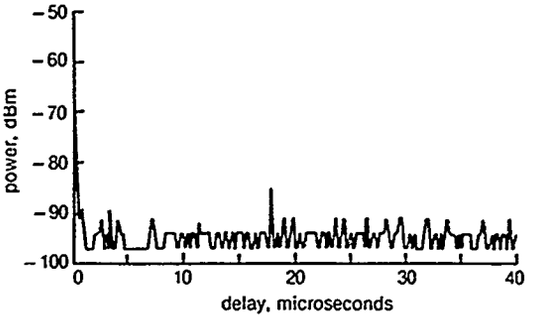

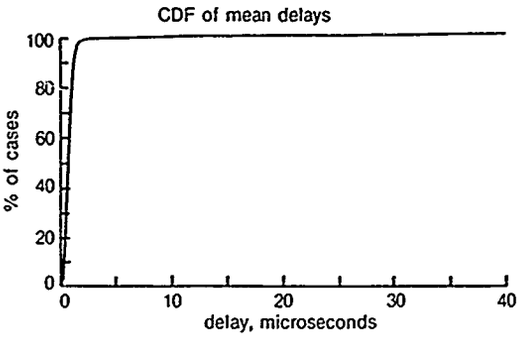

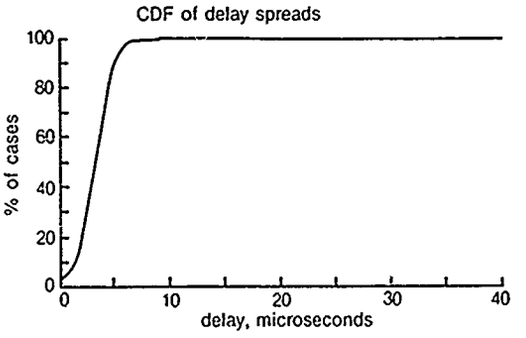

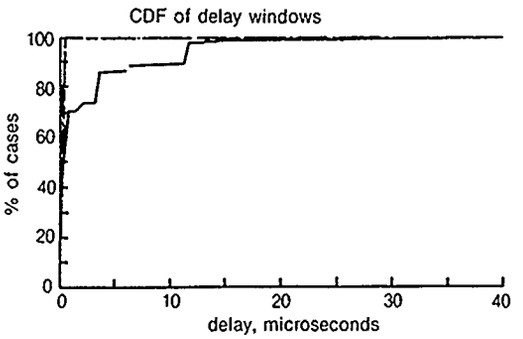

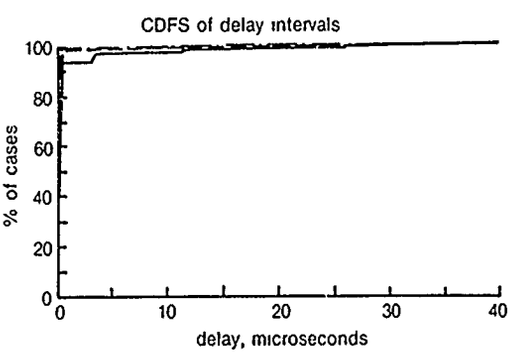

Fig 7 Keswick. sample impulse response and cumulative distributions representing better than typical sections of the route.

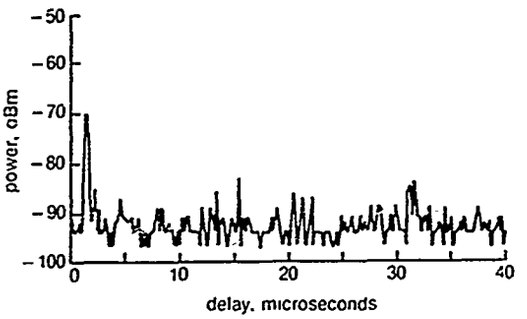

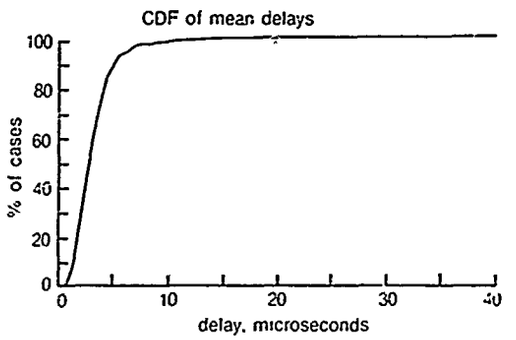

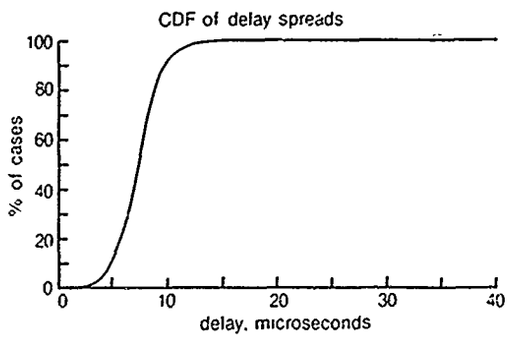

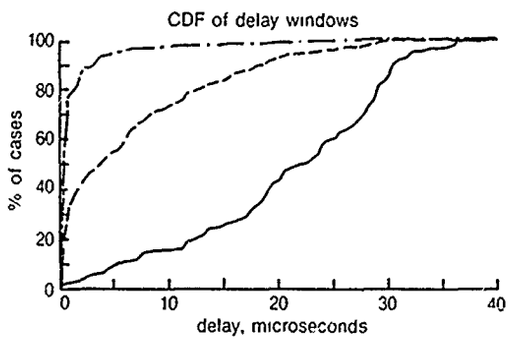

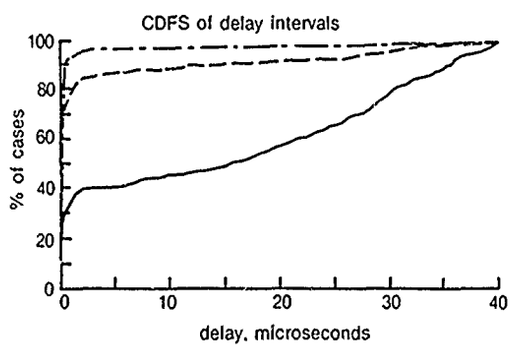

Fig 8 Keswick: sample impulse response and cumulative distributions representing worse than typical sections of the route.

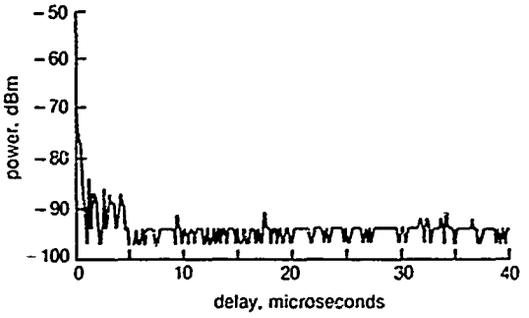

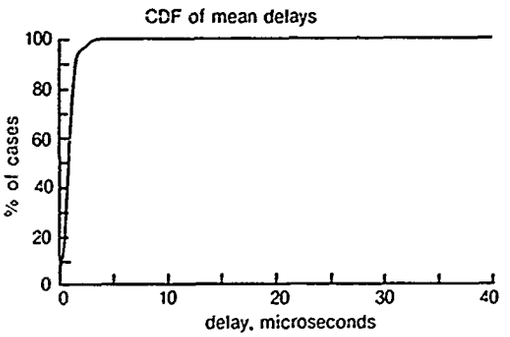

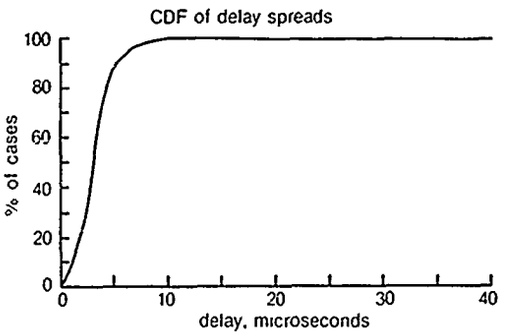

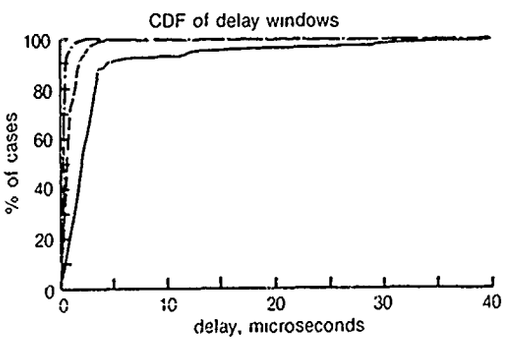

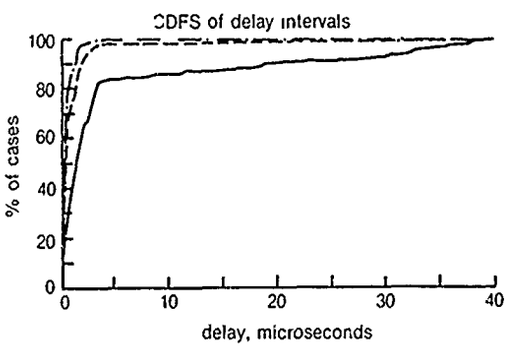

Fig 9 Keswick. sample impulse response and cumulative distributions representing the typical sections of the route.

a few microseconds. For the route around Keswick, a figure of 10 μs may be more appropriate despite the presence of longer echoes sometimes reaching 30 μs.

One significant feature of these results is the variability of the channel over relatively short distances (1—2 km). This means that the planning of the operational systems will require more location-specific information on the channel. Careful selection of the base station locations as well as the antenna heights and radiation patterns will help minimise the effects of multipath distortion and maximise the quality of service.

REFERENCES

1 Okumura Y, Ohmori E, Kawano T and Fukuda K. 'Field strength and its variability in VHF and UHF land mobile radio service , Review of the Electrical Communication Laboratory, 16, 9—10, (September—October 1968).

2 Ibrahim M F and Parsons J D. 'Signal strength prediction in built-up areas — part 1 — median field strength', IEE Preceedings, Part F, 130, No 5, (August 1983).

3 King R W and Causebrook J H. 'Computer Programs for UHF Co-channel interference prediction using a terrain data bank', BBC Research Report, BBC RD 1974/6.

4 Longley A G and Rice P L. 'Prediction of tropospheric radio transmission loss over irregualr terrain — a computer method', ESSA Technical report ERL 79 — ITS 67, (1968).

5 Lord Chorley (Chairman): 'Handling geographic information', HMSO, London, (1987).

6 Lorenz R W. 'Field Strength Prediction Program DBPR1, COST 207 technical document', COST 207 TD(86)#02, (1986).

7 Juul-Nyholm G. Land usage figures for use in field strength prediction as measured in Denmark', COST 207 technical document, COST 297 TD(86)28, (1986).

8 Zadeh L A: 'Frequency analysis of varible networks', Proc IRE, 38, pp 291—299 (March 1950).

9 Kailath T. Sampling models for linear time variant filters', MIT Research Lab of Electronics, Cambridge, Mass., Report no 352 (May 1959).

10 Bello P A. Characterisation of randomly time variant linear channels', IEEE Trans on Communication Systems, CS-11 pp 360—393 (December 1963).

11 Cox D C. Time and frequency domain characterisation of multipath propagation at 910 MHz in a suburban mobile radio environment', Radio Science, 7, No 12, pp 1069—1077, (December 1972).

12 Parsons J D and Bajwa A S. 'Wideband characterisation of fading mobile radio channels', IEE Proc Part F, 129, No 2, pp 95—101, (April 1982).

13 Berthoumieux D, Huish P W, Hultnen R and Mawira A. 'Wideband mobile radio channel characterisation', Proceedings of the International Conference on Digital Land Mobile Radiocommunications, Venice (June 1987).

14 Matthews P and Molkdar D. Wideband measurements of the UHF mobile radio channel', IEE International Conference on Antennas and Propagation, ICAP'87, York, UK (March 1987).

15 Bailey C C. 'Characterization of troposcatter channels by impulse response measurement', AGARD Conference Proc, Part II, pp 39-1 to 39-11, Germany (August—September 1970).

16 Lorenz R W et al. 'Evaluation of delay profiles in mountainous terrain', COST 207 technical document, COST 207 TD(87)16 (May 1987).

17 Lorenz R W '12th report of the working group on propagation', COST 207 technical document, COST 207 TD(87)#30 (May 1987).

ANALYSE LARGE BANDE DE LA PROPAGATION DES ONDES DE SOL DANS LA BANDE 150-400 MHz

D. SORAIS
THOMSON-CSF/DTC
66, rue du Fossé Blanc
92231 GENNEVILLIERS
France

RESUME

La propagation large bande par ondes de sol est étudiée dans une zone géographique semi-rurale en mesurant la réponse impulsionnelle complexe entre une station fixe et un mobile. On présente les distributions des principaux estimateurs statistiques pour 150, 250 et 400 MHz. Par ailleurs, l'analyse des multitrajets présents et l'identification de leur cause physique est réalisée pour des lieux de mesures particuliers.

1. INTRODUCTION

Pour une source d'émission donnée, un mobile ou une station tactique reçoivent l'onde directe ainsi que des échos dus à la topographie du terrain et aux constructions liées à l'activité humaine. Les multitrajets créés limitent les performances des systèmes de transmissions large bande ou de localisation. Lorsque l'on réalise une transmission numérique vers un mobile il existe, en absence d'égalisation, un rythme binaire de transmission maximum lié à l'étalement temporel dû aux multitrajets. Une transmission par étalement PN sera particulièrement vulnérable au moment de la prise de synchronisation lorsque le retard associé au pic dominant fluctue rapidement le long du chemin. Pour un système de goniométrie bande étroite par interférométrie un écho de faible amplitude relative peut causer une erreur de localisation importante.

Il résulte de ces éléments que l'analyse large bande de la propagation des ondes de sol est essentielle pour estimer les performances de matériels existants ou spécifier les caractéristiques de matériels nouveaux. Les systèmes radioélectriques liés à la propagation par ondes de sol et à des antennes omnidirectionnelles en azimut utilisent principalement des fréquences inférieures à 1 GHz. Pour les fréquences inférieures à 30 MHz la propagation par ondes de sol est plus ou moins fortement couplée à la propagation ionosphérique. Compte tenu de la complexité des phénomènes toute expérimentation devrait être spécifiquement développée en vue d'une application particulière. Les résultats d'expérimentations autour de 900 MHz étant nombreux, l'Administration française a donc décidé de faire réaliser des mesures dans la bande 30-400 MHz pour laquelle les données expérimentales disponibles sont insuffisantes. La première phase de l'expérimentation a été effectuée dans la bande 150-400 MHz. La seconde phase sera ultérieurement réalisée dans la bande 30-88 MHz.

On présente dans ce papier des résultats concernant la première phase de l'expérimentation réalisée dans une zone géographique semi-rurale (Vallée de Chevreuse) sur trois fréquences égales à 150, 250 et 400 MHz.

2. DESCRIPTION DE L'EXPERIMENTATION

La réponse impulsionnelle complexe du canal $h_c(\tau)$ est estimée par une technique de corrélation en transmettant une séquence binaire PN de longueur maximale modulée en BPSK. En réception le signal reçu est corrélé avec une réplique de la séquence transmise en utilisant une ligne SAW. On exploite uniquement le module $h_m(\tau)$ de l'enveloppe complexe en sortie du corrélateur :

$$(1) \qquad |h_m(\tau)| = |h_c * b|$$

La fonction $b(\tau)$ traduit l'influence des filtres d'émission et de réception ainsi que de la fonction d'autocorrélation de la séquence transmise .Les principales caractéristiques du banc de mesure sont résumées ci-après :

* Puissance moyenne émission : 100 W

* Antennes
  - Emission : Log-périodique G = 9 dBi
  - Réception : (150 MHz —> Ground-plane
    (250/400 MHz —> Dipôle
  - Polarisation verticale

* Séquence PN
  - 150 MHz —> 63 moments de 200 ns
  - 250/400 MHz —> 127 moments de 50 ns

Les antennes de réception placées sur le mobile ont un diagramme de rayonnement omnidirectionnel à $\pm$ 2 dB près.

Pour un chemin donné de déplacement du mobile on réalise l'enregistrement des modules de la réponse impulsionnelle complexe en des points régulièrement espacés de mètre environ. On effectue successivement cet enregistrement pour les trois fréquences d'expérimentation sur une distance d'environ 300 mètres. L'expérimentation a été réalisée sur 28 chemins de mesure répartis dans une zone géographique faiblement vallonnée et fortement boisée. Le paramètre Δh caractérise le degré d'irrégularité du terrain. Ce paramètre, estimé suivant le méthode de Longley et Rice ([15]) est compris entre 15 et 50 mètres. Les distances moyennes entre l'émetteur et les 28 chemins de mesures sont comprises entre 1.5 et 10 Km.

L'analyse des résultats expérimentaux requiert implicitement que la fonction de corrélation fréquence-temps du canal, formée à partir de la fonction de transfert équivalente basse fréquence, soit quasi-stationnaire en temps et en fréquence (canal QWSSUS [13]). La fonction diffusion retard du canal $u_c(\tau)$ exprime la puissance moyenne reçue en fonction du retard :

$$(2) \qquad u_c(\tau) = \frac{1}{2} \cdot E\left[|h_c(\tau)|^2 \right]$$

On notera $u_m(\tau)$ la fonction diffusion retard qui prend en compte l'influence du banc de mesure sur l'estimation de $u_c(\tau)$:

$$(3) \qquad u_m(\tau) = \frac{1}{2} \cdot \frac{E\left[|h_m(\tau)|^2\right]}{\int_{-\infty}^{+\infty} |b(\tau)|^2 d\tau} = \frac{|b(\tau)|^2 * u_c(\tau)}{\int_{-\infty}^{+\infty} |b(\tau)|^2 d\tau}$$

L'hypothèse ergodique permet d'estimer la valeur de la fonction diffusion retard $u_m(\tau)$ sur un tronçon de chemin de longueur 2 L centré sur l'abscisse curviligne So :

$$(4) \qquad u_m(\tau) \simeq \frac{1}{2} \cdot \frac{\frac{1}{2L} \cdot \int_{s_0-L}^{s_0+L} |h_m(\tau, s)|^2 \cdot ds}{\int_{-\infty}^{+\infty} |b(\tau)|^2 d\tau}$$

L'intégrale (4) est évaluée à partir des N échantillons de la réponse impulsionnelle mesures sur la distance 2 L.

La valeur moyenne P_{rm} de la puissance efficace reçue sur un tronçon de chemin (2 L $\geq$ 20 λ par exemple) lorsque l'on transmet une porteuse pure d'amplitude unité permet de définir l'atténuation de propagation de la liaison. Cette puissance P_{rm} s'exprime en fonction de $u_m(\tau)$:

$$(5) \qquad P_{rm} = \int_{-\infty}^{+\infty} u_m(\tau)\, d\tau$$

3. DISTRIBUTION DES PRINCIPAUX ESTIMATEURS STATISTIQUES DU CANAL

3.1. Retard moyen et étalement temporel

Le retard moyen $\bar{\tau}$ et l'étalement temporel σ_τ sont définis par les relations :

$$(6) \qquad \bar{\tau} = \frac{1}{P_{rm}} \cdot \int_{-\infty}^{+\infty} \tau \cdot u_m(\tau)\, d\tau \qquad (7) \qquad \sigma_\tau^2 = \frac{1}{P_{rm}} \cdot \int_{-\infty}^{+\infty} (\tau - \bar{\tau})^2 \cdot u_m(\tau)\, d\tau$$

Pour chaque tronçon de chemin élémentaire on obtient un profil puissance moyenne - retard (c'est à dire $u_m(\tau)$)pour lequel les paramètres $\bar{\tau}$ et σ_τ sont calculés. Les distributions du retard moyen et de l étalement temporel sont respectivement représentées par les histogrammes des Fig. 1 a -> c et des Fig. 2 a -> c pour les trois fréquences de l'expérimentation (150, 250 et 400 MHz). Le tableau ci-dessous fournit une synthèse des résultats :

Fréquences MHz	Nombre de profils	Retard moyen µs			Etalement temporel µs		
		Valeur moyenne	Ecart type	Valeur maximale	Valeur moyenne	Ecart type	Valeur maximale
150	152	0.5	1.2	5.6	0.85	1.3	5
250	336	0.2	0.5	4.1	0.4	0.55	3
400	252	0.15	0.4	2.2	0.3	0.45	2.6

Bien qu'en moyenne faible, l'étalement temporel prend des valeurs élevées pour quelques configurations de terrain pour lesquelles on obtient simultanément une onde de retard minimum fortement atténuée avec des échos arrière d'amplitudes élevées. Pour ces configurations les mesures à 250 MHz, et surtout à 400 MHz, étaient parfois trop bruitées pour être exploitées. L'accroissement de l'atténuation avec la fréquence est donc la principale raison de la diminution de la valeur moyenne de l'étalement temporel lorsque la fréquence augmente.

3.2. Bande de cohérence

Pour un canal QWSSUS la transformée de Fourier de $u_m(\tau)$ est égale à la fonction de corrélation fréquence $R_{Hm}(\Delta f)$. En utilisant la relation (3) on obtient :

$$(8) \qquad R_{Hm}(\Delta f) = \frac{R_{Hc}(\Delta f) \cdot R_B(\Delta f)}{\int_{-\infty}^{+\infty} |B(f)|^2 df} \; ; \qquad R_B(\Delta f) = \int_{-\infty}^{+\infty} B^*(u) \cdot B(u + f)\, du$$

avec $B(f) = \mathcal{F}[b(\tau)]$

La fonction d'autocorrélation $R_B(\Delta f)$ traduit l'influence du banc de mesure sur la fonction de corrélation fréquence $R_{Hm}(\Delta f)$ estimée. La bande de cohérence du canal B_c est définie comme la largeur du module de la fonction de corrélation fréquence $R_{Hc}(\Delta f)$ du canal (largeur à 0.9 ou 0.5).

La distribution des bandes de cohérence à 0.9 sont représentées par des fonctions cumulées pour les trois fréquences de l'expérimentation (Fig. 3). Les résultats obtenus sont résumés ci-après :

Fréquences MHz	Bande de cohérence à 0.9 (kHz)	
	Valeur minimale	Pour 10 % des lieux $B_c \leqslant$
150 MHz	15	30
250 MHz	24	130
400 MHz	27	110

4. ANALYSE DES MULTITRAJETS PRESENTS SUR DEUX LIEUX DE MESURES

4 1. Exemple 1

L'étalement temporel le plus élevé a été obtenu à 150 MHz pour un chemin de mesures situé dans le plan de propagation sur le flanc d'une colline (Fig. 4). Le retard moyen et l'étalement temporel demeurent très importants sur la totalité du chemin (Fig. 5).

Pour un écho de retard donné il est possible de déterminer, par continuité, l'évolution de ce retard sur le chemin de mesures. Le tracé des ellipses des lieux géométriques des diffuseurs au début et à la fin du chemin permet de localiser la zone géographique produisant l'écho. Les fonctions diffusions retard au début (Fig 6 a) et à la fin du chemin (Fig. 6 b) font apparaître un écho de forte amplitude dont l'évolution du retard $\delta\tau$ avec la distance est représentée sur la Fig. 7. Cette évolution $\delta\tau$ variant comme $2d/c$ il est probable que l'écho analysé est dû à une zone de diffusion arrière située dans le plan du grand cercle (voir Fig. 8). La puissance totale reçue (Puissance P_{rm} définie au § 2) sur le chemin d'analyse est d'environ 10 dB supérieure à la puissance de l'onde de retard minimum (Fig. 9). Les fortes erreurs de prévision des programmes de calcul d'atténuation de propagation sont notamment dues à ce type de configuration de terrain.

4.2. Exemple 2

Pour cet exemple le chemin de mesures est perpendiculaire au plan de propagation. Le profil moyen du terrain est représenté Fig. 10. L'évolution du retard moyen et de l'étalement temporel avec la distance (Fig. 11 a et b) montre que ces paramètres augmentent rapidement pour les distances supérieures à 180 mètres environ aux fréquences égales à 250 et 400 MHz, tandis que pour 150 MHz, les deux paramètres évoluent très peu. Le retard associé au principal écho qui détermine les fortes valeurs de l'étalement temporel à 250 et 400 MHz est quasiment constant sur toute la longueur du chemin. De même que pour l'exemple précédent l'écho est donc produit par une zone de diffusion arrière située dans le plan du grand cercle (la direction de ce plan varie très légèrement sur le chemin de mesure). Pour 250 et 400 MHz la puissance de l'onde de retard minimum décroît fortement pour les distances supérieures à 180 m tandis que celle de la fréquence 150 MHz reste constante (voir Fig. 12). L'atténuation par diffraction, plus faible à 150 MHz qu'à 250 MHz ou 400 MHz, semble donc expliquer la valeur quasi-constante de l'étalement temporel à 150 MHz.

5. CONCLUSIONS

Les multitrajets présents sur la zone géographique analysée sont très irrégulièrement distribués. Bien que faible pour la plupart des chemins de mesure, l'étalement temporel peut prendre de fortes valeurs lorsqu'il se produit simultanément une forte atténuation de l'onde de retard minimum et des échos arrière. L'étalement temporel moyen diminue lorsque la fréquence augmente du fait que pour les plus hautes fréquences on obtient souvent des enregistrements non exploitables (S/B insuffisant) pour les lieux où les multitrajets sont importants. L'examen de ces enregistrements bruités montre qu'avec une puissance d'émission nettement plus élevée l'étalement temporel moyen à 400 MHz serait du même ordre de grandeur qu'à 150 MHz. L'identification des principaux diffuseurs produisant des retards discernables par le banc de mesure est notamment très utile pour le développement des logiciels de calculs d'atténuation de propagation.

6. REMERCIEMENTS

Cette étude a été réalisée suite à un contrat émanant de la Direction des Recherches Etudes et Techniques (DRET).

7. BIBLIOGRAPHIE

1 C. COX * DISTRIBUTIONS OF MULTIPATH DELAY SPREAD AND AVERAGE EXCESS DELAY FOR 910 MHz URBAN MOBILE RADIO PATHS, IEEE Trans. on antennas and propagation Vol. : AP-23; March 75,

2 C. COX - P. LECK * CORRELATION BANDWITH AND DELAY SPREAD MULTIPATH PROPAGATION STATISTICS FOR 910 MHz URBAN MOBILE RADIO CHANNELS, IEEE Trans. on communications Vol. COM-23; November 75,

3 C. COX * 910 MHz URBAN MOBILE RADIO PROPAGATION : MULTIPATH CHARACTERISTICS IN NEW YORK CITY, IEEE Trans. on communications, Vol. : COM-21, November 73.

4 C. COX * TIME AND FREQUENCY-DOMAIN CHARACTERIZATIONS OF MULTIPATH PROPAGATION AT 910 MHz IN A SUBURBAN BILE-RADIO ENVIRONMENT. Radio Science, Vol. 7, Number 12, December 72,

5 DAVIES et al. * PROPAGATION AT 500 MHz FOR MOBILE RADIO -IEE Proceedings, Vol. 132 - August 85 -

6 W.R. YOUNG - L.Y. LACY *ECHOES IN TRANSMISSION AT 450 MHz FROM LAND TO CAR RADIO UNITS, Proceedings of the IRE, March 50,

7 TURIN et al. *A STATISTICAL MODEL OF URBAN MULTIPATH PROPAGATION. IEEE Transactions on vehicular technology, Vol. : VT-21; February 72

8 SUZUKI * A STATISTICAL MODEL FOR URBAN RADIO PROPAGATION IEEE Transactions on communications, Vol. COM-25, July 77.

9 BAJWA * UHF WIDEBAND STATISTICAL MODEL AND SIMULATION OF MOBILE RADIO MULTIPATH PROPAGATION EFFECTS. IEE Proceedings, Vol. 132 ; August 85.

10 ZANDER * A STOCHASTICAL MODEL OF THE URBAN UHF RADIO CHANNEL. IEEE Trans. on vehicular technology, Vol. : VT-30 November 81.

11 CLARKE * A STATISTICAL THEORY OF MOBILE-RADIO RECEPTION. BSTJ., Juillet-Août 68.

12 W.C. JAKES * MICROWAVE MOBILE COMMUNICATIONS. NEW YORK : WILEY 1974

13 BELLO * CHARACTERIZATION OF RANDOMLY TIME LENEAR CHANNELS. IEEE Trans. on communications. Vol. : CS 11 - December 63.

14 SCHWARTZ * COMMUNICATION SYSTEMS AND TECHNIQUES. MAC GRAW HILL 1966.

15 LONGLEY et RICE * PREDICTION OF TROPOSPHERIC RADIO TRANSMISSION LOSS OVER IRREGULAR TERRAIN. Institute for Telecommunication Sciences, NTIDS - AD - 676 874

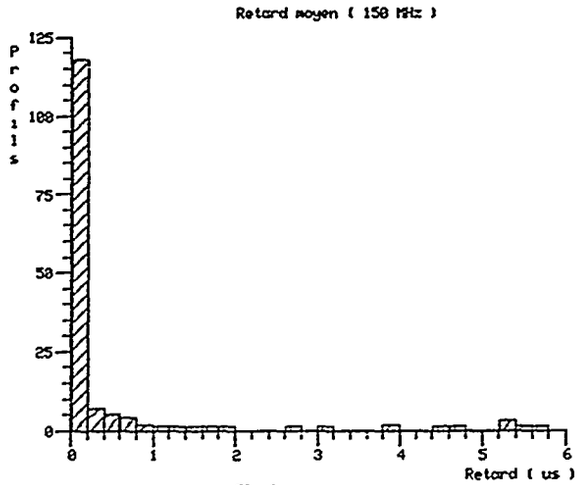

Fig 1 a

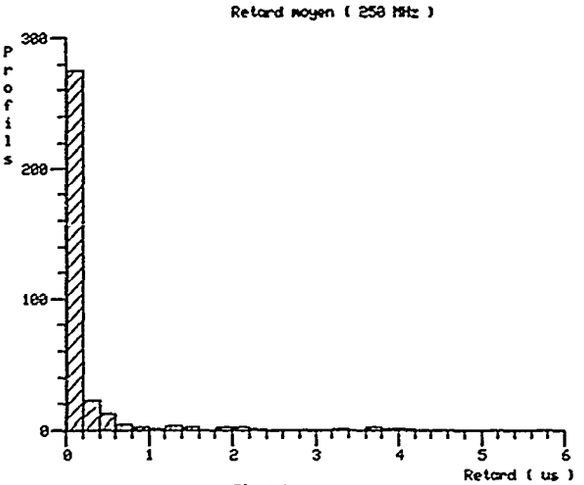

Fig 1 b

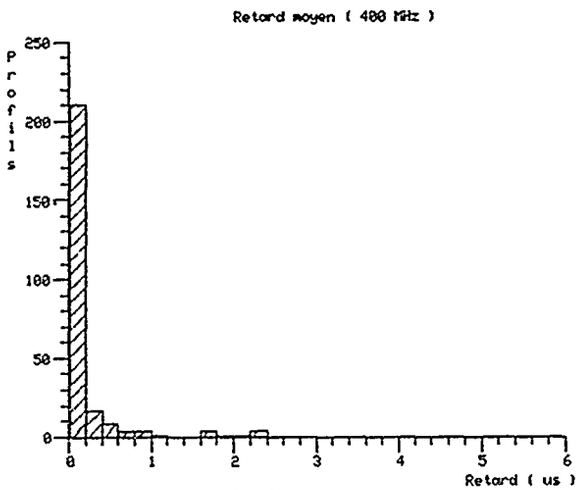

Fig 1 c

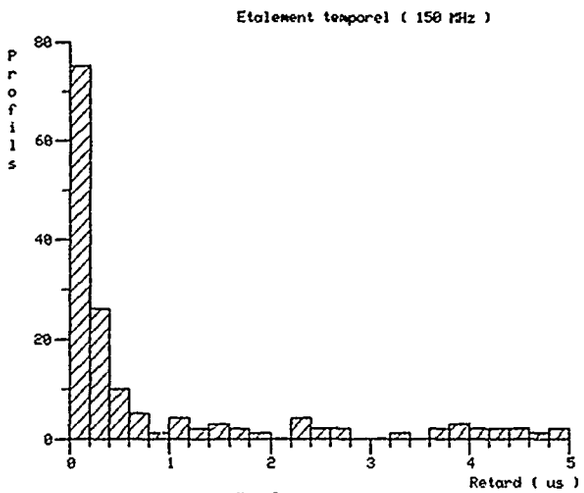

Fig 2 a

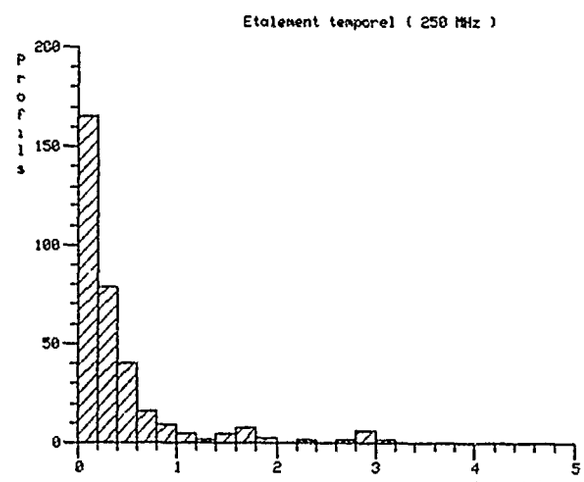

Fig 2 b

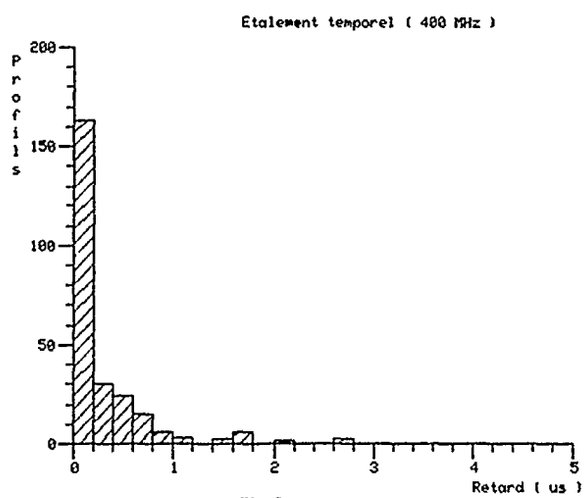

Fig 2 c

BANDE DE COHERENCE A 0.9

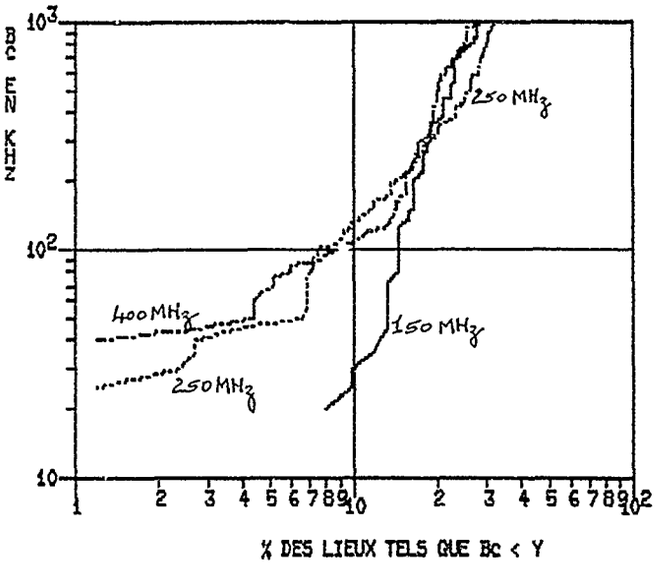

Figure 3

Exemple 1 - Profil du terrain

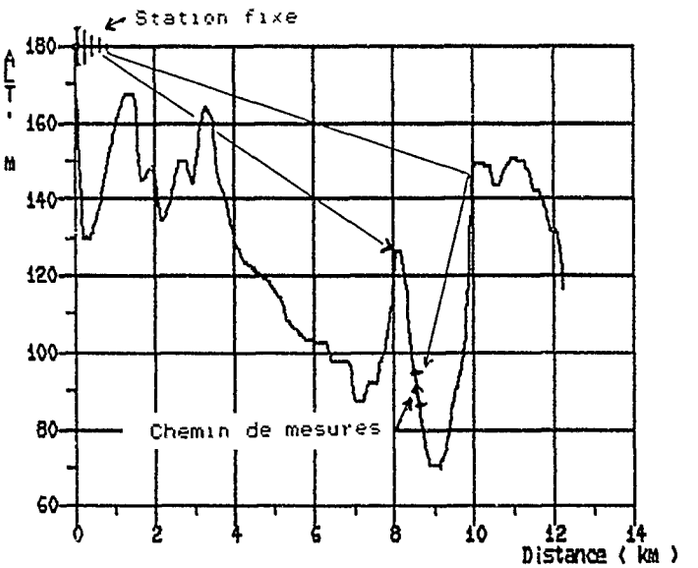

Figure 4

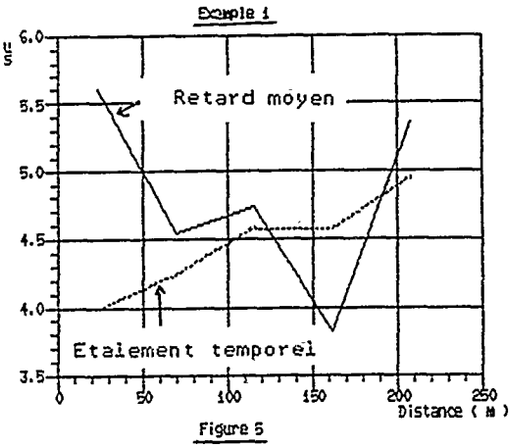

Figure 5

Exemple 1

Fonctions diffusion "retard" au debut et a la fin du chemin

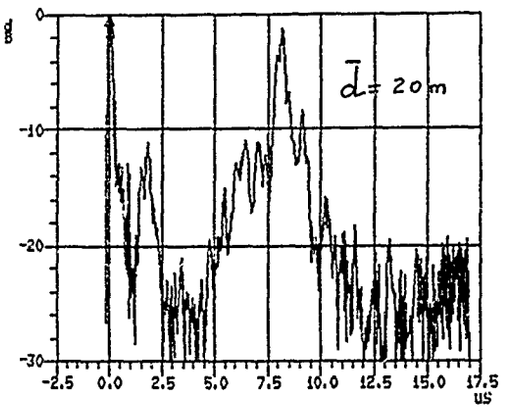

Figure 6 a

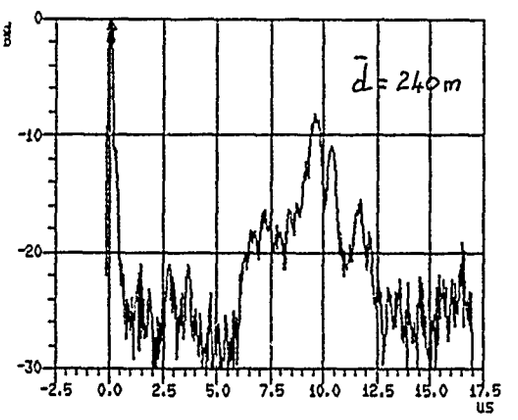

Figure 6 b

Exemple 1

Evolution du retard de l'echo principal le long
du chemin de mesures
(Valeurs successives liees a la fonction diffusion "retard")

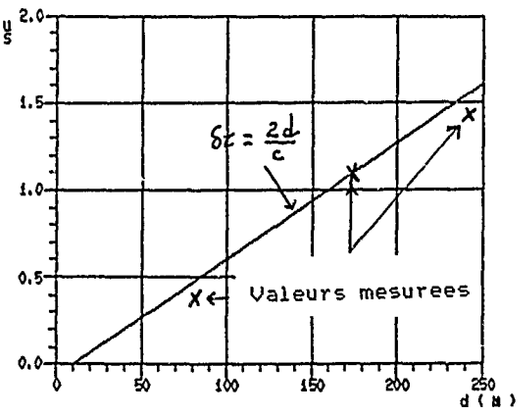

Figure 7

Exemple 1 - Identification de la cause de l'echo principal

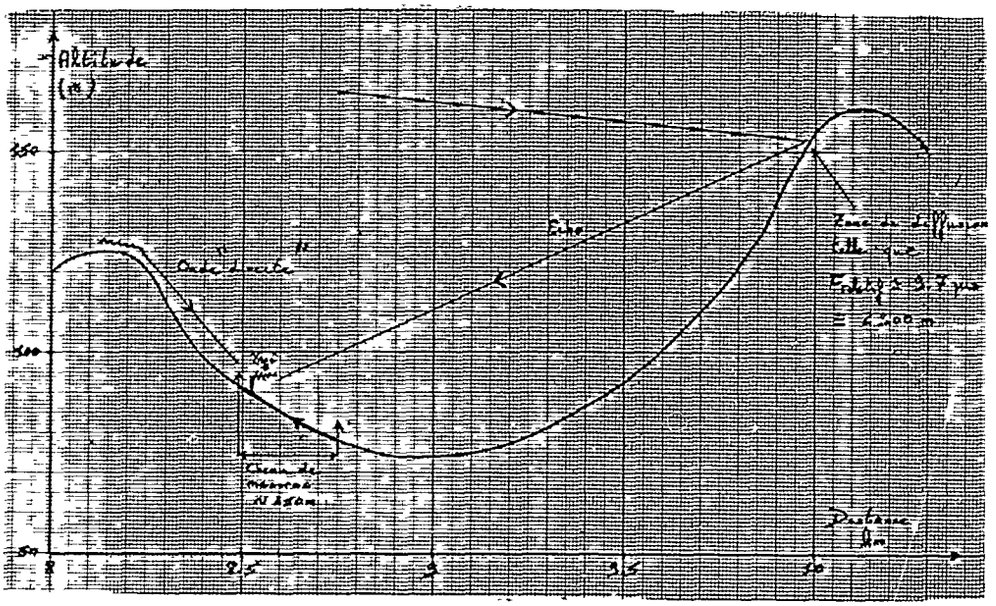

Figure 8

Exemple 1 - Puissances relatives recues

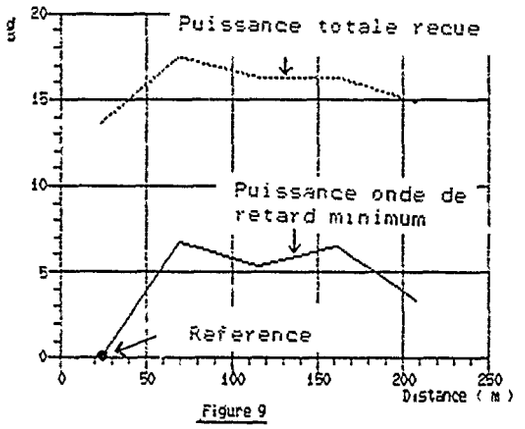

Figure 9

Exemple 2 - Profil du terrain

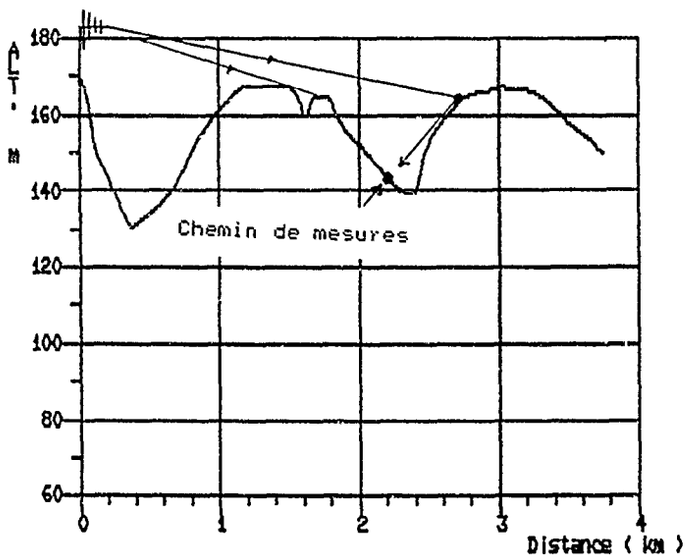

Figure 10

Exemple 2

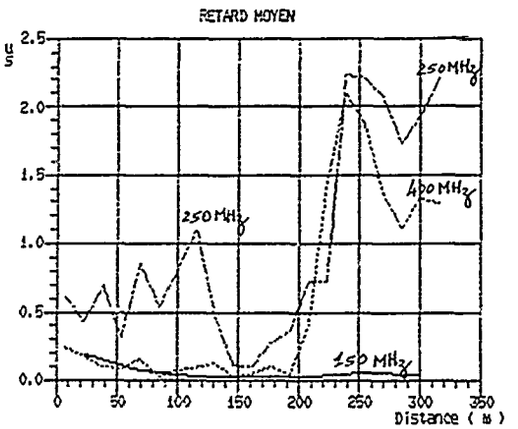

Figure 11 a

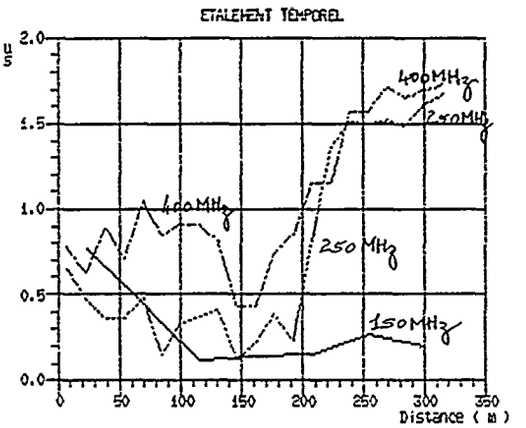

Figure 11 b

Exemple 2 - Puissances relatives de l'onde de retard minimum

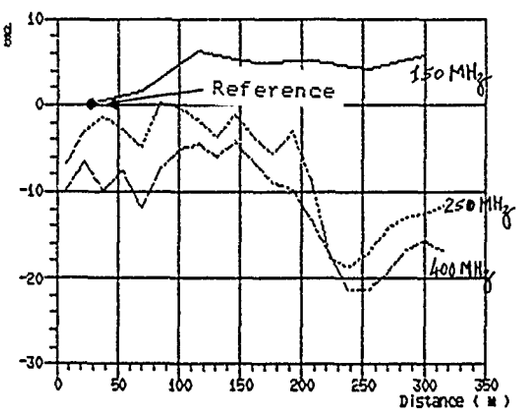

Figure 12

DISCUSSION

R.J. BULTITUDE

1 - I point out that the Fourier relation between Rn (τ, t) and R_H (Δf, t) is valid only for WSSUS channels. Its application can lead to very erroneous results if WSSUS conditions are not met, especially if a specular component is present in the received signal. A better procedure is outlined in paper 2 [BULTITUDE, 1983].

2 - What power threshold was used in rms delay computations. Workers in the U.S. suggest 40dB is required ?

3 - I also point out that I know no application for correlation Bw Bc results where Bc is defined by $|R_H(\Delta f,t)| < 0,5$.

AUTHOR'S REPLY

1 - La relation de Fourier ne peut en effet être appliquée que si les amplitudes des différents échos discernables par le banc de mesure sont deux à deux décorrélés. Cette non corrélation a été vérifiée pour quelques profils associés à des étalements temporels relativement importants. La probabilité que deux échos soient corrélés est d'autant plus forte que le retard relatif entre ces échos est faible. Il résulte de celà que la relation de Fourier peut éventuellement être inadaptée pour estimer les bandes de cohérences élevées. Par contre, les bandes de cohérence "moyennes" et "faibles", relativement à la bande d"analyse", sont sans doute correctement déterminées en utilisant la relation de Fourier.

2 - Les réponses impulsionnelles sont mesurées avec un seuil en puissance placé à S = - 20dB. Pour l'estimation de l'étalement temporel le seuil S doit être, à priori, d'autant plus faible que le retard relatif maximum mesuré τ max est grand. Un écho unique à 15 μs, d'amplitude relative égale à - 40dB, créé en effet un étalement temporel non négligeable (0,15 μs). Dans la mesure où de telles configurations de multitrajets sont fréquentes, la distribution des faibles valeurs de l'étalement temporel sera minimisée pour des seuils supérieurs à - 40dB. Pour des étalements temporels plus élevés l'erreur relative sera nettement plus faible. Par ailleurs, l'exigence d'une dynamique de 40dB conduit à une très faible zone de couverture qui limite la représentativité des résultats.

3 - Les bandes de cohérence à 0,9 et 0,5 sont des signatures radioélectriques du canal mesurées par différents auteurs. Les oscillations de la fonction de corrélation rendent plus aléatoire la détermination de la bande de cohérence à 0,5 que celle à 0,9.

K.S. KHO

The behaviour of narrow band signals 150-400MHz in terms of propagation characteristics is well known and information is available. Is it not possible to derive the behaviour of wideband signals from the available characteristics of narrow band signals ?

So, with computer simulations we will be able to predict the influences of propagations on wideband signals without carrying out expensive measurements.

If measurements are carried out, this simulation could be used to check the measurement results.

Please comment on this opinion ! Thank you !

DISCUSSION

AUTHOR'S REPLY

Le calcul des variations rapides du signal reçu par un mobile nécessiterait d'une part, d'obtenir une définition très fine du terrain et de sa couverture, et d'autre part, de disposer d'un logiciel capable d'exploiter ces données. L'effort considérable qu'il faudrait fournir pour développer de tels moyens de simulation semble inutile : les résultats expérimentaux permettent en effet de simuler les variations rapides par des modèles stochastiques ou déterministes (calculs de propagation à partir d'une distribution donnée d'objets). Il est par contre plus réaliste et plus intéressant de chercher à calculer les valeurs moyennes des puissances reçues en fonction du retard relatif (fonction diffusion retard) en utilisant un programme de simulation bande étroite. Bien que de nombreux travaux théoriques aient été réalisés sur ce problème [E. BAHAR, G.A. HUFFORD, R.H. OTT, A. BERRY] il n'existe pas, à ma connaissance, de logiciels permettant de traiter correctement la topographie d'un terrain décrit en 3 dimensions (pour les gammes V/UHF). Lorsque l'on réduit le problème du calcul de propagation au profil du terrain contenu dans le grand cercle passant par l'émetteur et le récepteur on trouve dans la littérature ouverte un grand nombre de méthodes semi-empiriques permettant d'estimer les atténuations de propagation. Ces méthodes testées sur les gammes de fréquence V/UHF et sur différentes classes de terrain fournissent toutes, en moyenne, des résultats notablement éloignés des mesures (écarts-types de 8 - 10dB). Les données expérimentales sont donc actuellement essentielles pour valider les hypthèses théoriques ou semi-empiriques faites dans les logiciels d'estimation de l'atténuation de propagation.

MEASUREMENT AND SIMULATION OF WIDEBAND MOBILE RADIO CHANNEL CHARACTERISTICS

Rudolf Werner Lorenz
Forschungsinstitut der Deutschen Bundespost
D-6100 Darmstadt

ABSTRACT

The general model of the transmission characteristics in mobile radio is derived. It is shown which abstractions are necessary to come up with the wide-sense stationary uncorrelated scattering (WSSUS) model. This model well known from troposcatter propagation is valid in mobile radio only for small vehicle travel distances. Nevertheless, the WSSUS model proved to be ideal for system test performance in mobile radio. The reasons are explained in the paper. A recently in France and Germany developed frequency-selective fading simulator is described which is based on the WSSUS model and proved to be a very suitable tool for hardware test of mobile radio equipment. The key dates of mobile radio channel charactistics standardized by COST 207 are briefly presented.

1. INTRODUCTION

When a new mobile radio communication system is specified a choice must be made out of a large variety of proposals concerning different methods of source coding, channel coding, modulation methods and access techniques. The implementation of microelectronics in mobile radio equipment makes feasible application of complicated algorithms for adaptive equalization, error detection and error correction. Modern receivers incorporate efficient microprocessors capable for several Mega-operations per second. But there is a limit to everything, and the more complicated the systems are, the more difficult is the optimum choice. It is impossible to find the best solution by theoretical considerations. Computer simulation is a powerful tool, but one is never sure, whether the models oversimplify the system reaction on the time- and frequency-variation of the transfer function and whether the computer simulation covers all aspects to be considered. Therefore, it is inevitable to perform hardware test measurements for varification of the results gained by theoretical analysis and computer simulation.

Test measurements in the field cannot yield results which are reproducible statistically. Too many uncontrollable distortions by man-made noise and interference of other radio services may affect the received signal. A reliable performance analysis of a mobile radio system can only be achieved if all parameters of the radio channel are controlled. This is the reason why hardware fading simulators were developed which reproduce the key characteristics of the mobile radio channel.

The general description of the transfer function of a mobile radio channel is given in section 2 of this paper. Bello /1/ has defined in 1963 the wide-sense stationary uncorrelated scattering (WSSUS) model for troposcatter propagation. The abstractions to apply this model on mobile radio are explained in section 3. It is shown in section 4 that the WSSUS model proves adequat for performance tests of digital mobile radio communication systems.

The Groupe Spécial Mobile (GSM) of the CEPT specified a Pan-European digital mobile radio telephone system in the 900-MHz band. Several different radio subsystems were proposed covering narrow-band FDM, narrow-band TDM and wide-band CDM access techniques. The GSM had to decide in a first step which access technique should be selected. This decision was mainly based on experimental comparison of different radio subsystems. The fading simulators proved to be essential parts of the experimental investigation of the GSM when bit-error ratio (BER) performance was compared. The application of frequency-selective fading simulators to model the mobile radio channel guaranteed that all radio subsystems were tested under equivalent propagation conditions.

COST 207 had coordinated the specification and development of two different types of hardware frequency-selective fading simulators, one of them made in France and the other one made in Germany. With respect to BER performance the results gained with one radio subsystem compared well when one simulator was substituted for the other one. However, both simulators suffered from some technical drawbacks which made it not recommendable to reproduce one of them. Therefore, the German and the French PTTs agreed to utilize the know-how gained and to co-sponsor the development of a new frequency-selective fading simulator called FS 900. This set-up is decribed in section 5 of this paper. It has been tested by an international group of experts and its performance fulfilled all requirements.

COST 207 coordinated in several parts of Europe measurement campaigns. Based on results gained from these measurements and published in the literature COST 207 defined parameter settings for the frequency-selective fading simulator to model mobile radio channel characteristics in rural, urban and mountainous areas. The key dates of the parameter settings are briefly summarized in section 6.

2. THE GENERAL PROPAGATION MODEL IN THE MOBILE RADIO CHANNEL

A propagation model has been suggested by Turin et.al. /2/. In this model it is supposed that the propagation medium acts as a linear filter with the property that, if $\mathrm{Re}(\underline{x}(t)\exp(j\,\omega_o t))$ is transmitted, where $\underline{x}(t)$ is a complex-valued low-pass signal and $f_o = \omega_o/(2\pi)$ is the carrier frequency, then $\mathrm{Re}(\underline{y}(t)\exp(j\,\omega_o t))$ is received, where

$$\underline{y}(t) = \sum_{k=1}^{K} \underline{x}(t - \tau_k)\, a_k \exp(j\, \vartheta_k) + \underline{n}(t). \qquad (1)$$

The propagation medium is determined by three K-dimensional sets of path parameters:

τ_k the excess delay,

a_k the resulting magnitude of the partial waves delayed by τ_k and

ϑ_k their phases.

In addition to these parameters the received signal is deteriorated by noise $\underline{n}(t)$ which is excluded from the analysis of the present paper.

Eq.(1) does not include the time dependence of the parameters. This has not been necessary for the purpose of Ref. /2/ because this publication was focused on the statistical distribution of τ_k, a_k and ϑ_k gained from point measurements. Concerning this objective Eq.(1) is a general description of the radio channel in multipath environment without considering any motion of either the scatterers, the transmitter or the receiver. It can be transformed into the frequency domain which results (omitting the additional noise) into the transfer function

$$\underline{H}(f) = \underline{Y}(f)/\underline{X}(f) = \sum_{k=1}^{K} a_k \exp(j\, \vartheta_k) \exp(-j\, \omega\, \tau_k) \qquad (2)$$

describing the frequency-selective fading, where $f = \omega/(2\pi)$ is the radio frequency.

For a general model the three sets of real parameters can be supposed to be time variant. It is well known that the time variation in mobile radio caused by the motion of the transmitter or the receiver consists of superimposed rapid and slow fading. These two time dependences differ by many orders of magnitude and they affect mobile radio communication in considerable different ways. The rapid fading is modelled by superposition of partial waves and the slow fading is modelled by time variation of parameters characterizing the partial waves.

The signal received at an excess delay τ_k consists of M partial waves

$$a_k \exp(j\, \vartheta_k) = \sum_{m=1}^{M} \underline{B}_{k,m} \qquad (3)$$

with $\underline{B}_{k,m}$ the complex amplitude of a partial wave generated by a distinct scatterer (k,m). If multiscattering is not considered all the scatterers with equal delay τ_k contributing to the received signal (a_k, ϑ_k) are located on an ellipsoid with the transmitter in one and the receiver in the other focus. Eq.(3) gives the superposition of all M scatterers which are located on the surface of the ellipsoid k.

Due to the motion of the mobile the scattering angle between the direction of incidence and the direction towards the mobile varies at the scatterer. The scatter diagram may cause a variation of the complex amplitude $\underline{B}_{k,m}$ in magnitude and phase. The magnitude $B_{k,m}$ is also affected by the variation of the distance between the scatterer and the mobile. More important for small displacements of the mobile, however, is the variation of the phase due to varying delay which is described by the last term in Eq.(2). The delays τ_k being equal for all scatterers located on the ellipsoid k at the instant of time t_1 differ in general at other times $t \neq t_1$. Therefore, double indices $\tau_{k,m}(t)$ must be introduced for the formulation of the variation of the delay of each individual partial wave. The variation of the delay after a small increment of time Δt can be formulated by a linear approximation

$$\tau_{k,m}(t_1 + \Delta t) = \tau_{k,m}(t_1) + w_{k,m}(t_1)\, \Delta t. \qquad (4)$$

The coefficient $w_{k,m}$ at the instant of observation t_1 is

$$w_{k,m}(t_1) = -(v(t_1)/c) \cos \gamma_{k,m}(t_1), \qquad (5)$$

where $v(t_1)$ is the speed of the mobile, c the velocity of light and $\gamma_{k,m}(t_1)$ is the angle between the direction of motion and the direction from the mobile to the scatterer. If these functions are known, the variation of the delay of the partial wave scattered from (k,m) can be computed

$$\tau_{k,m}(t) = -\int_{t_1}^{t} (v(t)/c) \cos \gamma_{k,m}(t)\, dt + \tau_{k,m}(t_1). \qquad (6)$$

By insertion of Eq.(3) and (6) into (2) the general formulation for the frequency and time dependence of the transfer function becomes

$$\underline{H}(f,t) = \sum_{k=1}^{K} \sum_{m=1}^{M} \underline{B}_{k,m}(t) \exp(-j\omega\, \tau_{k,m}(t_1)) \exp\left(j\, \omega \int_{t_1}^{t} v(t) \cos \gamma_{k,m}(t)\, dt/c\right). \qquad (7)$$

As mentioned the variation of $\underline{B}_{k,m}(t)$ results, in parts, from the variation of the scattering angle. This is related to $\gamma_{k,m}(t)$. Therefore, considering a single scatterer, the variation of the complex amplitude $\underline{B}_{k,m}(t)$ and the variation of its delay $\tau_{k,m}(t)$ are correlated in general. In tropospheric scattering a large number of almost equal scatterers contribute to the received signal. It may be assumed then that a scatterer moving to another place will be replaced by another one contributing the same power, on average.

In mobile radio, however, this situation will be observed only, if the mobile would drive within a dense forest. In all other cases the propagation medium consists of more or less prominent scatterers with deterministic relations between the variations of their amplitudes and delays with time. This is the reason why slow fading may not be modelled by the time variance of the complex amplitudes $\underline{B}_{k,m}(t)$ only but also the time variance of the delays $\tau_{k,m}(t)$ must be considered. Moreover, both variables must be correlated. Therefore, the model of slow fading in wide-band mobile radio channels is very complicated.

3. THE WIDE-SENSE STATIONARY UNCORRELATED SCATTERING (WSSUS) PROPAGATION MODEL OF THE MOBILE RADIO CHANNEL

A considerable simplification of the mathematical treatment as well as the feasibility to develop a frequency-selective fading simulator would be achieved if the wide-sense stationary uncorrelated scattering propagation model (WSSUS) /1/ were applicable.

A stochastical process is wide-sense stationary if its expectation value is constant and its autocorrelation depends on the difference of the variables only, in the case of $\underline{H}(f,t)$ only on (f_2-f_1) and (t_2-t_1) but not on f_1 or t_1. $\underline{H}(f,t)$ is according to Eq.(7) already stationary in frequency. For a more generalized formulation even that cannot be supposed. The scattering coefficients and the scatter diagrams are dependent on frequency. Within a bandwidth considered for wideband mobile radio, e.g. 10 MHz at 900 MHz, the variation of $\underline{B}_{k,m}$ with frequency, however, may be neglected.

Stationarity in time requires that v(t), $\underline{B}_{k,m}(t)$, $\gamma_{k,m}(t)$ and $\tau_{k,m}(t)$ are time <u>in</u>variant. It is obvious that the speed of the mobile should be constant for a stationary fading process. With respect to the other three variables stationarity can only be expected for short vehicle travel distances. The variation of $\gamma_{k,m}$ and $\tau_{k,m}$ strongly depends on the distance between mobile and scatterer. Cox /3/ has concluded from his measurements in New York City that the statistics of the mobile radio channel are usually quasi-stationary for vehicle travel distances in the order of 5 m to 30 m (small scale) but become grossly nonstationary for distances larger than 20 m to 150 m. Reducing Eq.(7) to small scale means that the time dependence of $\underline{B}_{k,m}(t)$, v(t), $\gamma_{k,m}(t)$ and $\tau_{k,m}(t)$ may be neglected and the integral has a trivial solution. Using for abbreviation the frequency shift (Doppler-frequency)

$$f_{D\,k,m} = \frac{v}{c}\, f \cos \gamma_{k,m} = \frac{v}{\lambda} \cos \gamma_{k,m} \qquad (8)$$

of the partial wave scattered by the scatterer (k,m) the stationary transfer function becomes

$$\underline{H}(f,t) = \sum_{k=1}^{K} \sum_{m=1}^{M} \underline{B}_{k,m} \exp(-2\pi j \tau_{k,m} f) \exp(2\pi j f_{D\,k,m} t). \qquad (9)$$

This is the quasi-stationary propagation model which is determined by four (K * M) - dimensional sets of parameters, constant in time and frequency:

$B_{k,m}$	the magnitude of the partial waves scattered from the scatterer k,m;
$\tau_{k,m}$	its excess delay, which is equal for all M_k partial waves scattered on the surface of the ellipsoid k, if multiscattering is not taken into account;
$f_{D\,k,m}$	its Doppler shift and
$\arc(\underline{B}_{k,m})$	its phase.

The distribution of the magnitudes versus excess delay and Doppler shift characterizes the behaviour of the stationary channel. It is called "time-delay Doppler-scattering function", for abbreviation "scattering function", for which an example reproduced from /4/ is plotted in Fig. 1. The scattering function depicts the power density level

$$p_D = 10\ \lg(P_{k,m}) = 10\ \lg(\underline{B}_{k,m}\,\underline{B}_{k,m}^{*}/\underline{B}_{max}\,\underline{B}_{max}^{*})\ \text{dB} \quad (10$$

versus delay τ and Doppler shift f_D. The power density p_D = 0 dB is referred to the partial wave having the maximum amplitude B_{max}.

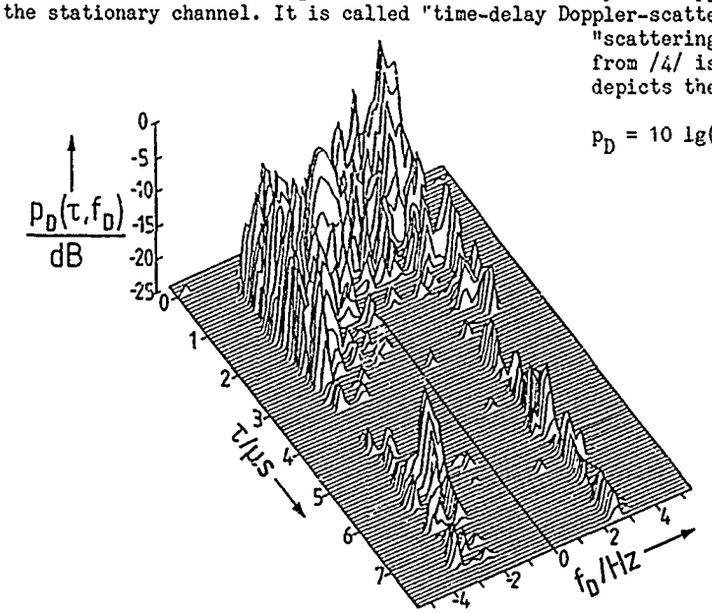

Fig. 1 Example of a measured scattering function /4/ depicting the distribution of power density versus delay τ and Doppler shift f_D.

The phases of the received partial waves, the fourth set of (K * M) - dimensional parameters, introduce the stochastical character into $\underline{H}(f,t)$. So far the scattering problem has been treated as a deterministic superposition of the contributions of each scatterer. However, due to the limited bandwidth Δf of the communication system the ratio of local resolution Δx to wavelength λ is approximately equal to the reciprocal relative bandwidth. Therefore, the minimum distance Δx for the distinct discrimination between two adjacent scatterers becomes

$$\Delta x \approx \lambda f_o / \Delta f \gg \lambda \quad . \tag{11}$$

The superposition of partial waves scattered at all obstructions located within the volume of resolution Δx^3 determines the phase of the resulting partial wave generated from that volume element. The resulting phase can be assumed to be a random figure equally distributed between 0 and 2π

$$\arg(\underline{B}_{k,m}) = Z^{(n)}_{k,m}(0,2\pi) \tag{12}$$

because the distribution of obstructions in the volume element is random. The suffix (n) indicates that $Z^{(n)}_{k,m}(0,2\pi)$ is a special sequence of (M * K) random figures. With each sequence (n) a different sample function can be computed:

$$\underline{H}^{(n)}(f,t) = \sum_{k=1}^{K} \sum_{m=1}^{M} \sqrt{P_{k,m}} \exp(-2\pi j \tau_{k,m} f) \exp(2\pi j f_{D\,k,m} t) \exp(j Z^{(n)}_{k,m}(0,2\pi)) \tag{13}$$

4. APPLICATION OF THE WIDE-SENSE STATIONARY MODEL ON SYSTEM PERFORMANCE TESTS IN MOBILE RADIO

A performance comparison of different digital mobile radio systems is based on the evaluation of the BER. An experimental determination of BER can be gained in a reliable way only if enough errors occur within one measured block of data. Therefore, the measurement must be extended to a certain length depending on the bit rate and the required level of resolution for BER. For example at a transmission rate of 16 kbit/s and a BER resolution down to 10^{-3} the measurement must endure for a period of 6.25 s to receive 100 errors on average. This measurement duration is required to determine in the statistical sense reliably the BER at one point of the curve versus signal to noise or signal to interference ratio. All points must be measured under the same statistical propagation conditions of the radio channel. Within 6.25 s the global parameters of the mobile radio channel may change tremendously because the mobile is displaced during the measurement so much. At 100 km/h, e.g., the mobile travels 174 m. Along such a run the mobile radio channel is nonstationary according to Cox /3/. Considering that the WSSUS model would not be applicable for determination of BER.

It is certainly true that a mobile radio system has to cope with nonstationary variations of propagation parameters. On the other hand, however, the length of data blocks is limited within which error correction procedures can be applied. In duplex telephony, e.g., the total delay must not exceed 100 ms. Otherwise the transmission system cannot be used for real-time conversation. In 100 ms the mobile is displaced only by $\Delta s = 2.8$ m at 100 km/h. According to Cox the mobile radio channel is stationary within that vehicle travel distance.

Errors occurring in mobile radio transmission are not equally distributed. Deep fades of magnitude of the transfer function, rapid variation of its phase and/or peaks of the group delay result in error bursts. This characteristic of the mobile radio channel is a result of the stationary model because deep fades of the transfer function are caused by interference of partial waves. The goal of system performance tests is to find out the reaction of the system on these critical conditions of the mobile radio channel likely to occur within one data block. Therefore, the reliable determination of BERs require the perpetuation of the statistical behaviour of the radio channel for the duration of a data block for which error correction can be applied. This means that transfer functions likely to occur statistically within a distance Δs along which the mobile travels during the transmission of one correctable data block should be reproduced for test measurements of BER performance. Even at high speeds of the mobile Δs is small or comparable to the travel distance within which the mobile radio channel is stationary. Because of this reason the WSSUS model is to be taken for determination of the BER.

In other words, the abstraction of the WSSUS model is necessary to determine the BER in small timeslots of transmission within which error correction procedure are applied. Obviously, this objective can only be obtained by a channel simulator, not by measurements in the real world which in addition to non-stationarity may be affected by uncontrollable events of propagation, interference and/or man-made noise.

5. THE FREQUENCY-SELECTIVE FADING SIMULATOR FS 900

The frequency-selective fading simulator FS 900 was developed in Franco-German cooperation. FS 900 was tested by an international group of experts /5/. It fulfilled all requirements. A simplified block diagram of the set-up is plotted in Fig. 2. The bandwidth of the fading simulator is 5 MHz. The center frequency can be set between 890 MHz and 960 MHz by adjustment of the frequency of the external local oscillator. The radio frequency signal is down converted to 10 MHz, digitised at a sampling rate of 40 MHz, split into 12 digital delay lines which can be delayed individually, digital to analog converted, controlled in power level in each tap and complex modulated by different random signals having specified Doppler spectra. The signals in the 12 branches are combined and up converted to radio frequency. The procedure for parameter setting is extremely simple and changes are performed quickly. Parameter sets can also be stored on magnetic disks. The 12 taps are described by

- the number of the tap;
- the file number of the Doppler spectrum of the noise sequence to be used for complex modulation;
- the attenuation of each tap transfer function and
- the delay of each tap.

The noise sequences are stored in EPROMs and one out of eight can be allocated to each tap. The noise sequences used in each tap are uncorrelated. The attenuation can be set between 0 dB and 31 dB in 1-dB steps and the excess delays between 0 μs and 51 μs in 0.2-μs steps. The speed of the mobile can be set between 0 and 300 km/h in 1-km/h steps. The Doppler spectra are computed according to Eq.(8) at a radio frequency between 890 MHz and 960 MHz which can be set in 1-MHz steps.

It can be programmed whether FS 900 operates in 12 taps or is split into two channels to each of which 6 taps are allocated. In the latter case three modes of operation can be selected:

- diversity;
- interference and
- simulation of two separated channels.

In the diversity mode the input signal at the radio-frequency input RF_{in} is split into two branches of uncorrelated channels for the two outputs RF_{out} A and RF_{out} B.

In the interference mode the signals from RF_{in} and the second input are transmitted after uncorrelated fading simulation to the output RF_{out} A. The second input operates at the center frequency of 10 MHz. This lay-out was selected because standardized interference spectra generated by a programmable signal generator may be used. For test measurements with interfering signals at radio frequency an external down converter must be connected to FS 900.

In the mode of simulation of two separated channels, FS 900 is split into two separate channels having 6 uncorrelated and individually programmable taps each. For this mode of operation the external up-converter is necessary. Both radio frequency bands must be within the bandwidth of 5 MHz.

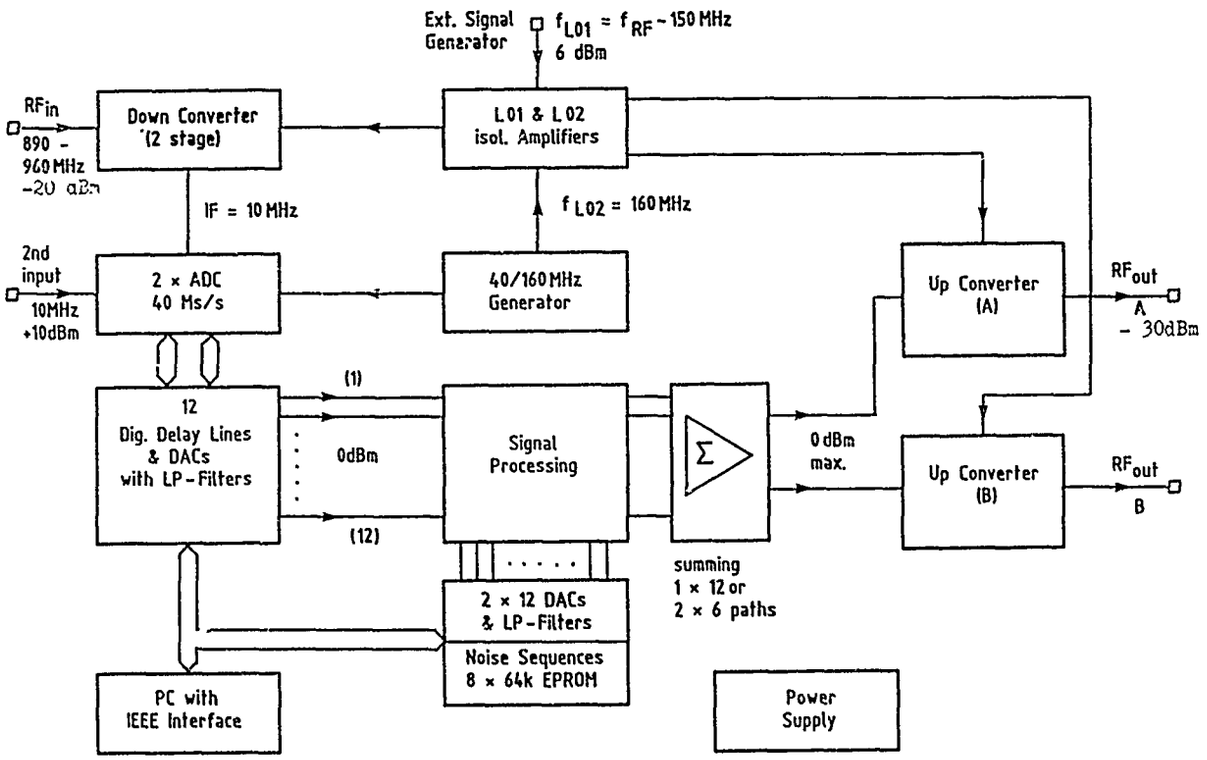

Fig. 2 Simplified block diagram of the frequency-selective time-variant fading simulator FS 900.

6. PARAMETER SETTING OF MOBILE RADIO CHANNEL CHARACTERISTICS IN DIFFERENT TYPES OF TERRAIN

COST 207 working group on propagation has defined parameter settings for the simulation of mobile radio channels /6/. They determine the simulation of propagation conditions which are typical

- in rural areas
- in urban and suburban areas
- in urban and suburban areas in mountainous terrain and
- in rural areas in mountainous terrain.

The average delay power profiles characterizing the four types of mobile environment are plotted in Fig. 3. These definitions of COST 207 were based on results published in the literature, on vast theoretical considerations as well as computer simulations and on propagation measurements performed in different countries participating in an international measurement campaign managed by COST 207. Some of the results gained recently in mountainous terrain under the coordination of COST 207 are published in /7,8/. The delay profiles $P(\tau)$, i.e. the power level allocated to different delays in the simulator are plotted in Fig. 3.

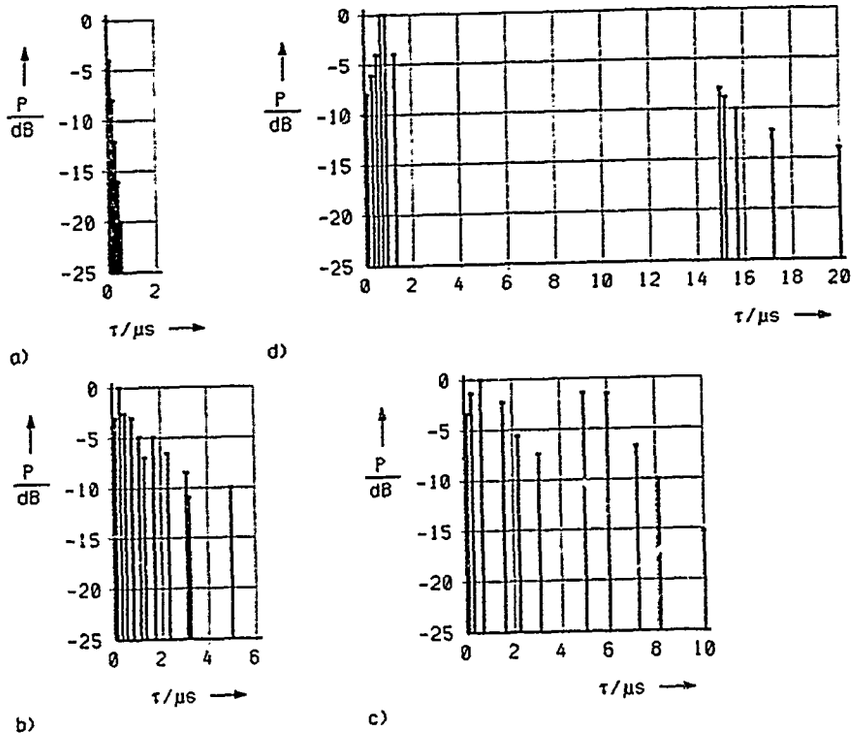

Fig. 3 Average power delay profiles defined by COST 207
a) in rural areas
b) in urban and suburban areas
d) in rural areas in mountainous terrain
c) in urban and suburban areas in mountainous terrain

The delay spread is the second central moment of the delay power profile. The delay spread S characterizes the frequency selectivity of the mobile radio channel. A brief overview is given in the following table:

Type of terrain	Delay spread S	Maximum excess delay
Rural area	0.1 μs	0.5 μs
Typical case for suburban and urban area	1.0 μs	5 μs
Typical bad case for suburban and urban area	2.5 μs	10 μs
Typical bad case for hilly terrain	5.0 μs	20 μs

The table shows the large variation of channel characteristics for frequency selectivity in mobile radio in different types of terrain.

7. CONCLUSIONS

The wide-sense stationary uncorrelated scattering (WSSUS) model describes the mobile radio channel along short vehicle travel distances, it is not valid for runs longer than 20 m to 150 m. Nevertheless, the importance of the WSSUS model is mainly to be a statistical perpetuation of short-term channel characteristics. Otherwise reliable tests of radio transmission system performance cannot be determined. Therefore, comparative test measurements can be carried out in a reproducable way only by use of fading simulators based on the WSSUS model and not by field measurements.

The frequency-selective fading simulator FS 900 developed in Franco-German cooperation proved to be a valuable tool for hardware test measurements of wideband mobile radio transmission systems. It is capable to simulate the different propagation conditions occurring in various types of terrain.

REFERENCES

1. Bello, P.A.: Characterization of randomly time-variant linear channels. IEEE Trans. COM-11 (1963) 360-393.
2. Turin, G.L., Clapp, F.D., Johnston, T.L., Fine, S.B. and Lavry, D.: A statistical model of urban multipath propagation. IEEE Trans. VT-21 (1972) 1-9.
3. Cox, D.C.: 910 MHz urban mobile radio propagation. Multipath characteristics in New York City. IEEE Trans. VT-22 (1973) 104-110.
4. Bajwa, A.S. und Parsons, J.D.: Small area characterization of UHF urban and suburban mobile radio propagation. IEE Proc. Pt.F 129 (1982) 102 - 109.
5. COST 207: Test measurements of the frequency-selective fading simulator. COST 207 TD (88) 40.
6. COST 207: Proposals on channel transfer functions to be used in the GSM tests. COST 207 TD (86) 51.
7. Lorenz, R.W., Kartaschoff, P., Lö..., K., Merki, P., Weber, M., de Weck, J.-P.: Excess delay power profiles measured in mountainous terrain, ALTA FREQUENZA Vol. LVII (1988) 57-64.
8. Damosso, E.: Wideband propagation measurements at 900 MHz, ALTA FREQUENZA Vol. LVII, (1988) 65-74.

DISCUSSION

R.J. BULTITUDE

I believe we agree that the QWSS assumption is acceptable for error rate analysis, but should not be used in the interpretation of propagation measurement results.

AUTHOR'S REPLY

Not really. The QWSS can be used also for the interpretation of wideband measurements, but only along short runs along several meters. The slow variation of attenuation and the variation of power delay profiles, however, are correlated. Therefore, a simulation of slow fading cannot be performed without the variation of the entire scattering function simultaneously. Since this is very difficult, both in description by a model as well as in hardware simulation such a model may not be used for error rate analysis. Moreover , as I have pointed out in the paper, the QWSS model is to be applied for duplex channels to perpetuate the short run characteristic of the mobile radio channel.

ESTIMATION DE LA REPONSE IMPULSIONNELLE DU CANAL RADIOMOBILE LARGE BANDE EN SITE SUBURBAIN A 910 MHz

M. SALEHUDIN, G. EL ZEIN, J.J. BAI, A. DANIEL, J. CITERNE.
Laboratoire "Stuctures rayonnantes"
UA au CNRS N° 834, INSA 35043 RENNES CEDEX

RESUME

Cette communication présente une méthode pour estimer la réponse impulsionnelle du canal radiomobile large bande, en UHF, à partir des paramètres relatifs à l'environnement. Ceux-ci comprennent la position relative des diffuseurs par rapport à celle du mobile. Ces diffuseurs sont répartis aléatoirement dans un environnement homogène et fonctionnent comme des sources secondaires d'ondes n'émettant qu'un seul rayon dans la direction du récepteur. Les paramètres de l'environnement sont extraits à partir des plans topographiques sectoriels existants. La hauteur des diffuseurs, conduisant à un modèle géométrique à trois dimensions, est introduite par la notion de section efficace radar bistatique. Cette dernière détermine les coefficients de réflexion sur les diffuseurs. La confrontation des résultats de l'estimation à ceux obtenus par la mesure sur le canal réel à été faite sous forme de fonction d'occupation de trajets dans un intervalle de retards donné. Elle démontre un accord prometteux dans des sites suburbains.

1. INTRODUCTION

La propagation radiomobile dans un environnement urbain est généralement affectée par la présence des trajets multiples. Dans ce cas, la propagation se passe à travers des réflexions et des diffusions sur des masques (bâtiments et autres obstacles). Ce phénomène se traduit sous forme d'évanouissements sélectifs en fréquence et en espace du signal reçu lorsque le mobile se déplace [1]. La connaissance des caractéristiques du canal comme, par exemple, sa réponse impulsionnnelle, s'avère alors utile pour améliorer la qualité de la liaison par la diversité de réception.

Divers modèles de canal sont mentionnés dans la littérature. Mais, très peu traitent des statistiques du canal large bande en tenant compte des paramètres relatifs à l'environnement. Ossanna [2] fut le premier à proposer un modèle basé sur des réflecteurs plans et parfaits, répartis d'une façon déterministe. Zander [3] a proposé un modèle géométrique - optique simple qui considère des diffuseurs scintillants et aléatoirement répartis. Récemment, Bajwa [4] a affiné le modèle de Zander en introduisant le principe de Huygen sur le rayonnement des diffuseurs discrets et aléatoirement répartis. Quelques soient leurs résultats, tous ces modèles n'introduisent pas encore la hauteur des diffuseurs.

Le modèle présenté dans cet article concerne un modèle géométrique à trois dimensions. La hauteur des diffuseurs y est introduite implicitement par la notion de leurs surfaces efficaces radar bistatique [5]. Celles-ci permettent de déterminer les coefficients de reflexions sur les diffuseurs. Les paramètres de l'environnement sont extraits à partir des plans topographiques sectoriels dont la numérisation a été effectuée au laboratoire. Enfin, la confrontation du modèle avec les statistiques du canal, obtenues à partir de nos campagnes de mesure effectuées sur le terrain, a été faite sous forme de fonction de probabilité d'occupation des trajets dans un intervalle de retards donné.

2. MODELE DU CANAL A TRAJETS MULTIPLES

Le modèle décrit ci après considère que le principe de diffusion est représenté par une simple réflexion. Les diffuseurs sont aléatoirement répartis suivant la même direction dans un environnement homogène et fonctionnent comme des sources secondaires d'ondes. Ces diffuseurs sont modélisés géométriquement par des parallélépipèdes ayant des surfaces planes verticales. Les coefficients de réflexion sur les diffuseurs sont déterminés par la surface efficace radar bistatique correspondant aux surfaces de ces derniers. Les ondes qui arrivent dans le voisinage du mobile sont supposées planaires et polarisées verticalement.

2.1. La géométrie des diffuseurs

Une vue générale des diffuseurs est donnée par la figure 1. Les vecteurs $\vec{r}_k$ = 1, 2, 3, ...N représentent les distances entre le mobile et les N diffuseurs. Chacun d'eux a un ou plusieurs coefficients de réflexion déterminés par la surface efficace radar bistatique des surfaces illuminées et s'exprime d'après [5]:

$$\rho = \frac{h^2}{\pi}\left[n\ l \cos\theta \frac{\sin(n l \sin\theta)}{n l \sin\theta} \right]^2 \qquad (1)$$

où h est la hauteur de la surface illuminée des diffuseurs, l est sa largeur, θ/2 est l'angle d'incidence de l'onde sur la surface et n = 0, 1, 2, ...

Le retard relatif τ_k dû à l'onde arrivant du k^{ème} diffuseur peut être calculé d'après la relation suivante,(voir fig.2):

$$\tau_k = \frac{r_k}{c} = \frac{\rho_k \sin\theta/2}{c \sin\phi_k \cos\beta_k} \qquad (2)$$

où r_k est la distance entre le k^{ème} diffuseur et le récepteur, ϕ_k et β_k déterminent sa position angulaire relative et c est la vitesse de la lumière.

Donc, la réponse impulsionnelle du canal est obtenue si les paramètres ρ_k, r_k, ϕ_k et β_k sont connus. Ces derniers sont des variables aléatoires.

Pour un modèle à deux dimensions, Zander a modélisé r comme un processus aléatoire stationnaire du second ordre, indépendant de ϕ, obtenu à partir d'un processus de Poisson planaire [3]. Bajwa a affiné ce modèle en introduisant la largeur des rues et aboutit à l'expression suivante [4]:

$$p(r) = \frac{1}{D} \exp\left[\frac{W}{2D} - \frac{r}{D}\right] \qquad ; r \geq W/2 \qquad (3)$$

où D est la séparation entre les diffuseurs et W est la largeur de la rue.

2.2. Les statistiques des paramètres de l'environnement

A partir des plans topographiques sectoriels ou des plans d'occupation du sol existants, à l'échelle de 1/2000, nous pouvons extraire des paramètres de l'environnement tels que:

a) la distance r séparant le diffuseur du récepteur mobile qui conduit à la connaissance de la densité de probabilité p(r).

b)- la position angulaire ϕ du diffuseur par rapport au récepteur mobile conduisant à la distribution $p(\phi)$.

Mais, la hauteur des bâtiments ne figure pas encore sur ces plans.

Ainsi, pour arriver à déterminer la distribution des coefficients de réflexion $p(\rho)$ et celle de l'élévation des diffuseurs $p(\beta)$, une inspection effectuée sur le site s'est révélée nécessaire. Tous les procédés d'extraction de ces paramètres ont été développés au laboratoire. Pour cela, un moyen de numérisation automatique des plans par ordinateur a été mis en œuvre.

3. SYSTEME DE MESURE

Des campagnes de mesure de propagation radiomobile à 910 MHz furent effectuées dans la ville de Rennes [6]. La technique choisie pour relever la réponse impulsionnelle du canal est basée sur le principe de corrélation .

A l'émission, fig.3, la fréquence intermédiaire (FI = 70 MHz) est modulée en B.P.S.K. par une séquence pseudo-aléatoire ayant un débit numérique de 10 Mbits/s et une longueur maximale de 127 bits. Une transposition à la radiofréquence (RF = 910 MHz) est ensuite effectuée avant d'attaquer l'étage amplificateur qui permet d'avoir une puissance d'émission de 10 W. Le signal est émis à partir d'une antenne omnidirectionnelle ayant un gain de 9 dBi et portée par un pylône de 43 m de hauteur.

Au niveau du récepteur , le signal est capté par une antenne omnidirectionnelle de gain 3 dBi placée sur le toit du mobile à 2,5 m du sol Afin d'améliorer la dynamique du récepteur, un amplificateur logarithmique est introduit à la fréquence intermédiaire. Ensuite, un corrélateur à ondes acoustiques de surface est mis en œuvre. Une détection cohérente est alors effectuée sur les deux composantes en phase et en quadrature de phase du signal reçu. La cohérence est garantie par la bonne stabilité des synthétiseurs de fréquence (10^{-10} / heure à 910 MHz).

La résolution temporelle obtenue avec ce système est de l'ordre de 100 ns, ce qui permet de dissocier des trajets différents de 30 m ou plus. Quant à la fenêtre d'observation, elle est de 12,7 μs environ.

4. SYSTEME D'ACQUISITION DES DONNEES

L'architecture générale du système d'acquisition et de traitement des données est montrée à la figure 4. Elle est construite autour d'un calculateur (TEK 4041). Les signaux reçus sont d'abord échantillonnés à l'aide d'un numériseur (TEK 7612 D) puis transférés dans une unité de stockage (TEK 4041 DDU) pour un traitement numérique différé. Un capteur de distance permet de relever, avec précision, le déplacement du récepteur mobile.

Les données ont été obtenues pour une vitesse constante du mobile de l'ordre de 1 m/s, sur des parcours de 30 m environ. La fréquence d'échantillonnage des signaux est de 50 MHz.

5. RESULTATS

Une caractérisation du canal radiomobile a été effectuée à petite échelle . Celle-ci portait sur la fonction de diffusion retard - Doppler et sur le profil moyen de la réponse impulsionnelle. Les figures 5 et 6 montrent des exemples de résultats obtenus. Ceux-ci permettent d'aboutir à une caractérisation globale portant, en particulier, sur la densité de probabilité d'occupation des trajets dans un intervalle de retards donné.

En pratique, cette probabilité est obtenue en comptant le nombre de profils où l'amplitude du trajet, dans un intervalle de retards de 100 ns, dépasse un seuil choisi. La figure 7 représente la probabilité d'occupation des trajets issue des résultats expérimentaux relevés dans un site suburbain. D'autre part, le résultat de l'estimation de cette probabilité, tiré à partir des paramètres de l'environnement du même site, est porté sur la figure 8. Une confrontation de ce résultat avec celui de l'expérience permet de constater un accord satisfaisant.

6. CONCLUSION

Cet article a concerné la présentation d'une méthode pour estimer la réponse impulsionnelle du canal radiomobile à large bande. La comparaison des résultats de l'estimation et l'expérience a été effectuée en considérant la probabilité d'occupation des trajets dans un intervalle de retards donné. Cette confrontation apparaît prometteuse. Mais, d'autres campagnes de mesure seront nécessaires pour valider la méthode dans des sites divers.

7. REFERENCES:

[1] W.C. JAKES
"Microwave Mobile Communications"
New York : Wiley, 1974.

[2] J.F. OSSANNA Jr.
"A model for mobile radio fading due to building reflections: Theoretical and experimental fading waveform power spectra"
BSTJ, 43, N° 6, pp. 2935-2971, 1964.

[3] J. ZANDER
"A stochastical model of the urban UHF radio channel"
IEEE Trans on Veh. Tech., VT - 30, N° 4, pp. 145-155, 1981.

[4] A.S. BAJWA
"A simple stochastical approach to wideband modelling of multipath propagation in mobile radio environments"
IERE International Conf. on Land Mobile Radio, Cambridge, 10-13 Dec., 1983.

[5] E.F. KNOT, J.F.SHAEFFER, M.T. TULEY
"Radar Cross Section"
Artech House Inc., 1985

[6] G. EL ZEIN, M. SALEHUDIN, J. CITERNE, J.M. FLOC'H
"Mesures de propagation radiomobiles à 910 MHz dans la ville de Rennes"
5èmes Journées Nationales Micro-ondes, Nice, Juin 1987, pp. 183-185.

8. REMERCIEMENTS:

Cette étude a été réalisée en l'exécution d'un contrat émanant de la Direction des Recherches Etudes et Techniques (DRET).

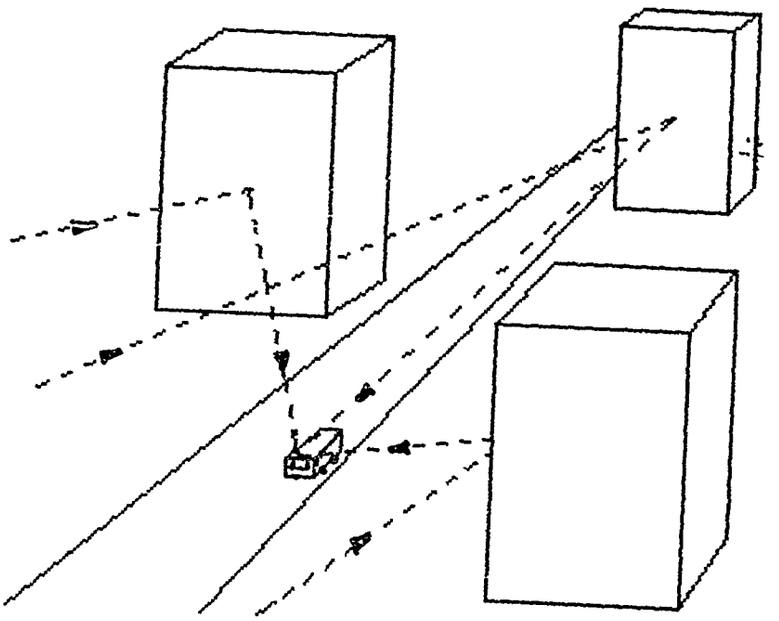

FIG.1 : Vue générale des diffuseurs.

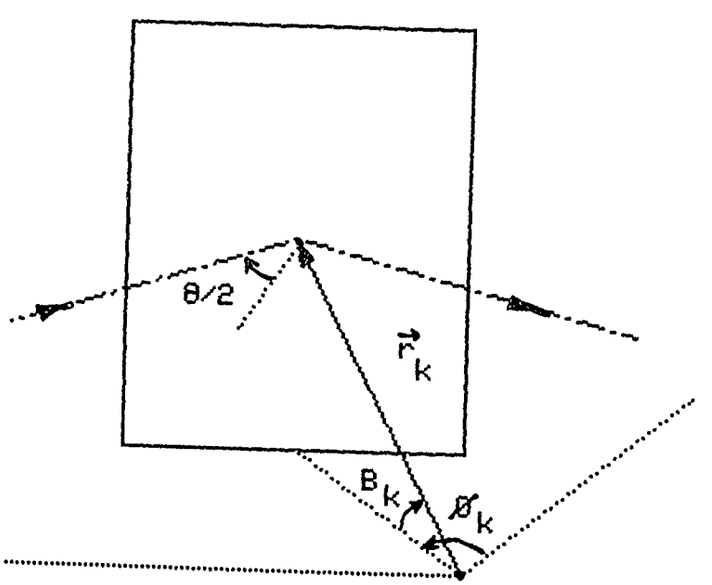

FIG.2 : Géométrie d'un diffuseur.

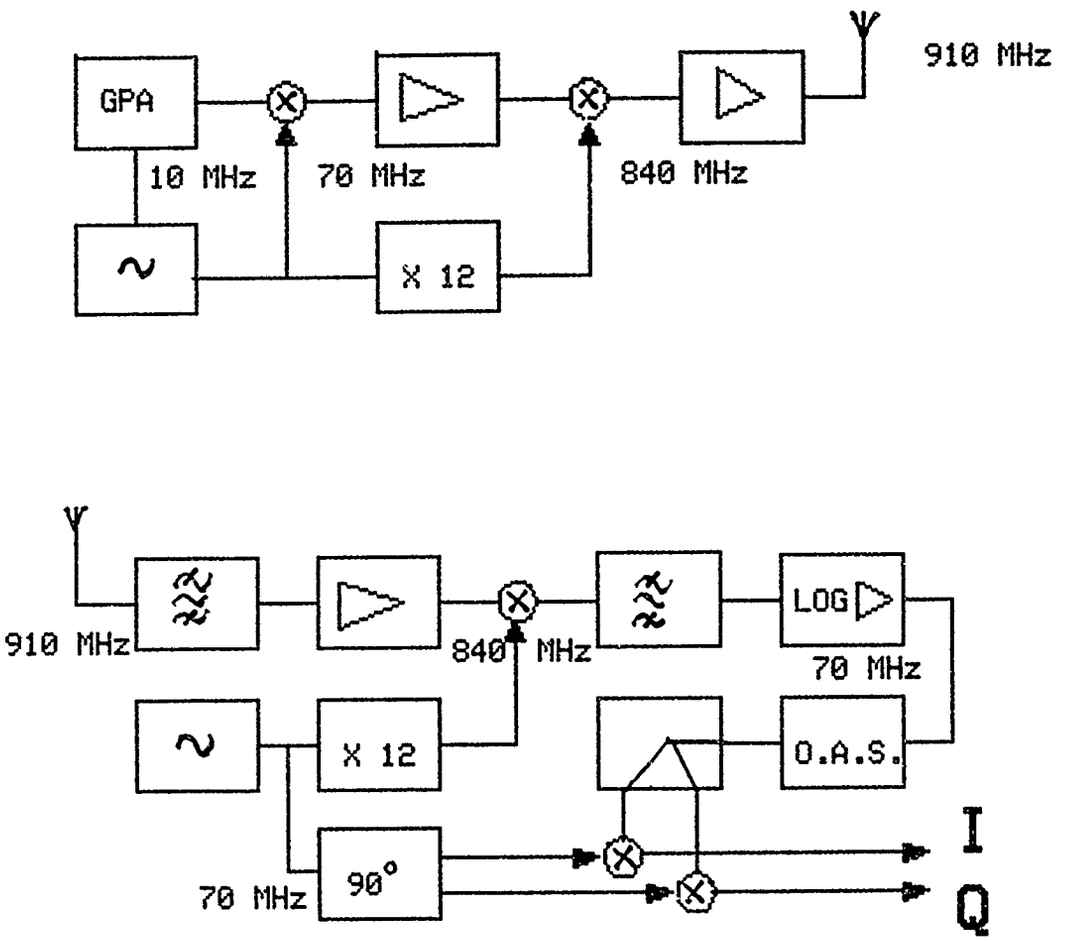

FIG.3 : Système de mesure.

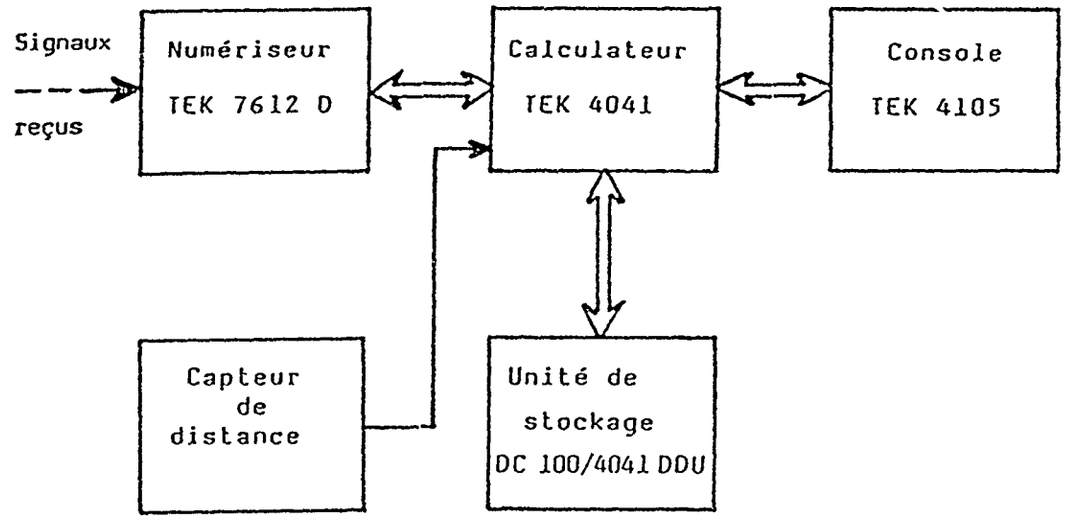

FIG.4 : Système d'acquisition des données.

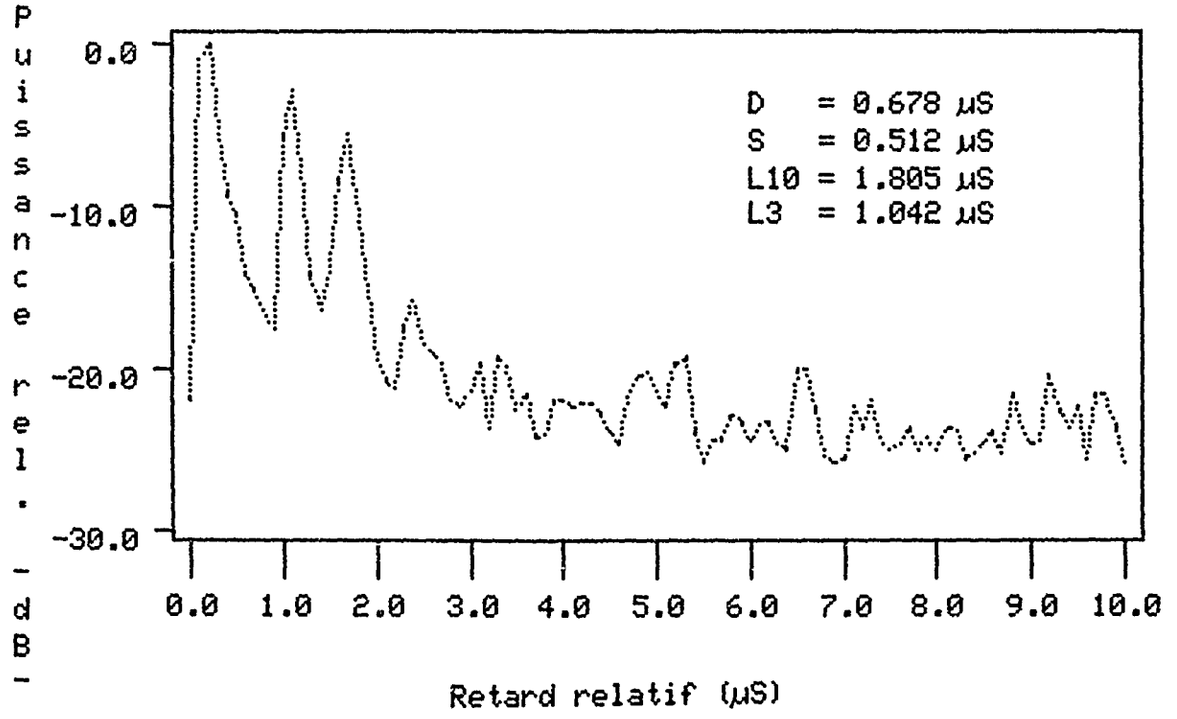

FIG.6 : Profil moyen de la réponse impulsionnelle.

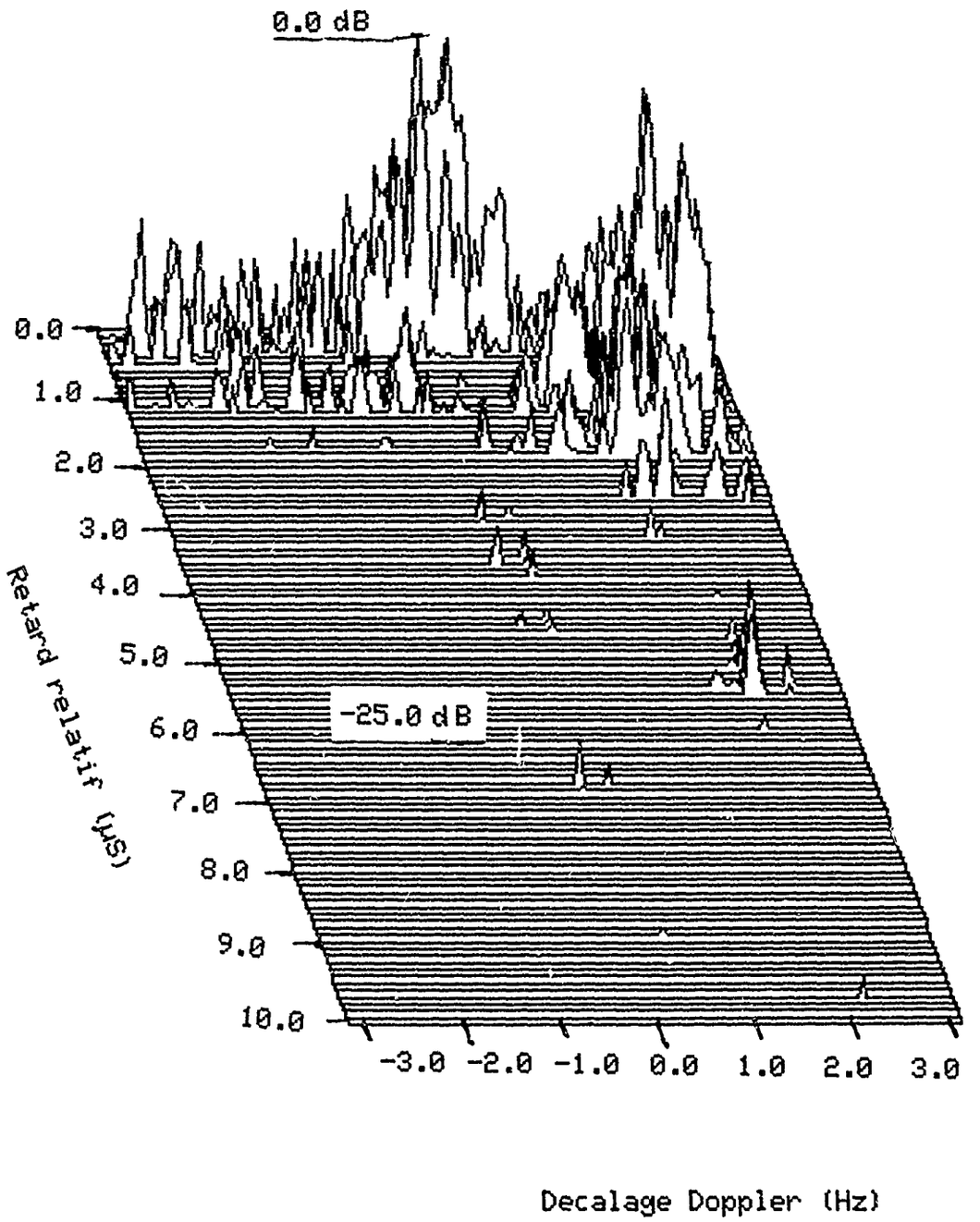

FIG.5 : Fonction de diffusion retard-Doppler.

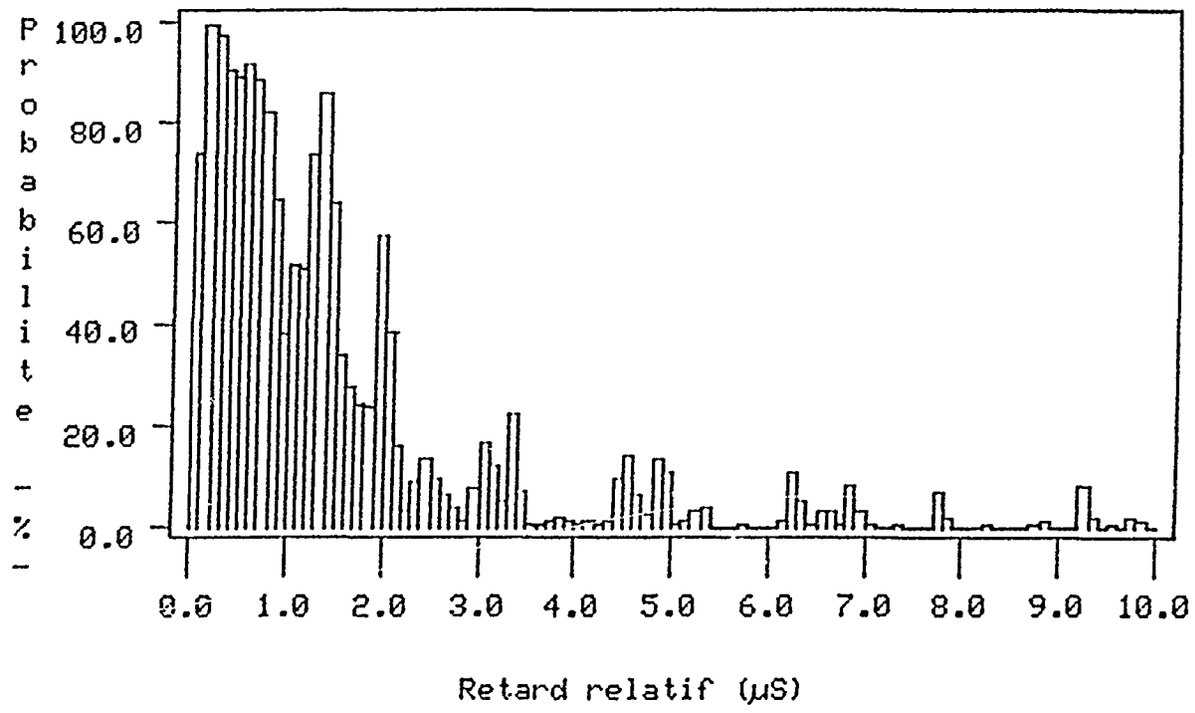

FIG.7 : Probabilité d'occupation des trajets (Expérience).

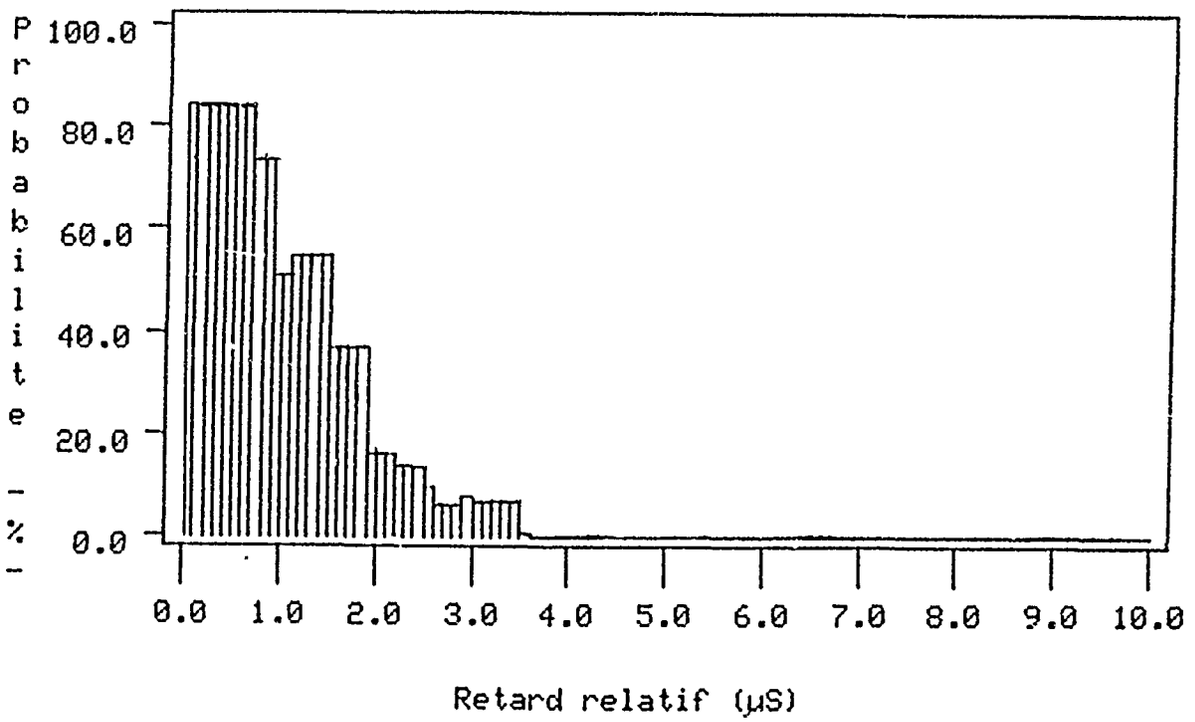

FIG.8 : Probabilité d'occupation des trajets (Estimation).

DISCUSSION

K.S. KHO

1 - There are two methods of wide band measurements :
- using pulses
- using PR patterns.
It seems to me that pulse measurements are the less complex one.
Can you give some rationale behind your PR pattern choice ?

2 - The narrowband propagation characteristics is quite wellknown. Is it not possible to extrapolate the narrowband characteristics to the wide band characteristics ?

AUTHOR'S REPLY

1 - Il est vrai que la mesure par l'émission d'impulsions est plus simple à mettre en oeuvre, par rapport à la mesure par l'émission d'une séquence pseudo-aléatoire.
Mais l'inconvénient majeur de cette technique s'exprime par la nécessité d'émettre des impulsions avec une puissance crête très importante. Ceci pour assurer une détection adéquate des impulsions reçues.
Quant à la mesure par l'émission d'une séquence pseudo-aléatoire, elle nécessite d'une part une puissance crête relativement plus faible et d'autre part, elle présente une meilleure immunité contre certains types de brouilleurs. Ceci est obtenu grâce au principe de l'étalement de spectre.

2 - Il est vrai qu'on ne peut pas extrapoler les caractéristiques de la propagation à large bande à partir de celles à bande étroite. Mais le contraire est toujours possible, du fait que l'émission à large bande est équivalente à plusieurs émissions simultanées à bande étroite.

E. GURDENLI

1 - Can you confirm that your model is an "extension" of Bajwa's ?

2 - Can you confirm that the only extension is the inclusion of the height of the scatterers ?

3 - What probability functions are used for the parameters of the model ?

4 - You described the use of topographic maps to extract the height information for specific scenarios. Do you have a probability density function for the height parameter ?

AUTHOR'S REPLY

1 & 2 - Notre modèle fait intervenir la hauteur des diffuseurs, tandis que le modèle de Bajwa est bidimensionnel et ne tient compte que de la surface d'occupation du sol par ces derniers.

3 & 4 - Les travaux actuels permettent d'envisager la détermination des densités de probabilité pour des paramètres tels que : la hauteur des diffuseurs, la distance diffuseurs-récepteur et la position angulaire des diffuseurs.
En pratique, l'extraction de l'information sur la hauteur des diffuseurs se fait par une inspection sur le site.

WIDEBAND CHARACTERIZATION OF FOREST PROPAGATION CHANNELS

Allan Schneider & Frederick J Altman
CyberCom Corporation
4105 North Fairfax Drive
Arlington, Virginia 22203, USA

Kevin Lackey
US Army CECOM
Center for C3 Systems
Fort Monmouth, NJ, USA

SUMMARY

Wideband propagation measurements within the frequency band 200 to 2000 MHz have been made through a coniferous forest of Douglas fir at Fort Lewis, Washington and through a deciduous forest of red maple in Coventry, Connecticut. Measurements were repeated at Fort Lewis in successive years following thinning of the forest, and twice within the same year at Coventry, before and after the autumn fall of leaves. These field measurements utilized wideband impulse-response measurements to characterize the UHF wideband forest propagation channel. The effort relied upon the US Army's Wideband Propagation Measurement System (WPMS), a self-contained, mobile, automated, wideband propagation data acquisition and recording system. This measurement program has been closely coupled to an analytic effort to develop a UHF forest propagation model suitable for predicting the transmission loss and delay spread experienced by a radiowave propagating through the forest. This paper will review both measured and predicted values of transmission loss and delay spread as they relate to distance, antenna height, frequency, polarization and biophysical forest parameters. Concepts bearing on the analysis and interpretation of the measured data will be discussed, and conclusions drawn relating to communication system deployment in forests.

1. INTRODUCTION/BACKGROUND

This program was initiated in response to the increasing comtemplated use of wideband techniques and the absence of definitive models to support the analysis of wideband performance. To date, link budget designs are still generally based on narrowband propagation analyses and models. Since narrowband models do not account for the increased vulnerability of wideband propagation to multipath and frequency selective fading, the use of narrowband models in the design of communication equipment employing wide bandwidths may result in under-design. Wideband measured data and a wideband propagation model were both needed to accurately represent the effects of the forest channel on wideband transmission. The motivations behind the Army's Wideband Propagation Program and its evolution are fully discussed by P. Sass (ref. 1).

The Wideband Propagation Measurement System (WPMS) has been designed (ref. 2) as a computer-controlled, self-contained measurement tool with which to conduct a series of comprehensive UHF ground communications channel measurements. The system covers a broad range of UHF frequencies and bandwidths, the transmitter and receiver portion of the system are housed in separate vehicles, and each vehicle is equipped with integral self-erecting antenna towers with an operating range between 12 and 65 feet. The complete characteristics and capabilities of the system are summarized in Table 1.

The transmitted signal is a wideband pseudonoise (PN) code-modulated phase-shift-keyed signal. After transmission through a carefully calibrated transmitter and antenna system, the wideband received signal is cross-correlated at the receiver with a locally-generated replica of the transmitted signal to produce the impulse response of the channel. The

Time-Varying Impulse Response (TVIR) is the primary means of channel measurement (ref. 3). The amplitudes and locations of the peaks in the TVIR provide data on the attenuation and delay of the received signal.

The measurement approach used to derive the TVIR of the communication channel is known as a "sliding correlator"; so-called because the receiver clocks its code sequence at a rate slightly different from the transmitter's. This causes the transmitter and receiver code sequences to slip in phase with respect to each other, so that the correlation function, when viewed on an oscilloscope appears to trace out the full length of a TVIR. The WPMS further reduces the long examination time inherent in such sliding correlator techniques by utilizing pairs of in-phase and quadrature correlators, the pairs offset by 1/4 chip intervals to reduce the total correlation time. Both in-phase and quadrature-phase components of the measured TVIR are recorded. For any given episode (a prescribed configuration of radio/antenna parameters), the TVIR is measured repeatedly until the data buffer overflows. Post-episode processing of the TVIRs involves calculation of the corresponding PTVIRs (sum of the squares of the in-phase and quadrature components) and their Fourier transforms. Also determined are the PTVIR_MIN, PTVIR_AVG, and PTVIR_MAX. Analogous operations are carried out on the Fourier spectra to determine SPEC_MIN, SPEC_AVG, and SPEC_MAX.

2. MEASUREMENT LOCALES

Propagation measurements were made in two distinctly different forest environments - a trunk dominated Douglas fir forest in the Pacific Northwest (Ft. Lewis, Washington) and a canopy dominated deciduous forest consisting of red maple in the Atlantic Northeast (Coventry, CN). Field propagation measurements were conducted twice at each site. Measurements were made at Fort Lewis prior and after thinning (some of the trees were harvested) allowing a unique opportunity to gauge the impact of tree density on a propagating signal. Measurements were made at Coventry during the summer and in the autumn (after the leaves had fallen) providing an opportunity to measure the seasonal effect of foliage on radio signals.

The propagation measurements conducted at Fort Lewis were made at a number of antenna heights providing propagation data from manpack-type deployment to just under forest canopy deployment. The first sets of measurements at Fort Lewis (ref. 4) were made during April-May 1986 and were conducted at two different sites. One site, Holden Woods, had older, less dense growth with taller (60-130 feet) larger (greater diameters) trees than the second site, South Perry, which had heights between 50 and 100 feet. The South Perry measurements were repeated in June 1987 after the trees had been thinned.

Measurements were made at Coventry, Connecticut in late August-early September of 1987 and identical measurements made again in early November (after the autumn fall of leaves) of the same year. The site is a flat wetland with a 30-year old stand of red maple with occasional white pine and aspen along the edges of the stand. The forest height is about 48 feet; the base of the canopy is about 28 feet above the forest floor.

3. FOREST BIOPHYSICAL CHARACTERISTICS

In order that measured data might be used both for model validation and trend analysis, the forests themselves were carefully characterized biophysically. For example, at Fort Lewis, a regular grid of tenth-acre plots was established

and within these plots the number of trees, tree trunk diameters, tree heights, and canopy thickness were all measured. The tree trunk number density and mean tree trunk diameter were then determined for each plot and used to construct the contour plots shown in Figures 1 and 2. These figures proved especially useful in assessing the homogeneity of the measurement sites and for deriving the path-averaged values of tree trunk number density needed for model validation and data interpretation. The tree trunk-diameter histogram (composite over all plots) and tree height-diameter regression curve are shown in Figures 3 and 4.

4. PATH-LENGTH EFFECTS

Path attenuation, as expected, increased with increasing path length. This is apparent from the (1986) Fort Lewis path attenuation data, measured at three frequencies (400, 850 and 1050 MHz) between three equal-height antennas (11.6, 14.6 and 17.6 m) and plotted in Figure 5. Regression of path attenuation against path length reveals only slight statistically significant differences according to frequency and polarization. With horizontal polarization, the least-squares attenuation/distance slopes at the higher frequencies of 850 and 1050 MHz are about 0.17 dB/m; for all other polarization-frequency combinations the slope is about 0.14 dB/m. There has been no evidence of any lateral wave, a forest propagation mechanism which often arises in dense forests at frequencies below 200 MHz. (The lateral wave is discussed further in Section 6.) Measurements conducted at Coventry prior to and after the autumn fall of leaves show an approximate 5 to 6 dB drop in attenuation loss with the leaves gone.

Delay spread, too, increases with increasing path length. This is apparent from the (1986) Fort Lewis delay-spread measurements shown in Figure 6. Generally, the delay-spread of horizontally polarized waves increases less rapidly with increasing path length than do the corresponding delay-spreads of vertically polarized waves. Especially notable is the rapid increase of delay-spread with increasing path length experienced by vertically polarized 400 MHz radiowaves.

5. ANTENNA HEIGHT/POLARIZATION EFFECTS

Both the Fort Lewis and Coventry data indicate attenuation to have some antenna height dependency. A plot of path attenuation versus antenna height for frequencies of 400, 850, and 1050 MHz for both vertical and horizontal polarization is shown in Figure 7 using data from the 1986 measurements at Fort Lewis. Note that no data are provided for South Perry for horizontal polarization at 850 and 1050 MHz and for vertical polarization at an antenna height of 65 feet. The path loss was so great at these frequencies and polarizations that no signal could be measured. The 400 MHz data showed little change with height, whereas the higher frequency data showed an increase in path loss with increasing antenna height. The high-frequency cases clearly refute the general wisdom that higher antenna heights are better. The increased path loss is most notable in the South Perry (shorter trees) data. This suggests that clearance-below-canopy is the effective parameter and not height. In addition, the Holden data indicate that horizontally polarized signals suffer more attenuation at the higher frequencies, most probably because of the effect of horizontally oriented branches.

Attenuation measurements through deciduous trees at Coventry showed just the opposite path-loss/polarization dependency. As stated earlier the conifers at Fort Lewis had branches that were practically horizontal while

the deciduous trees at Coventry had branches with a more vertical orientation. These two different results reinforce the contention that branches, and more specifically their orientation, strongly impact the path-loss/polarization relation.

At Fort Lewis (the only delay spread data processed so far) delay spreads up to 600 nanoseconds were observed. Delay spread was found to be greater with vertical polarization especially at 400 MHz. Although the Coventry data has not been formally processed delay spread was also noted to be greater with vertical polarization that with horizontal.

6. FOREST PARAMETER EFFECTS

Tree trunk number density appears to be the primary parameter affecting signal strength and multipath delay spread, although for antennas situated within the canopy, branch size and orientation statistics are likely to play a major role. The dominant propagation mechanism in the forest appears to be tree scatter. No ground effects were noticed, and it appeared that ground reflections were lost in multiple tree scatter. The existence of a "lateral wave" (a wave that propagates just above the canopy/air interface) was not seen.

A particularly useful measure for assessing the effects of the forest parameters on signal strength is specific attenuation. According to theory [7], the specific attenuation within a trunk-dominated forest increases linearly with increasing tree- trunk number. Theoretical curves showing the variation of specific attenuation with frequency are shown in Figure 8 based on the (1986) South Perry biophysical parameters. Also shown are the values of specific attenuation derived from measurement. Although order-of-magnitude agreement is excellent, the polarization dependence is extremely ragged, probably because the antennas were positioned only slightly below the canopy where scattering from branches could strongly affect polarization.

The much misunderstood lateral wave merits further discussion (ref. 5). First, a lateral wave is a signal that originates from an antenna within the confines of the forest, exits the forest through the canopy, propagates just above the canopy (experiencing essentially free space attenuation loss), re-enters the forest through the canopy, and is received at a second antenna also in the forest. Before addressing the lateral wave further some understanding of the propagation electromagnetics of a signal in foliage is necessary.

The propagating forest signal consists of an incoherent and coherent component. As a radiowave propagates through the forest, power associated with the coherent component is transformed to the incoherent component. The strength of the coherent wave is dependent on its ability to maintain coherence. It is the coherent component that gives rise to the lateral wave. As frequency increases (and wavelength decreases) the turbulence or roughness of the canopy/air boundary disrupts the coherent component causing it to lose coherence. Therefore, at frequencies above 400 MHz the strength of the coherent component has been reduced to such an extent by crossing the canopy/air interface that the lateral wave contribution to the received signal is negligible.

Measurements were conducted at Coventry specifically with the intent of finding a lateral wave. The measurements were made at a path length of 910 feet with both transmitting and receiving antennas at identical heights. The center of the canopy and the canopy/air interface were at

approximately 38 and 48 feet respectively. Most surprisingly, less loss was found at 38 feet than at 42 feet. A summary of the experiment characteristics and results are shown in the following table:

Antenna Height (ft)	Path Attenuation (dB) Vertical	Horizontal
38	15.2	4.4
42	17.3	10.2
47	10.5	6.3
52	9.6	10.6

Depending on forest canopy density, the portion of the transmitted signal giving rise to the lateral wave propagates upward from the transmitting antenna through the canopy and downward from above the canopy to the receiving antenna at an angle between 3 an 4 degrees relative to horizontal. Using this criterion with the measurements made in the canopy region at Coventry, a lateral wave should have been seen. At antenna heights of 52 and 47 feet no excess path loss should have been noted. Furthermore, the path loss should have increased as the antenna height was reduced to 38 feet. This last result certainly indicates that the signal travels along a direct path through the forest, experiencing path loss dependent on the density or number of scatterers present.

An additional problem when assessing data to determine the existence of a lateral wave is the homogeneity of the forest parameters (i.e., uniform tree height and number density for the entire transmission path). The plots in Figure 9 demonstrate the homogeneity problem. This figure contains plots of excess path loss vs distance for the Holden Woods site at Fort Lewis. Note that the excess attenuation exhibits a minimum at 800 feet attributable, most likely to path inhomogeneity. On long paths where the lateral wave has supposedly been seen an examination of the path should be made. Based on this project's experience in temperate forests, it is difficult to find a path of any great length that maintains constant density or height.

7. CONCLUSIONS

This paper has presented the initial findings of the Army's Wideband Propagation Measurement program. This effort is filling the void in wideband signal behavior and modeling; combining developing wideband theory and propagation models with actual field measurements to collect empirical wideband propagation channel data. Some notable observations from the field measurements are presented and a comparison of measured results to model-predicted signal behavior. The experiment results are by no means conclusive, since foliage measurements have been dominated by measurements in the trunk region of the forest, but the findings demonstrate the potential value of these measurements to understanding the wideband communication channel.

Most noteworthy are the antenna height/pathloss results and the polarization/pathloss results at both Fort Lewis, Washington and Coventry, Connecticut. These height/pathloss results clearly refute the general wisdom that higher antenna heights are better and may clearly impact tactical radio deployment philosophy. The Fort Lewis measurements made below the canopy in the trunk dominated portion of the forest, show a pronounced increase in path loss with increasing antenna height, especially with increasing frequency and horizontal polarization, Likewise the Coventry, Connecticut (deciduous forest) results show that path loss is less at

mid-canopy than just below the canopy interface.

These findings and others described in this paper will be examined further in an on-going analysis and presumably in future measurements. Specifically, measurements are planned around the canopy/air interface and through foliage over rougher terrain. These current findings, further analysis of existing data, and planned future measurements have expanded and will continue to expand wideband propagation models, and improve the utility of existing propagation models.

REFERENCES

1. P. Sass, "Propagation Measurements for UHF Spread Spectrum Mobile Communications," IEEE Transactions on Vehicular Technology, Vol. VT-32, No. 2, May 1983.

2. B. Fair, M. Frankel; "Design Plan for Wideband Propagation Measurement/Data Acquisition and Recording System," SRI Design Report 1, Contract DAAB07-82-C-J097, Sep 1982.

3. R.W. Hubbard, Linfield, Hartman, "Measuring Characteristics of Microwave Mobile Channels," US Department of Commerce, NTIA Report 78-5, Jun 1978.

4. J. Rino, J. Owen; "Wideband Propagation Measurements in Forested Media," SRI Technical Report, Contract DAAB07-85-C-K569 Aug 1987.

5. R.H. Lang, A Schneider, S. Seker and F.J. Altman, "UHF Radiowave Propagation through Forests," CyberCom Technical Report CTR-108-01, Sep 1982.

6. R.H. Lang, A. Schneider, F.J. Altman and S. Seker, "UHF Radiowave Propagation through Forests," CyberCom Technical Report CTR-115-02, Sep 1985.

7. A. Schneider, "UHF Communications through Forested Propagation Channels," AGARD Conference Procedings No. 363, pp 11-1 to 11-19, Jun 1984.

System Capabilities

GENERAL	
Carrier frequency range	200 to 2000 MHz
Delay-spread range	-1 to 20 us
Delay-spread resolution	2 ns
Doppler-spread range	-15 to 240 Hz
Doppler-spread resolution	<2 Hz
TVIR amplitude resolution	0.1 dB
TVIR multipath amplitude resolution	-20 dB min
Measureable path loss	155 dB min
ANTENNAS	
Omnidirectional	Biconical
Directional	Crossed LPAs
Transmitter polarization	V, H, RCP
Receiver polarization	V, H, RCP, LCP
Azimuth	0 to 360°
Height	5 to 65 ft
TRANSMITTERS	
Number	2
Frequency range	
Transmitter No. 1	200 to 1050 MHz
Transmitter No. 2	700 to 2000 MHz
Power output	100 W max
Modulation	PN sequence Bi-phase modulation or CW
Clock rate	50, 125, or 250 MHz
Instantaneous null-to-null bandwidth	100, 250, or 500 MHz
PN code length (chips)	255, 511, 1023, or 2047
Control	Local or receiver computer
RECEIVER	
Number	2
Frequency range (each channel)	200 to 2000 MHz
Sensitivity (23 dB SNR in 50 kHz BW)	-95 dBm
Modulation	PN sequence Bi-phase modulation or CW
Clock rate	50, 125, or 250 MHz
Instantaneous null-to-null bandwidth	100, 250, or 500 MHz
Code length (chips)	255, 511, 1023, or 2047
Control	Local computer
Instantaneous dynamic range	50 dB
Input signal range (at van wall)	0 to -95 dBm
AGC (receiver computer controlled)	Stepped in 1-dB increments

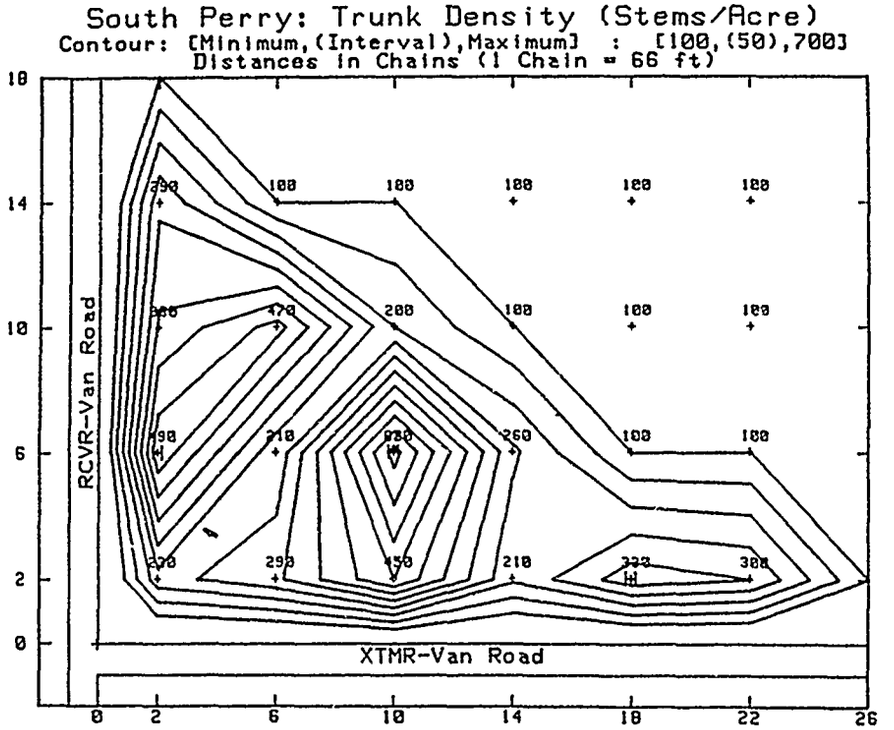

FIGURE 1. Tree-Trunk Number Density

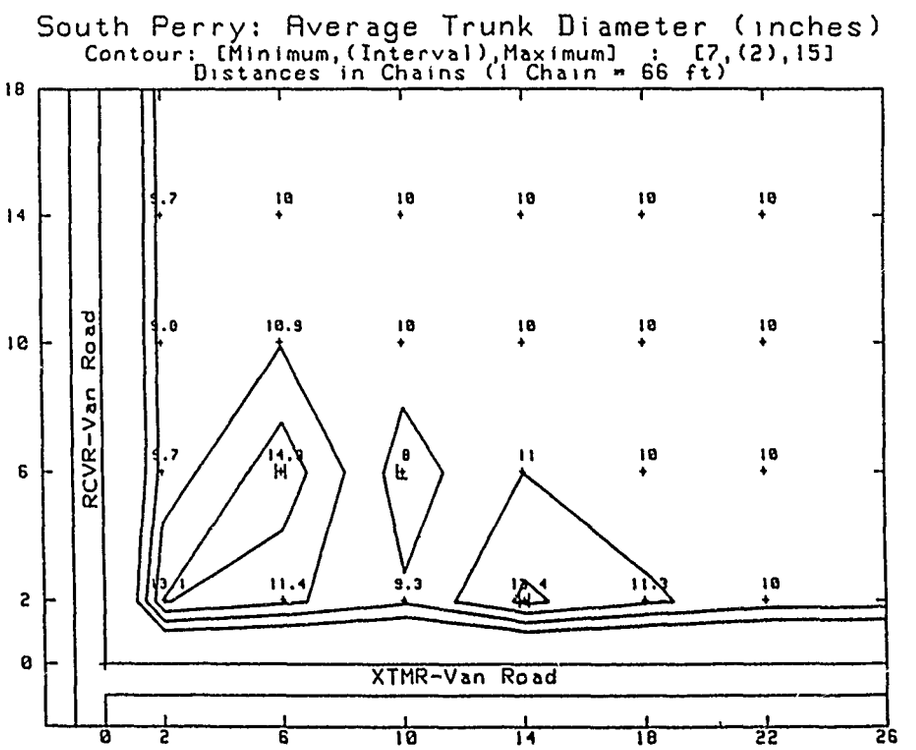

FIGURE 2. Mean Tree-Trunk Diameter

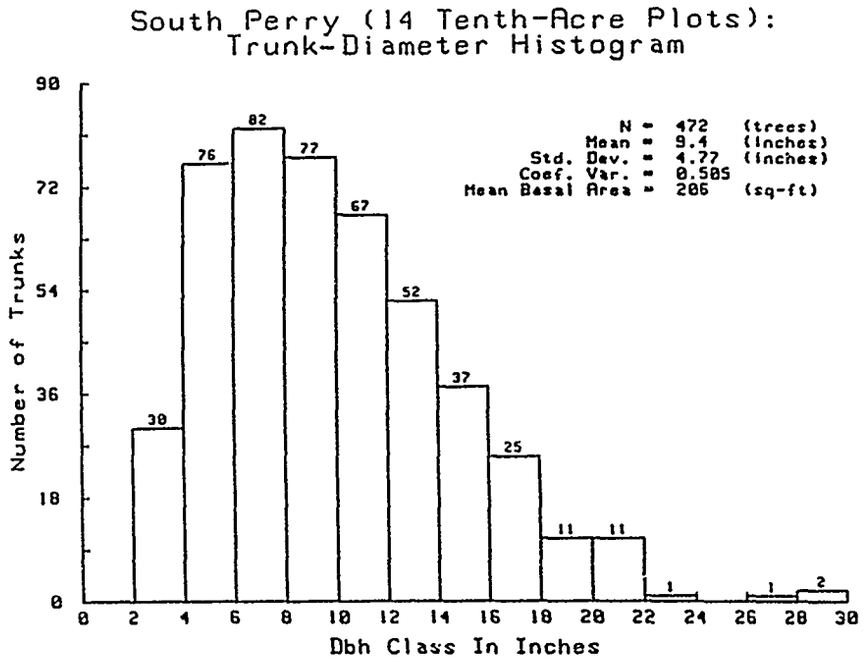

FIGURE 3. Tree-Trunk Diameter Histogram

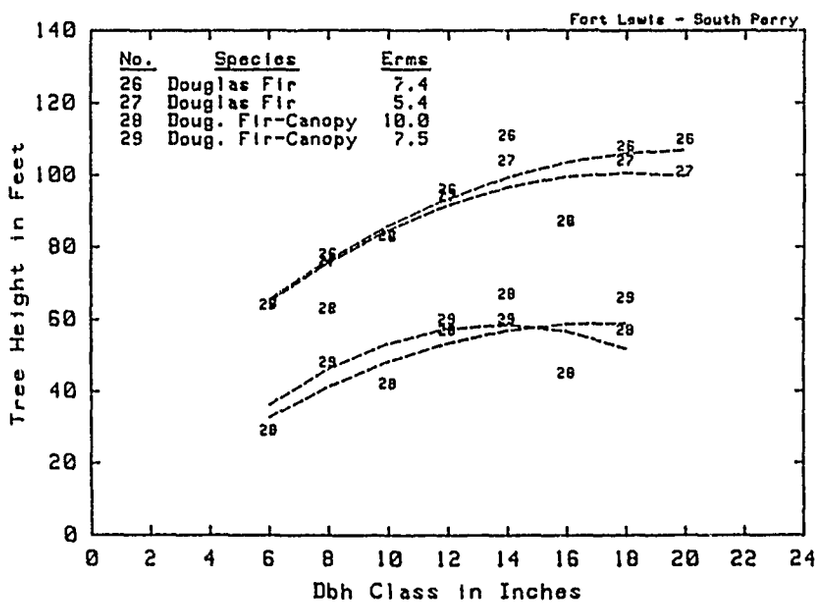

FIGURE 4. Tree Height-Diameter Curve

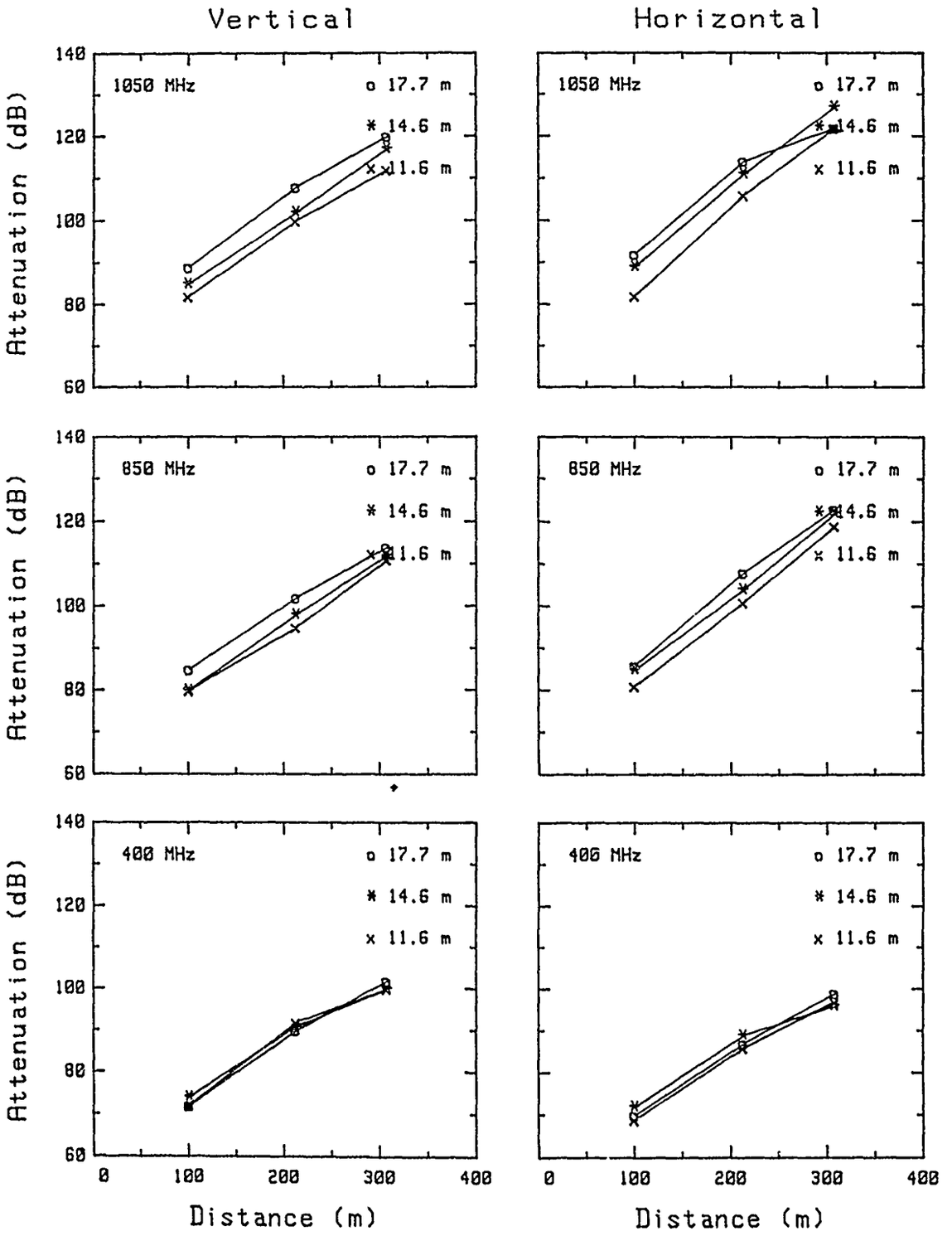

FIGURE 5. S.Perry attenuation vs distance

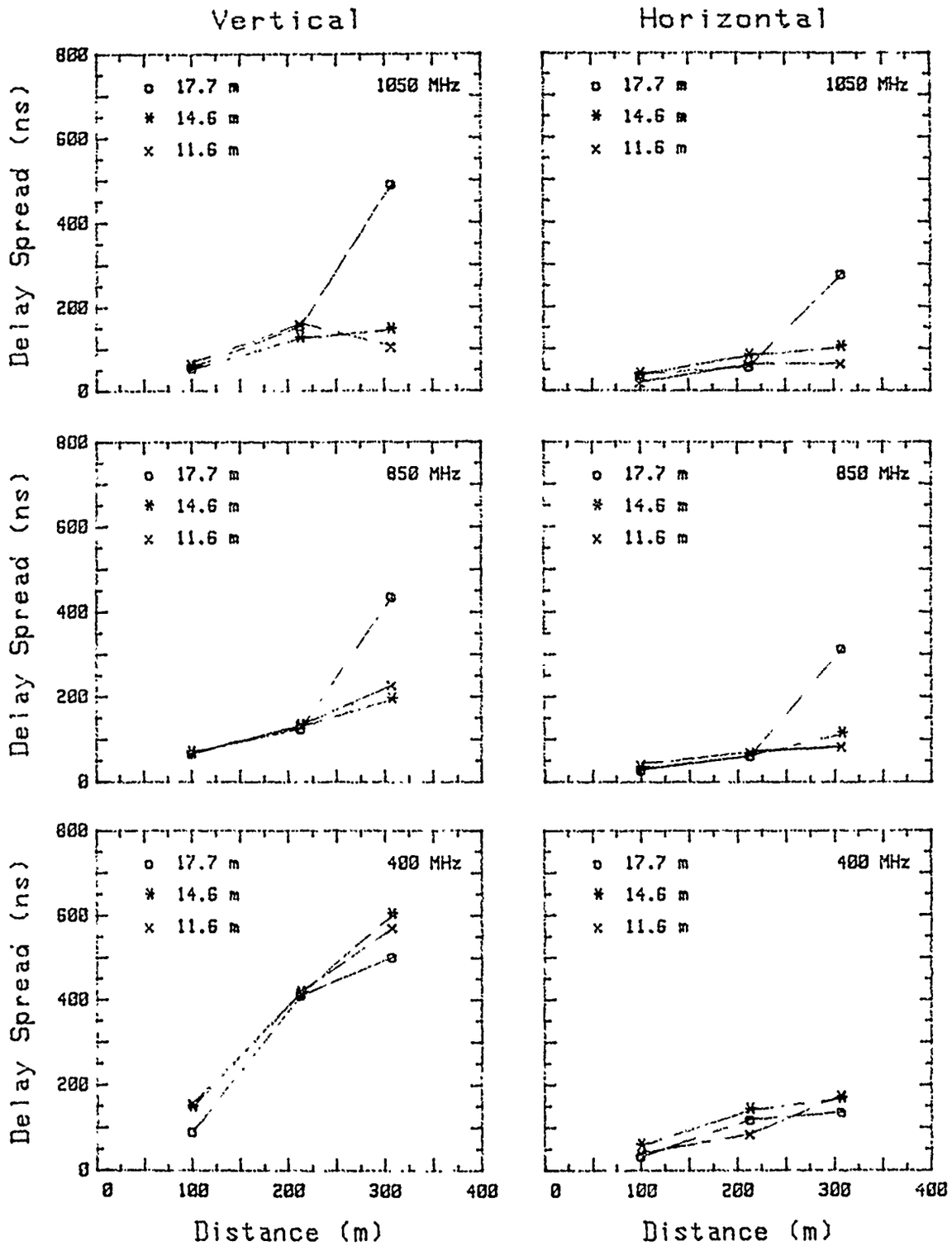

FIGURE 6. S.Perry delay spread vs. distance

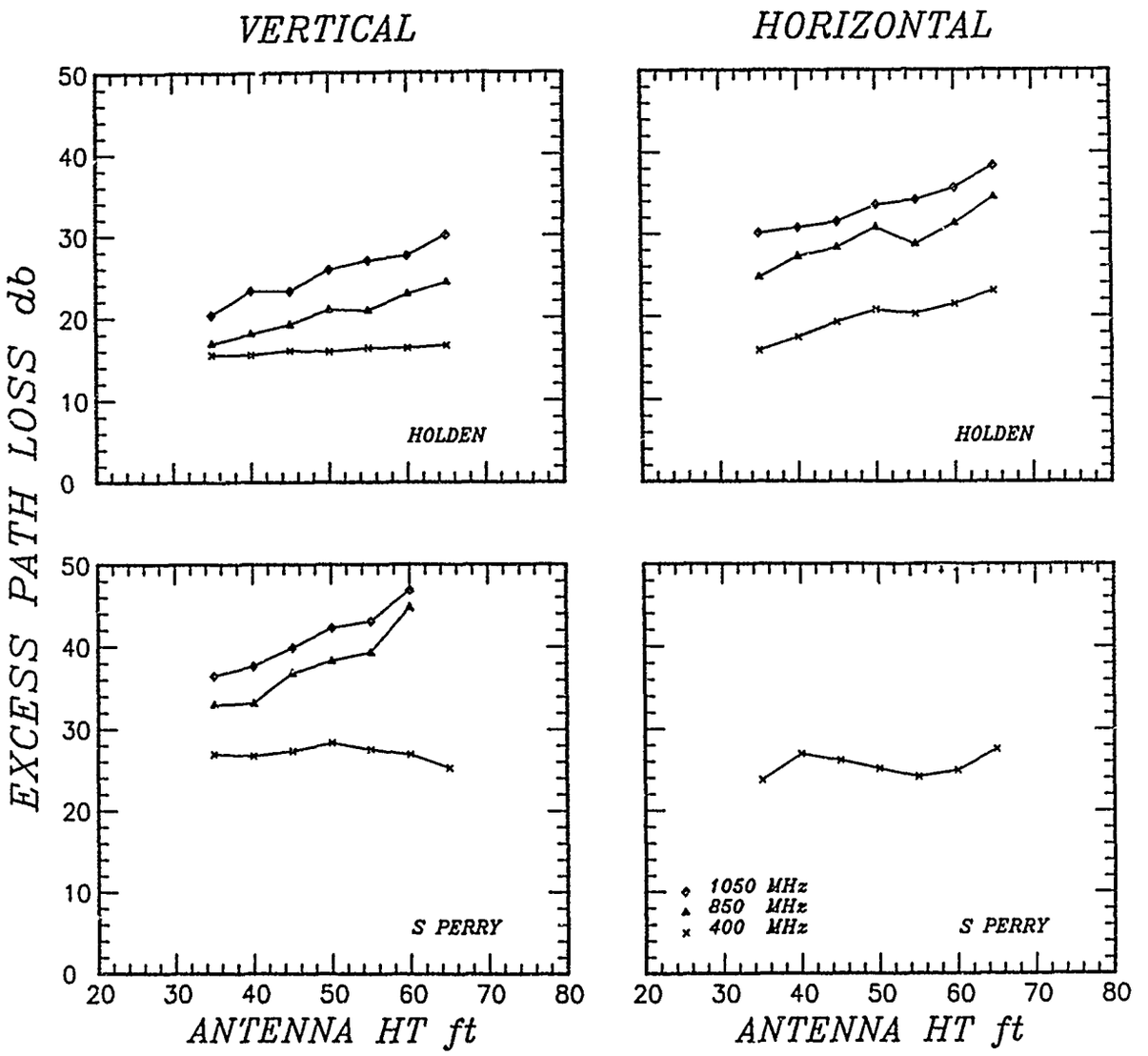

FIGURE 7. Comparison of height-gain patterns on comparable Holden Woods and South Perry paths.

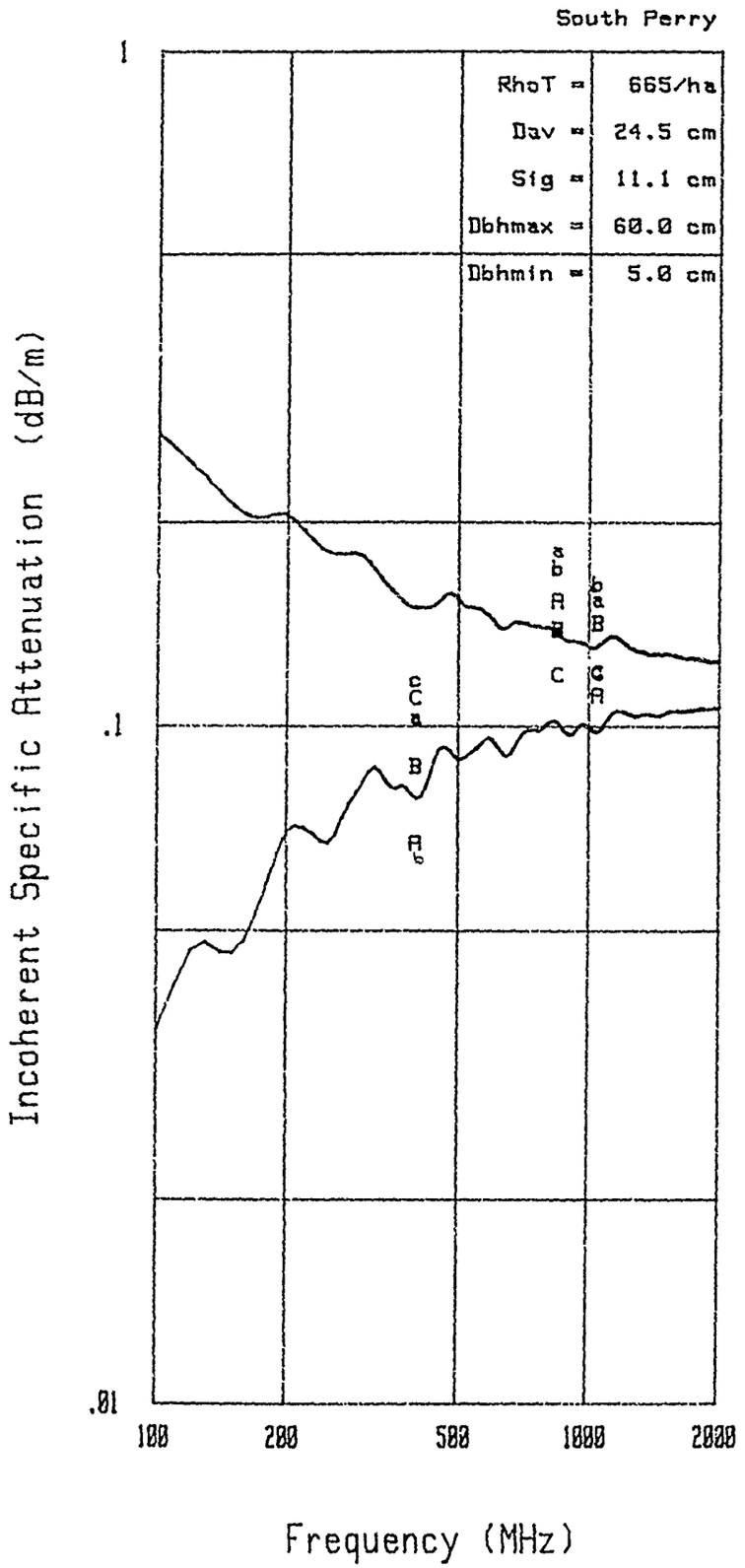

FIGURE 8. Theoretical and measured specific attenuation.

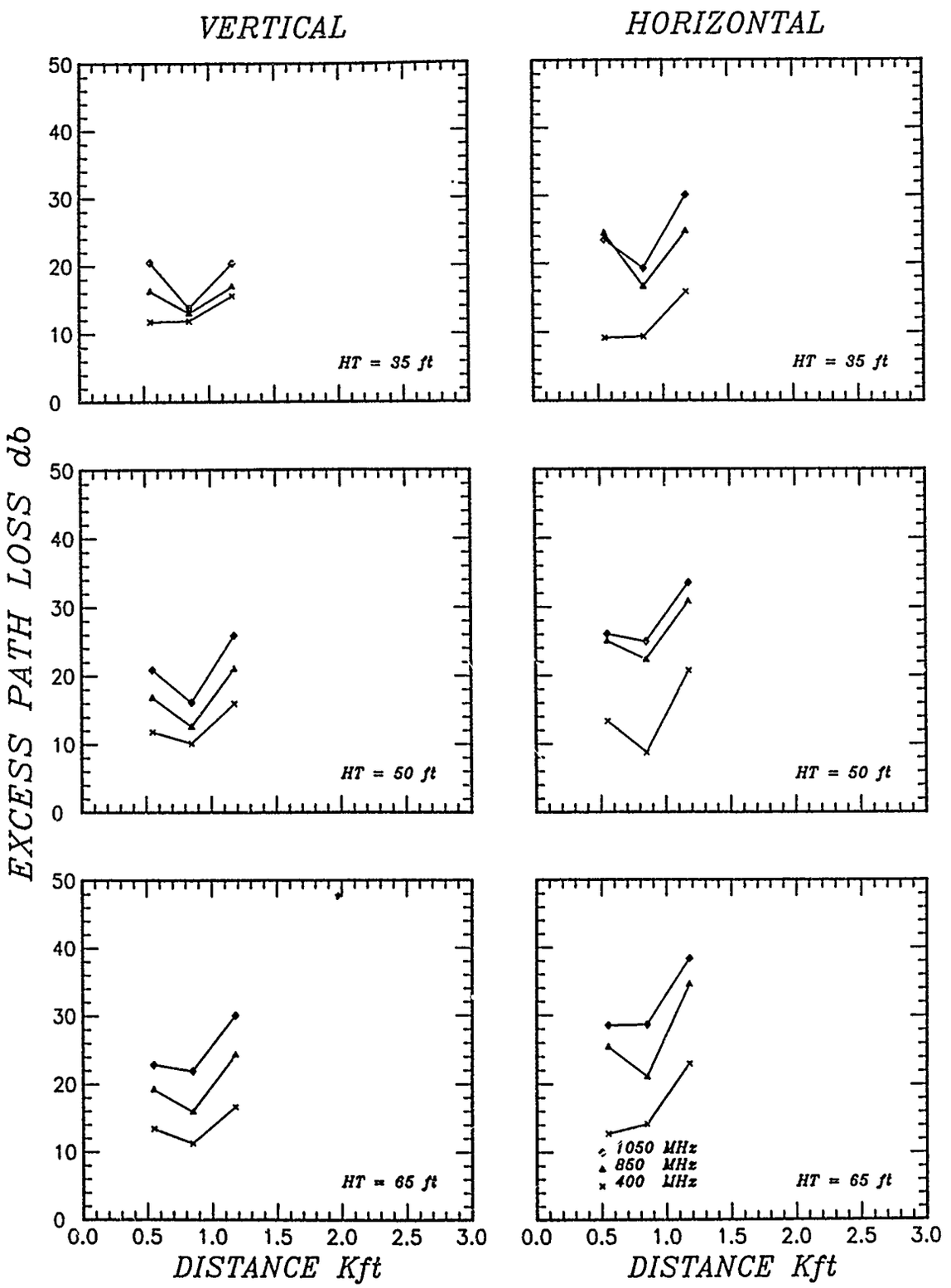

FIGURE 9. Excess path loss vs distance for Holden Woods.

IN-BAND AMPLITUDE DISPERSION ON A MICROWAVE LINK

by

Y.K.Li*, P.Gole and M.Sylvain
CNET/PAB/RPE
38—40 rue du Général Leclerc
Issy-les-Moulineaux
92131
France

ABSTRACT

Statistical results of in-band amplitude dispersion on a microwave link during 1985 with diversity reception in France are presented. The large time extent of our data base allowed an analysis of the seasonal variations of in-band amplitude dispersion distributions. Worst-month distributions are also presented for each channel. Idealized switch diversity is investigated with the decision criterion of in-band amplitude dispersion. It was found that the potential improvement due to the space diversity technique in terms of the reduction in amplitude dispersion was remarkable. The frequency correlation coefficient of received amplitudes and powers in the summer of 1985 was computed on the experimental data base. Comparisons between experimental results and theoretical results were made for the two non-diversity channels for the summer period of 1985.

I. INTRODUCTION

High-capacity digital microwave systems are very sensitive to in-band amplitude dispersion (IBAD) due to multipath fading. It was found from experiments and theoretical considerations that the bit error rate (BER) is closely correlated with in-band amplitude dispersion [4]. Because of its simplicity of measurement and its strong correlation with medium and high-capacity terrestrial microwave digital system performance, IBAD has also been chosen as a parameter to characterize the multipath propagation channel [7].

It has been previously shown that statistical characteristics of IBAD can be a basis to predict communication quality of microwave digital system due to multipath fading. Some experimental results have been published and empirical laws have been proposed for the distribution of this parameter. However, experimental results are still scarce, especially for space diversity systems, and theoretical research is far from being sufficient for the prediction of the statistical characteristics of this parameter.

This paper describes experimental results obtained in France on a space diversity microwave link. This experiment (PACEM 2 experiment) was set up for a period of several years in the Beauce region, and extends over a length of 50 km, with two receiving antennas at heights of 80 and 95 metres, respectively. The operating frequency is about 11 GHz, with a bandwidth of 64 MHz. Transfer functions (Automatic Gain Control Voltage and Group Delay Distortion) were recorded with a frequency sweep rate of 17.5 Hz on both diversity channels, and 128 samples per sweep. In order to reduce the amount of received data, only those transfer functions affected by multipath were kept, using a fade selection threshold of 6 dB. It should be noted that transfer functions from both channels were kept whenever one of the single channels exceeded this threshold. The topographic profile of the PACEM 2 experimental link is given in Fig.1; more details about this experimental set-up can be found in previous papers [3] [2].

From a theoretical point of view, a model is described, and the statistical characteristics of the IBAD parameter during serious multipath fading can be obtained. The comparisons between the cumulative distributions of measured IBAD and the calculated results for serious multipath fading periods is presented here.

II. EXPERIMENTAL RESULTS

In-band linear amplitude dispersion (IBLAD) is the difference between two levels in decibels at two frequencies.

In this paper, the statistical results of the in-band and linear amplitude dispersion in a 55 MHz frequency band in the whole period of the year 1985 are revealed.

The definition of IBLAD employed in this paper is,

$$\text{IBLAD} = 20\log(R_2/R_1) = 10\log(P_2/P_1) \quad (1)$$

where R_2 and P_2 are received relative amplitude and power corresponding to the higher edge frequency f_2 of the frequency band, R_1 and P_1 are received relative amplitude and power corresponding to the lower edge frequency f_1 of the band. For cumulative probability calculations, the absolute values of IBLAD are taken,

$$Z = 20\log[\max(R_1, R_2)/\min(R_1, R_2)]. \quad (2)$$

* Mr Li is a researcher of China Research Institute of Radiowave Propagation.

In the following, what is meant by the term diversity or third channel, is the one obtained supposing ideal switching, i.e. keeping that of the two single channels which has the lower IBLAD.

A. Monthly Distributions

Fig.2 and Fig.3 show the variations of the statistical distributions of IBLAD for the three channels from month to month. It should be noted that the curves for January and December are less reliable for the reason that insufficient data were recorded due to some failures of measurement system.

The probability values given in Fig.2 are relative or conditional probabilities. The probability given in Fig.3 was counted relative to the total experimental time during the month of interest. Fig.3 contains the total information, taking into account the difference in fading occurrence from one month to the next, the interest of conditional probability representation of Fig.2 is to stress the month difference in the strength of the events.

It should be noted here, in Fig.2 and Fig.3, that owing to the rejection of recorded data not satisfying the selection criterion, a certain distortion is introduced for small values of IBLAD. Indeed, we keep all transfer functions with IBLAD greater than 6 dB, because then the attenuation in the bandwidth is also greater than 6 dB. Portions of the transfer functions with IBLAD lower than 6 dB on the other hand may have an attenuation lower than 6 dB and thus be rejected by the data selection process, it results in a "distortion" of the IBLAD statistics at lower value. But this is of no practical consequence, if, as can be suggested, all possibly damageable transfer functions are retained.

In Fig.3, it appears that the probability values of small IBLAD for the diversity channel are greater than those of non-diversity channels. Since, during the calculation of cumulative probabilities of IBLAD, the same total time (experimental time) was used for the three channels, and since, moreover, the chosen IBLAD for the diversity channel is the smaller of IBLAD values between both non-diversity channels, there are much more small values of IBLAD on the diversity channel, this is the reason for such a result. In fact, diversity is useful only when IBLAD is large enough to induce outage. In that case, the curves always display a diversity improvement. This benefit could be better understood afterwards in part II-D of this paper.

B. Seasonal Variations

Seasonal variations for two selected thresholds of IBLAD are given in Fig.4. It can be clearly seen that there exists a broad maximum in the summer, which would be expected since it is known that atmospheric layering occurs more frequently during summer. Also, for the lower antenna, a high peak in February is noticeable, which can be explained by winter occurrence of atmospheric layers during short time periods.

Worst-month distributions for the three channels are given in Fig.5. They have been obtained as the envelope of the monthly curves of Fig.3. It shows that for worst-month a great improvement is provided by space diversity. The quantitative description of the diversity improvement will be found in II-D.

It can be noticed that the poor diversity improvement obtained on the level at centre frequency on the same data base [2] due to an abnormal behaviour of the events recorded in June, does not appear when considering the IBLAD here.

C. Yearly Distributions

The distributions of negative and positive values of IBLAD for the three channels are given in Fig.6. There seems to exist a slight dissymmetry for the three distribution curves.

Fig.7 gives the cumulative distributions all over 1985. They are almost linear for the three channels taken individually, the slope values are given in Table 1.

TABLE 1

Channel	Lower antenna	Higher antenna	Diversity
	0 ----- 24 dB	0 ----- 30 dB	0 ----- 12 dB
Slope (dB/decade)	6.2	7.5	2.2

From all of the above curves, is obvious that in our experiment the higher antenna is much more sensitive to multipath events, which is consistent with already obtained distributions of fade levels at centre frequency [2].

D. Diversity Improvement

The IBLAD parameter has been chosen in this paper as the decision criterion of the space diversity technique. The statistical results for the idealized switch diversity channel are computed. Diversity improvement factors which are defined as the probability ratios of the non diversity channels to the diversity channel at certain fixed dispersion thresholds for worst-month distributions are given in Table 2, and the diversity improvement factors I(ΔA) with month number for two dispersion thresholds are shown in Fig.8.

TABLE 2

Channel	Lower	Higher
I (6 dB)	30.78	38.43
I (10 dB)	95.36	142.78
I (20 dB)	532.73	1381.81

From Table 2 and Fig.8, it is very clear that the diversity improvement is remarkable. The space diversity technique is thus a very efficient method for overcoming in-band dispersivity due to multipath fading.

E. Frequency Correlations

The frequency correlation coefficient also is very important parameter for describing the severity of multipath fading effects and for estimating in-band linear amplitude dispersion. The correlation coefficient of received relative amplitudes and powers at the two edge frequencies separated by 55 MHz are computed for the summer period of 1985, and are given in Table 3.

TABLE 3

Antenna	Correlation Coefficient of relative amplitudes	Correlation Coefficient of relative powers	Parameters	
	$\rho_R = \frac{\langle R1R2\rangle - \langle R1\rangle\langle R2\rangle}{\sigma R_1\, \sigma R_2}$	$\rho_P = \frac{\langle P1P2\rangle - \langle P1\rangle\langle P2\rangle}{\sigma P_1\, \sigma P_2}$	$\lambda 11 = \langle R^2 1\rangle/2$	$\lambda 22 = \langle R^2 2\rangle/2$
Lower	0.786	0.731	0.069	0.074
Higher	0.407	0.246	0.081	0.084

From the above table we find out that the correlation degree of the higher antenna is smaller than that of the lower antenna. This also means that the effect of multipath fading on the higher antenna is greater than on the lower antenna. Moreover, for both antennas, the amplitude correlation coefficients are greater than the power correlation coefficients. The difference between the two parameters λ_{11} and λ_{22} is negligible, which shows that both frequencies are statistically equivalent, as it should be.

According to our general knowledge, for non-fading periods, the received powers at two frequencies of the same frequency band are almost completely correlated, and the frequency correlation coefficient is nearly unity. For fading periods, the frequency correlation coefficient is smaller than one, and the more serious the fading, the smaller the correlation coefficient. Here, only the correlation coefficients of fading periods upon the experimental data base are calculated. So, it is impossible to compare the frequency correlation coefficients here with those previously obtained by other authors. Because of the rejection of recorded data and using the total time of appearance of multipath events, the frequency correlation coefficients obtained here are much smaller than the results published before [6, 8].

III. THEORY

A. Theoretical Model

Considering that frequency selective fading occurs under the situation of comparatively deep fading, it is known that deep fading can be represented by a Rayleigh distribution [6]. Therefore, a mathematical model for a correlated two-dimensional Rayleigh distribution was employed to describe the distribution of the levels at two frequencies. The joint probability density function of amplitudes corresponding to the two edge frequencies of the frequency band can then be written as:

$$p(R_1, R_2) = \frac{R_1 R_2}{q\lambda_{11}\lambda_{22}} \exp\left\{-\frac{1}{2q}\left[\frac{R_1^2}{\lambda_{11}} + \frac{R_2^2}{\lambda_{22}}\right]\right\} I_0\left\{k\frac{R_1 R_2}{q(\lambda_{11}\lambda_{22})^{1/2}}\right\} \tag{3}$$

where $\lambda_{11} = \frac{1}{2}\langle R_1^2\rangle$, $\lambda_{22} = \frac{1}{2}\langle R_2^2\rangle$, $\lambda_{12} = \langle R_1 R_2 \cos\phi 1 \cos\phi 2\rangle$ $k^2 = \lambda_{12}^2/\lambda_{11}\lambda_{22}$, $q = 1 - k^2$, $I_o(x)$ is zeroth order modified Bessel function of the first kind. R_1 and R_2 are amplitudes corresponding to frequencies f_1 and f_2, respectively. $\phi 1$ and $\phi 2$ are the phases of the received signals at two frequencies f_1 and f_2, respectively.

With the definition of absolute in-band linear amplitude dispersion given by (2), the formula of cumulative distribution of in-band linear amplitude dispersion (dB) can be derived as

$$P(a > a_0) = 1 - \frac{\lambda_{11}a_0 - \lambda_{22}}{2[\lambda_{11}^2 a_0^2 + 2\lambda_{11}\lambda_{22}(1 - 2k^2)a_0 + \lambda_{22}^2]^{1/2}} + \frac{\lambda_{11} - \lambda_{22}a_0}{2[\lambda_{11}^2 + 2\lambda_{11}\lambda_{22}(1 - 2k^2)a_0 + \lambda_{22}^2 a_0^2]^{1/2}} \quad (4)$$

where $a_0 = 10^{Z_0/10}$.

With the approximation of $\lambda_{11} \doteq \lambda_{22}$ (which has been shown inb II-E to be reasonable), formula (4) can be simplified as:

$$P(a - a_0) \doteq 1 - \frac{a_0 - 1}{[1 + 2(1 - 2k^2)a_0 + a_0^2]^{1/2}}. \quad (5)$$

If we know the parameter k, the probability of amplitude dispersion can be calculated easily with formula (5).

B. Comparisons of Theoretical and Experimental Results

We discussed the calculations of the parameter k as it was defined in section III-A. It should be pointed out that this parameter is neither the correlation coefficient of powers, nor the correlation coefficient of amplitudes.

In fact, the kind of measurement available to us doesn't allow an exact computation of this theoretical parameter. We therefore investigated two approximation methods to derive an estimation of the parameter k.

First, fitting formula (5) to the experimental curves of probability of IBLAD by a least-square method, the values of parameter k for the two non-diversity channels are obtained, and found to be 0.948 and 0.827 for lower and higher antennas, respectively. The fitted curves are given in Fig.9 (black diamond-shaped symbols).

For the two channels, the values of parameter k determined this way are different, and it is smaller on higher channel than on lower channel.

The second approach is to consider that, though mathematically (R1, R2) and (ϕ1, ϕ2) are not strictly independent, with the assumption of weak correlation between them and of a statistically small difference between ϕ1 and ϕ2, the following approximated formula can be obtained for k:

$$k \doteq \frac{\langle R_1 R_2 \rangle}{\sqrt{\langle R_1^2 \rangle \langle R_2^2 \rangle}}. \quad (6)$$

The values of k for the two non-diversity channels based on our experimental data were calculated with the above formula. For the summer period, they are 0.974 and 0.912 for lower and higher antennas, respectively.

Comparisons of measured cumulative distributions of IBLAD with the calculated results for both non-diversity channels in the summer period (June, July, August) of 1985 are given in Figure 9, where the theoretical results are calculated by the formula (5), using the second estimation method for k (crosses).

Fig.9 shows that the agreement between the theoretical curve and the experimental result is better on higher channel than on lower channel, which again can be explained by the fact that there are much more strong events on the higher antenna than on the lower antenna.

IV. CONCLUSIONS

1 Statistical characteristics of in-band amplitude dispersion for one-year period is presented. Seasonal variations and worst-month distributions are obtained.

2. On this link, the higher antenna is much more sensitive to multipath events.

3. Space diversity technique is very efficient for overcoming in-band diversity as far as it is defined by IBLAD.

4 For different channels, the values of parameter k are different. Theoretical curves agree well with experimental results.

REFERENCES

1 Serizawa, Y.
Takeshita, S. *A Simplified Method for Prediction of Multipath Fading Outage of Digital Radio*, IEEE Vol. COM-31, No.8, pp.1017—1021, August 1983.

2. Gole, P.
Sylvain, M.
Ghahremani, T. *Long-term Multipath Effects on a Space-diversity Channel*, ISRP '88, Beijing, pp.464—467.

3. Gole, P. Lavergnat, J. Sylvain, M. — *Description and Preliminary Results of the PACEM 2 Experimental Program*, IEEE 1987, pp.38.5.1—38.5.5.

4. Sakagami, S. Hosoya, Y. — *Some Experimental Results on In-band Amplitude Dispersion and a Method for Estimating In-band Linear Amplitude Dispersion*, IEEE Vol. COM-30, No.8, pp.1875-1887, August 1982.

5. Vigants, A. — *Distance Variation of Two-tone Amplitude Dispersion in Line-of-sight Microwave Propagation*, IEEE pp.68.3.1—68.3.5.

6. Vigants, A. — *The Number of Fades in Space-diversity Reception*, B.S.T.J. Vol.49, No.7, pp.1153—1530, Sept. 1970.

7. Martin, A.L. — *Dispersion Signatures, A Statistically Based, Dynamic Digital Microwave Radio System Measurement Technique*, IEEE, Vol.SAC-5, No.3, pp.427—436, April 1987.

8. Martin, L. — *Statistical Data On Amplitude Dispersion Caused by Multipathing, Document* 5/107-*E*, CCIR Study Groups, Period 1986—1990, France, March 1988.

ACKNOWLEDGEMENT

The authors wish to thank Miss Ghahremani for the permission of using her previous data processing programme, and colleagues of CRPE for performing the PACEM2 experiment; one of us (Y.K.Li) is being supported by a CNET grant. We are also thankful to Mr J.C.Bic for helpful discussions.

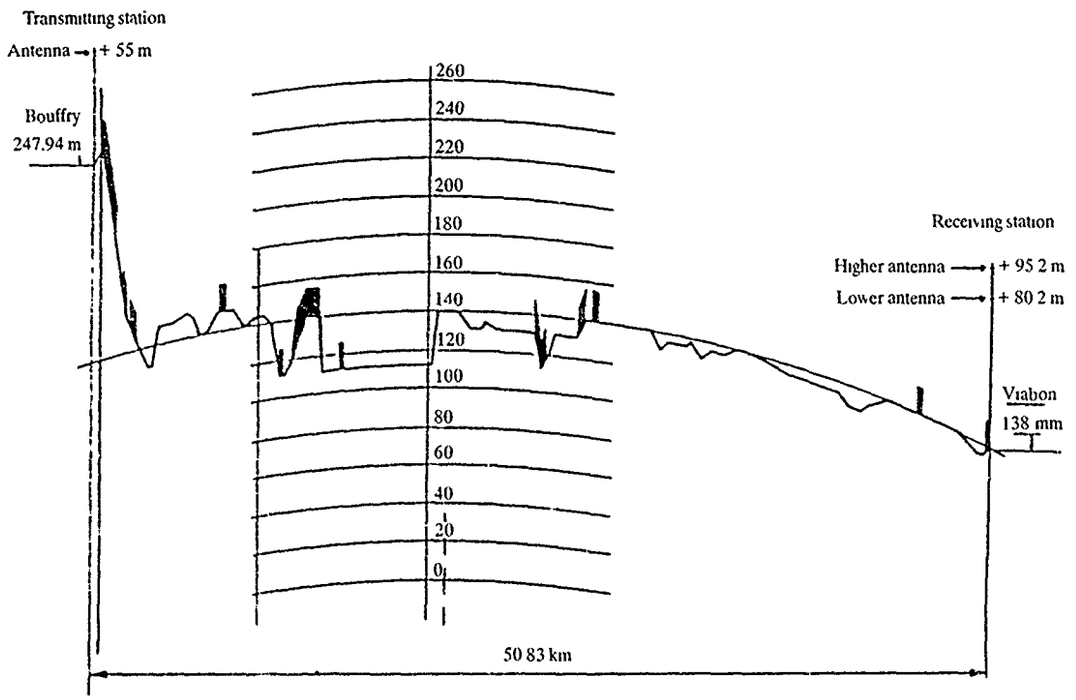

Fig.1 Topographic profile of the PACEM2 experimental link

a > Lower antenna

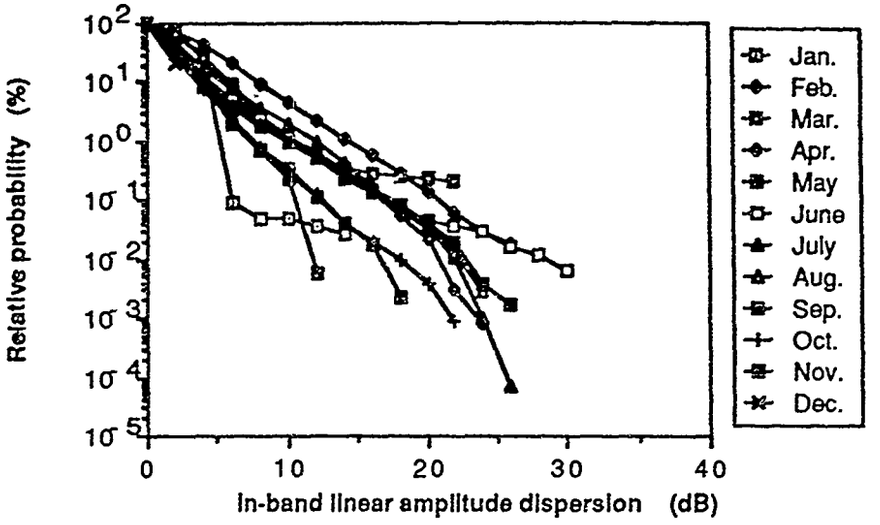

b > Higher antenna

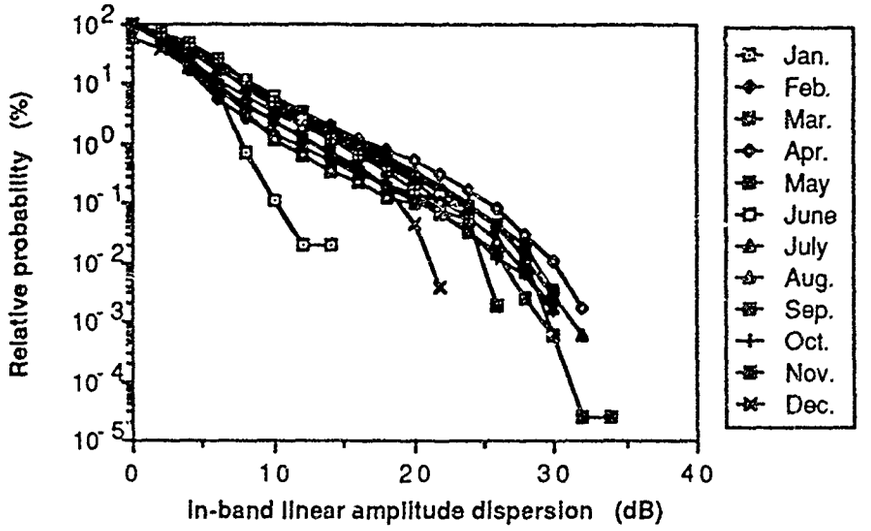

c > Diversity

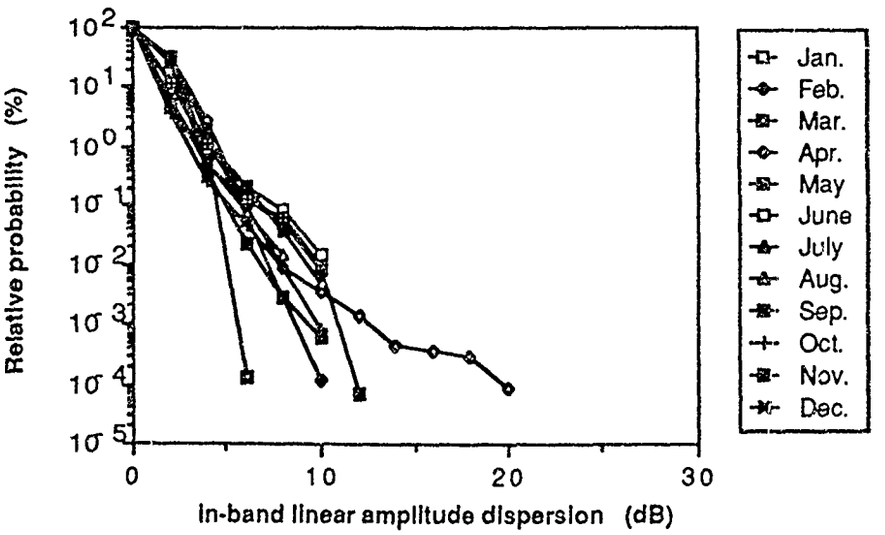

Fig.2 Relative probability curves

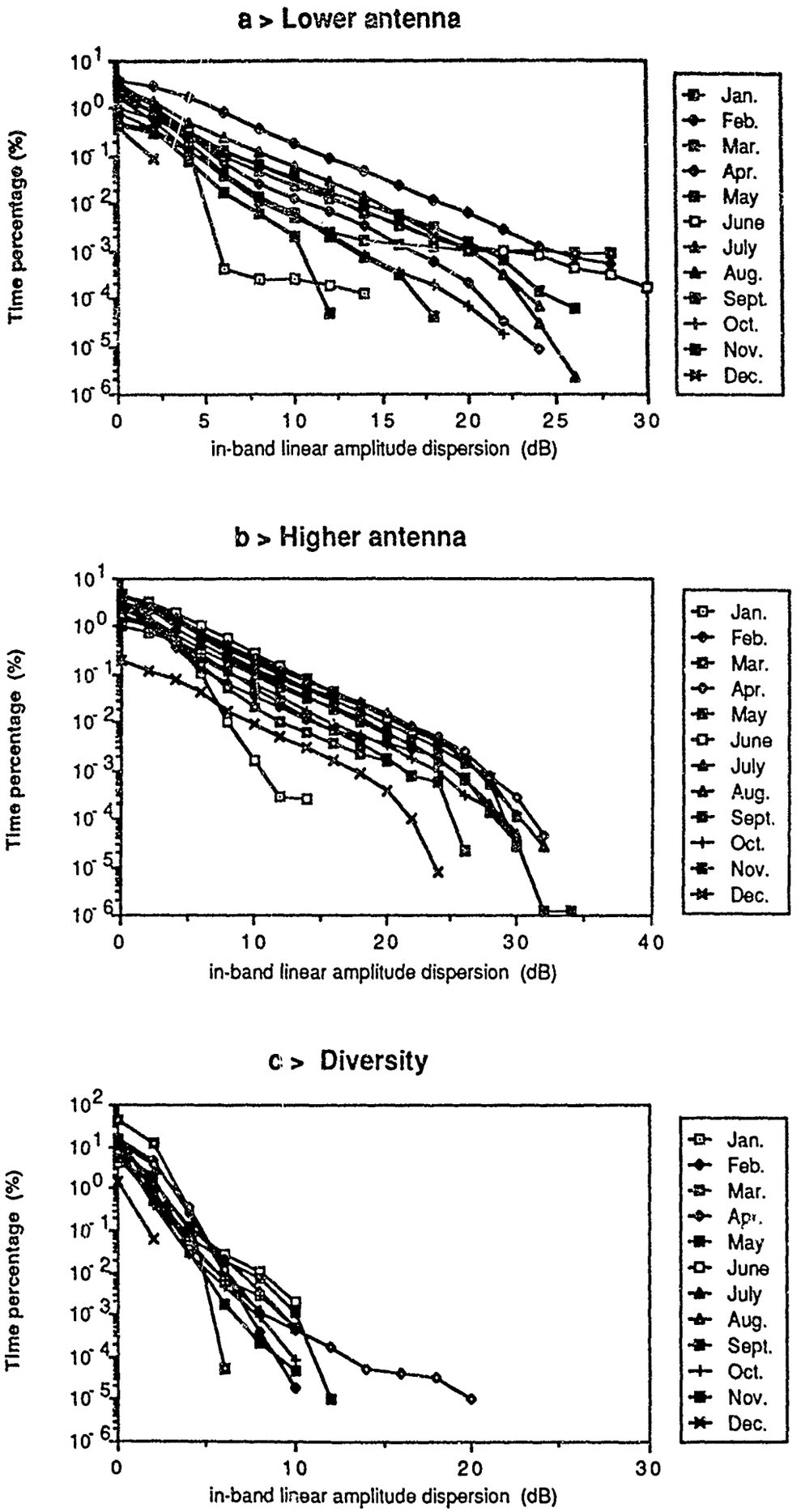

Fig.3 Cumulative probability curves

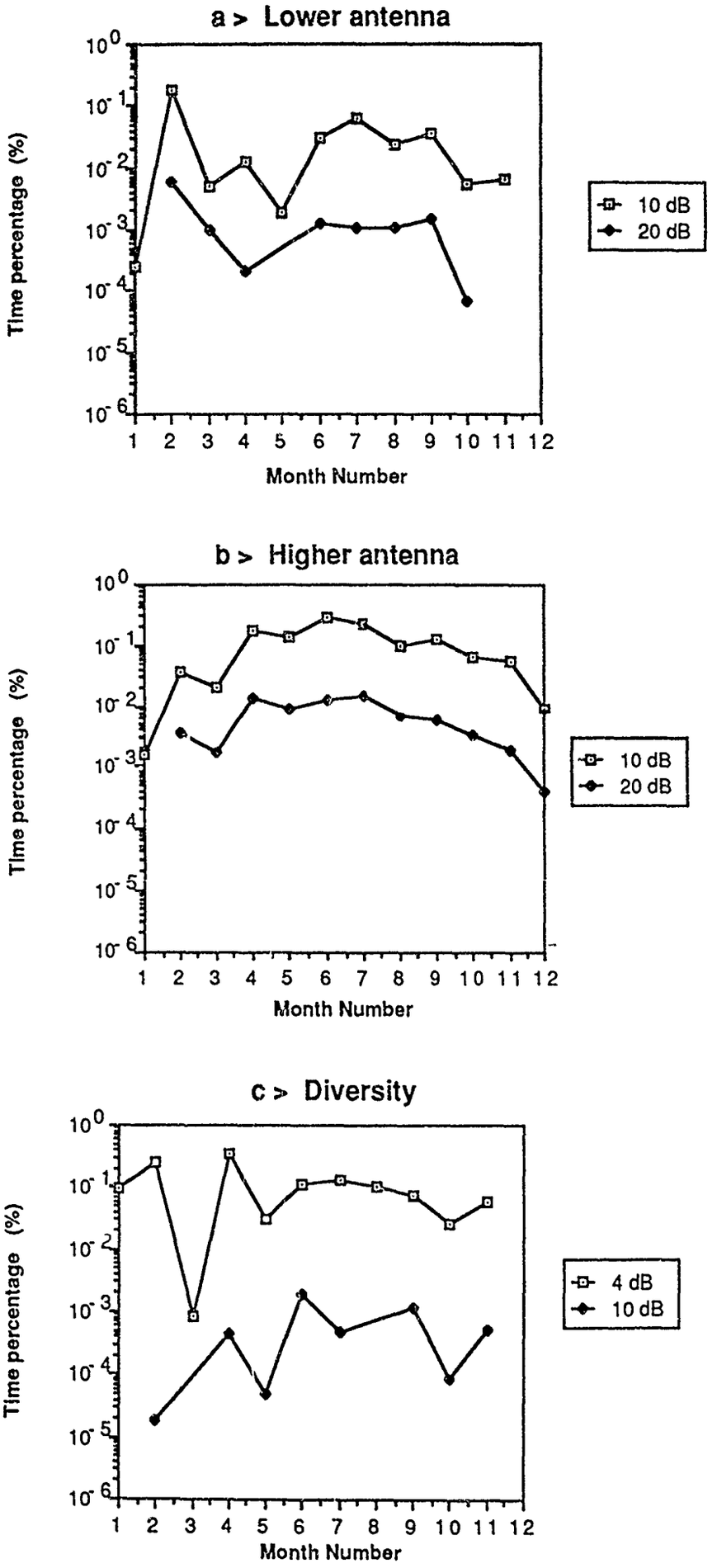

Fig.4 Seasonal variations

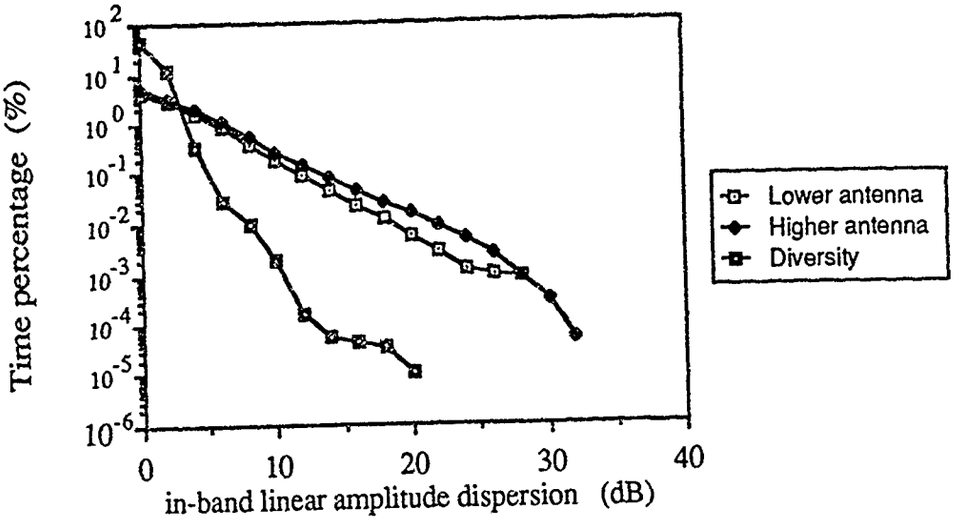

Fig.5 Worst-month distributions

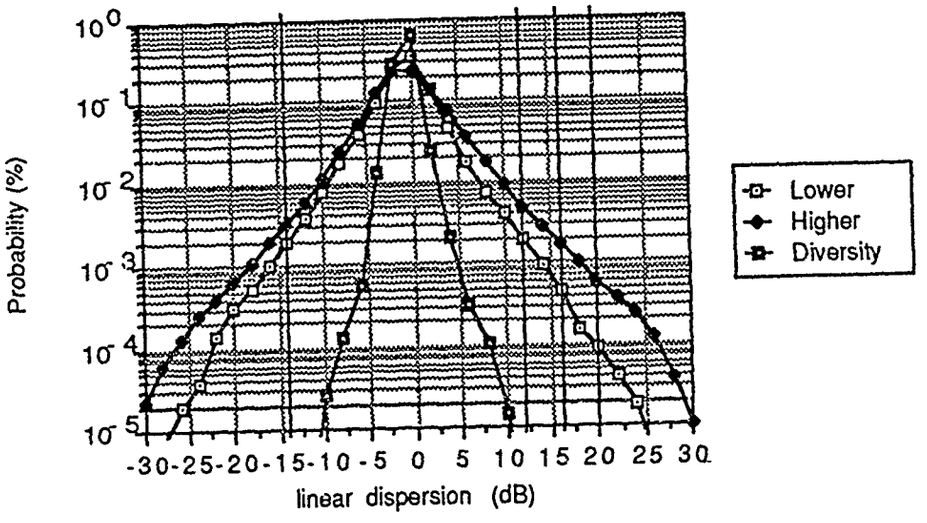

Fig.6 Distribution curve of IBAD for 1985

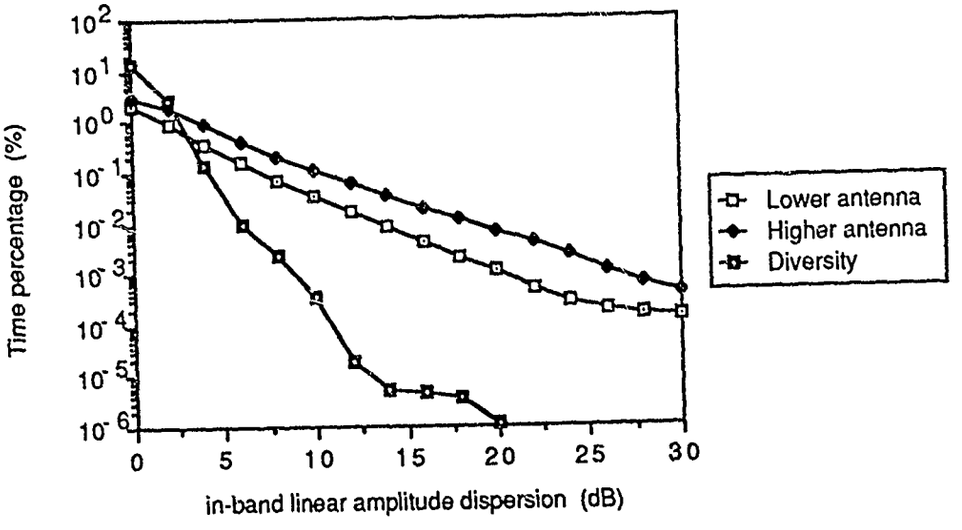

Fig.7 Cumulative probability curves for 1985

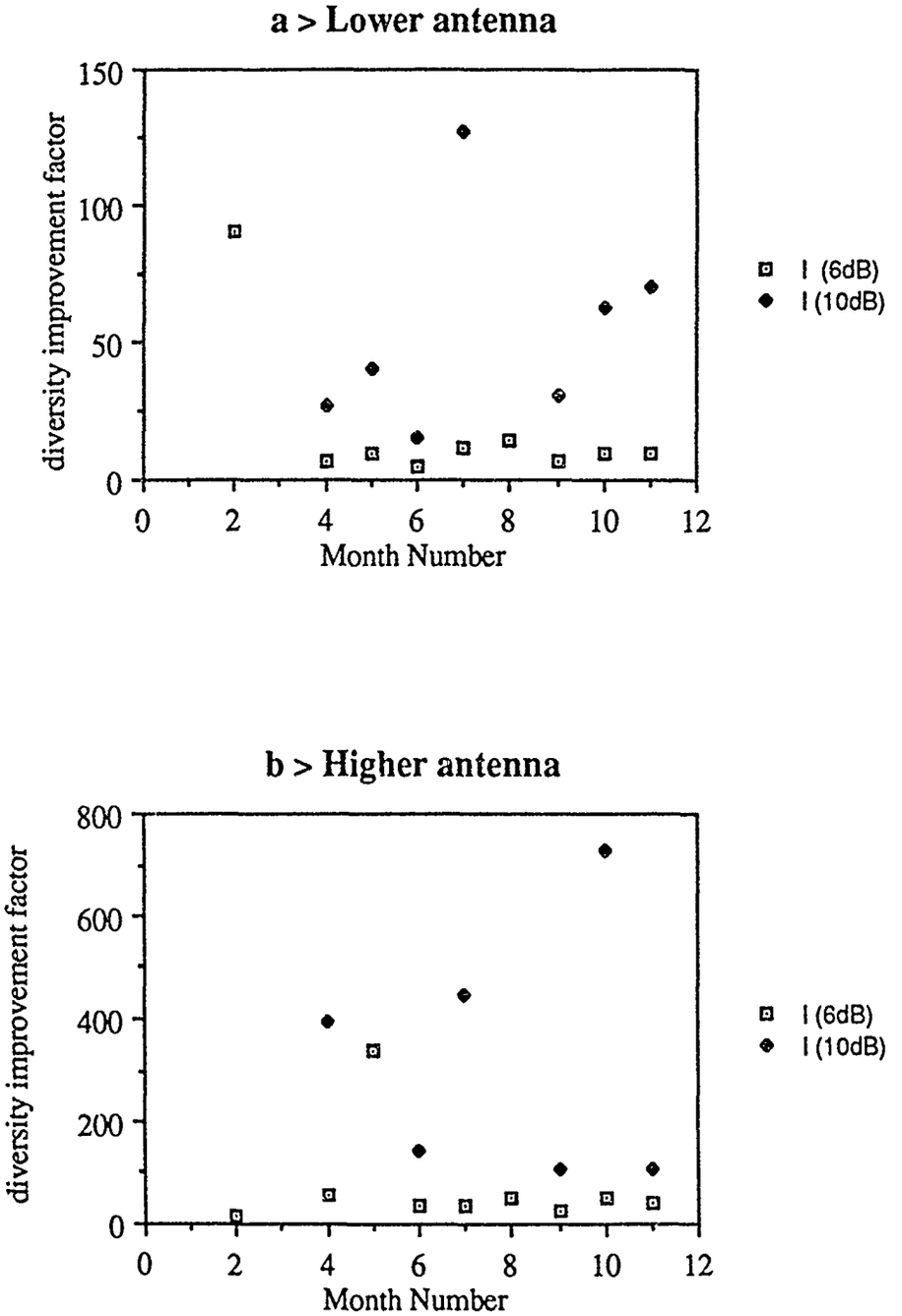

Fig.8 Monthly diversity improvement

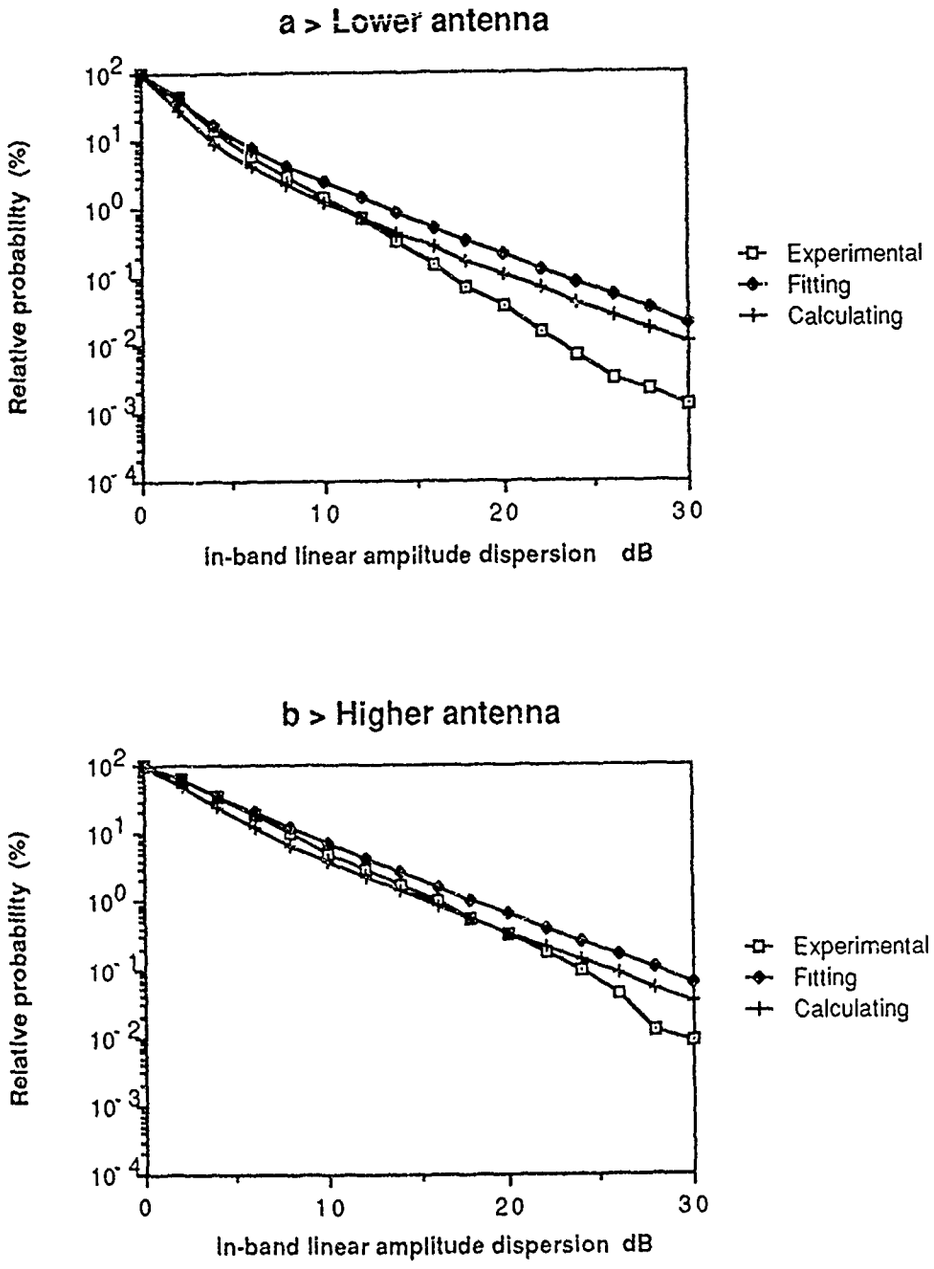

Fig.9 Comparisons with experimental results

DISCUSSION

K.S. KHO

You mentioned in your paper that you used space diversity because frequency diversity will fail because the frequencies are quite correlated. I think if the Freq. spacing is properly done using heightgain pattern, a correlation of - 0,5 could be achieved. I think the relation of space diversity and frequency diversity is nearly 1 to 1 relation.

AUTHOR'S REPLY

I don't think I have said that frequency diversity would fail because the signals at two frequencies would be too correlated. I agree that, in its principle, frequency diversity is very similar to space-diversity, the frequency spacing in one case corresponding to the antenna separation in the other. In both cases, the problem is to study how the selectivities on the two diversity-channels are correlated. To our knowledge, there has been a very few experiments concerning space diversity (Rummler, BST 61, n° 9, 1982, and our experiment since 1985) and no experiment at all on that aspect of frequency-diversity.

Moreover, space-diversity is more generally used than frequency-diversity because the latter requires twice as large a frequency bandwidth.

D.J. FANG

Could you state if your model (eq.(3) of your paper) applies to atmospheric multipath alone or applies to atmospheric multipath together with surface multipath ? If it applies only to atmospheric multipath, the model may have a value for universal application as the atmospheric multipath effect is less link specific. On the other hand, if it applies to atmospheric multipath together with surface multipath, the model may have little value for universal applications since surface condition varies greatly from one link to the other. Can you comment on that ? Specifically what do you see your model for design applications of a different link ?

AUTHOR'S REPLY

The modeling of fade levels at one frequency by a Rayleigh distribution applies to attenuations greater than about 15dB. The same restriction of course applies when the joint distribution of the levels at two frequencies is modeled by a bivariate Rayleigh distribution. When the atmospheric signal is attenuated so much by multipath effects, the ground-reflected rays are no longer negligible. The resulting signal is therefore a combination of several paths both from atmospheric and from ground-reflection origins, and it is not possible to separate them on the basis of single frequency or even medium bandwidth data.

The transfer function of the propagation channel is very sensitive to the smallest change in any of these paths, but from a statistical point of view, I don't think that on a bandwidth of a few tens of MHz, the paths effects depend on their physical origin. Therefore, a statistical model should be universal ; and in fact, statistical results from very different links are qualitatively similar.

The situation could be different on a link presenting permanent strong reflected rays (for instance over-sea link), but in that case, it is possible to determine the position of the antenna in order to reduce this effect.

DISCUSSION

E. GURDENLI

1 - Please clarify the difference between your "relative probability curves" and "cumulative probability curves".

2 - You have demonstrated how switched space diversity can reduce IBLAD. Can you comment on how this concept can be applied to the prediction of performance of radio relay systems ?

AUTHOR'S REPLY

1 - If T is the total period of observation, and T' (T' < T) is the part of the period during which multipath events occur, the "relative probability curves" relate to time percentages computed relative to T' (i.e. probabilities conditionned by the presence of a multipath event) whereas the "cumulative probability curves" relate to time percentages computed from T, and therefore taking into account the occurrence of the events.

2 - We have made in fact a propagation study of IBLAD on two channels which can be combined by space diversity. To apply the results to the prediction of performance of a radio-link, we need to know the relation between IBLAD and bit-error-rate (BER). This relation certainly depends on the system characteristics (modulation, power, ...), and is not a functional but an equiprobability relation. Its establishment is, anyhow, the job of systems designers, not of propagationists.
Morever, we have used (for its simplicity) the concept of "switched" space diversity when in fact real systems use a "combination" space diversity, the analysis of which would be more difficult.

C. GOUTELARD

Vous signalez une anomalie en Février, visible dans vos enregistrements. Avez-vous une explication de cette anomalie importante ?

AUTHOR'S REPLY

Nous observons sur l'antenne basse un extremum isolé d'occurrence pendant le mois de Février. Ce maximum correspond en fait à 1h20mn de dépassement d'une "distorsion linéaire dans la bande" de 10dB, et à 3 minutes et demi de dépassement de la valeur de 20dB.
On sait, par exemple par les observations faites par Louis MARTIN sur la liaison Lannion-Roc Tréduder, que des situations de trajets multiples se produisent l'hiver. On sait aussi qu'en climat tempéré la plus grande partie de l'activité de trajets multiples est concentrée sur quelques nuits du mois. Les observations de Février pourraient donc correspondre à seulement une ou deux nuits d'évènements. Il faudra donc :

1 - Rechercher les évènements individuels donnant cette forte occurrence.

2 - Attendre d'avoir traité les quatre années de mesure pour déterminer le caractère plus ou moins exceptionnel de tels évènements d'hiver, et dans la mesure du possible les conditions météorologiques leur ayant donné naissance.

A DIGITAL METEOR-BURST COMMUNICATION (MBC) PROPAGATION PATH SIMULATOR

K. Watson
Hull-Warwick Communications Research Group
Department of Electronic Engineering
University of Hull
Hull
HU6 7RX
UNITED KINGDOM

SUMMARY.

The Paper discusses an MBC propagation path simulator which has been developed by the author, and contrasts the specification of this simulator with that of a typical HF simulator. A discussion of how the simulator has been implemented and how it is to be employed then follows.

Finally, there is included a brief discussion of a few concepts which are to be investigated using the simulator. The final aim of the research is to produce an MBC system which makes more efficient use of the available capacity than previously reported systems.

1. INTRODUCTION.

The University of Hull is currently conducting research into adaptive channel encoding and signal processing applied to meteor-burst communications (MBC). Basically, this research is aimed at improving the performance of MBC systems by continually matching the transmission signal to the capacity of the inherently intermittent channel. Previously reported systems, are essentially non-adaptive; all have used fixed modulation formats, transmission rates and channel encoding schemes (Davis et al, 1957; Bartholme' and Vogt, 1968; Cannon and Reed, 1987).

As one would expect the research programme entails testing many different modulation formats, encoding schemes and complete system configurations. Basically such testing involves the grading of configurations according to their response to specific tests. For numerous tests to be performed and direct comparisons made it is necessary to have a readily available MBC test-bed which produces totally repeatable paths. Consequentally, it was decided that the most logical manner in which to start the research was to construct an MBC propagation path simulator. Such a simulator has many advantages over a real path during the development of a system. A basic summary of these advantages is given below:

(a) Repeatability.

As already stated this is a requirement of any form of comparative testing, which is required during the assessment of system configurations.

(b) Extreme Path Conditions.

With a realistic simulator it is possible to set up any conditions which can be found on an MBC path. Thus, it is possible with such a simulator to perform tests under conditions which only rarely occur over a 'real' channel. Consequentally, system configurations can be easily tested at their limits.

(c) Flexibility.

Due to the nature of the simulation it is possible to simulate any specific path with relative ease, including any localised noise and interference.

(d) Cost/Convenience.

The nature of the research programme implies that many different signal processing techniques, encoding schemes, modulation schemes etc need to be tested . Obviously, the use of a simulator for initial testing will save a considerable amount of reources in both time and finance.

(e) Replay Possibility.

It is possible to implement the simulator such that it has a "play through" mode. In

this mode the simulator uses on-air recordings of 'real' MBC paths, instead of simulated paths. Thus it is possible to reproduce specific conditions.

2. METEOR-BURST COMMUNICATIONS.

Meteorites and micro-meteorites continuously bombard the atmosphere, and as they do so they burn up in the atmosphere (lower ionosphere). As they burn up, they leave a trail of ionisation which, because of the speed of the meteorite, diffuses to form a cone of ionisation which persists for, typically, several tenths of a second. Meteorites which provide usable trails usually have masses in the range of 10^{-1} to 10^{-4} grammes. Meteorites with larger masses tend to be too infrequent to base reliable communications upon, and meteorites with smaller masses do not create enough ionisation whilst burning up. There are normally in excess of 10^{10} usable meteorites which bombard the earths' atmosphere every day, and thus between any two points within approximately 2000 km there are enough usable meteorites to provide a reliable (if intermittent) communication path.

The characteristics of communications via the ionised trails left by meteorites are variable, and are greatly dependent upon both the electron line density of the ionisation (which is itself dependent upon the mass of the incident meteorite), and the height at which the incident meteorite starts to burn up.

Electron line densities of 10^{10} to 10^{16} electron/m will provide useful forward scattering of radio waves. Within this range, meteor trails are traditionally classified as either underdense, or overdense. The dividing boundary is set at approximately $2x10^{14}$ electron/m.

When signals are propagated via underdense trails (electron line density less than $2x10^{14}$ electron/m) the received signal rises very quickly and then decays away exponentially. Signals which are propagated via overdense trails look totally different at the receiver, with a larger received power and longer duration. Usually overdense trails have durations greater than 0.5 second, and rarely up to as much as 30 seconds; Figure 1 exemplifies this point.

Although, overdense trails appear to be the largest constituent of system throughputs, it should be noted that the more attenuated underdense trails are far more numerous, and can account for in excess of 95% of the total number of usable meteor trails. Consequently, the vast majority of previously deployed MBC systems have been designed to make full use of these trails. Figure 2 shows a simulation of a typical MBC path over approximately 2 minutes.

Other physical phenomena can cause communication links to be established in the low VHF (very high frequency) region of the radio spectrum. The most common of which is sporadic-E layer propagation. This can 'open' links for up to 30-40 minutes and allow very high quality communications to be established. -70 dBm of received power is achievable with this mechanism, in comparison with -120 dBm of received power when the signal is scattered via meteor trails.

2.1 Noise and Interference.

As has been reported in other technical journals, noise in MBC systems is primarily galactic and man-made (Ostergaard, 1986) when receivers with low noise front ends are utilised. Man-made noise may be significantly greater than galactic noise, and can easily obscure low-power MBC returns. Special attention is needed when laboratory instruments and small computers are operated within proximity to MBC receivers. Measurement and analysis of the actual noise and interference experienced at the University of Hull site is currently underway and results should be available prior to the meeting.

2.2 Doppler Effects.

Reflection from the head of a meteor gives rise to doppler frequency shifts which can span the whole of the audio range. Doppler frequency shift from a meteor trail, which is a result of ionospheric and wind motions, can be of the order of 20 Hz at an operating frequency of 40 MHz. Doppler shift can also be a result of a specific application, eg an MBC system being used as an air-to-ground communication system. The movement of the aircraft could possibly introduce Doppler shifts up to 66 Hz for a 30 MHz operating frequency.

2.3 MBC in Brief.

MBC systems are inherently intermittent, and must be able to operate with very low received signal strengths. They are relatively phase-coherent, but can exhibit Doppler shift up to, say, 100 Hz. Obviously, any data communicated via this medium needs to be concatenated over several consecutive meteor bursts. During a burst, the capacity of the channel can be very high, but this does not tend to be fully utilised because of the short intervals involved. Most systems which have previously been deployed use a fixed transmission rate and a fairly low detection threshold. This allows a larger percentage of the burst to be used, but wastes a significant proportion of the available capacity.

3. AN MBC SIMULATOR.

If we compare the requirements of an MBC simulator to those of an HF simulator it can be seen that there are several important differences. Obviously, the major difference is that HF has a less variable attenuation over a fixed path than an MBC system over a similar path. Another very important difference is that the MBC simulator will have to cope with bandwidths of at least 20 kHz, whereas HF simulator only need to cover a little more than a standard 3 kHz HF channel. This will enable MBC systems which use large percentages of the available capacity to be tested on such a simulator. The other main differences between the requirements of an HF simulator and an MBC simulator are summarised below.

3.1 MBC.

(a) Due to the geometry of MBC, significant multipath is unlikely.

(b) The path propagation delay is equal to the sum of the delay between the transmitter and the meteor, and the delay between the meteor and the receiver.

(c) Excluding the end of the meteor trail, which is moved around by the wind, fading is not of great significance.

(d) Ignoring specific situations such as air-to-ground communications, Doppler shift is of relatively small magnitude.

3.2 HF.

(a) Multipath, which is caused by HF radio waves refracting from more than one of the ionospheric layers, is very important to HF communications. It is possible typically to have between 2-10 components.

(b) Each multipath component has an independent delay which is dependent upon the path taken.

(c) With HF communications fading, which is caused by the differing phases of multipath components combining in a random manner, can cause serious problems and is consequently of paramount importance.

(d) Doppler shift can be significantly higher in HF systems than in MBC systems.

On examination of the physical processes within MBC it can be seen that for a realistic simulation to be achieved there is a minimum number of processes which must be replicated. A summary of these is given below within the simulator specification.

3.3 MBC Propagation Path Simulator Specification.

Intermediate frequency(IF)	100 kHz.
Bandwidth	20 kHz.
Path delay range	0 - 12.8 ms.
Doppler shift	0 - 100 Hz.
Path attenuation	70 - 130 dB.
Noise sources (initially)	Gaussian white and impulsive.
Interference (initially)	Modem type interference.

3.4 Simulator Algorithms.

All simulator components are shown is Figure 3, together with the order in which they are applied. The individual algorithms are discussed below.

(a) Propagation Path Delay.

It is thought that, in order to fully test the functioning of the controlling algorithms and protocols, it is necessary to split the path delay into two distinct halves. This better represents the physical situation than would a single delay, which is how HF path delay is usually simulated. Figure 4 shows the geometry of a meteor scatter path. This case depicts the 'point of reflection' as the centre of the great circle path between the transmitter and the receiver. In the physical situation this will not always be the case, but is a reasonable initial approximation.

(b) Path Attenuation/Meteor-burst profiles.

The simulator must be able to generate a large number of differing path attenuations which realistically simulate an MBC path. It must therefore be able to vary the attenuation on the path by approximately 60 dB to cope with both rapidly varying normal underdense profiles, and also long periods of considerably less attenuated sporadic-E.

To achieve both of these requirements it was decided to generate path attenuations by randomly varying profiles taken from a standard library. It should thus be possible to obtain a very wide range of path conditions with relative ease. The simulator should also be able to operate in "play-through" mode, where a recording of a actual path is played through the simulator without modification.

(c) Doppler Shift.

In order that the simulator is able to test systems which are primarily designed for ground-to-air use, it is necessary for some form of Doppler shift to be included within the simulator. A reasonable range for simulated Doppler shift is 0 to 100 Hz.

(d) Noise and Interference.

During the initial stages of the simulator development (ie. before the MBC noise and interference characterisation work is complete), it was decided that the same type of noise/interference that is normally added to HF simulators would suffice. Consequently, Gaussian white noise, impulsive noise and modem-type interference were considered as reasonable.

3.5 Simulator Implementation.

During the simulator design stage, it was decided that it should be flexible enough to simulate both a typical HF path and also a typical MBC path - with only software changes. Consequently it was decided that the simulator should be software-based. After an examination of the microprocessors and digital signal processors (DSPs) currently on the market, it was decided to base the system around two TMS320C25 DSPs and a personal computer (PC). Each of the DSPs is used to represent one direction of the path.

(a) Sampling Rate.

When considering that maximum bandwidth which the simulator is required to accept is 20 kHz, it is reasonable to set the sampling rate at 80 ksamples/s. This also suits both the Doppler routine quadrature requirement and also the requirement to down-convert the incoming signal from its 100 kHz IF. By sampling the incoming signal in this manner it is modified from 100 kHz $\pm$ 10 kHz to 20 kHz $\pm$ 10 kHz, and consecutive samples have a phase difference of $\pi/2$.

(b) Path Delay.

Each of the two path delays which are included within the simulator are generated using a "RAM based delay line" similar to that used by (Matley and Bywater, 1977); this method is illustrated in Figure 5. A delay is introduced by reading the contents of the delay RAM, less a delay factor "Δ". Obviously, to function correctly the RAM must initially be zero-filled; the address pointers must increment at a constant rate, and they must wrap around when they reach the end of the RAM space.

Both of these delay RAMs are implemented on the TMS 320C25 DSP using 35 ns external RAM as storage. Use of the DSP's auxilary registers provides an efficient method of monitoring the state of these two RAMs.

(c) Doppler Shift.

As already mentioned consecutive samples have a phase difference of $\pi/2$, and thus it is relatively str aightforward to introduce a frequency shift to the input signal. By generating sin d and cos d, where d is described by equation 1, from a look-up table and multiplying these by consecutive samples it is possible to generate the required signal (equation 2).

$$d = w_{doppler} \cdot t \qquad [1]$$

$$\cos wt \cdot \sin d + \sin wt \cdot \cos d = \sin(wt + d) \qquad [2]$$

Doppler shift can thus be included by steadily incrementing d, at a rate determined by the selected doppler frequency. Figure 6 illustrates this algorithm.

If it were not considered insignificant to the operation of the simulator, phase variations could also be added using a similar method, with pseudo-random variations of d.

This algorithm can also be efficiently implemented on a DSP using on-chip RAM to store a sin/cos look-up table, and using the multiply/accumulate instruction to provide the appropriate arithmetic.

(d) Path Attenuation.

The hard disk of a PC is used to store a library of profiles. When initialising the simulator a number of profiles are copied into the memory of the PC. Each time a profile is required one is taken from memory and randomly modified in both magnitude and duration. This profile is then passed sample-by-sample, to the DSP. The DSP then applies the path attenuation to the signal along with other propagation path characteristics. A basic block diagram of the simulator implementation is shown in Figure 7.

(e) Noise and Interference.

The two types of noise which are to be initially included within the simulator can both be generated by digitally filtering the same maximal-length pseudorandom binary sequence. Gaussian white noise may be generated by digitally filtering a maximal-length pseudorandom binary sequence and operating on the resultant sequence to produce an approximately gaussian distribution. Impulsive noise may be generated as constant narrow width pulses. The time of arrival of the pulses can also be determined by digitally filtering a maximal-length pseudo-random binary sequence.

Modem-type interference may be generated by randomly summing together the outputs of 16, or so, tone generators of varying amplitude. A similar method was used by (Dawson, 1984).

4. MBC PROTOCOLS AND CHANNEL ENCODING.

MBC systems experience a very wide range of path conditions, and not just the traditional idealised underdense and overdense bursts. It is thus imperative that systems should not be designed with a particular type of burst in mind, but rather to take full advantage of any openings in the communication channel. Some previously deployed systems were not designed with this philosophy in mind, and the result was relatively inefficient operation.

Currently the MBC research programme at the University of Hull is planning to take account of the variable nature of the path by designing an adaptive transmission and control system. This system will be required to modify its modulation format, channel encoding scheme, and signal processing techniques in response to path conditions. The implementation of such an adaptive system is in no way straightforward, and much work is required in this field before an ideal solution will be found. Some of the concepts which are currently being examined by the research group are briefly discussed within this section (Darnell, 1987).

4.1 Real-Time Channel Evaluation (RTCE).

Obviously, RTCE is an essential element of any adaptive communication system. The more information that is possessed regarding a particular communication path, the more efficient can the encoding/decoding processes be made. For MBC systems two forms of RTCE would be advantageous, ie "pre-call" RTCE and "in-call" RTCE.

(i) Pre-call RTCE implies that before transmissions start, the system controller should have some information regarding the current nature of the path in terms of propagation and noise.

(ii) On-line RTCE requires the derivation of data from the transmissions themselves.

Due to the variable nature of MBC paths, (ii) has a major role to play in efficient MBC systems. Figure 8 shows one arrangement for enabling RTCE data to be made more precise. Basically, the traffic channel is delayed so that RTCE can be applied prior to signal processing. Derived information could thus be used to modify the signal processing algorithms. The complexity of the applied RTCE is obviously restricted by the amount of delay applied to the traffic channel. Relatively short periods of delay can be considered as insignificant to MBC systems, and still provide a reasonable amount of time for RTCE to be applied.

4.2 Embedded error control.

Much work has already been carried out by the communications research group on a concept known as "embedded error control" (Darnell, Honary and Zolghadr 1988). Basically, the same data is transmitted at a number of different rates. At the receiver the signal is decoded at the greatest rate possible for the current state of the channel. This technique is known to operate under very poor channel conditions. Figure 9 illustrates the principle of this technique, and Figure 10 gives an indication of the potential performance of such a technique.

4.3 Embedded modulation.

The concept of "embedded modulation" is similar to that of embedded error control in that the transmitted signal comprises robust elements and less robust elements.

Clearly, under poor path conditions only the robust elements will be demodulated, but when the path exhibits higher SNR's the less robust elements will be demodulated. Again, the technique offers the possibility of varying the information rate during a burst. Figure 11 illustrate two possibilities for implementing this technique, and Figure 12 illustrates the demodulation of one such technique.

5. CONCLUDING REMARKS.

The simulator has not as yet been fully compared against real paths, although the path profiles used are derived from real paths. It is planned to establish several actual paths from Hull for this reason. Updating the library of profiles is planned to be an ongoing project in order to make the simulator as realistic as possible.

It is hoped that real MBC noise and interference measurements will be available in the near future. The simulator will then be updated to be more representative of a true MBC path, both in terms of propagation and noise/interference.

When the simulator is completely validated it is planned for it to be used in 'bench testing' control and channel encoding algorithms which the group are currently investigating in the context of MBC systems. One of its first functions will be the testing of an MFSK modem which is currently in the design stage. Once this has been achieved, it is planned that the overall 'test facility' be used to compare several coding techniques which have been developed by the joint Hull University/Warwick University Communications Research Group.

It is hoped that this programme of research will result in the deployment of an MBC system which will be far more efficient in terms of its use of the available channel capacity than are existing designs.

6. REFERENCES.

1) Davis, G.W.L. et al , 1957: "The Canadian JANET System", Proc. IRE. Vol. 45(12).

2) Bartholme', P.J. and Vogt, I.M., 1968: "COMET - a new meteor burst system incorporating ARQ and diversity reception", IEEE Transactions on Communications, Vol. COM-16(2).

3) Cannon, P.S. AND Reed, A.P.C., 1987: "The Evolution of Meteor Burst Communications Systems", Journal of the IERE, Vol. 57, No.3, pp. 101-112.

4) Ostergaard, J., 1986: "Meteor Burst Propagation and System Design", AGARD Special Course on "interaction of propagation and digital transmssion techniques", AGARD Rpt. 744.

5) Matley, W. and Bywater, R.E.H., 1977: "A Digital High-Frequency Multipath Propagation Simulator", The Radio and Electronic Engineer, Vol. 47(7).

6) Dawson, J., 1984: "An HF Simulator For Use With Real Time Channel Evaluation Systems", AGARD, Conference on "Propagation Influences on Digital Transmission Systems - Problems and Solutions",Conference Proceedingsno. 363.

7)Darnell, M., 1987: "Signal Processing Strategies for Intermittent Communication Channels", Proceedings of the Symposium on "Meteor Burst Communications", SHAPE Technical Centre, STC SP-1, Vol. 1.

8) Darnell, M., Honary, B.K., Zolghadr, F., 1988: "Embedded Coding Technique: principles and theoretical studies", IEE Proceedings Part F, Vol.135, No.1.

7. ACKNOWLEDGEMENTS.

The author wishes to thank RAE Farnborough for financial assistance for the research programme from which this work is taken.

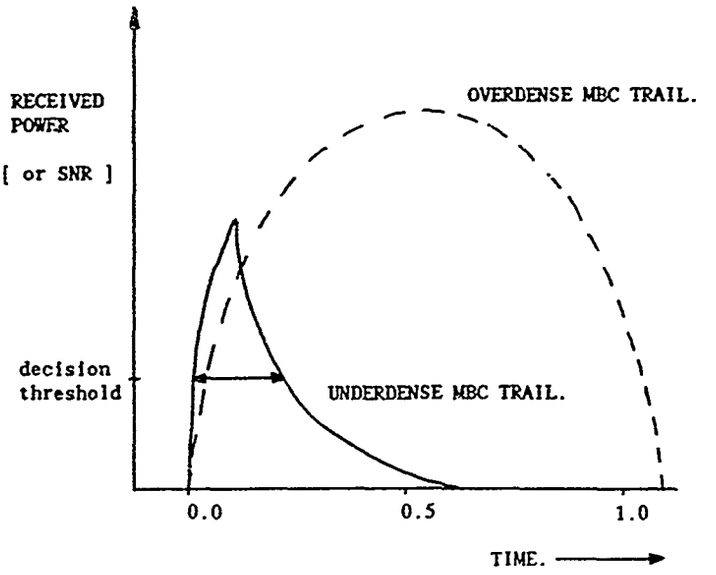

Figure 1: MBC Path Profile.

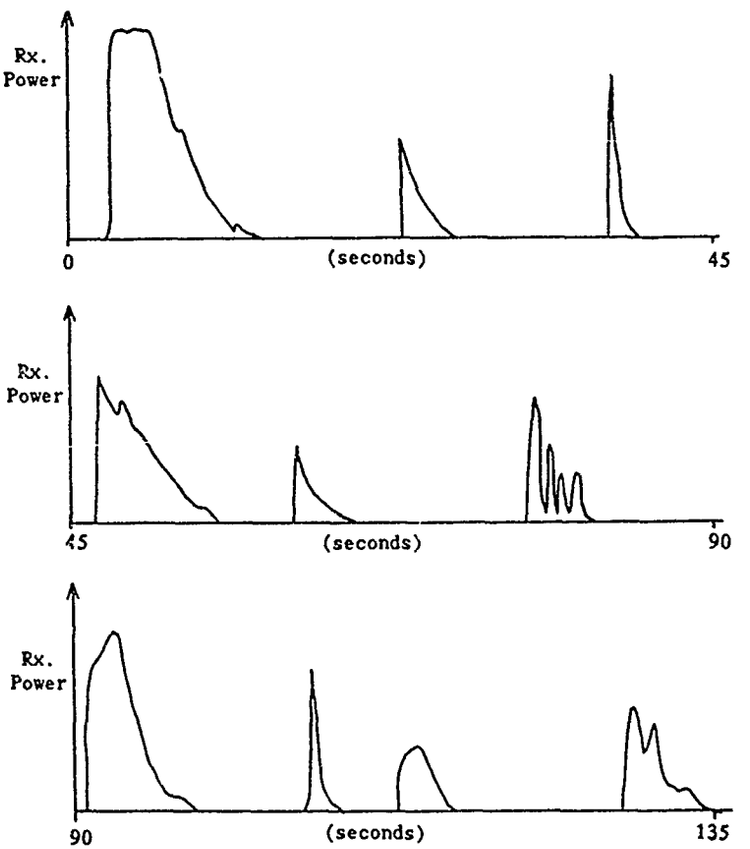

Figure 2 : Path Simulation.

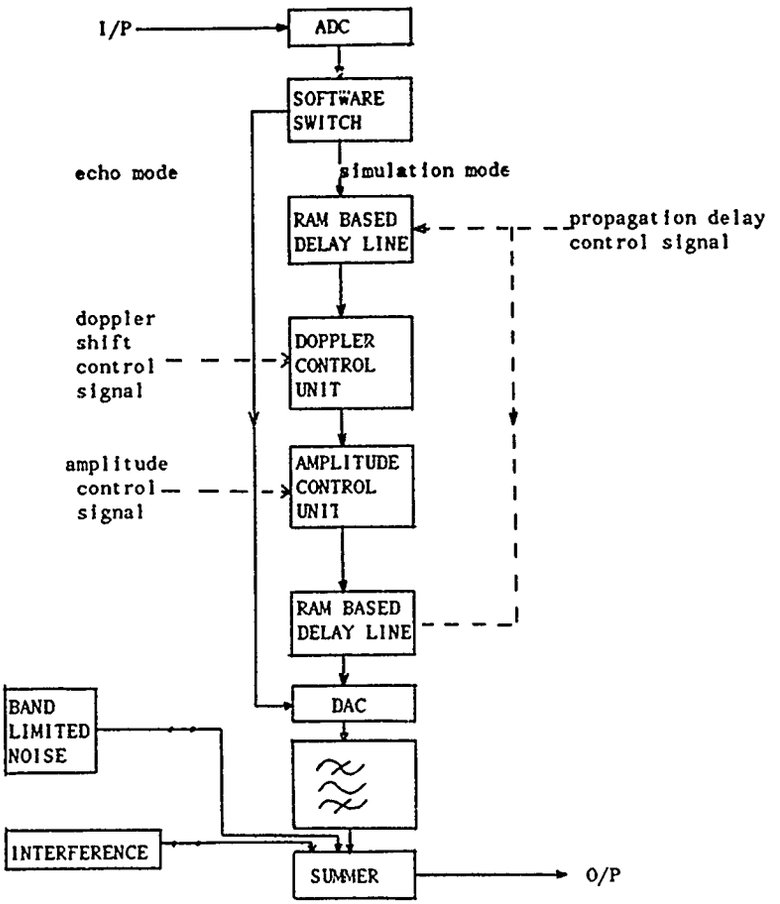

Figure 3: The Total MBC Simulator

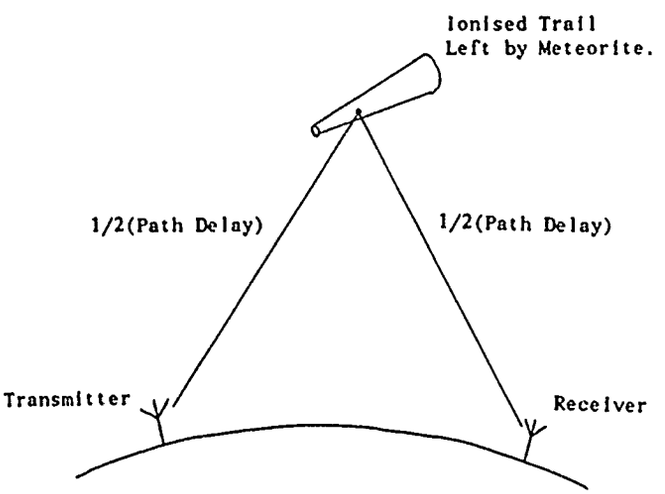

Figure 4: Splitting of the Path Delay.

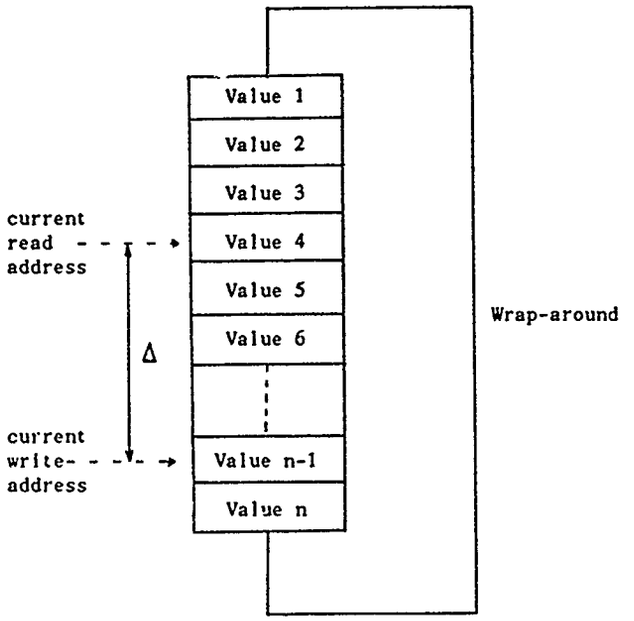

Figure 5: A "RAM Delay Line".

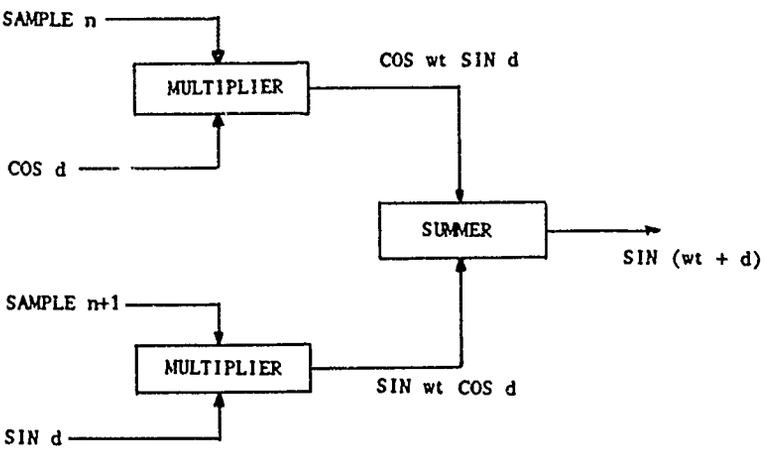

Figure 6: Doppler Routine.

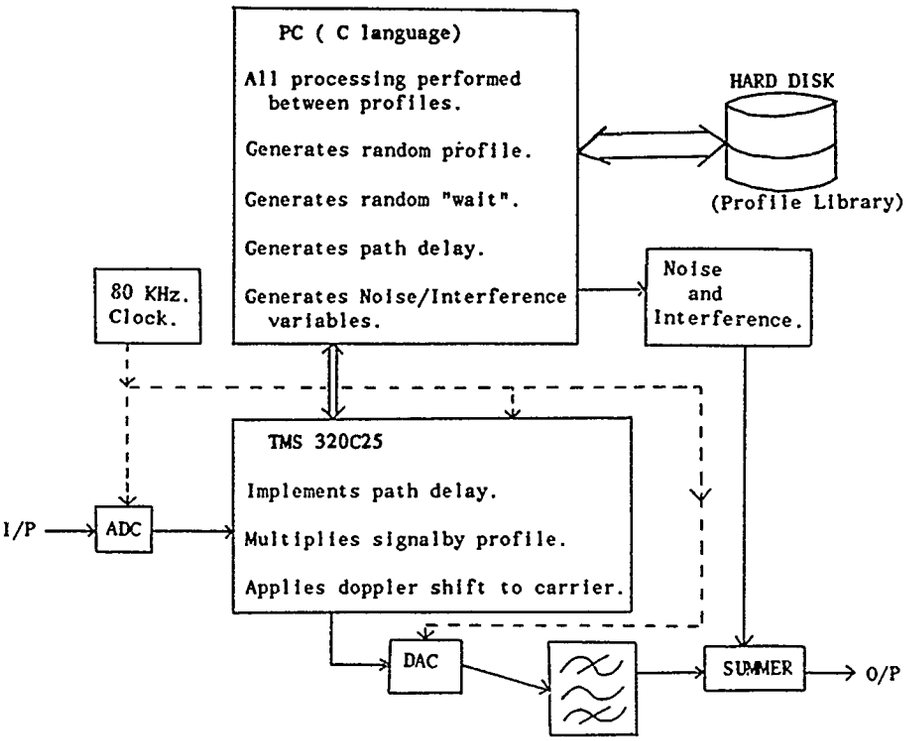

I/P = 100 KHz. + 10 KHz.

O/P = (100 KHz. + doppler + 10 KHz.)*Channel Profiles
+ Noise + Interference.

Figure 7: The Actual MBC Simulator.

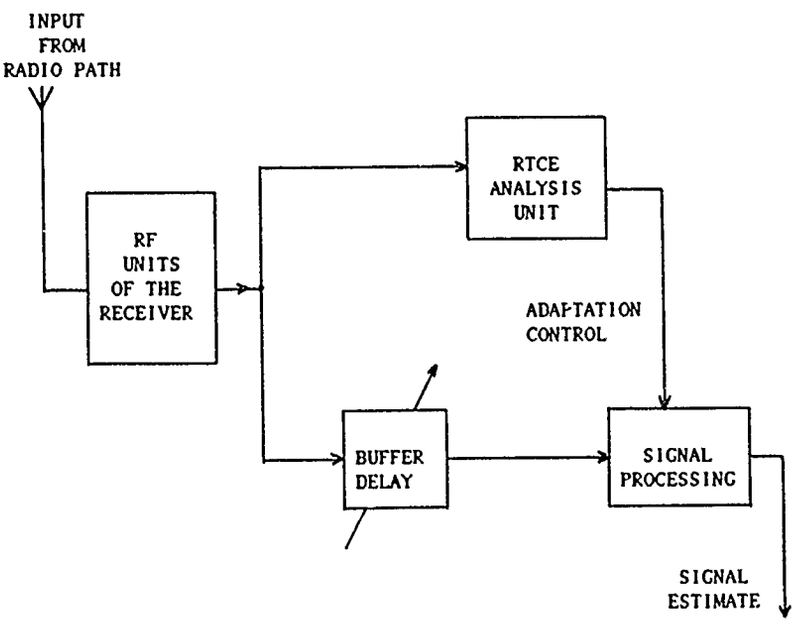

Figure 8: Use of Buffer Delay and RTCE to Assist Received Signal Processing.

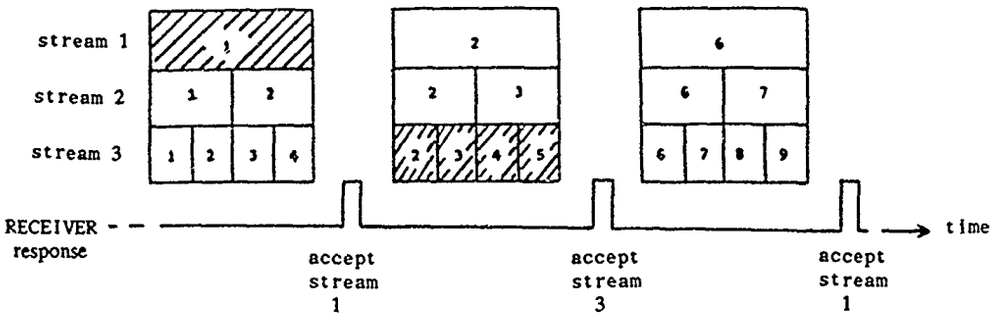

(a) Principle of embedded encoding.

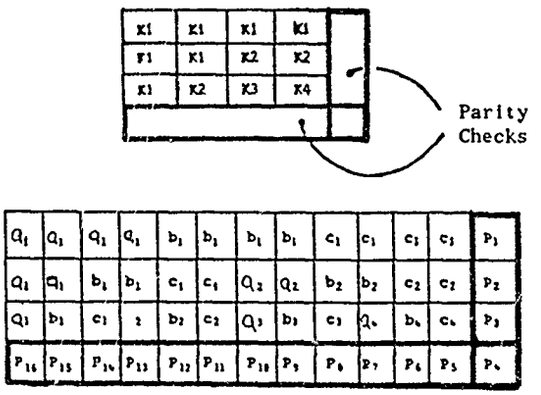

(b) (52,12) embedded array code block structure.

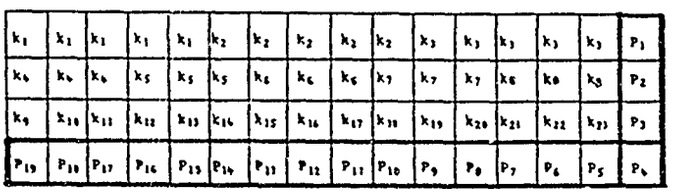

(c) (64,23) modified array code block structue.

Figure 9: Embedded Error Control.

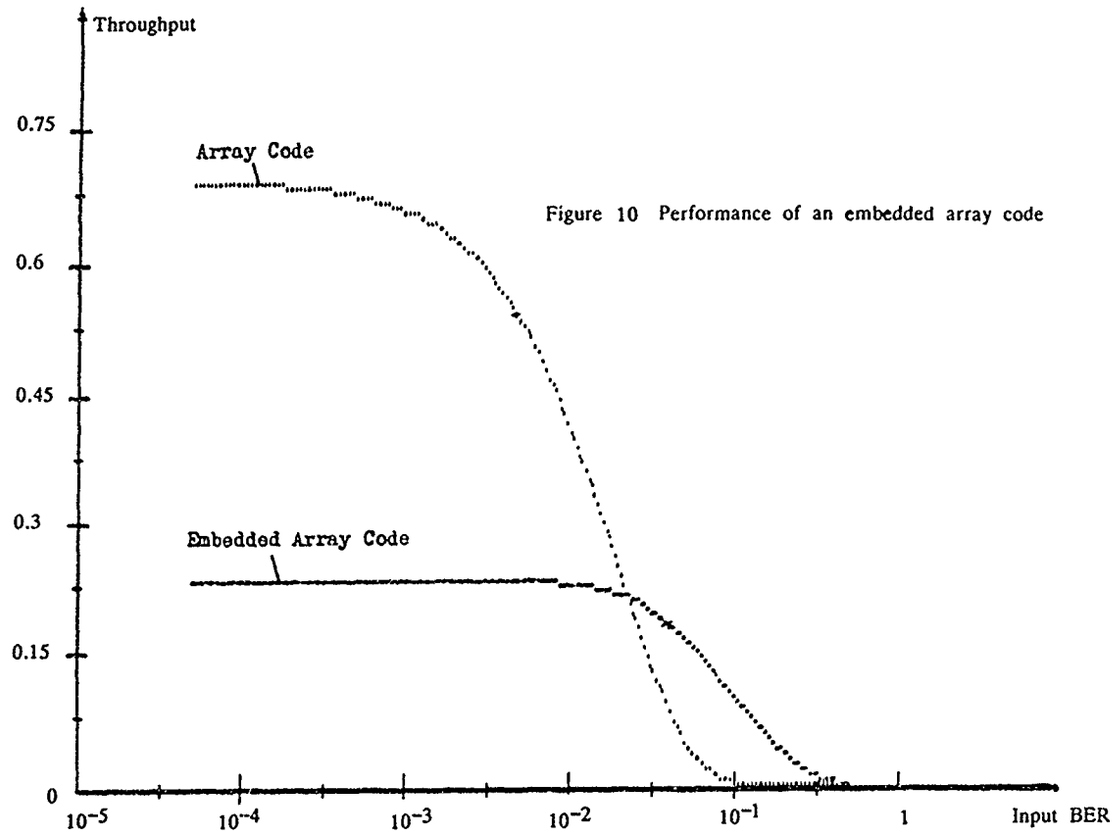

Figure 10 Performance of an embedded array code

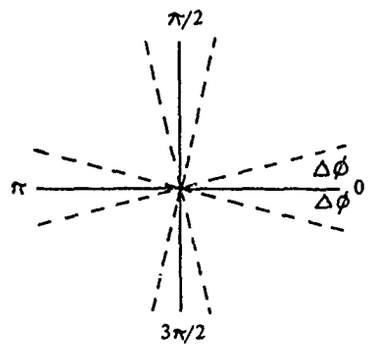

a) Low-Level Phase Modulation.

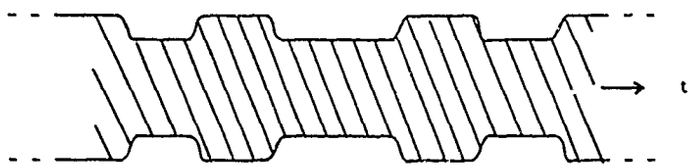

b) Low-Level AM

Figure 11: Examples of Embedded Modulation Schemes.

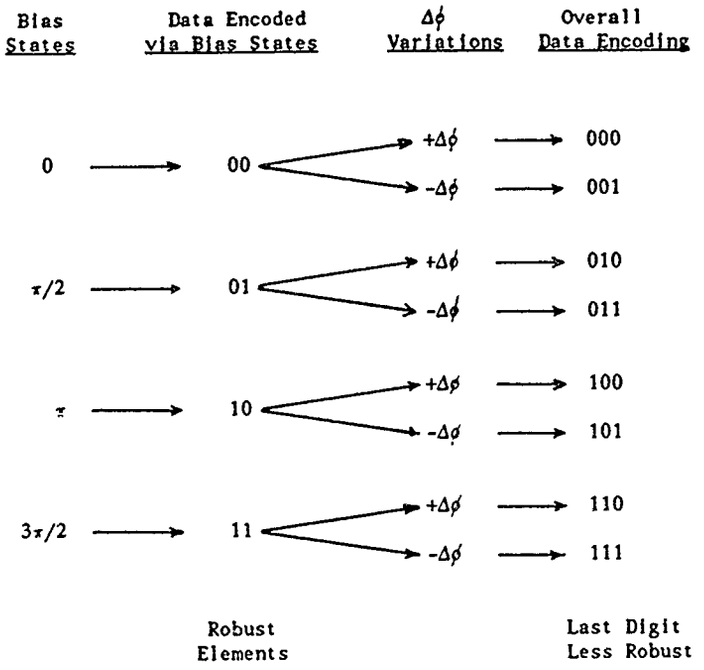

Figure 12: Embedded Modulation.

DISCUSSION

A. COIMBRA SANTOS

The system as presented is a simulator. Could you amplify on its applicability to develop or improve existing MBC systems, and could you provide details on equipment complexity i.e. modulation, antennae orientation, processing power, as well as practical system siting.

AUTHOR'S REPLY

1 - Using the simulator it should be possible to rigorously test very many protocols, encoding schemes etc; and by incorporating these into existing systems it should be possible to improve their performance.
2 - At present the envisaged MBC system will operate with MFSK type modulation and a low level of either amplitude modulation or phase modulation.
3 - Antennae orientation is path dependent, but generally both antennae should be directed towards the centre of the great circle path between the transmitter and the receiver.
4 - At present it is planned to provide both a personal computer (IBM PC Clone), and a TEXAS TMS320C25 digital signal processor for processing at either end of the link.
5 - Initially it is planned to site terminals at Cobbet Hill and the University of Hull, both in the UK.

K.S. KHO

MBC is a good alternative for long distance communications. But the interference of this transmitter to the others systems in the surrounding is very terrible. Thus should be a shortcoming of the system.
Security : I think typical shortcoming of long distance systems is anti jam capability. It could be jammed by a remote jammer.

AUTHOR'S REPLY

1 - The transmission power of MBC systems is not as high as your comment implies, and thus I would question whether such systems cause interference to surrounding users. Previously reported systems, such as those referenced in the text, use transmission powers of several hundreds of Watts.
2 - For meteor burst communication systems, a potential jammer would need to be within a definite footprint (approximately 200 km) around either the transmitter, or the receiver. This becomes apparent if one considers the geometry of the mechanism.

C. GOUTELARD

Votre simulateur paraît très bien, mais pouvez-vous nous dire quels paramètres allez-vous rentrer ? Forme des réponses des traînées, effet doppler sur la tête et la traînée, bruit...
Par ailleurs, je ne m'explique pas la forme dissymétrique de la fonction de distribution du bruit. Faut-il croire que son moment d'ordre 1 est différent de zéro ?

DISCUSSION

AUTHOR'S REPLY

1 - The simulator parameters will take two forms. They will include parameters which are currently being assessed at the University of Hull by recording and analysing on-air noise, profiles etc... Secondly, traditional parameters which have been published previously in several journals will be included.

2 - The non-symmetrical distribution function of the noise did have a zero mean.

MAN-MADE NOISE IN A MILITARY ENVIRONMENT

by

Ir. K.S.Kho and Mr P.A. van der Vis
Physics and Electronics Laboratory TNO
The Netherlands

1. INTRODUCTION

Over the last few years our laboratory has been involved in studies concerning the design of future radio systems and of Electronic Support Measures (ESM). Within the ESM-scope special attention is payed to Direction Finding (DF), as it offers a powerful means of locating enemy transmitters. Because environmental noise may seriously confine the range of reliable operation of both systems, the availability of relevant data is of crucial importance.

This paper pays attention to noise in the lower end of the VHF band, ie between 30 and 90 MHz. While statistics on atmospheric and galactic noise may be found in CCIR Report 322 and CCIR Report 258-3 provides information about man-made noise for areas described as urban, suburban, industrial etc., the 'military environment' is (understandably) not mentioned. As it goes without saying that military equipment must above all work well in wartime, there is an obvious need to gather information on what is to be expected if it comes to the worst. Because we cannot think of a better way of filling this information gap than by carrying out measurements during military manoeuvres, it was decided to make a start by making use of "Certain Strike", a large-scale NATO exercise in Europe in September 1987. The idea was supported by the Royal Netherlands Army (RNLA). The 4th division of the 1st NL corps hosted our team in Germany.

2. METHODS OF MEASURING NOISE

Man-made noise may be interpreted as:

"Interference produced by equipment or machines that unintentionally radiate electromagnetic waves".

There are many ways to measure the effects of noise and even more ways to present the results. In order to achieve what is useful for our aim, the following two methods were considered:

1. Record the noise envelope.
2. Measure how much extra signal power it takes to overcome the detrimental effects of the noise on a datalink.

Discussion of method 1

Although seriously considered, this method had to be abandoned because the time the realisation would take was not available before 'Certain Strike'. It is nevertheless briefly discussed here because we do not preclude using it in the future

A diagram of what we had initially in mind is given in Figure 1.

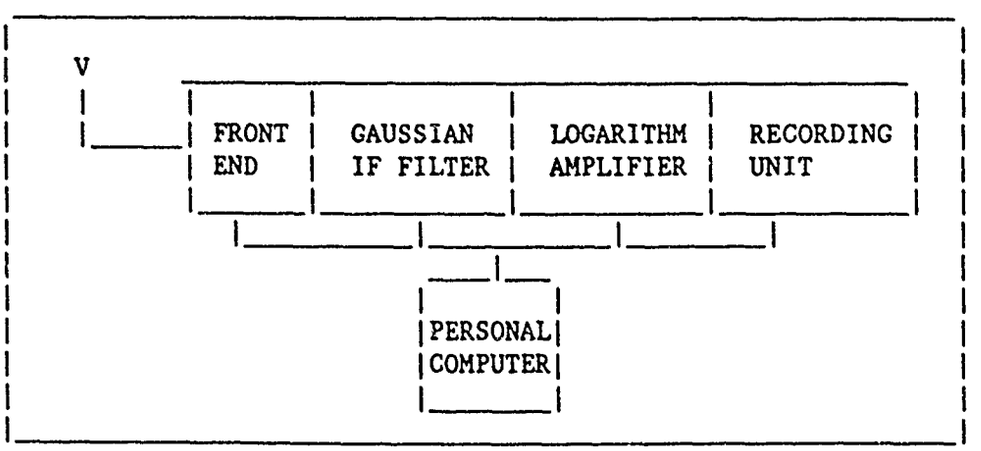

Fig.1 Recording the noise envelope

The logarithmic IF amplifier was inserted in order to obtain a sufficiently large dynamic range. The Gaussian response was meant to limit the amount of "ringing". Ringing in this case means that pulses arise in the IF filter that are responses to preceding stronger pulses. They are difficult to distinguish from others and will be erroneously recorded as received pulses An advantage of this method is that the noise envelope history remains available to any form of analysis at any time Because man-made noise is impulsive by nature and may contain very short pulses, a 'true' recording of the history will not be

possible because of the restricted receiver bandwidth. One reason for this restriction is that the bandwidth may not enclose 'intelligent' signals during the measurements. Another is that a larger bandwidth means more system noise and this limits the dynamic range at the lower end. The method is used by Parsons & Sheikh [1]. Figure 2 illustrates how they presented the results of some of their measurements. This presentation offers in statistical terms a very detailed picture of the received noise envelope. The method has the advantage that the results are applicable to various communication links. The application to a given link will however not always be easy.

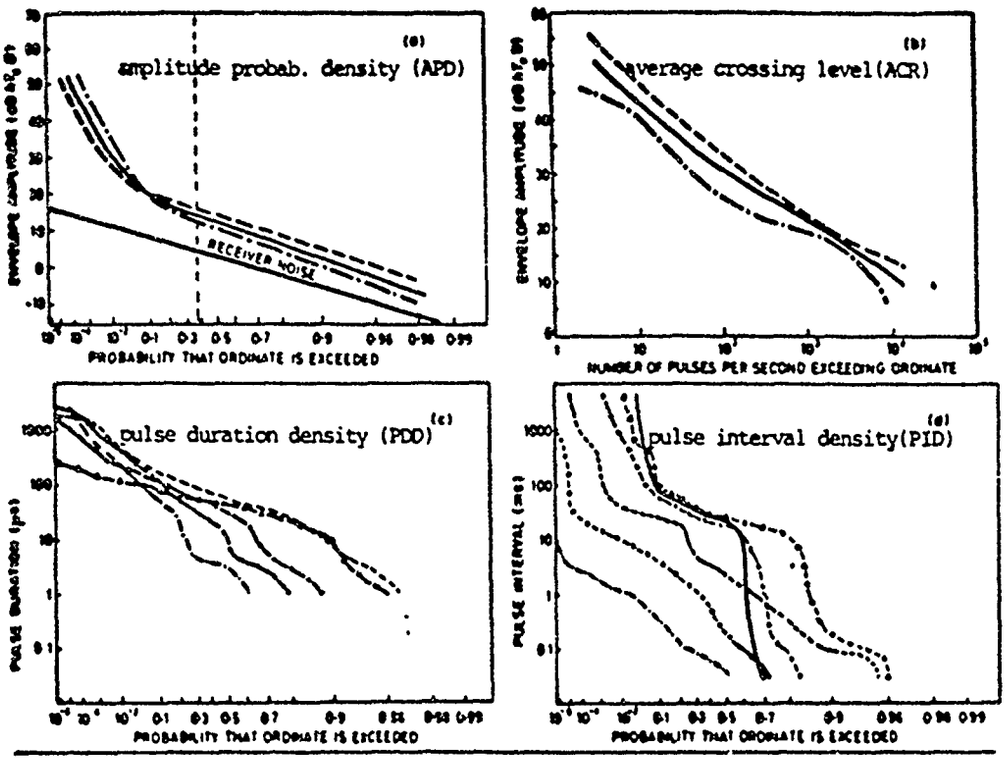

Noise measurements in suburban locations

(a) APD (b) ACR

--- Typical measurement in Bristol Road South
– – Typical measurement in Lordswood Road
— — Average curve representative of suburban locations.

(c) PDD (d) PID

Representative measurements in suburban locations.
Threshold levels relative to $k T_0 B$
· - · - 11 dB. —o—o 20 dB. --- 30 dB
x-x- 40 dB. —Δ—Δ 50 dB. —— 55 dB.

Fig.2 Results of measurements performed by Parsons and Sheikh [1]

Discussion of method 2. "Determine how much extra signal power is needed to compensate for the effects of the external noise"

This method has the drawback that it offers only in an indirect and coarse way information on the noise characteristics. On the other hand, the problem of applying the results to a given system — as arises with method 1 — is omitted, as the system used for the measurements can be made similar to that 'given system'. A diagram showing the principle of method 2 is depicted in Figure 3.

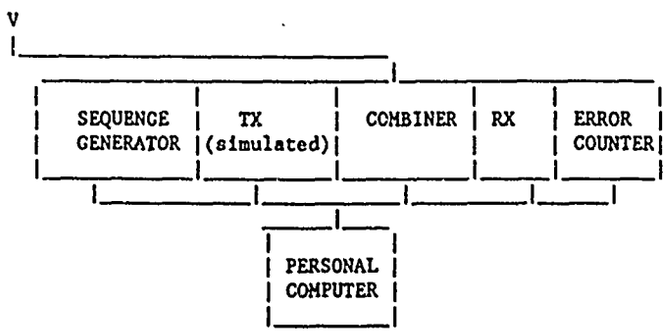

Fig.3 Setting the BER to a constant value by adapting the signal power

The principles followed here are simple and analogous to finding the noise figure of a receiver. By adapting the signal power, the BER is set to a constant value. Indirectly (assuming linearity) it is the signal to noise ratio that remains constant. This means that the applied signal power now is a measure for the (total) noise power.

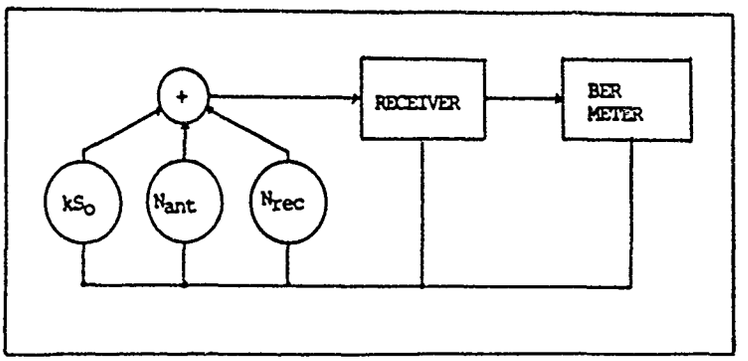

Fig.4 Measuring external noise indirectly.
The BER is held constant by adapting the signal power kS_o.

The receiver noise is represented by the source N_{rec}. The other symbols are described by:

N_{ant}: external noise power, picked up by the antenna.
S_o: signal power needed for a given BER if $N_{ant} = 0$.
$k*S_o$: signal power needed for a given BER if $N_{ant} > 0$.

Because the signal to noise ratio is constant, it follows that:

$$(k*S_o)/N_{rec} + N_{ant}) = S_o/N_{rec} \quad \text{or} \quad N_{ant} = (k-1)N_{rec}$$

3. TNO MEASUREMENT SET-UP

Figure 5 shows a more detailed block diagram of the measurement set-up. Important components were.

- A FM-3600 Combat Net Radio receiver of the RNLA.
- A centre-fed whip RF-3620, also of the RNLA.
- Interfacing hardware, designed for this mission.

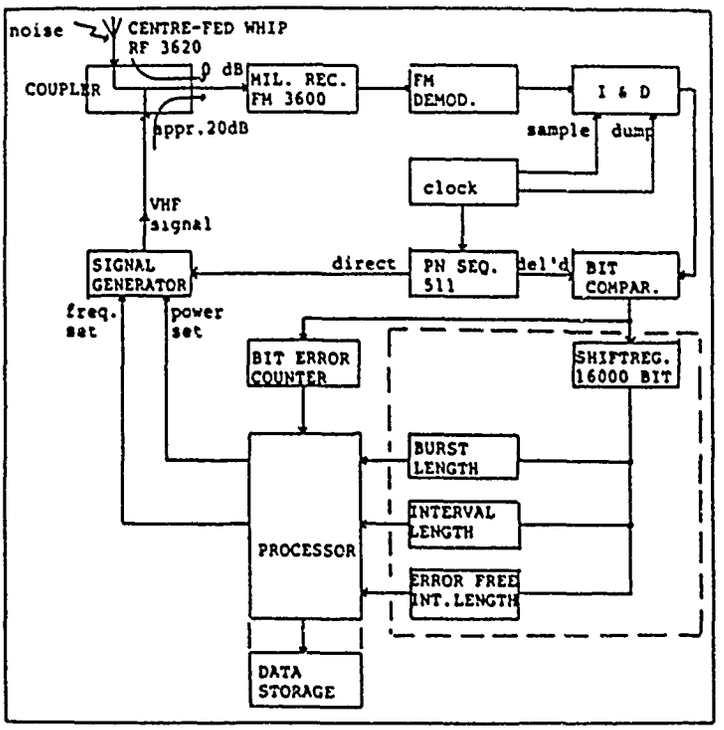

Fig.5 TNO measurement set-up

The bitrate was chosen to be 16000 b/s. Every 'trial' lasted 1 second. A Hewlett-Packard processor controlled the hardware, monitored the BER and changed the signal power kS_o when necessary. After each successful trial (ie BER .01 ± 10%) the value of kS_o was stored.

In addition to the described measures, circuits were added to enable collection of data regarding the distribution of errors within the 'successful' trials (ie BER approx. .01). This was done by sending the 16000 bits of each successful trial to circuits determining the lengths of 'bursts', 'intervals' and 'error-free intervals'.

Following [2] the mentioned quantities are defined as follows:

— *Burst:* A burst is a group of bits which begins with a bit in error and ends with a bit in error. A minimum number of errors Me are contained in this region; the minimum density of errors in the region is D.

— *Interval:* In an interval the minimum density of errors is less than D. The region begins and ends with a correct bit. An interval may contain errors.

— *Error-free interval:* This expression is self-evident.

The next figure illustrates the definitions.

In our measurements we have defined: Me = 2 and D = 15. Before possible measurements in the future, these values and also that of the critical BER, have to be carefully reconsidered and adapted to the protection coding scheme one intends to use.

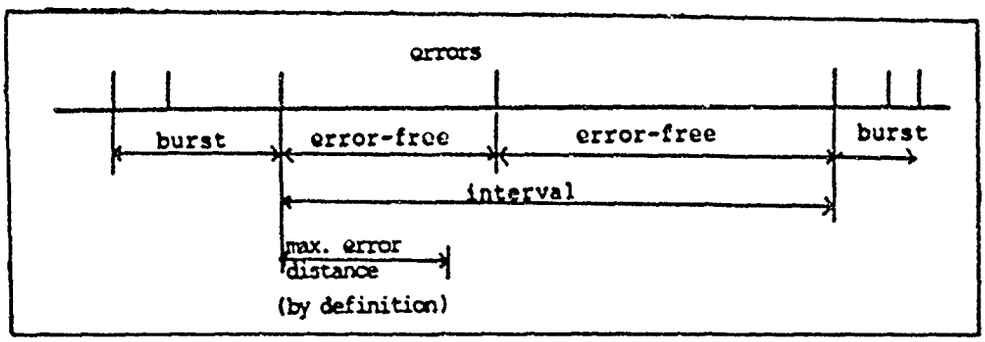

Fig.6 Illustration of error distribution definitions.

The results were stored on tape, together with the corresponding kS_o values.

4. RESULTS

4.1 Noise Level

The measurements were carried out on the Luneburgerheide. On September 15 between 00.00 and 10.00 hours local time, the equipment was placed in the centre of a great number of military vehicles of a RNLA brigade located in Unterluss. Most of them contained electronic equipment in operation. Data of 1800 trials were recorded in this period. Between 18.00 hours on September 15 and 09.00 hours September 16, our van was located in the middle of a command centre of a RNLA division that comprised an even greater number of vehicles. Most of these also contained electronic equipment in operation. The location was near Schneverdingen. Here the results of 3300 samples were stored on tape. Tables 1 and 2 show mean values and standard deviations for a number of sessions. Each session involves 300 'successful' trials. The noise levels found are so low that it is doubtful if the expression 'man-made' is applicable. For this reason the upper limits of galactic noise (CCIR) are also shown in the tables.

TABLE 1 Results in Unterlöss, being with the brigade

FILE	DATE	TIME	FREQ	CCIR	RESULTS	
				max. gal.	mean	st. dev.
NR	1987	LOCAL	MHz	dBkTo	dBkTo	dB
0	15.09	0045 tot 0326	45.00	13.4	6.1	1.3
1	15.09	0439 tot 0547	45.00	13.4	5.7	1.0
2	15.09	0550 tot 0651	45.00	13.4	5.5	1.3
3	15.09	0653 tot 0755	45.00	13.4	5.6	1.0
4	15.09	0815 tot 0916	45.00	13.4	6.0	1.3
5	15.09	0918 tot 1000	45.00	13.4	6.3	1.6

TABLE 2 Results in Schneverdingen, being with the Division Control Centre

FILE	DATE	TIME	FREQ	CCIR	RESULTS	
				max. gal.	mean	st. dev.
NR	1987	LOCAL	MHz	dBkTo	dBkTo	dB
6	15.09	1823 tot 1921	45.00	13.4	10.2	0.8
7	15.09	1923 tot 2210	45.00	13.4	10.4	1.1
8	15.09	2225 tot 2324	45.00	13.4	10.8	1.3
9	15.09	2328 tot 0021	35.00	16.1	7.3	1.6
10	16.09	0023 tot 0116	35.00	16.1	7.2	1.2
11	16.09	0123 tot 0221	40.00	14.7	10.0	1.0
12	16.09	0224 tot 0328	46.00	13.2	9.5	0.8
13	16.09	0330 tot 0432	45.00	13.4	10.5	2.3
14	16.09	0600 tot 0629	30.00	17.7	17.0	0.9
15	16.09	0630 tot 0731	38.00	15.2	7.2	2.7
16	16.09	0734 tot 0845	38.00	15.2	6.7	1.8

The unexpected results have led to a thorough re-examination of equipment after completion of our mission. As no indication of failing equipment was found, it must be concluded that even large concentrations of RNLR military vehicles cause very little man-made noise. For the moment there is no other explanation than assuming that measures like electric filtering and screening of equipment (tempest measures) and EMP screening of vehicles are not ineffective.

4.2 Distribution of bit errors

Figure 6 shows an example of the distribution of bursts etc. as observed between 19.23 and 22.10, September 15 in Schneverdingen. In addition to the quantities defined in 3.1 it shows also the distribution of 'guard space', by which is meant the ratio of the lengths of an error-free interval and of the succeeding burst.

It was found to be meaningless to show all plots. They are strikingly alike and also similar to what is found when Gaussian noise is applied. The most likely explanation is that most 'accepted' noise samples were of galactic origin. The circumstances that the measurement system was too slow to handle fast changes of noise level may also have contributed somewhat to these results, because this means that short bursts are overlooked. The operators reported that short bursts (perceptible on the display) occurred sometimes in Unterlüss and very scarcely in the woods near Schneverdingen.

A possibility to overcome the disadvantage of total neglection of short bursts may be overcome by dropping the fixed-BER concept. By changing the signal power stepwise within the power range of interest and recording bit errors independent of the BER level, error distributions including the effects of short bursts will be obtained.

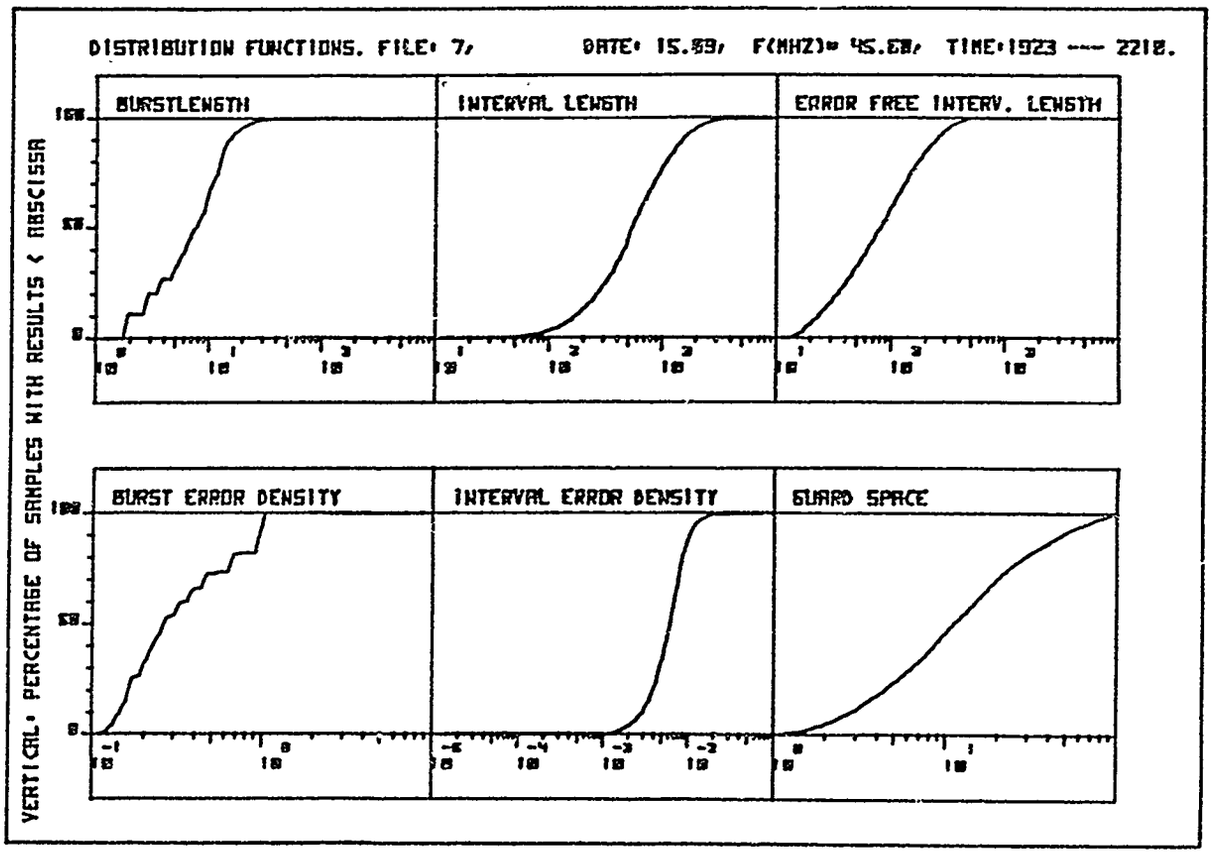

Fig.7 Example of measured distribution on bursts etc.

5. CONCLUSIONS

The results seem to indicate that:

1. The amount of VHF man-made noise, produced by concentrations of military vehicles of the RNLA is negligible.
2. The measured average noise level was 5 dB below the reported CCIR upper limit of galactic noise. The noise is Gaussian by character.
3. The effects of short bursts are not included in the results. These bursts were observed occasionally when being with the brigade and rarely within the division command centre.

6. RECOMMENDATIONS

After having gained this experience, it can be recommended to:

1. Collect more data on this subject.
2. Standardize measurement methods in order to improve the tendency to co-operate and to facilitate comparison of results.

7. REFERENCES

1. Parsons, J.D. Sheikh, A.U.H. *Statistical characterization of V.H.F. man-made radio noise.* The Radio and Electronic Engineer. Vol.53, No.3, pp.99-106, March 1983.

2. Brayer, K. *Error Correction Code Performance on HF, Troposcatter, and Satellite Channels*, IEEE Trans. Com. 19, 1971.

3. — CCIR (1963—1970—1974—1978). Report 258-3. (Study Program 29C/6)

DISCUSSION

C. GOUTELARD

L'étude que vous présentez est intéressante notamment dans la distribution des erreurs.

- Nous avons fait dans AGARD des publications similaires.
- Cependant vos mesures ne sont pas directement exploitables car les taux d'erreurs dépendent du modem. Il serait souhaitable de les traduire en niveau de bruit pour qu'elles le soient.

AUTHOR'S REPLY

Thank you for your comment.

1 - Could you inform me which AGARD publication is it ?

2 - Yes, as I have stated in the presentation ; the results are dedicated to the radio system (modulation schem used in the measurements. That's why I suggest to standardize measurement set-up for comparison of measurement results purposes. The enveloppe recording method could be a universal method and acceptable for others.

R.J. BULTITUDE

I commented on requirement to know error-rate-noise relationship in burst conditions. Also, I suggest that in field measurements in a changing environment, sufficient time will not be available to determine error rates accurately enough to determine noise power acculately.

AUTHOR'S REPLY

- You are right, the known C/N and BER relationship is based on Gaussian noise.
  As we know beside the Gaussian noise, there is also impulsive noise.
  The relationship between C/N ratio and BER in an impulsive noise environment should be deduced from measurements/calibrations on the testbench.
- We have chosen a BER value which is marginal. This means that the BER value is sensitive to a change in the C/N ratio. So, the BER adjusted should not be a certain value but it should a range of BER like between 5.10^{-3} to 5.10^{-2} BER. In this region for instance the C/N ratio variation will be within 1dB or less depending on the modulation scheme applied.

A. COIMBRA SANTOS

- How many sets of transmitters/receivers were under trial.
- Did you register the BER under noise conditions before adapting (raising) the transmitted power to obtain the preset BER, since raising the power is indeed a way to overcome difficulties while communicating.

AUTHOR'S REPLY

- There was one set of transmitter/receiver used for the noi e measurements.
- No, the BER before increasing the signal level was not recorded. The intention was to measure during radio silence, so that no interference signal will be recorded. It seemed that during our measurements there were only preparations and movements and very little communication activities. So we were lucky.

SUMMARY OF SESSION II

NEW APPROACHES IN COMMUNICATIONS SYSTEM DESIGN

by

D. ROTHER, Session Chairman

The program of this session shows some essential tendencies in the design and development of military radio communication systems. According to the military threat, especially jam-resistant transmission methods are used.

In the long-range HF-communication, automatic channel selection with adaptive processing and slow Frequency Hopping are the main new features.

In the VHF range, tactical radio normally use medium rate Hopping up to some hundred Hop/sec and coding/decoding principles to reduce Bit error rate in case of data transmission. A first new approach of Direct Sequence Modulation for tactical radio has been presented by "Thorvaldsen, NO".

In higher frequency ranges, the UHF and L-band around 1 Hz, more and more hybrid methods are used working with Direct Sequency Modulation and Frequency Hopping.

Besides these system characteristics a number of presentations were concerned with:

- coding/decoding methods
- synchronization methods
- frequency economic use of frequency bands
- correlation methods.

As a summary the session demonstrated very well the main tendencies in the design and development of advanced radio communication systems.

A NARROWBAND TACTICAL COMMUNICATION SYSTEM for the VHF and UHF MOBILE RADIO BANDS

A National Defence Sponsored Research Program

L. Boucher, Y. Jolly, J.H. Lodge
Communications Research Center, Department of Communications
P.O. Box 11490, Station 'H', Ottawa, Ontario, Canada, K2H 8S2

SUMMARY

A description of the research effort, performed in accordance with a National Defence (DND) sponsored Research Program, is presented. Goals fixed for the program aim at achieving good quality, encryptable voice communications in the VHF and UHF mobile bands within a channel spacing of about 3 kHz. A review of the desirable performance objectives of a land-mobile tactical voice communications system is presented, and the design strategy suggested to achieve this performance is described. Implementation includes the use of techniques such as frequency domain digital signal processing of single sideband speech, speech bandwidth reduction, and linear modulation. A study, and in some cases experimental evaluation, on promising bandwidth reduction techniques was done, and a method, called the dynamic frequency band extraction technique, was developed for this application. With this technique, a good voice quality is obtained by dynamically saving only about 1200 Hz of the original 3000 Hz voice spectrum. Taking into account the extra bandwidth required by the data, the frequency domain filtering, and the pulse shaping of the discrete-time samples, and using a highly linear power amplifier, the RF channel spacing of the modulated signal is expected to be approximately of 2.5 kHz.

1.0 INTRODUCTION

It is well known that the existing spectrum allocation in the mobile radio bands has become saturated There is a need for more allocation, but no more spectrum is available. The systems presently used utilized Frequency Modulation (FM) and need a RF channel spacing in the order of 15 to 30 kHz per station. A smaller channel spacing, made possible by more spectrally efficient signalling techniques, is one of the solutions that will help solve the spectral congestion problem. Efficiently reducing the amount of spectrum required for voice communications is this program's primary goal. Furthermore, the challenge of achieving such a narrow bandwidth is enhanced by the limiting factors imposed when the tactical requirements are taken into account. The design strategy can only be started after these requirements have been defined.

A reduction of the bandwidth allocated to the voice signal can help to reduce the RF channel spacing, and the chosen technique has a considerable impact on the overall design strategy. The research effort of the first phase of the program therefore consisted of using available digital signal processing techniques and finding the best compromise between good voice quality and baseband bandwidth reduction, keeping in mind that the narrowband voice signal had to be in a form that allows encryption, that keeps the spectrum spreading to its minimum, that may be mixed with data (side) information, and finally that contains enough information for the receiver to compensate for the radio transmission link (e.g., fading).

The voice bandwidth reduction technique that was developed for this application forms the backbone of the system, and through a versatile design implementation, various additional features can be grafted as needed

2.0 The PERFORMANCE OBJECTIVES

A number of design objectives originate directly from the kind of application this communications system will be used for, i.e., mobile tactical voice communications. A non-exhaustive list of immediate and future desired performance criteria is as follows:

- *Narrowband:* the Radio Frequency (RF) bandwidth used to transmit a given amount of baseband information through the communication channel should be kept to its minimum.
- *Good Voice quality:* although reduction in bandwidth is always associated with a degradation of the voice quality, this sacrifice in quality must be kept to its minimum. Good voice quality means that intelligibility, naturalness, and speaker recognition are preserved for a range of speaker types, volume levels, and emotional states. Still, for bandwidth conservation, the voice bandwidth should be the minimum needed for the degree of quality required.

- *Voice Security:* sophisticated encryption should be implementable, using as little extra bandwidth as possible.
- *Low Transmitted power:* in order to avoid transmission detection in spectrum monitoring activities, intelligible communications must be achieved with the lowest possible level of emitted power. (This also indirectly implies variable emitted power).
- *Resistance to interference:* must be able to function properly in the presence of high levels of noise and various kind of interference (e.g., jamming, co–located transmitter).
- *Robustness to background noise:* must be robust to background noise such as often encountered in mobile radio communications (for example, the sound of the engine when one is in a mobile vehicle, helicopter noise, etc.).
- *Power efficiency:* as power efficient as possible, for reasons of portability.
- *Data transmission:* the communications system must have the ability to transmute from voice to data transmission.
- *Concurrent voice and data transmission:*
  the advantages of a system that can send control information in the form of data before or after the voice are numerous; examples of possible applications in such a case are:
  - addressable squelch (selective calls),
  - adjustable transmitting power (automatic selectable power),
  - dynamic channel assignment (trunking) compatibility.

  Control information in the form of data mixed with the voice also has many advantages:
  - it is required for most forms of voice bandwidth reduction techniques,
  - it can help to increase the complexity level of the encryption, and
  - it is needed in the dynamic control of voice processing implementations such as level normalization, and for some companding and pre–emphasis schemes.
- *Fading compensation* and possibly adaptive equalization: to compensate for the time dispersion due to IF filters ripple, and frequ· lispersion/translation due to the multipath propagation of the land–mobile environment.
- *Vertical integration:* the system must be capable of vertical integration across the frequency bands, i.e. the system and spectrum configuration used at VHF must be those used, with minor modifications, at UHF.
- *Frequency Hopping:* the system should also be able to operate in the frequency hopping mode.

The final product will be four proof–of–concept prototype radios. Essentially, the prototype radios should show that such a system is feasible. At this stage it would be unreasonable to build a radio with all the above features. To prove that this narrowband radio is possible, only the basic features have to be included with the first prototypes, so proof–of–concept in this case means to demonstrate that a secure narrowband mobile voice communication system with good voice quality is possible. But in the initial design, one has to keep in mind future expansion. Although it is impossible to foresee all the possible implementation scenarios, the initial system must be versatile enough as to allow, as much as possible, future growth.

The prototypes will be available in about 1 1/2 years.

3.0 The DESIGN STRATEGY

3.1 Signal Processor

The feasibility of such a versatile system would have been impractical just a few years ago. But today, with the availability of very large scale circuit integration, digital signal processing in real time is possible. The simultaneous implementation of the various functions needed for this communications system can be implemented using Digital Signal Processing (DSP). With the commercial availability of powerful one–chip digital signal processors, real–time implementation is not only possible, but can be done in a compact economical fashion· voice bandwidth can be efficiently reduced using complex speech bandwidth reduction techniques, choice of voice or data transmission can be achieved by the simple throw of a switch that has the effect of loading a different program in the memories of the signal processor; in fact, all the performance objectives desired for this communications system can be simultaneously implemented using this state–of–the–art technology. This approach is not entirely new: a versatile ACSSB–LPC–Data modem has been recently successfully developed for mobile satellite applications [1–4], using first generation DSP processors. Based on this experience, and armed with more powerful DSP processors, sophisticated solution to the narrowband mobile tactical radio problem is feasible. (For other DSP applications to mobile radios, see also [5–6]).

3.2 Time and Frequency Digital Signal Processing

Alteration of an analog signal (e.g., filtering) is done by forcing the signal through a number of analog circuits designed to shape the signal to the desired form (or a close approximation of it). In contrast, in digital processing, the signal is sampled, and mathematical operations (algorithms) applied to the data perform the signal shaping. The altered signal is then reconverted to its analog form and changes equivalent to the ones obtained using analog processing are achieved. Generally, when the algorithms are applied directly to the untransformed digital (discrete) signal, the resulting data is in a form that can be directly reconverted to an analog (continuous) signal, and the sampled data is referred to as being a *time domain* representation of the signal (e.g., time domain filtering). In other instances, the data might undergo a major change in representation before the signal shaping algorithms are applied. An example of a representation transformation is the Discrete Fourier Transform — implemented using the Fast Fourier Transform (FFT). In this particular case, the data have been converted to a *frequency domain* representation, and the algorithms are applied in this domain. Before being reconverted to an analog form, the data is retransformed to its time domain representation by an Inverse Fast Fourier Transform (IFFT). Both processing methods yield similar results, however a particular alteration might be easier to implement in one domain than in the other.

3.3 The Modulation Scheme

Considering the basic requirements of the communications system, (i.e., the smallest possible RF bandwidth, communications with the lowest possible power, resistance to interference) it became clear that Single Sideband (SSB)-like forms of modulation (i.e., linear modulation) could be used advantageously for this application.

An argument that is often presented in favor of using wideband FM (i.e., with modulation index $\beta > 0.6$ [7]) is that it shows an improvement of the voice quality over the other analog modulation schemes (e.g., AM, SSB, or narrowband FM). However, this advantage, sometimes called the "capture effect", basically disappears in the presence of Raleigh fading [8]. Besides, there are two strong deterrents against the use of wideband FM for this application. The first one is that this voice improvement is only achieved through a sacrifice in RF bandwidth, and is currently implemented in the land-mobile bands with channel spacing in the range of 15 to 30 kHz. This is directly in conflict with the major objective; narrowband. The second one is related to the poor Signal to Noise Ratio (SNR) performance of this modulation scheme below the FM threshold of improvement. A wideband FM receiver with an input Carrier to Noise Ratio (CNR) well above threshold might generally have superior performance to that of SSB, however, as the input CNR falls below the threshold value, the output SNR of the FM receiver falls extremely rapidly. SSB, because of its linear nature, has a definitive advantage over wideband FM in this region. At CNR levels that yield unacceptable speech in the FM receiver, noisy, but intelligible speech is detectable in the SSB one. This advantage of SSB is accentuated in a Raleigh fading environment and in the presence of co-channel interference. In an FM receiver, as soon as the received signal fades below the receiver threshold, the audio output is heard to switch from signal to noise, a very disturbing effect that renders the speech unintelligible [9]. With SSB, the result will be an increase of the audio noise level, but the speech will still be readable [10] (unless the fade is of long duration, in which case any system will be unacceptable). In the presence of co-channel interfering signals and fast fading conditions, the audio output of the wideband FM receiver will switch between the wanted and unwanted signals and cause considerable distortion of the respective messages [9]. For SSB, provided the wanted signal is greater in magnitude than the unwanted signal for most of the time, occasional fades below the interfering level will not result in a loss of message. Even when the input CNR are identical, the wanted channel can be read, provided the signal has not faded below the receiver noise floor [10]. Therefore, communications with lower signal power and in the presence of high levels of noise (or interference) can be better achieved with SSB. This is very advantageous in situation such as broadband jamming.

Although FM has had, in the past, the advantages of economical design implementation and better performance, a number of recent studies have demonstrated that the traditional problems related to SSB usage (i.e., frequency stability, proper operation of the Automatic Gain Control (AGC) in a fading environment, sensitivity to impulsive noise, high costs, etc.), have been solved through the use of a pilot tone transmitted with the voice, and the use of a certain number of processing techniques that can be economically implemented with today's high level of circuit integration, to yield competitive SSB systems with performance similar to that of FM (e.g., [10-12]). This research lead to various pilot based SSB schemes, such as Amplitude Companded Single Sideband (ACSSB) [13] and transparent tone-in-band with Feedforward Signal Regeneration (FFSR) [14].

It seems reasonable to take advantage of the experimental experience that this extensive research yielded, and to apply the proven techniques to the baseline system. Although ACSSB was considered for this application, it was soon demonstrated that the implementation of the above mentioned objectives could not be fulfilled

using the conventional form of ACSSB. Nonetheless, the proposed implementation, called Digitally Processed ACSSB, has similarities with the SSB and ACSSB schemes. The use of a linear modulation scheme to implement a narrowband voice communications system is presented in more detail in the following sections.

One major problem related to the utilization of linear modulation schemes is the necessity of having highly linear power amplifiers. This problem is discussed in the next section.

Another consideration is the power efficiency of linear power amplifiers. Although constant envelope modulation schemes (e.g., FM) often use very power efficient class C amplifiers, it should be noted that this efficiency degrades significantly when the transmitted power is made to vary. Considering that variable power is part of the future performance objective, and taking into account the CNR/SNR gain (below the FM threshold) of SSB over FM, the power budget should be comparable.

4.0 LINEAR POWER AMPLIFIER

Although it is not difficult to show that of all the currently available analog schemes of modulation, Single Sideband (SSB) yields the best ratio between transmitted RF bandwidth and baseband bandwidth, the fact that a 3 kHz baseband voice signal, for example, produces more than 3 kHz SSB RF bandwidth is due to the non-linearities of the power amplifier used with such modulation scheme. If the power amplifier were ideal, a "one to one" ratio of RF to baseband bandwidth would be attainable (when no pilot is sent).

Designs of SSB and ACSSB systems have been aiming at a 5 kHz channel spacing. Unfortunately, their actual land-mobile implementation have yielded much larger bandwidth (e.g., 7.5 to 10 kHz [15–16]). The actual ratio of RF to baseband bandwidth for commercial land-mobile VHF ACSSB systems is therefore of about 3 to 1. This can be best seen in figure 1, where a "worst case emitted spectrum" of an above-band pilot ACSSB transmission is shown. The center frequency is about 145 MHz, and the "worst case spectrum" situation was obtained by talking continuously into the microphone (for about 2 minutes), and recording the maximum value of each RF frequencies. The assigned frequency in this figure is 1.8 kHz above the suppressed carrier frequency (that is, -1.8 kHz on this figure is the suppressed carrier frequency). The peak envelope power of this unit is 25 watts. One can see that the 3 kHz baseband bandwidth (that consists of the speech signal and the pilot tone) is directly translated into the RF bandwidth with an approximately ideal (one to one) ratio down to about 30 dB below the maximum power. Below this level, the non-linearities of the power amplifier give rise to spurious emissions that widen the spectrum, for example, up to 10 kHz at 65 dB below the maximum power. The spurious frequency components in the region about -4.5 to -2 kHz and +1.5 to +4 kHz relative to the assigned frequency are dominated by the third order intermodulation products; the spurious components outside this range are caused by the higher order products.

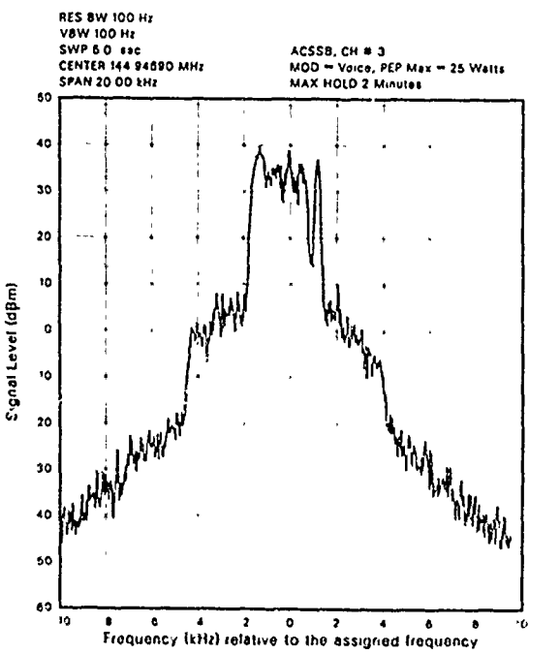

Figure 1 ACSSB Emitted Spectrum Long time Voice

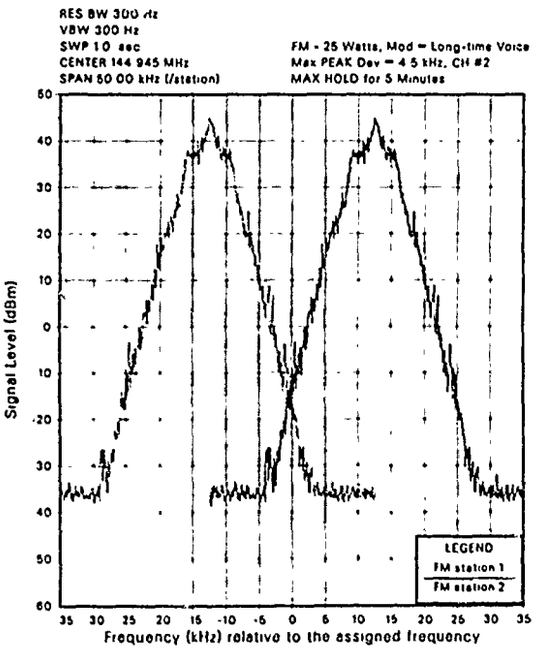

Figure 2 FM Emitted Spectrum, Long-Time Voice, 2 Stations (25 kHz)

The occupied spectrum at 60–70 dB below the maximum power is a criterion occasionally used to determine the channel spacing in land–mobile radios. This can be best seen looking at figure 2, where the worst case or long–time spectrum of 2 typical land–mobile FM transmitters is shown. The situation depicted in this figure is of 2 co–located FM transmitters, separated in frequency by one channel spacing (25 kHz). One can see that the emitted spectra meet at about 60 dB below the maximum power.

Therefore, in order to obtain the same kind of performances in terms of interference level and dynamic range for co–located ACSSB stations, a power amplifier with more linearity is definitively needed, because, as seen in figure 3, if we impose a 5 kHz channel spacing for the ACSSB transmitters, co–located stations interfere on each other at only about 35 dB below their maximum power. To get performance similar to that of FM, this value should be improved to at least 60 dB.

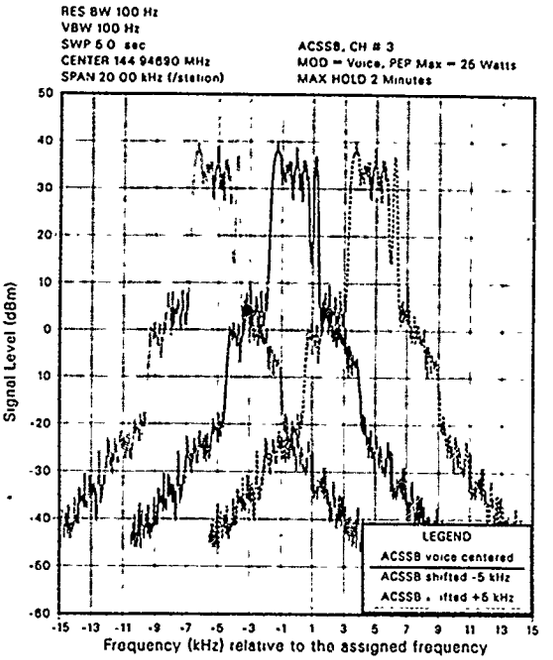

Figure 3. ACSSB Tx Spectrum, Long-time Voice - 5 kHz Channels

At the beginning of this research program, it was proposed to direct part of the efforts towards finding ways to improve the performance (or equivalently, improve the linearity) of the power amplifier. In addition to taking advantage of the past research in this field (e.g., [17–18]), the possibility of using digital signal processing at the baseband level in order to reduce the effects of the intermodulation products in the power amplifier had been suggested. Although these possibilities might still be explored, the task of finding an appropriate linear power amplifier was recently considerably reduced, since a Canadian Company working in this field was found. They produce a linear power amplifier that might be satisfactory for this application. We will soon be testing these amplifiers, and be able to judge if they meet our requirements.

Naturally, the width of the emitted spectrum is not the only factor to be considered to reduce the channel spacing, the receiver also has to be properly designed. But this part does not seem to cause major difficulty, and will most likely be handled with standard design techniques.

5.0 The BASEBAND BANDWIDTH REQUIREMENTS

It is generally accepted that for good voice quality, the baseband voice bandwidth should include the frequencies from about 300 to 3300 Hz. With an ideal power amplifier, an RF channel spacing of about 3 kHz could be obtained from a 3 kHz baseband speech signal. However, taking into consideration the demand resulting from the data information transmission required for the implementation of the desirable functions of a tactical communications system, and from the embedded reference signal (e.g., pilot tone) required for fading compensation, additional bandwidth is required. As stated, our basic objective is a channel spacing of about 3 kHz, hence, to achieve this goal, other means must be sought. The most obvious way to reach this objective is by reducing the baseband voice bandwidth. Therefore, one is facing the fundamental trade–off of narrowband versus quality. one would like to decrease the voice bandwidth, but not its quality. How can this dilemma be solved? Some form of bandwidth reduction can be used in order to save the major components of the speech that are important to maintain a relatively good voice quality.

Speech bandwidth reduction techniques are means of reducing the bandwidth needed to represent the human voice waveform. Bandwidth reduction methods introduce approximations and eliminate unneeded information in the speech signal. The possibility exists for techniques to reduce the voice bandwidth while maintaining relatively good voice quality, and they have been explored within this program. A brief overview of some of these techniques is presented in the next section.

6.0 SPEECH BANDWIDTH REDUCTION

6.1 Analog versus Digital Bandwidth Reduction Techniques

One distinction that should be made is the difference between analog and digital bandwidth reduction techniques.

Over the past decade, the overwhelming attention has been given to digital (i.e., vocoders) over analog techniques. Most activity today in speech bandwidth reduction is concentrated on digital techniques which provide bit rate reduction rather than direct audio bandwidth reduction. For example, Linear Predictive Coding (LPC), Adaptive Predictive Coding (APC), etc., are systems that use digital bandwidth reduction. Consequently, the reduced signal is transmitted using digital modulation techniques. Also, the need for security in voice communications has been met by converting the voice to a digital form so that sophisticated digital encryption is possible. Furthermore, digital techniques are attractive for transmission through Integrated Services Digital Networks (ISDN).

Digital bandwidth reduction techniques start with a big handicap with regards to bandwidth. At a sampling rate of 8000 samples per second and with a minimum of 8 bits per sample to characterize the amplitude of each sample, a total of 64000 bits per second is needed to represent the speech. A commonly accepted goal today is to reduce this bit rate to 2400–9600 bits per second (bps). While the lowest bit rate can be achieved, the quality of the voice generally suffers accordingly.

Linear Predictive Coding (LPC) for example is a digital bandwidth reduction technique that yields very good results in providing bit rate reduction in the digital transmission systems, and has been considered as satisfying some of the requirements of this application. However, at very low data rates (e.g., 2400 bps: LPC–10), although it yields a voice signal with relatively good *intelligibility*, it is often judged as lacking two very important attributes generally needed for the voice to be qualified as good quality speech: it is somewhat deficient in *naturalness*, the attribute of sounding natural, not machine–made, robot–like or synthetic, and also in *speaker recognition*, which is the ability of a listener to recognize the voice of someone he knows.

Most very low bit rate vocoders have the first of the above qualities (i.e., intelligibility), but lack the second and third (speaker recognition and naturalness). On the other hand, a very narrow band–limited voice signal (e.g., 200–2000 Hz) might conserve speaker recognition and naturalness, but lose a lot of intelligibility. Consequently, good voice quality is generally defined as having the 3 above attributes: intelligibility, speaker recognition, and naturalness, and the chosen bandwidth reduction method should preserve these 3 attributes.

A survey of the various bandwidth reduction techniques showed no digital voice coding techniques that result in less bandwidth for the same quality as analog. Although analog bandwidth reduction techniques have been tried in the past, with more or less satisfactory results, it is important to stress that a major element now makes these techniques easier to implement, more precise and powerful, and more economical than the implementations that were done in the late seventies: the implementation can now be done using digital signal processors.

Therefore, our efforts were not directed towards research in the actively studied field of digital bandwidth reduction. We chose rather to diversify and concentrate on using Digital Signal Processing (DSP) and apply it to the less explored analog bandwidth reduction techniques, because, for the typical land–mobile type of communication path, the best opportunity for baseband (bandwidth) reduction at present appears to be analog (although this could change in the future). Present status of analog reduction techniques indicates the possibility of obtaining good voice quality in less than half the actual transmitted baseband (bandwidth) of speech [19].

Another very important consideration with bandwidth reduction techniques is their performance in the presence of background noise. It is of prime importance that the technique utilized be able to function well in a noisy environment. Some techniques (e.g., LPC–10) yield completely unintelligible speech in many noisy environments, and this should be avoided.

A study of the available analog bandwidth reduction techniques that could be used for this application was done, and experimental evaluation using DSP was conducted with the most promising candidates. This is described in the next section.

6.2 Overview of Analog Speech Bandwidth Techniques

Analog bandwidth reduction techniques can be classified into two major categories. The principal difference between the two classes is that, in one case, an attempt is made to interpolate the missing speech components (time or frequency), whereas no attempt is made in the other case.

Because of their attractiveness in reducing the bandwidth of the voice signal, some consideration was given to frequency compression–expansion (companding) methods [20–22]. If frequencies could be easily divided and multiplied by two, bandwidth could be halved. That looks like a good approach, yet the implementation is not that simple. It is easy to compress and expand the amplitude of a signal. For example, the amplitude can just be divided by two at the transmitter, and multiplied by two at the receiver. However, dividing all the frequencies by two is another problem, because, by doing so, one essentially loses some of the frequency components. These missing components have to be interpolated in some way at the receiver and, as was

found, such interpolation can seriously affect the quality of the voice.

One technique of frequency companding consists of transforming the real and imaginary components of the FFT data into amplitudes and phases [23–24]. One out of two amplitude and phase components is rejected (put to zero) in the case of 2:1 frequency compression. The remaining components are then moved down and the resulting signal converted back to the time domain (IFFT), and transmitted using only half the bandwidth of the original signal. At the reception, an FFT is taken of the signal, the amplitude components are moved back to their original position, and the missing ones are linearly interpolated. The missing phases are replaced with random values (because of the low correlation of the phase, it can not be interpolated), and the signal reconverted to the time domain. The resulting signal is quite intelligible, and although amplitude interpolation error as well as discontinuities at the time domain block boundaries result, this is not the major problem: distortion and background noise are produced as a result of the incorrect phase associated with the interpolated amplitude components. This noise is sometimes referred to as audio phase noise. In a variation of this scheme, all the phase information is discarded at the transmission, and only the amplitude components are transmitted. At the reception, when the signal is converted back to the time domain using random or fixed phase values, a signal with background noise and/or with some form of amplitude modulation results. Finally, by reducing the FFT size, and by alternating the phase, for example between 0 and 180 degrees, a voice signal that is quite intelligible, but that has lost its naturalness is produced.

Other forms of interpolation such as the time domain speech gapping [25], and adaptive interpolation [26], or the frequency domain signal reconstruction from the Fourier Transform magnitude [27] were found to either yield relatively poor voice quality, and/or to be sensitive to background noise and/or to be highly susceptible to transmission errors.

Fewer problems are generated when no attempt is made to interpolate the missing (time or frequency) speech components. For example, in simple "fixed frequency band elimination", some of the frequency spectrum in the middle of the 3 kHz voice band is simply thrown away [28]. The frequency bands retained can be transferred into the frequency gaps created and the bandwidth of the speech signal thereby reduced. The major problem with this scheme is that important parts of the voice spectrum, located outside the kept bands, will be lost.

Another idea for frequency band elimination takes advantage of the fact that the voiced and unvoiced components tend to be separated in time and frequency [29]. But to function properly, this method requires a basic kept speech bandwidth in the order of 2 kHz. Note also that this technique is sensitive to background noise.

An improvement on the above two methods, the "dynamic frequency band extraction" has been successfully applied to digital speech bandwidth reduction techniques (in a technique called "sub-band coding" [30]), but has also its analog equivalent. The principle behind this scheme is simple: if one is going to throw away some frequencies, one might as well throw away the ones with the least energy. In this scheme, the speech energy in several frequency bands is analyzed continuously. Only the frequencies in the bands which contain the most significant energy are transmitted. This way, the formants of the voiced sounds, for example, can be tracked and included in the transmitted information. Naturally, means must be provided to inform the receiver which frequency bands are being transmitted and the signal is restored accordingly. This method is more complex to implement than the fixed frequency band elimination, yet yields much better voice quality. This method when optimized was found to yield results of a quality acceptable for this application and was adopted for the communications system.

Good voice quality was not the only criterion used for adopting this bandwidth reduction technique. Various other factors, for example, its behaviour in the presence of background noise, and its level of encryptability were also considered. A more detailed description of these factors, as well as an overview of the general principles behind the dynamic frequency band extraction method are given in the following sections.

7.0 The DYNAMIC FREQUENCY BAND EXTRACTION TECHNIQUE

The general principles of this method can be better explained by looking at the following figures:

Figure 4–a represents the frequency spectrum of a 4 kHz bandwidth voice sample, analysed over a short period of time (typical period values are between 16 and 128 milli-seconds (msec)). This period is hereafter called a frame. The frequency spectrum is obtained by first sampling the continuous-time voice signal, and by doing an FFT on a fixed-length block of sampled signal.

The vertical axis represents the amplitude squared (or equivalently, the energy) of the various frequency components (horizontal axis) present in this frame. One can see that many frequency bands are either empty or have very little energy. Thus, by eliminating these frequency bands, and by keeping only those

with significant energy, the voice quality should not degrade. In a possible form of transmission, the frequency bands that have been kept are translated down so that the bandwidth they occupy is reduced by a factor of 2 (from 4000 Hz to 2000 Hz), as shown in figure 4-b. From the original speech spectrum (4-a), one can also see that some frequency bands have relatively low energy; thus, by eliminating these low energy frequencies, a compression factor of 3 can be obtained (figure 4-c). When transmitted in this compressed form, the signal uses only 1/3 the original bandwidth. It is expanded back to its original frequency bands at the receiver to yield approximately the original voice signal frequency spectrum (figure 4-d). The approximate time domain speech signal is recovered by doing an inverse FFT on this spectrum.

Clearly, means must be provided to inform the receiver where to position the frequency bands. This requires the transmission of some data information along with the voice information. But, as mentioned before, data incorporated with the voice is an asset, and will help meet some of the objectives of this system. For example, by interlacing the data with the voice discrete-time frequency components, enough information would be provided at the receiver for it to "sound" the channel, and FFSR (Feed Forward Signal Regeneration) type of fading compensation could be performed using this "spread pilot" instead of an independent pilot tone.

Data can also be added to dynamically normalize the amplitude of the signal on a frame-to-frame basis, thereby yielding more efficient signal to noise ratios and lower peak to average power ratios.

Using an original voice bandwidth of 3 Khz (300-3300 Hz), and extracting statistics from a number of voice samples, it was found that most of the speech energy is concentrated in about a total of 750 Hz, therefore yielding the possibility of a 4 to 1 compression factor.

As mentioned, the speech energy in several frequency bands is analysed continuously, and only the frequency bands which contain the most significant energy are transmitted. Based on the statistics extracted from the voice samples, the technique was tried with different number of bands, with bands of various bandwidth, and with various optimization schemes.

Saving a total instantaneous bandwidth of 750 Hz (out of the original 3000 Hz) yielded relatively good quality voice for male speakers; but, because of the more dynamic and richer frequency content of the spectrum produced by female speakers, more distortion was introduced in their processed speech. This is mainly due to the higher number and larger excursion of the band movements in the female voice case. By careful planning of the movement of the bands, and by using a larger instantaneous bandwidth, the quality (specially for female speakers) was greatly improved. Thus, the final optimized version extracts only 1200 Hz per frame, out of the original 3000 Hz.

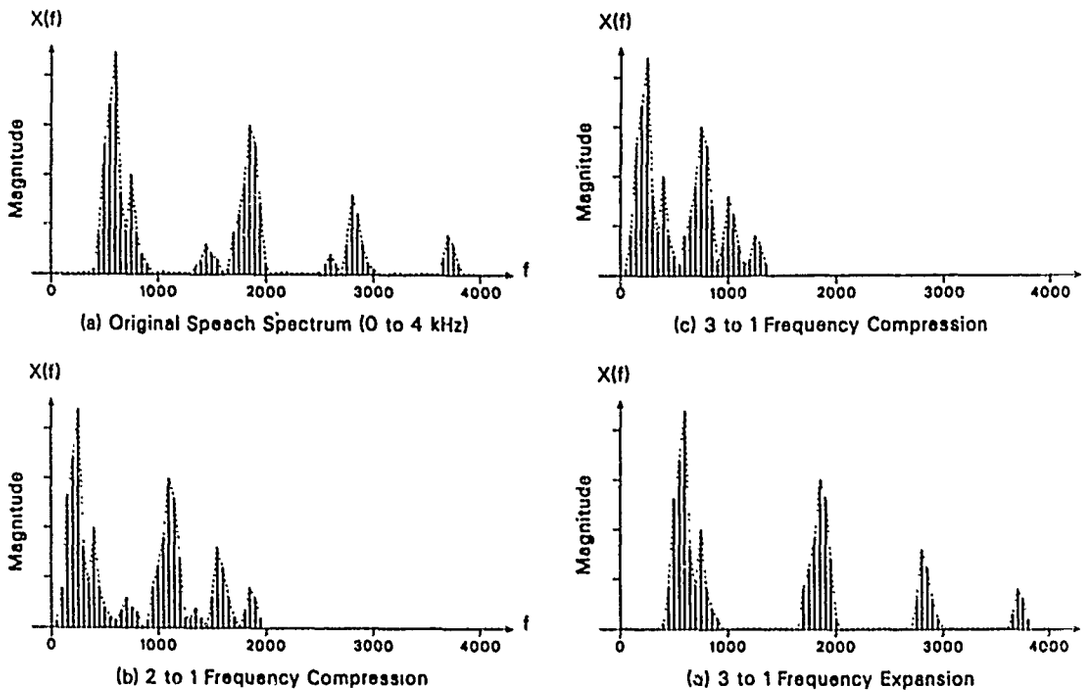

Figure 4. Compression/Expansion of the Speech Signal. Dynamic Frequency Band Extraction

This scheme was evaluated for a number of English speaking male and female voices, and was generally found to yield good quality speech signal. Finally, other languages (e.g., French, Japanese) were also tested and evaluated as of good quality. An audio cassette containing voice samples processed with this technique is available, and it illustrates the voice quality achieved.

Because the optimized 1200 Hz version produces good voice quality for both male and female speakers, and because this version also reproduces well other languages, it was considered a good candidate for our baseline system. But before being adopted, aptitudes to encryptability and resistance to background noise had to be demonstrated.

Therefore, a number of speech samples with various background noises were processed. The results showed that the dynamic frequency band extraction method was not only resistant to background noise, but in some instances could even help in reducing it. This is demonstrated in the following idealized representation: consider the original speech spectrum of figure 4–a. To this signal, some form of noise – let say white noise – is added. Figure 5–a is a representation of the noisy signal. Since only the highest energy bands are chosen and transmitted, at the receiver, the background noise that was present in the other bands has been eliminated (figure 5–b). Therefore, in this situation, the bandwidth reduction technique helped in reducing the background noise. Note also that various processing and optimization techniques can also be used to counter high energy spectrally limited noise.

The encryptability is also best demonstrated using a figure: Using the 3 to 1 frequency compressed speech spectrum representation of figure 4–c, applying amplitude compression and normalization to each frame, figure 6–a results. This processing serves two goals: to reduce the peak to average power ratio, and to remove the speech pattern. Normalizations bring the amplitudes of the high and low passages to the normalized level. Even for a very low level or a silent passage, the resulting signal ends up at the normalized level; consequently, the speech pattern is destroyed.

In addition, data, at the normalized level, is inserted with the voice components. This data is used for example to tell the receiver where to position the frequency bands, what normalization gain to apply to each band, etc. As can be seen in figure 6–b, the resulting frequency domain speech signal is already quite unrecognizable.

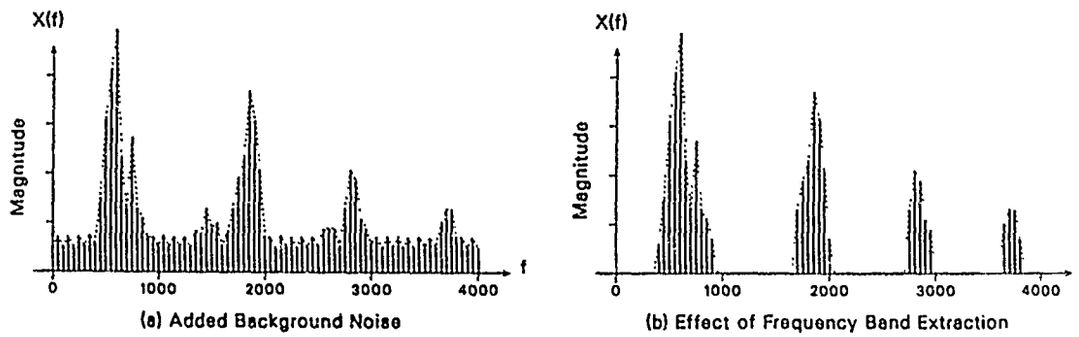

Figure 5: Dynamic Frequency Band Extraction in the presence of Background Noise

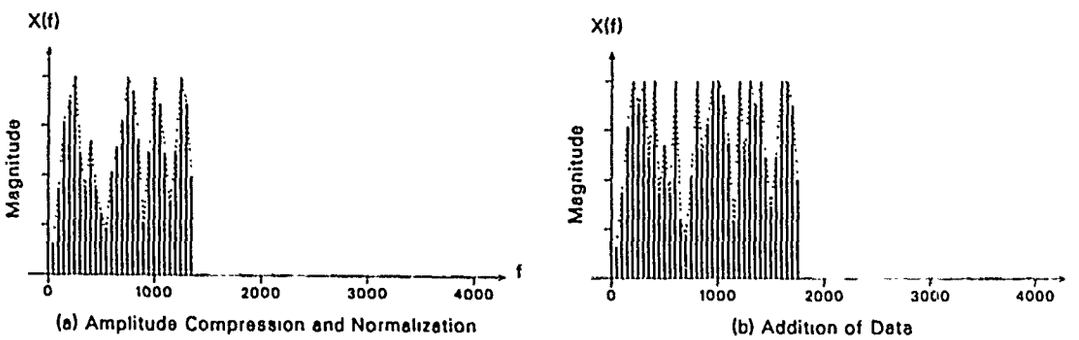

Figure 6: Amplitude Compression and Normalization, Addition of Data

To this signal different kinds of encryption can be added. for example, the position of the discrete frequency components can be mixed, or the phase can be scrambled, and independent encryption can be applied to the data and voice components. It has recently been shown that the FFT coefficients scrambling approach provides high-level security [31]. But if that is not enough, a second stage of encryption can be added by combining 2 or 3 frames together and scrambling everything together again. Most important, all this encryption can be done without further increase in the bandwidth.

8.0 The TRANSMISSION STRATEGY

As mentioned, a certain amount of data information has to be transmitted along with the reduced voice signal. The development of techniques for transmitting this information efficiently, without further distortion to the voice signal, is very important.

Another consideration, arising from the finite amount of processing that can be done in real time on the digital signal processor, is to keep the amount of processing at a practical level.

As we have seen, frequency domain processing is used to implement the voice bandwidth reduction. Therefore at least one Fast Fourier Transform (FFT) operation is required at the transmitter. Should conventional time domain modulation (e.g., ACSSB in its actual form) be used to transmit the signal, an inverse FFT before transmission would be required. FFT and IFFT transformations are computationally intensive operations that seize an important part of the time available for real time processing.

Relating the performance objectives to a time domain transmission, one finds implementation difficulties. For example, implementing encryption by scrambling the frequency components results in discontinuities in the frequency domain signal. If this signal is translated into the time domain, adverse oscillations will result and will cause additional distortion of the speech signal.

Incorporation of data with the voice would cause similar discontinuity problems, unless the data is modulated with the pilot, in which case the pilot would seize a relatively important part of the total bandwidth and transmitted power and would cause aggravated power amplifier intermodulation problems. Also, for anti-jamming purposes it has been suggested that the pilot be spread over the band, and implementation problems are anticipated if the time domain is used for the transmission.

Therefore, the mode of transmission strategy has to be carefully planned so that the performance objectives can be implemented without degradation of the voice quality.

By directly transmitting the amplitude and phase levels of the FFT components, as the amplitude and phase of the RF waveform, at uniformly spaced instances in time (instead of the continuous time domain IFFT amplitudes) [32], the above problems would be solved, and:

- data and FFT component levels can be mixed as a sequence of discrete-time complex (i.e., amplitude and phase) samples prior to modulation and transmission;
- since the conversion to the time domain is done only at the receiver, less processing is required, and an inverse FFT operation at the transmitter, as well as an FFT at the receiver are eliminated. Also, it is believed that transmitting the frequency domain samples will not only reduce the processing load, but also result in increased robustness;
- the discontinuity problem caused by the scrambling of the frequency components is eliminated, since the conversion to the time domain is done at the receiver after the FFT components have been descrambled,
- encryption can be more complex, in fact, similar techniques as the ones used for data encryption can be employed;
- data and known training samples (instead of a pilot) can be uniformly mixed with the FFT samples and used to sound the transmission link;
- the data and known training samples can be used to train an adaptive equalizer [33];
- finally, the data and known training symbols would effectively produce the effect of a spread pilot, yielding advantage not only in terms of anti-jamming performance but also in terms of avoiding inter-modulation in the linear power amplifier.

Therefore, bandwidth reduction in this case can be seen as a reduction of the number of spectral rays that have to be transmitted through the communication link. Although digital signal processing is used to implement the algorithms, the effect of the bandwidth reduction still results in the equivalent bandwidth reduction of the analog form.

In addition to the above mentioned advantages, another saving in bandwidth results from the fact that, if the voice signal was reconverted to the time domain before transmission, the pilot tone, inserted in the emitted signal, would need to be separated from the neighbour bands by a non-negligible frequency gap. The insertion of a non modulated, in-band, time-domain pilot tone necessitates a guard band of twice the maximum Doppler shift frequency, *on each side of it*, in order to compensate for the frequency spreading

that occurs during fading. We have an analogous, but smaller, penalty in that we have to "sound" the channel at a rate of at least twice the maximum Doppler frequency (Nyquist's sampling theorem).

9.0 The TRANSMISSION IMPLEMENTATION

This section briefly presents what is transmitted, how the transmission is accomplished, and how much RF bandwidth is required.

Data information, at a rate of about 550 bits per second, is needed to implement the majority of the performance objectives previously mentioned, including voice encryption and fading compensation. Part of this data is also used for the repositioning of the frequency bands at the receiver, and for amplitude normalization. As will be seen, the bandwidth used for the data occupies only about 1/4 of the total baseband bandwidth.

The reduced voice information consists of amplitude and phase components extracted from the original voice signal by using an FFT and applying the dynamic frequency band extraction to the high energy frequency bands. Although an instantaneous bandwidth of only 1200 Hz is kept (resulting in 1200 complex discrete-time samples per second), the overlap-and-add algorithm required when filtering in the frequency domain increases the number of samples per second by about 250. Therefore, a total of 1450 complex analog discrete-time samples per second is needed for the voice signal. The voice signal, therefore, takes about 3/4 of the total baseband bandwidth.

By coding the data information in terms of amplitude and phase, all the information to be transmitted is in the (complex) frequency domain form. The data is inserted between the voice samples. Consequently, a total of 550 + 1450 = 2000 complex discrete-time samples per second has to be sent.

Finally, the amplitude and phase levels of the voice and data frequency components are modulated as the amplitude and phase of the RF waveform. This is a form of quadrature SSB modulation. Allowing for the extra bandwidth required for the pulse shaping of this discrete time signal, and adding error detection and correction to our data, the modulated bandwidth will be about 1.25 times the discrete-time rate (this 1.25 factor is a function of the sharpness of the transmit filter). Consequently, supposing a very good linear power amplifier, an RF channel spacing in the order of 2.5 kHz is expected.

Should one be satisfied with the lower voice quality obtained by keeping an instantaneous bandwidth of 750 Hz instead of 1200 Hz, the RF channel spacing could be maintained below 1800 Hz.

This modulation scheme was simulated, and it was found that, as expected with linear modulation schemes, it provides intelligible communications in a very low RF carrier to noise environment.

10.0 CONCLUSIONS

The instantaneous 1200 Hz voice bandwidth, obtained using the dynamic frequency band extraction bandwidth reduction technique, has been chosen as the baseline voice representation for this communications system. A number of voice samples processed with this method has shown that such an instantaneous bandwidth accurately reproduces the majority of speakers. It is believed that the presented approach yield better voice quality and superior robustness to background noise, compared to digital vocoder techniques requiring similar bandwidths.

In terms of baseband bandwidth, some overhead data is required for channel tracking (fading compensation), voice encryption, dynamic control, error correction, and generally, to implement the various wanted options required for a versatile mobile tactical communications system.

At this time, assuming a highly linear power amplifier, it is felt that the total RF channel spacing, including voice, data, encryption, and fading compensation, can be maintained below 2500 Hz.

REFERENCES

[1] Lodge, J.H., *"A TMS32010-Based ACSSB modem for Mobile Satellite Applications"*, Proceedings of the Thirteenth Biennial Symposium on Communications, Kingston, Canada, June 1986, pp. B.1.5-B.1.8.

[2] Huck, R.W., *"Modulation and Voice Coding for Mobile Satellite Applications"*, Proceedings of an ESA Workshop on Land-Mobile Services by Satellite, held at ESTEC on 3-4 June 1986 (ESA SP-259, Sept 1986), pp 81-86.

[3] Lodge, J.H., Boudreau, D , *"The Implementation and Performance of Narrowband Modulation Techniques for Mobile Satellite Applications"*, IEEE International Communications Conference ICC '86, Toronto, June 1986

[4] Bryden, B , Hassanein, H , *"Implementation of a full-duplex 2.4 bps LPC Vocoder on a single TMS-320 Microprocessor Chip"*, ICASSP'84, Proceedings of the IEEE International Conference on Acoustics, Speech and Signal Processing, San Diego, CA , 19-21 March, 1984

[5] Hafez, H.M , Goubran, R., *"A Feasibility Study on the Adaptation of the SYNCOMPEX Concept to the VHF/UHF Land Mobile Communication System"*, Final Report, University Research Contract # OST 84-00173, Carleton Uni-

versity (Ottawa), Dept. of Systems and Computer Engineering, April 1985.

[6] Goubran, R.A., Hafez, H.M., Kerr, A.B., *"Adaptive Speech Companding for Speech Transmission over Mobile Channels"*, 37th IEEE Vehicular Technology Conference, Cat No. 87CH2429-9, Tampa, Fl, USA, 1-3 June 1987, pp. 13-18.

[7] Taub H., Schilling D.L.. *"Principles of Communication Systems"*, McGraw-Hill Book Co., New York, 1971, pp. 303-304.

[8] Lee, W.C.Y., *"Mobile Communications Engineering"*, McGraw-Hill, Inc., 1982, pp. 242-249.

[9] Juroshek, J.R., *"Measurements of FM Receivers in FM Interference"*, NTA Report 79-27, U.S. Dept. of Commerce, October 1979.

[10] Wells, R., *"SSB for VHF Mobile Radio at 5 kHz Channel Spacing"*, Proceedings of Conference Radio Receivers and Associated Systems 1978, IERE, London, 1978, pp. 29-36.

[11] Lusignan, B.B., Herro, M.A., Nocedal, F., Wala, P.M., *"Amplitude Companded Sideband for Land Mobile Radio"*, Conf. Proc. Intern. Telecom. and Computer Exposition, Los Angeles, 10-13 Nov. 1980, pp. 130-135.

[12] Gosling, W., McGeehan, J.P., Richardson, J.H., *"SSB as an Optimum Modulation for Land Mobile Radio"*, Proceedings of Intern. Conf. on Land Mobile Radio, IERE, Lancaster, Sept. 1979, pp. 325-334.

[13] Lusignan, B.B., *"The use of Amplitude Compandored SSB in the Mobile Radio Bands"*, Final Report, FCC Technical Report No. 29, Washington, DC, Federal Communications Commission, 1980.

[14] McGeehan, J.P., Bateman, A.J., Burrows, D.F., *"The Use of "Transparent" Tone-in-Band (TTIB) and Feedforward Signal Regeneration (FFSR) in Single Sideband Mobile Communications Systems"*, IEE Communications '82, Publication # 209, pp. 121-126.

[15] Belrose, J.S., *"Narrowband Technologies suited to the Transmission of Voice and Data for Mobile Radio Systems"*, First Canadian Mobile Radio Communications User Conference, Ottawa, Ontario, 13-14 May 1985.

[16] Burke, M.J., Boucher, L., *"An Amplitude Compandored Single Sideband Equipment Evaluation"*, IEE Inter. Conf. on Mobile Radio Systems and Techniques, University of York, York, UK, 10-13 Sept. 1984.

[17] Gosling, W., Petrovic, V., *"A High Efficiency VHF SSB Transmitter"*, Conference on Civil Land Mobile Radio, IERE Conference Proceedings No. 33, November 1975.

[18] Gosling, W., Petrovic, V., *"The Polar-Loop Transmitter"*, Electronics Letters, 15, No. 10, May 10, 1979, pp. 286-288.

[19] Gieseler, P B , O'Neal, J B., *"Speech Bandwidth Reduction"*, FCC Office of Plans and Policy Working Paper Series, Paper No. 3, November 1980.

[20] Bogner, R E., *"Frequency Division in Speech Bandwidth Reduction"*, IEEE Transactions on Communication Technology, Vol. COM-13, No. 4, Dec. 1965, pp. 438-451.

[21] Malah, D , Flanagan, J L., *"Frequency Scaling of Speech Signals by Transform Techniques"*, The Bell System Technical Journal, Vol. 60, No. 9, Nov 1981, pp. 2107-2156.

[22] Flanagan, J L , Christensen, S.W., *"Technique for Frequency Division/Multiplication of Speech Signals"*, J. Acoust. Soc. Am., 68 (4), Oct. 1980, pp. 1061-1068.

[23] Patrick, P J , Steele, R., Xydeas, C.S., *"Frequency Compression of 7.6 kHz Speech into 3.3 kHz Bandwidth"*, IEEE Transactions on Communications, Vol. COM-31, No. 5, May 1983, pp. 692-701.

[24] Wong, W C., Steele, R., Xydeas, C.S., *"Transmitting Data on the Phase of Speech Signals"*, The Bell System Technical Journal, Vol. 61, No. 10, Dec. 1982, pp. 2947-2970.

[25] An implementation of speech gapping was done by the Numa Corporation of Orlando, Florida, in the late seventies. See also reference [19].

[26] Steele, R , Benjamin, F., *"Sample Reduction and Subsequent Adaptive Interpolation of Speech Signals"*, The Bell System Technical Journal, Vol 62, No. 6, July-August 1983, pp 1365-1398.

[27] Nawab, S.H , Quatieri, T F , Lim, J S , *"Signal Reconstruction from Short-Time Fourier Transform Magnitude"*, IEEE Transactions on Acoustics, Speech, and Signal Processing, Vol. ASSP-31, No. 4, August 1983, pp. 986-998

[28] Harris, R W , Cleveland, J.F., *"A Baseband Communications System"*, Part 1, QST, November 1978, pp. 14-21.

[29] Patrick, P J., Steele, R., Xydeas, C.S., *"Voice/Unvoiced Band-Switching System for Transmission of 6 kHz Speech over 3.4 kHz Telephone Channels"*, The Radio and Electronic Engineer, Vol 51, No. 5, pp. 233-235, May 1981.

[30] Crochiere, R.E , Sambur, M.R , *"A Variable Sub-band Coding Scheme for Speech Encoding at 4.8 kb/s"*, The Bell System Technical Journal, Vol. 56, No. 5, May-June 1977, pp. 771-779.

[31] Matsunaga, A., Koga, K., Ohkawa, M., *"An Analog Speech Scrambler using the FFT Technique with High-level Security"*, IEEE International Conference on Communications '88 (ICC), Philadelphia, Pa, June 12-15, 1988, IEEE Publication # CH2538-7/88/0000-1619, Volume 3, pp. 1619-1625 (49.7.1-49.7.7).

[32] Logan, B.F , *"Bandwidth-Conserving Independent Amplitude and Phase Modulation"*, The Bell System Technical Journal, Vol. 62, No. 10, Dec. 1983, pp. 3053-3062.

[33] Lim, T L , Mueller, M.S., *"Adaptive Equalization and Phase Tracking for Simultaneous Analog/Digital Data Transmission"*, The Bell System Technical Journal, Vol 60, No. 9, Nov. 1981, pp. 2039-2063

DISCUSSION

M. DARNELL

Can you tell me how often the "dynamic windows" are re-assigned ? Is it more or less frequently than the 20-25ms of conventional digital vocoder systems ?

AUTHOR'S REPLY

The discrete Fourier transform is done about every 64msec., and the windows are allocated independently in each frame (i.e. every 64msec.). So this is about 3 times slower than with LPC-10. A compromise had to be made : in one hand you want a frame as long as possible in order to reduce the amount of "support" data sent per second. On the other hand you want a short frame in order to "grab" all the frequency variations.

R.D. STEWART

What techniques are you using for your "improved linear amplifier". Are you using novel techniques such as predistortion or feed-forward to improve linearity ?

What is the output power of your linear amplifier ?

AUTHOR'S REPLY

1 - Various techniques have been looked at. References are given in the paper. Basically we will use feed-forward techniques. Predistortion may be applied at the baseband level if this is easily done with Digital Signal Processing.

2 - The prototypes will have a peak envelope power of 10 watts. We want to be able to compete in terms of Range, with a 25 watts FM radio. SSB provides a CNR/SNR gain (below the FM threshold) over FM.

K.S. KHO

1 - What will be the size of the prototype terminal ?

2 - RF noise resistance. Do you consider the very bad C/N ratio in military environments ?

3 - To what kind of extend classification is possible with analog scrambling method ?

4 - Do you use speech pauses for transmitting the information (management) data ?

AUTHOR'S REPLY

1 - The first prototypes will fit in a 19 by 4 inches rack. But this size would be reduced a lot if the radio were commercialized. Almost all the processing is done digitally, and a small board with the TMS320C25 with A/D, D/A, and memory is used. Presently, the up and down conversions are the ones that require a lot of room because we have used a number of independently boxed 50 Ohms terminated devices. When this is put on PC boards, the room used will decrease significantly.

2 - Yes, tests were made with various level of white Gaussian noise, and our technique showed very strong resistance to it. Voice with the average speech power for example only 10dB above the average noise power is still very good. Also, the data is protected in 2 ways :

DISCUSSION

a) With error detection and correction, we now plan to use the extended (24, 12) Golay code which corrects 3 errors in 24 bits and detect the 4th one. But more sophisticated coding scheme could also be used later.

b) The data is transmitted at the rated peak envelope power level. Therefore, if the receiver can not detect the data because the received signal is too weak, it will not be able to demodulate the voice either, since the voice components are generally lower. In this case, we simply disable (silence) the audio output to avoid disturbing noise burst.

3 - There has been in the past questions about the level of security that can be achieved with an analog scheme. We believe that for our technique, it is very high, because, contrary to the traditional analog schemes, we work in the frequency domain and not in the time domain. In fact, our design, as well as the speech reduction technique were done and chosen keeping encryption in mind. Techniques used for data encryption can be used the same way with our technique. But tests will be done to try to determine the exact level of encryption that can be obtained. We will be able to answer better this question after these tests are completed.

4 - The possibility of using speech silences to transmit some overhead data has been looked at, and it might be part of future development, but for the moment we have to limit ourselves to the proof-of-concept prototypes. There are a few problems though with this method : you need very long processing delays (in the order of up to a few seconds) to take full advantage of the silences. Also you have more problems when dealing with (continuous) background noise.

CHANNEL SELECTION AND CONTROL PROCEDURES IN AN AUTOMATIC HF SYSTEM.

J. Hague
Hull-Warwick Communications Research Group
Department of Electronic Engineering
University of Hull
HULL
HU6 7RX
UNITED KINGDOM

1 SUMMARY

Conventional HF systems rely on a combination of human operators and off-line propagation prediction programs to determine an optimum operating frequency in what is a time-varying medium. Both these methods suffer drawbacks in that the rapidly varying nature of many HF paths leads to greatly reduced performance, since the system is unable to respond to the changing state of the medium.

An automatic HF system is described which is intended to overcome many of the drawbacks associated with conventional methods of control. By utilising cheap, amateur-grade equipment coupled with simple antenna systems, the system is able to carry data on one channel whilst assessing the usability of other channels assigned to that particular system. Measurements taken on alternative channels (probing channels) are compared with those of the current channel. The best channel currently available at each end of the link is then relayed to the other end by means of a robust data header on the user data channel. Thus each end of the link will always be transmitting on the optimum channel.

In order to assess the usability of the channel, some means of real-time channel evaluation (RTCE) is needed, both on the user's data and probing channels. This paper discusses the overall architecture of the automatic HF system, and details the methods of channel assessment performed. A description of a variable-redundancy coding scheme utilised by the system is also given, since this enables the system to optimise the data throughput. Finally, performance of various aspects of the system over an HF path are given.

2 INTRODUCTION

Due to the time-varying nature of the HF medium, a system which is to form part of a practical communications link must be able to adapt to it's environment if maximum throughput for the system is to be achieved. Current methods of control may involve a combination of the two techniques listed below:

i) Use of human operators to judge the optimum way in which to utilise the communications equipment at any one time.

ii) Use of off-line propagation procedures to set an optimum working frequency (OWF) on which communications should take place.

However, both of the above techniques suffer drawbacks which may render them inefficient under widely varying conditions. Use of human operators provides a satisfactory means of control when the state of the communications path is fairly well characterised, but under conditions of rapid, deep fading and heavy interference, the human operator may not be able to adapt the system sufficiently quickly to guarantee that optimum use is being made of the resources available to him/her.

Use of propagation analysis procedures may ease the above situation slightly, in that the user is given upper and lower frequency limits outside which communications has been predicted to be unreliable. However, such propagation predictions are based on mathematical models which aim to characterise the modes of propagation on a monthly median basis. Hence day-to-day variations by up to 50% from these figures may be found, thus limiting their usefulness. Also, such predictions are unable to predict such effects as localised interference, auroral blackouts, SID's and sporadic E, all of which have a major bearing on the quality of communications achieved.

A system which is able to automatically vary it's working frequency and error-control coding scheme in response to varying conditions will now be described.

3 AN AUTOMATIC SYSTEM CONCEPT

The system was designed to meet certain criteria, these being:

i) Use of simple antennas in conjunction with antenna tuning units, thus allowing the system to be used with non-resonant mobile antennas, and not relying on large

broadband arrays for successful operation.

ii) Use of transmitter/receiver units of cheap amateur grade. This enabled a workable system to be built at minimum cost by utilising 'off-the-shelf' units.

iii) Criterion (ii) above implies that the emitted power is at a minimum, thus reducing interference both to other spectrum users, and any co-sited radio terminals.

iv) Use of cheap processing power to control the overall system.

A block diagram of the system is shown in Figure 1. It comprises two transceivers, both of which are capable of being controlled by the 8085 control system. The basis of the system operation is that one of the transceivers carries the user's data with a certain degree of redundancy, on a channel that is determined to be optimum. The second transceiver performs alternative channel assessment. The results of this assessment enable the control system to determine the optimum channel/coding scheme to use for the user's data. The second 8085 system is dedicated to performing error-control coding/decoding on the user's data.

In order that both ends of the communications path are operating on the correct channel and with the optimum coding scheme, control data is appended on to each block of user data transmitted, as shown in Figure 2. This control data, known as the 'header', serves several purposes:

i) Bit reversals allow the receiver AGC to settle and also enable the error-control coding software to gain clock synchronisation.

ii) Use of a concatenated Barker (7,11) sequence enables the decoder to derive frame synchronisation [Barker, 1953]. It is also analysed further to enable the channels usability to be determined, as will be described in Section 4.1.1. For details of the system see [Hague, 1987] and [Hague, Jowett & Darnell, 1988].

The next two codewords are to inform the control software on which channel to transmit the next block of user data and with which coding scheme. The format of these control words is chosen to reduce the probability of false decoding occurring [Hague, 1987].

4 CHANNEL ASSESSMENT

In order that the optimum channel/coding scheme is chosen, some means of channel evaluation must be applied. For the alternative, or probing channel, this evaluation is continually being performed on each of the other channels in turn. For the current channel, assessment may take place at different stages throughout the data block. The method of channel assessment for each of the above two cases will now be described.

4.1 Current Channel Assessment

The way in which the current channel may be assessed are as follows:

i) Observing the correlation height of the sequence used for the decoder's frame synchronisation.

ii) Using the apparent error-rate derived from the decoder software.

iii) Deriving the channel signal-to-noise ratio from the modem.

The above methods will now be described in more detail.

4.1.1 Correlation Height of the Synchronisation Sequence

The sequence used to enable the decoder software to derive frame-synchronisation is the concatenated Barker (7,11) sequence. This sequence was chosen because of its high immunity to false synchronisation under high error rates. A plot of its autocorrelation is shown in Figure 3. This illustrates that the expected maximum for the autocorrelation value is 77, obtained at zero shift. However, as errors are introduced into the sequence, this height decreases by 2 for every error added. This phenomenon may be explained by the equation:

$$h = mn(1 - p) \qquad (4.1)$$

where, h is the peak correlation height, m and n are the lengths of the two sequences used in the concatenation (7 and 11 in this case), and p is the probability of a bit error occurring.

Thus for a concatenated Barker (7,11) sequence, being used over a Gaussian white channel, this equation becomes:

$$h = 77(1 - 2 \exp[-E_b/2N_o]) \qquad (4.2)$$

where E_b is the signal energy per bit, and N_o is the noise power spectral density.

It can now be seen that by observing the height of the synchronisation sequence matched filter peak output, then a measure of the channel's signal-to-noise ratio may be determined. Ideally, this figure is taken as an average for the channel over approximately 5 samples. This is due to the fact that during periods of high noise, the spread of the samples tends to be large, and analysis of the channel using just one synchronisation sequence may be misleading. Figure 4 illustrates this point by showing the results of laboratory trials obtained using a Gaussian white noise source as the only means of corrupting the sequence (the sequence was transmitted at 75 bits-per-second in a 3 kHz channel).

However, due to time constraints, it is impractical for the user's data channel assessment to be based on an average number of samples. Thus it is necessary to employ other methods of channel evaluation in conjunction with the synchronisation height in order to achieve a more reliable figure of assessment.

4.1.2 Error-rate Measurement Using the Decoder

The coding scheme used by the system employs variable redundancy to optimise throughput; this will be explained further in Section 5. The decoder software operates by utilising matrix techniques to detect and correct errors in the codewords - see Appendix A for further details on matrix coding/decoding of data. Since matrices are used, it is a simple matter to determine the most likely error-pattern added to a corrupted codeword. This is because the matrix operations involved in the detection and correction of errors produce a codeword which is calculated to be the most likely error-pattern to have been added to the user's data codeword. Thus by observing the error-patterns produced, a measure of the error-rate present on the channel may be determined.

However, under very high error-rates, a false indication of the number of errors present may be given, as the decoder may be attempting to detect errors above its capability. Thus again, this type of measurement should be used in conjunction with other forms of RTCE available.

4.1.3 Signal-to-Noise Ratio Using the Modem

A detailed description of the modem used will not be given here; for further details refer to [Hague, 1987].

A typical circuit diagram for the detector stages of a two-tone FSK demodulator is given in Figure 5. The output at points A and B may be used to derive the signal-to-noise ratio for each sub-channel within the receiver bandwidth.

Considering only point A at present: during interval 1, the output at point A represents the noise level, N_a for that sub-channel. Also, during interval 2, the output represents the (signal+noise) level, $(S_a + N_a)$ for that sub-channel. Thus the signal-to-noise ratio may be calculated by:

$$\frac{S_a}{N_a} = \frac{\text{level at interval 2} - \text{level at interval 1}}{\text{level at interval 1}} \qquad (4.3)$$

$$= \frac{(S_a + N_a) - N_a}{N_a} \qquad (4.4)$$

Similar equations may be applied to point B, and thus the signal-to-noise ratio of sub-channel B may also be derived.

As stated in Section 4.1.1, use of the synchronisation sequence correlation height alone is not reliable enough to provide an accurate means of channel evaluation. This method of evaluation provides the control system with an estimated S/N ratio for the channel. This figure may be used to predict an error-rate for the encoded data blocks which follow the synchronisation sequence. This may therefore be used in conjunction with the estimated error-rate , as measured by the decoder software, to reinforce the assessment figure.

Both of these methods may be further reinforced by comparing their calculated S/N ratio, with the S/N ratio as calculated using measurements taken from the modem output. The most easily derived means of RTCE are those using the synchronisation sequence and the decoder software, since they produce these figures during normal system operation. Therefore calculation of the S/N ratio using the modem should only be performed if there is a discrepancy between the other two channel evaluation figures.

4.2 Probing Channel Assessment

Two of the above methods may also be applied to enable alternative channel assessment to be performed; these are the synchronisation height, and modem output levels. However, the probing sequence does not contain any encoded data, and thus the error-control coding scheme will not be operational on this data.

In Section 4.1.1, it was stated that in order to gain a more realistic figure for the error-rate by using the synchronisation height, then it would be necessary for an average over several sequences to be taken. By analysing the results of several tests carried out under laboratory conditions (3 kHz channel with additive Gaussian white noise), it was found that an ideal figure over which to average was 5 sequences. This was because a smaller figure than this would give a channel estimate that could fluctuate widely under high error-rates, and a larger figure than this may not give a quick indication if the error-rate suddenly decreases - i.e. the average is too heavily influenced by it's past history. These deficiencies would be more noticable under deep-fading conditions.

The results of the trials over 5 sequences are shown in Figure 6, and it can be seen that the measured figure for each level of signal-to-noise ratio falls into reasonably distinct bands.

Probing channel assessment may be reinforced by using a signal-to-noise ratio figure derived by the method given in Section 4.1.3.

5 VARIABLE-REDUNDANCY CODING SCHEME

It was decided to use a variable-redundancy coding scheme to encode the user's data. It has been shown [Hellen, 1985] and [Goodman & Farrell, 1975] that the use of a variable-redundancy coding scheme is beneficial when the medium's capacity is likely to vary with time. Figure 7 shows the performance of 3 error-correcting coding schemes at increasing error-rates. At zero and very-low error rates, the use of <u>no</u> redundancy is optimum since adding redundancy serves no useful purpose except to reduce the overall throughput. A similar condition occurs at very-high error-rates: the error-rate is too high to be corrected successfully by even the most redundant coding scheme, and thus again serves no useful purpose except to reduce the overall throughput. Between these two extremes exist several points where the same conditions apply for medium-redundancy coding schemes. Thus the optimum coding scheme at any one time may be found by using that marked by the bold line in Figure 7.

A coding scheme which attempts to meet these conditions is to employed in the automatic HF system. Three, or more levels of redundancy, including no redundancy, may be employed at each end of the link to suit prevailing conditions. Analysis of the channel conditions using the methods detailed in Section 4 enable the system to determine the most suitable coding scheme to employ. Information regarding the coding scheme to be used by the other end of the link is passed in a robust format in the data header on the user's data channel, along with the optimum channel number. Selection of different levels of redundancy is accomplished by changing the generator matrix in the encoder, and the parity-check matrix in the decoder (see Appendix A).

6 SYSTEM INITIALISATION

When the system is to be used after a long period of radio-silence, it is necessary for both ends of the link to find a usable channel on which to commence communications. After this initialisation period, the system may then operate as normal. It is assumed that one end of the link will assume the role of 'master' station to allieviate the need for channel contention problems, and also to allow for the provision of a network of systems. Also, a real-time clock is provided at each end of the link to allow for synchronous operation. Two methods by which this initialisation may be performed are now detailed.

6.1 Scanning All Channels

One method by which this initialisation may be performed is to scan all the available channels in turn. Information regarding the quality of the channel in each direction is passed between each end of the link. Once all the channels have been evaluated, then communication commences on the optimum channel for each direction. Each scan takes 15 seconds, and therefore up to 16 channels may be evaluated every 4 minutes. Figure 8 details the format of such a scanning operation.

Transmission between master and slave takes the form of 3 robust sequences (the Barker 13-bit sequence, for example). These sequences are encoded by inverting all the bits to represent a 0, or leaving the sequence unaltered to represent a 1. At the receiving site, these sequences are passed into a matched filter, which produces a positive peak when the uninverted sequence has been received. In this manner up to 8 levels of information may be passed between sites regarding the usability of the channel. The operation of this protocol is as follows:

i) The processor waits for 3 seconds to enable the automatic antenna tuning unit

to match the antenna to the channel being used.

ii) The processor then waits for a further 1 second to allow for any time discrepancies between the master and slave systems.

iii) Three sequences are then transmitted at 75 baud to the slave station. These sequences need not carry any information.

iv) At the slave site, the processor is in the 'listen' phase, and inputs data at four times the bit-rate into a matched filter which has been 'stretched' by a factor of four in order to allow for the oversampling. Oversampling is necessary to alleviate the need for a clock-synchronisation section within the data stream, which may alter the correlation characteristics of the robust sequences being received.

v) Analysis is performed on the incoming data, to give the channel a figure of merit (see Section 4.2). This figure of merit is then scaled to give a level of between 0 and 7.

vi) During the 'transmit' phase at the slave site, the 3 sequences are encoded to give the figure of merit calculated during the 'listen' phase.

vii) The master site receives these sequences, and compiles a table indicating the ranking order of the channels scanned.

viii) This process is repeated until all the channels have been scanned. The system is then able to commence data transfer between master and slave sites on the best channel(s) found.

The main disadvantage of this method is that all of the available channels are scanned prior to the normal operation of the communications link. Thus when a large number of channels are available, the scanning time becomes appreciable and may require the use of off-line propagation predictions to set the lower and upper frequencey limits in which to scan. However, the advantage of using this method is that it has a fall-back channel in case the initial channel becomes unavailable.

An alternative method of system initialisation will now be discussed.

6.2 Initialisation On the First Available Channel.

This method operates by utilising the first available channels in each direction on which to commence normal data transfer. The format used is shown in Figure 9. It is similar to the previously described format, however the 'transmit' phase uses 4 instead of 3 sequences. The use of 4 sequences enables up to 16 levels of information to be conveyed. The sequences are used to indicate whether propagation between master and slave sites exists on the channel being scanned. The scanning time per channel is identical to that taken for the other protocol. The flow of operation using this protocol is depicted in Figure 10, and is now described.

i) Initially both the transmitter and receiver channels at both sites are set to channel 1.

ii) The master station sends out 'null' channel information to the slave during its 'transmit' phase. This represents a call set-up message to the slave.

iii) The slave site attempts to analyse any incoming data in a similar fashion to that described in Section 4.2. Assume for this example that the slave does not obtain a satisfactory result.

iv) As the call has not been received, the slave does not respond to the master during its 'transmit' phase.

v) The channel for both transmitter and receiver at both sites is incremented, and the master station calls the slave station once more on the new channel.

v) Assume that the slave station evaluates this channel and finds it to be satisfactory, based on the results obtained during its 'listen' phase. It now responds to the master by transmitting back 'channel 2' as a means of confirmation. The slave receiver now stays on channel 2 until it receives a confirmation of its response from the master.

vi) The master now increments its transmitter and receiver channels (likewise for the slave station's transmitter). If the master has not received the response from the slave, it continues to transmit a 'null' channel.

vii) During the master station's 'listen' phase, it detects the slave station transmitting 'channel 2'. The master station will now transmit its next block on channel 2. It must also inform the slave station on which channel it heard the slave's response. This is achieved by transmitting 'channel 3' (in the example shown) instead of the 'null' channel during it's 'transmit' phase.

Once the slave station has received this acknowledgement, then the system may begin

to operate in it's normal data transfer mode, since both sites will now know on which channel(s) satisfactory communications are possible.

The main disadvantage of this method is that neither site has a fall-back channel in case the initial channel becomes unavailable. However, since normal system operation will commence after the initialisation phase, this is not considered to be a problem, since during normal operation evaluation of alternative channels takes place.

7 Concluding Remarks

This paper has discussed methods of real-time channel evaluation to be employed in a previously described automatic HF system. The emphasis on the overall system has been to provide a simple and cheap means of utilising the HF spectrum, to provide a relatively reliable means of data transfer betwween two sites. Protocols to enable system initialisation have been discussed, and these reflect the non-optimum nature of the system configuration, i.e. simple antennas, a limited channel allocation and low radiated powers. Utilising these protocols would enable such a system to be used in a variety of situations.

Testing of the protocols described is to take place in the near future and it is hoped to detail results of these trials at the meeting.

APPENDIX A

1.1 Error Control Coding Using Matrices

In order to fully understand the principle of error-control coding using matrices, a description of the process using the code's polynomial will be given.

For any given error-control coding scheme, there exists a polynomial g(x), known as the generator polynomial. In order to produce a codeword, c(x) of an (n,k) cyclic code from a message word, m(x) it is necessary to evaluate the following equation:

$$c(x) = x^{(n-k)}.m(x) \ , \ p(x) \qquad (A.1)$$

The above describes the concatenation of the original message shifted up by (n-k) places, and the parity bits. The parity bits are formed by:

$$p(x) = \text{rem} \ [\ x^{(n-k)}.m(x) \ / \ g(x) \ ] \qquad (A.2)$$

where rem is the remainder resulting from the division.

The first bit output to the channel is the most-significant bit of the message.

Upon reception at the decoder, a similar operation takes place in order to form the syndrome, s(x).

$$s(x) = \text{rem} \ [\ c(x) \ / \ g(x) \ ] \qquad (A.3)$$

It can easily be seen by examining A.2 and A.3 that if the codeword is received error-free, then the syndrome, s(x) is evaluated to be zero. In cases when the syndrome is found to be non-zero, then a detectable error-pattern has been added to the codeword, and the syndrome may be used to find the most likely error-pattern added; this may then be used to correct the erroneous word. However, if the error-pattern is of a greater weight than the error-control code can detect, then the syndrome may also be evaluated to be zero, implying to the decoder that an error-free codeword has been received, resulting in an error to the user.

A similar principle applies to error-control coding using matrices. For a given code, there exists an (n,k) matrix, G which descibes the generator polynomial. This matrix is formed as:

$$G = [\ I \ P \ ] \qquad (A.4)$$

where, I is the k bit identity matrix, and P is the parity matrix for the code. The matrix may be generated using several methods. One method is to apply each identity matrix word to the generator polynomial and use the reults to form the matrix. Another method is to generate a subset of the total number of matrix elements and produce the others by shifting and adding these elements.

The codeword, C which exists for a message, M may be formed by the matrix muliplication:

$$C = M \ G \qquad (A.5)$$

At the decoder the syndrome, S is again calculated by another matrix operation:

$$S = R \ H^T \qquad (A.6)$$

where, R is the received codeword, and H^T is the parity-check matrix transposed:

$$H = [\ P^T\ I\ ] \qquad (A.7)$$

The syndrome is used, as in the polynomial method to correct errors occurring during transmission over a noisy channel. Since an error-pattern is calculated with which to correct erroneous words, then the decoder can inform the user of the average bits in error per codeword. Matrix operations have been used for the implementation of the coding system since is is relatively straight forward to perform in software. Also a change in the coding scheme only requires a change in the generator matrix.

REFERENCES

[1] Barker R H, 1953, 'Group synchronising of binary digital signals', Communication Theory, Butterworth, London, pp 273-287

[2] Hague J, 1987, 'Improved coding and control of HF systems in a non-Gaussian noise environment', AGARD Conference No. 420, 'Effects of Electromagnetic Noise and Interference on Military Radio Communication Systems', Lisbon

[3] Hague J, Jowett A P, Darnell M, 1988, 'Adaptive control and channel encoding in an automatic HF communication system', IEE Conf. Proc. No. 284, 'HF Radio Systems and Techniques', London

[4] Hellen P, 1985, 'The provision of computer quality data transmission on HF', IEE Conf. Proc. No. 245, 'HF Communication Systems and Techniques', London

[5] Goodman R M F, and Farrell P G, 1975, 'Data transmission with variable-redundancy error control over a high-frequency channel', Proc. IEE, Vol. 122, No. 2, February

ACKNOWLEDGEMENTS

The author would like to thank the Science and Engineering Research Council for funding the above research.

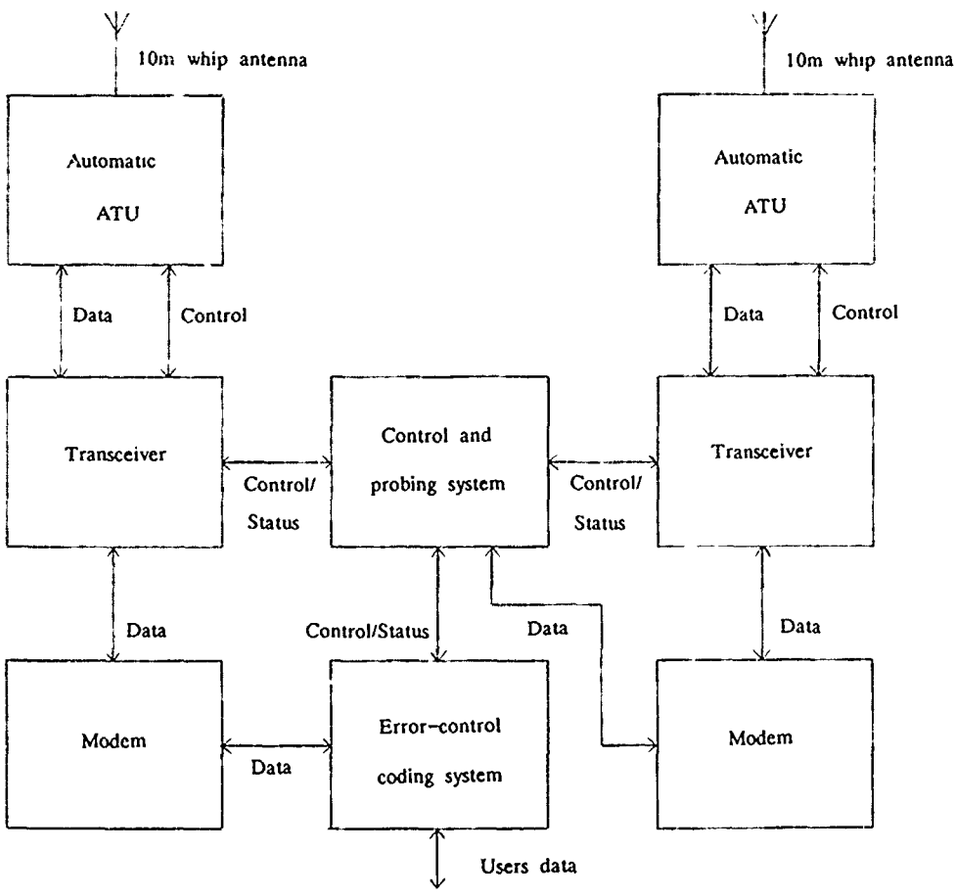

Figure 1 Block diagram of automatic HF system

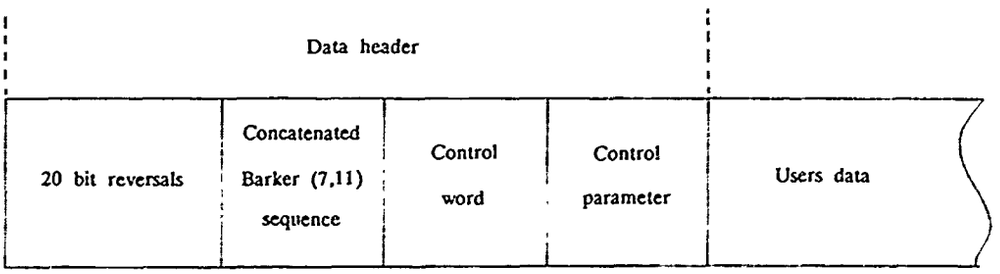

Figure 2 Format of data header

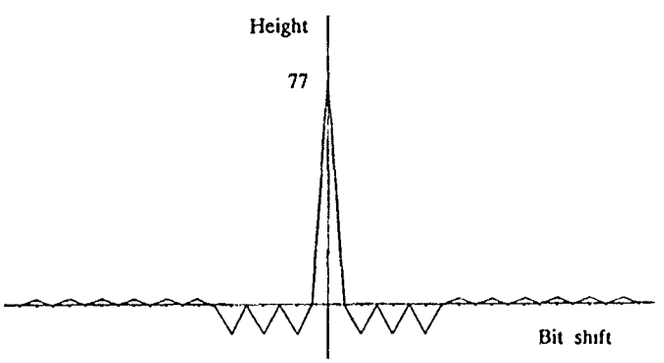

Figure 3 Autocorrelation of a concatenated Barker (7,11) sequence

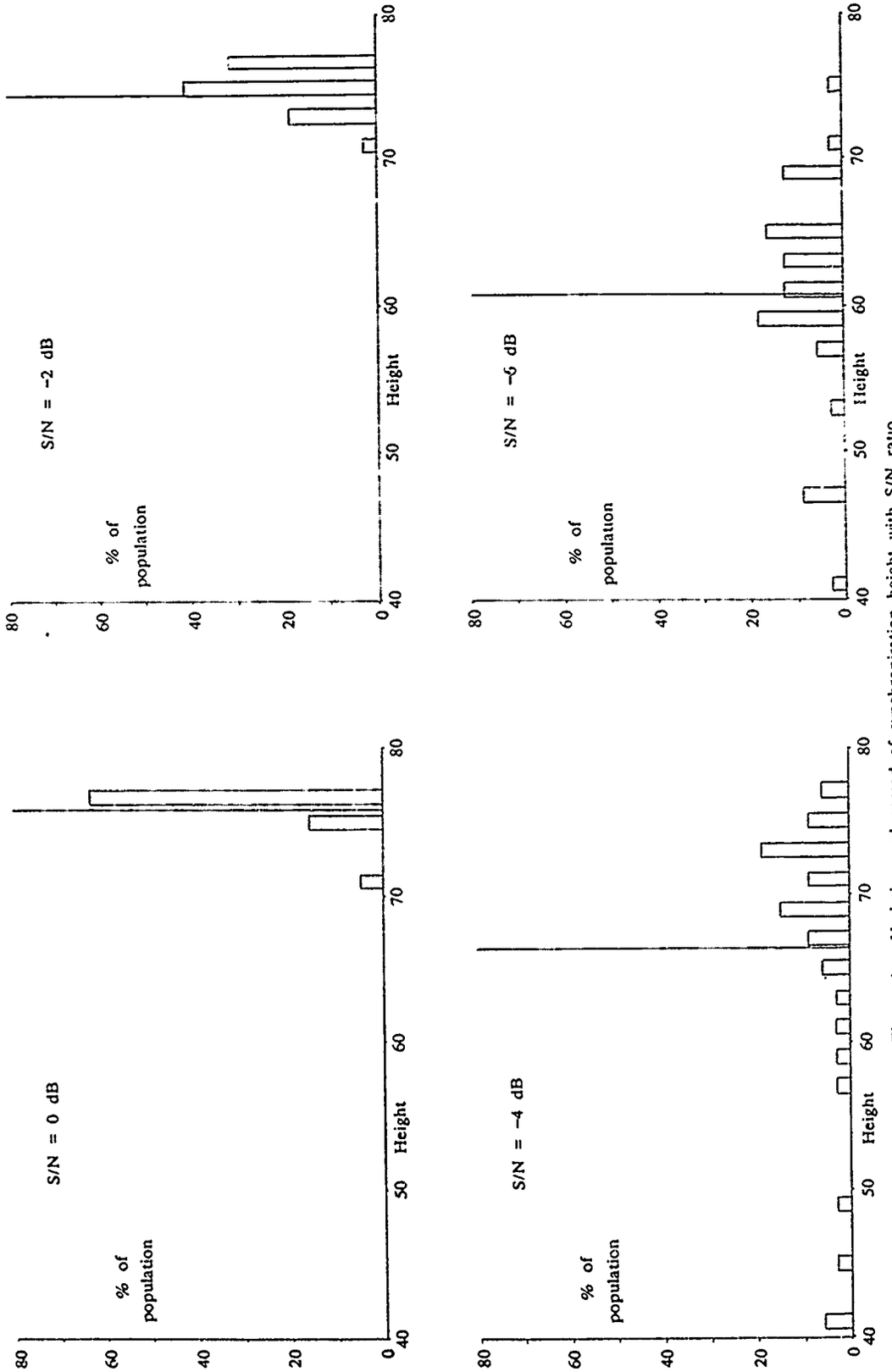

Figure 4 Variation and spread of synchronisation height with S/N ratio

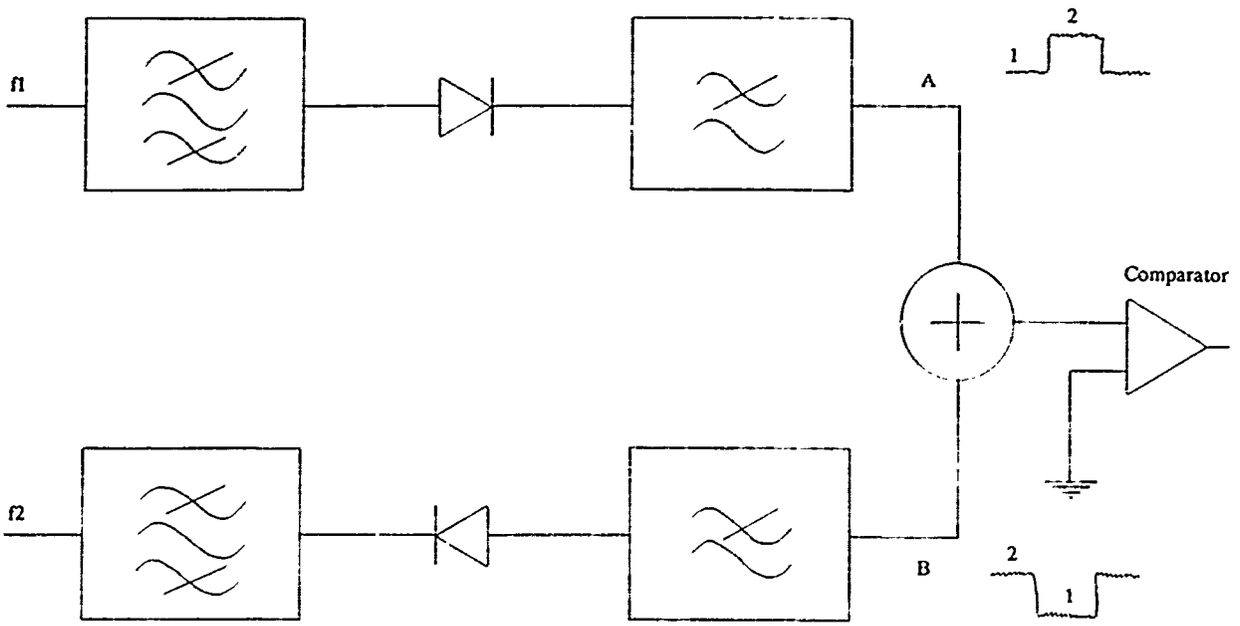

Figure 5 Extraction of S/N ratio from the FSK demodulator

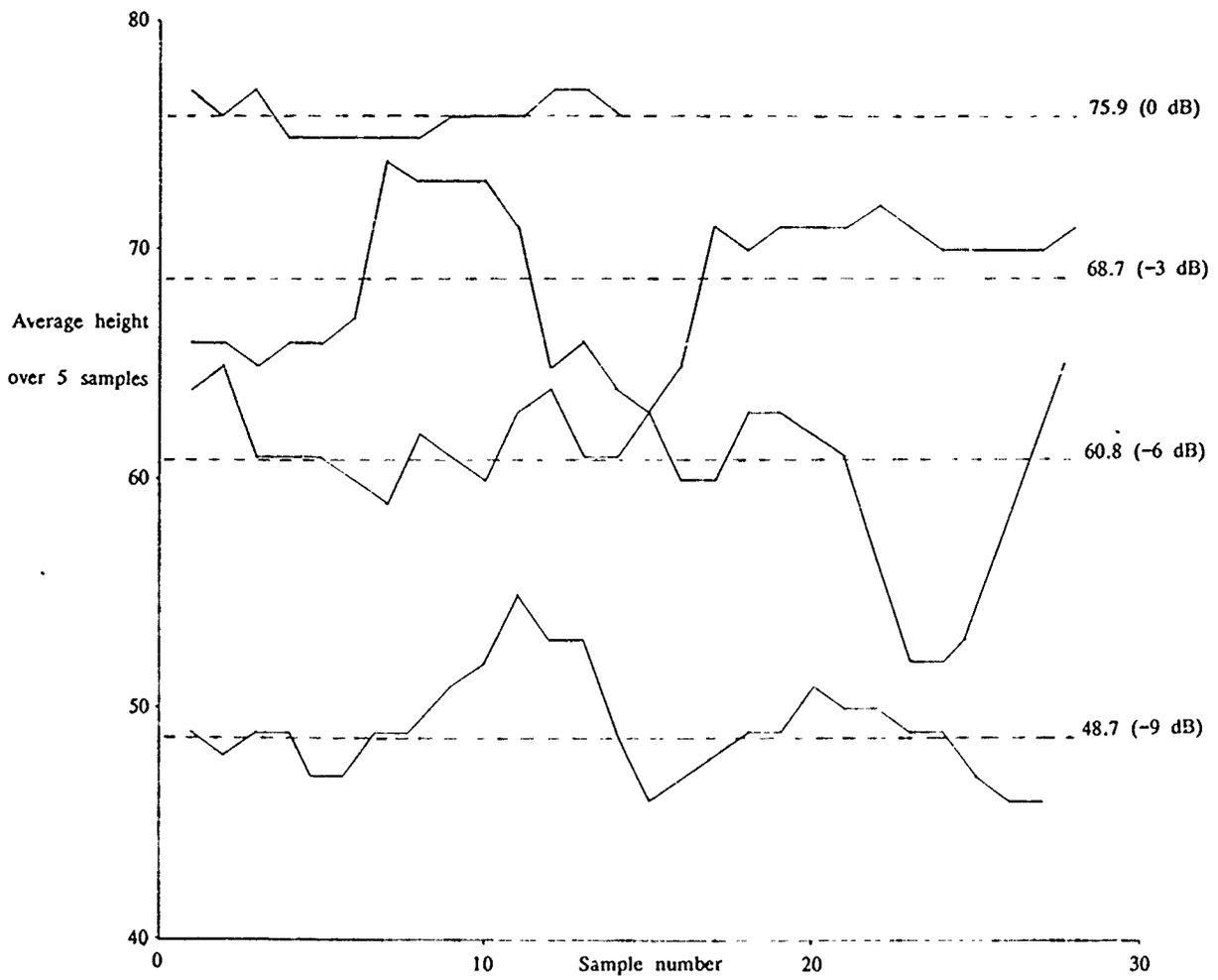

Figure 6 Average Barker (7,11) synchronisation height for decreasing S/N ratio

(population average indicated by a dotted line)

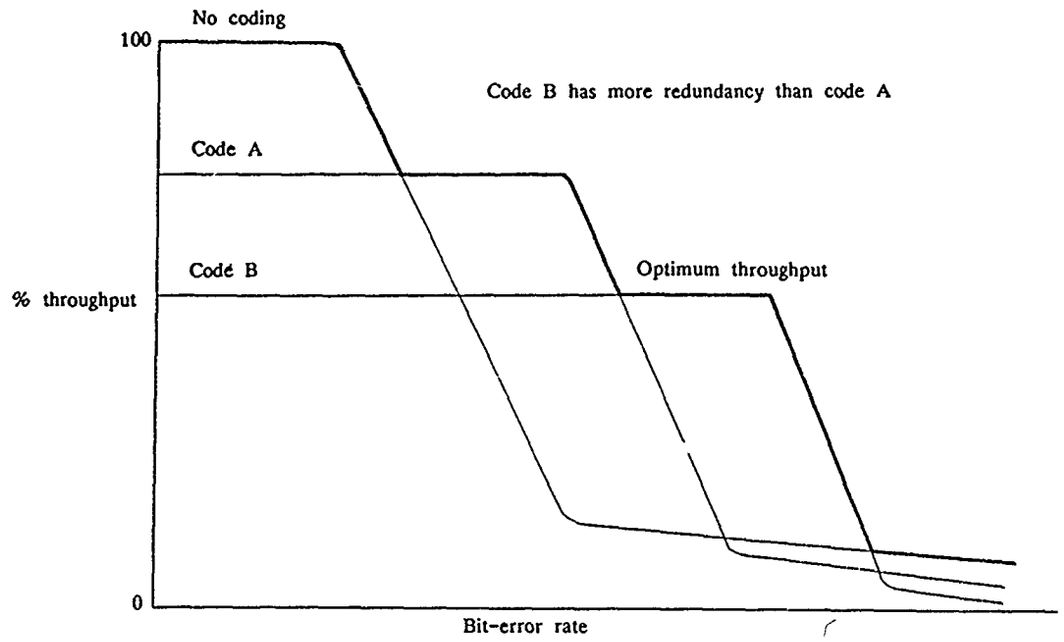

Figure 7 Use of variable-redundancy coding to optimise throughput

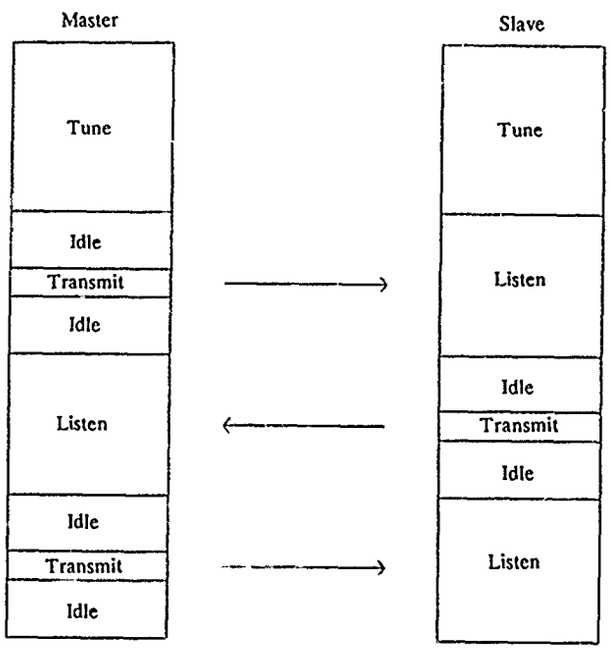

Figure 8 A protocol for automatic call set-up

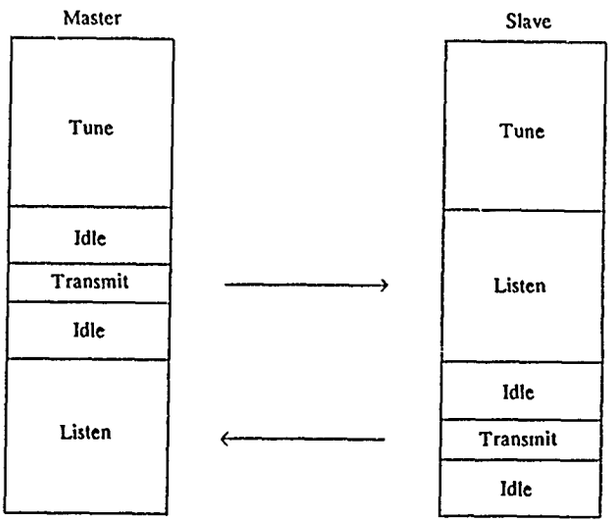

Figure 9 An alternative protocol for automatic call set-up

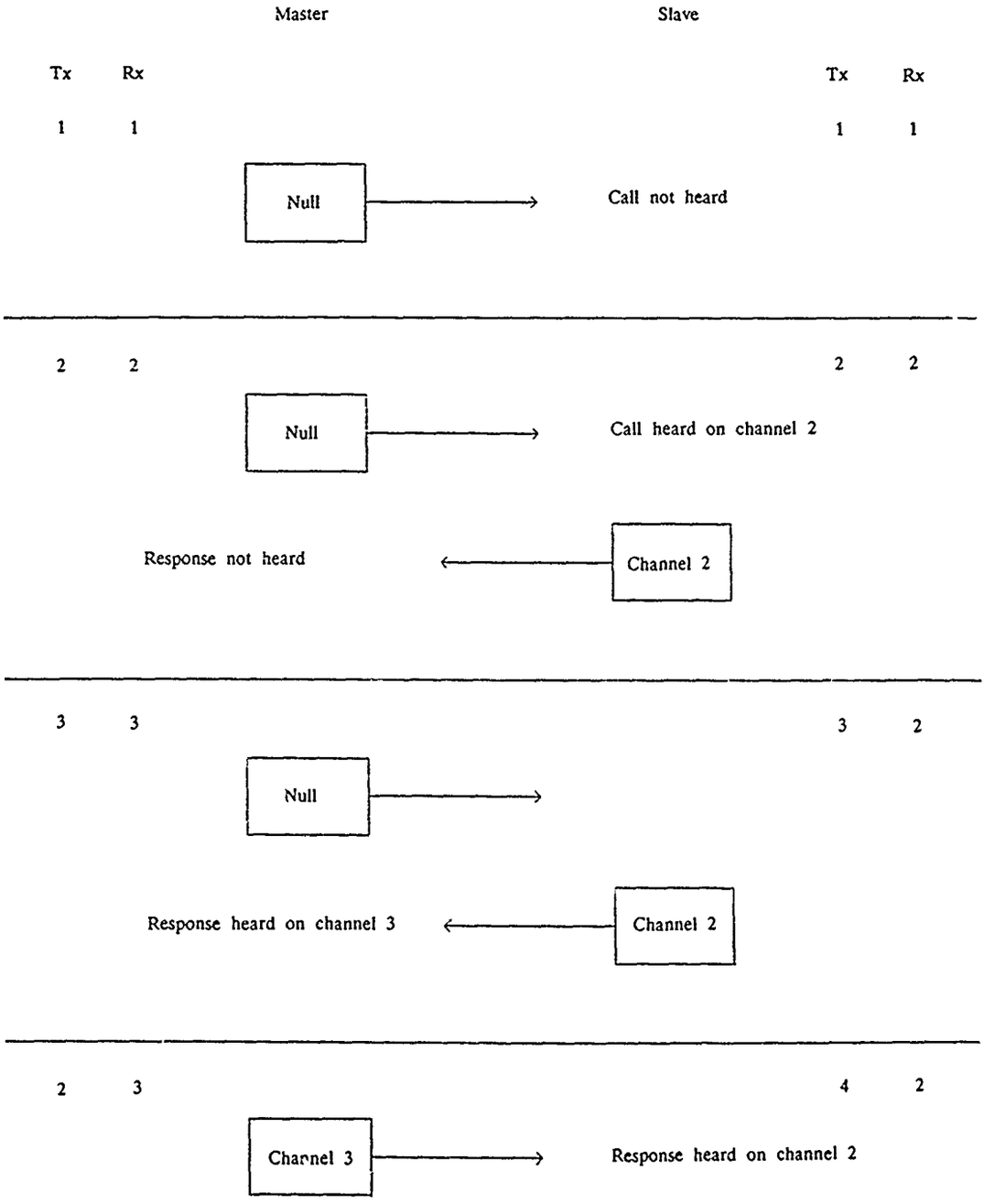

Figure 10 Flow of operations for an automatic call set-up protocol

DISCUSSION

C. GOUTELARD

Ma question comprend 2 parties :

1 - Dans votre figure 7 les axes ne sont pas gradués. Pourriez-vous préciser les points d'intersection des courbes et comment vous faites vos choix.

2 - Dans les planches qui montrent la diminution de la valeur maximum de la fonction d'autocorrélation vous ne tenez pas compte des trajets multiples qui existent la plupart du temps dans le canal HF. Dans ce cas l'altération de la fonction de corrélation est importante et vous n'avez pas toujours une décroissance monotone de la courbe de probabilité d'erreur.

AUTHOR'S REPLY

1 - Figure 7 is meant to show the technique of variable-redundancy coding and therefore the exact points of intersection and the labelling of the axes are not indicated.

2 - Concerning the use of the autocorrelation height as a method of RTCE, multipath components may not be derived using the described method, since the baud rate is 75 bits per second, which would only allow a resolution of $\simeq$ 13ms. This is not compatible with multipath delays on HF of $\simeq$ 2-4ms.

K.S. KHO

The various coding scheme in figure 7 is a dynamic scheme, I expect.
Could you give some more detailed information about the coding synchronization procedures ?

AUTHOR'S REPLY

The coding system incorporated within the overall system design is dynamic in nature. Selection of a particular degree of redundancy is made by analysing RTCE data both on current and alternative channels.
Coding synchronisation is in the form of a Barker concatenated (7.11) sequence. Both ends of a link are informed of the coding scheme in use by means of a robust data header (see "Effects of Electromagnetic Noise and Interference in performance of military Radio Communication Systems" - AGARD CPP 420, Lisbon 1987).

AN EXPERIMENTAL MEDIUM SPEED WIDEBAND MODEM

by
Alastair N Brydon and Geoffrey F Gott
Department of Electrical
Engineering and Electronics
UMIST
PO Box 88
Manchester
M60 1QD
England

SUMMARY

This paper describes an experimental high frequency (HF) modem which uses chirp signals swept across a voice channel bandwidth. The modem is able to adaptively excise interference from other HF users, and has inherent tolerance to frequency selective fading and additive white Gaussian noise. A number of experimental chirp signal formats have been incorporated so as to achieve data transmission at rates of 75, 150, 300 and 600 bits per second, and error correction via interleaved Golay (23,12,3) code is included. The paper outlines the principles behind the experimental formats, and indicates how they performed during 156 hours of tests over a 125km HF sky-wave link.

1 INTRODUCTION

Reliable digital communication in the HF environment requires a modem with tolerance to frequency selective fading, atmospheric noise, and interference from other users. One approach is to employ wideband signals to convey the data.

Wideband signals have an advantage over narrowband signals in frequency selective fading, but are more likely to encounter interference within their wider bandwidths. Figure 1 illustrates a demodulator which is able to identify and remove such interference by adaptive filtering of the received signal. The adaptive filter is essentially a bandpass filter which can be configured to selectively reject parts of the signal spectrum. An interference assessor continuously monitors the signal level across the bandwidth, and should the interference level in any region rise above a given threshold, the adaptive filter is reconfigured to reject all frequency components lying in that region. Although useful signal components are also lost, the elimination of large interferers from the data decision process is advantageous. The process is demonstrated by figure 2, where notches are inserted into the passband of the adaptive filter in areas where interference is severe.

The experimental modem to be described applies adaptive filtering. Data are conveyed by chirp signals which sweep linearly over a 2.7kHz bandwidth. This frequency sweep corresponds to a voice channel bandwidth, and hence the signals are compatible with existing voice communications equipment. The aim of the work has been to investigate ways of achieving medium data rates - up to 600 bits per second (bps) - using serially transmitted chirp signals.

2 BACKGROUND

2.1 The chirp signal

Detailed analyses of chirp and related signals have been published previously (1). Briefly, a chirp signal existing in the period $-T/2<t<T/2$ can be defined by

$$f(t) = \cos(\omega_0 t + \pi F t^2/T)$$

where ω_0 = centre radian frequency (rads/s)
F = frequency sweep (Hz)
T = chirp duration (s)

An important parameter of the chirp signal, affecting a number of its properties, is its FT product - otherwise known as its dispersion factor.

In particular, if $FT>>1$,

(i) Nearly all the signal energy lies within the bounds of the frequency sweep, and it is distributed uniformly within that region. Figure 3 illustrates a chirp signal and its approximate spectrum.

(ii) Chirp signals which ascend in frequency are approximately orthogonal to chirp signals which descend in frequency.

If a chirp signal is passed through a unity gain matched filter (i.e. a filter whose impulse response is proportional to the time reverse of the signal), then the output is given approximately by

$$g(t) = \sqrt{FT}(\sin(\pi Ft)/\pi Ft)\cos(\omega_0 t)$$

This signal has a (sin x)/x envelope and a peak value of $\sqrt{FT}$. 90% of its energy lies within the central lobe of the envelope, which has a duration of 2/F.

2.2 DPSK chirp

Gott and Karia proposed differential phase shift keying (DPSK) as an efficient chirp modulation scheme (2). Figure 4 illustrates the binary case. A relative phase of 0 between successive chirp signals represents a binary 1, while a relative phase of π represents a 0.

Figure 5 is the block diagram of a detector and figure 6 shows the associated waveforms. The matched filter compresses the chirp signals, increasing their peak value. This provides processing gain, without which the performance of the system would be inferior to a narrowband DPSK system. The differential phase information is extracted by multiplying each compressed chirp signal with a delayed version of the previous one. At this stage a positive pulse represents a binary 1 and a negative pulse represents a 0. The integrator accumulates the energy of each pulse over a short period around the peak and its output polarity then indicates the data.

Under multipath conditions, each signal path yields a discrete pulse at the output of the matched filter and multiplier. By widening the integration window it becomes possible to capture each of these, at the expense of white noise performance (2). The choice of integration period becomes a compromise between a wide window, which captures all multipath components, and a narrow window, which minimises the degradation caused by additional noise entering the integration process.

2.3 Adaptive filtering

Sepehri built and tested a DPSK chirp modem which included adaptive excision (3). The adaptive filter unit comprised 15 adjacent Tchebyshev bandpass filters across the chirp signal bandwidth. During breaks in signal transmission the signal level at the output of each filter was measured. Those contributing high levels of interference were omitted from the composite filter during reception of the subsequent message. Large ripples in the amplitude/frequency and phase/frequency response of the filter led to severe signal dispersion even in the absence of excision. As a consequence, significant intersymbol interference was introduced at a keying rate of 80 bauds.

Darbyshire used analogue transversal filter circuits to synthesise an adaptive filter with a linear phase/frequency response (4). This largely eliminated the dispersion problem. The chirp bandwidth was treated as 16 contiguous sub-channels each 170Hz wide, any combination of which could be removed to a depth in excess of 50 dB.

A problem with performing interference assessment during breaks in transmission was that changes in interference structure during a message could not be tolerated. Darbyshire used an analogue spectrum analysis technique to analyse the 2.7kHz swept bandwidth with a resolution of 120Hz every 26.6ms. Using a microprocessor to interpret the received signal spectrum it was possible to perform continuous interference assessment and filter updating during message reception.

2.4 Adaptive chirp versus FEK

Darbyshire compared on an HF link an adaptive DPSK chirp modem employing voice bandwidth chirp signals, with a conventional frequency exchange keying (FEK) system. He discovered that adaptive DPSK chirp was superior to FEK at a data rate of 75 bps. Its average performance was better, and it achieved almost continuous useful communication, whilst there were extended periods during which the FEK format failed repeatedly.

3 INCREASING THE DATA RATE

There are two solutions to the problem of increasing the data rate of a serial DPSK chirp modem. The first is to increase the number of phase states. The alternative is to reduce the chirp keying period (while retaining the full frequency sweep).

A reduced keying period can be a problem when operating under multipath propagation conditions. If the multipath delay is of the same order as the keying period, then severe intersymbol interference occurs. Minimum keying periods of around 10ms are typical in HF modems. Figure 7 illustrates a signal format which alleviates the problem. Two independent DPSK chirp sequences are interleaved; one using ascending frequency chirps (denoted forward sweeps), and the other using descending frequency chirps (denoted reverse sweeps). In the composite waveform alternate chirp signals sweep in opposite directions. Figure 8 indicates how the demodulator operates on the received signal. Two independent DPSK chirp detectors are used, one matched to the forward sweeps and the other matched to the reverse sweeps. Since opposite sweeps are approximately orthogonal, each matched filter compresses its matched signals, but

disperses the orthogonal signals to a low level, as shown in figure 9. If the dispersion factor is large, the orthogonal chirp signals have little effect on the data decision. As a result of this processing, the effective keying rate in each detector is half the transmitted chirp signal rate.

4 THE EXPERIMENTAL SYSTEM

The experimental modem combines the features discussed above so as to achieve data transmission at rates of 75, 150, 300 or 600 bps. In all cases DPSK modulation of chirp signals swept across 2.7kHz is employed and adaptive filtering is applied. Table 1 describes the 8 signal variations included in the modem.

Note: At 75 bauds, keying period = 13.3ms
dispersion factor = 36
At 150 bauds, keying period = 6.7ms
dispersion factor = 18
At 300 bauds, keying period = 3.3ms
dispersion factor = 9

Format 1 (FB75) is identical to that used by Darbyshire (4). With format 8 (AQ300), the combination of quaternary DPSK and alternating chirp sweeps gives an effective serial rate of 150 bauds at the decision point of each detector, for a data rate of 600 bps.

Interference assessment is achieved by a spectrum analyser/microprocessor unit based on that used by Darbyshire. The adaptive filter is identical to Darbyshire's (4).

The demodulator includes a microprocessor which performs frame synchronisation, data logging, de-interleaving to a level of 88 bits and Golay (23,12,3) decoding of received data.

5 SYSTEM MEASUREMENTS

5.1 LABORATORY TESTS

The modem was subjected to conventional white noise tests to ensure that the detectors for the individual formats performed equally. Analysis of the performance of DPSK chirp using an integrator is difficult, but measurements compared well with previously published results.

5.2 THE FIELD TRIAL

The modem was tested over an HF radio link between RSRE Malvern in Worcestershire (England) and Jodrell Bank radio astronomy site in Cheshire (England) - a distance of 125km. Tests were performed at a number of 'Fixed and Mobile' frequency allocations in the region of the predicted optimum working frequency (OWF). Typically, a signal power of 3W was fed into a Racal RA1003 Difan wideband antenna at the transmitting site. Reception was via a horizontal active dipole wideband antenna. The system operated day and night under a variety of propagation and interference conditions for a total of 156 hours in the period from 16th June 1988 to 26th June 1988.

The modulator and demodulator were each equipped with a microprocessor provided with accurate timing information derived from the MSF transmission at Rugby. The microprocessors facilitated automatic testing by sequentially selecting each of the 8 signal formats. In each minute the modulator and demodulator were configured to operate with the same format and a single, fixed length message was transmitted. Hence, the modem cycled through each of the experimental formats every 8 minutes.

De-interleaving/Golay error correction was applied to each message, and all results were dumped to a BBC microcomputer for storage and analysis.

Each message comprised:

33 bit frame synchronisation code
2047 bits of information (either pseudo-random sequence or alternate 1s and 0s)

The duration of a complete message ranged from 30s at 75 bps down to 3.25s at 600 bps.

6 RESULTS

The histograms of figures 10 and 11 represent the overall performance of the system during the tests. They indicate the success achieved by each format, with regard to the percentage of messages obtaining synchronisation, and the percentage which were decoded with zero errors by Golay code interleaved to a level of 88.

7 CONCLUSIONS

Darbyshire found that adaptive DPSK chirp was superior to FEK at 75 bps (4). The work reported here compared a number of experimental chirp signal formats in an effort to deduce the best way of achieving higher data rates using this approach. The following points summarise the results of 156 hours of HF tests:

(i) 69% of messages transmitted at 75 bps using format 1 (FB75) were decoded with 0 errors.

(ii) To operate at 150 bps, there is little to choose between using 4-phase DPSK chirp at 75 bauds (FQ75) and 2-phase DPSK chirp at 150 bauds (FB150).

49% of messages transmitted at 150 bps using format 2 (FQ75) were decoded with 0 errors.

(iii) To achieve 300 bps, 4-phase DPSK at 150 bauds (FQ150) is preferable to 2-phase DPSK at 300 bauds (FB300). On average, with 4 phases, the unidirectional chirp sweeps (FQ150) performed better than alternating sweeps (AQ150).

43% of messages transmitted at 300 bps using format 5 (FQ150) were decoded with 0 errors.

(iv) At 600 bps it is essential to use alternate sweeps and 4-phase DPSK at 300 bauds (AQ300).

20% of messages transmitted at 600 bps using format 8 (AQ300) were decoded with 0 errors.

The experimental results suggest that rather than reducing the keying period it is preferable to increase the number of phase states in a DPSK chirp system to achieve greater data rates. However, stringent requirements on the demodulator and the stability of the channel are likely to make 4 phases a practical limit.

At 150 bauds the forward sweep systems were generally superior to the alternate sweep systems. The greater tolerance of the latter to multipath propagation was apparent only occasionally, and did not compensate for their inherently inferior white noise performance.

8 REFERENCES

1 KLAUDER J.R., PRICE A.C., DARLINGTON S. and ALBERSHEIM W.J.: 'The Theory and Design of Chirp Radars', Bell System Technical Journal, Vol.39, July 1960, pp.745-808

2 GOTT G.F. and KARIA A.J.: 'Differential phase-shift keying applied to chirp data signals', Proc.IEE, Vol.121, No.9, Sept.1974, pp.923-928

3 SEPEHRI M. and GOTT G.F.: 'An Adaptive Chirp Modem', IEE Conference Publication Number 206, '2nd Conference on HF Communication Systems and Techniques', London, February 1982, pp.121-124

4 DARBYSHIRE E.P. and GOTT G.F.: 'Robust data transmission at HF', IERE Conference, 'Radio Receivers and Associated Systems', Bangor, 1986

9 ACKNOWLEDGEMENTS

This work has been financially supported by the UK Ministry of Defence (RSRE), and has been carried out in the Department of Electrical Engineering and Electronics, UMIST. The authors would like to thank Clive Harding, John Spicer and colleagues at RSRE for their assistance with the experimental work. Thanks also to Bob Pritchard and colleagues at Jodrell Bank for the use of their facilities and for their assistance during the field trial.

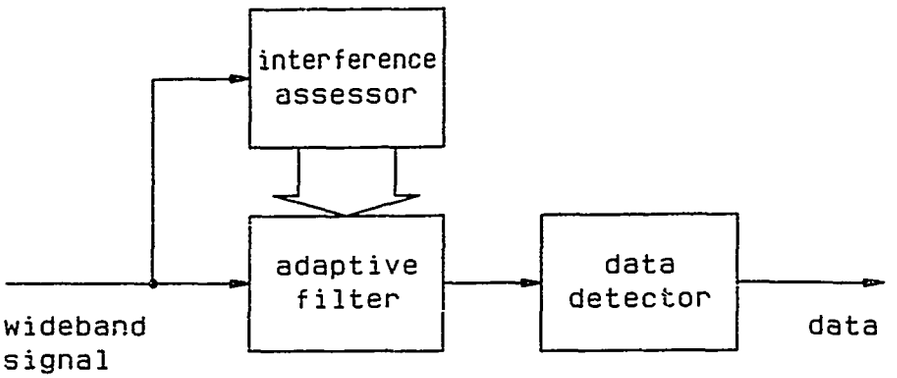

Figure 1

Adaptive demodulator

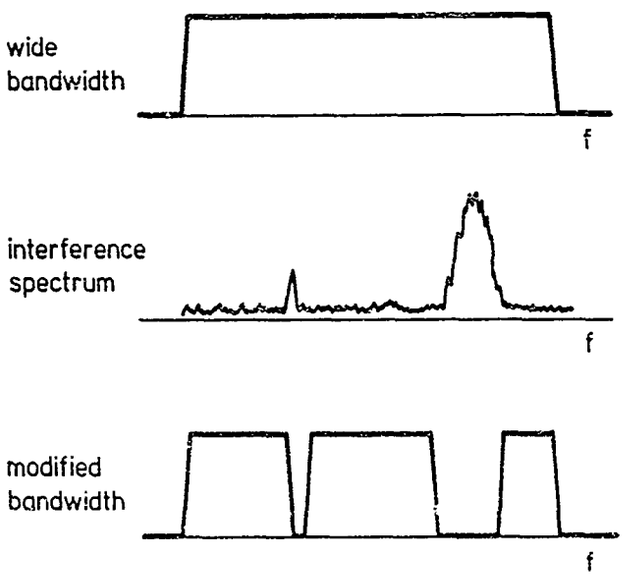

Figure 2

Interference rejection

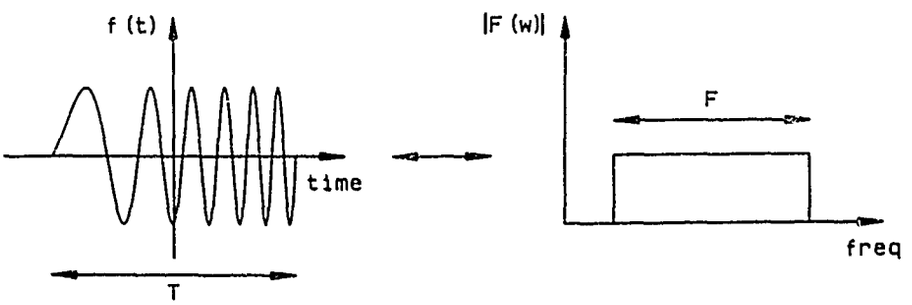

Figure 3

Chirp signal and approximate spectrum

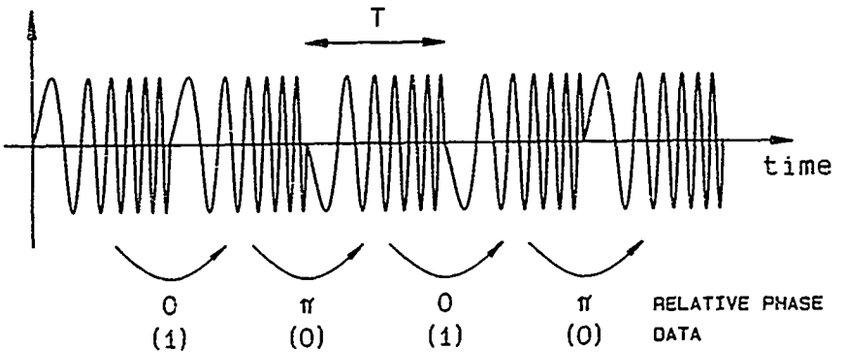

Figure 4

Binary DPSK chirp signal

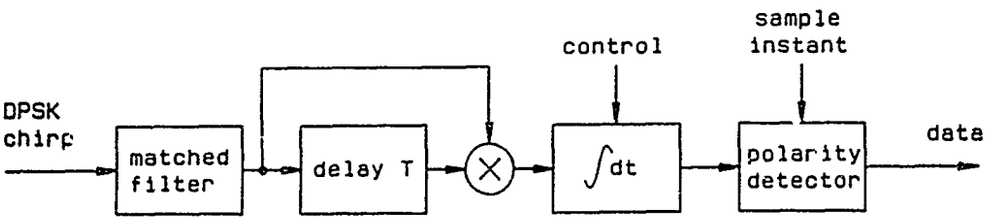

Figure 5

Binary DPSK chirp detector

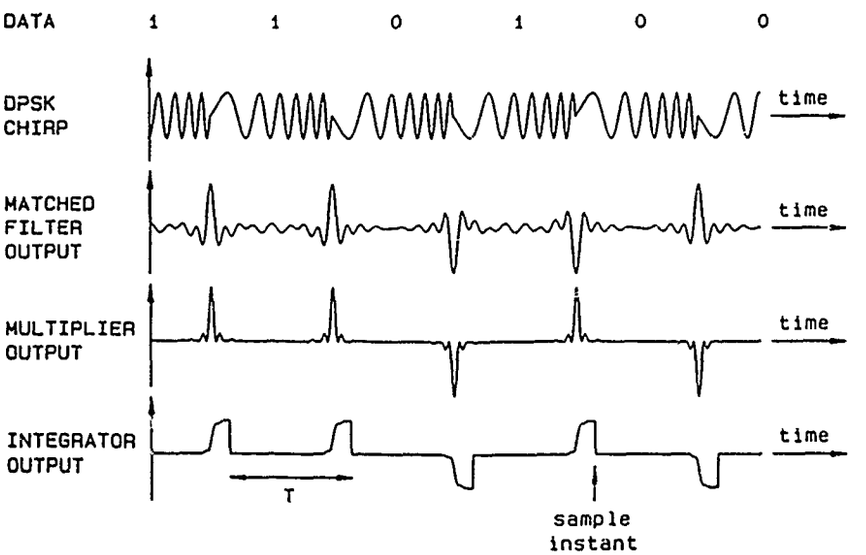

Figure 6

Waveforms produced by binary DPSK chirp detector

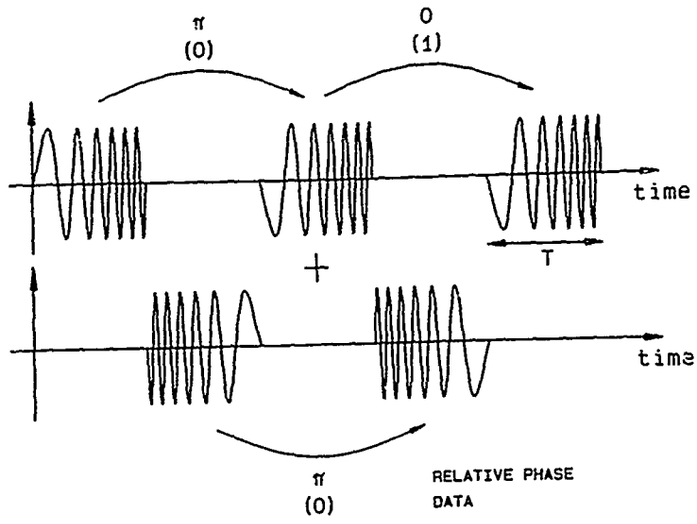

Figure 7

Alternate sweep binary DPSK chirp signal

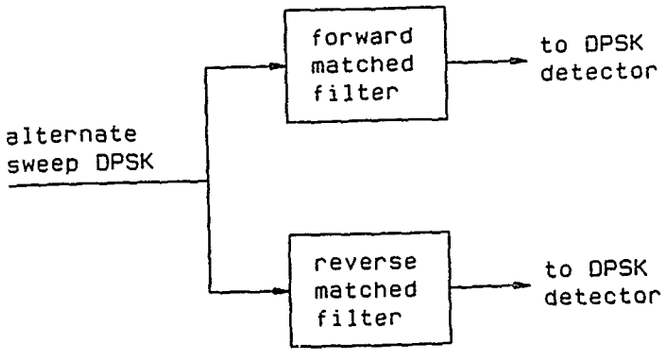

Figure 8

De-interleaving of forward and reverse chirp signals

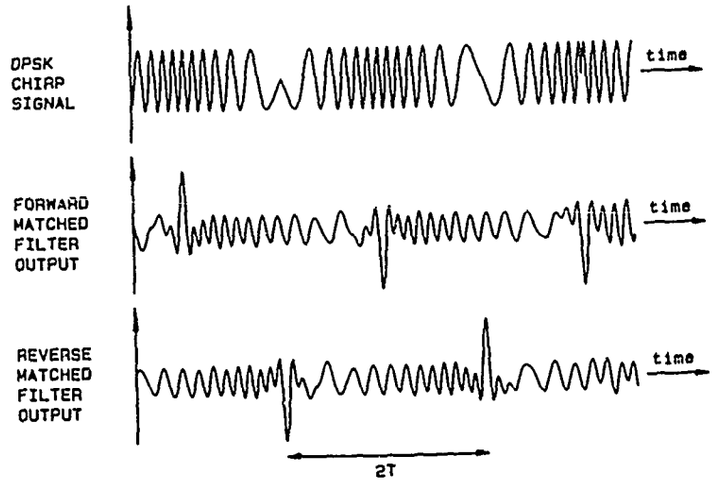

Figure 9

Waveforms produced by alternate sweep detector

Figure 10

Percentage of transmitted messages which synchronised

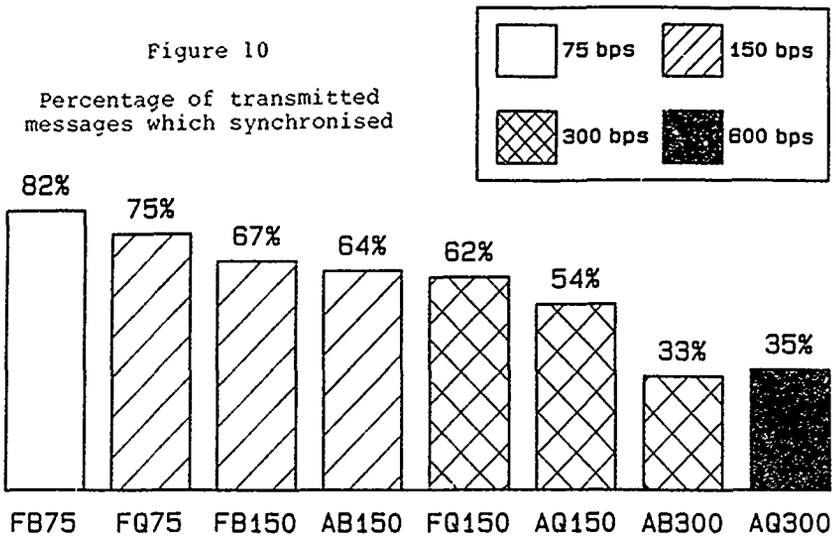

Figure 11

Percentage of transmitted messages which were decoded with zero errors

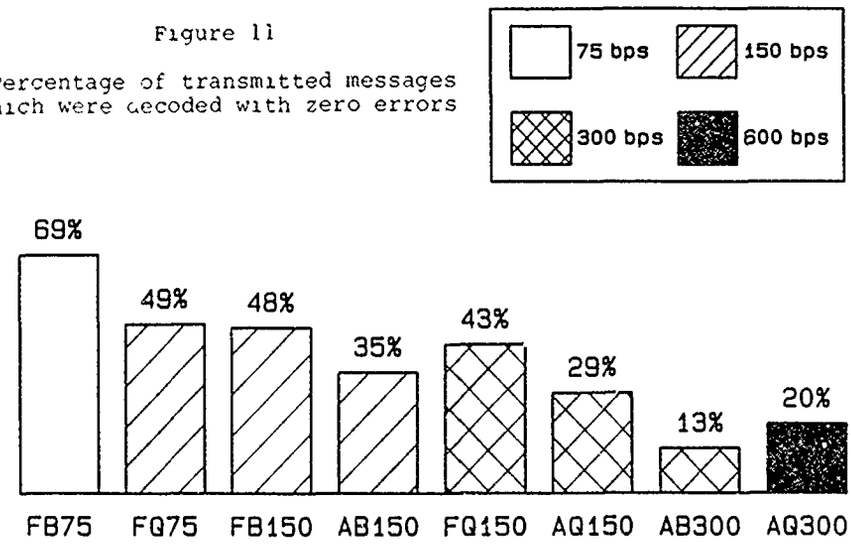

CHIRP MODEM SIGNAL FORMATS				
FORMAT	SWEEPS	DPSK TYPE	KEYING RATE	BIT RATE
1. FB75	Forward	Binary	75 bauds	75 bps
2. FQ75	Forward	Quaternary	75 bauds	
3. FB150	Forward	Binary	150 bauds	150 bps
4. AB150	Alternate	Binary	150 bauds	
5. FQ150	Forward	Quaternary	150 bauds	
6. AQ150	Alternate	Quaternary	150 bauds	300 bps
7. AB300	Alternate	Binary	300 bauds	
8. AQ300	Alternate	Quaternary	300 bauds	600 bps

Table 1

DISCUSSION

C. GOUTELARD

I would like to comment on the interventions of Mr OSSEWAARD and Prof. DARNELL, and to ask a question.

First, when digital modulation is superimposed on the chirp signal sequence the result is the convolution of the spectra. The digital modulating signal is narrow-band (typically 80Hz) and is therefore almost a Dirac impulse - the neutral element of convolution. Thus only the secondary effects which widen the spectrum by twice 80Hz modify the spectrum.

I agree with Prof. DARNELL. Extrapolating, this leads to an optimisation problem. The best compromise between interference rejection and its effect on the output autocorrelation function must be chosen. Have you investigated this problem ?

AUTHOR'S REPLY

As indicated in the reply to Prof. DARNELL's question, computer simulations have been performed in order to investigate the effects of the excision process. In particular, it is important to appreciate that the dispersion of the chirp signal, due to excision, did not cause significant chirp signal energy to fall outside the integration window.

M. DARNELL

1 - Was the interference excision filter in operation during the practical trials described ?

2 - Can you say something about the nature & magnitude of the group delay distortion produced by the filter when excising say multiple narrow band pass signals ? How significant is this ?

3 - In the practical trials, the excision filter might have been configured differently for each data type. In this case, to what extent would this influence the comparative results ?

AUTHOR'S REPLY

1 - Adaptive interference excision was included throughout the field trials.

2 - The effect of excising narrowband sections of the chirp signal spectrum is to disperse the energy of the compressed pulse at the matched filter output. The degree of dispersion is dependent both on the total bandwidth rejected, and also the position of the individual sections. Computer simulations have shown that the dispersion introduced by excision patterns typically necessary for HF interference structures is less than that introduced by multiplath propagation. As a consequence, the integrator in the detector successfully gathers together the dispersed energy of the pulses, such that performance is not adversely affected.

It may be noted that the transversal filters used to achieve interference rejection have a linear phase/frequency response, and hence do not introduce group delay distortion.

3 - Observations of interference within voice bandwidth channels at HF have shown that the interference structures are relatively static (refs. 1, 2, 3). A given interference pattern might exist for hours, and the modem cycled through each of its experimental formats every 8 minutes. Coupled with the 156 hours duration of the tests, it is fair to assume that on the whole the experimental formats experienced similar interference conditions.

References :

1 GOTT G.F. and STANIFORTH M.J.D. : "Characteristics of interfering signals in aeronautical HF voice channels", Proc IEE, Novembre 1978.

2 GOTT G.F., DUTTA S.,and DOANY P. : "An analysis of HF interference with application to digital communications", Proc IEE Part F, August 1983.

3 DARBYSHIRE E.P. and GOTT G.F. : "Robust data transmission at HF", IERE International Conference on 'Radio Receivers and Associated Systems', Bangor, July 1986.

G. OSSEWAARD

The spectrum of the chirp signal was block-shaped. Is this not an idealisation of the real spectrum ? The modulated chirp signal can be considered as a multiplication of the unmodulated chirp and the random binary signal.
In the frequency domain this results in the convolution of the respective signals.

AUTHOR'S REPLY

The spectrum of a chirp signal with bandwidth-duration product much greater than I closely approximates the idealised spectrum illustrated in the paper.

The spectral analysis technique employed in the experimental modem derives each spectrum from a single chirp signal. It is therefore independent of the spectrum of the modulating signal. (See also Prof. GOUTELARD's comment regarding the effect of the modulation).

CORA. A DIRECT SEQUENCE SPREAD SPECTRUM RADIO FOR VOICE AND DATA

by

T Thorvaldsen
Norwegian Defence Research Establishment
Division for Electronics
N-2007 Kjeller, Norway

1. INTRODUCTION

For many years the ordinary FM radio (e g the VRC 12 family) has been the workhorse in military forces throughout the world. This type of radio has some advantages; it is relatively simple and cheap, it has a low power consumption as man-pack and an excellent voice quality. Since the modulation type and details are known by everyone, however, the meassages are easily intercepted and even rebroadcasted in order to fool the enemy. Age is also becoming an important argument for introducing a new radio generation on the market.

2. REQUIREMENTS FOR A NEW RADIO GENERATION

In this paper we are mainly talking about radios operating in the military VHF band 30 - 88 MHz. The requirements for such a radio will of course vary from country to country and the following list contains requirements we at NDRE feel are the most important ones.

a. Resistance to interceptance

This means different things to different people. The most important aspect is that it must be imposssible to tap the information off the transmission for anyone else than those the transmission is intended for. Cryptographic equipment is available for todays radios, but new radios should have such a possibility built into the radio and in addition the modulation format should make it very difficult to listen to the traffic without knowing some kind of key in advance. Interceptance could also mean detection of radiation, location of transmitters and logging of the traffic intensity of certain transmitters. These factors should also be taken into consideration when evaluating the signal format of new radios.

b. Resistance to jamming

The new radio generation should be more resistant to jamming. The importance of various types jammers must be evaluated. Jammers may be broadband and powerful, but stupid, like stand-off barrage jammers, or the may be narrowband and less powerful, but more intelligent like follower jammers capable of measuring frequencies and directing its transmitter to this frequency in a very short time. New radios should offer resistance to the jammer(s) considered most important.

c. Suitability for data applications

Everyone agrees that use of voice to transfer information in military systems is inefficient an unreliable. Standard messages

such as position, own adress, receiver adress, transmitted and received signal power could be transferred much more efficient with the use of data. This decreases the chances of being detected and then again jammed, if we assume that the enemy does not jam until he detects the transmission. Since many messages are very short in nature (like firing commands in weapon control systems), it is important that the radio is efficient for short meassages like for instance 20 byte. More use of data will also lead to a much more efficient use of the available spectrum, which in some places is overcrowded.

d. Suitability for colocation of many radios

Some applications require that radios are installed very close to each other, for instance in the same vehicle, either using antennas very close to each other or sharing the same antenna through some sort of multiplexer. In either case the isolation between the radios that can be obtained is very limited, on the order of 20 dB. This requires that the radios are equipped with suitable filters both in the transmitter chain and in the receiver path so that transmitting from one or more radios on one frequency does not disturb the receiveing radio and restricts the range of that radio on some other frequency. Since received signals can be of the order of -120 dBm and transmitted signals on the order of 47 dBm this puts some very tough requirements both on the receiving and transmitting chain in the radios.

e. Low power consumption

New radios introduced on the market so far definitely consumes more power than a simple FM radio. It seems that the price to pay for new requirements is increased power consumption. We feel that this is an important issue, of course most important for the man-pack version of the radio. Part of the problem can be solved by using other types of batteries e. g. lithium.

f. Low price

New requirements inevitably seems to lead to a higher price on the product. New radios introduced are all more expensive than the simple FM radio. This is serious of course, since it means that less radios can be bought for the same amount of money.

g. Suitable for antenna null-steering

Antenna null-steering is a completely passive means of acheiving jam resistance. If a null-steering system can be constructed cost-effectively, the radio should be prepared to work together with such a system. Remember that if a null-steering system raises the signal-to-noise ratio by 10 dB, this is equivalent to a bandspreading of ten times, and an increase in the range of the radio by a factor of approximately two. So if such a system could be made at a moderate cost, the radio signal format should not prevent the use of it. On the contrary, the radio format should be such that introducing a nullsteering system is made more easily.

3. NEW RADIOS ON THE MARKET

Leading industries of the world have introduced the Frequency Hopper (FH) on the market, mainly as an answer to requirements a and b. We will briefly discuss the frequency hopper in view of the above requirements.

a. It is definitely more difficult to tap the information off an FH system than a fixed frequency FM system. When it comes to the enemy`s ability to detect and locate various transmitters, we feel that little is gained by hopping in the way now implemented. Low Probability of Interceptance (LPI) requires low output power for a given bandwidth, large hop-set, short messages and low hop-rate. The hoppers on the market for VHF today do not have these characteristics.

b. The number of frequencies in the hop-set is often quoted as the so called Processing Gain (PG) of the frequency hopper. This is very misleading indeed. Let us define processing gain for the hopper as the number of frequencies necessary to jam in order to acheive a certain (bad) quality on the link between the hoppers. If the hop-set is 1000 and the data-rate 16 kb/s (this data rate is standard for all the hoppers on the market) we still need only jam one single of these frequencies in order to achieve a BER of 10-3 on that channel. The PG is therefore in this case 0 dB. Voice can with-stand a higher BER. Typically, the number of blocked channels tolerated is 25%, which leads to a PG of 250 (24 dB). We therefore see that the PG of the hopping system is heavily dependent on the mode of the frequency hopper. We also see that an FH channel with 16 kb/s data rate is virtually impossible with quality requirements necessary for data transmission. The 16 kb/s data stream will have to be coded. Then again, the PG for the system will depend on the type of code to be used and can not be stated generally from the number of frequencies in the hop-set.

   The PG experienced in a typical scenario will vary according to how many nets are on the air at the same time. In a crowded situation the jammer will not have to be turned on at all. The hopping nets will jam themselves. Let us try to illustrate this situation in a figure, see fig 1. This is valid for voice, which we assume tolerates 25 % blocked channels. We assume that the available spectrum for the hoppers is 256 x 25 kHz. (We feel very strongly that when the hoppers are fielded, they will not be allowed to use a very large percent of the available spectrum). Let us now assume that we start to introduce FH nets in this bandwidth. The goal of the jammer is to jam all nets, and the vertical scale indicates how many frequencies he has to jam in order to acheive this goal. (This equals the number of times he has to increase the power from his transmitter source). The first nets on the air are easily jammed by a follower jammer. The jam resistance according to the above definition is therefore 1 (0 dB). When the follower jammer no longer is able to operate satisfactorly, the jammer must resort to tone-jamming over as many frequencies as necessary. The PG rises sharply to 64, and with these frequencies the jammer is able to jam all nets on the air in

this frequency range. As the number of nets exceeds approximately 64, self-jam starts to become important, and the jammer does not have to transmit on 64 frequencies any longer.

When approximately 128 nets are on the air, the jammer is not needed any longer. Here, we have excluded the possibility for the different nets to apply orthogonal hopping.

Let us compare this to what happens when the same radio is used as a fixed frequency radio, each net introduced being allocated to a new 25 kHz slot. The jammers goal is still to jam all nets in the band. (He is not able to sort out the important ones). The jam resistance of the total system of radios is now increasing linearly as the number of nets increases. We see that the "Processing Gain" is passing the FH system as the number of nets exceeds approximately 64. We feel that the lesson to be learned from this is that very little is to be gained by hopping as long as many nets are on the air simultanously and the enemy must jam all nets in order to be sure to acheive his goal.

Finally, hopping around with the center frequency of a system does not increase the resistance to barrage jammers. Take as an example a 10 kW jammer 50 km away located in an aircraft. The advantage of putting the jammer in an aircraft is tremendous when it comes to propagation which then becomes approximately free space. The jamming input power to each radio could be on the order of -60 to -70 dBm, which is enough to wipe out any communication system in the whole VHF band but the most short ranged and powerful ones. The FH radio does not offer any increased performance in such a scenario.

c. Frequency hoppers were introduced on the market as voice radios with increased resistance to interceptance and jamming. The basic data rate is slightly more than 16 kb/s to support delta modulated voice. We have already seen that it is hopeless to achieve a high quality 16 kb/s data link with a frequency hopper. The data have to be coded in order to tolerate blocked channels. Reasonable tolerance to blocked channels can be achieved at data rates on the order of 1.2 kb/s. The high rate coder implemented to do this is very inefficient in white noise applications leading to relatively poor range capabilities when the noise is evenly spread over the spectrum as is the case when a barrage jammer is operating or no interfering signals are operating at all.

The efficiency for short data messages is very poor due to long synchronization preambles and the coding and interleaving nescessary to tolerate blocked channels. The shortest possible message length for some frequency hoppers is around 0.5 second. It is therefore impossible to use frequency hoppers in packet radio networks which use short message formats.

Since the coding used can tolerate only a certain amount of blocked channels at a certain data rate and quality of channel, the throughput offered by a certain bandwidth, say 256 x 25 kHz channels, will start to decrease when the density of nets reaches a certain level. This is illustrated in figure 2. As we start to introduce nets in the given bandwidth, the

total throughput increases linearly. If we exclude the possibility of using orthogonal hopping, these nets will start to interfere with each other and the throughput will decrease. If the radios were Fixed Frequency (FF) however, this will not happen if we assume a good frequency planning, and the throughput will increase linearly.

d. Colocating Frequency Hoppers is not an easy task. It is impossible to plan the frequency allocation to avoid direct hits and spurious responses in transmitter and receiver. The solution offered is most often to confine one hopping net in one band separated by a guard band from the next hopping band. The separation must be on the order of 5 MHz or more. Doing this is the same as breaking a very important principle for frequency hoppers: the frequencies should be selected totally random over as large a bandwidth as possible. The band allocation principle makes it easier for an enemy to sort the traffic and then jam the important nets.

e. The frequency hoppers on the market definitely burn more power than the ordinary FM radios. Whether a new type, new radio generation can be constructed having a power consumption comparable to the FM radios remains to be seen.

f. The price for new radios will be higher, if these radios meet the new requirements to some extent.

g. Antenna null-steering has been a subject of discussion for a long time. Hardware has been introduced on the market by various companies. It is no doubt that such a system can increase the Signal to Noise Ratio by a large amount in certain scenarios. However, the time to establish a null in a given direction will be considerable compared to the time on one frequency for frequency hoppers and also some method for not nulling friendly signals must exist. These circumstances both tend to make it difficult for the FH system to implement Antenna Nulling systems.

4. DESCRIPTION OF THE CORA RADIO

In this chapter we describe the CORA radio developed at NDRE, Norway. This development started in 1986. The objective was to develop a radio suitable for both voice and data, especially packet data. The development has resulted in one transmitter and one receiver, which has been tested by the Norwegian Army in June 1988. The radio is one of the competitors when the Norwegian Army shall decide what radio will be the next radio generation to replace the VRC 12 family now in use.

CORA is a Direct Sequence Spread Spectrum (DSSS or DS) radio utilizing orthogonal coding. For a reminder of the DS principle, we refer to figure 3, which shows a series of data bits (010) each coded with a 7 bit (chip) Pseudo Random code. The conventional DS system represent each data bit with a code according to the modulation principle, which may be Differential Phase Shift Keying (DPSK). If the number of code bits is L, the bandwidth of the system then approximately increases L times, the jam resistance increases L times and the receiver needs a correlator of length L. The correlator may be looked upon as a

coherent integrator and increases the SNR at the output L times. The PG of the system is said to be L, which most often is associated with the increase in bandwidth and not the correlator length which from a physical point of view is the most correct way to look at it.

For a reminder of what orthogonal signaling is, we refer to figure 4. In this example each code transmitted represents two bits of information. As can be seen we then need 4 different codes to represent any data sequence, and the receiver must be able to distinguish between these codes. The advantage with this type of modulation is dramatic. The bit rate may be doubled or the bandwidth of the system may be half the original bandwidth if the bit-rate is constant. If we prefer the last choice, the range of the radio is increased, since the amount of noise in the receiver is half the original noise and the necessary increase in signal power to detect the codes correctly is very small compared to the reduction in noise power. Note that the correlator length is constant. Except for the small loss due to the extra signal power needed to detect codes correctly, this means that the PG against the narrowband jammer being able to concentrate all his power into our bandwidth, is approximately the same. Against a broadband jammer the performance has increased by approximately 3 dB. DS systems are often said to have a Low Probability of Interceptance (LPI) since their output power spectral densities are lower. In a system employing orthogonal coding the spectral density has increased. The thing to remember is that the range for the same output power has also increased. So if we choose to keep the range constant, the LPI performance is approximately the same as before ie given by the correlator length.

The codes used should ideally be perfectly orthogonal, ie the output from the correlator should be zero when the reference code is not the same as the transmitted code. In a practical communication system, the necessary level of the crosscorrelation needs only be some 20 dB down. This means that the number of codes available is more than adequate. The receiver will be slightly more complex in order to search for the codes in the alphabet used, but this is a small price to pay compared to what is gained by reducing the bandwidth of the system. CORA is therefore using orthogonal signalling at a very high level, ie 256-ary for 2.4 kb/s and 128-ary for 16 kb/s.

We now proceed by explaining the CORA dataformat shown in figure 5. To establish chip synchronism, the data are preceeded by a preamble consisting of two long codes. These are correlated in the receiver and the results are incoherently integrated. Synchronism is established therefore in a very short time, less than 10 msek. The synchronizing codes are followed by codes for information to the radio, F codes, giving information about what type of signal is coming, ie 16 kb/s voice or data, 2.4 kb/s data etc. This means that the radio does not have to know in advance what is to be transmitted to it. The information symbols I can be codes of variable length, and the total number of codes in a frame can vary with the application. The frame may be ended with Message End codes if this is necessary.

The CORA main specifications are shown in figure 6. These should

be more or less selfexplaining bearing in mind what have been said about the multilevel orthogonal signalling.

A point that needs comment is perhaps the channel separation. In the VRC 12 family the bandwidth of the radio is approximately 25 kHz and the channel separation is 50 kHz. In CORA we claim that the channel separation and the bandwidth is approximately the same. Here one must bear in mind that we deal with a direct sequence spread spectrum system with processing gain. The tolerable noise power at the input of the receiver from a radio with a different code is at the center frequency more than 10 dB above the correct signal. In terms of channel separation this means that we can define a "new" channel closer to a certain frequency than in conventional systems. The PG is reducing the necessary filtering. (For a high enough PG we could have operated the system as true Code Division Multiple Access (CDMA), and have channel separation 0 Hz!)

Let us now run quickly through the CORA radio block diagram shown in fig 7. We will follow 8 bit of information from the data input to the transmitter to the output of the receiver. When a stream of data is presented to the radio at its input ports the first thing the radio does, is to sort the data in blocks of 8 bits. These 8 bits represent a number between 0 and 255. The code corresponding to this number is then read from a memory and put forward to the MSK modulator which is modulating some intermediate frequency according to the code. Then follows a conventional up-converter with associated filtering and amplification. Extensive filtering is employed to improve colocation performance. The maximum output power in the prototype is 5 watts.

In the receiver chain extensive preselection filtering is used to improve the colocation performance. The radio is a of the double superheterodyne type with linear IF amplifiers. After downconversion to baseband, follows the correlator bank with associated synchronization and demodulation circuitry. The correlator is controlled from this circuitry to look for the synchronizing codes and then select the code that gives the highest correlation peak and declare this as the code transmitted. The associated number of the code is forwarded to the processor as the data. The data is either routed to the terminal or used internally to test the performance of the radio such as Bit Error Rate measurements.

5. THE CORA PERFORMANCE IN VIEW OF THE REQUIREMENTS

We now discuss the CORA radio performance in view of the requirements given in section 2.

a. It is extremely difficult to demodulate the data from the CORA transmission without knowing the codes being used, even if you have a CORA radio at hand. The number of codes that can be used for the alphabets is very large. Furthermore it is perfectly feasible to change synhronizing codes and alphabets at a rather fast rate making it virtually impossible to demodulate the data for anyone not knowing the key for changing the codes. As for detection of traffic going on, the LPI performance of the CORA radio is approximately as for conventional DS systems if the output power is decreased

according to the sensitivity gained in the receiver due to the multilevel signalling. Also very important is the ability of CORA to transmit very short data messages. This ability decreases the total time on the air which again reduces the possibility of being detected at all. A message containing 100 bits of information does not take more than approximately 10 msek, including synchronization, in the 16 kb/s mode. This time is comparable to the "on time" in many frequency hopping radios.

b. The resistance to jamming is approximately the same as for a conventional DS radio system. The PG is 24 dB in 2.4 kb/s mode and 15 dB in 16 kb/s mode. To furthermore increase the resistance to narrowband jammers, a system with Automatic Channel Selection and slow frequency agility will be employed.

   Because of the multilevel signalling the performance against the broadband barrage jammer is very good compared to other radios not using this technique. A comparison is given in figure 8. In this figure we compare CORA with an ordinary frequency hopper using noncoherent FSK in a scenario limited by a white noise background. The performance of the frequency hopper is very dependent upon the coding being used and the figures are for the average system. As can be seen, the range performance of CORA is superiour.

c. The ability of CORA to transfer data messages is very good. The reason is the short synchronization times needed, the Fixed Frequency format and the modulation method. Also the radios ability to find out itself whether data or voice is transmitted is important.

d. As for colocation performance, this is to a large extent decided by the filtering employed in the transmitter chain and the receiver chain. Here, the CORA radio performs very well compared to ordinary frequency hoppers. The general result is that despite the higher modulation rate and the larger bandwidths involved, the spectrum of CORA and the receiver selectivity of CORA compared to frequency hoppers is the same or better farther from the center frequency than approximately 100 kHz. In the receiver greater selectivity is obtained because of the DS principle involved. Finally the fixed frequency format is a must when it comes to avoid spurious responses by frequency management both in transmitter and receiver.

e. Power consumption in the CORA radio will in a production model be comparable to, or lower than most frequency hoppers on the market. The reduction in power has been possible because of the low clocking speeds involed and the relatively narrow bandwidths. This again is a consequence of the multilevel signalling used in CORA.

f. Pricing of a production radio must be decided by the company involved. It may be said, however, that the price of the radio unit itself could be comparable to or slightly higher than frequency hoppers on the market. The reason for a higher price could be the slightly increased complexity due to the use of the DSSS principle involving correlators and a more stable oscillator in the system. Because of the narrow bandwidth

employed, large deviations from the prices on radios already on the market as Frequency Hoppers is not expected.

g. A fixed frequency DSSS radio is the ideal partner for an antenna nullsteering system. The reason is firstly that the slightly increased bandwidth makes a shorter adaptation time for the nulling possible. The fact that the system is fixed frequency (at least for a single message) makes the null, once established, valid for a long period of time. Furthermore, the DSSS principle means that the radio may work with negative Signal to Noise Ratios (SNR) at the input. This means again that the algorithm finding the null does not have to take into account the possibility that the signal it works on is a friendly signal. The chances that the nulling system is able to push the signal level so much below the background noise that the data is undetectable, can be made very small.

5. TESTING OF THE CORA PROTOTYPES

The prototype transmitter and receiver have been tested extensively in the laboratory and also range tests have been performed by the army various places in Norway. In the laboratory tests very good performance regarding narrow spectra and selectivity in the receiver has been measured. Figure 9 shows the transmitted output spectrum in dB relative to the carrier, as a function of the offset from the carrier frequency. From 200 kHz it is comparable to most frequency hoppers on the market and better than PRC 77 in spite of the faster modulation rate employed.

Figure 10 shows the selectivity of the radio as measured against an interferer which in this case was a signal generator frequency modulated with 12.5 kHz deviation and 500 Hz frequency. The curve shows the tolerated interference level in dBm when the friendly signal level received by the radio under test is -120 dBm, as a function of the frequency offset of the interferer. Here the CORA radio outperforms most frequency hoppers on the market from approximately 100 kHz.

The sensitivity measured in the laboratory for 2.4 kb/s and BER 10-3 is approximately -126 dBm. This figure is expected to improve in the future due to improvement in certain components in the receiver and transmitter. The BER as a function of the signal power received by the radio is extremely steep as expected for the multilevel signalling employed. We have so far not been able to measure any residual Bit Error Rate, because it is too small. This means that for a packet radio network with messages of reasonable lengths the residual BER in the radio is unimportant. The sensitivity level for readable voice is approximately 6 dB higher than for 2.4 kb/s, and for 16 kb/s data with BER 10-3 approximately 10 db higher

In the field tests, the result was that 2.4 kb/s data was received with BER 10-3 or better with the same or smaller power than PRC 77, when the voice in the latter system was just readable. Somewhat higher power was necessary for voice in the CORA radio, and 16 kb/s (BER 10-3) data communication was demonstrated with approximately 10 dB higher power. Because of

the DS principle involved multipath was not a problem. Delays up to 100 usecs was measured with the CORA radio.

The last two figures show the prototype radio with an external terminal and a private soldier using the CORA radio both for voice and data purposes during the trials. (Note that CORA can receive FM voice and DSSS data at the same time and at the same frequency!)

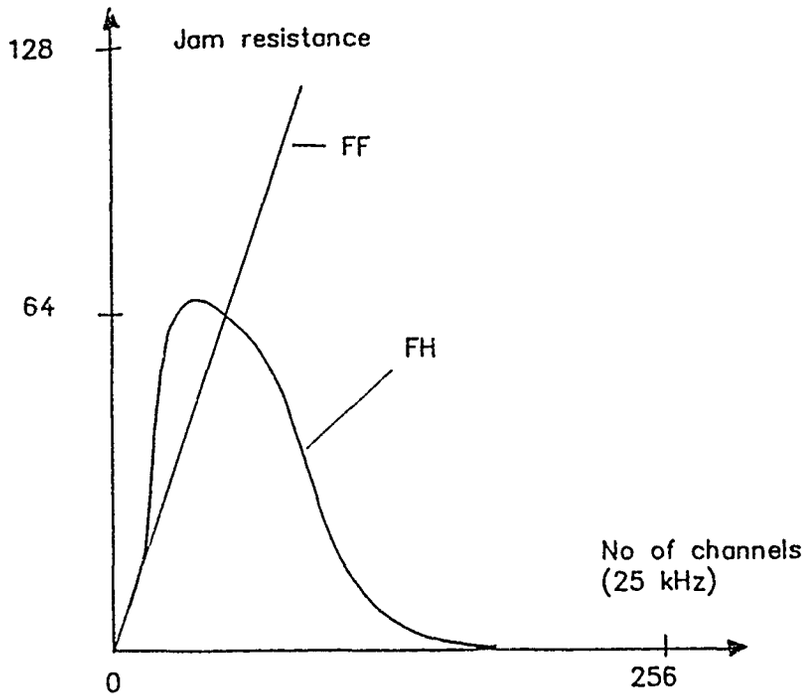

Fig. 1 Jam resistance of FF and FH radios

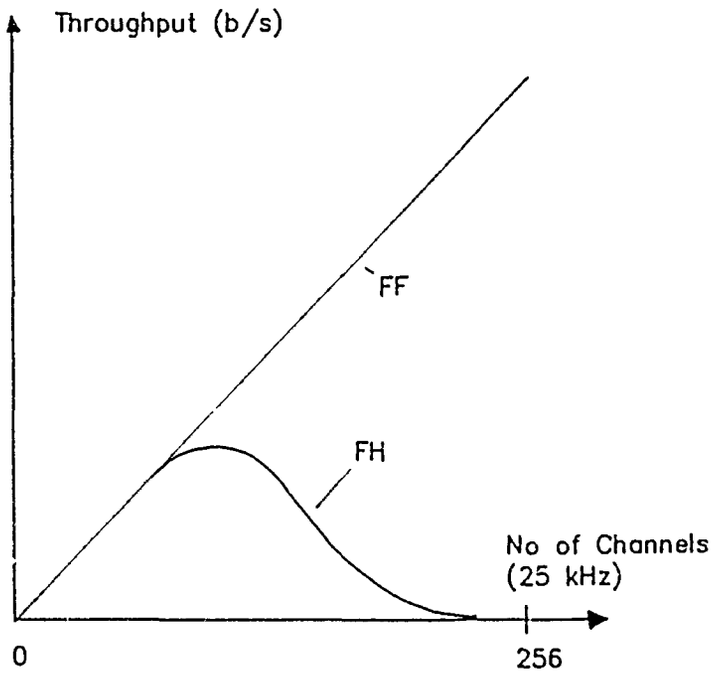

Fig. 2 Throughput of FF and FH radios

DIRECT SEQUENCE SPREAD SPECTRUM:

INFO BITS:	0	1	0
CODE BITS:	0001101	1110010	0001101

REQUIRES CORRELATOR LENGTH L

REQUIRES INCREASED BANDWIDTH

JAM RESISTANCE INCREASES L TIMES

Fig. 3 Direct Sequence Spread Spectrum principles

ORTHOGONAL SIGNALING:

EXAMPLE: 4 LEVELS:

DATA BITS	CODE TRANSMITTED
00	1
01	2
10	3
11	4

. TWO BITS PER CODE TRANSMITTED
. BANDWIDTH REDUCED BY FACTOR 2
. RANGE INCREASED
. CORRELATOR LENGTH THE SAME
. RECEIVER MORE COMPLEX

Fig. 4 Orthogonal Signalling principles

CORA DATAFORMAT :

Fig. 5 CORA Dataformat

RADIO TYPE: FIXED FREQUENCY, DIRECT SEQUENCE SPREAD SPECTRUM

FREQUENCY RANGE: 30 – 88 MHz IN 25 kHz STEP

TX BANDWIDTH: 40 kHz

RX BANDWIDTH: 45 kHz

CHANNEL SEPARATION: 50 kHz

DATA RATES: 2.4kb/s, 16 kb/s and low rate data, 150 b/s

VOICE: FM AND 16 kb/s DELTA

PROCESSING GAIN: 24 dB and 15 dB plus coding gain for lower rates

SENSITIVITY: BETTER THAN – 120 dBm for 2.4 kb/s

MODULATION TYPE: NONCOHERENT ORTHOGONAL, DSSS, MSK

PLANNED PRODUCT IMPROVEMENTS :

ANTENNA NULLSTEERING SYSTEM

FORWARD ERROR CORRECTION BY RS CODING

Fig. 6 CORA Specifications

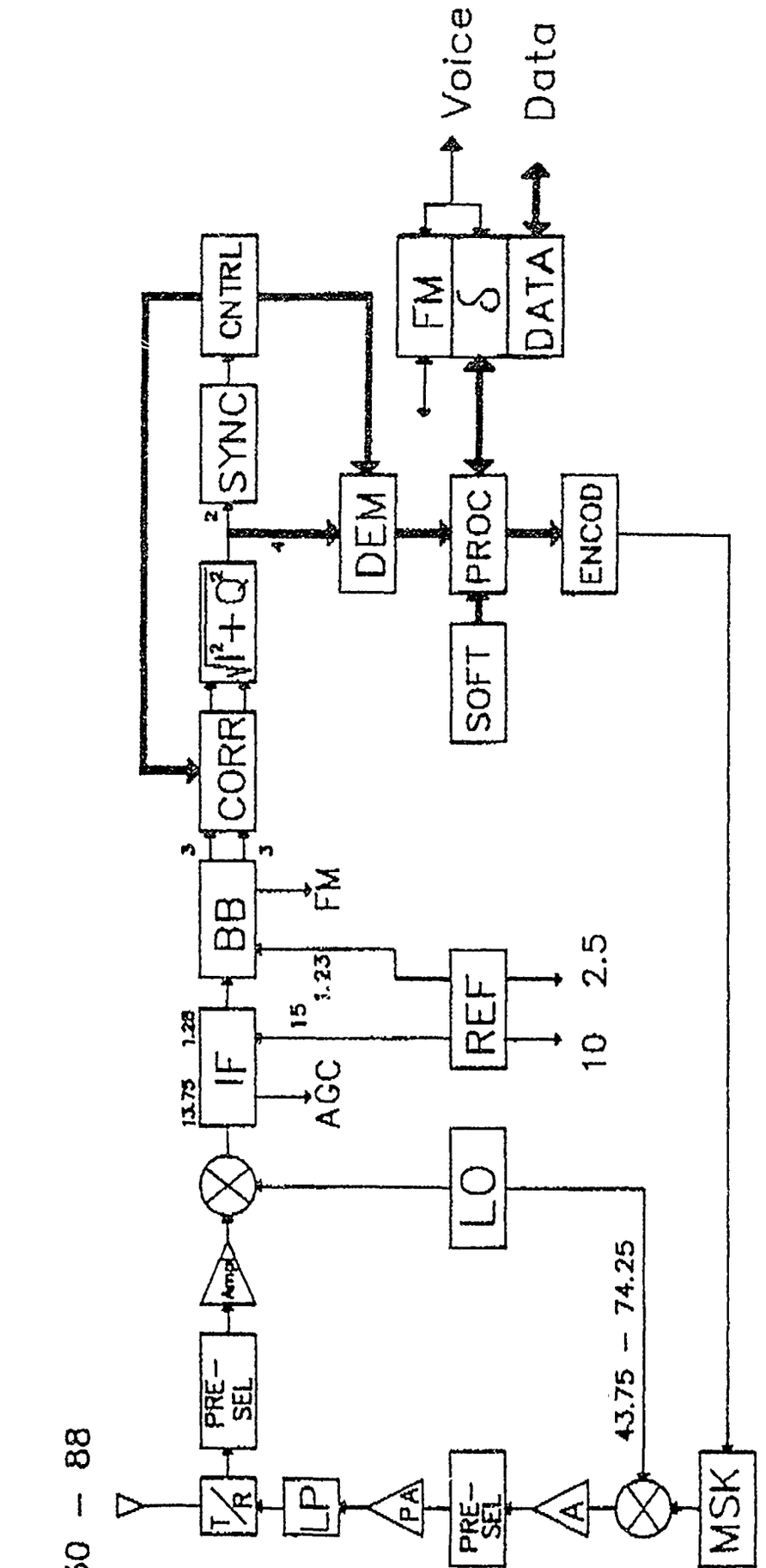

Fig 7. CORA Block Diagram.

RANGE COMPARISON, CORA/FSK

1. 16 kb/s BER 10 – 3

	FSK	CORA	RANGE GAIN
Eb/N_0:	11 dB	5.5 dB	36 %

2. 2.4 kb/s BER 10 – 3

	FSK	CORA	RANGE GAIN
Eb/N_0	13.2 dB	4.5 dB	66 %

Fig. 8 Range Comparison CORA - FSK

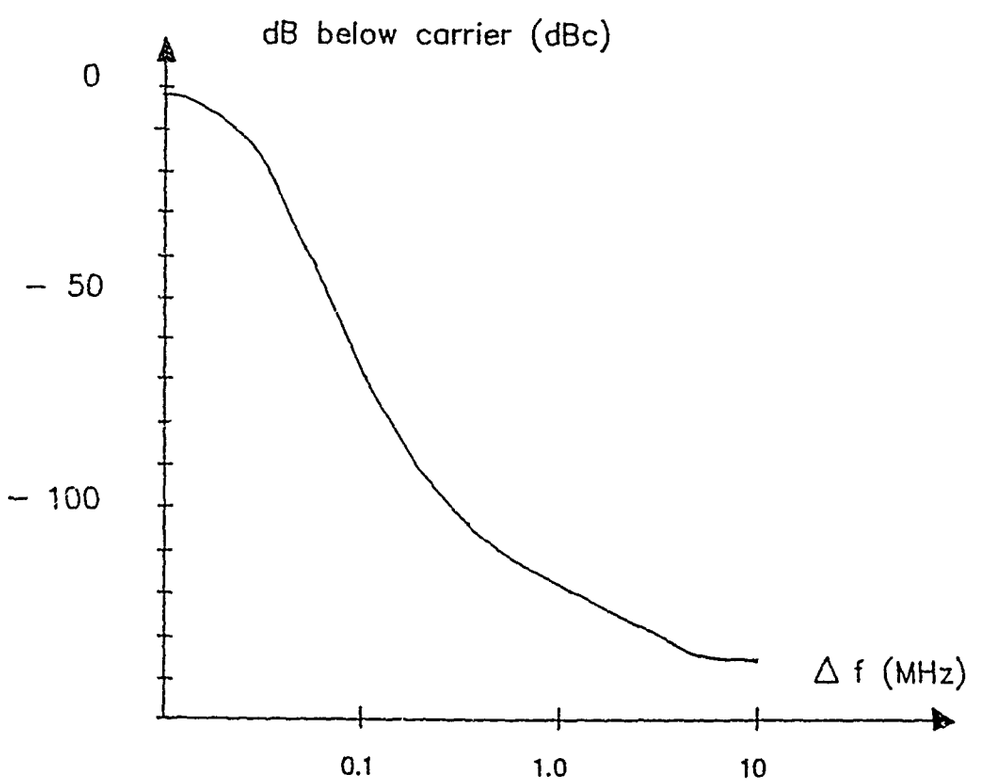

Fig. 9 CORA spectral characteristics

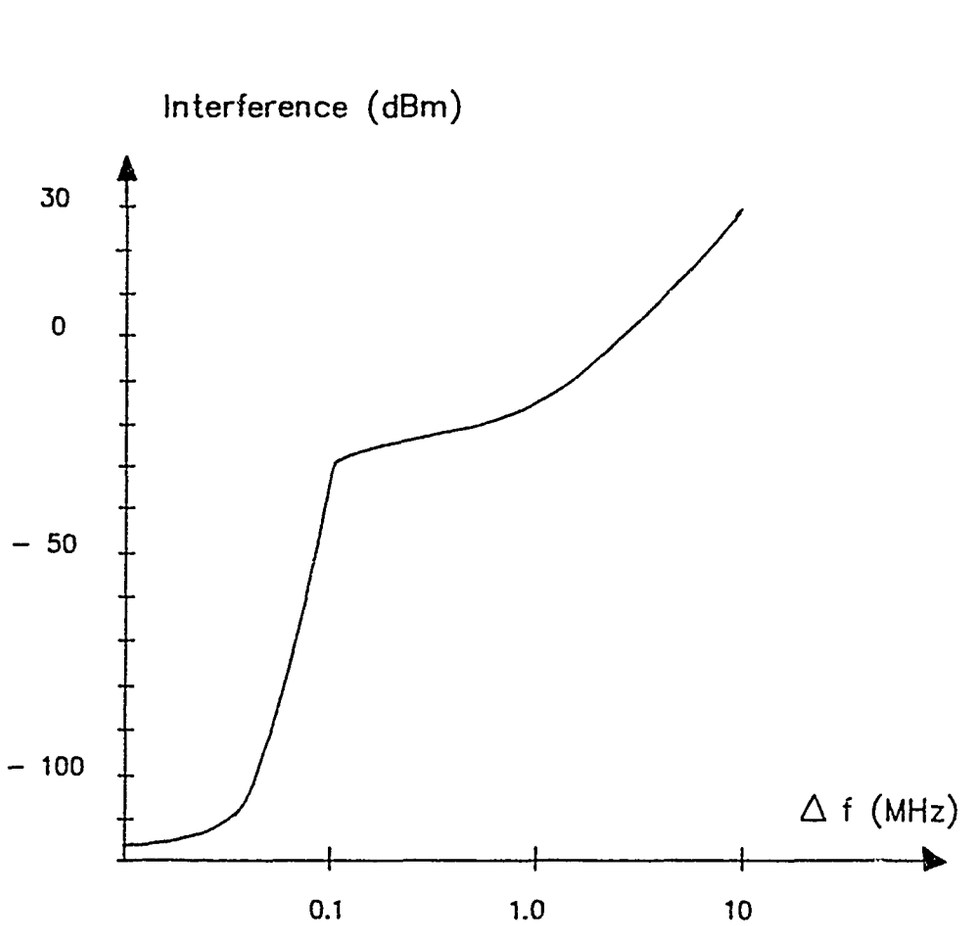

Fig. 10 CORA selectivity curve

Fig. 11 CORA Prototype Radio

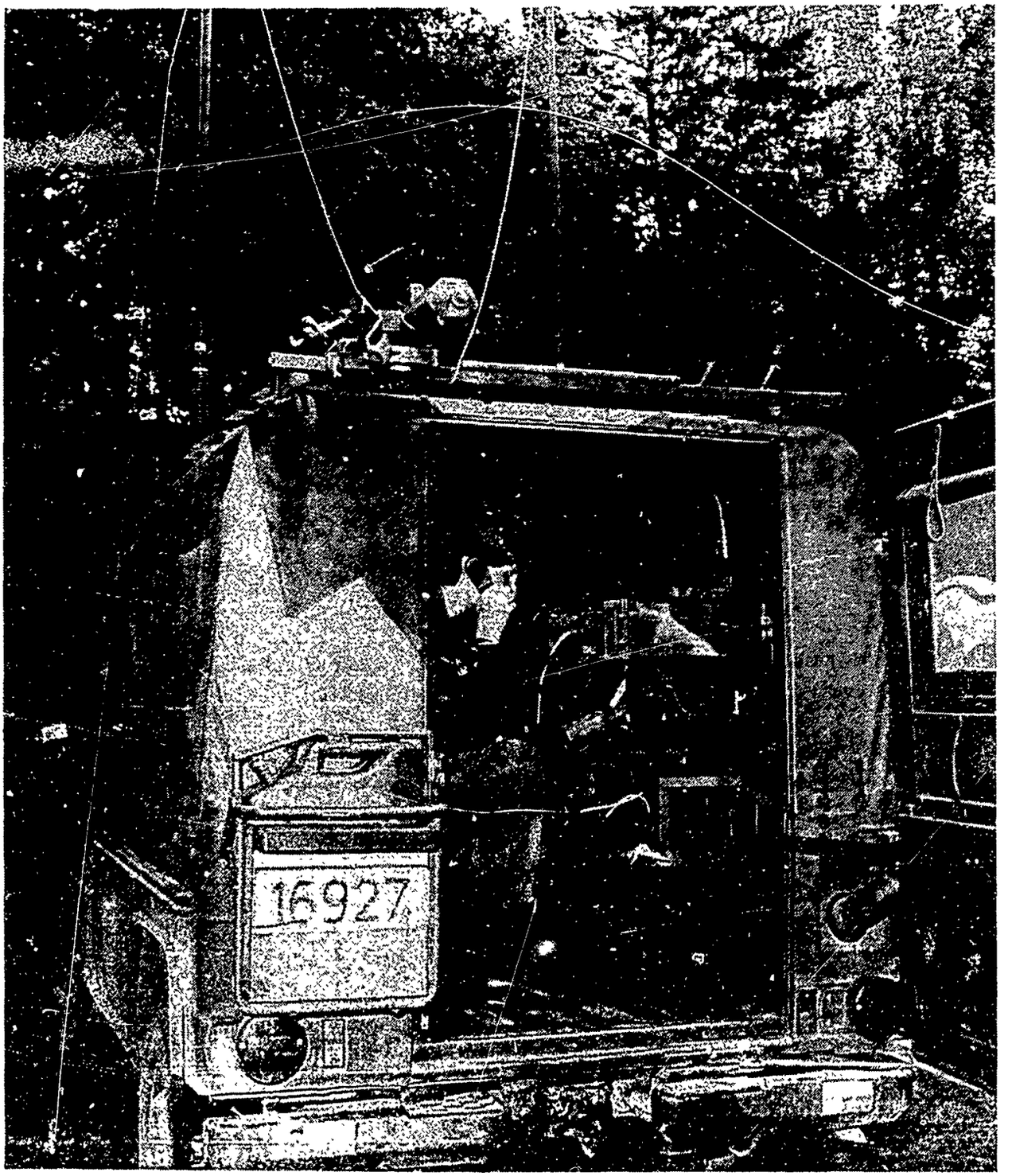

Fig. 12 From Field Trials of CORA

DISCUSSION

D. ROTHER

What is your anti-jam margin in a 50KHz channel bandwidth ?

AUTHOR'S REPLY

It we define : Margin M = acceptable S/I BER 10^{-3}, then
Margin M $\simeq$ - 10dB for white noise case.
M much better for sinusoïdal case.

P.J. MUNDAY

The comments made by the author on the following aspects of frequency hopping are injustified :

1 - Anti-jam margin.
2 - Synchronization time.
3 - Coloration of radios.
4 - Working with antenna nulling.

My question is : how can you get a processing gain of 15dB by spreading a 16kb/s signal up to only 50KHz ?

AUTHOR'S REPLY

No reply was given in the meeting.

K.S. KHO

1 - How about the frequency allotment . Today allotment is based on 25KHz rastering.
2 - For the backward interoperability, you implement FM mode. It means two radios in one case. What is your comment !
3 - You said FH can not cope with multipath. I think before the multipath is coming, the radio will already be at another frequency.

AUTHOR'S REPLY

1 - Depends on required isolation : 25KHz ⟶ 10dB
50KHz ⟶ ~25dB
100KHz ⟶ ~90dB
2 - FM voice /2.4 kb data can be received simultaneously at same center frequency. FM sensitivity : - 115dBm.
3 - FH dwell time $\simeq$ 10ms
Multipath delay < 100 μs
You are therefore wrong.

MULTIPLE-USER MULTIPLE-ACCESS TECHNIQUES FOR COMMUNICATION OVER DISPERSIVE RADIO CHANNELS

M. Darnell* & B.Honary**

Hull-Warwick Communications Research Group

*Department of Electronic Engineering
University of Hull
HULL HU6 7RX
UK

**Department of Engineering
University of Warwick
COVENTRY CV4 7AL
UK

SUMMARY

The paper first reviews "conventional" multiple-user/multiple-access techniques which have been employed on various types of radio channels. These techniques are time-division multiple-access (TDMA), frequency-division multiple-access (FDMA) and code-division multiple-access (CDMA).

Attention is then turned to CDMA-type systems which appear to offer promise of reliable operation over dispersive radio paths. Two main aspects are considered:

(i) The use of completely uncorrelated, as opposed to near-uncorrelated, code sets. In practical CDMA systems designed to date, the latter class of codes has been used. It is shown that completely uncorrelated sets have distinct advantages - particularly for packet data operations.

(ii) The use of collaborative coding techniques to permit simultaneous transmission by several users sharing a common channel, with overall transmission rates in excess of that achievable with say TDMA. The paper describes the performance of three new collaborative coding multiple-access (CCMA) schemes, each with two users, under Gaussian noise conditions.

1. INTRODUCTION

Historically, radio communication has been concerned primarily with single-transmitter/single-receiver configurations and with broadcast modes. Any multi-user requirements have tended to be satisfied via combinations of these architectures. However, this can be an inefficient way of exploiting available bandwidth and channel capacity. Consequently, in recent years, more sophisticated multi-user architectures have been developed which allow a number of transmitters to communicate on a multiple/random-access basis with a number of receivers - as illustrated in Figure 1. Here it is required to establish communication over a multiple-access channel (MAC) between n sources and m destinations in a flexible manner. In practice, n and m may, or may not, be equal.

It is the purpose of this paper to describe a number of methods of achieving this objective in the context of dispersive radio channels, eg in the HF (2 - 30 MHz) band. Digital data, as opposed to analogue, communication is assumed; the ability to generate information in packet data format when necessary is also assumed. It is required to pass the information with as small a delay as possible, and with acceptably low error rates.

2. CONVENTIONAL MULTIPLE/RANDOM-ACCESS SCHEMES

For many years, multi-user packet data communication has largely been confined to combinations of simple single-user systems designed primarily for continuous data streams. The major systems of this kind are frequency-division multiple-access (FDMA) and time-division multiple-access (TDMA).

In the case of FDMA, the message sources are each assigned distinct frequency sub-channels in parallel within an overall system bandwidth; each sub-channel can be utilised continuously, but the bandwidth - and hence proportion of total system capacity - available to each user is obviously restricted. The need to allow "guard bands" between sub-channel also reduces system efficiency. FDMA can operate with multiple transmitters, or with a single broadcast transmitter radiating all sub-channels simultaneously.

The TDMA technique, in contrast to FDMA, allows each source access to the complete system bandwidth in uniquely defined time slots. When a slot assigned to a given source expires, the system protocol forces it to wait until its next assigned time slot in order to continue its transmission.

In packet systems with priority and low transmission delay requirements, basic FDMA and TDMA systems perform relatively poorly. As an example, consider an FDMA system with 100 transmitters: if, at some instant, only one station has a packet to transmit, it will be constrained to use its own sub-channel representing about 1% of the total system capacity available at that time. Hence, the transmission time is expanded by a factor of 100 in comparison with what is theoretically achievable. An

analagous situation would arise in the case of TDMA, with a single transmitter only having access to its assigned time slots. A protocol which has been designed to reduce this problem in lightly loaded systems involves the detection of packet collisions, when two or more sources attempt to transmit at the same time.

An example of this architecture is the ALOHA system; here, terminals exchange data packets via a single radio channel. The basic concept is that, at low packet generation rates, there will rarely be more than one terminal ready to initiate a packet transmission at a given instant. Each terminal is allowed to transmit an uncoded packet as soon as it is available using the entire system bandwidth. By an appropriate feedback mechanism, terminals learn if their packets have arrived successfully at the intended destinations. If two or more terminals transmit simultaneously, their packets are likely to be corrupted and must be re-transmitted at a more favourable time. The ALOHA protocol invokes random time delays in order to avoid repetitive collisions. At low packet generation rates, the system works well since for most of the time there is only a single active source which can act as if it were the sole system user; packet delay is minimal. However, as generation rates increase, so delays increase. Since the advent of ALOHA, many more sophisticated and efficient schemes have been devised (Massey, 1985), their basic goal being to exploit any knowledge of the packet arrival statistics in order to keep the transmission delays as low as possible.

One major problem with the existing range of collision algorithms is that they have usually focussed on packet arrival statistics, but largely ignored the effect of channel noise on transmission delays; if there is no collision, packets are assumed correctly received. Some error control in the form of cyclic redundancy checks (CRC's) may be appended for efficient error detection, but little attention is paid to correction of errors. This is evidently a more important consideration with dispersive radio channels with relatively high levels of noise - which may be significantly non-Gaussian.

Another conventional form of multiple-access strategy which has been exploited practically, particularly in the field of satellite communication, is that of CDMA. Here, all transmitters share the same overall transmission bandwidth, with isolation being achieved by an appropriate choice of codes for the terminals. Figure 2 is a schematic diagram of a generalised CDMA system: the sources S(1) - S(n) are assigned unique channel codes, $x_1(t)$ - $x_n(t)$, which have the following 2 properties:

(i) that their crosscorrelation functions (ccf's) are zero, or near-zero, over the detection interval T, ie

$$\phi_{ij}(\tau) = 1/T \int_0^T x_i(t)\, x_j(t+\tau)\, dt \neq 0 \qquad (1)$$

where

$$1 \leq i \leq n$$
$$1 \leq j \leq n \qquad (2)$$
$$i \neq j$$

with τ being a delay variable;

(ii) that their autocorrelation functions (acf's) are impulsive, or approximately impulsive, over the detection interval T, ie

$$\phi_{ii}(\tau) = 1/T \int_0^T x_i(t)\, x_i(t+\tau)\, dt = \delta(\tau) \qquad (3)$$

where

$$1 \leq i \leq n$$

and $\delta(\tau)$ is a unit impulse centred on $\tau = 0$ (4)

At the receiving sites, matched filters, or correlation detectors, are employed which effectively compute the ccf's between the incoming composite received signal, y(t), and each of the x(t) reference signals. In general, y(t) will be a combination of different numbers of transmitted x(t) components, depending on how many of the sources S(1) - S(n) are active at any time. Thus

$$y(t) = x_a(t) + x_b(t) + \ldots + x_i(t) + \ldots + x_k(t) \qquad (5)$$

where

$$1 \leq a \leq n$$
$$1 \leq b \leq n$$
$$\vdots$$
$$1 \leq i \leq n \qquad (6)$$
$$1 \leq k \leq n$$
$$a < b < \ldots < i < \ldots < k$$

The matched filters MF(1) - MF(n) compute the ccf's

$$\phi_{x_i y}(\tau) = 1/T \int_0^T x_i(t)\, y(t+\tau)\, dt \qquad (7)$$

where $1 \leq i \leq n$. Because the group of x(t) signals forms an uncorrelated set over T, the matched filter detectors will only respond when y(t) contains the x(t) component to which they are matched. Therefore, substituting from (5) into (7) yields

$$\phi_{x_i y}(\tau) = \phi_{x_i x_a}(\tau) + \phi_{x_i x_b}(\tau) + \ldots + \phi_{x_i x_i}(\tau) + \ldots + \phi_{x_i x_k}(\tau) \qquad (8)$$

In the absence of noise/interference, it is clear that the only non-zero (impulsive) term will be $\phi_{x_i x_i}(\tau)$.

If the x(t) set is chosen correctly, all transmitters can transmit simultaneously in the same overall channel bandwidth without interaction, and the matched filters will only extract those components to which they are matched.

In practice, sets of periodic pseudorandom (pr) sequences have been employed as the x(t) signals in CDMA systems. The ccf's within such a set are normally near-zero, rather than identically zero; hence, the superimposed ccf components in (8) will be a source of system "self-noise" which will eventually cause a limit on the number of simultaneous users. A further practical problem with such periodic sequence sets is the need to acquire and maintain synchronisation between transmitting and receiving terminals (Darnell & Honary, 1986). The CDMA architecture described in the following section attempts to overcome both of these problems.

3. AN APERIODIC CDMA SYSTEM

The system to be described here is based upon the use of sets of aperiodic (non-periodic) waveforms, known as "complementary sequences", as the x(t) codes in the architecture of Figure 2. The design minimises the problems of self-noise and synchronisation inherent in many CDMA systems implemented to date.

3.1 Complementary Sequences

A pair of binary aperiodic complementary sequences is defined as comprising two, equal-length sequences which have the property that the number of pairs of like elements with any given separation in one sequence is exactly equal to the number of pairs of unlike elements with the same separation in the other sequence (Golay, 1961). This property leads to the characteristic form of the summed aperiodic acf's of the sequences, ie that the sum of the individual acf's is zero at all corresponding time shifts, except at the in-phase (zero-shift) position where it takes the value 2N, N being the number of bits in each sequence. Normally

$$N = 2^n \quad (n \text{ integer}) \qquad (9)$$

Reference 4 (Darnell, 1975) describes further developments of Golay's basic binary sequence theory, together with methods for the synthesis of completely uncorrelated sets of binary complementary sequences and practical applications of such sets.

When it is required to synthesise complementary sets of more than two sequences and more than two levels, the original definition is no longer appropriate and a modified definition related directly to the set acf properties must be adopted, ie that the sum of the individual sequence aperiodic acf's for all members of the set should be zero at all corresponding shifts, except at the zero-shift position where it takes a value equal to the sum of the squares of all digits of all sequences in the set. Figure 3 illustrates typical individual and summed acf's for a set of 4 sequences.

For completeness, a pair of uncorrelated aperiodic complementary sequence sets is defined as a pair of sets for which the aperiodic ccf values for corresponding sequences in each set sum to zero at all time shifts. For example, the two binary sequence sets, each comprising 4 sequences

Sequence 1:	+1 +1 +1 +1	-1 +1 -1 +1
Sequence 2:	+1 +1 -1 -1	-1 +1 +1 -1
Sequence 3:	-1 +1 -1 +1	+1 +1 +1 +1
Sequence 4:	-1 +1 +1 -1	+1 +1 -1 -1

(10)

are both complementary and uncorrelated in the senses indicated previously.

3.2 Synthesis Procedures for Binary Sets

In Reference 4, recursive procedures for synthesising sets of binary complementary sequences are described. Assuming that the length of each sequence in a set is N, then if A and B are sub-blocks of length N/2, a pair of complementary sequences can be synthesised from the block structures

```
(a)  +A +B    (b)  +A +B    (c)  -A +B    (d)  +A -B
     +B -A         -B +A         +B +A         +B +A        (11)
```

For example, if A = +1 and B + +1, then applying 11(a) and 11(d) yields the 2-bit sequence sets

```
          (a)  +1 +1    (b)  +1 -1
               +1 -1         +1 +1                          (12)
```

which are both complementary. Also, the summed non-periodic ccf between the corresponding sequences of 12(a) and 12(b) is zero at all time shifts, thus demonstrating that the two sets are uncorrelated. Note that the structures of 11(b) and 11(c) also provides a pair of uncorrelated complementary sets, whereas (a) - (b), (a) - (c), (b) - (d) and (c) - (d) do not.

If A and B are now redefined as 12(a) and 12(b) respectively, and the basic structure of 11(a) and 11(d) again employed, two uncorrelated sets, each comprising four 4-bit sequences result ie

```
(a)  +1 +1 +1 -1          (b) +1 +1 -1 +1
     +1 -1 +1 +1              +1 -1 -1 -1
     +1 -1 -1 -1              +1 -1 +1 +1          (13)
     +1 +1 -1 +1              +1 +1 +1 -1
```

This procedure can again be applied recursively with 13(a) and 13(b) respectively now representing the basic blocks A and B.

3.3 Synthesis Procedure for Multi-level Sets

The same basic recursive procedure can also be employed to synthesise multi-level (non-binary) complementary sets. If +1 and +2 are now chosen as A and B in the structure of 11(a), and +3 and +4 as A and B in the structure of 11(d), the sets

```
          (a) +1 +2   and   (b) +3 -4
              +2 -1               +4 +3                    (14)
```

are produced, which are each complementary. However, the two sets are not now uncorrelated because of the different digit weightings in the two sets. If 14(a) and 14(b) are now redefined as A and B respectively within the structures of 11(a) and 11(d), the following sequence sets are produced:

```
(a) +1 +2 +3 -4          (b) +1 +2 -3 +4
    +2 -1 +4 +3              +2 -1 -4 -3
    +3 -4 -1 -2              +3 -4 +1 +2          (15)
    +4 +3 -2 +1              +4 +3 +2 -1
```

These sets are both complementary and uncorrelated, the latter property arising because the two sets now have identical digit weight distributions. Again, the synthesis algorithm can be applied recursively to give sets of longer sequences.

The multi-level synthesis procedures described above can equally well be applied to produce non-integer sequence sets if A and/or B are chosen to be non-integer "seeds".

Further work has been carried in the following areas:

(a) the synthesis of odd-length complementary sequence sets (Darnell & Kemp, 1988);

(b) the synthesis of more than two uncorrelated sets of complementary sequences, all having the same dimensions;

(c) the synthesis of non-square complementary sequence sets.

3.4 Application of Complementary Sequence Sets

The application to which uncorrelated sets of complementary sequences is being put is that of aperiodic CDMA packet data communications over dispersive radio channels. Here, the sets have a multi-functional capability in the sense introduced in (Darnell & Honary, 1986), ie they can simultaneously provide a capability for error control, synchronisation, multiple-access and channel evaluation in an adaptive communication system architecture. In the first instance, a multiple frequency-shift keying (MFSK) transmission scheme of up to 8 levels has been chosen to interface with multi-level complementary sequence sets; simple digital matched filter (tapped delay line) detectors are employed at the receivers.

A CDMA system is being implemented in which uncorrelated sets of complementary sequences are assigned to multiple transmitting terminals; thus, a single radio frequency channel can be shared by a number of users - theoretically without interaction since the sets have identically zero ccf's, rather than simply having low crosscorrelation. The number and weighting of sequence levels, the number of sequences in a set and the sequence lengths are all adaptable in response in response to channel state and user requirements. The need for synchronisation preambles etc is

removed by the impulsive nature of the aperiodic acf's of the sequence sets. Also, the outputs of the matched filter detectors can provide information on channel state (RTCE data) to initiate adaptive variation of system parameters.

The system being implemented is seen as a vehicle for robust, relatively low-rate packet data transmission over poor quality radio channels, eg with low-power HF mobile terminals.

4. COLLABORATIVE CODING MULTIPLE-ACCESS TECHNIQUES

The collaborative coding multiple-access (CCMA) technique permits potentially efficient simultaneous transmission by several users sharing a common channel, with transmission rates, in terms of bits/channel, greater than TDMA (Farrell, 1981). However, such coding schemes require a MAC with an output symbol value equal to the arithmetic sum of the users' input symbol values.

As shown in Figure 4, the data from source i, U(i), where i = 1, 2, 3, ... , T, is encoded by encoder i according to a uniquely assigned block code C(i). The resulting codeword vector X(i) is then transmitted over the channel where it combines with the other (T - 1) codeword vectors, codeword synchronisation being assumed, to produce a composite codeword vector Y. The single decoder at the receiver decodes Y into estimates of the T original data streams U(1), U(2), ..., U(T).

The T codes C(1), C(2), ... , C(T) together are called a "T-user collaborative code", where each of the T components is termed a "constituent code". If the code C(i) contains M(i) codewords, each of length N, then the rate of the ith constituent code, assuming all codewords are equiprobable, is given by

$$R(i) = [\log_2 M(i)]/N \qquad (16)$$

and the rate sum for all the T users' codes

$$RS(T) = R(1) + R(2) + \ldots + R(T) \qquad (17)$$

$$= \sum_{i=1}^{T} [\log_2 M(i)]/N \qquad (18)$$

If all the constituent codes are binary block codes, then the codeword vector X(i) is an N-symbol binary vector, ie each symbol S(i) belongs to the set [0, 1]. Therefore, the channel output symbol S is a composite arithmetic sum of all the T input symbols

$$S = S(1) + S(2) + \ldots + S(T) \qquad (19)$$

$$= \sum_{i=1}^{T} S(i) \qquad (20)$$

4.1 Channel Models

(a) Baseband

The baseband channel considered here is a T-input noiseless adder MAC. Each user's input alphabet is the integer set [0, 1], and the output Y is the sum of the T inputs X(1), X(2), ... , X(T), ie

$$Y = \sum_{i=1}^{T} X(i) \qquad (21)$$

where the summation sign denotes real addition. Therefore, each output symbol is an integer from the set [0, 1, 2, ... , T]. For example, Figure 5 illustrates the case where T = 2: each user input symbol is taken from the set [0, 1], whilst each output symbol will be an integer from the set [0, 1, 2].

The collaborative code used in this particular case is formed from the two constituent codes, each of block length 2; user 1 is assigned the codewords C(1) = [00, 11] and user 2 the codewords C(2) = [00, 10, 01], as shown in Table 1 below.

		USER 1: C(1)	
C(1) + C(2)		00	11
USER 2: C(2)	00	00	11
	10	10	21
	01	01	12

TABLE 1

It can be seen from this table that each of the 6 possible composite codewords, resulting from symbol-wise addition in the channel, is distinct and can therefore be unambiguously decoded into its constituent codewords. The rate pair achieved by this

scheme is (R(1), R(2)) = (0.5, 0.792); thus the overall rate sum RS(2) = R(1) + R(2) = 1.292 bits/channel use.

(b) Bandpass

The channel model considered here is a T-user, M-frequency, bandpass MAC. It is assumed that the T users have available M sinusoidal carriers, each at different frequencies F(1), F(2), ... , F(M), and that phase-coherence is maintained at the receivers. During any symbol interval, I, each of the users selects one of these frequencies to transmit and the receiver must then decide which combination of frequencies have been transmitted during the symbol interval. It is also assumed that all the T users are time synchronised so that each user transmits its frequencies within the same symbol time intervals as all other users. Each tone must be separated from adjacent tones in frequency by an amount sufficient to allow rejection of those other tones by the receiver. Hence, choosing a frequency separation of 1/I would give a tone raster guaranteeing a fixed energy per tone within the symbol interval, I, and allowing M orthogonal tones to be placed in an overall bandwidth of M/I.

It should be noted here that the collaborative code used in the work described in this paper is based upon the codes constructed by (Kasami & Lin, 1976) and (Kasami, Lin & Yamamura, 1975). For the 2-user case, the User 1 code C(1) is any linear (n, k) code which contains the "all-ones" word 11...1; the User 2 code C(2) then comprises the "all-zeros" word, all the coset leaders of a coset array of C(1), but not including C(1) and the complements of those coset leaders. This construction results in rate sum of 1.292 bits/channel use; when N = 4, User 1 has four codewords and User 2 nine codewords. For simplicity of simulation, only 8 codewords are employed for User 2 to match sources with k-bit symbols, ie

2^k states (where k is an integer).

Such a code construction for the 2-user case is shown in Table 2 below.

USER 1: k = 2		USER 2: k = 3	
[00] --	0000	[000] --	0000
[01] --	0011	[001] --	0001
[10] --	1100	[010] --	0010
[11] --	1111	[011] --	1000
		[100] --	0100
		[101] --	0101
		[110] --	0110
		[111] --	1001

TABLE 2

where the square brackets show the users' original data of length k bits.

Three specific schemes for the bandpass MAC are considered in the following section.

4.2 Specific CCMA Schemes

(a) 2-User Bandpass MAC with Matched Filter Detection

Figure 6 shows the general configuration for a T-user bandpass MAC system. The ith user is assigned transmission states F1(t) and F2(t) as follows:

$$F1(t) = \cos(w_1)t \quad \text{for symbol } S(i) = 0$$

$$F2(t) = \cos(w_1 + 2\pi/I)t \quad \text{for symbol } S(i) = 1 \qquad (22)$$

assuming a convenient tone frequency w_1 and zero phase angle.

During any symbol interval, the ith user transmits its tone frequency according to the above, ie

$$s_i(t) = S(i)\, F2(t) + [1 - S(i)]\, F1(t) \qquad (23)$$

where i = 1, 2, 3, ... , T. This signal then combines over the channel with the signals transmitted by the other system users; hence, the resulting demodulator input, in the absence of noise, is

$$s_r(t) = \sum_{i=1}^{T} S(i)\, F2(t) + [1 - S(i)]\, F1(t) \qquad (24)$$

from which the users' collaborative codeword symbols must be recovered. It is clear that only two frequencies are required for the complete T-user system. For the 2-user case, the composite signal at the receiver is of the form

$$s_r(t) = S(1)\, F2(t) + [1 - S(1)]\, F1(t) + S(2)\, F2(t) + [1 - S(2)]\, F1(t) \qquad (25)$$

A matched filtering technique is then employed to recover the collaborative codeword symbols. For example, to recover F1(t), the signal of expression (25) is multiplied

by F1(t) and integrated over the symbol interval, I, giving

$$\int_0^I s_r(t)\, F1(t)\, dt \qquad (26)$$

The same form of processing is used to recover F2(t). The result of the matched filter processing indicates which frequencies are present in a given symbol interval and how many of each frequency component are present. This type of MAC is also referred to as a MAC with intensity information (Chang & Wolf, 1981) (Omura, 1979).

(b) 2-User Bandpass MAC with Square-Law Detection

A simple modulation scheme which provides users' data symbol addition over the channel is proposed in (Brine & Farrell, 1985); the arrangement is shown in Figure 7. Here, the ith user is assigned the carrier

$$Fi(t) = \cos [(w_o + i\,\delta w)t + \phi(i)] \qquad (27)$$

where i now can take values 0, 1, 2, ... , (T - 1) and

w_o is the carrier frequency assigned to User 0;

δw is a fixed frequency increment;

$\phi(i)$ is an arbitrary phase angle.

During any symbol interval, I, the ith user transmits an on-off keyed (OOK) signal

$$s_i(t) = S(i) \cos [(w_o + i\,\delta w)t + \phi(i)] \qquad (28)$$

where S(i) is the ith user's constituent codeword symbol taken from the set [0, 1]. Assuming a noise-free channel, the resulting demodulator input is

$$s_r(t) = \sum_{i=0}^{T-1} S(i) \cos [(w_o + i\,\delta w)t + \phi(i)] \qquad (29)$$

from which it is required to recover the collaborative codeword symbols. Therefore, for a 2-user example, the demodulator input has the form

$$s_r(t) = S(0) \cos [w_o t + \phi(0)] + S(1) \cos [(w_o + \delta w)t + \phi(1)] \qquad (30)$$

If δw is chosen to be $2\pi/I$, this corresponds to the minimum allowable frequency separation for tone orthogonality, irrespective of the values of $\phi(0)$ and $\phi(1)$. Making this substitution in (30) gives

$$s_r(t) = S(0) \cos [w_o t + \phi(0)] + S(1) \cos [(w_o + 2\pi/I)t + \phi(1)] \qquad (31)$$

In this system, the demodulation scheme used to recover the collaborative codeword symbol [S(0) + S(1)] is to square-law detect and then integrate over the symbol interval, I.

(c) 2-User Bandpass MAC with Average Zero-Crossing Detection

A simple modulation technique to provide CCMA via amplitude/frequency assignment is now considered. This technique is designed to operate in conjunction with a demodulation scheme based upon zero-crossing counting. The block diagram of this system is shown in Figure 8. The ith user of the system is assigned the carrier

$$A_j \cos[(w_o + S(i)(i + 1)\,\delta w)t + \phi_j] \qquad (32)$$

where i = 0, 1, 2, ... , (T-1) and j = 0, 1, 2, ... , (M-1), with M being the total number of frequencies available. The amplitude of the jth assigned carrier is denoted by the coefficient A_j.

During any symbol interval, I, the ith user transmits the signal

$$s_i(t) = S(i)\, A_j \cos [(w_o + S(i)(i + 1)\,\delta w)t + \phi_j] + (1 - S(i))\, A_j \cos [(w_o + S(i)(i + 1)\,\delta w)t + \phi_j] \qquad (33)$$

Assuming a noise-free channel, the overall demodulator input with T users is

$$s_r(t) = \sum_{i=0}^{T-1} [S(i)\, A_j \cos [w_o + S(i)(i+1)\delta w)t + \phi_j]$$

$$+ (1 - S(i))\, A_j \cos [(w_o + S(i)(i+1)\delta w)t + \phi_j]] \quad (34)$$

from which it is required to recover the desired collaborative codeword symbols. This is achieved by counting the number of zero-crossings of the signal (34) per unit time at the receiver, from which the transmitted frequency components can be deduced.

For the case when the composite signal at the channel output comprises the sum of two separate sinusoidal components, the average number of zero-crossings per second (ANZCPS) of this composite signal (Blachman, 1975)

$$s_r(t) = A1 \cos (2\pi F1\, t + \theta) + A2 \cos (2\pi F2\, t + \delta) \quad (35)$$

is given by

(i) K1 = 2 F1 if A1 A2 and A1 (A2 F2)/F1 (36)

(ii) K2 = 2 F2 if A2 A1 and A2 (A1 F1)/F2 (37)

(iii) K3, where K3 is between K1 and K2, if F1 F2 and A1 A2 (A1 F1)/F2 (38)

For the 2-user case MAC with ANZCPS demodulation, three frequencies are needed and only regions (i) and (ii) above are of interest, ie K1 and K2. By appropriate amplitude and frequency assignment, the demodulator output can be made to follow one of the frequencies of the composite signal in each symbol interval. Therefore, the only possible values of ANZCPS for the composite signal which can occur at the demodulator input are

K0 = 2 F0
K1 = 2 F1 (39)
K2 = 2 F2

The amplitude and frequency assignment of the 2-user, 3-frequency MAC system simulated was such that F0 F1 F2 and A0 A1 A2; Figure 9 shows this assignment.

5. RESULTS OF MAC SYSTEM TESTS

A simulation has been carried out of the situation in which multiple users are attempting to communicate with a number of destinations in the presence of additive Gaussian white noise (AGWN); T users, each radiating power P are assumed, as shown in Figure 10. Let

$$Y = \sum_{i=1}^{T} X(i) + Z \quad (40)$$

where Y is the channel output symbol, X(i) is the ith user constituent codeword symbol and Z is Gaussian white noise with zero mean and variance N.

The general method used for the simulation of this situation for all three bandpass MAC systems introduced in the previous section is to generate many test message bits over a range of normalised signal-to-noise ratio E_b/N_o.

In all three cases, the demodulators are preceded by bandpass filters to define the bandwidth of the demodulator input noise. The general decoding procedure in all three cases is based upon minimum-distance decoding in which the received codeword vector, Y, is compared with all the possible outputs. Typical plots of performance for the three 2-user systems are shown in Figures 11 - 16, in terms of each users bit error rate (BER) and overall system throughput efficiency, both as a function of E_b/N_o.

6. CONCLUDING REMARKS

This paper describes a number of CDMA-type systems that are being developed and tested for use in the dispersive radio channel environment. The system based upon aperiodic complementary sequence sets would appear to offer considerable potential for reliable and adaptive operation over poor paths.

The CCMA scheme has the potential for use with a multi-user radio MAC, although much more work remains to be done to increase the number of simultaneous users. Theoretically, it allows a greater efficiency of channel use than TDMA. Simple modulation/demodulation schemes have been implemented for practical 2-user CCMA systems to provide symbol recovery at the receiver without ambiguity. The performance

of the three systems tested is identical under noise-free conditions - as can be seen from the results of Figures 11 - 16; with AGWN, however, the bandpass MAC with intensity information and optimum demodulation gives the best results.

It should be noted that Figures 11 - 16 are obtained using a particular coding scheme. Improvements in performance resulting from the use of coding responsive to channel state are currently being evaluated.

7. ACKNOWLEDGEMENT

The authors wish to thank the UK Science & Engineering Research Council for its support of the work described in Section 2 of this paper.

8. REFERENCES

1. Massey, J.L. (Ed): IEEE Trans. Special Issue on Random-access Communications, Vol. IT-31, March 1985.

2. Darnell, M. & Honary, B.: "Multi-functional coding schemes applicable to secure communication", Proc. IEE Int. Conf. on "Secure Communication Systems", IEE CP-269, pp 74 - 81, London, 1986.

3. Golay, M.J.E.: "Complementary series", IRE Trans. Vol. IT-7, pp 82 -87, 1961.

4. Darnell, M.: "Principles and applications of binary complementary sequences", Proc. of Int. Symp. on "Theory and applications of Walsh and other non-sinusoidal functions", Hatfield, UK, 1975.

5. Darnell, M. & Kemp, A.H.: "The synthesis of multi-level complementary sequences", submitted for publication in Electronics Letters, 1988.

6. Farrell, P.G.: "Survey of channel coding for multi-user systems", in "New concepts in multi-user communication", Ed. by J.K. Skwirzynski, Sijthoff & Noordhoff, 1981.

7. Kasami, T. & Lin, S.: "Coding for a multiple-access channel", IEEE Trans. Vol. IT-22(2), pp 129 -137, 1976.

8. Kasami, T., Lin, S. & Yamamura, S.: "Further results on coding for a multiple-access channel", Proc. of Hungarian Colloquium on "Information theory", pp 369 - 391, Keszthely, August 1975.

9. Chang, S.C. & Wolf, J.K.: "On the T-user M-frequency noiseless multiple-access channel with and without intensity information", IEEE Trans Vol. IT-27(1), 1981.

10. Omura, J.K.: "Random coding bounds for non-coherent MFSK multiple-access channels", ITC/USA/79, Int. Telemetering Conf., ISA, Pittsburg, 1979.

11. Brine, A. & Farrell, P.G.: "Bandpass adder channel for multi-user (collaborative) coding schemes", Electronics Letts., Vol. 21(22), pp 1030 -1031, 1985.

12. Blachman, N.M.: "Zero-crossing rate for the sum of two sinusoids or a signal plus noise", IEEE Trans., Vol. IT-21, 1975.

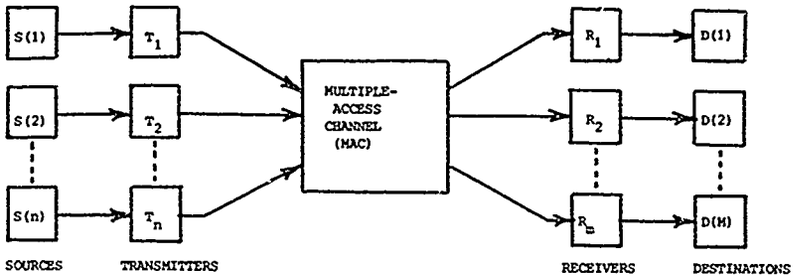

Figure 1: General Multi-User Communication System

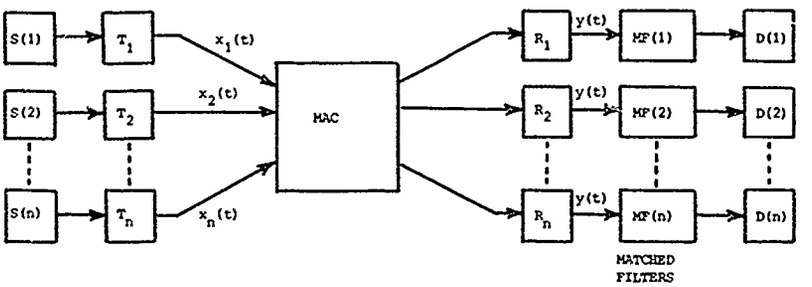

Figure 2: Generalised CDMA System

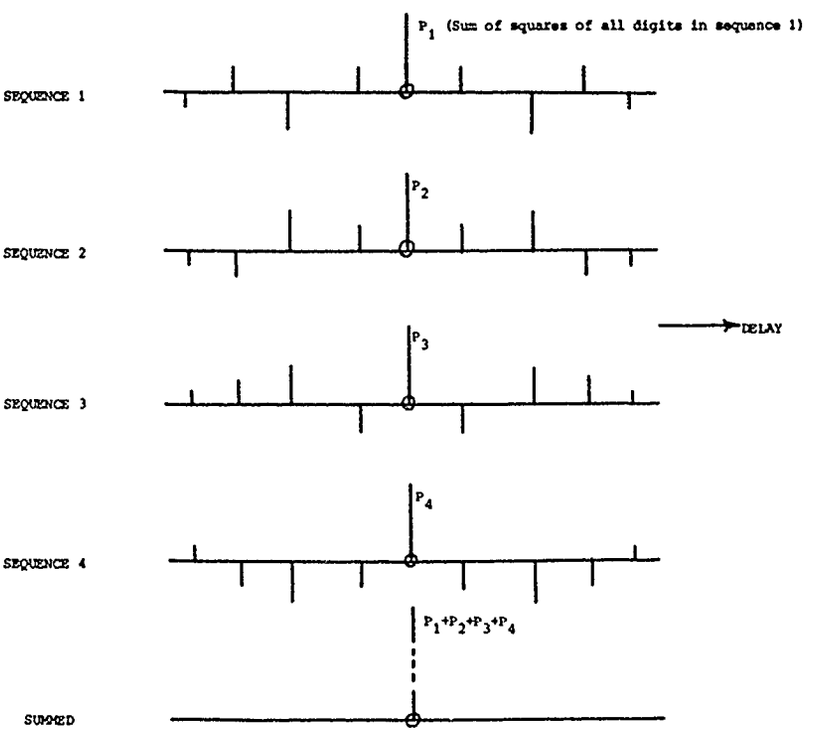

Figure 3: ACF's for a Set of 4 Complementary Sequences

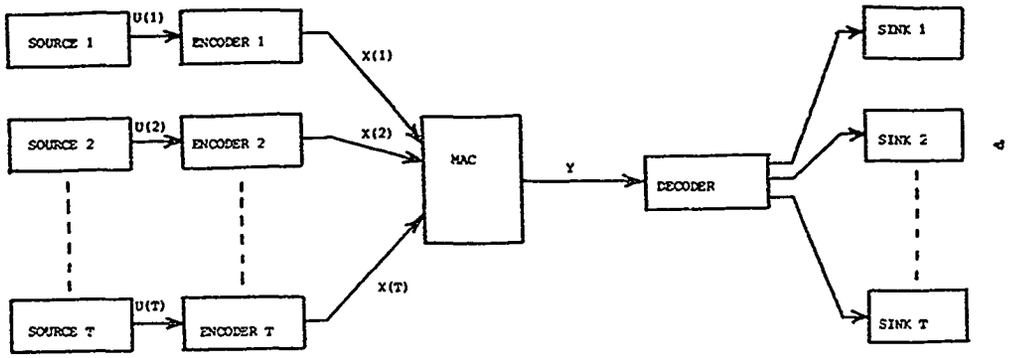

Figure 4: T-User Multiple-Access System

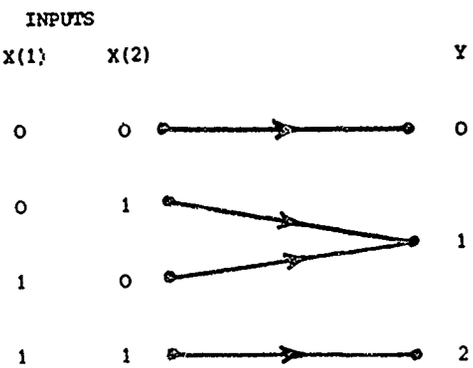

Figure 5: 2-User Baseband MAC Symbols

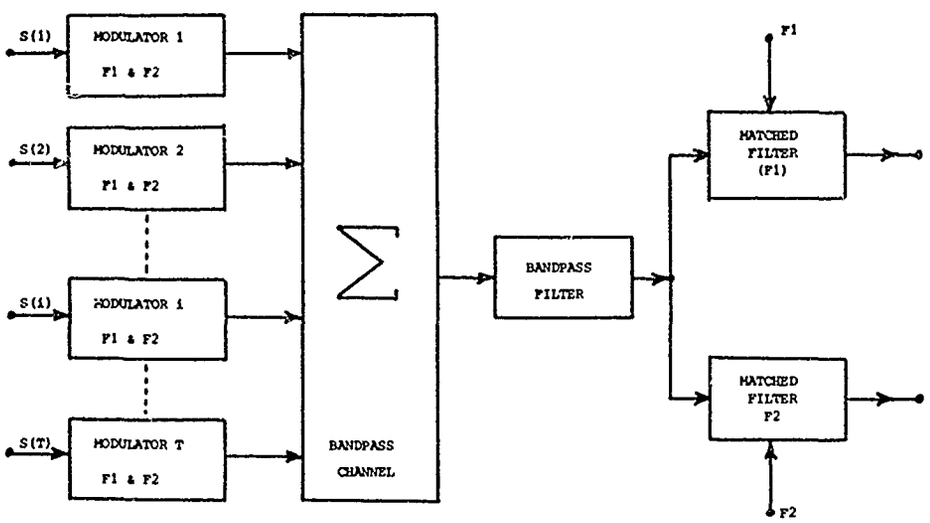

Figure 6: T-User Bandpass MAC with Matched Filter Detection

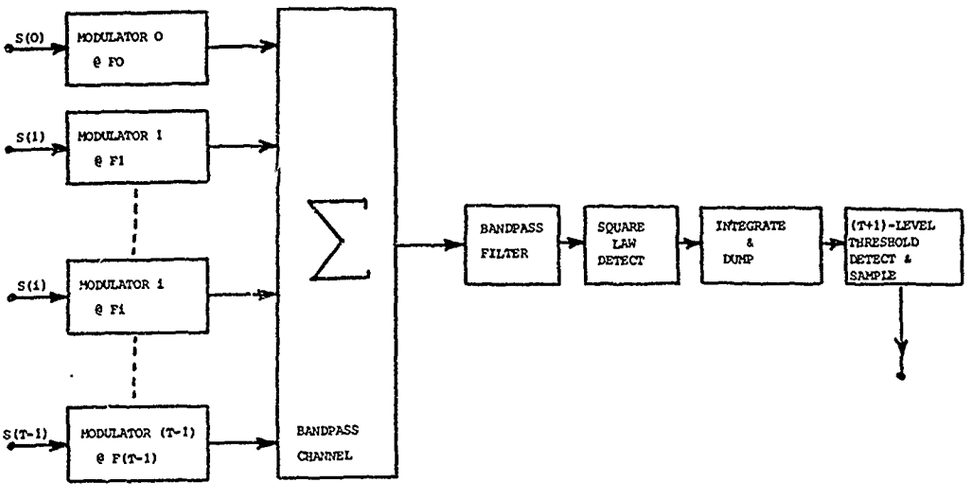

Figure 7: T-User Bandpass MAC with Square Law Detection

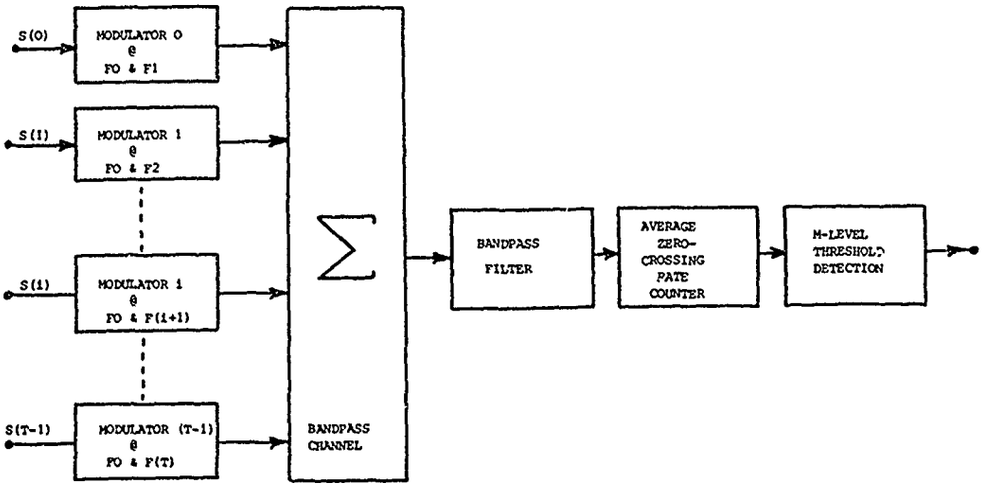

Figure 8: T-User Bandpass MAC with Average Zero-Crossing Rate Detection

S(0)	(S1)	AMP & FREQ USER 0	USER 1	ANZCPS
0	0	A0,F0	A0,F0	K0 = 2F0
1	0	A1,F1	A0,F0	K1 = 2F1
0	1	A0,F0	A2,F2	K2 = 2F2
1	1	A1,F1	A2,F2	

Figure 9: Amplitude & Frequency Assignment in 2-User 3-Frequency MAC

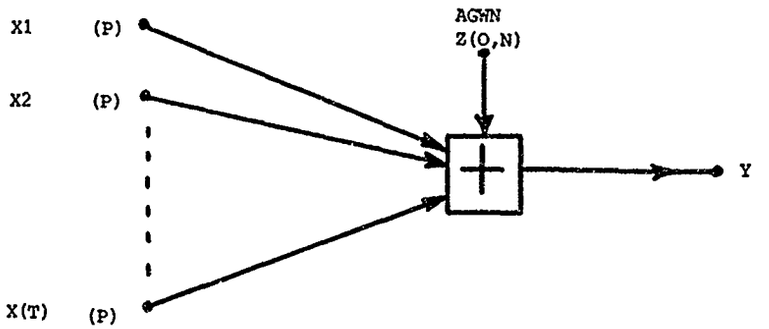

Figure 10: Noise Contamination Mechanism

Figure 11 2-User System One Log Output BER against Eb/No

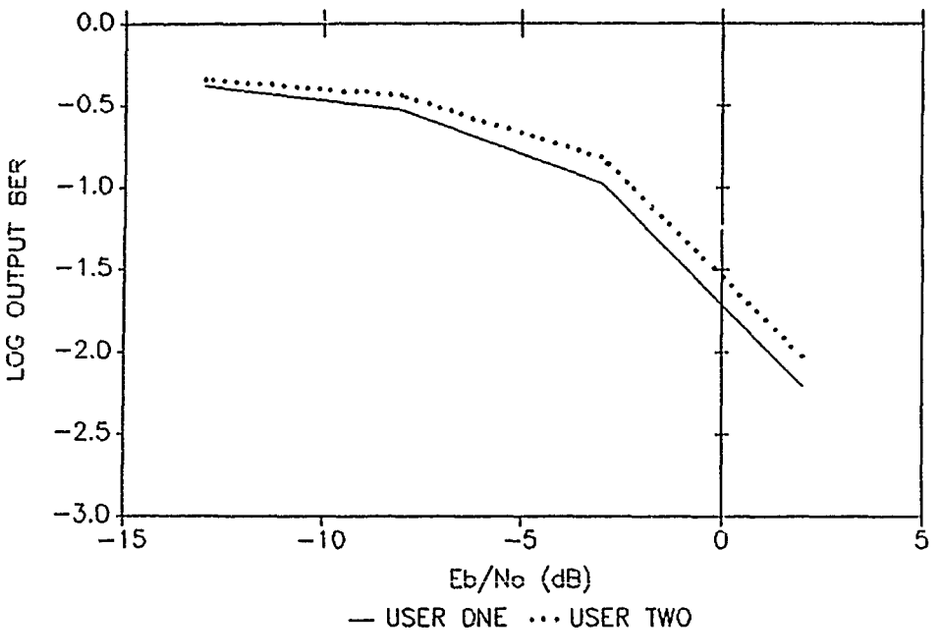

Figure 12 . 2-User System One Overall Throughput against Eb/No.

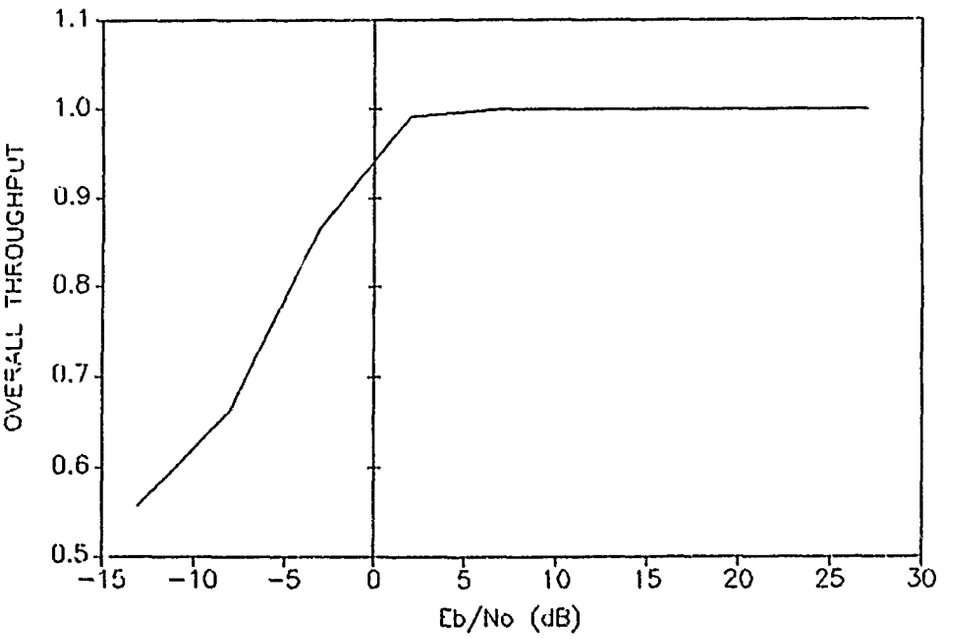

Figure 13 . 2-User System Two LOG Output BER against Eb/No

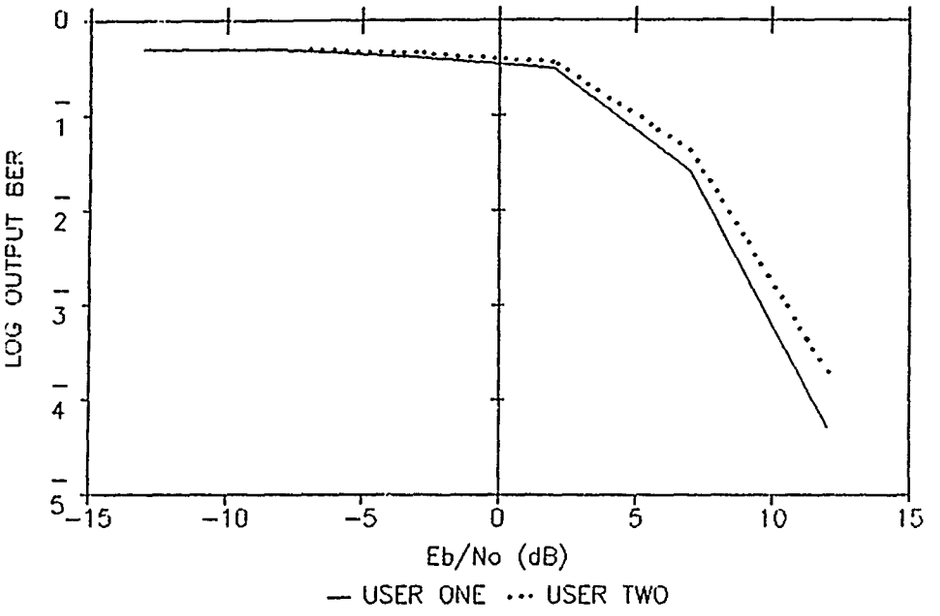

Figure 14 . 2-User System Two Overall Throughput against Eb/No

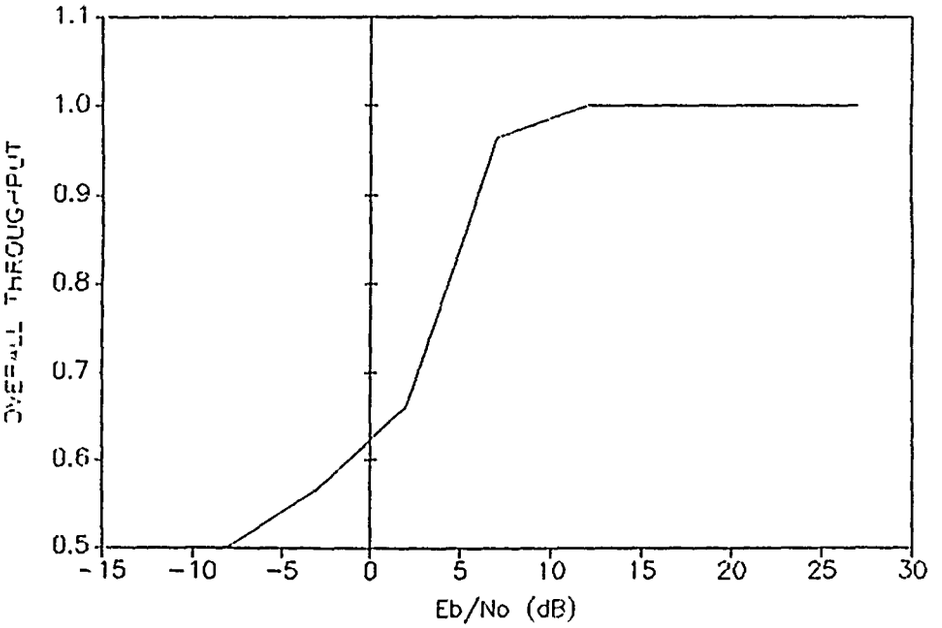

Figure 15 . 2–User System Three Log
Output BER against Eb/No.
(Freq Separation= 1/Ts)

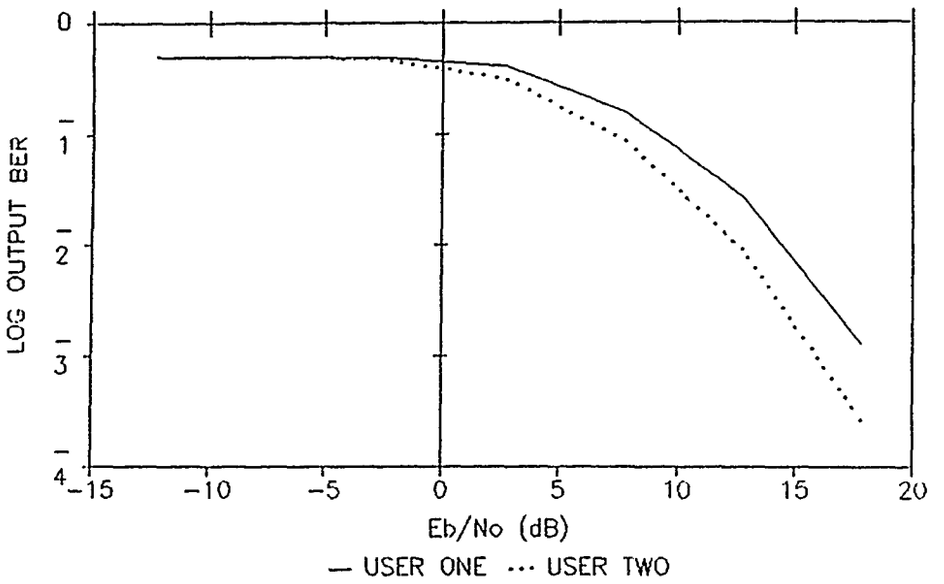

Figure 16 . 2–User System Three Overall
Throughput against Eb/No.
(Freq. Separation= 1/Ts)

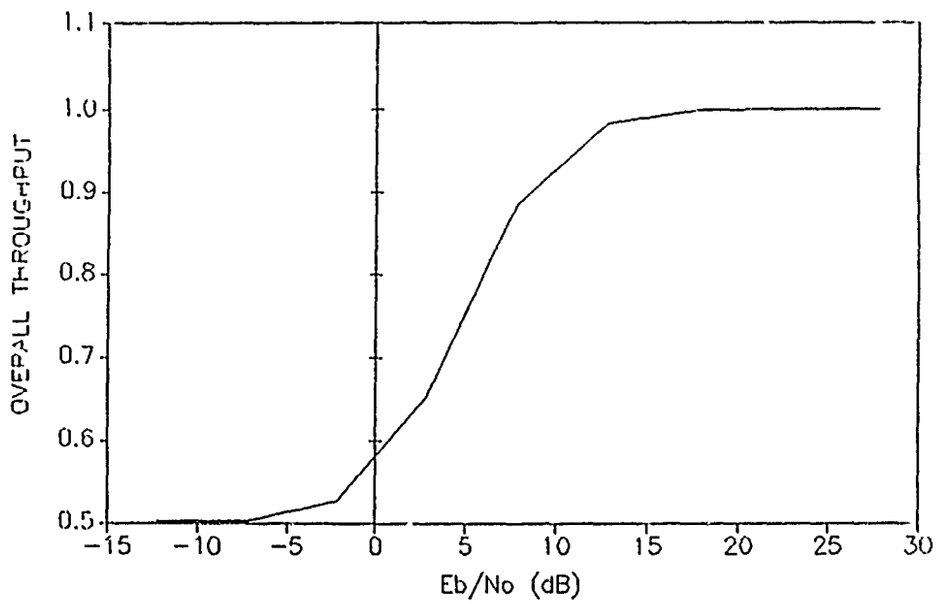

DISCUSSION

C. GOUTELARD

Des séquences complémentaires multiphases ont été étudiées, mais ma question porte sur les suites que vous proposez : vous formez un code. Quel est le nombre de vecteurs que vous obtenez pour une longueur de vecteurs (nombre de symboles) donnée ? Enfin, obtenez-vous des fonctions d'intercorrélation nulle et avez-vous comparé vos résultats avec la borne de Welch ?

AUTHOR'S REPLY

I should be most grateful if you could let me have the references you mention : we have not previously been aware of these.
In theory, the number of completely uncorrelated sets of sequences that can be synthesized is unlimited. In practice, larger sets require longer sequences, which may present a practical problem of transmission efficiency. Since the sets are totally uncorrelated, any practical limit on number of sets will be produced by channel effects which will depend on channel type.
At present, we can synthesize sets with even numbers of sequences of odd and even length, both binary or multi-level.

D.J. FANG

What size and what level of collision rate allowed for your networks. Is your transmission going to be slotted or unslotted ? My general comment is that your statment "No sync preamble is needed" may be reasonable only for small size and low collision rate system.

AUTHOR'S REPLY

We envisage initially networks of perhaps 5 or 6 HF terminals. Since the complementary sequence sets are completely uncorrelated, it is not necessary to use slotted transmissions : simultaneaous CDMA is possible to the extent that channel imperfections will allow.
No preambles are required because of the self-synchronization properties of the sequence sets by virtue of their ideal summed aperiodic autocorrelation functions.

A VERSATILE INTEGRATED BLOCK CODES ENCODER-DECODER
Codeur-Décodeur Intégré de Codes en Blocs

P.A LAURENT

THOMSON-CSF Division Télécommunications
66, rue du Fossé Blanc - 92231 GENNEVILLIERS Cedex - FRANCE

SUMMARY

This paper presents a new VLSI circuit which is designed to perform encoding and decoding of almost all Reed-Solomon and BCH codes (including generalized BCH) using symbol sizes from 1 bit to 8 bits.

It is fully programmable by many standard microprocessors which consider it like any other more common co-processor.
Its architecture allows a high bit rate and a great flexability.
The interfacing protocol is optimized for minimizing timing constraints (mail boxes) and limiting programming effort : no advanced knowledge of codes is required to use it.

RESUME

On présente ici un nouveau circuit VLSI conçu pour effectuer le codage et le décodage de la plupart des codes Reed-Solomon et BCH (dont les codes BCH étendus) utilisant des symboles comportant entre 1 et 8 bits d'information.
Ce circuit est entièrement programmable par différents microprocesseurs standard qui le considèrent comme un co-processeur de codes.
Son architecture permet à la fois un débit élevé et une grande flexibilité.
Un soin particulier a été apporté au protocole d'interfaçage qui minimise les contraintes temporelles (système de "boîte aux lettres") ainsi que l'effort de programmation qui ne nécessite aucune connaissance approfondie des codes.

1. PRESENTATION

Les systèmes de transmission de données numériques sont de plus en plus nombreux et de plus en plus exigeants : on cherche à transmettre sur un canal donné de plus en plus de communications simultanées, et pour chacune d'entre-elles, un débit utile de plus en plus élevé.
Lorsque la qualité des données reçues est fondamentale pour l'efficacité de la liaison, ce qui est courant, ceci conduit à la nécessité d'utiliser des procédés permettant de corriger les perturbations dues au canal lui-même (ex : canal HF), aux autres usagers (canal encombré) et/ou à des brouilleurs volontaires(liaisons tactiques ou stratégiques).
De même, pour un canal donné, la théorie montre que l'utilisation d'un système de codage permet d'accroître le débit d'information utile, du moins lorsque la qualité de départ n'est pas trop dégradée.

Dans les deux cas, le codage à utiliser doit être adapté au niveau des perturbations que l'on doit supporter, à leur structure (dispersées ou en paquets), et aussi au système de modulation utilisé : il est évident que l'on doit utiliser deux codes différents pour une transmission FSK 1200 bauds filaire classique et pour un système évolué à étalement de spectre par séquences orthogonales.

Enfin, dans beaucoup d'applications, il est souhaitable que, si une partie du message est trop perturbée pour être correctement restituée à la réception, ceci n'ait aucune conséquence facheuse pour les parties adjacentes : ceci suppose l'utilisation de codes détecteurs et correcteurs d'erreurs structurés en blocs.

On expose ci-après les principes de ce type de codage et la nature des algorithmes utilisés, avant de décrire le circuit RSBCH (du nom des codes qu'il met en oeuvre) et d'en donner les performances dans quelques cas significatifs.

Le lecteur désirant davantage de détails sur les codes se reportera avec profit aux références [1], [2], [3] et [4].

2. CODAGE ET DECODAGE

2.1. DEFINITION D'UN CODE

Le message à transmettre est composé de SYMBOLES, qui peuvent être des bits isolés ou des caractères regroupant 2 bits ou plus (typiquement, de 2 à 8 bits).

Les symboles sont regroupés par paquets de K symboles auxquels on rajoute N-K symboles de même nature pour former des MOTS DE CODE de longueur K, notés (N,K).

Le nombre de symboles rajoutés, appelés symboles de redondance, est fonction croissante des performances du code : plus ils sont nombreux, plus grand est le nombre d'erreurs qu'il sera possible de corriger.

Ces symboles de redondance sont en effet déduits des K symboles originaux (symboles d'information) par une série d'équations connues à la fois de l'émetteur et de récepteur. Le récepteur, ne connaissant pas avec certitude le contenu du message est obligé de supposer qu'il comporte un certain nombre d'errata acceptables.

Les errata sont de deux sortes :

1. Les EFFACEMENTS : le démodulateur a un doute sur la qualité d'un symbole donné, et il le signale au décodeur, qui devra en reconstituer la vraie valeur (une inconnue) ;
2. Les ERREURS : le démodulateur a commis une erreur franche et ne s'en est pas aperçu, si bien que le décodeur devra à la fois trouver la position de l'erreur (une inconnue) et sa valeur (deuxième

inconnue)

Le nombre total d'inconnues ne pouvant dépasser le nombre d'équations disponibles, le décodeur pourra corriger n'importe quelle configuration d'errata telle que la somme du nombre d'effacements et du double du nombre d'erreurs soit inférieure ou égale au nombre d'équations indépendantes disponibles.

D'une manière générale, on choisit le système d'équations définissant le code de telle sorte que le nombre d'équations indépendantes pour des valeurs de N et de K données soit le plus élevé possible et que le codage et le décodage soient faisables de la façon la plus simple possible (donc la plus rapide).

Les codes de base choisis ici sont les codes Reed-Solomon (RS), qui présentent ces caractéristiques, et qui sont les plus connus, donc les plus utilisés.
Ces codes traitent intrinsèquement des symboles à plusieurs bits (par exemple, des octets).
On peut les contraindre à n'utiliser que des symboles plus courts (donc pouvant prendre moins de valeurs différentes), ce qui conduit aux codes BCH (symboles de 1 bit) et a tous les codes intermédiaires (appelés ici BCH étendus). ceci a pour effet de rajouter aux équations définissant le code RS de base des équations supplémentaires, non indépendantes (donc n'améliorant pas les performances en nombre d'errata corrigés) et d'augmenter le nombre de symboles en redondance et réduire le débit utile.
La figure 1 montre, pour des codes (N = 63, K variable), le nombre de symboles de redondance qu'il faut rajouter en fonction du nombre d'erreurs à corriger, pour un code RS et les codes BCH (étendus ou non) qui s'en déduisent.
La figure 2 donne la probabilité que le décodage ne soit pas correct pour deux codes de redondance voisine de 2 (autant de symboles d'information que de symboles de redondance) de types RS et BCH en fonction de la probabilité d'erreur par symbole (de 6 bits ou de 1 bit) en entrée du décodeur.

On notera - et ceci est le cas général - que,lorsque cette probabilité d'erreur est par trop élevée (par exemple, 10% avec un code BCH), l'utilisation d'un code dégrade les performances au lieu de les améliorer. Il convient donc de choisir soigneusement le code en fonction de la qualité de bas de la liaison.
Une manière efficace de procéder dans les cas difficiles est d'interdire au décodeur de corriger s'il détecte un nombre d'errata supérieur à un seuil donné. On doit alors procéder plus souvent à des répétitions du message, mais ceci optimise globalement le rendement de la liaison.

2.2. ALGORITHMES DE CODAGE

Le codage se fait comme indiqué plus haut, en calculant les symboles de redondances en tant que combinaisons LINEAIRES pondérées des symboles d'information.
Ceci suppose l'utilisation de multiplications et d'additions, sur des nombres (les "valeurs" des symboles) qui ne peuvent prendre qu'un nombre fini de valeurs : en effet, un symbole de m bits ne peut prendre que 2^m valeurs différentes. Ceci est possible en convenant que les symboles représentent des éléments d'ensembles finis appelés Corps de Galois, ou de telles opérations sont possibles.

2.3. ALGORITHMES DE DECODAGE

Le décodage consiste à écrire toutes les équations disponibles en supposant la configuration d'errata maximale, puis à les résoudre.
Bien que les équations de départ soient linéaires, les équations du décodage sont non linéaires pour les positions des erreurs (assimilables à des exponentielles inconnues). Il existe cependant plusieurs algorithmes pour les résoudre en fournissant la solution la plus vraisemblable parmi toutes les solutions possibles. On utilise ici une combinaison de l'algorithme de Berlekamp [1] (pour déterminer les positions des erreurs) et du décodage par transformée [4] (pour reconstituer les symboles faussés) en raison de leurs performances : rapidité pour l'un, possibilité de "vectorisation" pour l'autre, mise à profit dans le circuit.

2.4. CODES TRAITES

Le circuit peut traiter la plupart des codes RS, BCH et BCH étendus dont les symboles comportent entre 1 et 8 bits d'information.

D'une manière générale, lorsque le code Reed-Solomon de base est construit sur des symboles de m bits, la longueur N des mots de code est au maximum égale à 2^m-1 (255 pour des octets).
Toutes les longueurs inférieures sont autorisées, par la méthode du raccourcissement du code : on met implicitement à zéro les premiers symboles du code de plus grande longueur, et l'on ne les transmet pas.
De même, presque toutes les capacités de correction (dont se déduit K, nombre de symboles utiles par bloc) sont autorisées. Seules sont interdites les capacités très élevées (qui ne se justifient pas dans la pratique) qui conduiraient à un sur-dimensionnement inutile des mémoires internes au circuit.

De plus, conformément à ce qui a été dit plus haut, il est possible de demander au circuit de corriger moins d'erreurs qu'il ne pourrait le faire pour améliorer les performances de la liaison.

Enfin, pour tous les codes, on fournit en entrée du décodage, et pour chacun des symboles reçus (y compris les symboles binaires) un bit de validation qui indique si le symbole est présumé bon ou non (gestion des effacements) et le décodeur fournit en retour si on le désire des informations sur le décodage : détection de dépassement de capacité, ou nombre/nature des errata détectés et corrigés. Ceci permet de gérer la liaison, notamment en adaptant le code aux conditions de transmission, ou encore en détectant les mauvaises synchronisations (cadrage erroné des mots de code).

3. CIRCUIT RSBCH

3.1. ARCHITECTURE

L'architecture générale du circuit RSBCH a été partiellement déduite de celle du codeur-décodeur présenté dans [5], et est différente decelles proposées dans [6], [7], [8] et [9], les trois dernières références étant plus particulièrement consacrées à la définition de composants élémentaires des-

tinés à réaliser des processeurs adaptés à de très hauts débits.

Cette architecture est présentée figure 4.
Elle comporte quatre ensembles distincts, décrits ci-après.

* SEQUENCEUR : le circuit est du type microprogramme, au même titre que d'autres co-processeurs plus connus (ex : 68881). Il nécessite donc un séquenceur, qui est chargé de la lecture et de l'exécution du programme stocké en mémoire morte (ROM), assisté d'un "compteur de boucle polynômiale" pour la vectorisation de certaines opérations de codage/décodage.

* PROCESSEUR ARITHMETIQUE : ce processeur est essentiellement une unité arithmétique et logique (UAL) simplifiée chargée de faire les calculs simples (additions, soustractions, comptages,...) nécessaires dans les algorithmes et les entrées-sorties.

* PROCESSEUR GALOIS : c'est lui le coeur du dispositif, spécialement conçu pour les traitements scalaires et polynomiaux dans les Corps de Galois (CG).
Outre des mémoires pour les mots de codes et les vecteurs intermédiaires, il comporte un multiplieur combinatoire et entièrement programmable pour s'adapter à n'importe quel CG (la définition d'un CG se fait en précisant la valeur binaire d'un élément particulier, appelé générateur du corps, comportant un nombre de bits égal à la largeur des symboles dans le code RS de base). L'ensemble est optimisé pour les opérations de multiplication/division polynômiales qui sont la base des algorihtmes utilisés.

* INTERFACE : cet interface comporte des registres accessibles directement de l'extérieur, la logique de dialogue, et une "boîte à lettres" (FIFO : Fisrt In, First Out) servant de tampon avec le processeur hote.
Des connexions du circuit sont réservées à la configuration des échanges pour s'adapter à différents microprocesseurs hôtes : PSM, 68XX, 680XX, ADSP2100, TMS320XX, 8066,...

3.2. TECHNOLOGIE

Le circuit est réalisé en technologie CMOS à géométrie de 1.25um.
Sa surface est de l'ordre de 50mm^2 , et il est présenté dans un boîtier DIL 40 broches.
Sa consommation est de 25mW par MHz, soit 250mW à la fréquence maximale d'horloge qui est de 10MHz.

Lorsqu'il n'est pas en train d'effectuer des opérations d'initialisation, codage ou décodage, il se met automatiquement en mode veille, ou il ne consomme plus que 5mW.

Enfin, il comporte un auto-test intégré qui peut être activé de l'extérieur au démarrage.

3.3. UTILISATION DU CIRCUIT

Le circuit est entièrement paramétrable.

Le processeur hote est à tout instant en mesure de redéfinir son mode de fonctionnement, en précisant les points suivants :

- nombre de bits par symboles ;
- nature du code : RS, BCH, BCH étendu ;
- générateur du Corps de Galois ;
- capacité de correction théorique des codes à utiliser ;
- capacité de correction effective (inférieure ou égale à la précédente) ;
- longueur des codes (deux longueurs : code normal, et code raccourci, ce dernier étant généralement utilisé en tant qu'en-tête (Header) des blocs de messages relatifs à un échange donné).

Cette redéfinition est suivie d'un temps d'initialisation après lequel le circuit est disponible pour des opérations de codage ou décodage sur l'un ou l'autre des deux codes, sans phase de ré-initialisation.

Pour chaque opération de codage, l'extérieur fournit les symboles d'information du mot de code (K symboles) et lit en sortie le mot de code complet (N symboles).
Pour un décodage, il écrit les N symboles reçus accompagnés de leurs indicateurs de validité, et lit en sortie le résultat de décodage : succès/échec, nombre d'errata en cas de succès, et bien entendu le mot décodé.

3.4. PERFORMANCES

Le circuit RSBCH a été conçu de telle sorte que le fait qu'il soit entièrement paramétrable n'enlève rien au niveau des performances.
En effet, à sa fréquence maximale d'horloge (10MHz), le débit utile (symboles d'information seuls) dépasse aisément 100 Kbits/s même pour des codes de forte capacité de correction.

La figure 5 donne des exemples dans quatre cas caractéristiques.

- code RS (31,15) à symboles de 5 bits (utilisé dans les systèmes JTIDS et SINTAC), véhiculant 15 x 5 = 75 bits d'information par mot de code, et capable de corriger 8 erreurs parmi 31 (ou 16 effacements, ou une combinaison d'erreurs et d'effacements où le nombre d'erreurs Nberr et le nombre d'effacements Nbeff sont tels que 2.Nberr + Nbeff < 17) : l'initialisation prend 70us, un codage nécessite 73us, et un décodage 410us, ce qui conduit à un débit utile de 183Kbits/s.

- Code BCH (31,15), qui ne corrige que 3 erreurs et un effacement supplémentaire ou 7 effacements ou erreurs et effacements, déduit du précédent (code binaire) : la durée d'initialisation est légèrement supérieure à celle du code RS, et, bien que la durée d'un décodage soit plus faible (270us), le débit utile est inférieur au tiers du précédent, puisque le code ne véhicule que 15 bits d'information par mot de code.

- Code RS (255,223), à symboles de 8 Bits, corrigeant 16 erreurs (utilisé par la NASA), dont chaque mot de code véhicule 1784 bits d'information (!) ce qui fait que, même avec une durée de décodage de 7.5ms, le débit maximum est de 238 Kbits/s.

Code BCH (255,223), code binaire déduit du précédent et ne corrigeant que 4 erreurs, pour lequel le débit est réduit de moitié environ (112 Kbits/s).

On rappelle que le circuit RSBCH n'est pas limité aux seuls codes cités ci-dessus (voir figure 3) et que ses performances sont fonction du code choisi : longueur des mots de code, capacité de correction, nombre de bits par symboles.

4. CONCLUSIONS

Le codeur-décodeur de codes en blocs objet du présent article doit être considéré comme un composant standard, d'usage général dans les transmissions de données, tant en raison de sa très grande flexibilité que parce qu'il est d'emploi aisé et de performances élevées.

Il assure a lui seul toutes les tâches habituellement réalisées à grands frais par des processeurs standard mal adaptés donc lents, et permet donc de laisser le processeur de gestion faire ce pour quoi il est conçu.

Il représente pour cela un important pas en avant par rapport à l'état de l'art antérieur où des codes plus simples (répétition) étaient souvent mis en oeuvre pour cause de difficulté (sinon impossibilité) de mise en oeuvre.
Son intégration est actuellement en phase finale, et les premiers prototypes seront disponibles au début de 1989.

BIBLIOGRAPHIE

|1| E.R BERLEKAMP, Algebraic Coding Theory, Mc Graw-Hill, 1968

|2| W.W.PETERSON & E.J.WELDON, Error Correcting Codes, MIT Presse, 1972

|3| G.C.CLARK & J.B.CAIN, Error correction Coding for Digital Communications, Plenum Press, 1982.

|4| R.L.MILLER, T.K.TRUONG & I.S.REED, Efficient Program for Decoding the (255,223) RS Code over GF (2^8) with both Errors and Erasures, using Transform decoding, IEE Proc. 127, Pt E, N°4.

|5| E.LENORMAND, Réalisation d'un Codeur-Décodeur (31,15) de Reed-Solomon, Revue Technique THOMSON-CSF, 12, 1980 .

|6| L.M.H.E.DRIESSEN & H.T.KANTERS, A High Speed Encoder-Decoder for a RS Code with Minimum Distance at most seven, International Zurich Seminal on Dig. Comm., 1984.

|7| P.G.FARREL, Influence of LSI and VLSI Technology on the Design of Error-Correction Coding Systems, IEEE proc, 129, Pt F, N°5, October 1982.

|8| K.Y.LIU, Architecture for VLSI Design of RS Encoders, IEEE Trans on Computers, C-31, N°2. Feb. 1982.

|9| K.L.LIU, Architecture for VLSI Design of RS Decoders, IEEE Trans on Computers, C-33, N°2, Feb.1984.

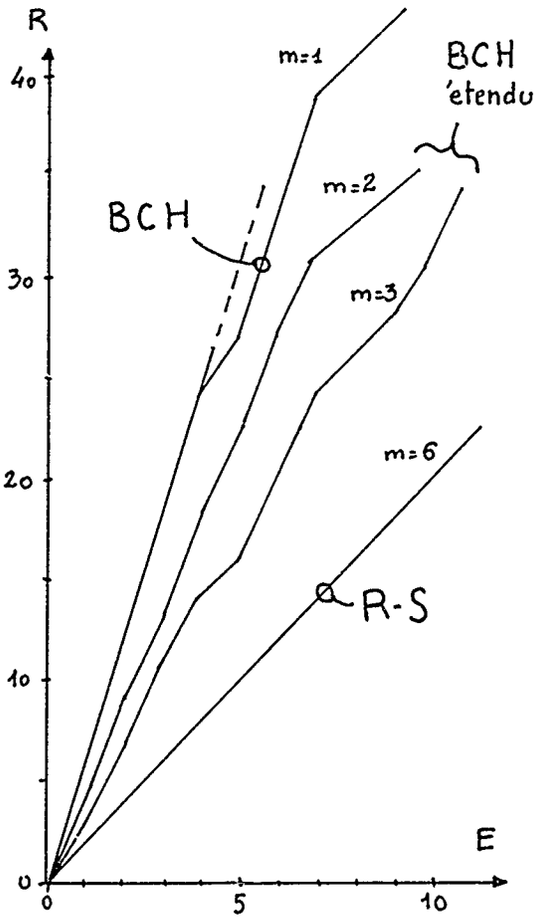

Figure 1

Comparaison des codes RS et BCH.
Nombre de symboles de redondance necessaires pour corriger le nombre d'erreurs figurant en abscisse.
Le code de base est du type RS(63,K).
Le parametre m est le nombre de bits par symbole.

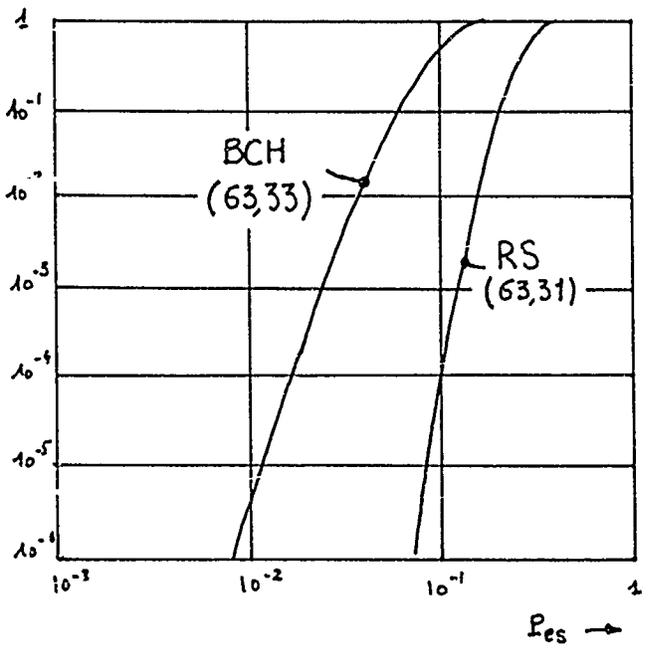

Figure 2

Performances comparees de deux codes de redondance voisine de 2:
-Code RS(63,31) corrigeant 16 erreurs;
-Code BCH(63,33) corrigeant 6 erreurs.
Les courbes donnent, en fonction de la probabilite d'erreur en entree du decodeur, la probabilite que la capacite de correction soit depassee.

CODES Reed-Solomon et BCH

Nature du code	N max (longueur des plus grands mots de code)	Capacite de correction maximale et code correspondant
Reed-Solomon et BCH (*)	7, 15, 31, 63 (RS: 3, 4, 5, ou 6 bits par symbole)	Pas de limite
Reed-Solomon	127 (7 bits/symb.)	C <= 113 : RS (127,14)
BCH (*)	127	C <= 63 : BCH (127,7)
Reed-Solomon	255 (8 bits/symb.)	C <= 120 : RS (255,135)
BCH (*)	255	C <= 119 : BCH (255,12)

(*) Codes BCH: 1 bit par symbole

CODES BCH ETENDUS

Nombre de bits par symbole	N max (longueur des plus grands mots de code)	Capacite de correction maximale et code correspondant
2	15	Pas de limite
2	63	Pas de limite
3	63	Pas de limite
2	255	C <= 119 : BCHe (255,33)
4	255	C <= 119 : BCHe (255,80)

Figure 3

Tableaux donnant la liste des codes RS et BCH traites par le circuit BCH, ainsi que les codes BCH etendus.
La capacite de correction C est le nombre maximum d'effacements qui peuvent etre corriges; le code peut corriger quand la relation suivante est verifiee:

$$2.\text{Nb erreurs} + \text{Nb effacements} < C+1$$

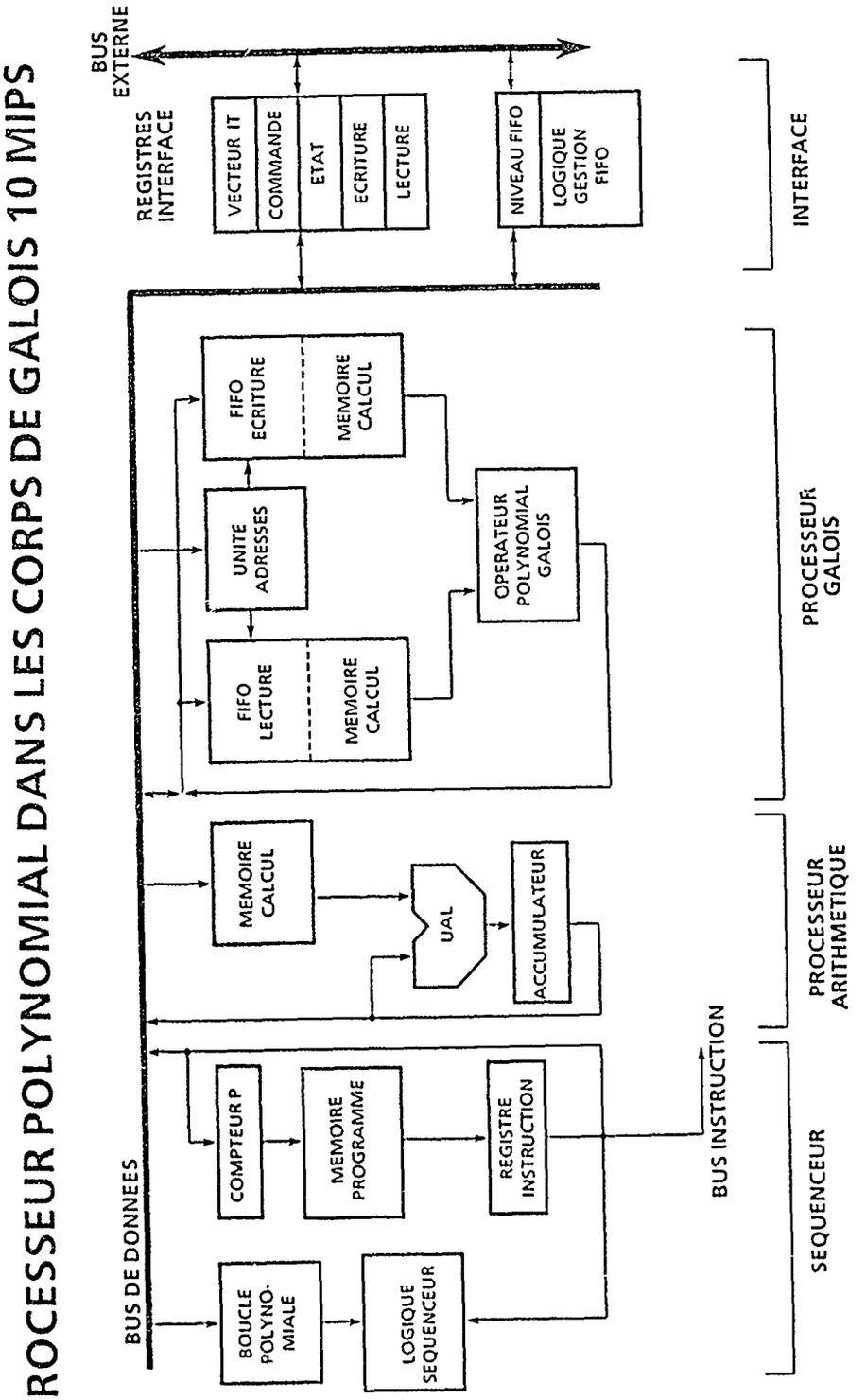

Figure 4

Architecture generale du circuit RSBCH.

Code utilise	C	Init (us)	Codage (us)	Decodage (us)	Debit UTILE (Kbits/s)
RS (31,15)	16	70	73	410	183
BCH (31,15)	7	100	73	270	56
RS (255,223)	32	4000	1500	7500	238
BCH (255,223)	8	5500	800	2000	112

Figure 5

Temps d'execution des differentes operations et debit utile maximum possible pour 4 codes BCH et RS. L'initialisation ne doit etre effectuee que lorsqu'il y a changement de codes.
La capacite de correction C a la meme definition que celle utilisee figure 3.

DISCUSSION

K.S. KHO

1 - Could give me some reasoning behind the choice of RS and BCH coding schemes.

2 - Could we make a combination of RS & RS instead of RS and BCH, based on your graph which shows that RS performs better than BCH. What would be the problem if you make a RS & RS combination ?

AUTHOR'S REPLY

1 - RS codes are among the most powerful error/erasure correcting codes. They are also the best known ones and there exists simple and efficient algorithms for coding and decoding.
BCH codes are a subset of RS codes, where the symbols are constrained to be binary (two valued).

2 - The graph shows that RS performs better than BCH and that intermediate codes have intermediate performances.
No code combination is investigated here.

C. GOUTELARD

Comment programmez-vous vos codes : par le polynôme générateur ou par un autre moyen ?
Par ailleurs comment faites-vous les multiplications sur les corps de Galois ? Est-ce par Tables ?

AUTHOR'S REPLY

1 - La programmation des codes se fait en indiquant au circuit :
- la nature du code (BCH, RS, ...)
- la longueur des mots de code (deux codes différents)
- la capacité de correction théorique et la capacité de correction effective demandée (inférieure ou égale)
- l'élément α générateur du corps de Galois souhaité.

2 - Le multiplicateur est de type combinatoire, avec "pipe-line" : une multiplication/accumulation se fait en une seule instruction.

D.J. FANG

Have you developed the external processor required for given instructions to your monolithic processor discussed in your paper, the coding algorithm (BCH-RS concatenation, blocksize, etc...) on an instantaneous basis ? If this external processor is yet to be developed, how can one use your coding processor for real-time adaptive application ?

AUTHOR'S REPLY

1 - The external processor is a standard off-the-shelf processor (68xx, 68xxx, TMS320, 8086, ADSP2100) ; it considers the RS BCH like any other coprocessor/peripheral (ex : 68881/2, ACIA, SSDA, MMU, ...).

2 - It can change the codes at any time, and this change is under its own responsibility, considering for example the number of errors detected by the RS BCH, which is available as a by-product of decoding.

DISCUSSION

U. SEIER

How did you solve the synchronization problem under the aspect of block lengths of up to 255 symbols/block ?

AUTHOR'S REPLY

The host processor can read the number of errors which have been detected by the circuit.
If the demodulator or any external device indicates good reception conditions and if the RS BCH detects systematically errors, this is an out-of-lock condition : the external processor has to shift the symbol input streams.

MINIMISATION DU COUT DE TRANSFERT DE L'INFORMATION DANS LES TRANSMISSIONS HF A ETALEMENT DE SPECTRE

C. GOUTELARD - J. CARATORI
Laboratoire d'Etude des Transmissions Ionosphériques
94230 CACHAN - FRANCE

RESUME

L'étalement de spectre est une technique bien connue qui prend cependant un aspect particulier en HF à cause de la dispersivité du canal et des interférences particulièrement importantes.

Les contraintes imposées par ce canal et leurs effets sur le signal sont analysés. Les caractéristiques du bruit et des interférences sont déterminées par une série de mesures sur lesquelles est appliqué un calcul statistique.

Les effets des contraintes dues au canal et aux interférences sont pris en compte pour définir différentes stratégies possibles. Il est alors montré qu'il est possible de minimiser le coût de transfert de l'information défini par la quantité d'énergie nécesaire pour transmettre un Shannon d'Information dans le cas d'un étalement du spectre parfait ou semi parfait.

La comparaison des différentes stratégies est faite. Le choix peut être effectué par la complexité tolérée des opérations à effectuer pour la détection.

I. - INTRODUCTION -

L'utilisation de larges bandes dans le domaine des ondes décamétriques se heurte à deux types de problème.

Le premier est lié directement aux caractéristiques du canal dont la dispersivité, si elle n'est pas corrigée, introduit des distorsions inadmissibles.

Le second est causé par les interférences extrêmement fortes dans ce domaine et qui font que la puissance du bruit ne varie pas linéairement en fonction de la largeur de bande utilisée, mais plus rapidement.

Le transfert de l'information par étalement de spectre pose le problème du choix optimum de la bande utilisée et des taux de compression susceptibles d'être atteints.

On examine dans cet article les limites imposées par le canal et l'encombrement spectral sur les bandes d'étalement possibles dans la zone Europe occidentale. Il ressort de cette étude que les bandes utilisables sont inférieures à celles que souhaitent les utilisateurs. Une stratégie consistant à masquer les parties brouillées du spectre est alors examinée. Le compromis entre l'altération du signal et la réduction du bruit fait apparaître la valeur optimale de la bande d'étalement à choisir.

L'application aux cas concrets du spectre HF donne les ordres de grandeur de ce que l'on peut attendre.

II. - LIMITATIONS APPORTEES PAR LE CANAL IONOSPHERIQUE -

Les ondes électromagnétiques décamétriques sont utilisées dans les propagations par réfractions ionosphériques pour les liaisons grandes distances et le mécanisme de ces propagations est bien connu.

Différents facteurs affectent ces propagations :

- Le milieu est dispersif et les effets des variations du temps de groupe ont d'abord été étudiés par les distorsions introduites sur la propagation des impulsions de courte durée par BUDDEN [1961], SUNDE [1961], EPSTEIN [1968] et autres. MILSON et SLATOR [1982] ont cherché les limites des bandes utilisables dans le cas de transmissions en étalement de spectre par des séquences directes et par des sauts de fréquence. Ces auteurs donnent pour des séquences directes une vitesse de modulation $Cr = (\frac{1,5}{dTg/df})^{\frac{1}{2}}$ symboles par seconde pour une perte de 3dB du rapport signal/bruit, où dTg/df est la dérivée du temps de propagation par rapport à la fréquence. Pour des pentes de 10 μs/MHz la vitesse de modulation est de 387 kbands et de 122 kbauds pour une pente de 100 μs/MHz.

  Dans le cas d'étalement par modulation de fréquence ces mêmes auteurs donnent une bande utilisable :

$$Be \leqslant \frac{1}{10\ Hr\ \frac{dTg}{df}}$$

  où Hr est la fréquence des sauts.

  Cette bande est imposée par les limites de la gigue de phase qui ne doit pas excéder le dixième de la durée d'un palier.

  Ainsi, pour une pente de 10 μs/MHz et Hr = 3KHz, la bande utilisable est Be = 3,3MHz et elle vaut encore 330KHz pour une pente de 100μs/MHz.

- Le milieu est anisotrope et les deux modes de propagation, ordinaire et extraordinaire, inséparables par les critères temporels, altèrent la fonction de transfert dans laquelle apparaissent les caractéristiques des évanouissements sélectifs. Ce phénomène, l'effet Faraday, introduit des évanouissements profonds lorsque les deux modes sont, au lieu de réception, d'amplitudes comparables. La fréquence d'émission joue un rôle important et les bandes utilisables [Salons 1985] délimitées par les évanouissements dépassant 6dB, peuvent varier dans une grande plage s'étendant jusqu'à 1MHz avec des valeurs typiques de 100 à 200KHz.

- La non stationarité du canal introduit des variations de sa fonction de transfert dont la correction par des systèmes auto adaptatifs est particulièrement ardue en large bande.

- Les trajets multiples peuvent être séparés par des critères temporels si la bande d'étalement est suffisante.
  Dans le cas où ils ne le sont pas, comme par exemple au voisinage des fréquences de jonction, ils introduisent des évanouissements sélectifs dans la fonction de transfert.

- La présence d'irrégularités ionosphériques introduit des focalisations secondaires, des effets Doppler, des absorptions qui sont susceptibles de modifier encore les caractéristiques du canal.

Ces effets sont bien connus et ont été étudiés, pour certains, depuis très longtemps. Des modems ou des systèmes expérimentaux développés dans les dernières années [6] [7], ont montré que des bandes d'étalement de l'ordre de 100KHz pouvaient être utilisées sans que celà constitue une borne supérieure.

Les caractéristiques de transmission du canal ne sont pas les seules limites imposées à l'étalement de spectre dans le domaine décamétrique. L'encombrement spectral y est très important et l'élargissement de la bande d'étalement se traduit par une diminution du rapport signal/bruit [8].

La figure 1 donne un exemple de l'encombrement spectral que l'on peut observer en Europe occidentale.

La puissance de bruit mesurée dans la bande d'étalement Be est, évidemment, une fonction croissante de Be. Lorsque le bruit est blanc, il est bien conu que sa puissance croît de 10dB par décade et que le rapport signal à bruit après décompression est indépendant de la largeur de bande.

Une étude de l'accroissement du bruit en fonction de la bande d'étalement montre que celui-ci croît avec une pente supérieure à 10dB/décade [8]. La courbe de la figure 2 représente un exemple de variation de la puissance de bruit dans la plage de largeur Be la moins brouillée choisie dans un intervalle de 1MHz.

Ces résultats montrent que la croissance du brouillage, par rapport au bruit blanc augmente de 3dB pour des bandes d'étalement de l'ordre de 20KHz et qu'elle peut atteindre 20dB pour une bande d'étalement de 1MHz.

Dans ces conditions, on conçoit que le brouillage apporte une limitation à l'augmentation de la largeur de la bande d'étalement. En dessous de 20KHz, l'augmentation n'apporte pas de pénalisation sensible, mais pour des lageurs plus grandes l'augmentation de la puissance du brouillage devra, à qualité de réception constante, être compensée par une augmentation égale de la puissance d'émission qui rend, à la limite, inutile l'étalement du spectre.

Le problème traité dans cet article concerne la présentation d'une méthode de masquage des brouilleurs qui a été proposée par différents auteurs [9], [10]

III. - OPTIMISATION D'UNE RECEPTION PAR MASQUAGE DES BROUILLEURS -

Nous considérons :

- Que le signal obtenu après étalement du spectre possède un spectre $S(\omega)$ dont le module est uniforme sur l'intervalle $[-\Omega_0, \Omega_0]$ et définissable par

$$|S(\omega)|^2 = \frac{A_0}{2} \int_{-\infty}^{+\infty} [\delta(\omega+\omega_0+\Omega_0) - \delta(\omega+\omega_0-\Omega_0) + \delta(\omega-\omega_0+\Omega_0) - \delta(\omega-\omega_0-\Omega_0)]\, d\omega$$

où $\delta(x)$ est l'impulsion de Dirac.

Cette loi correspond aux parties utiles des spectres des principales techniques d'étalement, et est optimale dans le cas d'un bruit blanc.

- Que la détection effectuée est optimale en présente de bruit blanc.

- Que le masquage consiste à éliminer les parties du spectre où le niveau de brouillage est trop important.

Avec ces hypothèses, on considèrera que la détection est optimale si la marge de détection est maximale. Cette marge est réduite par le masquage du fait de l'altération du signal mais accrue par l'élimination des brouilleurs. Le compromis optimum résulte des actions inverses de ces deux effets.

La démodulation du signal étalé transposé en bande de base se ramène donc à une opération de corrélation du signal reçu avec la réplique du signal émis. En l'absence de brouilleur, le spectre du signal en bande de base $So(\omega)$ dont le carré du module s'exprime par

$$|So(\omega)|^2 = Ao \int_{-\infty}^{+\infty} [\delta(\omega+\Omega o) - \delta(\omega-\Omega o)]\, d\omega$$

a pour fonction de corrélation

$$C(\tau) = 2Ao\,\Omega o \quad \text{sinc}\,(\Omega o\,\tau)$$

où sinc $(x) = \sin x/x$.

Si on effectue un masquage des brouilleurs en plaçant N fenêtres de largeur $2\,\Delta\Omega i$ centrées sur des pulsations Ωi (figure 3) la fonction de corrélation s'exprime par :

$$C(\tau) = \frac{2Ao}{\tau} \sin(\Omega o\,\tau) - \sum_{i \in N} \frac{2Ao}{\tau} \sin(\Delta\Omega i\,\tau)\cos(\Omega i\,\tau) \qquad (1)$$

Le second terme représente la déformation de la fonction de corrélation provoquée par les masquages.
Si l'on note :

$$C_p(\tau) = \sum_{i \in N} \frac{2Ao}{\tau} \sin(\Delta\Omega i\,\tau)\cos(\Omega i\,\tau)$$

cette quantité représente une grandeur aléatoire dont le moment d'ordre 1 est nul, à des effets secondaires près, et dont on peut calculer la variance :

$$\sigma^2 p(\tau) = E\left\{C^2 p(\tau)\right\}$$

où E(x) dénote l'espérance mathématique de la variable aléatoire x.

Le calcul peut être mené en supposant que le nombre de fenêtres, compte tenu de l'encombrement spectral, est important. On admet d'autre part que les variables aléatoires $\Delta\Omega i$ et Ωi sont statistiquement indépendantes et ont des distributions uniformes respectivement notées $p_\Delta(x)$ et $p_\Omega(x)$, telles que :

$$p_\Delta(x) = \frac{1}{(1-c)\,\Delta\Omega o} \qquad \text{pour } x \in [c\,\Delta\Omega o,\ \Delta\Omega o]$$

$$p_\Delta(x) = 0 \qquad \text{pour } x \notin [c\,\Delta\Omega o,\ \Delta\Omega o]$$

et :

$$p_\Omega(x) = \frac{1}{(b-a)\,\Omega o} \qquad \text{pour } x \in [a\Omega o,\ b\Omega o] \qquad b < a$$

$$p_\Omega(x) = 0 \qquad \text{pour } x \notin [a\Omega o,\ b\Omega o]$$

Alors :

$$\sigma^2 p(\tau) = \frac{4Ao^2N}{\tau^2}\{1-\text{sinc}((1-c)\,\Delta\Omega o\,\tau)\cos((1+c)\,\Delta\Omega o\,\tau)][1+\text{sinc}((b-a)\,\Omega o\,\tau)\cos((b+a)\,\Omega o\,\tau)]$$

Cette expression se simplifie si c = 0, a = 0 et b = 1, c'est-à-dire dans le cas où les distributions sont uniformes à partir de 0.
Alors :

$$\sigma^2_{p(\tau)} = \frac{4\alpha\Omega_o A_o^2}{\Delta\Omega_o \tau^2}\,[1-\mathrm{sinc}\,(2\Delta\Omega_o\tau)][1+\mathrm{sinc}\,(2\Omega_o\tau)] \qquad (2)$$

où :

$$\alpha = \frac{N\Delta\Omega_o}{\Omega_o} = \frac{\text{somme des bandes masquées}}{\text{bande totale}}$$

Cette expression qui suppose Ωi et $\Delta\Omega i$ indépendants n'est plus valable quand α tend vers 1.

La conséquence de l'existence des fenêtres de masquage se traduit par :

- Une diminution de la valeur de $C(\tau=0)$ qui, compte tenu de la relation (1) et du fait que la valeur moyenne de $2\Delta\Omega i$ est $\langle 2\Delta\Omega i\rangle = \Delta\Omega_o$, s'écrit :

$$C(\tau=0) = 2A_o(\Omega_o - N\Delta\Omega_o) \text{ soit}$$
$$C(\tau=0) = 2A_o\Omega_o(1-\alpha)$$

- Un accroissement de l'amplitude des lobes secondaires de la fonction de corrélation dont la variance donnée par (2) peut être bornée par une valeur σ^2_m en remarquant que sinc $(2\Omega_o\tau)$ tend rapidement vers zéro. Il vient alors :

$$\sigma^2_m = \frac{8}{3} A_o^2\,\Omega_o\,\Delta\Omega_o\,\alpha$$

Il est intéressant de faire apparaître le rapport :

$$R = \frac{\text{Energie du signal sans masquage}}{\text{Densité spectrale de bruit moyen sans masquage}} = \frac{Eo}{no}$$

Alors on dispose de trois fonctions :

$$C_1^2\,(\tau=0) = R\,no\,(1-\alpha)^2$$

$$\sigma_1^2{}_m = \frac{2}{3} R\,no\,\left(\frac{\Delta\Omega_o}{\Omega_o}\right)\alpha$$

$n(\alpha)$ densité spectrale moyenne de bruit qui prend la valeur no pour $\alpha = 0$.

Le critère d'optimisation conduit au choix de α optimum qui maximalise le rapport signal/bruit après démodulation :

$$S/N = \frac{C_1^2(\tau=0)}{\sigma_1^2{}_M + n(\alpha)}$$

Ce rapport apparaît comme une fonction de α qui peut, selon les variations de $n(\alpha)$, présenter un maximum.

Si le bruit est blanc S/N est maximum pour $\alpha = 0$. Dans les autres cas le maximum existe si $\frac{d(S/N)}{d\alpha} > 0$ pour $\alpha = 0$.

Il est simple de voir que si R est élevé le masquage est inutile.

La figure 4 montre les résultats d'un cas typique d'encombrement spectral (figure 4-a) dans une plage de 400KHz dans laquelle on a cherché la meilleure position d'une bande d'étalement de 200KHz. On a tracé (figure 4-b) les courbes $n(\alpha)$, $\sigma^2_{1m} + n(\alpha)$ et

C_1^2 ($\tau = 0$) qui permettent de déduire la courbe (S/N) = f(α) (figure 4-c) où apparaît la valeur optimale α opt.

La figure 5 donne les résultats pour 3 cas typiques rencontrés dans le spectre décamétrique. Les courbes (S/N) = f(α) montrent, pour différentes bandes d'étalement, les valeurs optimales des α .

IV. - CONCLUSION -

L'encombrement spectral de la gamme décamétrique apporte une pénalisation importante dans les systèmes à étalement de spectre dès que la bande dépasse 20KHz.

Le procédé de masquage des brouilleurs apporte une solution acceptable. Le compromis entre l'altération du signal et la réduction du bruit conduit à un choix optimum des parties masquées.

Ce choix peut être fait à la réception par l'analyse locale du spectre à l'aide d'un système adaptatif.

BIBLIOGRAPHIE

[1] K. BUDDEN - Radio waves in the ionosphere. Cambridge University Press. New York 1961.

[2] E. SUNDE - Pulse transmission by AM.FM and PM in presence of phase distorsion. Bell Syst. Tech. JO. 50 1961.

[3] H.R. EPSTEIN - The effects of polarization rotation and phase delay with frequency on ionospherically propagated signals. IEEE Trans Antennas Propag. AP. 16 1968.

[4] J.D. MILSON and T. SLATOR - Consideration of factors influencing the use of spread spectrum on HF skywave paths. IEE Conférences Publication 206 1982.

[5] S. SALOUS - Measurement of the coherent bandwidth of HF skywave radio links. IEE Conferences Publication 245 1985.

6 R. SKAUG _ An experiment with spread spectrum modulation on an HF channel IEE conf publ. 206 1982

[7] R. SCHEMEL A. INCE - An experimental modem for HF channel using spread spectrum and bloc encoding AGARD Conf Proc. 244 - 1978

[8] C. COUTELARD - Allocation of frequecies in the decametrique band for ECM resistant communication systems 5ème symposium ARFA - Frequency provision for ECM resistant communications systems - Bruxelles dec 1986

[9] C. COUTELARD A. JOISEL - Protection adaptative des systèmes de détection fonctionnant par étalement de spectre. AGARD Conf Proc. 345 - 1983

[10] G.F. GOTT P. DOANY E.b. DARBYSHIRE - Experimental robust HF modem incorporating adaptative excision AGARD Conf Proc. 420 - 1987

FIGURE 1 : Exemple d'encombrement spectral de la gamme décamétrique

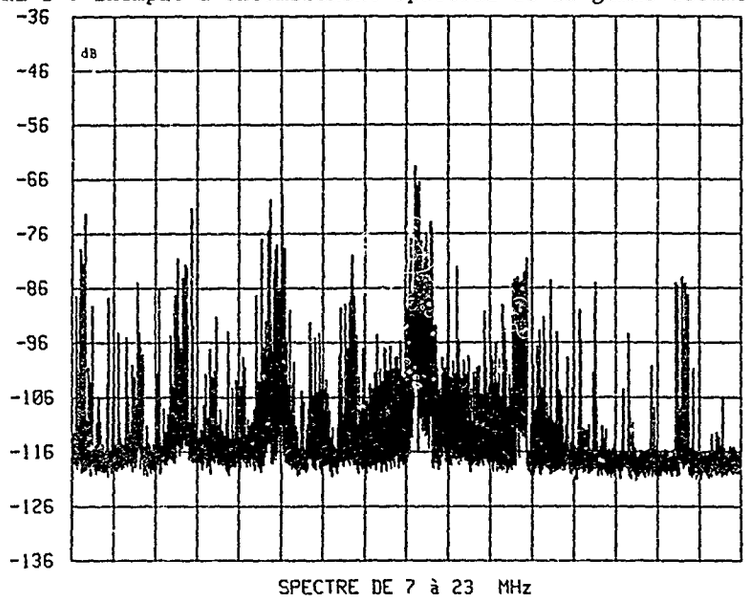

FIGURE 2 : Variations de la puissance de bruit
en fonction de la bande d'étalement Be

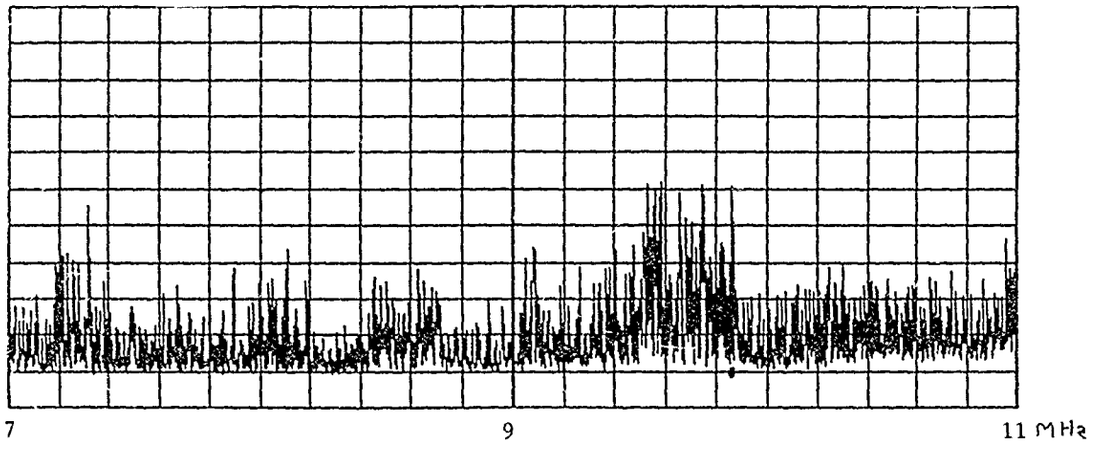

a) Spectre de la gamme

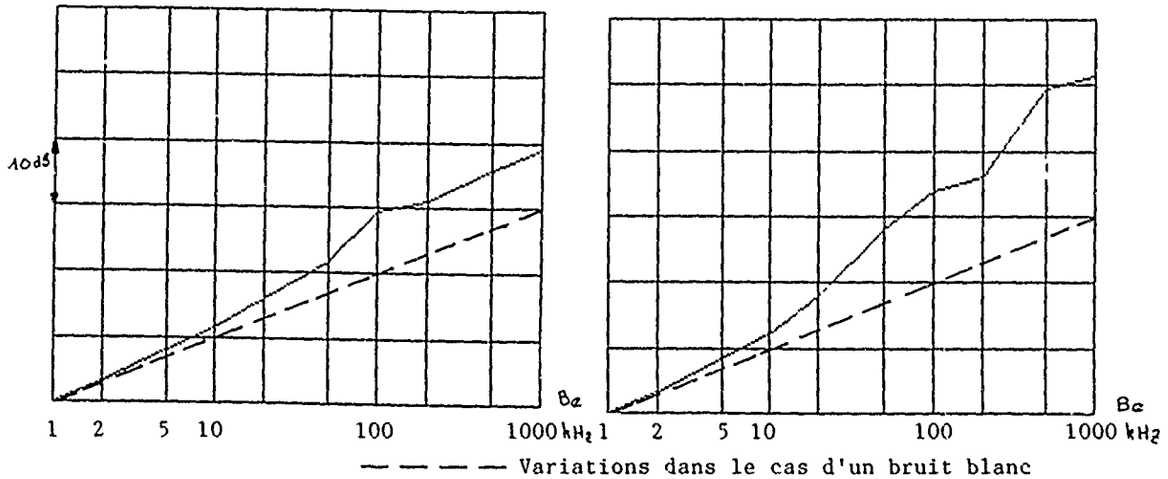

b) Variations dans le cas d'une plage peu perturbée 8-9MHz

c) Variations dans le cas d'une plage fortement perturbée 9-10MHz

FIGURE 3 : Masquage du spectre d'étalement

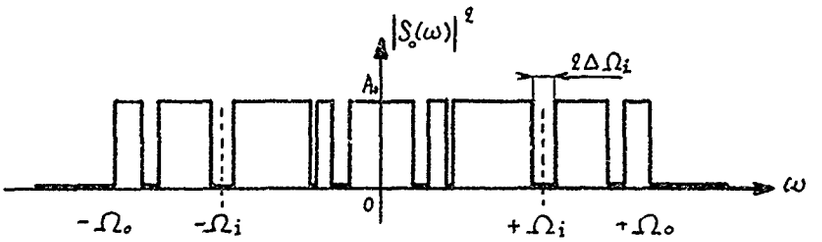

FIGURE 3

FIGURE 4 : Détermination de la valeur optimale de alpha

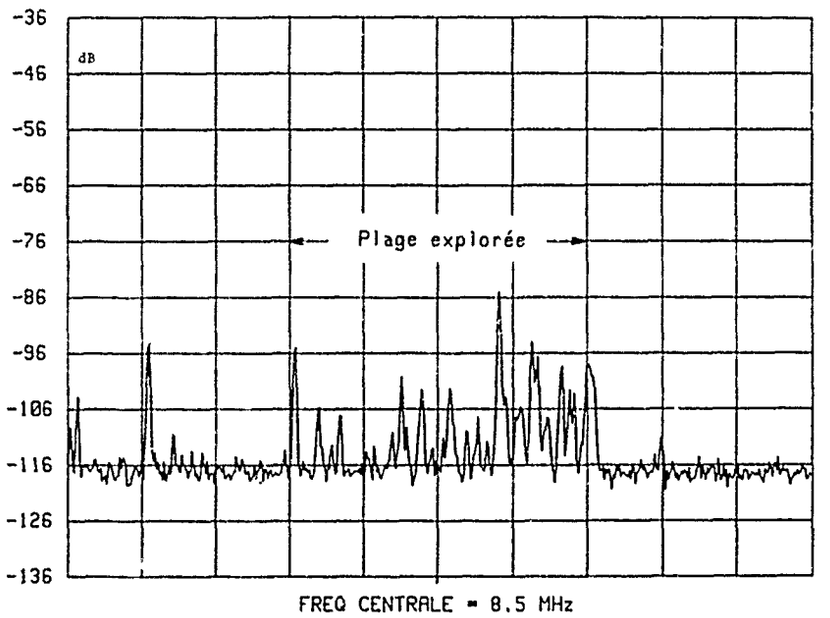

a)

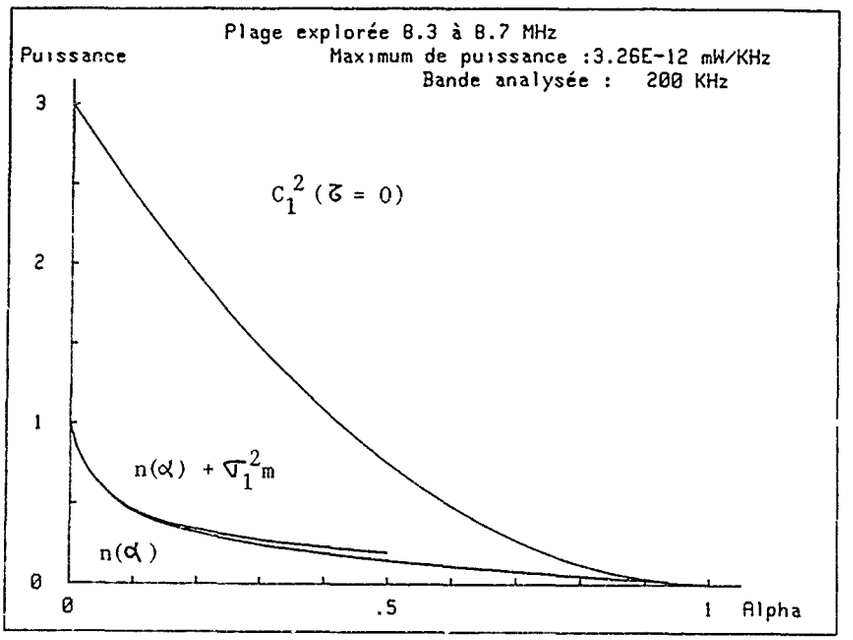
Plage explorée 8.3 à 8.7 MHz
Puissance
Maximum de puissance :3.26E-12 mW/KHz
Bande analysée : 200 KHz
3
2
1
0
C_1^2 (τ = 0)
n(α) + σ_1^2m
n(α)
0
.5
1
Alpha

b)

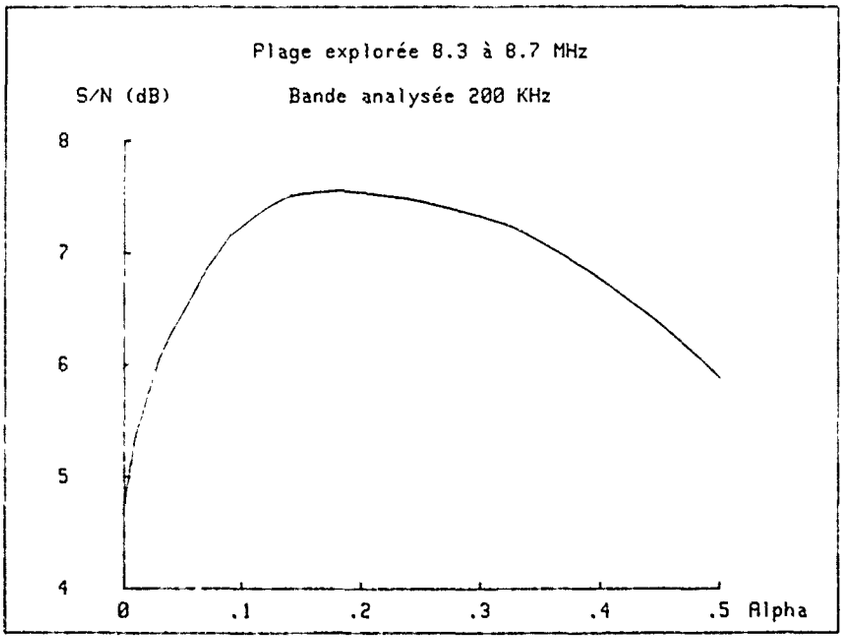
Plage explorée 8.3 à 8.7 MHz
S/N (dB)
Bande analysée 200 KHz
8
7
6
5
4
0
.1
.2
.3
.4
.5
Alpha

c)

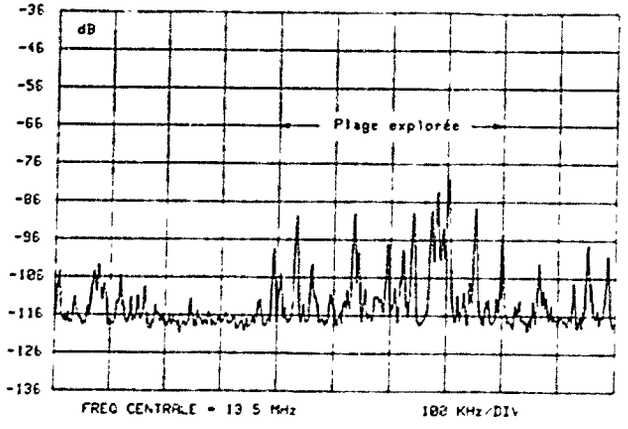

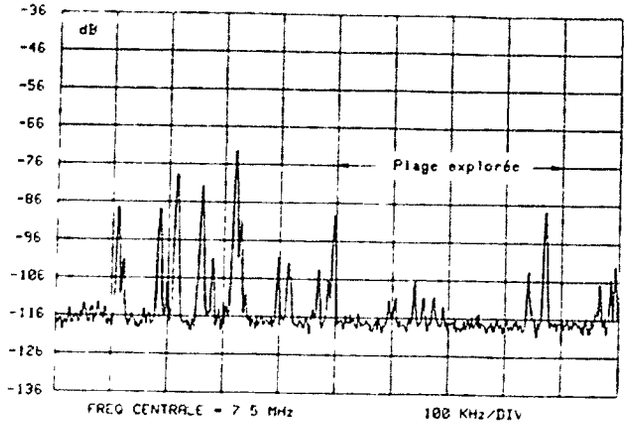

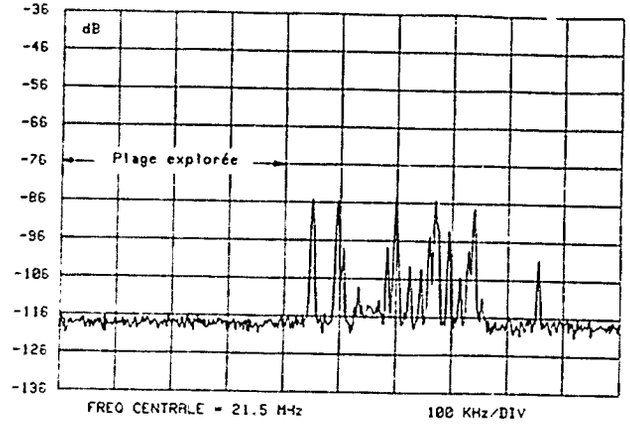

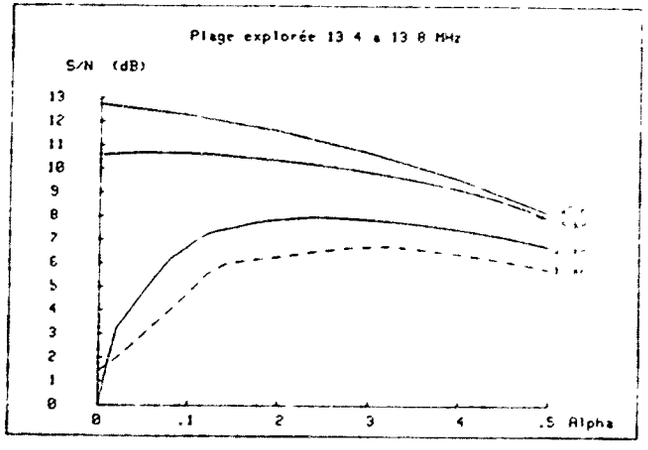

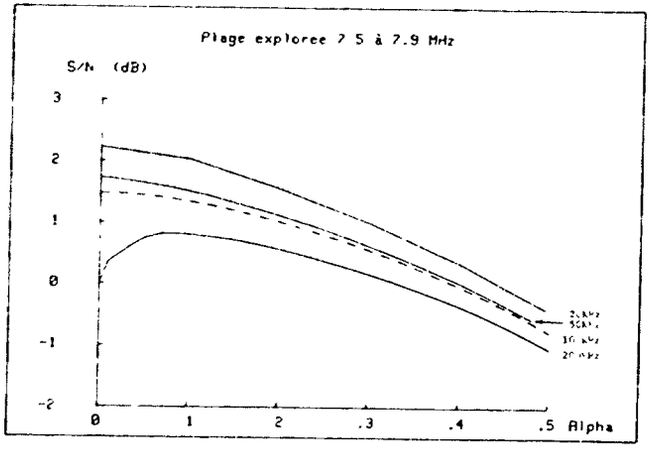

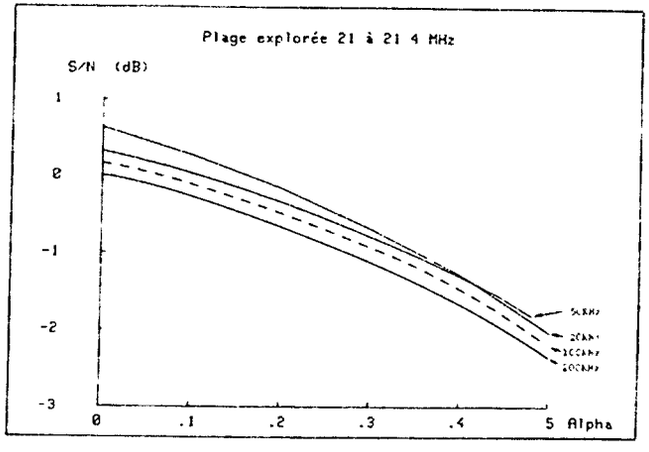

FIGURE 5 : Résultats typiques

a) Plage fortement perturbée 13,4-13,8MHz

b) Plage moyennement perturbée 7,5-7,9MHz

c) Plage très peu perturbée 21-21,4MHz

DISCUSSION

J. HOFFMEYER

Do you plan to construct a prototype direct sequence spread spectrum HF system and interference suppression system and do you plan on making experimental measurements of the effect of interference suppression on spread spectrum system performance ?

AUTHOR'S REPLY

Nous sommes des Universitaires et nous n'avons pas la vocation de construire des systèmes qui doivent être étudiés par des industriels dont c'est le métier. Par contre nous avons fait des mesures et nous avons réalisé des expériences pour juger des performances. Il est facile également de faire des simulations. Les résultats que nous avons obtenus sont en bon accord avec le calcul.

G. OSSEWAARDE

The use of spectral gaps turns out to be very effective. The gaps give a very high suppression of certain parts of the spectrum.
Other parts of the spectrum on the other hand are not attenuated at all.
The transition between the two areas is quite abrupt.
How can these spectral gaps be realised ?

AUTHOR'S REPLY

Il est bien évident que lorsque l'on effectue des calculs il faut se définir un modèle. Celui que nous avons adopté répond bien aux critères que vous citez et ils peuvent être approchés avec d'excellentes précisions par les traitements numériques du signal ou d'autres méthodes. Par exemple pour citer un cas simple, dans le cas d'un étalement par rampe linéaire de fréquence (chirp) ce type de filtre est simplement réalisé par une fenêtre temporelle. Dans d'autres cas on peut recourir avec efficacité aux techniques numériques.

Geoffrey F. GOTT

Although this has been a theoretical paper, the experimental work outlined in paper 18 has shown that the instrumentation of effective excision is feasible, certainly for the narrower bandwidth suggested. Prof. GOUTELARD has indicated alternative instrumentation philosophies for excision, namely the use of transversal filters, and the time gating of the output of a real time spectrum analyser, with subsequent real time transformation to the time domain. I believe that both of these approaches are entirely equivalent, and suffer from the same inherent problems.
It is also relevant to add that our experience on spectral analysis of HF interference indicates that significant gaps, at the atmospheric noise floor level, clearly exist between signals (outside the broadcast bands). Such gaps persist typically for substantial periods, occasionally for hours when the ionosphere is in a stable condition.

DISCUSSION

AUTHOR'S REPLY

Je partage tout à fait votre opinion, Dr GOTT. L'excision du spectre est techniquement réalisable par différents procédés dont le choix doit être fait de façon spécifique pour obtenir la complexité minimale.
D'autre part, les relevés expérimentaux le prouvent, il est possible, sur les bandes d'étalement envisageables dans cette bande, de pratiquer des excisions qui n'altèrent pas trop les signaux tout en détruisant la plupart des brouillages.

NEW SYNCHRONISATION TECHNIQUES APPLICABLE TO MULTI-TONE TRANSMISSION SYSTEMS

M. Darnell* & B. Honary**
Hull-Warwick Communications Research Group

* Department of Electronic Engineering,
University of Hull,
Hull HU6 7RX,
U.K.

** Department of Engineering,
University of Warwick,
Coventry CV4 7AL,
U.K.

SUMMARY

The synchronisation techniques described in this paper are applicable to both narrowband, multiple frequency-shift keyed (MFSK) digital transmission systems and wideband frequency-hopping systems. The techniques do not require specific synchronisation "overheads" to be incorporated into the transmissions, but operate using the normal traffic signal formats. It is required that digital signal processing is employed at the receiver for the procedures to be effective. Three distinct synchronisation methods are discussed:

(a) modulation-derived synchronisation;

(b) code-derived synchronisation;

(c) combined modulation- and code-derived synchronisation.

1. INTRODUCTION

Imperfect synchronisation is one of the major causes of error in digital communication systems. There are typically two elements to the synchronisation problem, ie

(a) bit or symbol synchronisation;

(b) block or frame synchronisation.

The establishment of bit/symbol synchronisation does not necessarily remove the need for block/frame synchronisation because of timing drifts due to effects such as changing Doppler shift, varying multipath structure, etc during the block/frame interval. In this paper, both block/frame and bit/symbol synchronisation procedures are described.

Traditionally, most radio communications synchronisation requirements have been met by a process of "initial" synchronisation, via say a preamble code, followed by a "flywheel" synchronisation procedure involving timing extraction from symbol transitions and/or the use of inserted segmenting information. The techniques for synchronisation described here require no synchronisation "overheads", such as preambles or inserted segments, but function entirely on the unmodified, information-bearing signal formats. If reception is interrupted for any reason, the procedures will recover synchronisation automatically after the discontinuity.

The concept of "multi-functional coding" has been defined by the authors (Darnell & Honary, 1986) to describes source and channel coding schemes designed to perform two or more simultaneous functions within the overall architecture of a communication system, eg error control, multiple-access coding, modulation, etc. The techniques described in the following sections are simple examples of multi-functional coding in that they involve combinations of modulation, error control, real time channel evaluation (RTCE) and synchronisation.

2. TECHNIQUE I: MODULATION-DERIVED SYNCHRONISATION

The modulation-derived synchronisation (MDS) procedure is a new symbol synchronisation method with a multi-functional capability for synchronisation acquisition and maintenance, demodulation and RTCE. It can be applied in modems that employ digital signal processing techniques to operate on the received waveform. The method was originally developed for multiple frequency-shift keyed (MFSK) transmission systems, but can, with simple modification, also be applied in other binary and multi-level modem types.

The principle of MDS will now be described by reference to a specific example of an 8-tone MFSK system. Consider the received signal to be sampled at intervals of δt, with n successive samples being equivalent to one symbol (tone) interval. The procedure outlined below effectively implements a digital matched filter at every sampling instant. This is achieved at any sampling time T_s, by computing the integral (or summation) of the product of the most recent n samples with the sampled sine and cosine components of the M tones. The summations are then processed to define M-dimensional vectors in M-dimensional signal space (MDSS); this is achieved by evaluating the modulus of the summation, I, for corresponding sine/cosine pairs, ie at time T_s

$$I_{(T_n,m)} = \{[\sum_{i=1}^{n(n\delta t=T_n)} f(i)\sin(w_m i\delta t)\,]^2 + [\sum f(i)\cos(w_m i\delta t)\,]^2\}^{1/2} \quad (1)$$

where $1 \le m \le M$, $f(i)$ are the samples of the received signal and w_m is the tone frequency.

When T_n coincides with a symbol transition, with tone w_m being transmitted, then

$$I_{(T_n,m)} = E_m \quad (2)$$

the total symbol energy. For other tone frequencies w_k, ($k \neq m$)

$$I_{(T_n,k)} = 0 \quad (3)$$

If T_n does not coincide with a symbol transition, and tone w_m is transmitted, then

$$I_{(T_n,m)} < E_m \quad (4)$$

and

$$I_{(T_n\ ,\ k)} = 0 \quad (5)$$

The above applies to the case of a perfect, noise-free communication channel. For practical channels, the ratio

$$C_n^2 = \frac{[\ I^2 \text{ for the tone giving maximum } I\ ]^2}{[\ \text{sum of } I^2 \text{ values for all M tone detectors}]} \quad (6)$$

is computed, ie

$$C_{(n)}^2 = \frac{I_{(T_n,\text{best tone})}^2}{\sum_{j=1}^{M} I_{(T_n,j)}^2} \quad (7)$$

C_n is thus a measure of detection confidence at instant T_n. As the instant T_n advances, so the detection vector describes a stepped course through MDSS.

In order to derive the phase of the data clock at the receiver, it must be assumed that, within reasonable limits, the period of the transmitter clock is already known - a reasonable assumption in most practical situations. It is then required that the I values obtained at the receiver should be processed to yield clock timing. The series of C_n values is suitable for this purpose since it contains a strong component at the clock frequency which is independent of the sequence of tones transmitted.

It can be seen that, under noise-free conditions, C_n will take the value unity when T_n coincides with a symbol transition; when this coincidence does not occur, C_n will be less than unity. Hence a clock periodicity is present as long as symbols are being transmitted sequentially. When a sequence of similar symbols occurs, the value of C_n will remain constant, but this is likely to be a sufficiently infrequent event so as not to inhibit the maintenance of correct synchronisation.

In the case of an 8-tone MFSK transmission system, the maximum and minimum values for C_n are 1 and $1/\sqrt{8}$. Figures 1 and 2 show plots of C_n, both filtered and unfiltered, for conditions of additive Gaussian White noise. Also shown are the corresponding digital matched filter outputs M_1 - M_8. In Figure 1, the effective overall signal-to-noise ratio (SNR) in the total channel bandwidth is 3 dB, whilst in Figure 2 it is 0 dB.

In practice, the nature of the C_n and the matched filter outputs will be determined by channel and noise characteristics. It can be seen that the value of C_n for each of the symbols in the MFSK tone array is in fact a measure of detection confidence and can be used as a source of RTCE data. Such RTCE data can be used to improve the performance of both demodulation and decoding procedures; it can also assist in the optimisation of the number of MFSK tones, M, in response to channel state (Shaw, Honary, & Darnell, 1988).

3. TECHNIQUE II : CODE DERIVED SYNCHRONISATION

Code-derived synchronisation (CDS) is an effective method of block synchronisation. In this scheme, the power of the code is used for both error control and time-drift correction. CDS is basically a decoding method which not only correlates the received codewords with all the possible codewords, but also per-

forms correlation in time (over one code word interval) for every possible codeword. The CDS system operates in the following manner. Assume a code of dimension (n,k) is used (where n is the block length of the code and k is the number of information bits in a codeword); the number of codewords is then 2^k. At the receiver 2n bits of the received data are stored, the decoder then uses these bits to decide the best time-shift and the best codeword, so as to minimise the number of errors for that particular codeword interval. This is achieved by comparing all the possible 2^k codewords with the received sequence. For each codeword, the received sequence is compared against the time-shifted versions (by γ, where $0 \leq \gamma < n$) of the codeword, the number of errors for each of the n time-shifts is then recorded. In this way, a two-dimensional array can be formed for every decoding pass, the contents of which give the number of errors for codeword i, at time shift γ. The format of this array is shown in Table 1.

		time shift γ					
		0	2	3	4	5	n-1
codeword i	0						
	1						
	2						
	. .						
	2^k-1						

Table 1

The decoder then searches through this array and determines the best codeword/time-shift combination.

As an example, the CDS system has been implemented using the (7,4) Hamming code. Fig. 3 shows the decoding pass for one such codeword, where block synchronisation occurs at time shift 4, with no errors. Fig.4 shows a similar graph, but for all the codewords for one decoding pass. The y direction on the graph of Figure 4 depicts all the 16 codewords, with the deviation from the horizontal lines indicating the number of errors. It is seen that synchronisation occurs with codeword 13 at time-shift 4, and with codeword 10 at time-shift 5. This ambiguity could be eliminated if more than one codeword is considered.

The major application of the CDS approach would appear to be in supporting, or enhancing, other synchronisation techniques.

4. TECHNIQUE III : COMBINED MODULATION & CODE-DERIVED SYNCHRONISATION

The combined modulation- and code-derived synchronisation (CMCDS) scheme contains elements of both the MDS and CDS approaches described in the previous two sections. A particular realisation, termed code-assisted bit synchronisation (CABS), is described here in the specific context of a 4-tone MFSK transmission system.

The tone frequencies are chosen such that they are orthogonal over the symbol interval. In CABS, the processes of demodulation and decoding are combined; hence the need for a separate timing recovery (either carrier or symbol) is eliminated. In combining the processes of demodulation and decoding, a half-rate binary convolutional code is used in conjunction with a soft-decision Viterbi decoder, rather than a block code, to perform the main function of CABS. The decoder therefore performs both symbol timing recovery and error correction. This is achieved by dividing every trellis in the decoder trellis diagram into n sub-trellises, where n is the number of samples within a symbol interval. The decoding is then carried out for every L sub-trellises separated in time by the symbol interval (where L is the search length of the decoder); this process is repeated for all the sub-trellises within any arbitrary symbol time. The soft-decision information to the decoder is obtained via a set of matched filters whose outputs are sampled n times within every symbol interval.

In an attempt to reduce the complexity and the processing load of the system, a simple 4-state convolutional code is used. The CABS transmitter system operates in the following manner:

(a) A message sequence is encoded using the 1/2-rate convolutional code into a code sequence.

(b) To each code word, $C \in \{00,01,10,11\}$, an MFSK tone is allocated and transmitted in the allocated symbol time interval, T_s. The tone allocation is as shown in Table 2 below.

Codeword	Tone frequency
00	f_0
01	f_1
10	f_2
11	f_3

Table 2

The receiver in the CABS environment take the following steps :

(a) The incoming baseband tones are sampled n times at a sampling frequency of f_s.

(b) For each of the tones, the in-phase (I_{ij}) and the quadrature (Q_{ij}) components are evaluated, where i is the tone number ($0 \leq i \leq 3$) and j is the sample number within a symbol ($0 \leq j < n$) where

$$n = T/f_s. \tag{8}$$

(c) At each sampling instant, k, within an arbitrary frame, a 4-tuple magnitude vector M_k is evaluated, where M_k is given by

$$M_k = \{M_{0k}, M_{1k}, M_{2k}, M_{3k}\} \tag{9}$$

where M_{ik} is the magnitude of the output of the matched filter i ($0 < i < 3$) at the sample reference number, k (where ($0 \leq k < n$)), within an arbitrary frame of duration T_s, integrated over the past n samples. M_{ik} is therefore given by:

$$M_{ik} = \sum_{j\,=\,k-n+1}^{k} \sqrt{(I_{ij}^2 + Q_{ij}^2)} \tag{10}$$

In this manner, for any arbitrary symbol interval T_s, n 4-tuple magnitude vectors can be evaluated.

(d) Starting at any arbitrary point in time, magnitude vectors, M_k, for L successive symbol intervals are stored.

(e) The Viterbi decoder is then used to resolve both time and symbol ambiguities. The decoder operates on L successive M_k vectors, separated in time by exactly one symbol interval T_s. The soft-decision metric assignment is as follows:

$$\Gamma_{00k} = M_{0k} \quad \Gamma_{01k} = M_{1k} \quad \Gamma_{10k} = M_{2k} \quad \Gamma_{11k} = M_{3k} \tag{11}$$

where Γ_{ijk} is the metric assigned to the code word {ij} at time slot k within an arbitrary symbol interval.

(f) The decoder then determines the most likely path through the trellises. The confidence of this path, the decoded bit and the time-shift are stored. The above operation is then repeated n times with a time-shift of $1/f_s$ being applied at each step. In this way, the decoding is performed for all the possible available time-slots within any arbitrary symbol interval.

(g) Finally, the most likely path (ie the one with the highest confidence) among the n possible stored paths is chosen as the CABS system's decision for that particular symbol interval. The decoded bit associated with this path is then output. Symbol timing information is then derived from the time-shift associated with the chosen path.

The performance of the CABS system has been studied, using simulation techniques, over an additive white Gaussian noise channel. For this simulation study the following system parameters have been used:

Parameter	Value
L	15
T	3.9 mSec
f_s	10KHz
f_0	1285Hz
f_1	1542Hz
f_2	1799Hz
f_3	2055Hz

Table 3

Fig.5 shows the output bit error rate (BER) of the CABS system as a function of E_b/N_o. E_b/N_o is given by:

$$E_b/N_o = 10\ \mathrm{Log}_{10}(9.75/\sigma^2) \qquad (12)$$

where E_b is the energy per information bit, N_o is the one-sided noise power spectral density and σ is the standard deviation of the noise. The size of the test message was 10^5 bits.

The performance of the CABS algorithm and conventional demodulation schemes, both coherent and noncoherent (Proakis 1983), for 4-tone MFSK data detection is plotted in Fig.5 for Gaussian noise conditions. In addition the output of CABS detector provides information on symbol timing, in the same way as the MDS system described previously, thus giving a multi-functional capability.

5. CONCLUDING REMARKS

The three synchronisation schemes described in this paper, ie MDS, CDS and CABS, all depend for their operation on the availability of digital signal processing at the communications system receiver. They illustrate how the digital processing architecture at the receiver can be used in a manner that is uniquely digital, rather than simply simulating classical analogue processing procedures.

All three synchronisation procedures have the major practical advantage of requiring no specific synchronisation overheads in the form of preambles or segmenting information. They can be applied either individual or in combination. Although discussion has centred on MFSK transmission, the techniques can be easily adapted for other binary or multi-level transmission formats.

6. REFERENCES

1. M. Darnell & B. Honary, " Multi-Functional Coding Schemes Applicable to Secure Communication", Proc.IEE Int. Conf. on "Secure Communications", Conf. Proc. No.269, October 1986.

2. M. Shaw, B. Honary & M. Darnell, "Optimisation of Parameters in an MFSK Transmission System", Electronics Letters, Vol.24, No. 12, 9th June 1988.

3. Proakis, J. G., "Digital Communications", McGraw-Hill, 1983.

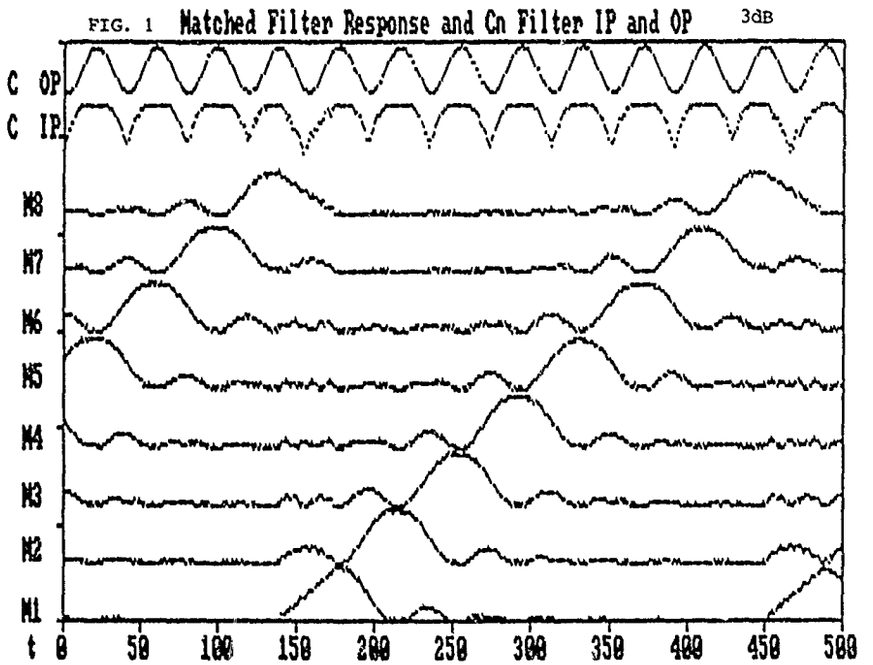

FIG. 2 **Matched Filter Response and Cn Filter IP and OP. 0dB SNR.**

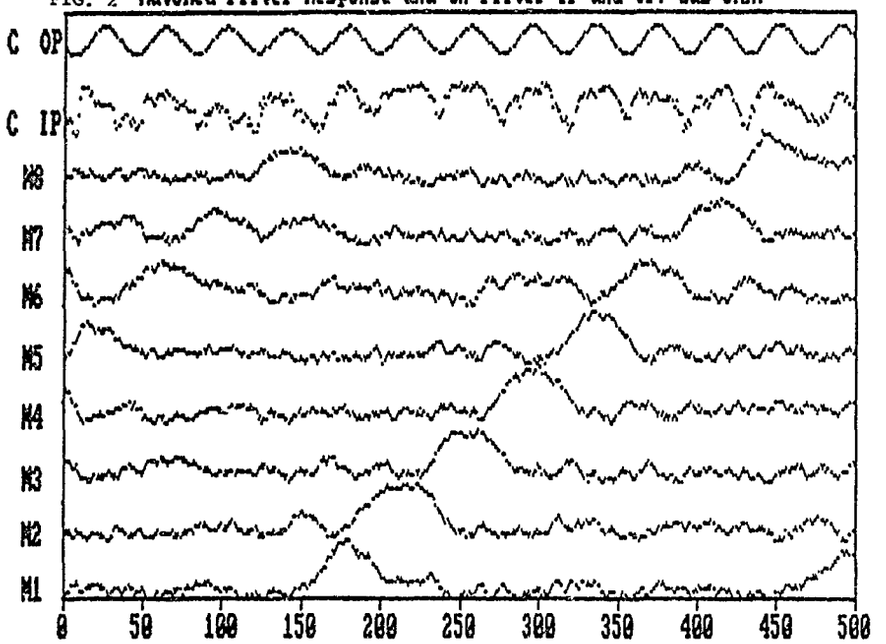

Fig. 3 Example of code derived synchronisation

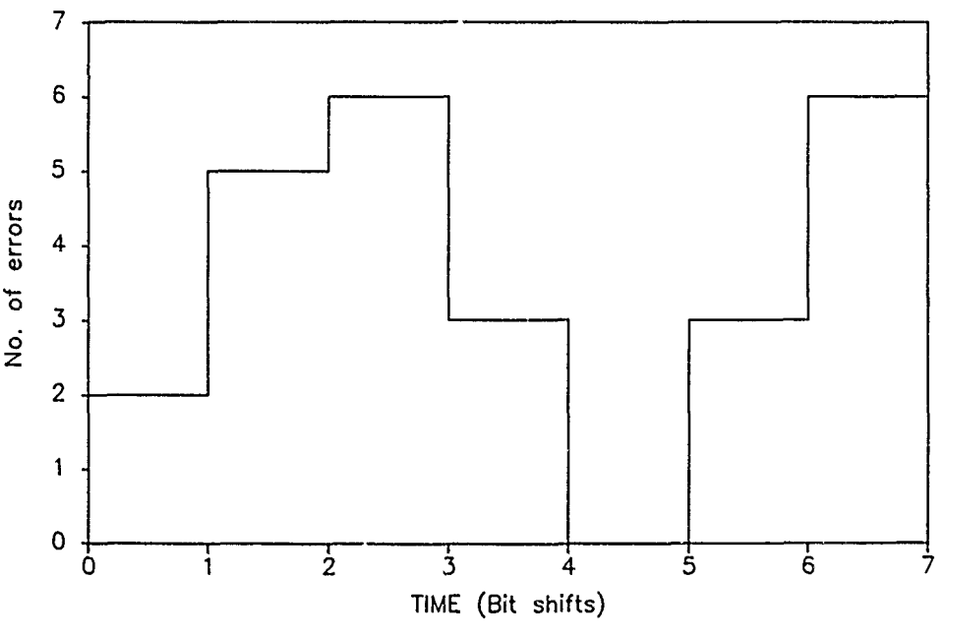

(7,4) Hamming code
synch loss of 4 bits

FIG. 4 Example of code derived synchronisation for all possible codewords

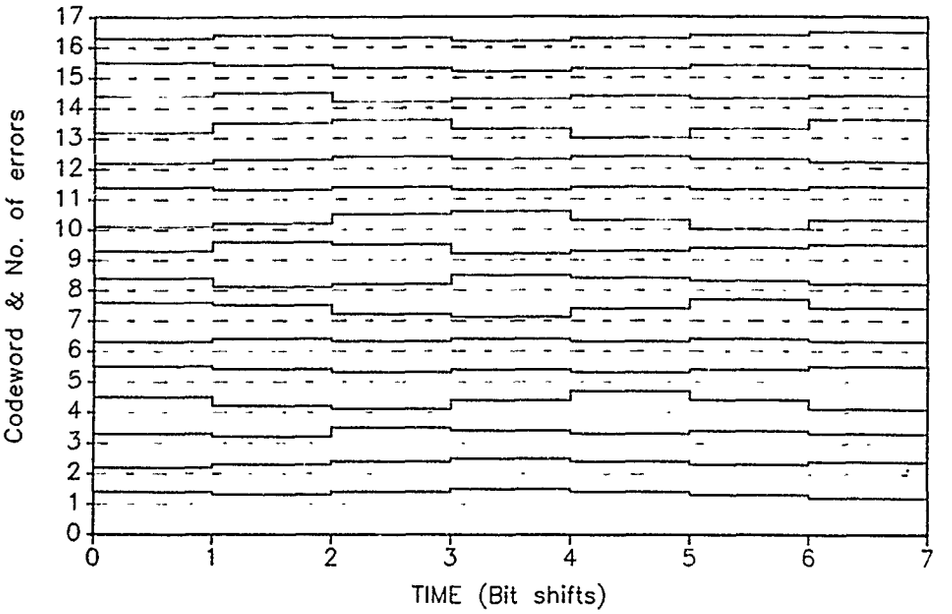

(7,4) Hamming code
Sync. loss of 4 bits
Synchronised to codeword 13 at shift 4

FIG. 5 Probability of error of coherent, noncoherent MFSK systems and the CABS system vs Eb/No (dB).

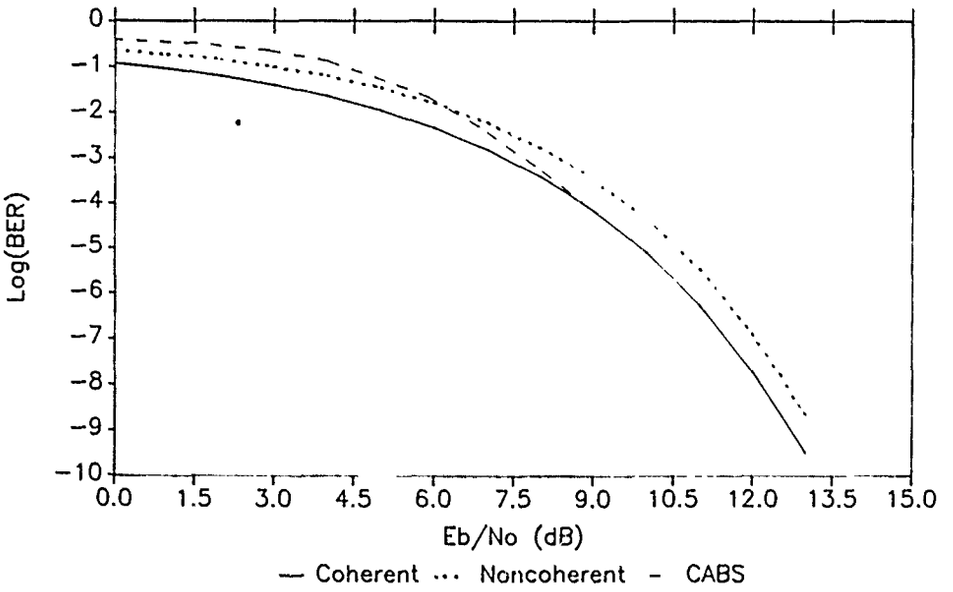

Note that the coherent and noncoherent detection methods assume perfect symbol synchronisation (theoretical values)

DISCUSSION

Geoffrey F. GOTT

The code-derived synchronization appears to be based on the principle of fundamental decoding, whereby the received codewords are compared to stored replicas of all possible codewords. The Hamming code, used as an example by the authors , may be instrumented simply, but the technique may rapidly become impracticable as the code complexity increases.

AUTHOR'S REPLY

This a valid comment. However, in the HF context, the codeword size is usually relatively small, thus the decoding complexity is not impracticable.
Certainly, at low transmission rates (less than a few hundreds of bits/s) this is not likely to be a computational problem.

D.J. FANG

I assume you are still talk about HF applications. For an HF network even that consists of 5 terminals, it is a complicated one in the aspect of clocking. The multipath effect practically shifts the clock timing all the time and it is not possible to establish a standard clock for an HF network such as the case for a satellite network. In view of that, I have problem to accept your conclusion that "Synchronization overhead is not required". Please comment.

AUTHOR'S REPLY

The techniques described in the paper are essentially to enhance the accuracy of "flywheel" synchronization by providing additional synchronization information from other sources such as demodulators and decoders. If fast initial synchronization is required, it may well be necessary to attach preamble sequences,i.e.overheads. In general, I believe that the more sources of synchronization that are available at the receiver, the better.

SYNCHRONISATION DES TRANSMISSIONS EN EVASION DE FREQUENCE
EFFET DU SURECHANTILLONNAGE

J.P. VAN UFFELEN

TRT, 5 Avenue Réaumur, 92350 LE PLESSIS-ROBINSON, France

1 - INTRODUCTION

Toutes les communications numériques nécessitent pour leur établissement la synchronisation du récepteur par rapport au message à recevoir. Au cours de cette période d'initialisation, plusieurs phases sont à distinguer :

- . La synchronisation de séquence de saut de fréquence dans le cas d'une communication utilisant l'évasion de fréquence.
- . La synchronisation de mot ou de trame dont le but est de définir l'instant d'arrivée du message et de retrouver la trame de celui-ci.
- . La synchronisation de symboles quelquefois appelée synchronisation de bit et qui permet de définir l'instant de prise de décision.
- . La synchronisation de porteuse dans le cas de démodulation cohérente.

On peut également considérer la synchronisation du chiffre dans le cas de communications cryptées et la synchronisation de la séquence d'étalement de spectre pour les transmissions de ce type.

Dans cette communication, nous nous intéressons principalement à la synchronisation de mot et de séquence de saut de fréquence et de son impact sur la synchronisation symbole.

2 - POSITION DU PROBLEME

Pour synchroniser une séquence de saut de fréquence ou la trame du message, le récepteur doit reconnaître un mot dit mot de synchronisation, identifiant le début de la communication ou un instant caractéristique de celle-ci. Selon les contraintes retenues pour le temps d'établissement de la liaison ou le rythme de saut de fréquence, il peut être nécessaire que la synchronisation de mot soit faite sans que la synchronisation symbole soit acquise. Il convient dès lors d'effectuer simultanément les deux types de synchronisation.

Plusieurs techniques sont utilisables pour la détection de mots, elles sont toutes basées sur la corrélation du signal reçu avec la réplique locale du mot de synchronisation, et diffèrent selon que cette corrélation utilise les signaux reçus avant ou après décision.

Si la synchronisation utilise le signal après décision, le récepteur bénéficie d'une plus grande simplicité. Pour évaluer les performances de ce traitement nous avons eu recours à des simulations pour déterminer les probabilités de non détection et de fausse alarme, lorsque le signal reçu est suréchantillonné.
Pour réaliser simultanément la synchronisation de mots et de symboles, celles-ci peuvent être effectuées séquentiellement après avoir mis en mémoire le signal reçu échantillonné à raison de 4 ou 8 échantillons par symbole. Une autre technique consiste à calculer en temps réel la fonction de corrélation suréchantillonnée. Le maximum de cette fonction détermine la phase optimale d'échantillonnage et, après comparaison à un seuil, détecte la présence éventuelle du mot de synchronisation attendu.

3 - RECEPTEUR

Le récepteur dont le schéma est donné en figure 1, est composé par :

- Les parties haute fréquence (RF) dont le but est d'amplifier le signal reçu et de transposer sa fréquence sur une fréquence intermédiaire où est effectuée la démodulation.
- Le démodulateur (FSK, PSK, MSK...) adapté à la nature du signal reçu.
- Le filtre de démodulation qui limite la bande du signal et optimise son rapport signal à bruit avant la prise de décision.
- L'échantillonneur et la prise de décision.
- Le corrélateur utilisé pour la reconnaissance du mot de synchronisation.
- Un comparateur permettant de décider si le signal attendu a été reçu ou non.

4 - EVALUATION DES PERFORMANCES

4.1. Critères d'évaluation

Les performances sont appréciées par la probabilité de non détection (Pnd) du signal attendu et par la probabilité de fausse alarme (Pfa) lorsque le signal n'est pas présent. Le couple Pnd, Pfa permet de comparer entre elles les différentes hypothèses de traitement.

4.2. Caractéristiques des traitements

Les divers traitements sont définis par les paramètres suivants :

- La longueur du mot de synchronisation,
- La longueur de corrélation du filtre de démodulation,
- La fréquence d'échantillonnage.

Le tableau 1 précise les valeurs de paramètres qui ont été retenues lors des simulations :

Mot de synchronisation	16 ; 32 ; 48 et 64 symboles
Largeur de corrélation du filtre de démodulation	$\frac{T}{2}$; $\frac{2T}{3}$; T
Fréquence d'échantillonnage	$\frac{1}{T}$; $\frac{2}{T}$; $\frac{4}{T}$; $\frac{8}{T}$

T : la durée d'un symbole

TABLEAU 1

4.3. Simulations

Les simulations dont les principes sont donnés en annexe 1 ont été effectuées en absence de signal pour déterminer la probabilité de fausse alarme et en présence de signal affecté de taux d'erreur compris entre 2 et 15 % pour déterminer les probabilités de non détection. Ces simulations ont été conduites avec les traitements dont les caractéristiques sont données dans le tableau 1.

Quelques résultats de ces simulations sont présentés à titre d'exemple sur les courbes des figures 2 à 5. La figure 2 présente la probabilité de fausse alarme obtenue avec un mot de synchronisation composé de 32 symboles, une fréquence d'échantillonnage de $\frac{4}{T}$, la longueur du filtre adapté étant de $\frac{T}{2}$. Les figures 3, 4 et 5 donnent avec les mêmes hypothèses de traitement la probabilité de non détection lorsque le signal est reçu avec un taux d'erreur de 2,5 %, 4 % et 11 %.

5 - ANALYSE

L'analyse des résultats a été conduite pour apprécier l'influence de la fréquence d'échantillonnage sur les performances d'un système de détection de mots. Parmi l'ensemble des résultats acquis, nous présentons ceux correspondant au mot de longueur 32 en fonction du taux d'erreurs et du filtrage effectué sur le signal.

Pour comparer les résultats obtenus en fonction du filtrage, le principe du taux d'erreur constant a été retenu de préférence au rapport signal à bruit constant. Ce critère a été choisi, car la limite de portée d'une liaison est définie par la dégradation maximale de qualité admissible. Or, celle-ci s'évalue par un taux d'erreur maximal quelque soit le type d'utilisation : parole numérisée, transmission de messages brefs, transmission de données, avec ou sans codage, correcteur d'erreurs. C'est ce taux d'erreur qui définit le rapport signal à bruit nécessaire, compte tenu de la nature de la modulation utilisée du procédé de démodulation ; la limite de portée se détermine alors par la connaissance de la fréquence de transmission et de la puissance rayonnée.

Ainsi qu'il l'a été indiqué au paragraphe 4.1., c'est le couple Pnd Pfa qui est utilisé pour évaluer les performances du traitement. La figure 6 représente pour des mots de 32 bits reçus avec un taux d'erreur de 2,5 %, l'évolution des probabilités de non détection et de fausse alarme lorsque le seuil de décision varie. Les cinq courbes correspondent aux fréquences d'échantillonnage égales à $\frac{1}{T}$, $\frac{2}{T}$, $\frac{4}{T}$, et $\frac{8}{T}$, le filtrage étant égal à $\frac{T}{2}$.

Ces courbes montrent que les performances s'accroissent lorsque la fréquence d'échantillonnage passe de $\frac{1}{T}$ à $\frac{4}{T}$ et $\frac{8}{T}$. Par contre, lorsque cette fréquence est égale à $\frac{2}{T}$, les performances obtenues peuvent être en retrait, ceci s'explique par la phase de l'échantillonnage. En effet, dans le cas représenté sur la figure, le signal est échantillonné (courbe a) au milieu du symbole et à l'instant correspondant aux transitions cette configuration est la plus pénalisante. Si le peigne d'échantillonnage est décalé de $\frac{T}{4}$ (courbe b), les performances s'avèrent meilleures que celles obtenues avec une fréquence d'échantillonnage égale à $\frac{1}{T}$. L'écart de performances pour les deux phases de l'échantillonnage permet de gagner trois ordres de grandeur sur la probabilité de fausse alarme, lorsque la probabilité de non détection est égale à 10^{-2}.

Il faut noter également que cet effet lié à la phase d'échantillonnage existe également, lorsque la fréquence d'échantillonnage est égale à $\frac{4}{T}$ et $\frac{8}{T}$, mais l'amplitude de la variation de performance se réduit lorsque la fréquence d'échantillonnage croît.

La figure 7 permet d'apprécier l'influence du filtrage sur les performances. Elle indique pour un taux d'erreur de 2,5 %, la probabilité de fausse alarme associée à une probabilité de non détection de 10^{-4} pour une fréquence d'échantillonnage égale à 4, lorsque la bande passante du filtre avant décision passe de $\frac{1}{T}$ à $\frac{2}{T}$. Dans ces conditions, la probabilité de fausse alarme associée à la fréquence d'échantillonnage de 1/T est de 10^{-2}. Il apparaît clairement que le gain apporté par le suréchantillonnage augmente rapidement, lorsque le filtrage est caractérisé par une bande égale à $\frac{2}{T}$, et que le gain dû au suréchantillonnage demeure important (supérieur à deux ordres de grandeur) lorsque la bande de bruit est réduite à 3T/2 puis à 1/T. La figure 8 présente les mêmes paramètres lorsque le taux d'erreur est égal à 6 %.

6 - CONCLUSION

Le procédé de synchronisation étudié cumule les avantages de :

- . La simplicité du traitement,
- . La possibilité de synchronisation mot et symbole simultanée,
- . Le gain de performance.

Ce dernier point a fait l'objet d'une évaluation par simulation prenant en compte, en particulier, la fréquence d'échantillonnage et la bande passante du filtre avant décision.

Nous avons mis en évidence que l'utilisation de quatre échantillons par symbole permet un gain de trois ordres de grandeur sur la probabilité de fausse alarme pour une probabilité de non détection égale à 10^{-4}. La comparaison avec un traitement par corrélation avant décision permet d'obtenir théoriquement des performances supérieur au traitement proposé au prix d'une complexité accrue dans la synchronisation et d'une plus grande difficulté pour déterminer le seuil de décision de synchronisation.

ANNEXE 1

Principes de la simulation

La simulation a pour but de déterminer la probabilité que la valeur du signal de sortie du corrélateur soit égale à x ($0 < x < nL$ que L = longueur du mot de synchronisation et n le taux d'échantillonnage 1 ; 2 ; 4 ou 8).

Le programme de simulation comprend 5 modules.

1. Génération du signal de test. Le signal de test est une séquence composée de 8 symboles fixes 1.0.0.1.0.1.1.1.0., chaque symbole est échantillonné à la fréquence $\frac{8}{T}$.
2. Génération du bruit, le bruit utilisé est blanc, gaussien à valeur moyenne nulle. 8 échantillons indépendants de bruit par symbole sont calculés soit en tout 64 échantillons.
3. Filtrage

   Les 64 échantillons de signal auxquels ont été ajoutés les échantillons de bruit sont filtrés par un filtre adapté de durée $\frac{T}{2}$; $\frac{2T}{3}$ ou T.

   Ce filtre effectue le calcul suivant :

$$y(k)=\sum_{i=0}^{n-1} S(k-i)+n(k-i) \qquad 0 \leqslant k \leqslant 63$$

Pour éviter les effets de bord, un symbole supplémentaire est ajouté au début de la séquence, et huit échantillons supplémentaires de bruit sont calculés.

4. Corrélation

Le signal filtré puis décidé est corrélé avec la séquence de test. Ce calcul est effectué pour les quatre valeurs "n" du taux d'échantillonnage.

$$C(n)= \sum_{\substack{k=0 \\ \text{par pas de n}}}^{63} S(k).\mathrm{sgn}[y(k)]$$

Les modules 2, 3, 4 sont répétés un grand nombre de fois (10^4 à 10^5) permettant d'attribuer à chaque valeur de corrélation une probabilité d'apparition et d'obtenir la densité de probabilité de la corrélation. La figure A1 présente les résultats de la simulation pour un mot de 8 bits échantillonné à la cadence $\frac{1}{T}$, $\frac{2}{T}$, $\frac{4}{T}$ et $\frac{8}{T}$.

5. Evaluations des probabilités

A partir de la densité de probabilité obtenue par simulation pour un mot de longueur 8 symboles, les densités de probabilité liées aux mots de 8, 16, 32, 48 et 64 symboles sont calculées par la formule suivante :

$$p(x,L)= \int_{-\infty}^{+\infty} p(y,L/2).p(y-x,L/2)\,dy$$

L : longueur du mot de synchronisation

Remerciements :

Je tiens à remercier Monsieur François BEAUDOUIN pour son aide dans la préparation de cette communication.

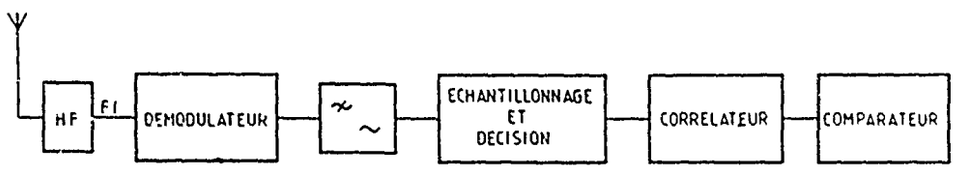

FIG 1
CHAINE DE RECEPTION

Rapport signal à bruit +3 0

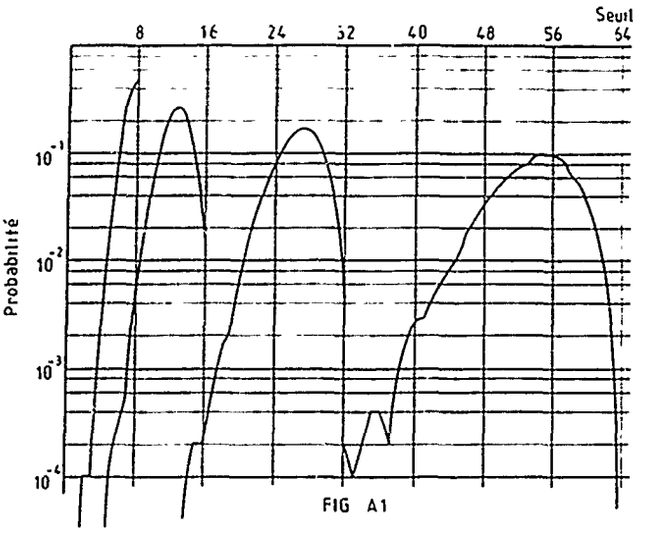

FIG A1

Longueur du mot 32
4 echantillons par symbole

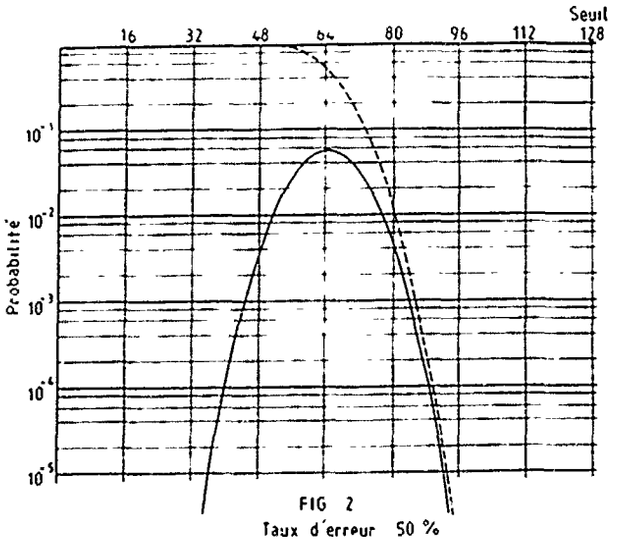

FIG 2
Taux d'erreur 50 %

Trait plein Probabilite que la corrélation soit égale à l'abscisse
trait pointillé Probabilité de non detection

Longueur du mot 32
4 echantillons par symbole

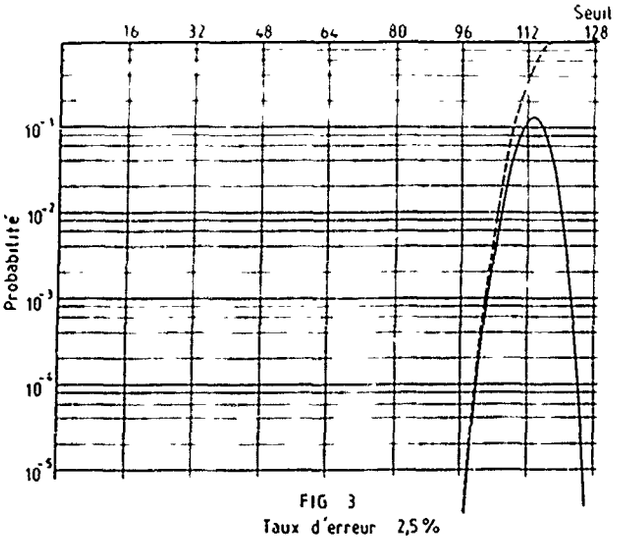

FIG 3
Taux d'erreur 2,5 %

Trait plein Probabilite que la corrélation soit égale à l'abscisse
trait pointillé Probabilité de non detection

Longueur du mot 32
4 echantillons par symbole

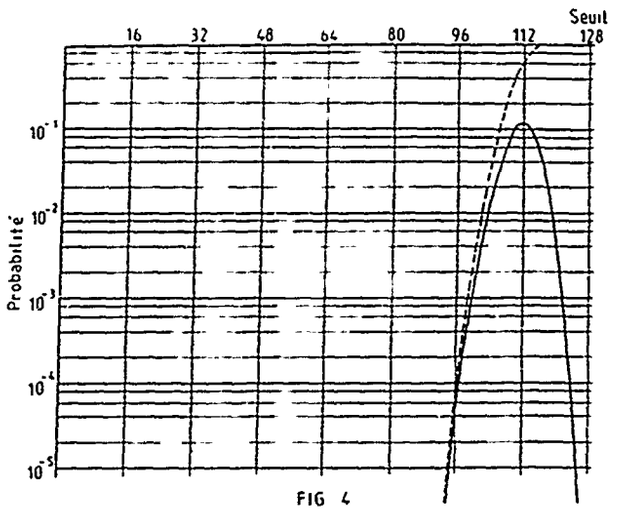

FIG 4
Taux d'erreur 4 %

Trait plein Probabilité que la corrélation soit égale à l'abscisse
trait pointillé Probabilité de non detection

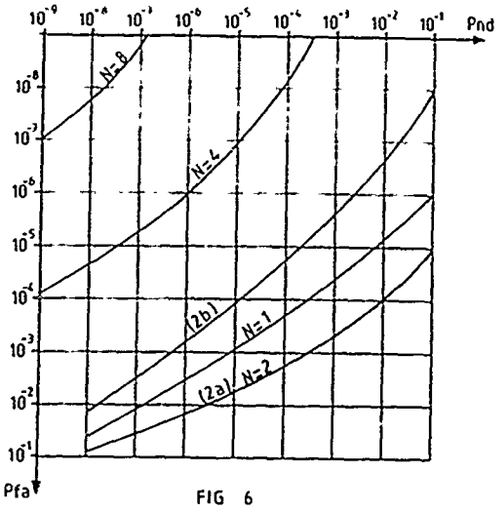

FIG 6

N nombre d'échantillons par symbole
Longueur du mot : 32
Taux d'erreur 2,5 %

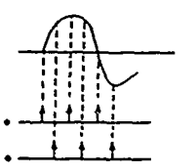

Courbe (2a)
Courbe (2b) optimale

Longueur du mot 32
4 echantillons par symbole

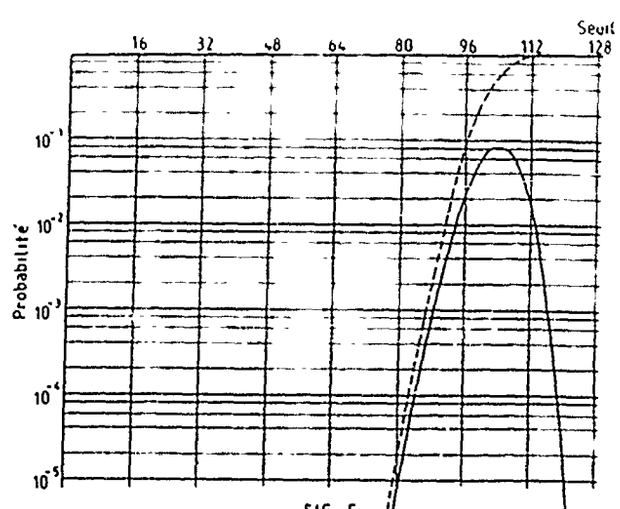

FIG 5
Taux d'erreur 11 %

Trait plein Probabilité que la corrélation soit égale à l'abscisse
trait pointillé Probabilité de non detection

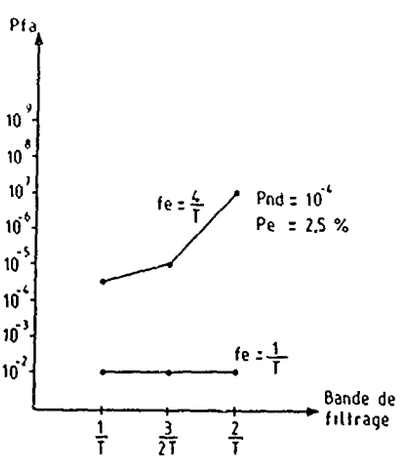

FIG 7

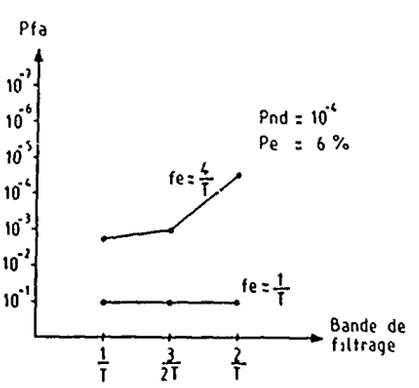

FIG 8

DISCUSSION

C. GOUTELARD

Vous utilisez des symboles numériques de durée T. Lorsque vous utilisez un échantillonnage à une fréquence $\frac{1}{T}$ en réalité vous sous-échantillonnez. Qu'en est-il pour le signal et le bruit ?

AUTHOR'S REPLY

Lorsque le signal est échantilloné, après une décision ferme, à un rythme $\frac{1}{T}$ nous supposons que la phase de l'échantillonnage est optimale. Vis-à-vis du signal nous nous trouvons dans le cas classique d'une transmission de données. Pour le bruit : une variable aléatoire est ajoutée au signal. Il est bien évident que ce traitement ne permet pas (sous-échantillonnage et opération non linéaire) de conserver le spectre du signal originel.

NEW APPROACHES FOR RAPID SYNCHRONISATION FREQUENCY HOPPERS

by
Mr A D Bisset BSC (Hons)
Marconi Defence Systems
Browns Lane
The Airport
Portsmouth
PO3 5PH
U.K.

SUMMARY

This paper describes in detail the analysis and simulation of a typical synchronisation protocol employed in a medium rate frequency hopper, specifically under poor signal conditions.

Bit slippage within the initial synchronisation frame was identified as the major source of reduced performance of synchronisation protocols. A set of performance curves is presented to enable the dependance on correlation threshold, and the ultimate receive probability for a given protocol, to be evaluated.

The dependance on bit synchroniser PLL bandwidth was simulated, indicating that improvement was possible at limit signal conditions. However, this was off-set by a reduced performance for better signal conditions.

An effective solution to such a problem can be achieved by employing a combined bit and frame synchroniser. Simulation results for such a technique are also presented for comparison.

INTRODUCTION

Synchronisation of any digital communication link, whether frequency hopping or single frequency, requires the operations of Bit, Frame and Message synchronisation to be successfully completed.

Bit synchronisation is essentially a demodulation process which ideally reproduces the data sequence originally transmitted, thereby providing the link between the analogue channel and the digital circuits in the receiver. Frame and message synchronisation is then required to enable specific blocks in this received data sequence to be identified. These are necessary operations, if, for example, the received data is encrypted.

Frame and Message synchronisation are obtained from the result of digital processing of the received data. For example, correlation of the received data against certain expected patterns is a technique commonly employed, synchronisation being obtained when a correlation yielding less than a defined number of errors is received. Given the bit error rate (BER) for the received data, the probability of obtaining a successful correlation may be readily evaluated.

To increase the message receive probability (MRP) synchronisation protocols can be employed which enable Frame and Message synchronisation to be obtained over a number of frames; i.e. multiple opportunities for sync at each stage (Frame and Message sync) are allocated. With the probability of correctly receiving a successful correlation known, the message receive probability can be readily evaluated for the synchronisation protocol employed.

The function of a bit synchroniser, described as a demodulation process above, is essentially a two stage operation. Initially the transitions in the received data need to be identified, and an internally generated clock, phase locked to them. This clock is then used to sample the received signal at an optimum point, to produce a value for the received data for the entire current bit period, thereby providing the necessary bit synchronisation.

Under poor signal conditions the transitions present in the received data will be noisy. Indeed the noise present will introduce additional transitions in the received data. It is therefore essential that the identified transition location is the result of averaging many transitions. A failure to do this will result in excessive random movements of the identified transition location with the result that the received bit error rate will be degraded.

Random movements in excess of +/- half a bit period cause an extra bit to be inserted/deleted from the received data. Such bit slips cause an instant loss of frame and message synchronisation, invariably rendering the remainder of the message ineffective. The synchronisation protocol must provide additional Frame and Message synchronisation opportunities to recover from such a breakdown.

For the purpose of introduction it can be assumed that some form of phase locked loop (PLL) is employed to provide the necessary transition identification and filtering. As with any PLL, such a configuration will have a certain transient performance dependent on its bandwidth. Hence, prior to the initial transient decaying sufficiently, the bit error rate of the first part of the received message will be degraded on the steady state value. This produces a reduction in the frame acceptance probablity, which can be minimised if the settling transient is rapid. However, a good steady state performance is achieved with a low bandwidth PLL, whilst for a fast transient performance a high bandwidth is required. With such a dichotomy, optimisation to meet both requirements is not possible and a compromise must be made.

A common solution to the above problem is to precede the message synchronisation preamble with a string of reversals. Analysis is relatively straightforward to evaluate the length of such a string of reversals necessary to achieve an acceptable steady state bit synchroniser performance for a defined link BER. The message receive probability expected is then readily evaluated, as discussed above. However, the penalty for such a simple strategy is an increase in the length of the message preamble.

In systems where the preamble length is constrained, the overhead of such a reversal string can be unacceptable and is therefore removed. Typical examples where such a strategy is required are:

(a) Medium Rate Frequency Hopping. Receivers wait for numerous hops on selected channels, for the single initial sync frame expected on that channel. On obtaining an acceptable correlation, bit and frame/hop sync are assumed. The receiver is then able to hop in synchronism with the transmitter and search for message sync.

(b) Packet Radio Synchronisation. In this example a single frame is allocated to provide the entire synchronisation for the following data packet. A principal factor in obtaining the maximum utilisation of the packet network is the performance of the synchronisation scheme. It is therefore essential that an optimal utilisation of the single frame is achieved.

PERFORMANCE BOUND OF SYNCHRONISATION PROTOCOL

The synchronisation protocol of a typical medium rate frequency hopper described above may be represented diagrammatically as shown in Figure 1a. Two possible outcomes for synchronisation to a message are shown: that of detecting the message, or failing. Also shown are the possible paths from the starting unsynchronised state to each outcome. Each path element has a probability associated with it, as shown. This enables the probability of traversing between any chosen states to be readily evaluated.

Figure 1a may be reduced to show the breakdown of requirements necessary to receive a message. Figure 1b represents such a reduction, showing the message receive probability as the probability of obtaining initial sync and then confirmation.

With the assumption that the bit error rate is constant from start to the end of a message, i.e. no degradation due to reconstitutor, the frame probability may be readily evaluated and Figures 1a and 1b used to evaluate the message receive probability. An upper bound on message receive probability may therefore be produced.

INCORPORATION OF FAILURE MECHANISMS

The synchronisation outcome path diagram may be readily modified to include the effects of bit slips, as shown in Figure 2a. Here bit slips occurring after initial sync have been represented by an additional element in the forward path, conveying the requirement that a bit slip must not occur in the remainder of the message.

Bit slips occurring within the frame which yields initial sync require a different inclusion as shown. The basis for this method of inclusion is significantly different than for bit slips after initial sync detection, due to the constraint that detection of initial sync is required to qualify possible bit slips.

The frame acceptance probability P_{FA}, frame rejection probability P_{FR}, frame acceptance with bit slip probability P_{FBS}, and bit slip probability P_{BS} are evaluated in the analysis sections below. The analysis presented is targeted at a typical production medium rate frequency hopper employing an early/late type PLL for data reconstitution, the operation of which may be represented by the decision process shown in Figure 3. Early or late transitions are shown to modify a counter, which acts as a form of filter. Phase adjustments of 1/28th of a bit period are made after an excess of 1, 4 or 16 transitions:

High bandwith	1 transition/adjustment	Pre Initial Sync
Medium bandwidth	4 transitions/adjustment	Post Initial Sync
Low bandwidth	16 transitions/adjustment	Tracking

SIMULATION ANALYSIS

The probability that a data transition is received earlier or later than expected is a function of the phase error, $\emptyset_e$, between the received data clock and the reconstituted data clock.

Hence, the late probability may be defined $P_l(\emptyset_e)$.

With the decision process contained in Figure 3, modifications to the reconstituted data clock phase cause the phase error $\emptyset_e$ to be increased or reduced. This in turn causes the probability of the type of the next transition to be changed, as P_l is a function of $\emptyset_e$. For a sequence of transitions the output phase distribution P_o can be evaluated by considering all possible paths that can be taken to get from the initial phase $\emptyset_i$, to the final output phase $\emptyset_o$. Movement between phase states is dependent on the filter output. Hence, the output phase distribution is also dependent on the counter's initial state.

With a phase adjustment of 1/28th bit period, the range of possible phase values may be defined by the set:

$$P_{VAL} = \{\emptyset : \emptyset = -13, -12 \ldots, 0, \ldots, +14\}$$

and the initial counter states:

$$C_{STATE} = \{C : C = 0, \ldots, NADJ-1\}$$

where: NADJ = number of transitions required/adjustment

We may therefore define the probability that the output phase is n after the sequence of transitions, which is conditional on the initial conditions, $\emptyset_i$ and C_j, as:

$$P_o(\emptyset = n/\emptyset_i, C_j)$$

where: $n \in P_{VAL}$

$i \in P_{VAL}$

$j \in C_{STATE}$

BIT SLIP

By the same method employed above, the probability of a bit slip resulting from the sequence of transitions may be defined, as:

$$P_{BS}(SLIP/\emptyset_i, C_j)$$

where: $i \in P_{VAL}$

$j \in C_{STATE}$

A bit slip being deemed to have occurred if an odd number of crossings of the -13, +14 phase state boundary are observed in the analysis interval.

BIT ERROR RATE

Each possible sample of the input signal across the bit period will have a error rate associated with it. This will range from 50% at the transitions up to the optimum for the channel conditions. This optimum sample point occurs with some fixed offset on the transition location. By accounting for this offset it is possible to associate each phase state with a resulting bit error rate. Hence the bit error rate is a function of the current phase state, expressed:

$$BER\ (\emptyset)\ ,\ \emptyset \in P_{VAL}$$

Each path traced from an initial phase to output phase, under the influence of the sequence of transitions, will yield a bit error rate which is dependent on the path taken. To account for all possible phase changes within a path, a quality measure must be assigned to each path, enabling the effect of the chosen path on the received bit error rate to be quantified. The path mean bit error rate was considered an acceptable approximation and therefore employed as the path quality measure. It is accepted that such an approximation will reduce the effect of values significantly above the mean. However, for conditions of interest there will only be a few elements within paths, hence the path variance will be low, justifying such an approximation.

Over the analysis interval, many possible paths can be taken from an initial phase state. Each path has a certain probability of being taken, and will yield a unique path mean bit error rate quality measure as discussed above. Hence a probability distribution representing the mean path bit error rate can be produced to combine the two factors.

To evaluate such a probability distribution it is necessary to introduce some form of quantisation, and evaluate the discrete probability distribution. Half percent sections were employed for the simulation, commencing at the optimum channel bit error rate and extending a further 13.5%. Values outside this range were constrained to be at the maximum value. The range of possible bit error rate values is defined by the function:

$$BER\ RANGE = (BER\ OPT + 0.5\ x) : x = 0, 1 \ldots 27$$

where: BER OPT = optimum bit error rate for the channel

B_{VAL} is defined to be the set of possible x values.

We may therefore define the probability that the mean bit error rate is n, after the sequence of transitions as:

$$P_b(BER = n/\emptyset_i, C_j)$$

where: $n \in B_{VAL}$

$i \in P_{VAL}$

$j \in C_{STATE}$

which is conditional on the initial conditions, $\emptyset_i$ and C_j.

ANALYSIS INTERVAL CONSTRAINTS

The arrays P_o, P_{BS} and P_b, discussed above, describe the probability of all outcomes expected due to the application of a sequence of transitions, commencing from defined initial conditions. The length of this sequence or analysis interval significantly effects simulation time. With a sequence of 16 transitions, approximately 10 minutes is required to produce the necessary data for the above variables. This extends to approximately one year for a sequence of 32 transitions, which is clearly unacceptable.

A further constraint on the sequence length is the number of transitions required per phase adjustment. If the filter size is comparable to the sequence length, then there will be negligible phase movement produced. An analysis interval of 16 transitions is acceptable for use in the highest bandwidth mode, as with 28 samples per bit a peak coverage of 57% of the bit period can be achieved, reducing to 14% with 4 transitions per adjustment. An alternative simulation is therefore employed to evaluate the 4 and 16 transitions per adjustment cases in the steady state (tracking) mode.

Sixty-three bits are employed for synchronisation frames in the target system. On average such frames will contain approximately 32 transitions, which is conveniently two analysis intervals of 16 transitions. Therefore, to meet the constraints of simulation time and phase adjustment, initial sync frames were approximated by two analysis intervals of 16 transitions each.

DEFINITION OF PHASE MOVEMENT OVER FRAME

The arrays P_o, P_{BS} and P_b describing the reconstitutor movement for half frames, are readily employed to evaluate similar arrays representing movement over entire frames. Defining:

$\emptyset_i$ = initial reconstitutor phase error.

$\emptyset'_o$ = reconstitutor phase error at the end of first analysis interval.

$\emptyset_o$ = final reconstitutor phase error at the end of a frame.

The output phase probability distribution at the end of a frame, P_F, given an initial phase is defined as:

$$P_F(\emptyset_o = n/\emptyset_i) = \sum_i \sum_j \sum_k P_o(\emptyset_o = n/i,k)\, P_o(\emptyset'_o = i/\emptyset_i,j)\, P_c(j)\, P_c(k)$$

where: $\emptyset_i \in P_{VAL}$

$\emptyset'_o = i \in P_{VAL}$

$n \in P_{VAL}$

Initial counter state for first interval $j \in C_{STATE}$

Initial counter state for second interval $k \in C_{STATE}$

and: $P_c(.)$ = discrete probability distribution representing the initial counter state.

With such a definition the conditioning imposed by the initial counter state has been eliminated. Hence the output phase probability distribution for a frame is conditional on the initial phase value only, as shown.

In high bandwidth mode NADJ = 1, and every transition produces a phase adjustment and the set $C_{STATE} = 0$. Hence, with a single state, $P_c = 1$, and there is no dependance on the counter state. However, for other values of NADJ the result is not trivial, and some approximation is required of the discrete probability distribution representing the initial counter state, to eliminate this variable.

DEFINITION OF MEAN BIT ERROR RATE OVER FRAME

If it is assumed that the path bit error rate, as evaluated above, is solely dependent on the initial phase conditions, i.e. there is no dependance on the final phase state. Then the probability distribution representing the effective mean bit error rate over a frame may be defined:

$$P_{BER}(BER = n/\emptyset_i) = \sum_{j}\sum_{k}\sum_{l}\sum_{m=o}^{n} P_b(BER = (2n-m)/1,k)\, P_b(BER = m/\emptyset_i,j)$$

$$P_o(\emptyset_o = 1/\emptyset_i,j)\, P_c(j)\, P_c(k)$$

where: $\emptyset_i \in P_{VAL}$

$1 \in P_{VAL}$

Initial counter state for first interval: $j \in C_{STATE}$

Initial counter state for second interval: $k \in C_{STATE}$

and the resulting mean bit error rate: $n \in B_{VAL}$

Where the resulting mean bit error rate has been produced as the average of the two constituents, i.e.:

$$n = \frac{m + m'}{2}$$

where: n = mean element BER indicator

and: m and m' = constituent BER indicators

$n, m, m' \in B_{VAL}$

hence: $m' = 2n-m$

DEFINITION OF TRANSIENT FRAME ACCEPTANCE PROBABILITY

The frame acceptance probability is a function of the required threshold for the 63 bit code; and the bit error rates for the two constituents i.e.:

$P(\text{frame acceptance}) = P_{OK}(m, m', th)$

m & m' = BER indicators

th = correlation threshold

The initial synchronisation probability, given the threshold and initial phase state, is defined:

$$P_{SYNC}(th,\emptyset_i) = \sum_{j}\sum_{k}\sum_{l}\sum_{m}\sum_{n} P_{OK}(m,n,th)\, P_b(BER = n/1,k)\, P_b(BER = m/\emptyset_i,j)$$

$$P_o(\emptyset_o = 1/\emptyset_i,j)\, P_c(j)\, P_c(k)$$

with parameters defined as previously.

This definition takes no account of possible bit slips occurring within the frame. Hence further conditioning on the synchronisation event is required, to partition the synchronisation event into those containing a bit slip and those not, represented by P_{FBS} and P_{FA} respectively in Figure 3a. With a frame represented by two halves, the possible outcome may be illustrated:

BIT SLIP

1st Half	2nd Half	RESULT
0	0	NORMAL OPERATION - NO BIT SLIP
1	0	50% BER ASSUMED 1ST HALF, NO FURTHER DAMAGE
0	1	SYNC ACCEPTANCE WITH BIT SLIP - MESSAGE SYNC WILL NOT BE ACHIEVED
1	1	ACCEPTANCE PROBABILITY VERY SMALL

0 = No Bit Slip

1 = Bit Slip Occurred

The bit slip probability is also conditional on the initial phase and counter states. Hence, $P_{FA}(\emptyset_i,th)$, the frame acceptance probability as a function of $\emptyset_i$ and the correlation threshold th, may be defined:

$$P_{FA}(\emptyset_i,th) = \sum_j \sum_k \sum_l P_c(j)\, P_c(k)\, P_o(\emptyset\delta = 1/\emptyset_i,j)\, \underbrace{(1-P_{BS}(SLIP/1,k))}_{\text{NO SLIP SECOND HALF}} *$$

$$\sum_m P_b(BER = m/1,k) \Big[\underbrace{P_{OK}(50\%,m,th)\, P_{BS}(SLIP/\emptyset_i j)}_{\text{SLIP FIRST HALF}} +$$

$$\sum_n P_{OK}(n,m,th)\, P_b(BER = n/\emptyset_i j)\, \underbrace{(1-P_{BS}(SLIP/\emptyset_i,j))}_{\text{NO SLIPPAGE}} \Big]$$

Similarly $P_{FBS}(\emptyset_i,th)$, the frame acceptance probability that will not result in confirmation, may be defined:

$$P_{FBS}(\emptyset_1,th) = \sum_j \sum_k \sum_l P_c(j)\, P_c(k)\, P_o(\emptyset\delta = 1/\emptyset_i,j)\, (1-P_{BS}(SLIP/\emptyset_i j))$$

$$P_{BS}(SLIP/1,k) \sum_n P_{OK}(n,50\%,th)\, P_b(BER = n/\emptyset_i,j)$$

DEFINITION OF PHASE STATE ON FRAME ACCEPTANCE

Analysis has shown that the bit slip probability post initial synchronisation is significantly dependant on the PLL phase state existing at acceptance.

Additionally, a significant PLL bandwidth reduction is invoked at acceptance, which will result in a long settling transient. The confirmation synchronisation codes will be passed during this period. Hence a further mechanism for loss in message receive probability exists. The phase state on acceptance is therefore defined:

$$P_{TERM\emptyset}(\emptyset_T=h/\emptyset_i,th) = \sum_j \sum_k \sum_l P_c(j)\, P_c(k)\, P_o(\emptyset_o = 1/\emptyset_i j)\, P_o(h/1,k)$$

$$\underbrace{(1-P_{BS}(SLIP/1,k))}_{\text{(NO SLIP SECOND HALF)}} \sum_m P_b(BER = m/1,k) \Big[\underbrace{P_{OK}(50\%,m,th)\, P_{BS}(SLIP/\emptyset_i,j)}_{\text{(SLIP FIRST HALF)}} +$$

$$\sum_n \underbrace{P_{OK}(n,m,th)\, P_b(BER = n/\emptyset_i,j)\, (1-P_{BS}(SLIP/\emptyset_i j))}_{\text{(NO SLIP FIRST HALF)}} \Big]$$

Due to the conditioning imposed by the frame acceptance requirement, this function will not sum to unity. Normalization is therefore required for events post initial synchronisation.

TRANSIENT ANALYSIS

The output phase probability distribution P_F developed above, is conditional on the initial phase. By defining the initial conditions, P_F may be employed to evaluate P_F, the actual output phase distribution:

$$P_F^1(\emptyset_o = n) = \sum_i P_F(\emptyset_o = n/i)\, P_i(\emptyset_1 = i)$$

where the initial phase $\emptyset_i = i \in P_{VAL}$

and $P_i(.)$ = initial phase probability distribution

Although not strictly a matrix, P_F in the expression above is readily visualised as such. Hence in the following discussion, P_F is referred to as the phase transition matrix.

The phase settling transient may be iteratively produced by successive evaluation of the output phase distribution, from the phase transition matrix and current input phase distribution, and by employing the previous output phase distribution as the input phase distribution for the next iteration. Defining:

Pi_n = Initial phase probability distribution for nth frame

$P'F_n$ = Output phase probability distribution for the nth frame

With no apriori of the received data clock phase it is reasonable to assume the initial phase distribution for P_{i_1} is uniform. The first frame received causes some settling to occur and P'_{F1}, results. The effect of further frames may be evaluated by defining:

$$P_{i_{n+1}} = P'_{F_n}$$

where: n = frame number in settling transient

LOW BANDWIDTH TRANSIENT ANALYSIS

In this mode typically less than one phase adjustment is made per frame. Hence the effect of frames is essentially represented by the change in the counter state that occurs across the frame. Extension of the above analysis is therefore required to include this aspect. However this is not realistic for very low bandwidths, due to the excessive simulation time required.

For this analysis the current PLL state was represented by the set of two-tuples defined:

$$P_{STATE} = \{(X_1, X_2)\}$$

where: $X_1 \in P_{VAL}$

$X_2 \in C_{STATE}$

The application of a transition will cause the adjacent state to be adopted. The probability of this new state may be defined, as shown in Figure 5, for cases when no phase adjustment is made. More rigorously the new state for all initial states may be defined:

$$P_{\substack{STATE \\ n+1}}(\emptyset,K) = \begin{cases} \left.\begin{array}{l} P_{\substack{STATE \\ n}}(\emptyset,K+1)\, P_1(\emptyset) \\ + P_{\substack{STATE \\ n}}(\emptyset,K-1)\, \overline{P}_1(\emptyset) \end{array}\right\} \text{for } 0 < K < C_{MAX} \\ \left.\begin{array}{l} P_{\substack{STATE \\ n}}(\emptyset,1) P_1(\emptyset) \\ + P_{\substack{STATE \\ n}}(|\emptyset-1|_{PMAX}, C_{MAX})\, \overline{P}_1(|\emptyset-1|_{PMAX}) \end{array}\right\} K = 0 \\ \left.\begin{array}{l} P_{\substack{STATE \\ n}}(|\emptyset+1|_{PMAX}, 0)\, P_1(|\emptyset+1|_{PMAX} \\ + P_{\substack{STATE \\ n}}(\emptyset, C_{MAX}-1)\, \overline{P}_1(\emptyset) \end{array}\right\} K = C_{MAX} \end{cases}$$

After initialisation, successive application of the above rule enables the output phase distribution to be iteratively evaluated, for as many transitions as required.

The above analysis is readily extended to accommodate bit slip evaluation if the range of P_{VAL} is extended. Bit slippage is then indicated by a reduction in the main lobe probability, Figure 6.

SIMULATION VALIDATION

Message receive probability versus link signal to noise ratio (SNR) is shown in Figure 7, for simulated and experimental results. Due to the practical limitations of obtaining measurements of sync probability, the number of trials over which the sync probability was measured is significant. To account for this a 90% confidence interval, evaluated from the trial conditions and results, is shown on the performance curves. Such a bound defines a region where there is a 90% chance of the actual MRP being situated.

In view of practical problems associated with measurements at low signal to noise ratios, the half dB error at low signal to noise, between experimental and simulated results, was considered an acceptable error. The simulation results were therefore considered consistent with the experimental results available.

DISCUSSION

The probability of obtaining initial sync versus SNR, for various correlation thresholds is shown in Figure 8; where the synchronisation protocol employed requires a minimum of one sync frame from four to be obtained to achieve initial sync. This graph indicates that at 3dB SNR (approx 10% BER) the optimum correlation threshold is 52 to 53. At 3dB SNR initial sync detection probability is quite insensitive to correlation thresholds. However below 3db SNR the correlation threshold is very critical as shown.

Also shown in Figure 8 is the performance of a combined bit synchroniser and frame synchroniser. This employed a simple maximum bin technique to identify the transition locations present in the input data; enabling the data to be extracted from a stored unsynchronised version of the input data. The transition location was therefore fixed for each frame correlation.

At 1dB SNR (approx 18% BER) there is negligible improvement with this type of synchroniser with such a simple selection algorithm employed. However at 3dB the improvement is significant. Additionally a reduction in the correlation threshold produces an increase in detection probability. This is not the case with the PLL synchroniser, as shown in Figure 8.

With the PLL type synchroniser bit slips occurring in the latter half of the sync code will prevent detection of the rest of the message, as detection of initial sync is employed to define the bit sync phase (which is then preserved by a bandwidth change); illustrated in Figure 2a as PFBS. For a given correlation threshold and SNR, this loss limits the effectiveness of multiple synchronisation opportunities.

For a SNR of 1dB (approx 18% BER) the initial sync detection probability versus the number of attempts is shown in Figure 9. This graph clearly illustrates the trade off between correlation threshold, and the number of sync attempts allocated. The maximum bin synchroniser is not limited by this effect. Hence the sync probability approaches unity as the number of sync attempts are increased, as shown.

To operate in a scenario which provides a good signal when unjammed, but where 70% of hops are jammed and unusable. Then nine initial sync attempts would be required to provide a 95% chance of gaining initial sync. With nine initial sync attempts the maximum bin synchroniser at 18% BER will provide a 99% chance of gaining initial sync. Hence as far as initial preamble length is concerned, the requirements for 70% jamming and a limit signal defined as 20% BER are similar.

Post initial sync detection a low bandwidth PLL synchroniser is employed to obtain accurate bit synchronisation, and to enable signal fades to be bridged. The transient response at 1dB SNR is shown in Figure 10 for the medium bandwidth employed, i.e. 4 transition required/adjustment. With no apriori of the bit phase the settling transient lasts in excess of 14 frames. The conditioning on the initialization imposed by the requirement to detect initial sync significantly reduces the settling transient as shown. The maximum bin selection technique indicates approximately a 12 or 6 frame settling advantage over the no apriori and sync acceptance cases respectively. This could be increased further if the maximum bin selection process was employed for further frames, prior to switching to PLL timing maintenance.

TRANSITION FILTER MODIFICATIONS

The effect of reducing the bit synchroniser PLL bandwidth is shown in Figure 11. At 3dB SNR, (10% BER) a change from a 1 transition/adjustment to a 4 transition/adjustment filter will produce an improvement in message receive probability of approximately 1%. However, below 5dB SNR this improvement is lost. Additionally the rate of improvement in MRP with increasing SNR is negligible compared with the 1 transition/adjustment filter case.

Bit slips in the latter half of the initial sync frame are causing these effects, as shown in Figure 12. Below 5dB SNR the 1 transition case is significantly worse than the 4 transition case. Which is reflected in an improved initial sync detection probability as shown in Figure 11. However, above 5dB SNR the transition case is better with a faster rate of reduction. This is producing the increasing performance in Figure 12 for the 1 transition case, when the 4 transition case has settled out.

CONCLUSIONS

Bit slippage in the latter half of the initial sync frame with a PLL type bit synchroniser is a major failure mechanism of synchronisation protocols. Its effects may be minimised only by the careful selection of both correlation threshold and number of initial synchronisation opportunities, (Figure 9). The bandwidth of the bit synchroniser PLL must be selected with respect to good signal and limit signal conditions, to avoid an unacceptable levelling off of synchronisation probability, Figures 11 and 12.

A correlation type bit and frame synchroniser is required to eliminate this effect.

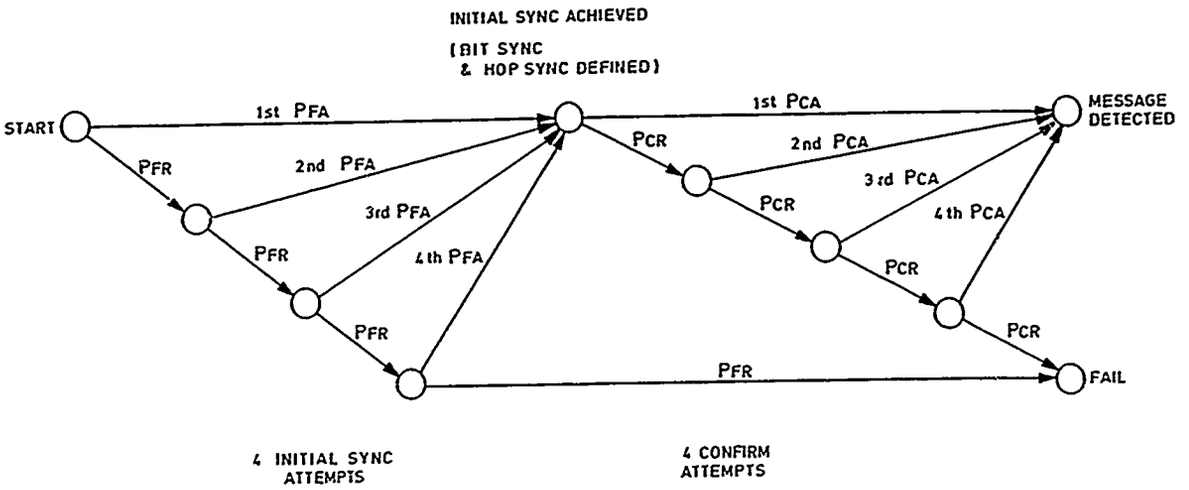

Figure 1a Representation of Synchronisation Scheme

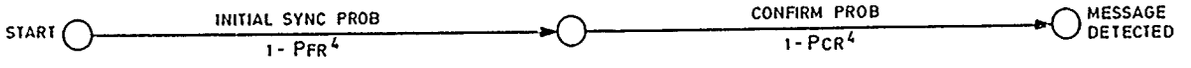

Figure 1b Minimisation

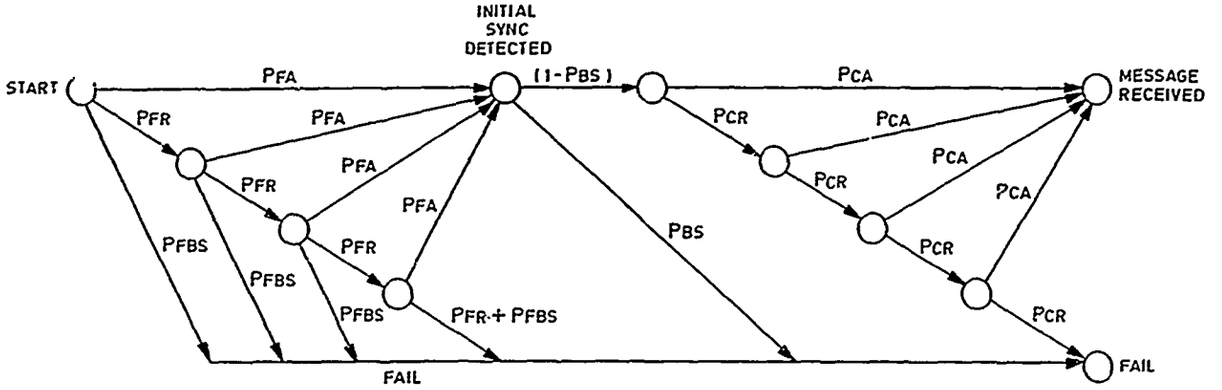

Figure 2a Representation of Synchronisation Scheme with Failure Mechanics

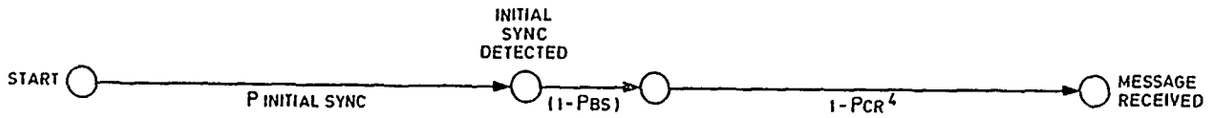

$$P_{\text{INITIAL SYNC}} = P_{FA}\left[1 + P_{FR} + P_{FR}^2 + P_{FR}^3\right]$$

Figure 2b Minimisation

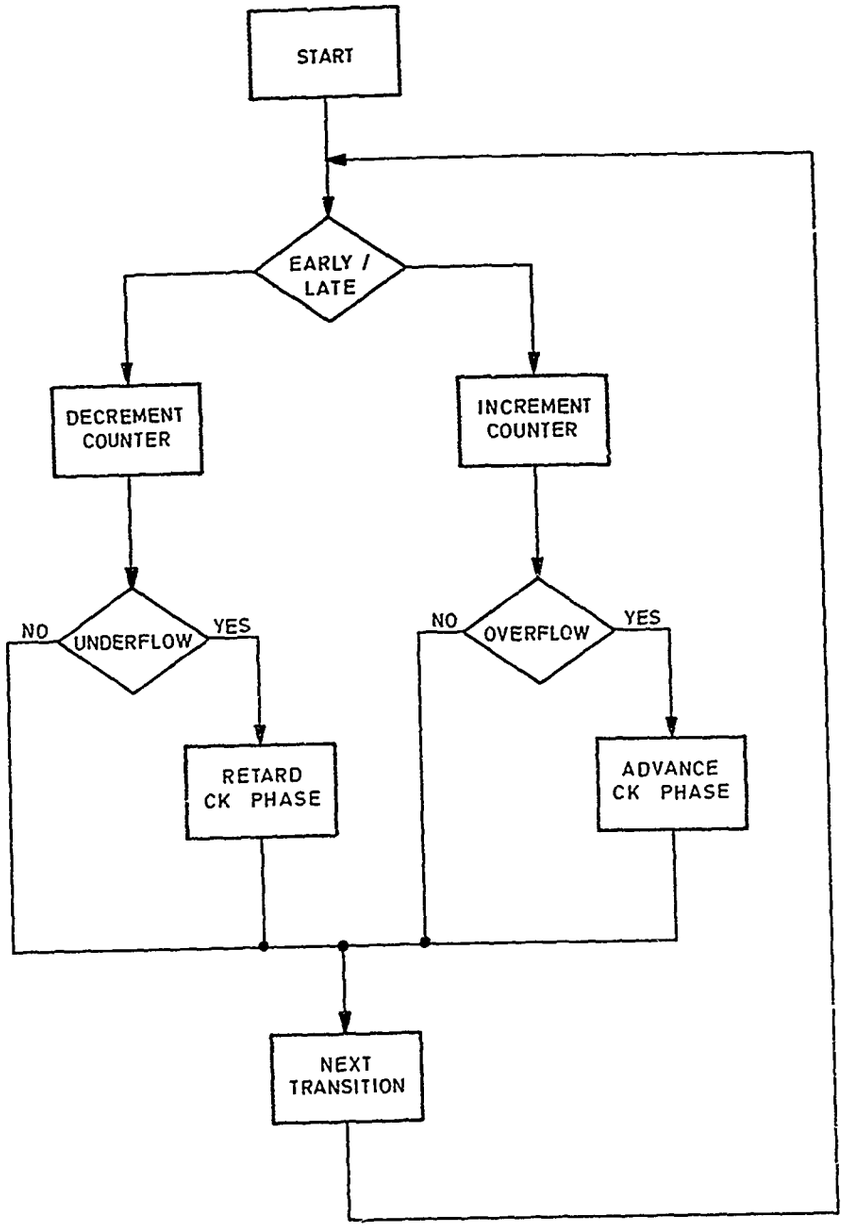

Figure 3 Bit Synchroniser Decision Process

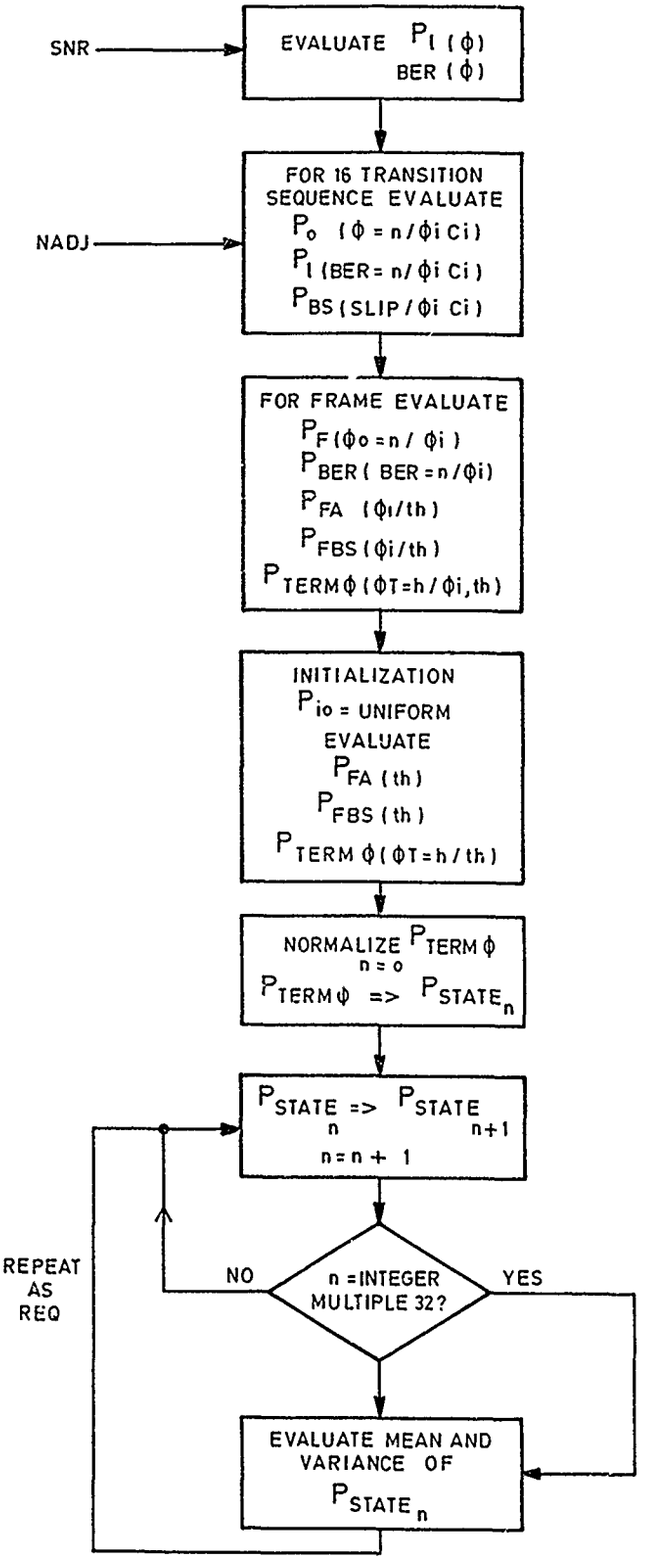

Figure 4 Simulation Flow Chart

PROBABILITY OF NEW STATE

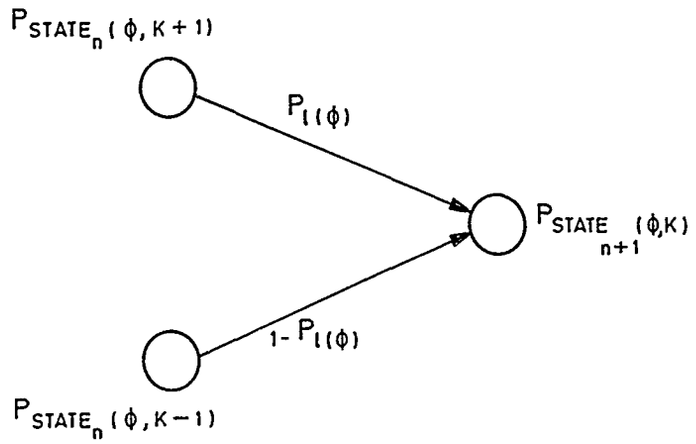

NOW STATE DEFINED

$$P_{STATE_{n+1}}(\phi,K) = P_{STATE_n}(\phi,K+1)\,P_l(\phi) + P_{STATE_n}(\phi, K-1)(1-P_l(\phi))$$

(FOR NO PHASE ADJUSTMENT CASE)

Figure 5 Probability of New State

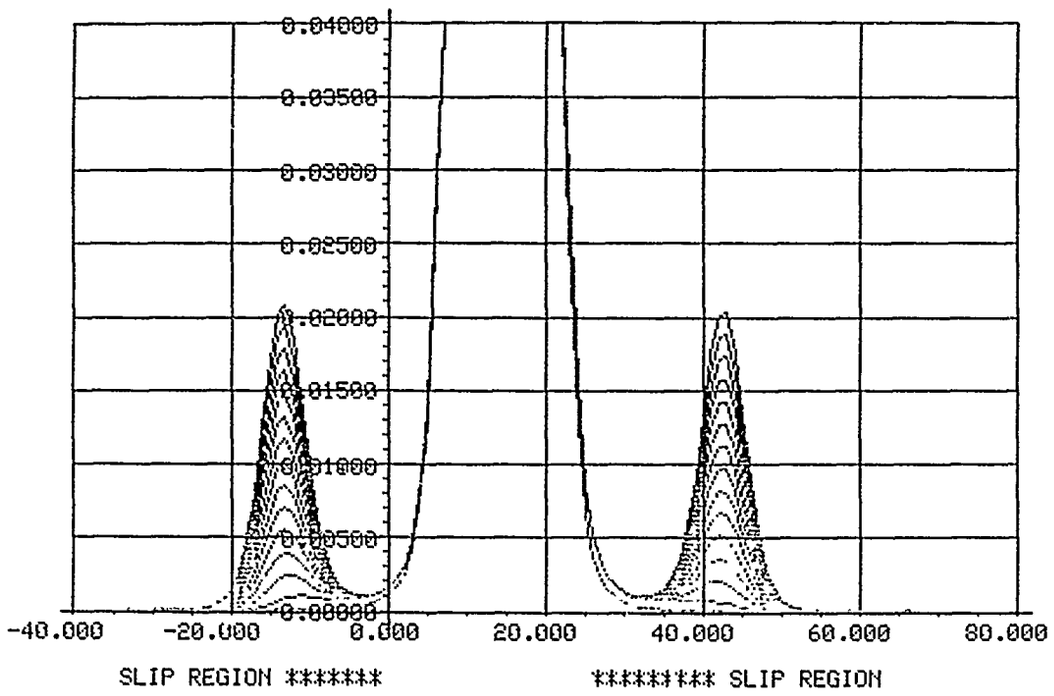

Figure 6 Transient Phase Probability Distribution

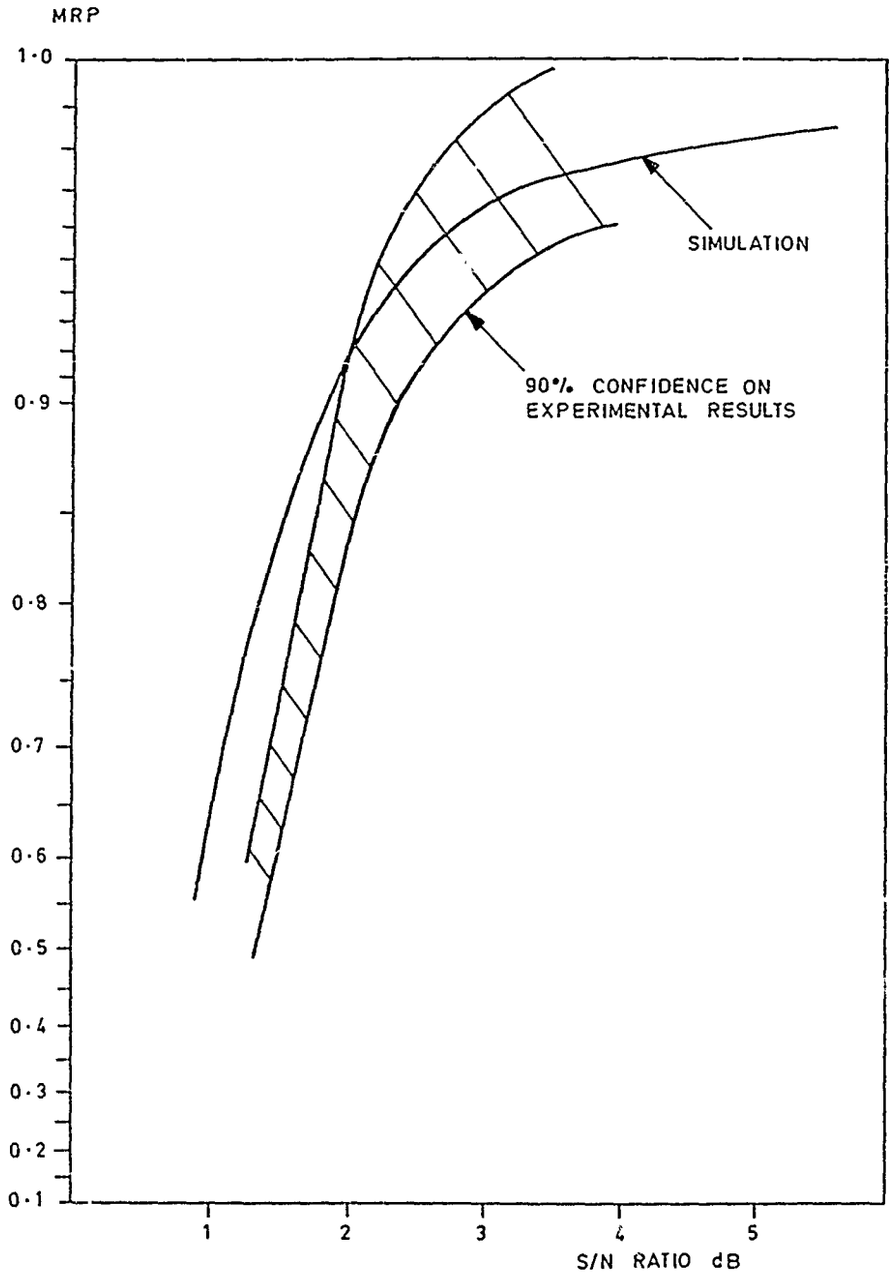

Figure 7 Message Receive Probability Vs Signal to Noise Ratio

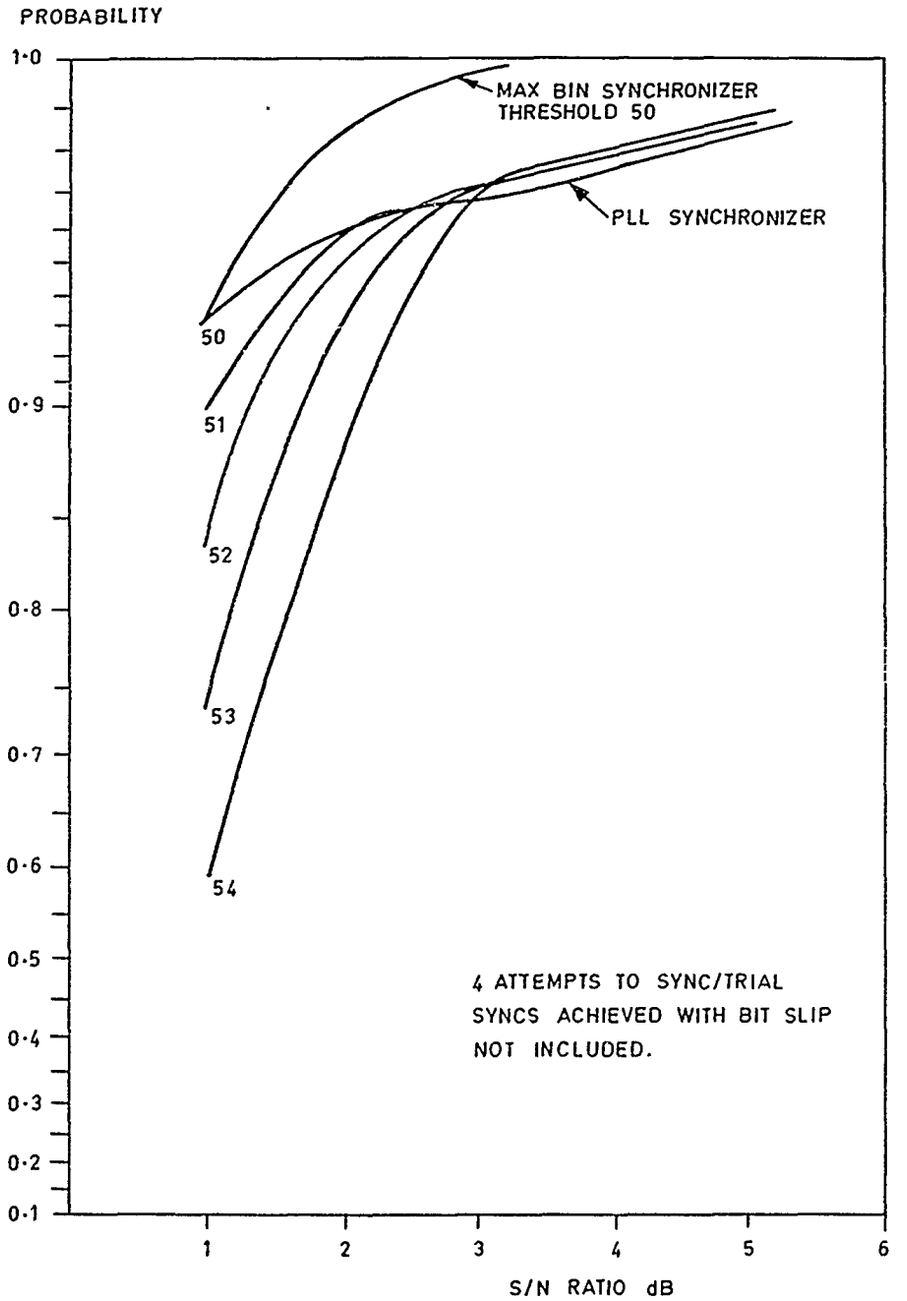

Figure 8 Probability of Detecting Initial Sync Vs Signal to Noise Ratio

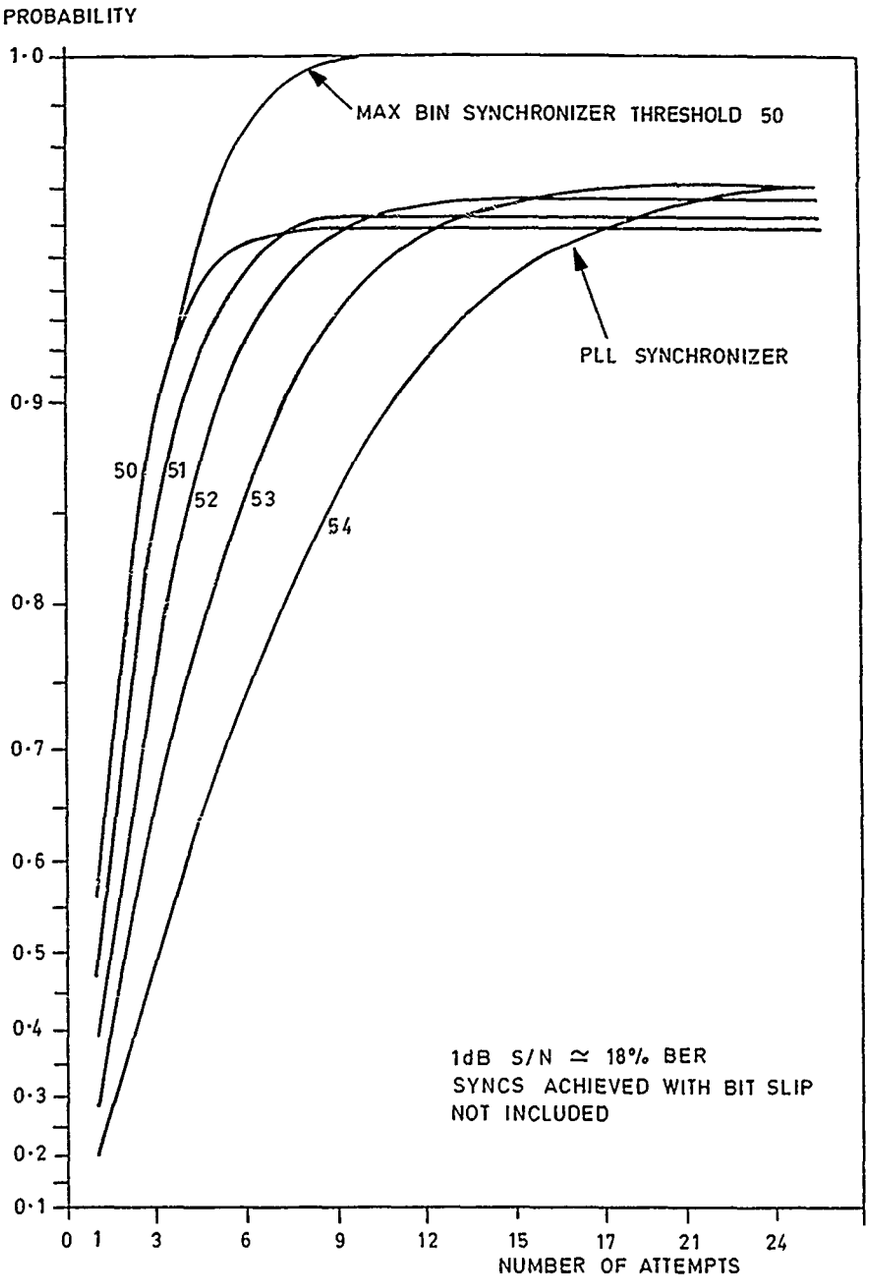

Figure 9 Probability of Detecting Initial Sync Vs Number of Attempts for Various Correlation Thresholds

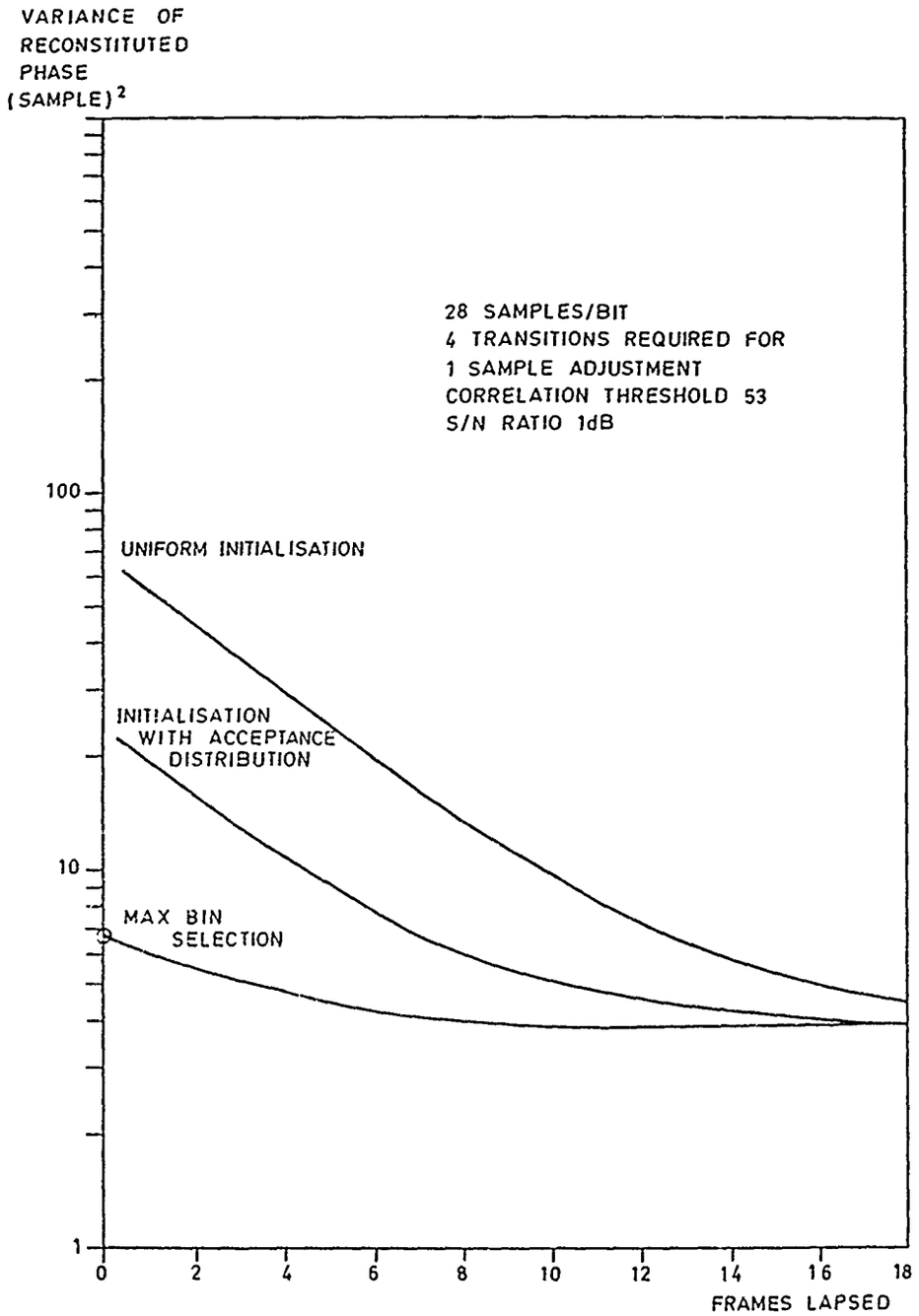

Figure 10 Transient Response at 18% BER

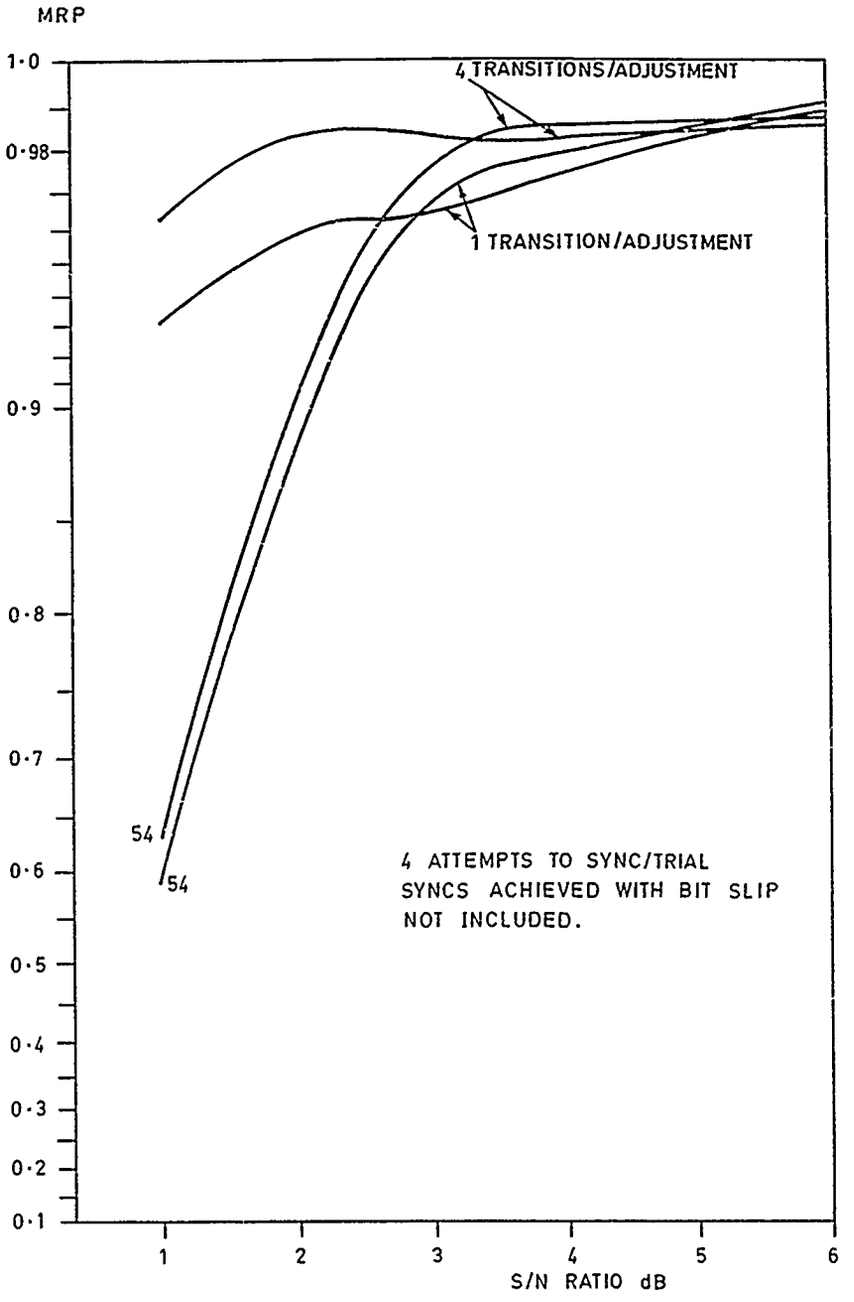

Figure 11 Probability of Detecting Initial Sync Vs Signal to Noise Ratio

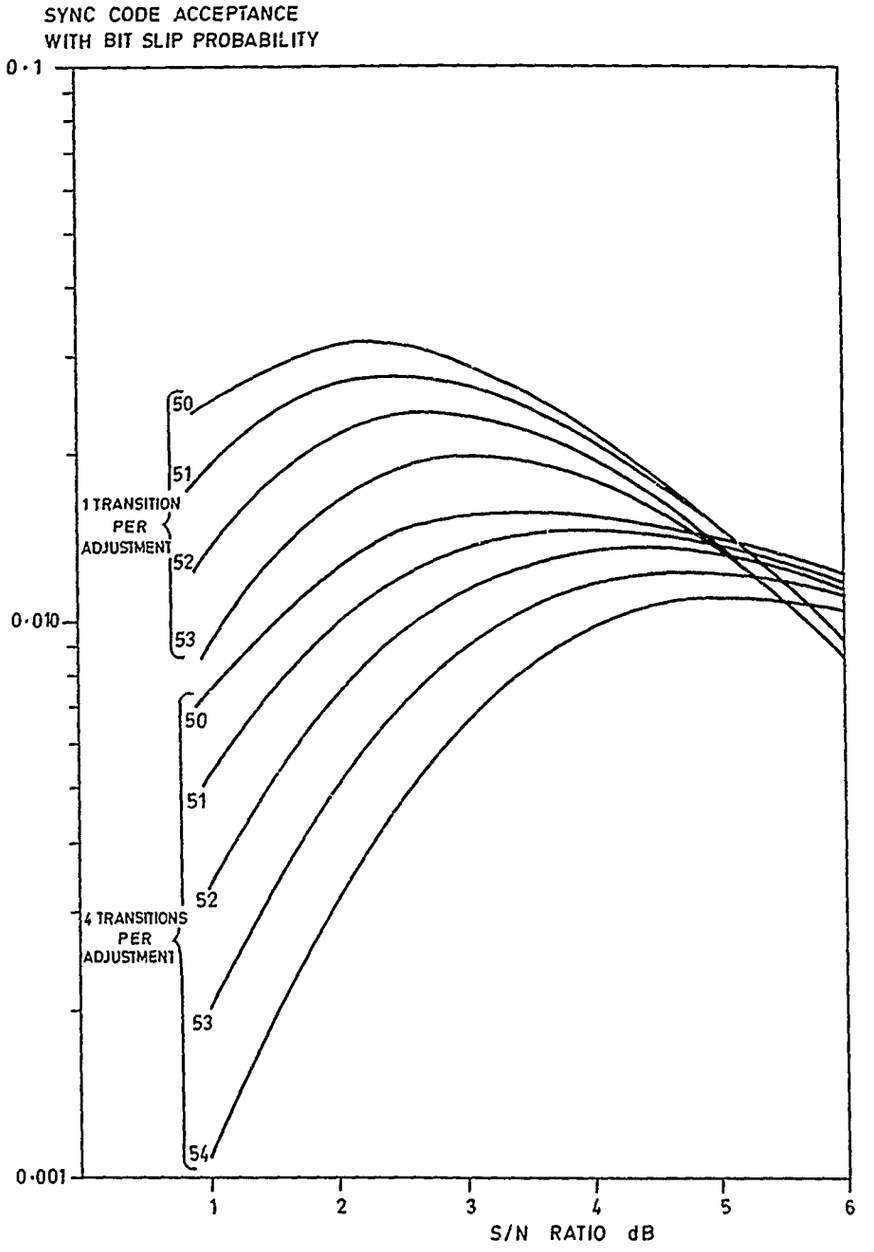

Figure 12 The Probability of Sync Detection with Bit Slippance
Vs Signal to Noise Ratio

SUMMARY OF SESSION III

SYSTEM PERFORMANCE

by

H. VISSINGA, Session Chairman

Seven papers were presented in this session covering a wide range of aspects of system performance. These papers are summarised below.

"Effects of Ionospheric Modification on System Performance"
(I have neither an abstract nor a preprint available on this paper).

"HF Spread Spectrum, an Audit of Power Requirements and LPI Vulnerability".
In this paper the consequences of the congestion of the HF band are considered when introducing spread spectrum systems. In order to maintain an acceptable data throughput the radiated power has to be increased to such a level that this has a significant influence on the probability of exploitation by the adversary. Parallel diversity is proposed as a means that offers a significant improvement in this aspect.

"Combined Effects of Fast and Selective Fading on Performance PSK and MSK with Coherent Detection".
In this paper theoretical results for the required threshold for a given errorrate are given for a WSSUS channel. For both QPSK and MSK results are presented for different Doppler shifts and path delays.

"Etude expérimentale d'une liaison numérique radiomobile à étalement de spectre en site urbain".
In this paper results are presented of the measured bit errorrate of a direct sequence spread spectrum system for the following interfering signals : white noise, sinusoidal, d.s.s.s. and multipath under simulated conditions. On the radiochannel narrowband measurements were performed on the mean decrease of the fieldstrength with distance and the fast variations of it in a moving car. In the wideband configuration the channel impulseresponse was measured.

"Packet Radio Network Concepts for the Norwegian Field Army".
In this paper mobile packet radio (PR) network concepts are described and discussed. Many PR networks are connected through radio access points to a tactical communications area network. Each PR network has its own frequency, access to the common channel is governed by the CSMA technique. The radio equipment makes use of direct sequence spread spectrum modulation. The inherent capture effect of this has a beneficial effect on throughput.

"Experimentation d'un système de transmission de données par canal météorique : Théorème".
In this paper the first phase of an experimental programme of a meteor burst system on a frequency of some 40MHz over a distance of 350 km is described. The modulation is FSK, the bitrate 16Kbit/s. With a transmitter power of 1KW the mean throughput is 100 to 150 characters per second, while the maximum is 300 to 400.

"System Factors to be Considered in Assessing Propagation Effects on Modern Satellite Communications Systems".
In this paper, system factors to be considered in the assessment of propagation effects are outlined. The essence is to point out that for modern digital satellite communications systems propagation assessment has to have proper system reference in order to provide readily useful conclusions for system engineers.

EFFECTS OF IONOSPHERIC MODIFICATION ON SYSTEM PERFORMANCE

Suman Ganguly
Center for Remote Sensing
8200 Greensboro Drive, Suite 503
McLean, VA 22102
USA

Controlled ionospheric modification can be used for disrupting as well as facilitating communication and radar systems. After briefly describing the results achieved with the present day ionospheric modification facilities, we present a scenario for the genertion of strong and significant ionospheric modification. We present a few schemes for the development of modern high power facilities using the state of the art technology and then describe the impact of such facilities on the system performance.

1. INTRODUCTION

Artificial modifications of the ionospheric plasma induced by high power radio waves have been studied for the last two decades, and these investigations have shown strong promise of utilizing these ionospheric modifications for practical benefits as well as understanding the involved physics of the wave-plasma interactions. Interaction between the e.m. wave and the ionized plasma could be hard or soft. This depends on the R.F. frequency (f). For hard interaction, when $f > f_p$, the plasma frequency, strong interaction can take place at the crossing of two r.f. beams. This was first proposed by Ganguly and Gordon (1984)[1]. The beat frequency produced by the two UHF or VHF beams could ultimately cause plasma breakdown and unlimited energization of the plasma (see Fig. 1).

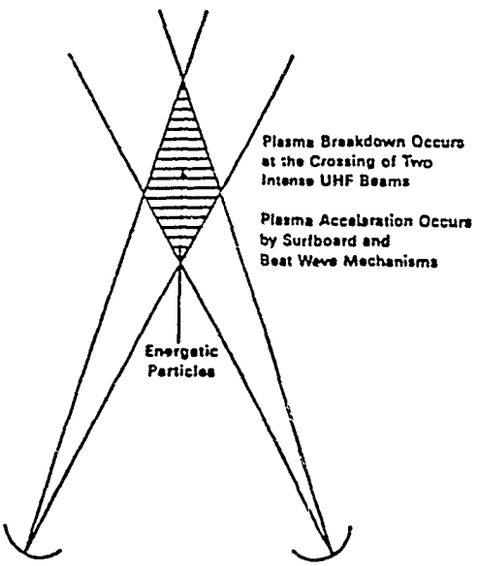

Figure - 1.

Although these concepts are well established in laser fusion studies, there has been no practical experiment in the earth's ionosphere. All the ionospheric modification by ground based wave injection has been done with H.F. beams (soft interaction). This is mostly because for H.F. frequencies the electric field is enhanced near the region of reflection. For low wave energies, nonlinear forces arising through collisional forces have been well known since the early days of radio waves. As the power density increases, the ponderomotive force effects manifest. A good measure of this force is determined when the quiver velocity becomes comparable to the thermal velocity. In the H.F. range this can happen with power densities of only mw/m^2. Currently, ionospheric modification facilities exist in Arecibo, Puerto Rico, in Alaska, in Tromso, Norway and in several places within the U.S.S.R. During these modification processes we have observed the following features :

a) Electron temperature increases by a factor of up to about two to five.

b) Large and small scale density irregularities are generated by thermal and ponderomotive forces. Typically one to ten percent. Depending on the scale size.

c) Several plasma waves, instabilities and turbulences are generated.

d) Electron energization results in enhanced optical emission.

e) Nonlinear processes give rise to wave mixing and wave generation.

The effect of these physical changes on radio waves are summarized in Table I. The available power densities in all of these facilities are too small to create any dramatic change. With large enough power densities the ionospheric plasma will breakdown (Gurevich, 1978)[2] and artificial layers and patches can be generated. (See Figure 2). Once the plasma breakdown is attained, relatively modest power should be able to sustain it.

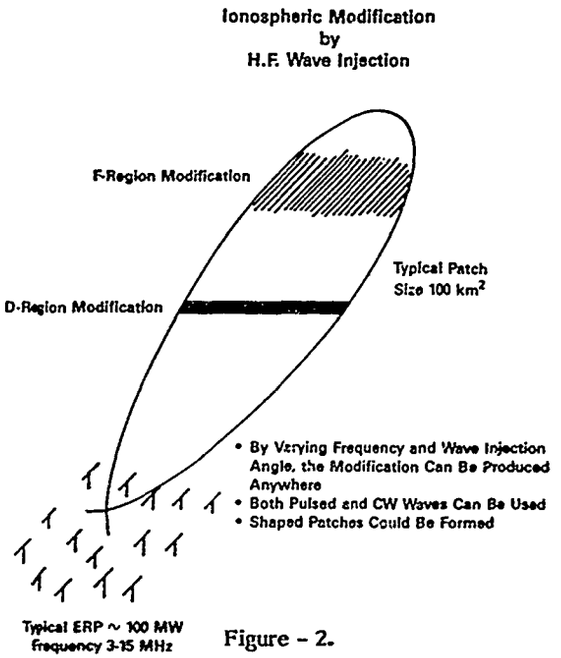

Figure – 2.

TABLE I

EFFECTS OF IONOSPHERIC MODIFICATION ON RADIO WAVES

UHF BAND	Plasma waves and related instabilities produce weak backscatter signals. Scintillation of radio waves by large (Km) scale irregularities are well documented.
VHF BAND	Strong backscater from field aligned irregularities observed. Scintillation for transionospheric propagation.
H.F. BAND	Spread F, Multiple Traces, Z-Mode Propagation, Ducting, Caviton & Turbulence, Changes in H.F. Spectra, Doppler Shift, Backscatter, Nonlinear Effects. Changes in Attenuation (WBA) and phase in the F-region and D & E regions. Strong HF signals can occasionaly penetrate the ionosphere.
WAVE GENERATION	Generation of beat frequency wave, Helicon, Alfven, Whistler, Ion Chyclotron and Electron Cyclotron modes. Beat wave generated at the H.F. frequency can produce plasma breakdown and can accelerate electrons. ULF-HF propagation can be affected by changes in lower ionosphere, where the most dramatic effect can take place.

2. CURRENT UNDERSTANDING

In spite of our demonstrated ability to use the artificial ionospheric modifications for the control of communication, radar and related areas and the significant understanding of the wave plasma interactions, our understanding of the involved physical processes has been mearge. Earlier observations at Platteville initiated investigations on HF and VHF scattering processes, whereas the investigations at Arecibo prompted some interesting theoretical studies on the involved parametric and several other plasma instabilities. The parametric instability was first discovered at Arecibo and significant amounts of theoretical and experimental research has been conducted in these areas.

The incoherent scatter diagnostics at Arecibo also attracted some (although very limited) interests from the plasma physics community. The interaction of strong e.m. waves with the plasma can produce a wealth of plasma instabilities and other effects that are difficult to study in the laboratory. Thus, oscillating two-stream instabilities, caviton formation and decay, stimulated Brillouin scattering, thermal self-focussing, particle acceleration, Z-mode propagation have all been observed at Arecibo. Two major areas that have been neglected are aeronomical implications of ionospheric modifcations and the search for new events.

Very little has been achieved in terms of interfacing the radio engineering communities with the plasma physics group. Utilization of the wealth of plasma physics knowledge, particularly that gained through laboratory and theoretical studies related to high energy physics and laser fusion, into the scaled version of the ionosphere, has been attempted in a limited manner. Very little knowledge exists in the modifications of the lower ionosphere, generation of ULF, ELF and VLF waves, possible generation of the F-region cavitons or plasma instabilities and plasma turbulence, and their relationship with the H.F., VHF scattering process is still unclear. Scintillation of the radio signals and even the backscatter of VHF signals are not yet well understood.

In its upward journey, (Figure 3), the first encounter of the radiowave takes place in the lower ionosphere, where it raises the electron temperatures and loses most of its energy. It is here that the ULF-VLF waves could be generated either by modulating the ambient current or by the dynamo effect. Modification of the D-layer also affects ELF-VLF propagation. Creation of artificial layer is also most efficient at these heights. If the radio wave survives with significant strength, it produces detectable interaction in the F-region, where, because of the resonance swelling of the E-field and because of low collisional damping, wave plasma interactions manifest themselves in creating an array of plasma waves, instabilities and density perturbations created by thermal and ponderomotive forces.

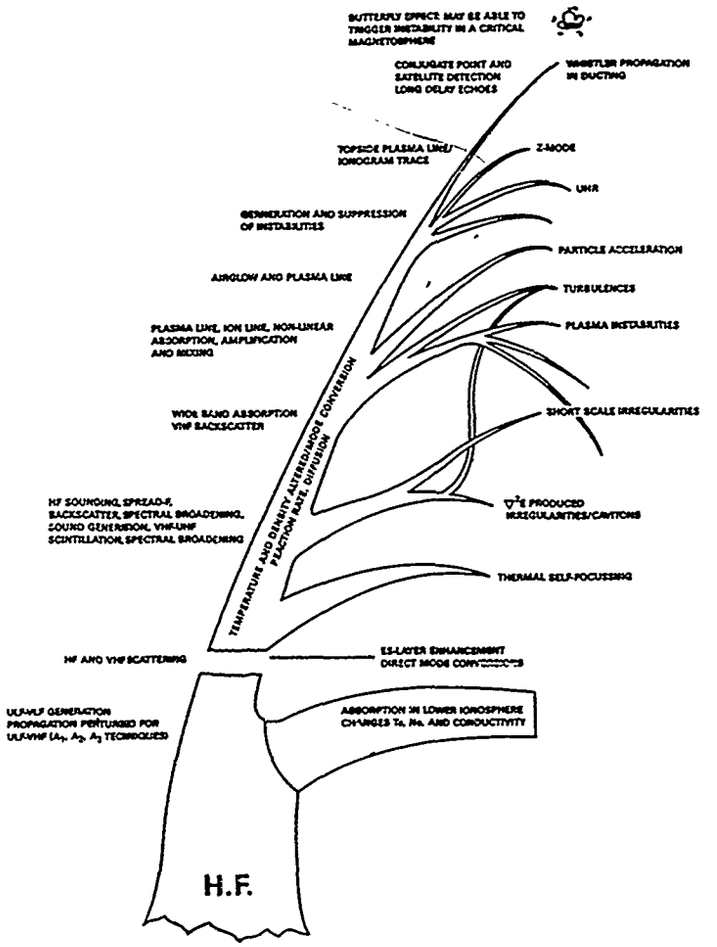

Sketch of Interaction of HF Wave in the Ionosphere

Figure - 3.

The large and small scale density perturbations could be created by thermal self-focussing, by formation of cavitons, by interaction with ion-sonic waves or by various other instabilities. Although parametric instability has been reasonably well investigated at Arecibo, the relative roles of the other processes such as resonance instability, drift instability, oscillating two stream instability, two stream and plasma fluid instability, ExB instability, etc. and also the decay of dissipative parametric instability, dissipation of decay instability, nonlinear thermal coupling of decay instability, trapping of plasma waves inside cavitons, possible formation of solitons, formation of clumps, etc. are almost unexplored. Collapse of the caviton and decays of various instabilities could eventually lead to plasma turbulence and accelerate the ambient plasma. Our current state of knowledge of these plasma processes is almost in a state of flux.

Experimental observations of the formation of cavitons and large - and small-scale density fluctuations have been meagre. Little is known about their growth, decay, threshold E dependence, on polarization and orientation to the magnetic field lines. Even the conversion of e.m. waves into the e.s. wave modes and vice versa in the inhomogeneous plasma is little understood. It has been suggested that excitation at UHR region could inhibit the formation of plasma wave and instabilities. Coordined theoretical and experimental studies are needed to understand the various instabilities and their relationships with irregularity generation.

There are observations that showed the strong plasma oscillation generated by penetration of high power radiowave through the overdense plasma (Ganguly and Gordon,)[3]. Proper understanding of the processes are lacking although this has a profound implication in the application of space borne systems.

Beat frequency excitation and periodic modulation of the electric field generate whistler and Alfven mode waves. These could trigger several instabilities in the magnetosphere and there are evidences that auroral particle precipitation is enhanced due to similar triggering. The auroral situation also offer exciting opportunity of studying field aligned electric field effects. Cornwall and Vesecky (1984)[4] critically reviewed the generation of $E_{\parallel}$ by non MHD effects such as kinetic Alfven waves and anomalous resistvity as well as phenomena expected from E. These include beam driven instabilities such as electrostatic ion cyclotron or ion acoustic waves which can cause trapping of upward moving bomb generated plasma, as well as precipitation into the ionosphere of naturally occurring energetic plasma. The field aligned electric field and currents are known to be associated with ion acceleration.

VLF waves injected into the magnetosphere from Siple Station, Antarctica was amplified by 30 db or more and triggered intense emissions with bandwidths extending up to several hundred Hz (Helliwell[5], 1983). This was possibly produced by a feedback interaction between the waves and counterstreaming cyclotron resonant electrons in the magnetosphere. Possibilities produced by whilstler type mode or Alfvenic modes and associated electron precipitation can potentially trigger a critically unstable magnetosphere and precipitate a large scale magnetic storm. (See Fig. 4 and 5)

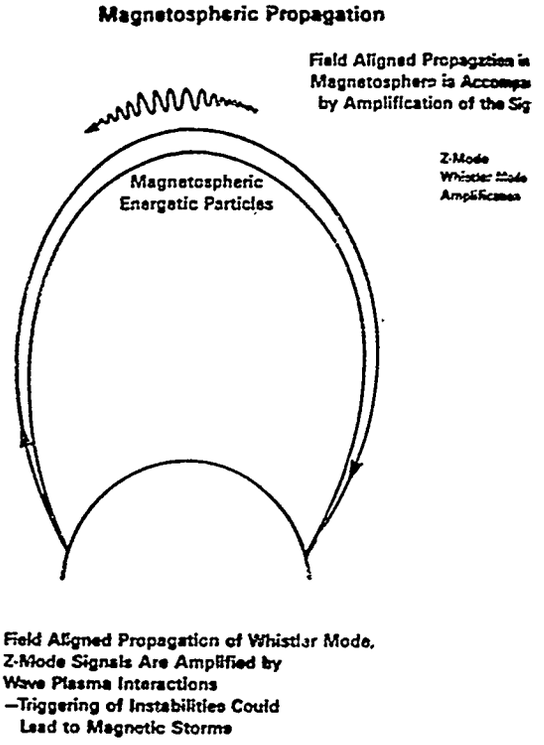

Figure - 4.

Large acceleration of electron population by magnetic mirroring in the magnetosphere could result. Ducts produced during the ionospheric modification favour radiowave propagation over long distances in the magnetosphere. Around the world propagation and reflection from conjugate points have been reported.

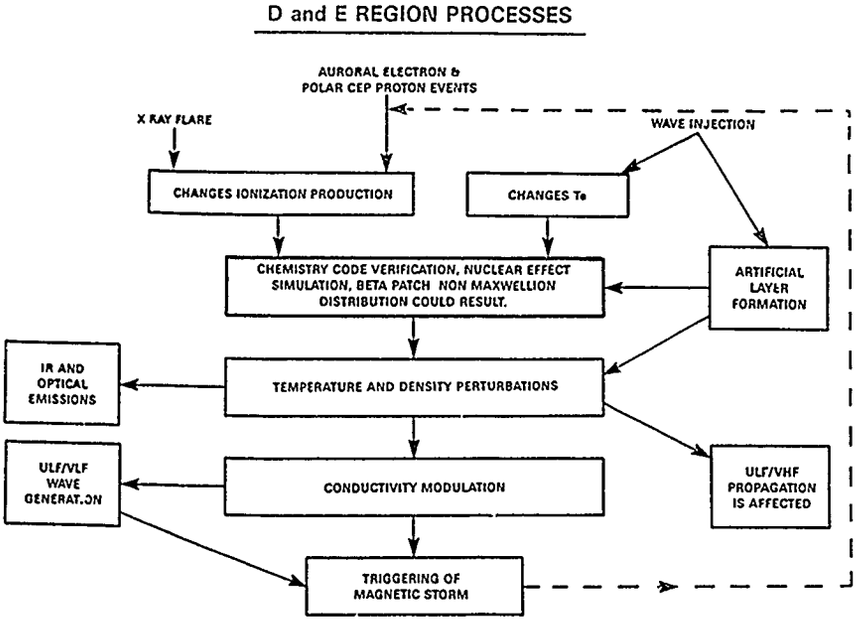

Figure - 5. Ionospheric modification by natural processes and wave injection experiment. Also note the feedback loop connection magnetic storm generation & auroral electron events.

It is apparent that a proper understanding of the wave-plasma interaction would require a range of diagnostics covering a wide spectrum of scale sizes and a considerable amount of effort.

2A. D- AND E-REGION HEATING - TEMPERATURE AND CHEMISTRY CHANGES

Holway and Meltz[6] and Tomko et al.[7] predicted large increases in electron temperature in the D- and E-regions when irradiated by a high-power high-frequency radiowave. Shlyuger[8] reported the temperature rises by a factor of 20 to 40. Absorption increases of 25 to 30 db have been reported and there have been suggestions of a saturation effect. The time constants for these heating processes vary from tens of microseconds in the lower D-region to several milliseconds in the E-region. If the enhanced temperature is maintianed for a considrable period, ion concentrations, (both positive and negative) as well as the electron number densities, would possibly

be altered[2,7]. Suggestions of complex changes involving Ne and Te have been observed at Platteville using radio-wave absorption as a diagnostic[9] and also during Soviet heating experiments. During a preliminary experiment at Arecibo, the HF heater was cycled on/off every 10 secs and the diagnostics signals were used at several frequencies adjacent to the heater frequency of 5.1 MHz (Figure 6). Strong evidence of density changes in the lower ionosphere was obtained. Similar investigations regarding time scales for these heater-induced changes and their relative amounts would be invaluable in our understanding of the lower ionospheric processes. The disassociative recombination rates for O_2^+ and NO^+ are reasonable well known to decrease with increasing Te as Te^{-k}, with K 0.5 to 0.6. Thus increased electron densities are predicted with increase in Te. There has been no experimental evidence to support the density increase. Only indications suggest a decrease in density.

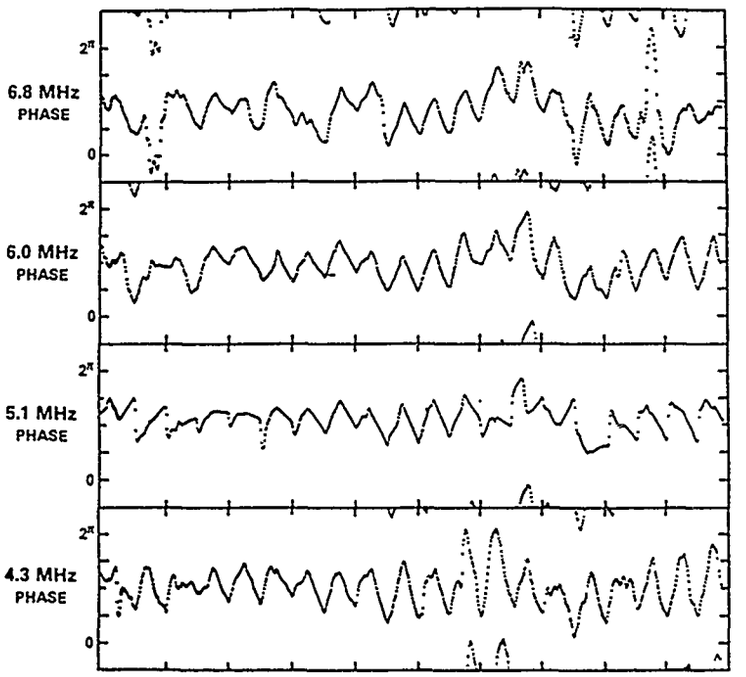

PHASE PERTURBATIONS OBSERVED BELOW AND ABOVE THE HEATER FREQUENCY (5.2 MHz). HEATER IS CYCLED ON/OFF EVERY 10 SECS. DATE: 07/06/81, TIME 1506 AST.

Figure - 6.

The lower ionosphere is further complicated by the presence of negative ions. Dependences of the perturbed densities in elevated Te can be predicted using the temperature dependences in the chemistry code. However, most of these rates and their temperature dependences are highly uncertain and significance improvements can be made using ionospheric observation[10]. Such studies will be aimed towards demonstrating the capabilities of our current understanding of lower ionospheric chemistry and predict therefrom the situations that could result during Beta Patch or Artificial Ionization Patch generation. This will help to estimate the threshold and maintenance power requirements for artificial layer formation.

2B. STRIATIONS, CAVITONS, INSTABILITIES

In the F-region, density perturbations are produced by the striction or radiation pressure forces and also by the thermal forces. Evidence for the formation of quasiperiodic irregularities in electron density due to the presence of a powerful HF wave reflection in the ionosphere has been presented by Belikovich et al (1977)[11]. A sketch describing the relevant processes is shown in Figure 7.

The thermal forces act in creating density perturbations and irregularities with a much larger scale length. The first direct evidence of the thermal self-focussing effect was observed at Arecibo by Duncan and Behnke[12] (1982). Recent observations by Duncan indicate large density perturbations amounting to about 50% or so and suggestions have been made that "thermal cavitions"[13] were generated. Vertical extent of these patches could be several hundred km. Both theoretical and experimental studies are needed to understand the formation of these irregularities. Experiments have revealed a lowering of the electron density in the wave reflection region, a shift of the reflection point[9], and a decrease of the density in the region of the F-layer maximum piercing a "hole" through the ionosphere[14]. Severe focusing and defocusing of radio wave beams can take place.

Recent observations show the presence of cavitons and plasma bubbles and suggest the formation of solitons. Plasma inside these large plasma bubbles or cavitions are known to move with acoustic or ion thermal velocities. Several plasma instabilities can result near the boundaries of these large scale density perturbations. These cavitons have been known to trap several plasma oscillations inside them and suggestions of soliton like characteristics have been reported.

Understanding of the plasma instabilities are crucial to any wave-plasma interaction. The wealth of plasma instabilities excited in the ionospheric modification could be studied for advancing our knowledge in these areas. A thermal instability or thermal caviton or ionospheric blob can be easily produced by heating. The ExB instability

operates mostly around the edge of the plasma blobs, the thermal instability could structure the ionospheric irregularities throughout the region of plasma enhancements.

SCENARIO OF IONOSPHERIC MODIFICATION IN THE F-REGION

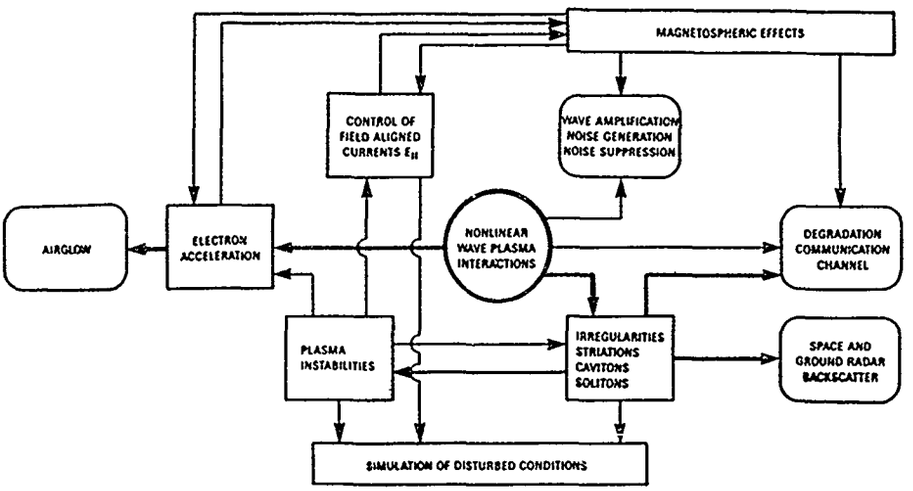

Figure - 7.

Very little is understood regarding plasma turbulence. A wealth of such turbulences are generated in the ionosphere. The plasma could move with speeds around the thermal speed of the ions. Considerable drift between electrons and ions could occur and several plasma instabilities and cross field instabilities have special relevance to nuclear explosions simulation.

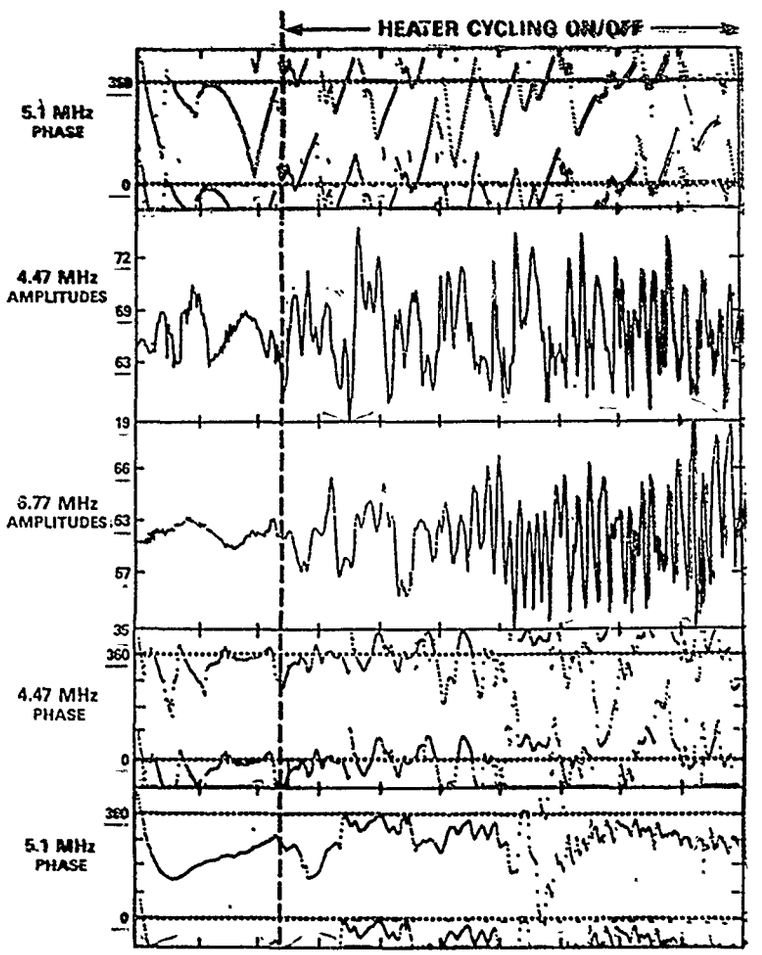

AMPLITUDE AND PHASE FLUCTUATIONS

In 6.77 and 4.47 MHz Signals. Heater Cycled On/Off Every 10 Secs.
NIGHT TIME Observation at Arecibo.

Figure - 8.

Formation of spread F induced by the H.F. heater was observed during the early experiments at Plateville. Although it has been believed that the spread F occurs as a manifestation of thermal self focussing a proper theoretical understanding or a thorough experimental observation has never been attempted. During some preliminary observations at Arecibo, we did not find any evidence for the formation of spread-F at Arecibo. Occasional occurences take place when the $f_0F_2 \approx f_{HF}$ and when the F-layer is at lower altitude.

H.F. diagnostic experiments at Arecibo also failed to show any evidence of Wide Band Absorption. Figure 8 shows the amplitude and phase perturbations produced by the H.F. heater. No significant changes are observed in the level of probing signals when the H.F. heater is turned on. However, there are strong amplitude and phase fluctuation produced by the heater induced formation of irregularities. By using several diagnostic frequencies around the heater frequency, we could determine the vertical extent of these large scale irregularities.

Irregularities can be diagnosed by using several other interesting H.F. probing techniques. These include sky map and high resolution spectral observation. The scattering from the artificial irregularities (with scale sizes of the order of first Frenel zone) shows a doppler broadening of $\approx$ 8 Hz (Fig. 9). This would indicate the scattering region moving away with speeds near the acoustic speed. When the reflection takes place in the Es region, a large scattered field (20-30 db below the main signal) is often observed.

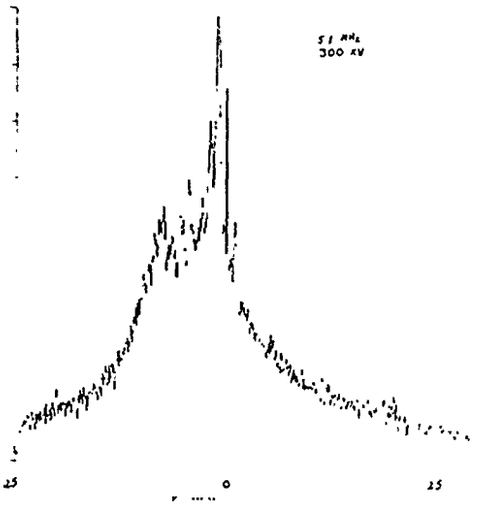

Figure - 9. Spectrum of the reflected signal from the ionosphere. Vertical scale is 80 db. Horizontal scale is 50 Hz centered at the heater frequency of 5.1 MHz.

Use of pulse and cw sounding at several frequencies around the heater frequency is a very powerful diagnostic. Our experiences at Arecibo have shown strong promise for this technique and further studies are suggested towards obtaining data on striated plasma structure and understanding the role of various instabilities, cavitons, solitons and their roles on HF-UHF systems.

One of the most important of the plasma instabilities e.g. the parametric instability was first discovered it Arecibo[15]. This manifests itself as a strong plasma line at a frequency which is offset from the radar frequency by almost equal to the H.F. frequency. Inspite of significent developments being made in understanding these plasma processes our knowledge is still almost in a state of flux. Recent observations by Ganguly show that these instabilities are generated from a few localized centers near the region of reflection of the H.F. signal. Typically, the affected region is less then 1 Km. in extent.

2C. NONLINEAR MIXING PROCESSES

When the ionosphere is illuminated with two strong HF signals, nonlinear mixing processes can take place near the region of reflection. The first direct experimental evidence of such processes occurring in ionospheric plasma have been presented[16]. The experiments were performed at Arecibo, where the HF ionospheric modifier was split to operate as two pure isolated and indepenedent pumps over the frequency range of 3-8 MHz and the frequency difference between the two pumps was varied between a fraction of a Hz and several kHz. The purity of the transmitted signals was always ensured. Strong nonlinear effects were observed when the frequency difference was several Hz.

Specifically, the HF signal from the ionosphere contained sidebands which were multiples of the difference (Δ f) between the two pumping frequencies. The first sidebands were typically 20-40 db below the pump signal (see Figure 10). The strengths of the first sidebands increased, when the difference (Δf) between the two pumping frequencies decreased. Below about 5-10 Hz, the power in the first sidebands varied almost in f^{-n} fashion, with n between 1 and 2. The power in the sidebands was also a strong nonlinear function of the incident pump field strength, showing the presence of a threshold. It is suggested that studies of such nonlinear mixing process[17,18] would be valuable both for diagnostic and practical usage of ionospheric plasma.

With high spectral resolution it is often possible to identify multiple hops of the main cw signal. The individual peaks are separated by small doppler shifts, which may be as low as 0.1 Hz. We also measure the attenuation for the first hop 3-7 db larger than the subsequent hops. This is the nonlinear absorption which depends on the incident field and our results demonstrate the importance of precise frequency matching for this energy to be mode coupled to stable plasma waves.

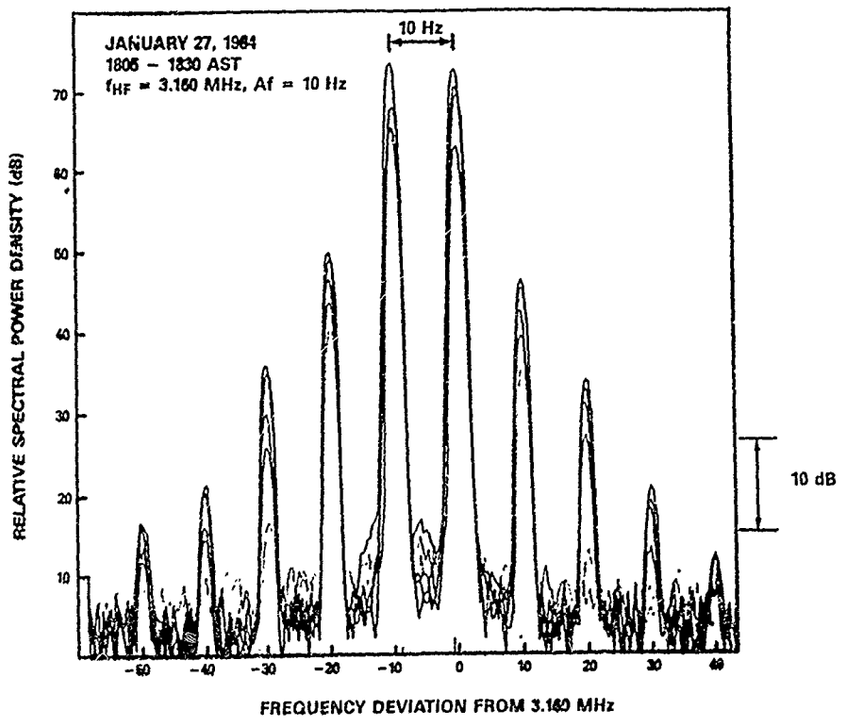

Figure - 10. Spectrum of the signal received at Arecibo. The frequency difference between the two pumps was 10 Hz.

2D. ULF-VLF GENERATION

The nonlinear process could also generate the beat frequency itself. Several processes exist. These are :

a) Modulation of ambient ionospheric currents

b) Ponderomotive force effects

c) Dynamo effects.

Generation of ULF-VLF waves is a subject of topical research[19]. There are strong suggestions that modulation of ambient currents give rise to VLF-ELF signals. Proper experiments need to be performed for the ULF band.

3. STRONG HEATING

With the advent of very high power microwave sources such as gyrotron or free electron lasers, GW levels of power can be generated. This creates a situation where hard interactions might be utilized as suggested by Ganguly and Gordon for beat wave acceleration or for microwave breakdown suggested by Gurevich[9].

Artificial breakdown suggested by Gurevich[2] and original by Bailey (1937) has recently been the subject of some interest. With large enough power densities the air will breakdown. The technology of developing proper antenna feed system to handle the necessary power density needs to be developed.

The artificial ionized layer however may not be able to support useful radio ware propagation. This is because of the diffuse boundary of the layer and the tremendous losses associated with such a boundary in a highly collisional regime. Thus instead of an ionized mirror it will turn out to be an absorber. Prediction of the power requirement for the creation of artificial layers would also require a better understanding of the ionizing processes in the presence of several minor constitutents. As the ambient electrons are heated, some of them (in the tail of the distribution) will start ionization by collision. To be effective, the rate of ionization must be larger then the predominent losses e.g. the attachment and consequent formation of negative ions. Unfortunately our understanding of the negative ion chemistry of the ambient D-region is in a state of flux and further studies are needed regarding the formation and detachment of the negative ions. Both in the presence and absence of sunlight.

Our current knowledge about ionospheric processes needs to be properly and critically assessed before we can understand the complex forces that would be responsible in affecting the artificial ionized layer. The relevant forces include turbulence, drift, diffusion, motion of various sorts, inhomogeneties in both horizontal and vertical dimensions and furthermore the complex chemistry of both the positive and negative ions.

Several other possible uses of the very high power radio waves have been suggested. These include :

a) Directing Radio Waves.

By artificial ionization and scatterers one could produce new paths for radio waves. By varying the frequency and angle of the modifying beam, shaped reflecting or scattering region could be produced. Some of these potential uses are :

a. OTH Radar
b. Covert communication
c. ELOS communication
d. Setting up unattainable communication or radar links.

b. Create Scintillation & Scattering :

Irregularities, localized patches, density perturbations and plasma oscillations degrade communication channels. Scale size of km to cm are involved. All the radio frequencies will be affected to some degree. Effects at HF, VHF, UHF and S-band have been observed. For the UHF and S-band the plasma oscillations with wavelengths of cm or so produce strong Bragg scattering.

Space borne radars are strongly affected by scattered signal from these irregularities and plasma fluctuations. These would appear as strong clutter with large doppler shifts. The heated plasma could have speeds comparable to the sound speed. By directing the modifier wave injection angle one could produce a shield against space Radars. Even weak backscattered signal is significant because of the large beamwidth of space radars. Because the motion of the irregularities can be up to kms, MTI technique will not be able to resolve the clutter (See Figure 11).

SHIELD AGAINST SPACE RADAR

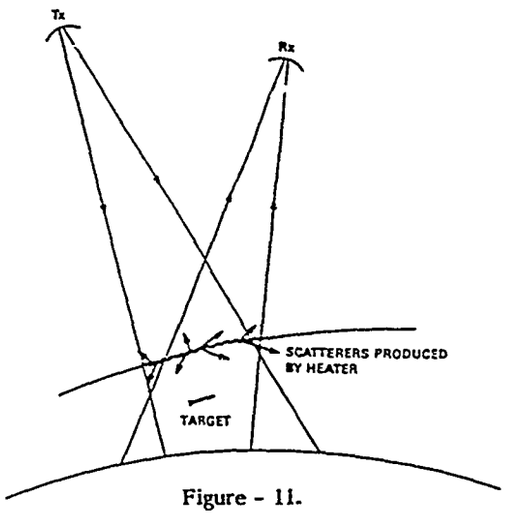

Figure - 11.

c). The energised plasma could create optical and I.R. emissions to blind the space based sensors. If sufficiently energised they might initiate a lighting bolt effect from the ionosphere.

d) Control of irregularities (both generation and suppression) and triggering of magnetic storm would allow a similar control over the HF/VHF propagation channels. The affected parameters are attenuation, fading and loss of coherency.

4. CONCLUSION

The existing ionospheric modification facilities both in U.S.A. and in U.S.S.R. do not produce any significant effect in the practical communication system. To be effective, the oblique "heating" must be utilised. We in U.S.A. have not observed significent manifestations of oblique heating. With the vertical heating, the ionosphere overhead the heater can be perturbed to some extent. For a communication system, the irregularities with the size of a Fresnel size are generally of significence. Thus scintillations of a few percent can be produced for VHF-UHF band transionospheric signals. This applies for both the amplitude and phase. For H.F. signals the worst case fading of some 20-30 dB might be introduced with overhead heater. Although there has been no quantitative measurement, it is believed that attenuation can be increased by some 20 dB or so both with vertical and oblique heating.

When the technology for GW power heating becomes available, we do expect some interesting changes. However, it is believed that more detailed knowledge about specific areas of the ambient ionosphere is desirable before we can start understanding the behavior of the disturbed ionosphere. This is particularly evident in the lower ionosphere and in the wave plasma interaction studies in the F-region.

It must be realized that the subject of ionospheric modification is almost in an embryonic state and does not allow conclusive inferences to be drawn as to the potential applications of the techniques for C^3 and related systems. For one, the facilities needed to create useful ionospheric modification with the present day technology do not appear to be transportable. Development of microwave facilities would require technology improvement in feed design. The impact of such systems on the various aspects of C^3 need to be judiciously evaluated by responsible radio scientists.

5. REFERENCES

1. Ganguly, S., and W. Gordon, "Generation of Intense Electric Field in the Ionosphere", presented at "The effect of the ionosphere on C^3I systems", Alexandria, VA, April 1984.

2. Gurevich, A.V., "Nonlinear Phenomenon in the Ionosphere, Physics & Chemistry in Space", Vol. 10, Springer Verlag, New York, 1978.

3. Ganguly, S. and W.E. Gordon, Heater Enhanced topside plasma line, Geophys. Res. Lett., 10, 977-978, 1983.

4. Cornwall, M.S., and J.F. Vesecky, "Communication Effects of Ionospheric and Magnetospheric Plasma Injection," JASON Technical Report, JSR-82-401, 1984.

5. Helliwell, R.A., "VLF Wave Injection from the Ground", Proc. Int. Symp. on Active Experiments in Space", Alpbach, Austria, 1983.

6. Holway, L.H., and G. Meltz, "Heating of the Lower Ionosphere by Powerful Radio Waves", JGR, 78, 8402, 1973.

7. Tomko, A., A. J. Ferraro, H.S. Lee, and A.P. Mitra, J. Atmos. Terr. Phys., 1980.

8. Shlyuger, J.S., "Self Modulation of a Powerful Electromagnetic Pulse Reflected from the Upper Layers of the Ionosphere", JETP Lett., 19, 162, 1975.

10. Ganguly, S., and J. Zinn, presented at AGU Spring Meeting, Baltimore, MD, (1987).

11. Belikovich, V.V., E.A. Benediktov, M.A., Itkina, N.A. Mityakov, G.I. Terina, A.V. Tolmacheva and B.P. Shavin, "Scattering of Radio Waves by Periodic Artificial Ionospheric Irregularities," Radiophys. Quantum Elect., 20, 1250-1254, 1977.

12. Duncan, L, and R. Behnke, Phys. Rev. Lett., 1982.

13. Dysthe, K.B., Mojlhus, H. Pesceli and K. Rydel, "Thermal Cavitons", Physics Scripta, T2/2, 548, 1982.

14. Fialer, P.A., "Field-Aligned Scattering From a Heated Region of the Ionosphere - Observations at HF and VHF", Radio Sci. 9., 923-940, 1974.

15. Carlson, H.C., W. E. Gordon, and R. L. Showen, "High Frequency Induced Enhancements of the Incoherent Scatter Spectrum at Arecibo", J. G.R., 77, 1242, 1972.

16. Ganguly, S., and W. E. Gordon, 1986, Geophys. Res. Lett., 13, 503-505.

17. Fejer, J. A., H. M. Ierkic, M. P. Sulzer, C. A. Tepley, L. M. Duncan, F. T. Djuth, S. Ganguly, W. E. Gordon, C. A. Gonzales, "Ionospheric Modification Experiments with the Arecibo Heating Facility", J. Atmos. Terr. Phys., 1985.

18. Papadopoulos, K., K. Ko, and V. Tripathi, "Efficient parametric decay in dissipative medium", Phys. Rev. Lett., 51, 463-466, 1983.

19. Ganguly, S., W. E. Gordon, and K. Papadopoulos, "Active Nonlinear ULF Generation in the Ionosphere", Phys. Rev. Lett., 1986.

DISCUSSION

K.C. YEH

Are there calculations that show the power density required in the ionosphere in order to enhance the ionization density to such an extent so as to shield a ground based radar ?

AUTHOR'S REPLY

Yes. GUREVICH published the power densities needed to create and maintain air breakdown. Generally, with enough power one can create ionization up to the frequency of the disturbing or ionizing source. Thus with S-band heating ionization is possible that could reflect or absorb frequencies up to S-band.

Specific applications in relation to reflecting the radar waves from such an artificial layer are being looked into by AFGL, ARCO and SAIC.

D.J. FANG

I like to follow-up Prof. K.C. YEH's question. If the strong ionization by heating is to be created at a height of about go to 50 km, then the diffusion, all kinds of diffusion, would kill it quickly. What is the time scale of damping ?

And is it worthwhile to create an ionization by an order of Giga-Watt power for only a short period of time ?

AUTHOR'S REPLY

With sustained heating the ionization could be maintained. But the ionization will diffuse and thus create heavy attenuation for radio waves passing through the region. Thus instead of a mirror it will be an absorber. AFGL thinks it will get a mirror.

HF SPREAD SPECTRUM, AN AUDIT OF THE POWER REQUIREMENTS AND LPI VULNERABILITY

C S den Brinker
Redifon Ltd
Newton Road
Crawley
West Sussex RH 10 2TU
England

SUMMARY

Electronic Counter Measures and the response to ECM has been widely introduced in frequency bands other than HF. The unique characteristics of HF generate a different set of problems. In this overview, the normal hygienic measures that can be adopted for communication are reviewed. Force fitting of trends in spectral occupancy has revealed that the power penalty to be paid for low error rate frequency hopping could be prohibitive. The arguments used here may shed new light on the differing views taken with respect to the VHF band, where the choice of location could influence the efficacy assessment. Parallel diversity over a restricted bandwidth appears to offer a low probability of intercept in the case of dense occupancy and thus negate the need for excessive frequency hopping powers.

1 Introduction

For some years now the communication industry as well as the Military Establishments have been active in evaluating different Electronic Warfare communication systems. Widely differing views are taken of the efficacy of such systems, surprisingly this even applies in cases where transmissions are limited by propagation laws such as are encountered in the VHF and UHF bands.

The High Frequency band by its very nature produces a far more complex set of problems:

a) Skywave propagation means that the transmission range is significantly greater than line of sight and hence the spectral occupancy is greater.

b) The Bandwidth of HF is greater than those encountered in the VHF and UHF bands and moreover the physical laws governing propagation vary considerably across the band.

Because of this, any discussion about the approach to Electronic Warfare (EW) in the HF band should be two pronged. The first and obviously the most significant aspect evolves around operational needs for communications; ie are we primarily concerned with strategic or tactical communications? In the case of VHF and UHF, unless these frequency bands are part of a satellite system, the attainable range (line of sight) fairly puts their usage in the tactical category.

HF could offer both strategic and tactical communications as either skywaves or groundwaves. In fact the groundwaves range at the lower end of the HF band offers a greater reach than either VHF or UHF.

The second leg of the two pronged argument is entirely concerned with the physical constraints imposed when using HF. And here, as will be also shown, the arguments yet again bifurcate. Is it Anti-Jam (AJ) that should dominate our thoughts or it is Low Probability of Intercept or Exploitation (LPI/LPE)? AJ may well have an LPE feature implicit in its nature, but as will be shown later in this paper, it is apparent in HF that one cannot have it both ways.

Therefore, in order to bring some order into the reasoning with regard to physical limitations, it is important that one first considers the common features to which both AJ and LPI will be subjected, and then separately the specifics that could apply to either. It is the intention in this paper to bring some logic to bear on what might otherwise turn into a rather chaotic discussion. To start with we must consider the boundaries of the operational logic as this covers the approach that the users would really wish to pursue if all other considerations were to be equal. At the same time it is assumed that LPE due to specific platform signatures can be ignored as not being part of this treatise's argument.

2 Operational Considerations in Terms of the Physical Environment

If one assumes that the primary requirement of any communication system is to convey intelligence, then the possibility and worry that an adversary might achieve any sort of advantage by listening in on a conversation must take second place. The widespread use of Cryptography implies that an adversary does not have immediate access to the type of intelligence that is being conveyed, he is therefore mainly limited in his exploitation to the location and discernment of the nature of the platforms from which any communication emanates. Ideally, we wish to reduce the limited probability of exploitation, while still securing good link reliability.

To set the scene for the subsequent reasoning, some well established truisms must first of all be revisited. The methodology for reducing the probability of exploitation is by no means clear cut. It is only fair to state that groundwaves intercepts tends in general, to provide better results to an interceptor than skywaves. Ignoring such effects as for example the diffraction at the sea to land coastal interface, one can say that for groundwaves, bearings tend to be more accurate and propagation distortion is avoided. But LPE is never assured and resorting to skywave transmissions per se, merely increases the difficulty for an adversary. It is also self-evident that the further away from any communication link that an interceptor is forced to work, the more difficult that exploitation becomes. Thus the choice of frequency and hence the skip distance will play an important role in lowering the probability of exploitation, particularly so

as a consequence of skywave selection, the skip distance will or can also preclude members of a task force from access to the general interchange of data. In other words, the complement of the truism that any transmission is bound to be vulnerable to interception is also true. Denial of access to an adversary by employing physical phenomena such as skip distance also denies access to friendly users caught in these denied areas. All of these discussions are self evident, but they do lead towards a conclusion that the choice of frequencies, groundwaves versus skywaves, etc, are essentially those for specific operational conditions. It is only in the case where extremely high data or chip rates are concerned, that groundwave transmission is indicated, unless single frequency adaptive modems are to be employed. But the latter cannot easily be employed in a networked situation as the idiosyncrasies of each of the skywave paths are likely to be unique for each of the network connections.

Thus far it appears that few choices are available to anyone in the search for an LPE advantage. This picture changes rapidly when we add interference into the picture. It is interference which offers the mechansim for hiding transmissions.

3 Operational Considerations in Terms of Interface

Communications can be interfered with deliberately as in the case of ECM, or accidentally by legitimate users of the spectrum. Indeed Gott et all have demonstrated that the latter form is a major effect in the HF spectrum. (Refs 1 and 2).

Since World War II power levels of transmission seem to have crept up to where we now employ power levels that correspond to some 10 Joules per Baud over major theatres of operation. In other words the cocktail party syndrome, where people gradually increase their audio power level until the reliance on directional diversity dominates, is also prevalent in the HF spectrum. System designers must recognise this fact in that omnidirectional transmission links are no longer subject to common sources of noise such as atmospherics, but rather they are likely to be subjected to interference where the sources will tend to favour one side of a link more than another. In the northern hemisphere, for example, atmospheric noise or remnants of the thunderstorms which originate in the tropical land masses, produce a noise plateau which appears to be more or less common to all the participants. The origins of interfering transmissions cannot be treated as such. To illustrate this, a rather extreme case will be used. Ignoring at this stage the EW methodologies that could be employed, one can describe a typical fleet landing task. Probably the most precarious situation that arises occurs at the time of command handover from the senior officer of the fleet to this Army/Marine counterpart. At this time, the task force position may be as indicated in Figure 1. The landing fleet is crucially dependent on receiving unequivocable orders (Rx). These are likely to derive from say, a Flagship which is positioned behind the landing task force (Tx). If, as illustrated in Figure 1, the distances are 2 : 1, then if a coastal interferer (deliberate or otherwise) manages to create a situation where the Flagship needs to increase its power significantly, (to be effective vis a vis the Landing Fleet), then a potential interceptor has attained a significantly improved advantage geographically. In this simplistic case, it is assumed that the received power from the 'interceptor' at least equals the initial power received from the Flagship. It is also implicitly taken that the inverse power law of path attentuation will prevail in this situation. The resultant geometrical relationships need not be expounded on here as they are the classical case of the 'Circle of Appollonius'. Similar pictures can be derived for, say, a Battle Fleet in transit. Here too, the directionality of the transmission paths plays an important role, but more so, the dispersal of platforms add yet another dimension. For example, a Flagship in the middle of a communication-active cluster is subject to greater interference than say, a far off platform which may be on picket duty. The transmission power demanded from the picket platform will be dictated by the noisy cluster containing the command platform and this may make the the picket platform more vulnerable to counter EW measures. In the final analysis, the decision of risk must be an operational one, ie, how vulnerable is the command structure without the intelligence derived from the picket position?

Precise in situ, mechanical analysis is not possible nor is it in the opinion of the author necessary. One cannot precisely analyse the effect of mutual interference within a vast fleet, particularly as the situation is a dynamic one. There are some operational alternatives which will be discussed later on.

It is at this stage important to have some measure of the dynamics that can occur in a real situation and this is a subject to be dealt with next.

Reciprocity Versus Interference

A danger exists in believing that the reciprocal behaviour of any one transmission path could in any way imply identical conditions for both participants. This was recognised by Redifon and as a result of an unsolicited proposal to the Royal Navy, the RN through ARE, carried out some trials with a demonstrator system in which the power was adjusted 'on demand' by a simple revertive protocol. (Reference 3).

The trial was carried out on land, its range was relatively short at some 300km. Even at this short range, the diversity of power demand between the notional slave and master station was far greater and dynamically variable than was expected, ie the maxium range in favour of the master was 48 dB and the maximum range in favour of the slave was some 24 dB. Thus the total dynamic range experienced was some 72 dB. All of the experiments were carried out with a block repeat system, such that the traffic plus the repeat overhead would be restricted to the order of 1.35 times the primary traffic.

The experimental results were limited in terms of time, diurnal and seasonal variations. Nevertheless the wide dynamic range experienced is in itself sufficiently indicative of the considerable variations that can occur in the stochastic environment of the HF spectrum.

Last but not least, it may be worth quoting that on average, local interference conditions tended to persist typically for some 14 minutes at more or less constant levels.

With this indication of the dynamics of local variability it is worth to review the behaviour of channel occupancy as reported by Gott et al, without the concern of the actual power reference.

5 Channel Occupancy

Probably the best reference sources of channel occupancy information are those provided by Gott et al (Ref 1 and 2), and these will be referred to in the following discussions. In both the references, measurements performed in 1981 and 1982, a cursory glance at the tabulated results show that there is an orderly trend in the behaviour of channel occupancy in spite of a pronounced scatter. It is this trend which one may wish to discern, as it is indicative of the overall occupancy versus power relationship.

Using the results of the 1982 observations and starting at 3 MHz, (while precluding the broadcast channels), the figures provided were subjected to a forced fitting exercise and the outcome of this is shown in Figure 2. Initially all the results were gathered in classes of some 5%, ie 90 - 95%, 85 - 90% occupancy and then their trends in terms of 10dB increases were grouped. Because of the uncertainty of channel occupancy versus atmospheric noise as noted by Gott et al the class of 95 - 100% occupancy was also ignored.

It must be appreciated that for the purposes of this exercise, the values as presented by Gott were only used to discern dynamic trends. Detailed behaviour versus bandwidth as presented by Moulsley (Ref 4) further endorses that the dynamic trends remain the same for differing bandwidths, only the absolute values alter. The conclusions being that over a restricted bandwidth interference can be treated as quasi-Gaussian. This proposition is further supported, although indirectly, by the practical results reported at the same conference in a paper by D D McRae and F A Perkins. In their final set of curves, they relate power versus power distribution for different Baud rates and the 50% or mid point exhibits more or less a constant Joules per Baud relationship.

Thus if we were to consider a frequency hopping system, where it may not be possible to selectively predict the occupancy state of all the channels to be used, the cocktail party syndrome could demand a very high power price to achieve an error rate of say only a few percent. The unpredictability of channel occupancy on either side of a link was discussed earlier, resulting from a variability of some 72 dB. Consequently, minimising the probability of error rate to 2%, will require power levels in the hopping range where the transmitter on average becomes visible to anyone by some 10 dB in 98% - or by some 40 dB in well over half (84%) of potentially used channels, at a range equivalent to the 'legitimate' receiver, more so of course if the interceptor is even closer and less if he is further away. This is by no means a satisfactory scenario. Further forced fitting exercises also reveal that bandwidth reduction make very little difference in this power versus occupancy relationship until the bandwidth is reduced to 300 Hz and below, but even here, the apparent improvement (based on limited data) is that only 0.4 of channels remain occupied for 10 dB increase in power.

Although the previous numerical example is self-explanatory, it is of value to provide a range of worked data as shown in Table 1. The higher tolerable error rates would be permissible if some form of error correction is included in the communications protocol.

Table 1

	% Visibility of Channels to Interceptor @ Power Level above Background				
Error Rate (%)	10dB	20dB	30dB	40dB	50dB
1	99	98	96	92	84
2	98	96	92	84	64
3	97	94	88	76	52
4	96	92	84	68	36
5	95	90	80	60	20
6	94	88	76	52	4

Although Table 1 is only an arithmetic extension of the previous example, it illustrates graphically the potential vulnerability of a hopping system to interception. Consider, for example, the last line. If the link can tolerate a 6% intrinsic error rate, which is probable the norm in case of a simple error detection system, then provided the interceptor has the physical capacity, he could discern some 52% of the hopped signals even if he is geographically disadvantaged by the equivalent distance of 40 dB. Any LPE advantage that a hopper offers in the

HF band, appears to be one of physical resources needed to intercept, ie, the investment differential between the communication and interception.

More than anything else, these examples show that the normal variability of power .evels in the channels would put an HF AJ hopping system at a clear LPE disadvantage as against a system where the background noise level is truly Gaussian and hence more or less uniform, or for that matter non-orthogonal.

This problem, although specifically acute in the HF band, would equally apply to VHF close to the FEBA. Indeed in Middle Europe, where potential adversaries use an identical band of frequencies, the problem is further complicated by congestion. In the case of HF, the 'status of conflict' has yet a further effect on this syndrome. In an all out conflict large numbers of civil transmitters would be off the air, although during the transition period between peace and war one might expect that HF activity would be even higher than during peace time. These above examples illustrate that a potential interceptor may be quite successful in his exploitation at distances considerably greater than those dictated by the error rates that are intrinsically tolerable to the communicators. It must not be forgotten either that the interceptor may yet have at least a further 10 dB advantage in his location techniques as he is likely to employ some form of directional technology which would eliminate the effect of other 'interferers'.

Last but by no means least, we must consider the implications of the scatter illustrated in Figure 2.

At low level error rates, the direct relationship between blocking channels and potential errors, as shown in Table 1, is wholly justified. At higher levels of error, or in effect lower power blocking levels, the situation is not the same. For a start, blocking power levels are not evenly distributed. Also it is normal for AJ systems to have channel bandwidths well in excess of communication bandwidths. Thus if each one of the hopped channels is significantly wider than a normal communication channel, it is likely that every so often several high levels will occur within one hopped channel. Consequently, we are likely to experience significantly more pronounced low level occupancy bunching. Indeed the min max scatter of Figure 2 confirms this.

To cater for this, we would need to introduce a statistical relationship, which in a simplified form states that the yield of good data chips is likely to be:

$$\text{Yield} = \exp(-n/N)$$

where n is the number of error producing channels
N is the number of hopping channels

As stated before this modification applies to situations where the dimensions of error or fault sources are significantly smaller than the operating dimensions.

The implications of this modification are not particularly helpful to the error rate considerations for a frequency hopping communication link. However, as Figure 2 would indicate, they have a profound effect on the interceptor, in fact they could considerably improve his changes of exploitation.

If a suspected hopper is operational, an interceptor could indeed pay particular attention to those channels which appear to him to be free from high level sources of interference.

The first conclusions that can be drawn from the above, somewhat convoluted, arguments are:

1 Any hopping system that relies on power levels only, to reduce the error rate of communications to acceptable levels, will be vulnerable to exploitation.

2 Using the dynamic power versus occupancy results, the indications are that for good LPE, the tolerance to potential causes of error may have to be in the order of 25%

3 The variability, both in terms of locality and dynamics indicate that some form of automatic power management structure is highly desirable.

4 Any error correcting technque ideally should not occur at the cost of an excessive overhead in transmission time.

These issues will be reviewed in the subsequent sections.

6 Diversity Considerations

Significant improvements have been achieved in power containment using diversity. Wilkinson described such a system (Ref 6) and Chapman discussed the results in terms of a morse comparison (Ref 7). The demonstrator, which was developed by Redifon, employs multiple tone and time diversity schemes, but was limited to a single speech channel. According to Skaug (Ref 8), wider bandwidths can yield a consistently better performance, as is shown in Figure 3, which was derived from Ref 8. If however, the sporadic nature of the middle curve can be ignored and provided that the mid operating frequency lies well below the MUF, then limited BW diversity may be sufficiently efficacious to consider for a hopped system.

The additional BW required may have to be considered in terms of the windowing function. Figure 4, illustrates the difference in dynamic signal range that is achievable moving from a non windowed to a windowed situation. The dynamic range of the actual discernable signal changes

from some 25 dB to nearly 60 dB. In terms of the windowing BW however, to achieve the latter results this BW may have to be an order greater than the chip rate. Thus a serial system having a Baud rate of 75 would require a windowing BW of 750 Hz if one chip per Baud were to be used.

Parallel diversity has not received the attention that it deserves. This may be largely due to the peak to mean ratio which also does not favour parallel modems where the system may be limited by peak power considerations. It is however, possible to design a tone structure where the peak to mean ratio is contained. For example the equation:

$$V = \sin(2\pi f_1 t) + \sin(2\pi f_2 t) - \sin(2\pi f_3 t)$$

could be used to limit the minima and maxima.

Within a speech channel for example, the following results could be obtained for a 75 Baud system:

Table 2

	Marks	Spaces
Tone 1	740	225
Tone 2	1725	1275
Tone 3	2700	2325
Minima	-2.234	-2.229
Maxima	+2.231	+2,229

Probably better structures can be obtained but the above is only used as an example of an approach. Structures such as these can now be considered, since Silicon Digital Signal Processing Technology is coming of age and hence the complexity is no longer an insurmountable problem.

Windowing each individual tone would permit us to employ diversity without too great a price having to be paid in terms of increased interference from the effective increase in BW in a hopping system. The real complexity does arrive when we consider the assessment of the quality of the individual channels.

Considerable differences by probably up to 6 dB are attainable by moving from a simple switch and examining scheme towards and an equal gain and maximal ratio protocol for this.

A three tone pair may not be quite adequate for a 25% occupancy situation is as shown in Figure 5. A four tone pair system would also avoid the regular problem of 2 out of 3 choices arising (Ref 10). In the latter case, the uncertainty of the mean remains problematic. Moreover, if the purpose of the exercise is to harden the system against deliberate jamming, then the introduction of time diversity (in which each parallel chip carries, say three different symbols related in time) may be indicated.

SUMMARY CONCLUSIONS

In an environment where potential interferers occupy orthogonal channels for relatively prolonged periods, diversity can yield a better result than a mere resort to increased power to obtain a good communication link.

Our previous discussions have shown that reducing the occupancy level from 30% to 4% would require a power increase of 41 dB. The three tone diversity scheme which can achieve the same would increase the mean power by approximately 5 dB. The average net gain in choosing the latter approach is significant. This becomes even more significant if one considers what the jammer is required to muster in terms of his resources.

It cannot be stressed enough that if the initial response to a jammer is to hop, then having been discovered and earmarked, one should not be pushed into responding by having to reply in such a fashion that one's presence will be known to an even greater potential audience than was encountered prior to the jamming situation. This indeed was the starting point described in our first figure.

Implicit in diversity system is the option to assess the quality of reception prior to decryption and this is an operational advantage which cannot be ignored, particularly as it also allows the use of automatic emission control thus also enhancing the LPI/LPE quality.

REFERENCES

1 Geoffrey F Gott et al

Occupancy Measurement Across the Entire HF Spectrum. AGARD Conference Proceedings 332 Paris 1982.

2 Geoffrey F Gott et al

Experimental Observations of Spectral Occupancy at HF, AGARD, Lisbon 1983.

3 R Dines

A Variable Radiated Energy Control System for Maritime HF Telegraphy Circuits - Trials Report ARE TM (AXA) 87014 February 1988.

4 T J Moulsley

HF Data Transmission in the Presence of Interference, IEE Conference on HF Communication Systems and Techniques, Feb 1985, publication number 245

5 D D McRae and F A Perkins

Results of Link Tests of Serial HF Modems Employing Forward Error Correction Coding

6 R G Wilkinson (ARE)

A Modem for More Reliable Communications at HF. IEE HF Communication Systems and Techniques Number 206, pp 116-120 1982

7 P S Chapman (ARE)

Comparison of 10 B P S Modem with Man-Read Morse. IEE HF Communication Systems and Techniques Number 245, pp 136-140 1975

8 R Skaug

Experiment with Spread Spectrum Modulation on an HF Channel Proc, IEE Vol 131 February 1984, pp 87-91

9 GRT Hill and Anna Loise Scott

LPI Pre-feasibility Study Report, November 1987. Redifon Limited

ACKNOWLEDGEMENTS

Although the opinions expressed are the responsibility of the author, he cannot but acknowledge the help that he received from his colleagues. In particular, he wishes to thank Mr Neil Hoey for his patient support.

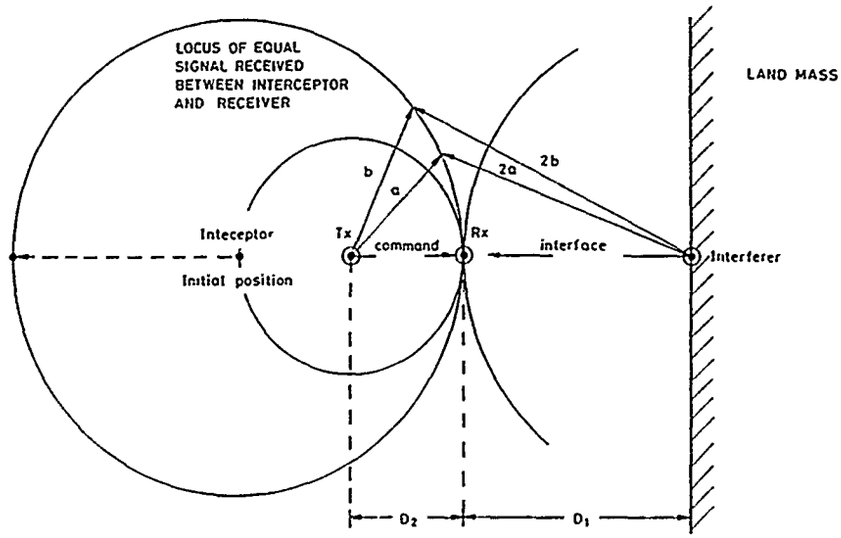

Figure 1 A Landing Scenario

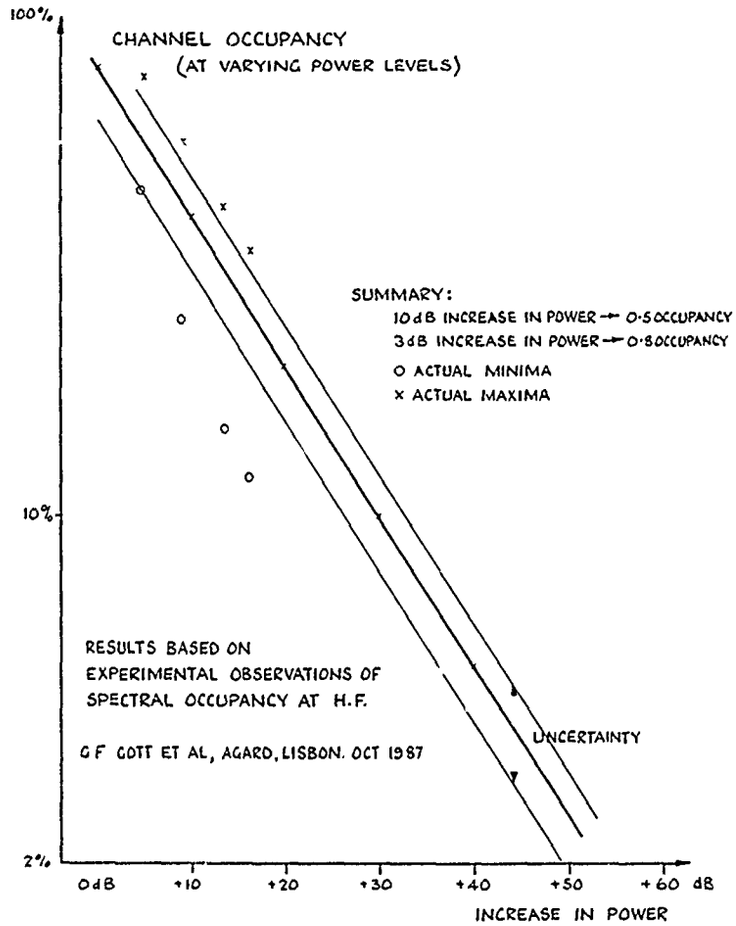

Figure 2 Channel Occupancy versus Power Level

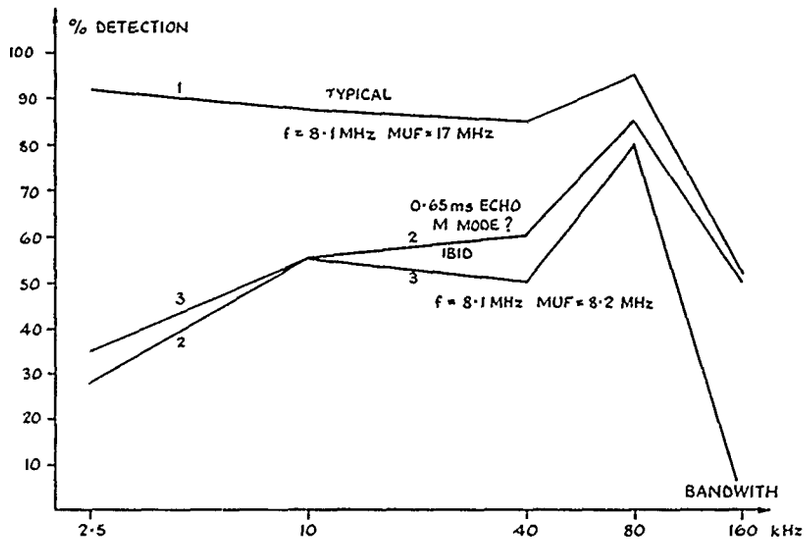

Figure 3 COMMUNICATION PERFORMANCE VERSUS BANDWITH EMPLOYED

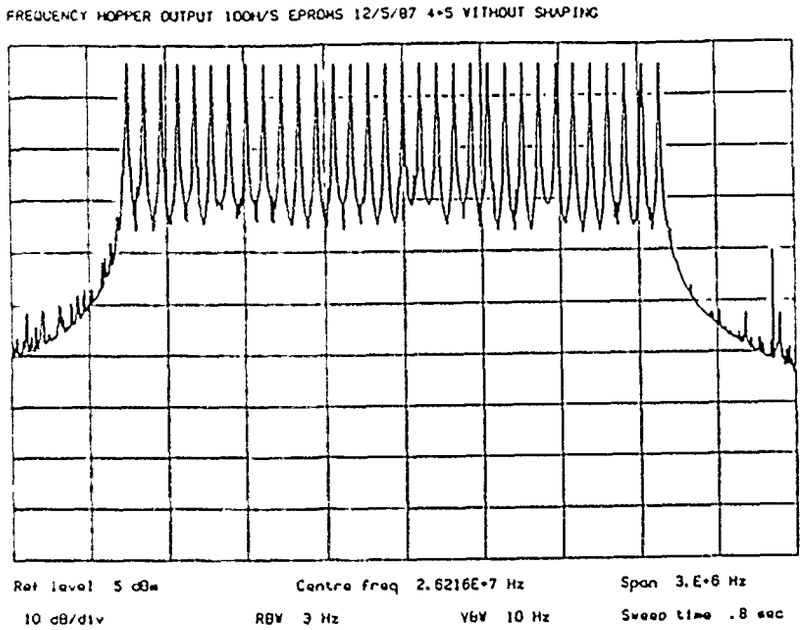

Figure 4a Unwindowed Frequency Hopping

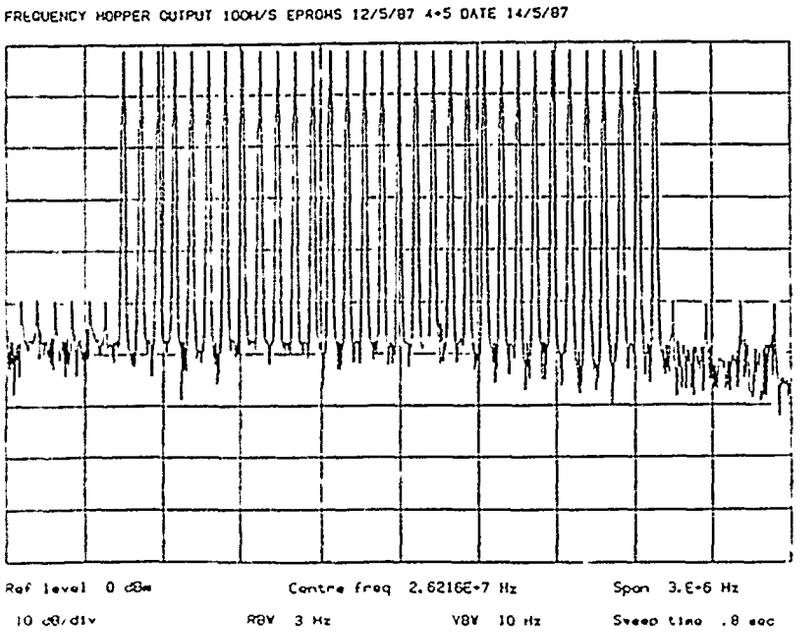

Figure 4b Windowed Frequency Hopping

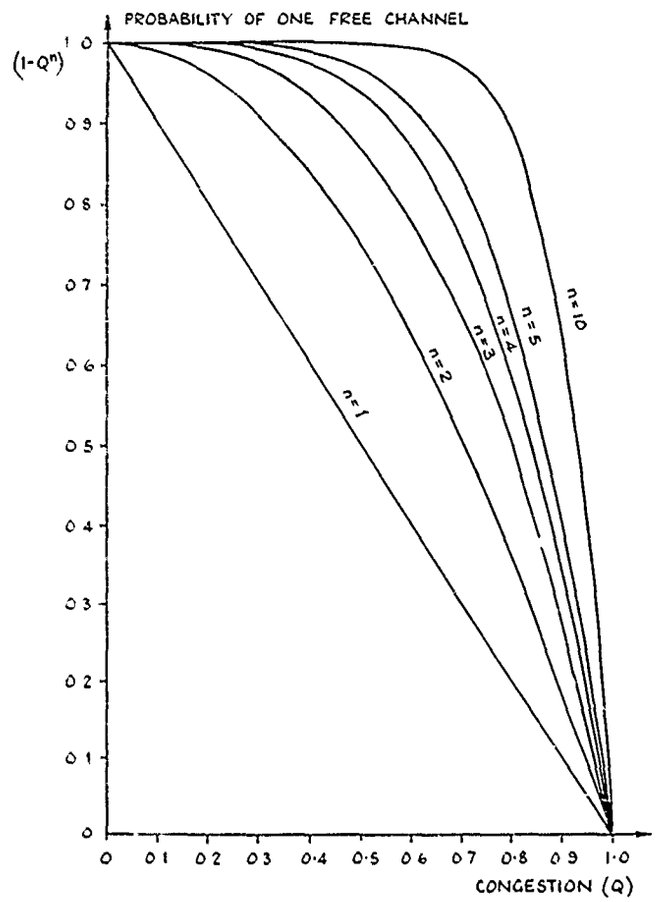

PROBABILITY OF FINDING A FREE CHANNEL
IN A CONGESTION OF N CHANNELS

Figure 5 Diversity - Occupancy Probability

Combined Effects of Fast and Selective Fading on Performance of PSK and MSK with Coherent Detection.

Armand J. Levy
Centre National d'Etudes des Télécommunications, PAB-RPE
38-40, rue du Général Leclerc - 92131 ISSY LES MOULINEAUX FRANCE
Téléphone : (1) 45 29 40 04 Télex 200570F

Summary

Depending on the symbol rate and on the particular channel conditions, mobile radio communications can be affected by fast fading, by selective fading or by both of them. In order to determine when each effect should be considered, the performance of PSK and MSK with coherent detection is theoretically evaluated in the presence of a fast and selective fading channel. A numerical method of analysis is derived for a Gaussian Wide Sense Stationary Uncorrelated Scattering channel, taking into account the phase recovery error induced by the degraded channel. Results are presented for cases of practical interest. It appears that for some severe channel conditions, none of the fast and selective fading can be neglected.

Introduction

Radiomobile communications can be affected on one hand, due to the mobile movement, by fast fading (the channel is time varying) and on the other hand, due to the multipath phenomenon, by selective fading (the channel is frequency selective).

Depending on the symbol rate, one or the other of these two phenomena can be neglected while the other dominates.

Consequently the performance evaluation of these communications usually adopt either the assumption of a fast fading only [1-3] or the assumption of a selective fading only [6-8]. Countermeasures are different in both cases. For instance differential or non-coherent detection performs better in fast fading while selective fading can require the use of adaptive equalization. Thus it is usefull to know, for a given channel and system, what is the effective context between the "good" slow and flat idealization, and the difficult fast and selective situation.

To this end we propose in this paper an analysis which can apply to a communication simultaneously affected by fast and selective fading. We assume a WSSUS channel characterised by its complete scattering function. Two kinds of modulation are analysed: the PSK modulation (2-PSK and 4-PSK) and the MSK modulation. In both case, signals are coherently detected.

System features and impairements taken into account include:

- the presence of any equipment filters at emitter and receiver,
- a PLL carrier recovery device disturbed by the fading channel,
- a possibly highly selective channel: many intersymbols interference (ISI) coefficients are taken into account.

1. The channel

The Gaussian WSSUS channel is characterised by the correlation function S of its varying impulse response. Let $s(t,\tau)$ be the channel impulse response at time t.

$$< s(t,\tau)\ s^*(t',\tau) > = S(t-t',\tau)\ \delta(\tau-\tau')$$

The function S and the more usual scattering function are related by a single Fourier transform on the variable t.

2. The signals

For the linear analysed modulations, the complex envelope of the emitted signal e(t) can be expressed

$$e(t) = \sum_k c_k\, p(t-kT)$$

where the symbols c_k and the pulse shape p(t) depend on the modulation used and on the equipment filters. For binary, resp. quaternary, PSK modulation, symbols will take the values $c_k=\pm1$, resp. $c_k=\pm1\pm j$, while p(t) will be a bandpass filtered rectangular pulse of duration T. The MSK modulation can be defined by $c_k=\pm(j)^k$ and $p(t) = \mathrm{Rect}_{[0,2T]} \sin(\pi t/2T)$.

The emitted signal is successively filtered by the time varying channel and by the receiver filter (impulse response q(t)). The receiver bases its decision on a sample at time t_s of the resulting signal r(t) corrupted by thermal noise.

$$r(t) = \left[\sum_k c_k \int p(t-\tau-kT)\, s(t,\tau)\, dt \right] * q(t) + n(t)$$

$$r(ts) = \sum_k c_k \iint q(t_s-t)\, p(t-\tau-kT)\, s(t,\tau)\, dt\, d\tau + n_s$$

$$= c_o h_o + \sum_k{}' c_k h_k + n_s$$

3. Error probability evaluation

The sample $r(t_s)$ clearly includes an ISI term. Since the channel is Gaussian, the coefficients h_k are jointly Gaussian random variables. The correlation between these coefficients can be derived:

$$\langle |h_o| \rangle \triangleq a^2$$

$$R_{ik} \triangleq \langle h_i h_k^* \rangle / \langle h_o h_o^* \rangle$$

$$= 1/a2 \iiint q(t_s-t)\; q^*(t_s-t')\; p(t-\tau-iT)\; p^*(t'-\tau-kT)\; S(t-t',\tau)\; d\tau\; dt\; dt'$$

An error free carrier recovery device would ideally determine the phase of h_0, and consequenly minimize the error probability. An error on the estimated phase of h_0 degrades the performance of the decision device by rotating the decision regions in the complex plane.

In order to evaluate the symbol error probability let us fix h_0 and consider the ISI term conditionally to h_0. From properties of jointly Gaussian variables it can be stated that the mean value of ISI is

$$m \triangleq \langle \sum_k{}' c_k h_k \;\Big|\; h_o \rangle$$

$$= \sum_k{}' c_k R_{k,o} h_o$$

It is noticeable that this mean value has a form similar to the ISI term in a fixed channel condition (deterministic coefficients).

The standard deviation of the interference can also be derived

$$\sigma_{ISI}^2 \triangleq \langle \left| \sum_k{}' c_k h_k - m \right|^2 \;\Big|\; h_o \rangle$$

$$= a^2\, C^t\, U\, C^*$$

with $C^t=(...c_{-2},c_{-1},c_0,c_1,c_2,...)$ and where U is a matrix given by

$$U_{i,k} = R_{i,k} - R_{i,o} R_{k,o}^*$$

Rigorously this standard deviation depends on the symbol sequence (c_k). However we observed by simulation that this dependance is weak and that σ_{ISI} is almost constant. Morover it can be easily overbounded. The normalized vector C which maximizes C^tUC^* is the eigenvector V of U corresponding to the highest eigenvalue. Consequently σ_{ISI} takes its maximum value σ_m for the sequence $c_k=\mathrm{sign}(v_k)$, for binary PSK, and $c_k=(1+j)\ \mathrm{sign}(v_k)$ for quaternary PSK (v_k are the component of the eigenvector V). In

the case of the M'SK modulation, two submatrix can be extracted from U on which a similar derivation holds.

Consequently $r(t_s)$ an be rewritten as

$$r(t_s) = h_o \, (c_o + \sum_k{}' c_k R_{k,o}) + n_{ISI} + n_s$$

where n_{ISI} is a Gaussian variable of approximate variance σ_m

The receiver uses the estimated phase φ of h_0 and derives a decision concerning the real part of c_0, from the sign of $Re(r(t_s) \exp(-j\varphi))$. Let $\Delta\varphi$ be the error on this phase estimation. Assuming $Re(c_0)=1$, the bit error probability can be written

$$Pe = Pr\{ c_o^{(r)} \cos\Delta\varphi + [c_o^{(i)} \sin\Delta\varphi + \sum_k{}' (c_k^{(r)} (R_{k,o}^{(r)} \cos\Delta\varphi - R_{k,o}^{(i)} \sin\Delta\varphi) - c_k^{(i)} (R_{k,o}^{(r)} \sin\Delta\varphi + R_{k,o}^{(i)} \cos\Delta\varphi))] + n_{eq} < 0 \}$$

where $X^{(r)}=Re(X)$ and $X^{(i)}=Im(X)$.

The noise term

$$n_{eq} = Re((n_{ISI} + n_s) \exp(-j\varphi) / |h_o|)$$

is a random variable, ratio of a gaussian to a rayleigh variable. Its distribution function is

$$f(x) = 1/2 \; (1 + x/(x^2 + \sigma_{eq}^2)^{1/2})$$

$$\sigma_{eq}^2 = (\sigma_{ISI}^2 + \sigma_n^2) / a^2$$

The error probability presented in that way is that of a symbol corrupted by an interference term (with fixed coefficients and thus a simple characteristic function) and by an equivalent noise term n_{eq} with a known distribution function. A computation technique previously proposed precisely apply to that case [9-10] and thus complete the error rate evaluation for a given phase recovery error.

4. Phase recovery error

In a fast fading environment and for a coherent detection, phase error in carrier recovery can be an important source of disturbance. While the incidence of noise on PLL devices was widely studied, few works were devoted to the operation of a PLL when the input signal is corrupted by fast fading.

Consequently, rather than theoretical results, we used the experimental data proposed by T. Fitch [11] and we derived, using a polynomial regression method, the following formula for the phase error distribution function.

$$f(\varphi) = (0.05 / (\varphi + 0.05))^{2.15} \quad (1 + 20\,\varphi / K) / (1 + 20\,\varphi)$$

with $K = 0.04\ B/f_d$ and for $B/f_d \gtrsim 10$

where B is the loop filter bandwidth.

This expression is in good agreement with the curves presented in [11] for a damping factor of one.

In order to evaluate the average error rate, taking into account the phase error distribution, we used the previously described derivation for sampled fixed phase errors and we realized a numerical integration. It should be noticed that the method is rigorously valid only if the phase error distribution is not dependant on the particular random channel.

5. Numerical results

The error probabilities of 2-PSK, 4-PSK and MSK were calculated using the method derived in the previous sections. The channel correlation function used correspond to an exponential delay distribution with random uniform rays incidence angle.

$$S(t,\tau) = k \, . \, J_o \, (2\pi \, f_d \, t) \exp(-\tau/\tau_o)$$

The filter loop bandwidth B, which is an important system parameter, is systematically adjusted to the twentieth part of the symbol rate (B= 1/20T). For PSK modulation, emitter and receiver equivalent filters are identical, and their combination gives a cosine rolloff pulse shape with rolloff factor α= 0 3 . The MSK signal is filtered only at receiver by a fourth order equalized butterworth filter with a 3 dB excess bandwidth of 20% .

The dependance of the error rate on a fixed phase error (not considering the fluctuations of the phase error) is first presented in figures 1 and 2.

The following figures present the minimum signal to noise ratio necessary to attain an error rate of 10^{-2}, varying the delay spread τ_0 characterizing the selectivity, and the doppler frequency f_d characterizing the fast fading rate. The phase error distribution and six adjacent interfering symbols are taken into account.

The first observation concerns the sharp edges of these figures : a small variation of the symbol rate can lead to a very different sensitivity to fast or selective fading. Secondly it is noticeable that a range of symbol rate generally exists for which the channel can be considered ideally flat and slow. However an essential observation is that in some severe but not unrealistic channel conditions, and for some intermediary symbol rates, none of the fast and selective fading can be neglected.

References

[1] P. A. Bello and B. D. Nelin, "The effect of frequency selective fading on the binary error probabilities of incoherent and differentially coherent matched filter receivers," IRE Trans. on Comm. Systems, pp. 170-186, June 1963.

[2] C. C. Bailey and J. C. Lindenlaub, "Further results concerning the effects of frequency selective fading on differentially coherent matched filter receivers," IEEE Trans. on Comm. Technol., pp. 749-751, Oct. 1968.

[3] B. Glance and L. J. Greenstein, "Frequency selective fading effects in digital mobile radio with diversity combining," IEEE Trans. on Comm., vol. COM-31, no. 9, pp. 1085-1094, Sept. 1983.

[4] P. A. Bello and B. D. Nelin, "The influence of fading spectrum on the binary error probabilities of incoherent and differentially coherent matched filter receivers," IRE Trans. on Comm. Systems, vol. CS-10, pp. 160-168, June 1962.

[5] K. Hirade, M. Ishizuka and F. Adachi, "Error-rate performance of digital FM with discriminator detection in the presence of cochannel interference under fast Rayleigh fading environment," Trans. of the IECE of Japan, vol. E.61, no. 9, Sept. 1978.

[6] K. Hirade, M. Ishizuka, F. Adachi and K. Ohtani, "Error rate performance of digital FM with differential detection in land mobile radio channels," IEEE Trans. on Vehicul. Tech., vol. VT-18, no. 3, pp. 204-212, Aug. 1979.

[7] S. Elnoubi and S. Gupta, "Error rate performance of noncoherent detection of duobinary coded MSK and TFM in mobile radio communications systems," IEEE Trans. on Vehicul. Technol., vol. VT-30, no. 2, pp. 62-75, May 1981.

[8] M. Yokoyama, "BPSK system with sounder to combat Rayleigh fading in mobile radio communication," IEEE Trans. on Vehicul. Technol., vol. VT-34, no. 1, Feb. 1985.

[9] A. J. Levy, "Fast error rate evaluation in the presence of intersymbol interference," IEEE Trans. on Comm., vol. COM-33, no. 5, May 1985.

[10] A. J. Levy, "Performances en probabilité d'erreur des modulations à grand nombre d'états en période d'évanouissements sélectifs," Ann. des Telecomm., vol. 40, no. 11-12, pp. 617-625, Nov. 1985.

[11] T. A. Fitch, "The effect of rayleigh distributed multipath fading on carrier recovery performance," Vehicul. Technol. Conf. record , pp. 252-255, 1986.

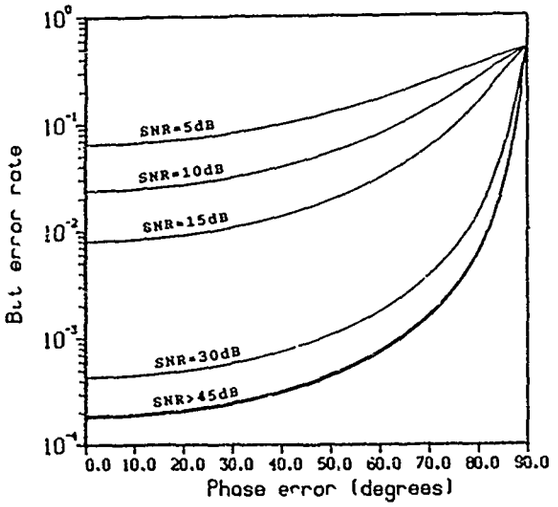

Figure 1 Bit error rate shown as a function of a fixed phase recovery error, for different signal to noise ratio, in a fast and selective fading channel (BPSK modulation, τ_o=2 µs, D=15kb/s, f_d=50Hz)

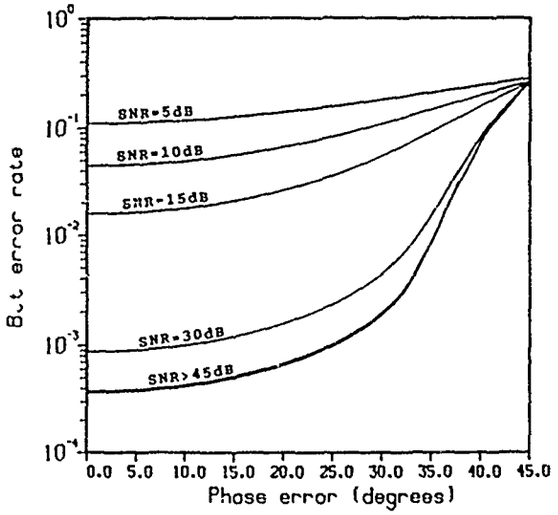

Figure 2 Bit error rate shown as a function of a fixed phase recovery error, for different signal to noise ratio, in a fast and selective fading channel (QPSK modulation, τ_o=2 µs, D=15kb/s, f_d=50Hz)

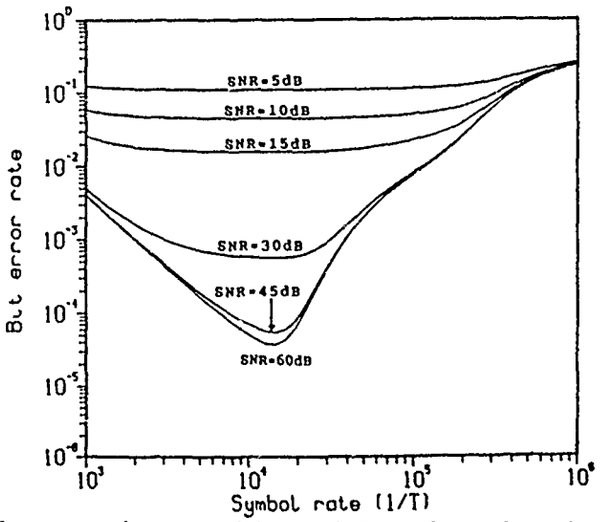

Figure 3 Bit error rate shown as a function of the symbol rate for various signal to noise ratio (QPSK modulation, Doppler frequency f_d=20Hz, delay spread τ_o=1 µs)

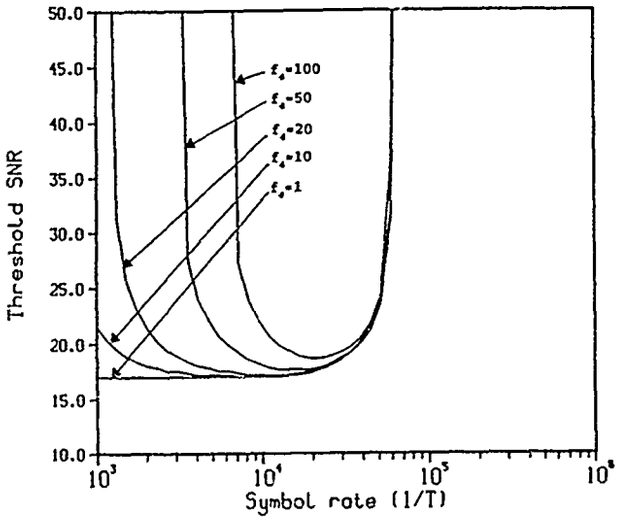

Figure 4 Required signal to noise ratio for an error rate of 10^{-2} (QPSK modulation, delay spread τ_o=2μs)

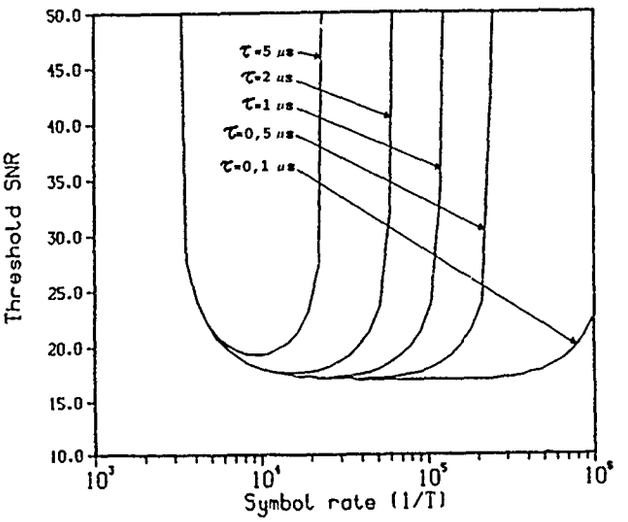

Figure 5 Required signal to noise ratio for an error rate of 10^{-2} (QPSK modulation,f_d=50Hz)

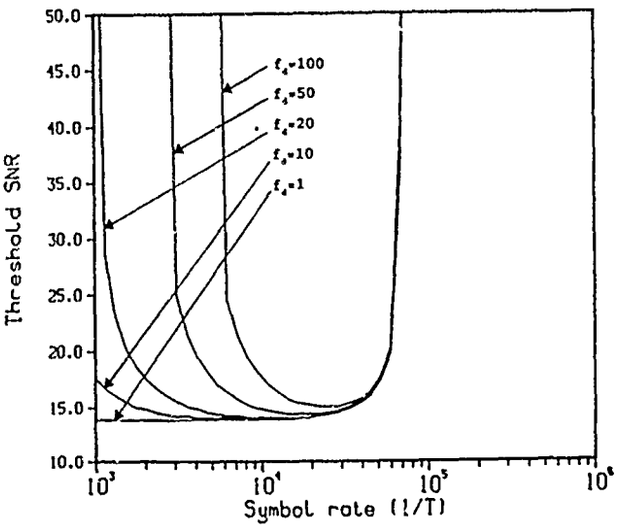

Figure 6 Required signal to noise ratio for an error rate of 10^{-2} (MSK modulation, delay spread τ_o=2μs)

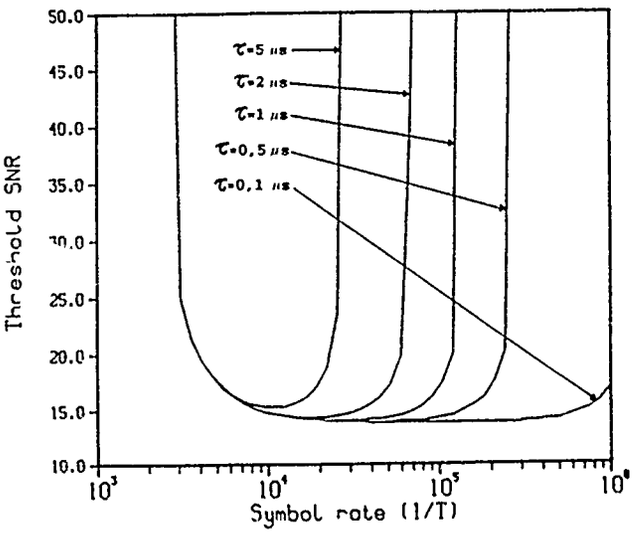

Figure 7 Required signal to noise ratio for an error rate of 10^{-2} (MSK modulation, f_d=50Hz)

DISCUSSION

G. OSSEWAARDE

In your graph (figure 5) you have taken the BER criterion at 10^{-2}.
Is the behaviour different for other BER's (e.g. 10^{-3}) ?
The graph shows a fast increase of threshold SNR for the different values of τ.
Is there a "physical" explanation for this ?

AUTHOR'S REPLY

The graphs depend of course of the BER chosen, but the general behaviour do not, as it can be seen on the following figure computed in the same condition as figure 5 but with a BER criterion 10^{-3}.
The fast increase of threashold SNR with the bit rate is due to the existence of a so-called "irreducible error rate". Once this error rate overpass the BER criterion the threshold SNR becomes infinite.
The dependance of the bit rate limit with τ_0 follows as expected a law of the form : $BER_{limit} \cdot \tau_0 = constant$.

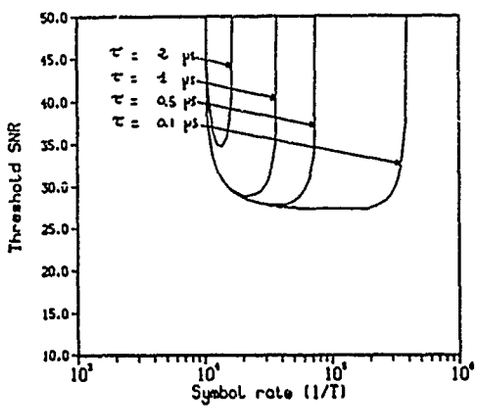

D.J. FANG

I understand the assumption of your paper that synchronization and carrier locking are always achieved. May I ask the errors of 45° or bigger as investigated in the paper can indeed be synchronized by a standard PLL (Phase-Locked-Loop) in the first place. Can you tell me the state-of-the-art PLL for HF circuits in terms of maxima carrier locking phase error in degree.

AUTHOR'S REPLY

I am not a specialist of HF circuits but I hope the following will answer the question. Your oral question mentioned the fact that PLL on satellite links loose synchronization for phase error far less than 45°.
Actually PLL on satellite links faces noise. The design constraints and caracteristics of a PLL when facing noise and those in the presence of a strong signal but with a varying channel are very different. That's probably the reason why Fitch [Ref. 11] can measure non negligeable probability density of phase error for values as large as 80 degrees and with a synchronized PLL. A PLL able to follow a rapidly varying channel will recover such a phase error while for a PLL designed to resist to noise, and in the presence of that noise, a much lower phase error is the sign of an insufficient SNR and of a probable loose of synchronization.

ETUDE EXPERIMENTALE D'UNE LIAISON NUMERIQUE RADIOMOBILE A ETALEMENT DE SPECTRE EN SITE URBAIN

G. EL ZEIN, M. SALEHUDIN, A. DANIEL, J.J. BAI, J. CITERNE.
Laboratoire "Stuctures rayonnantes"
UA au CNRS N° 834, INSA 35043 RENNES CEDEX

RESUME

Cette communication concerne l'étude et la réalisation d'une liaison numérique radiomobile à 910 MHz, utilisant l'étalement de spectre par séquence directe. La mise en œuvre de cette liaison est faite soit en tant que système de communication à étalement de spectre, soit en tant que système de mesure employant l'étalement pour une caractérisation fine du canal radiomobile urbain.

Les mesures de performances effectuées en laboratoire ont révélé un bon accord théorie expérience et ont mis en évidence différents avantages de l'étalement de spectre. Les mesures de propagation effectuées sur la liaison réelle ont montré d'une part, les variations spatiales et temporelles sur l'enveloppe du signal reçu et d'autre part, les fluctuations instantanées de la réponse impulsionnelle du canal de transmission.

Ces mesures permettront d'aboutir à une modélisation statistique du canal de transmission et à l'amélioration de la qualité de la liaison par la diversité des multitrajets.

1. INTRODUCTION :

Les nouveaux systèmes numériques, destinés aux communications radiomobiles civiles ou militaires, sont appelés à fonctionner dans un environnement de plus en plus hostile comme l'est, par exemple, un site urbanisé. Dans cette situation, le canal de transmission acquiert un caractère de non-stationnarité et évolue rapidement dans l'espace temps-fréquence [1].

Dans un système de communication à étalement de spectre, la bande passante du récepteur est en général suffisamment large pour couvrir l'inverse de la différence entre les deux plus courtes durées caractéristiques de la propagation. Il est donc possible de discriminer les différents trajets de la propagation. Dès lors, plutôt que de considérer les réflexions multiples comme une nuisance, il devient possible, en principe, de tirer profit de leur présence pour tenter d'améliorer la qualité de la liaison, à partir du concept de diversité [2].

Cet article présente une liaison radiomobile à étalement de spectre réalisée à 910 MHz. Les premières mesures effectuées sur table ont porté sur l'évaluation des performances du système en présence de diverses perturbations. Ensuite, la liaison réelle est mise en œuvre en vue de caractériser le canal radiomobile urbain. Dans ce cas, les mesures de propagation effectuées ont porté sur l'étude du phénomène des trajets multiples.

2. PRESENTATION DE LA LIAISON :

2.1. Le modem :

Le principe du modulateur utilisant la séquence directe est simple, il s'agit d'additionner modulo 2 l'information binaire à un code pseudo aléatoire ayant un débit numérique (Rc = 1/Tc) beaucoup plus important que celui du message à transmettre (Rm = 1/Tm). Ensuite, il est procédé généralement à une modulation à déplacements de phase [3].

Les données véhiculées sont à bas débit (Rm = 7,2 Kbit/s). Un codage direct par séquence pseudo aléatoire (Rc = 10 Mbit/s) à longueur maximale est introduit avant de réaliser une modulation à deux états de phase (M.D.P.2) à la fréquence intermédiaire (Fo = 70 MHz).

En réception, pour éliminer l'effet de l'étalement, le démodulateur doit assurer une synchronisation parfaite entre le code reçu et un code généré localement, identique au premier. Une fois le décodage effectué, on procède à une démodulation classique M.D.P.2.

En ce qui concerne l'opération de synchronisation, elle est réalisée en deux temps. D'abord, l'acquisition de la synchronisation est obtenue en faisant glisser, bit par bit, le code local par rapport au code reçu. Si la tension détectée à la sortie du corrélateur est inférieure au niveau du seuil, le processus de recherche continu. Sinon, ce processus s'arrête pour enclencher celui de la poursuite en mettant en œuvre une boucle à verrouillage de retard. Dans ce cas, le signal reçu est corrélé avec deux versions, l'une avancée l'autre retardée d'un demi bit, du code généré localement. Cette boucle réagit donc en discriminateur avance retard pour maintenir le déphasage entre les codes nul et corriger ainsi des écarts éventuels de synchronisme.

Après le décodage, une démodulation cohérente M.D.P.2 est effectuée. La récupération de la porteuse est réalisée grâce à une boucle à verrouillage de phase à doublement de fréquence. Pour la reconstitution du message binaire émis, le signal démodulé est remis en forme puis échantillonné au rythme de l'horloge récupérée. Un codage-décodage par transition, introduit respectivement à l'émission et à la réception, permet de lever l'ambiguïté sur la phase de la porteuse récupérée.

2.2. Le sous-ensemble radiofréquence:

Les fréquences généralement utilisées dans les systèmes récents de radiocommunications avec les mobiles se situent vers le haut de la bande U.H.F.

Un schèma synoptique de la liaison radiomobile réalisée est montré sur la figure 1. C'est une liaison unilatérale entre une base d'émission fixe située au laboratoire L.C.S.T à l'I.N.S.A de Rennes et un récepteur mobile.

Le signal issu du modulateur est transposé à la fréquence d'émission (RF = 910 MHz). Un étage amplificateur de puissance permet d'obtenir 1 Watt à la sortie de l'émetteur. L'antenne d'émission est portée par un pylône de 43 m de hauteur. Elle est omnidirectionnelle et présente un gain Ge=9 dBi, avec un angle d'ouverture verticale de 7,5°.

A la réception, l'antenne est verticale omnidirectionnelle avec un gain Gr=3 dBi. Elle est placée au centre du toit du mobile à 2,5 m du sol. Le signal reçu est ramené à la fréquence intermédiaire avant d'être appliqué à l'entrée du démodulateur.

3. EVALUATION DES PERFORMANCES DU SYSTEME :

Le taux d'erreur constitue un indicateur précis de la qualité de la transmission. Il a tout d'abord été mesuré en présence de bruit blanc puis avec un brouilleur sinusoïdal ou modulé à spectre étalé n'utilisant pas le même code et enfin en présence de trajets multiples.

3.1. Taux d'erreur en présence de bruit blanc:

Ces mesures sont effectuées avec le montage de la figure 2. Le rapport signal à bruit de la liaison est modifié en changeant l'atténuation placée dans la chaîne de bruit. La mesure de ce rapport est faite après le filtre de réception précédant le démodulateur.

Le taux d'erreur a été mesuré avec et sans étalement de spectre, le contrôle automatique du gain étant hors service. Les résultats sont représentés graphiquement sur la figure 3 par des traits continus. Pour situer les performances obtenues, elles sont confrontées à la courbe de la probabilité d'erreur théorique de la démodulation cohérente M.D.P.2. (Codage-Décodage par Transition).

On constate que pour un taux d'erreur de 10^{-5}, la dégradation du rapport (E/No) par rapport à la théorie est égale à 1 dB sans étalement, causée essentiellement par le filtrage de prédétection (Bm = 9 KHz). Avec l'étalement, il apparaît une dégradation supplémentaire de 1,2 dB, due principalement au filtrage de réception (Bc = 12 MHz) et à la gigue de synchronisation.

Après l'introduction du sous-ensemble radiofréquence, ces mesures ont été refaites sur table. Dans ce cas, le bruit blanc est injecté à l'entrée du récepteur. Les résultats obtenus sont montrés en tirets sur la figure 3 et font apparaître, pour un taux d'erreur de 10^{-5}, une dégradation de 0,7 dB par rapport aux courbes obtenues pour le modem seul, avec et sans étalement.

Cette dégradation est due essentiellement aux distorsions apportées par l'étage amplificateur de puissance (conversion AM-PM, variation du gain).

3.2. Taux d'erreur en présence de brouilleur sinusoïdal:

Le brouilleur pur est injecté à la place du bruit blanc (fig.2). Les performances sont mesurées en fonction du rapport signal à brouilleur $(S/J)_{dB}$ et de la fréquence centrale du brouilleur $(Fj)_{MHz}$.

Les résultats montrés sur la figure 4 font apparaître un brouillage plus efficace lorsque celui-ci est centré sur $Fj = Fo \pm Rm$, conformément à la théorie [4] . D'autre part, lorsque Fj = Fo, le système peut maintenir la synchronisation pour des rapports (S/J) supérieurs à - 20 dB.

3.3. Taux d'erreur en présence de brouilleur large bande:

Le brouilleur utilisé est un modulateur à spectre étalé. Le code C2 utilisé pour le brouilleur a le même débit (10 M bits/s) et la même longueur (2 047 bits) que le code du signal utile C1 ([2,11]), mais se distingue par son polynôme générateur ([2,5,8,11]).

Le taux d'erreur est relevé en fonction du rapport $(S/J)_{dB}$. Le résultat est montré sur la figure 5. Le système peut donc maintenir la synchronisation pour des rapports (S/J) supérieurs à - 24 dB.

3.4. Taux d'erreur en présence de trajets multiples:

Pour pouvoir tester le comportement du système face aux trajets multiples, un simulateur de canal radiomobile à large bande a été réalisé [5]. Ce simulateur permet de reproduire en laboratoire un canal de RICE à neuf rayons (un trajet direct et huit trajets réfléchis) avec un retard maximal de 10 µs.

Le montage de mesure utilisé est montré sur la figure 6. Le taux d'erreur a été mesuré en présence d'un trajet direct caractérisé par un facteur d'atténuation γ_0^2 et de cinq trajets réfléchis (N = 5) ayant la même puissance relative ($\gamma^2 = 0.4$) . Les résultats sont portés sur la figure 7 en fonction de $(E/No)_{dB}$ et du paramètre γ_0^2. Ils sont confrontés aux courbes théoriques obtenues d'après [6] et permettent de constater un bon accord théorie-expérience .

4. MESURES DE PROPAGATION RADIOMOBILE:

Pour les mesures de propagation, la liaison radiomobile réalisée (Emetteur fixe - Récepteur mobile) est mise en œuvre. Ces mesures sont effectuées en deux parties :

- mesures en bande étroite,
- mesures à large bande.

4.1. Mesures en bande étroite:

Les mesures en bande étroite (porteuse pure) permettent la description des variations spatiales et temporelles du signal reçu à petite et grande échelle [7].

En particulier, la puissance moyenne du signal reçu en milieu urbain est relevée en fonction de la distance émetteur-récepteur. Les résultats expérimentaux sont montrés en pointillé sur la figure 8 et font apparaître une décroissance suivant $d^{-3,2}$. On peut constater également que, pour un milieu suburbain ($d < 2,5$ Km), ces valeurs s'approchent plus du modèle théorique de prédiction développé par EGLI [8]. Lorsque le récepteur est situé en zone urbaine, les résultats tendent vers le modèle d' OKUMURA - HATA [9].

Ensuite, des fluctuations rapides, régulièrement espacés de $\lambda/2$, sont observées sur le niveau du signal reçu en fonction de la vitesse du mobile (Fig.9).

4.2.Mesures à large bande:

Les mesures à large bande permettent de déterminer la réponse impulsionnelle instantanée du canal de transmission. Ainsi, trois techniques ont été mises en œuvre.

La première consiste à émettre un train d'impulsions de 100 ns avec une période de 10 µs, et à détecter l'enveloppe du signal reçu. Pour les deux autres techniques, basées sur le principe de corrélation, le signal émis est un code pseudo-aléatoire avec un débit numérique de 10 Mbit/s. La longueur du code est de 2047 bits lorsqu'on utilise un corrélateur discret proposé par COX [10]. Dans le cas où un corrélateur à ondes acoustiques de surface est introduit, la longueur du code est de 127 bits. Dans ces trois méthodes, les mesures sont effectuées avec une largeur de bande d'environ 10 MHz, ce qui permet de discriminer des trajets différents de 30 m ou plus.

La figure 10 montre une réponse impulsionnelle obtenue par l'émission d'impulsions dans un site urbain modéré. Un exemple de quatre profiles, relevés avec le corrélateur de COX à des intervalles réguliers de 10 cm, est montré sur la figure 11. Ces profiles sont représentatifs de la réception dans un terrain plat, en présence de quelques réflexions spéculaires arrivant au voisinage du mobile. Dans ces conditions, de fortes variations spatiales peuvent apparaître sur les trajets multiples [11]. La figure 12 représente un profile obtenu avec le corrélateur à ondes de surface et fait apparaître une réflexion avec un retard d'environ 10 µs. Cette valeur correspond au retard maximal observé sur les trajets lors de nos campagnes de mesures et semble prévisible pour un site en zone non montagneuse [12]

5. CONCLUSION:

Ce papier a concerné la présentation d'une liaison numérique radiomobile à étalement de spectre par séquence directe. Cette liaison a été expérimentée pour la transmission de données numériques à bas débit. Ensuite, elle a été mise en œuvre pour effectuer des mesures de propagation en milieu urbain.

L'évaluation des performances du système est effectuée en considérant diverses perturbations pouvant affecter la liaison réelle. D'autre part, l'application de modèles de prédiction de la propagation radiomobile est faite en tenant compte de la nature hostile du canal de transmission urbain. Les mesures de performances et de propagation réalisées permettent de constater que le système actuel constitue aussi bien un système de communication performant qu'un système de mesure précis.

De nombreuses campagnes de mesures seront nécessaires pour aboutir à une modélisation statistique complète du canal urbain. L'amélioration de la qualité de la liaison sera ensuite envisagée grâce à des techniques de diversité de réception, notamment celles qui utilisent la sélection ou la combinaison des trajets multiples.

6. REFERENCES:

[1] W.C. JAKES
Microwave Mobile Communications.
New York : Wiley, 1974.

[2] G.L. TURIN
"Introduction to Spread-Spectrum Antimultipath Techniques and their Application to Urban Digital Radio".
Proc. IEEE, vol. 68, N° 3, pp 328-353, March 1980.

[3] R.C. DIXON
Spread Spectrum Systems.
New York : Wiley, 1976.

[4] G.EL ZEIN
"Etude et réalisation d'une liaison numérique radiomobile à étalement de spectre en site urbain".
Thèse de Doctorat de l'Université de Rennes I, Juin 1988.

[5] A . DANIEL, G. EL ZEIN, M. SALEHUDIN et J. CITERNE
"Etude et réalisation d'un simulateur de canal radiomobile à large bande".
L'Onde Electrique, vol. 68, N° 2, pp 82-89, Mars 1988.

[6] E.A. GERANIOTIS and M.B. PURSLEY
"Performance of Coherent Direct-Sequence Spread-Spectrum Communications over Specular Multipath Fading Channels"
IEEE - Trans. Commun., vol. COM-33, N° 6, pp 502-508, June 1985.

[7] D.L. NIELSON
"Microwave Propagation Measurements for Mobile Digital Radio Application".
IEEE - Trans. Veh. Technol., vol. VT-27, N° 3, pp 117-131, Aug. 1978.

[8] J.J. EGLI
"Radio Propagation Above 40 Mc over Irregular Terrain".
Proc. IRE, vol. 45, pp 1384-1391, Oct. 1957.

[9] M. HATA
"Empirical Formula for Propagation Loss in Land Mobile Radio Services".
IEEE - Trans. Veh.Technol., vol. VT- 29, N° 3, pp 317-325, Aug. 1980.

[10] D.C. COX
"Delay-Doppler Characteristics of Multipath Propagation at 910 MHz in a Suburban Mobile Radio Environment".
IEEE - Trans. Ant. Prop., vol. AP-20, N° 5, pp 625-635, Sept. 1972.

[11] D.C. COX
"910 MHz Urban Mobile Radio Propagation : Multipath Characteristics in New York City".
IEEE - Trans. Veh. Technol., vol. VT-22, N° 4, pp 104-110, Nov. 1973.

[12] W.C.Y. LEE
"Mobile Communications Engineering".
Mc Graw-Hill, 1982.

7. REMERCIEMENTS:

Cette étude a été réalisée en l'exécution d'un contrat émanant de la Direction des Recherches Etudes et Techniques (DRET).

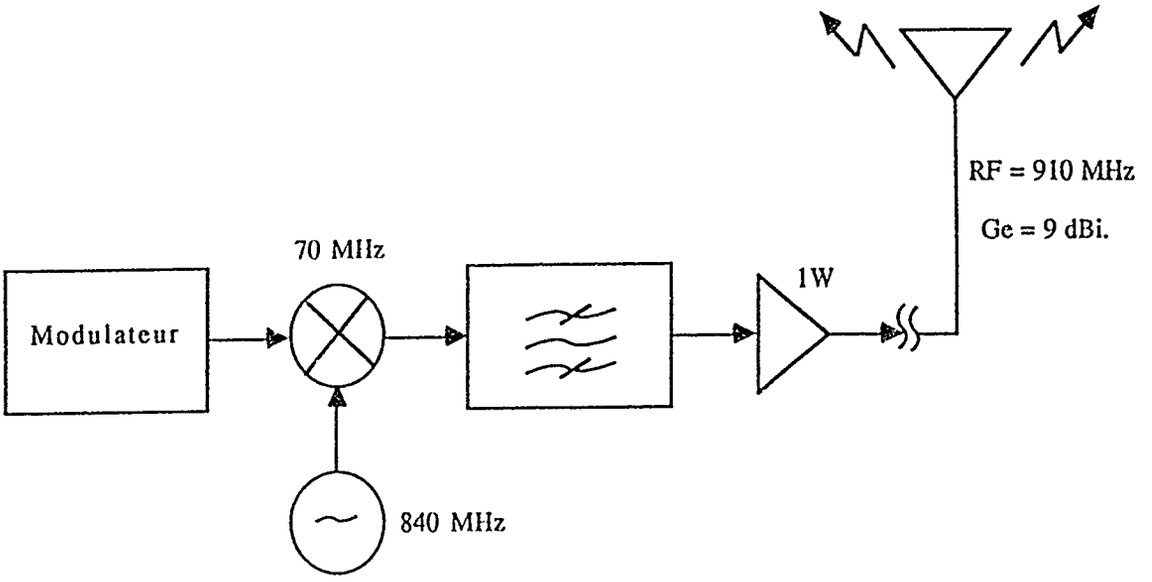

a) Emission

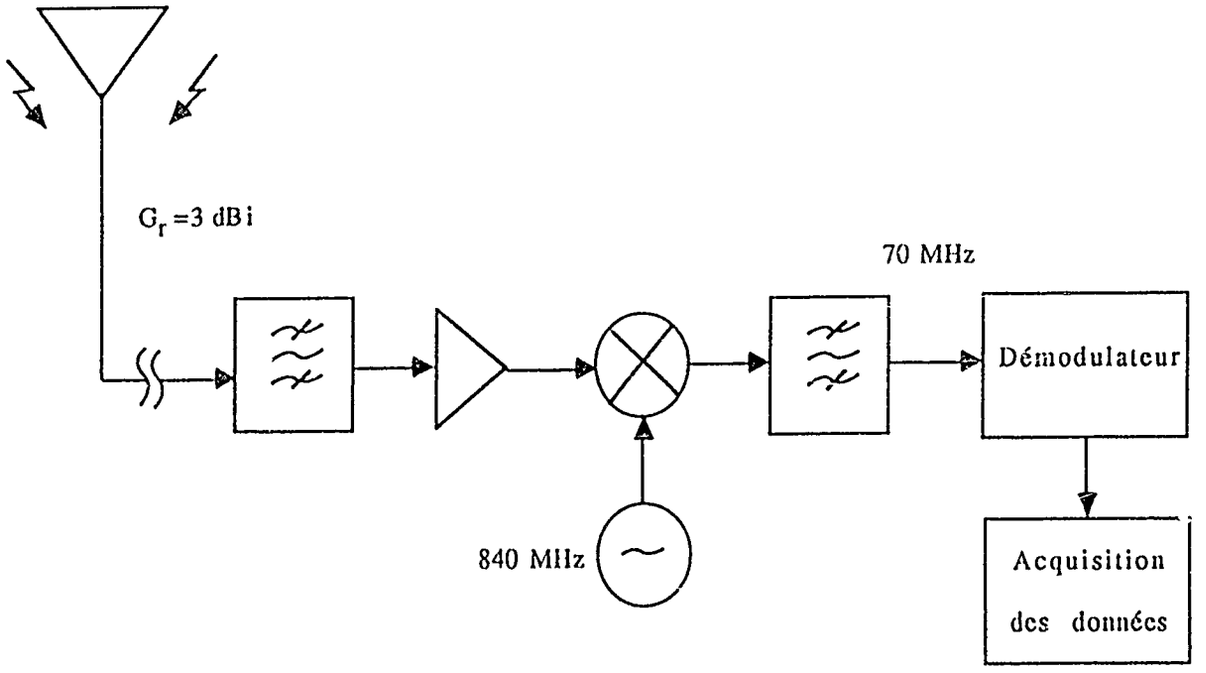

b) Réception

FIG.1 : Structure de la liaison réalisée.

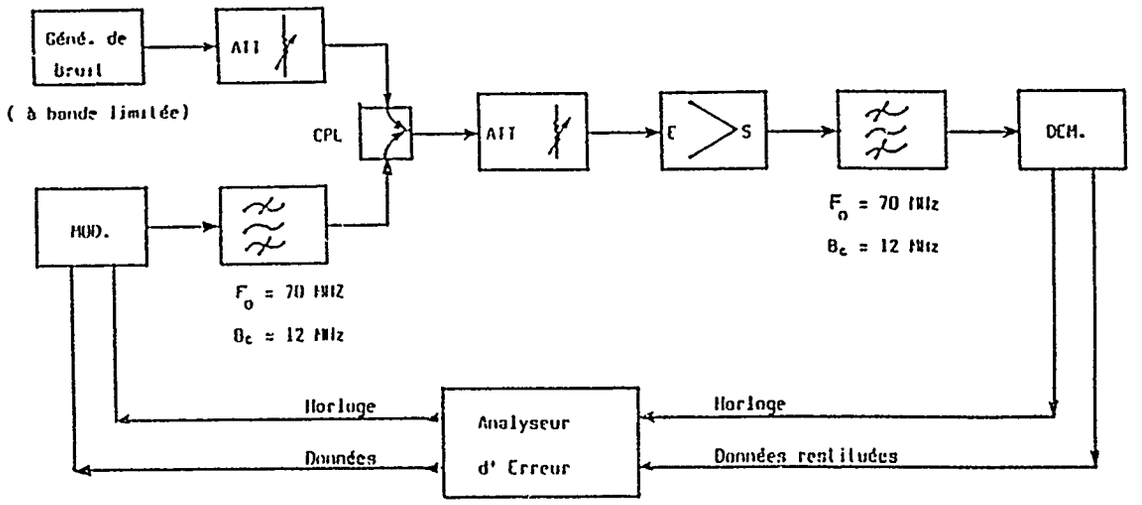

FIG.2 : Synoptique de la chaîne de mesure du taux d'erreur en fonction du rapport signal sur bruit.

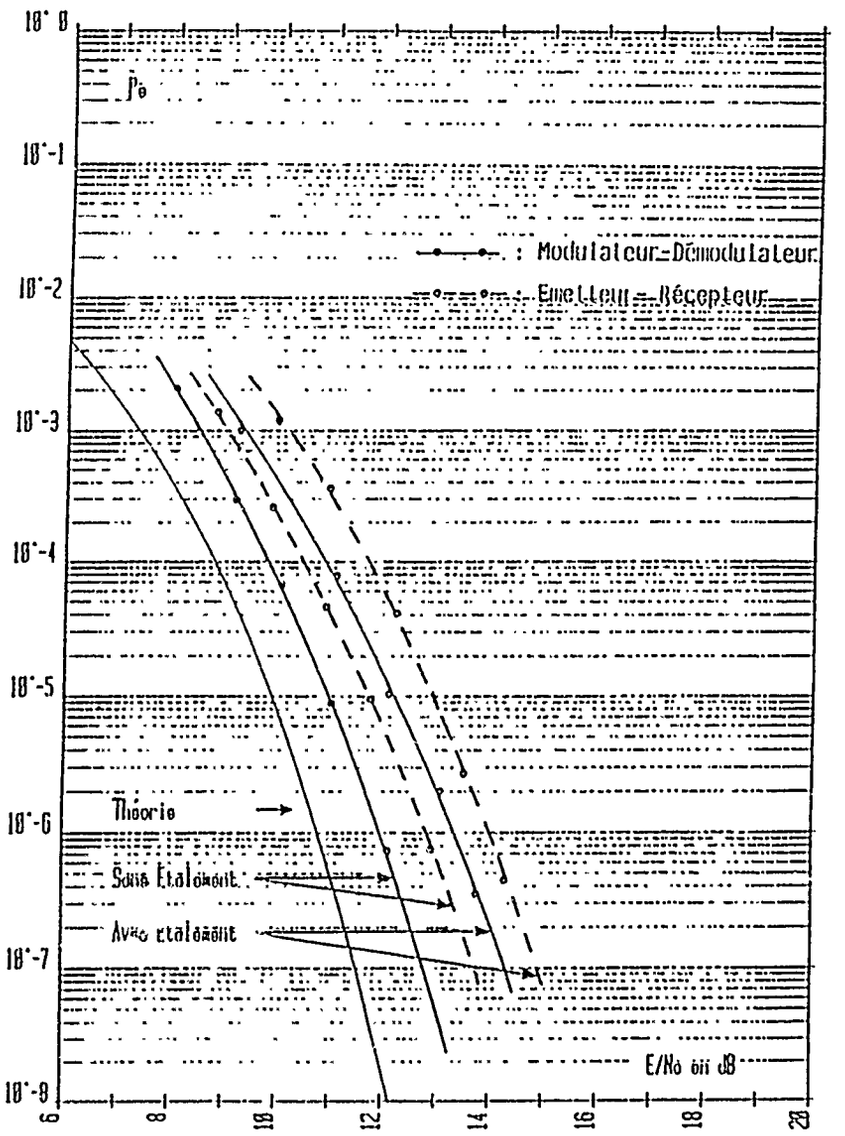

FIG.3 : Taux d'erreur en présence de bruit blanc. Comparaison Théorie-Expérience.

$\left(\frac{S}{J}\right)$dB \ F_j MHz	$F_0 - \frac{1}{Tc}$	$F_0 - \frac{1}{2Tc}$	$F_0 - \frac{1}{Tm}$	F_0	$F_0 + \frac{1}{Tm}$	$F_0 + \frac{1}{2Tc}$	$F_0 + \frac{1}{Tc}$
	60	65	69,9928	70	70,0072	75	80
-20	🚶	🚶	🚶	🚶	🚶	🚶	🚶
-19	🚶	🚶	🚶	6.10^{-3}	🚶	🚶	🚶
-18	🚶	🚶	🚶	8.10^{-5}	🚶	🚶	🚶
-17	🚶	🚶	🚶	🚶	🚶	🚶	🚶
-16	🚶	🚶	🚶	🚶	🚶	🚶	🚶
-15	🚶	🚶	🚶	🚶	🚶	🚶	🚶
-14	🚶	🚶	🚶	🚶	🚶	🚶	🚶

FIG.4 : Influence d'un brouilleur sinusoïdal.

🚶	: Perte de synchronisation.
🚶	: Pe $\leqslant 10^{-6}$

$\left(\frac{S}{J}\right)$dB	Pe
-24	🚶
-23	1.10^{-4}
-22	1.10^{-5}
-21	3.10^{-7}

FIG.5 : Influence d'un brouilleur large bande.

🚶	: Perte de synchronisation

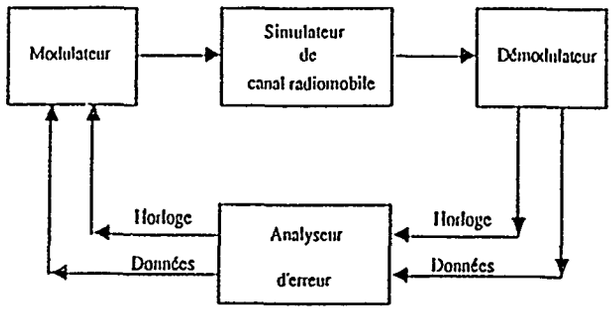

FIG.6 : Montage de mesure en présence de trajets multiples.

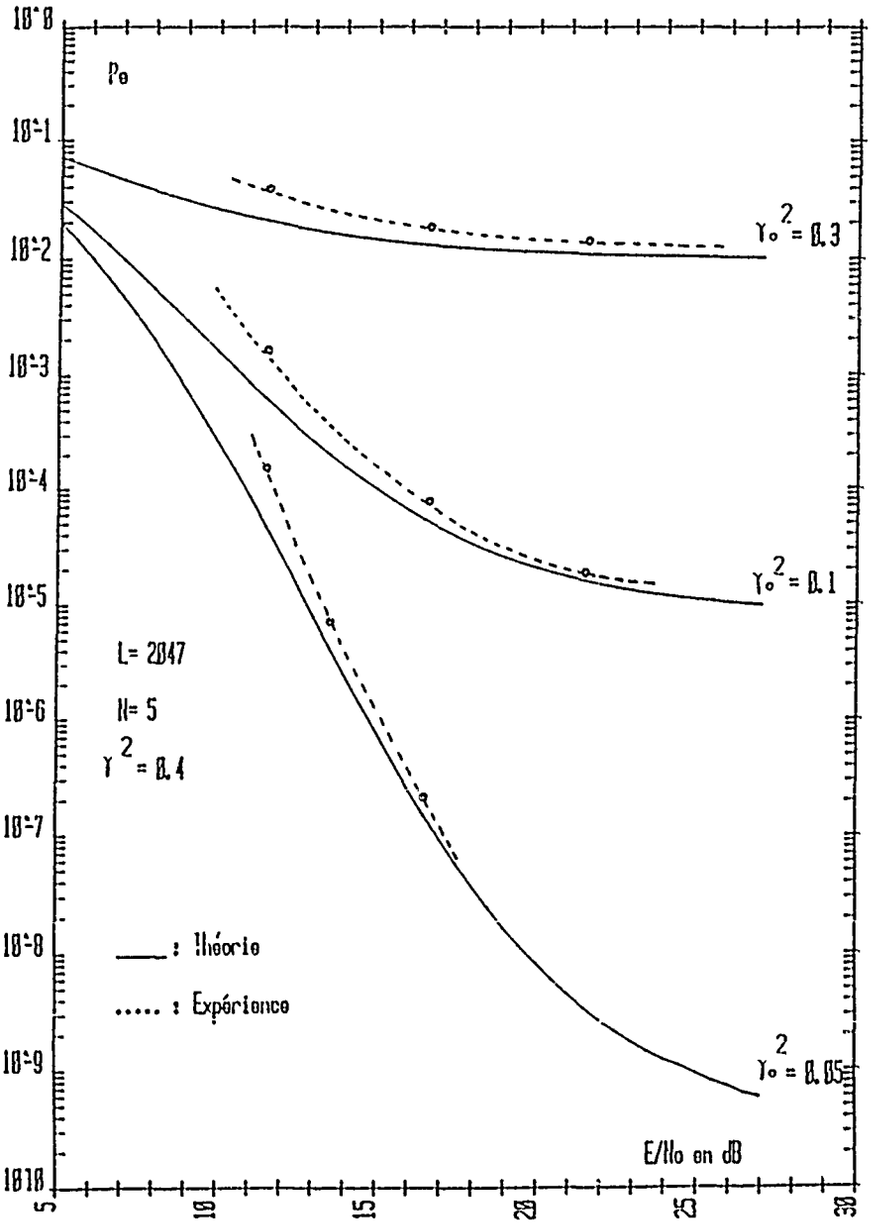

FIG.7 : Taux d'erreur en présence de trajets multiples.
Modèle de RICE.

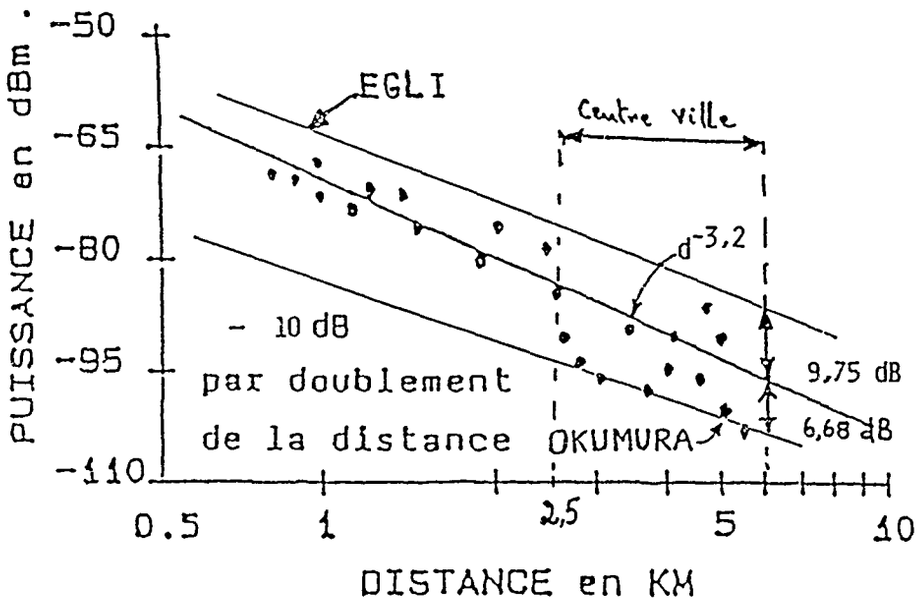

FIG.8 : Puissance moyenne reçue en fonction de la distance Emetteur-Récepteur.

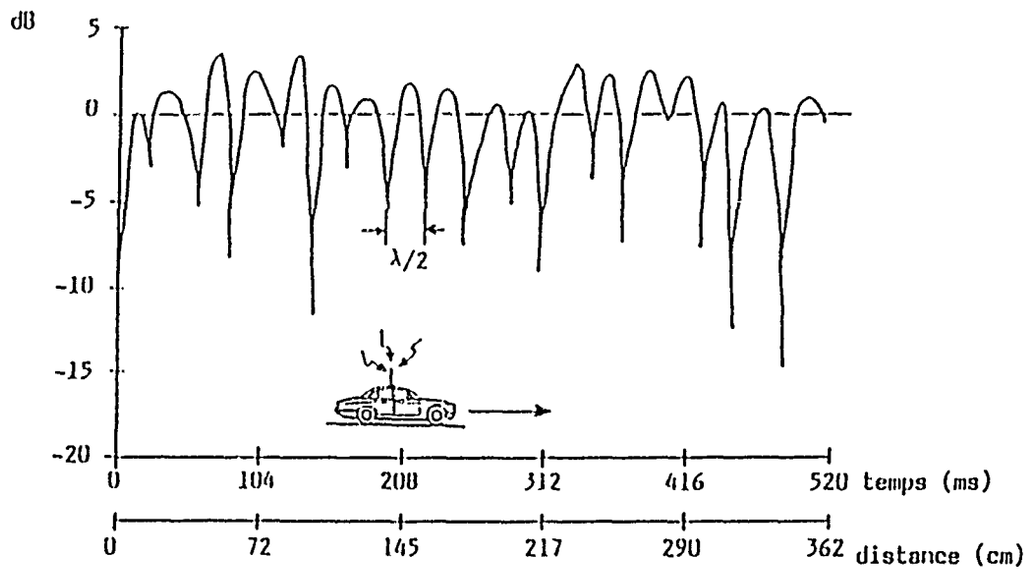

- Vitesse du mobile = 25 Km/h.

FIG.9 : Evanouissements caractéristiques du signal reçu par le mobile.

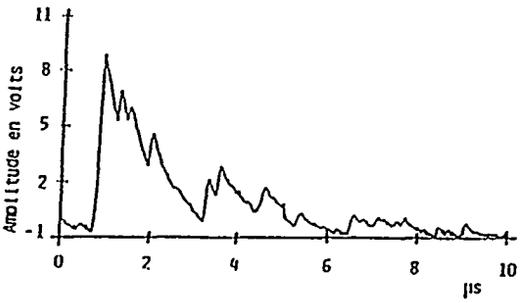

FIG.10 : Réponse impulsionnelle obtenue par la transmission d'impulsions.

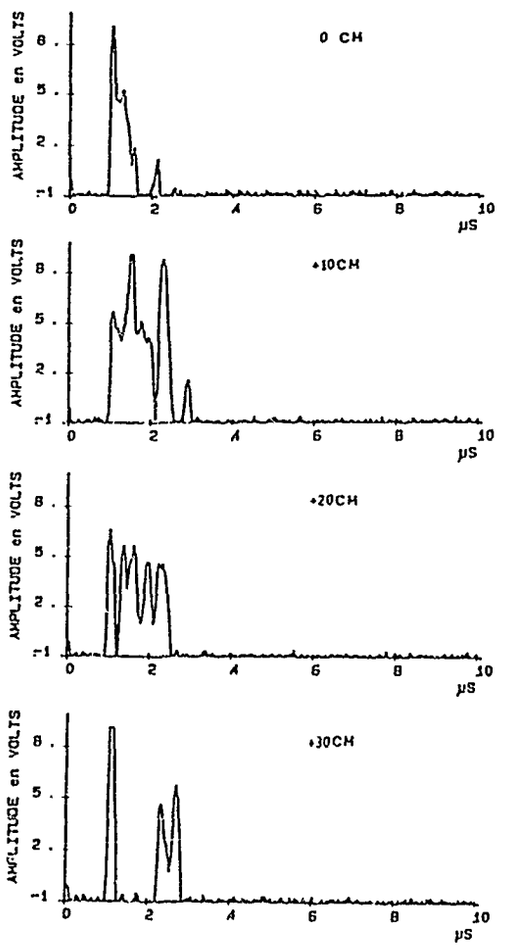

FIG.11 : Evolution spatiale de la réponse impulsionnelle à la sortie du corrélateur de COX.

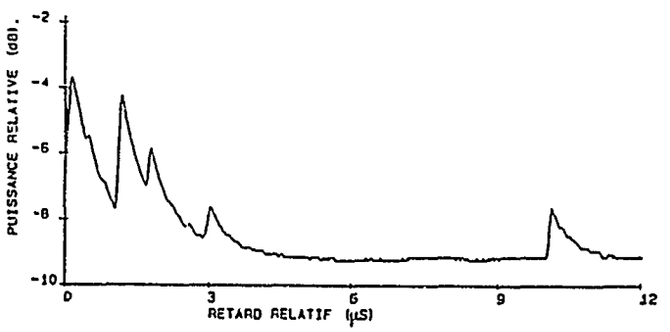

FIG.12 : Profil de trajets multiples relevé à la sortie du corrélateur à ondes de surface.

DISCUSSION

R.M. HARRIS

Pouvez-vous dire quelque chose au sujet du contrôle automatique de l'amplificateur du récepteur ?
Y avait-il deux boucles ou une boucle ?
Comment se comporterait-il en présence du brouillage ?

AUTHOR'S REPLY

Le contrôle automatique du gain (C.A.G.) est réalisé en FI par une boucle où la réaction est la puissance détectée du signal reçu. Pour améliorer les performances du C.A.G. en présence de brouilleurs, le point de détection a été placé après l'opération de désétalement. La dynamique ainsi obtenue est de l'ordre de 45dB et le temps de réponse est de l'ordre de 100 μs.

R.W. LORENZ

You have compared very nicely the different methods for wide-band measurements in mobile radio. However the methods presented are restricted to 10 μs and 12,7 μs, respectively for delay lengths. In mountainous terrain, especially at lower frequencies, longer delays are likely to occur.
Did you consider measurement systems to obtain results in mountainous terrain ?

AUTHOR'S REPLY

Lors de la propagation radiomobile dans des régions montagneuses, il est possible de relever quelquefois des trajets multiples avec des retards qui dépassent 12,7 μs. Dans ce cas, le corrélateur à ondes de surface utilisé dans notre système ne peut plus servir pour effectuer les mesures. Par contre, les deux autres techniques, qui consistent à utiliser le corrélateur discret de COX ou à émettre des impulsions, peuvent être mises en oeuvre à condition d'augmenter la fenêtre d'observation.

U. SEIER

1 - What kind of modulation is used by the realized transmission system ?
2 - How do you explain the characteristic behaviour of the described spread spectrum system in case of a CW-jammer (figure 4 in preprint) ? Why is the system rather sensitive for jammer-frequencies equal to Fo $\pm \frac{1}{Tm}$, but less sensitive (about 4-5dB) for a jammer-frequency equal to Fo, although the CW-jammer is spreaded over a wide bandwith in the receiver ?

AUTHOR'S REPLY

1 - La modulation utilisée dans notre système est la modulation à deux états de phase B.P.S.K. associée à un codage-décodage par transition.
2 - Lorsque le rapport G/L est proche de l'unité, (G étant le gain de traitement et L la longueur du code pseudo-aléatoire), comme c'est le cas dans notre application, l'influence du brouilleur n'est pas maximale pour Fj = Fo. En effet, en examinant la densité spectrale de puisance de l'interférence après étalement illustrée par la figure 1, il est simple de constater que, pour Fj = Fo et $(G/L) \approx 1$, seule la raie centrée sur Fo de puissance $(1/L^2)$ va contribuer au brouillage de l'information utile. Si par contre, Fj = Fo $\pm$ (1/Tm), cette puissance devient pratiquement L fois plus importante $[(L+1)/L^2 \approx 1/L]$.

DISCUSSION

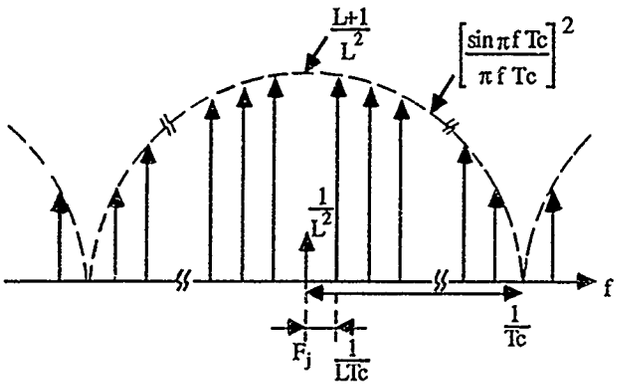

FIGURE 1 : Spectre de l'interférence sinusoïdale après étalement.

PACKET RADIO NETWORK CONCEPTS FOR THE NORWEGIAN FIELD ARMY

by

Tore Berg, John Erik Rustad, Ole Henrik Støren
Norwegian Defence Research Establishment
P O B 25, N-2007 Kjeller, Norway

SUMMARY

The Norwegian army has taken a very close look at the advantages in integrating weapon control systems, general CCIS and tactical communication. All these services are provided by the communication area system TADKOM consisting of a nodal trunk part and a mobile radio part. The concept laid down for TADKOM is based on the idea of a unified system with decentralized net-control and where voice and data are integrated into one system. This paper will present the mobil radio part of TADKOM and concentrate on what is identified as the most critical design issues.

1 INTRODUCTION

Tactical communication shall support the operational units in the field and must therefore reflect the strategy of the forces. A flexible threat reaction demands very mobile units which may be spread over a large geographic area. Placement and reconfigurations of communication units should not delay or limit the manouvrability of the forces to be served. If the forces shall operate under a centralized management and at the same time retain their mobility, this will put heavy demands on the communication system. The demands will be in the form of security, survivability and protection against electronic warfare.

The increasing use of mobile and data-supported units will lead to an increased use of electronic equipment on the battlefield and increased operational dependance on radio communication. The increased use of radiocommunication will in turn lead to an increased physical and electronic threat against these radiosystems. To withstand this threat an extensive use of autonomous communication systems being protected against electronic countermeasures are required.

The Norwegian army has taken a very close look at the advantages in integrating weapon control systems, general CCIS and tactical communication. The integration is resulting from the wish to see the communication demands for existing and future CCIS systems closely connected to tactical communication which anyway must be established within the brigade and division areas. The integration also reflects a wish to optimize the CCIS services by providing a communication system which can be given high efficiency, good coverage and with simple access to a large number of users spread around in the brigade area.

Both Norwegian and international user inquiries have revealed an increasing need for data services. There are two major reasons for this:

- the need to economize with a scarce frequency resource. The frequency use can be reduced by orders of magnitude if voice

is replaced by data. Userwise quantifying and describing kind of messages of objective nature are well suited for data messages

- a large part of messages exchanged in CCIS and communication systems are generated and terminated in some form of data hardware.

However the same inquiries also show that the need for the subjective form of voice communication will be needed for a long time in the future. It is obvious advantages both of technical and economical nature in integrating these services in one communication system.

Early in the 70's, NDRE with support from the Army, carried out study regarding a tactical communication system for the Army post 1980. The study outlined a communication concept which had a number of interesting features regarding mobility, distribution and capacity. The study was carried further in the Army's own organisations and in the Norwegian industry and resulted in the tactical area system TADKOM.

A simplified outline of the system is shown in Figure 1. TADKOM is based on digital modulation which offers voice and line switched or packet switched datasevices. TADKOM makes up the backbone in a communication system for the field army at brigade and division level. TADKOM and its different components will as far as possible and as long as it is cost-effective also serve the subunits within a brigade and division.

The trunk system is based on digital switched connected by line of sight radio relay circuitry. Between the switches the traffic is routed so that it is possible to obtain a minimum of blocking of messages. This concept also assures good survivability in the case of physical or electronic dropout of switches, or radio relays at one or more nodes.

Already at an early stage in the development of TADKOM, it became obvious that a number of users would require mobile radio access to the sytem. In 1984/85 several user related studies were carried out, and the Army initiated an activity to clarify the possibilities for harmonizing the concept for the mobile radio access and the user requirements emerging from the studies. The Army now expected that the mobile radio access to TADKOM would be used as:

- mobile access for mobile subscribers in the area system TADKOM. As subscribers, one is here thinking of the traditional command and control functions with voice and data requirements as well as firecontrolsystems with high demands wrt reliability and capacity of data transmissions

- as replacement for conventional combat net radios, especially for users which do have or will develope a need for data transmission.

The concept laid down for TADKOM is based on the idea of a unified system where voice and data are integrated into one system, and where fire control and future CCIS are seen as part of the tactical communication system. The major demands on the mobile radio access system are:

Considerable resistance to Electronic Warfare
Integrated Voice/Data facilities
Decentralized net-control (Autonomy)
Packet switching of data traffic

The bitrate for datatransmission is 2.4 kbit/sec., which means that we have a very limited capacity on the radiochannel. The overall network topology is therefore divided into subnetworks, each with a preassigned frequency within the VHF band. Hence the traffic loads on each subnetwork is at a level so that the throughput/delay characteristics meet the capacity requirements. This subnetwork strategy makes it possible to allocate users with related application traffic to one dedicated frequency.

Each of the packet radio subnets (PR-subnets) are connected to the trunk part of the tactical communication area network TADKOM through a radio access point (RAX). The TADKOM trunk network must therefore have a geographical structure that covers most of the brigade area. As shown in Figure 2 we see that each of the PR-subnetworks cover a certain dedicated area of the brigade, and in connection with the trunk network all the PR-subnetworks will together give a complete coverage of the brigade area. It is important to note that many of these subnetworks will geographically overlap since the generated traffic might require more capacity than one subnetwork can provide in the same area.

All nodes are allocated in a specified subnetwork depending on their application interests which will reduce the need for inter subnetwork communication (communication between subnetworks).

In performing inter subnetwork communication the RAX is responsible for finding a route to the destination address. The RAX must therefore have a global routing capability, see Figure 3. This Figure illustrates the relaying function between two subnetworks which are connected to the same RAX. This relaying will also be possible when the two subnetworks are connected to different RAX'es.

This paper is going to discuss three topics of the packet radio network:

- the first chapter presents the subnetwork services. An important design objective is to be able to connect a standard X.25 terminal to the network. Some problems of using X.25 in inherent connectionless type of application have been identified. The necessary changes in X.25 to circumvent these problems are highlighted in this chapter

- the second chapter introduces the network functions which is needed for packet forwarding within a network. Some details regarding the routing table structure and the distribution of routing information is presented

- the third chapter discusses the medium access protocol in some detail. A special emphasis on the capture effect is made. The channel capacity is evaluated based on simulations done for the Carrier Sense Multiple Access (CSMA) protocol.

2 SUBNETWORK SERVICES

A major design objective for the mobile radio system is to make possible an attachment of standard X.25 terminals, Figure 4. Even

inherent connectionless type of applications, such as e.g. radar/weapon control systems, shall apply X.25. Problems related to the use of X.25 in connection with weapon control systems in a narrow-band PR-network have been identified. To circumvent these problems, some deviations from the X.25 are made. These deviations consist in making restriction in the way a Data Terminal Equipment (DTE) may use the "X.25 Fast Select with Restriction on Response" and on the Data Circuit-Terminating Equipment (DCE) operation. The recasted service is named Reduced X.25 Fast Select with Restriction on Response (Reduced X.25 FS w/RR).

2.1 Reduced X.25 FS w/RR

The reduced X.25 FS w/RR allows a call request packet to contain a call user data field up to 128 octets. This call user data field is transferred to the called DTE by the intra network layer protocols without end-to-end (DCE-to-DCE) control. The call user data may be lost or duplicated, and a sequence of X.25 FS w/RR with call user data may be received out-of- sequence; all without notification to the DTEs. After a time L the DCE issues an X.25 clear indication packet containing no user data and the DTE shall respond with an X.25 DTE clear confirmation. Figure 5 to 7 shows the time-sequence diagrams for the Reduced X.25 FS w/RR. The receipt of an X.25 clear indication FS w/RR shall only be interpreted to have local significance i.e. the call user data may or may not be delivered to the called DTE.

When a DTE receives an X.25 incoming call packet with FS w/RR it shall immediately issue an X.25 disconnect request on the same logical channel number. This packet will be stopped at the local DCE and not conveyed to the calling DTE by the intra network layer protocols.

In summary, the reduced X.25 FS w/RR has the following restrictions compared with the CCITT/X.25 FS w/RR:

- the receipt of the clear indication has only local significance

- a called DTE may never include called user data in the clear request packet

2.2 Enhancements to X.25 (1984)

Certain facilities not specified by CCITT are required to fulfil military requirements. The non-standard facilities have been specified such that they place no constraints on DTEs not making use of the facilities. Some services (e.g. fixed priority) can be agreed for a period of time. In such cases the services do not require any non-standard call handling. The following non-standard services are provided:

- Precedence and Pre-emption

- Maximum Lifetime

- Semi-Broadcast

Precedence and Pre-emption

Priority

Priority is an essential service in the PR-network, and all traffic is to be marked with priority. There are 4 levels of priority (0 - 3), zero indicating the lowest priority. The priority mechanism is used in both call setup and traffic handling. Call attempts with high priority are processed before call attempts with lower priority. If there are no available channels for setting up a logical connection, an existing connection with the lowest priority is disconnected, provided that a connection with lower priority than the new call exist. Both subscribers involved are informed about the reason for the disconnection. This is done in the Clearing Cause and the Diagnostic code fields.

Selection and Indication of priority

As an optional user facility it is possible to select priority for virtual calls. A maximum limit of priority must be agreed upon in advance. From then on the selection of priority occurs on a per call basis using the service field in the X.25 call request packet.

Maximum Lifetime

As an optional user facility it is possible to select lifetime on a per call basis. The lifetime denotes the maximum time a packet may live in the network. It is possible to set the maximum lifetime to a maximum of 60 seconds with a resolution of 200 ms. If the DTE does not set a lifetime value the network will add a default value agreed upon in advance (i.e. at the subscription time).

To be able to provide X.25 VCs without corruption, every packet must be enforced a maximum lifetime at the intra network level. By allowing a DTE to select this value on a per call basis (or per "data packet" basis in conjunction with Reduced X.25 FS w/RR), network capacity is saved by discarding (i.e. no more store-and-forward operations are performed) packets that are too old to be usable for the application (DTE). Further, by including the remaining lifetime in an X.25 incoming call packet, DTEs have a mechanism to measure the network transit delay, which is needed by some applications, e.g. such as radar/weapon control systems.

Semi-Broadcast

In a PR-network where the network topology constitutes a complete graph (i.e. every pair of nodes is adjacent) a broadcast facility may be implemented without the need to introduce additional network functions. Generally, the network topology does not constitute a complete graph and the broadcast protocol needed in such a case does not only introduce additional complexity, but also uses too much bandwidth in a narrow-band PR-network. For these reasons only a semi-broadcast facility (i.e. a packet transmitted on the radio channel is only received by nodes one hop away) is implemented.

Packets transmitted as semi-broadcast packets are conveyed by means of the Reduced FS w/RR at the DTE/DCE interface (Semi-

broadcast can not be used in case of standard X.25 VCs!). The semi-broadcast facility is requested by setting a dedicated called DTE address in the X.25 call request packet. A packet conveyed by X.25 FS w/RR is identified as semi-broadcast by the special called DTE address value in the X.25 incoming call packet. The calling DTE address field shall, as usual, contain the address of the DTE that issued the packet.

At the intra network level no acknowledgement/retransmission procedure is applied on semi-broadcast packets.

3 A DISTRIBUTED ROUTING ALGORITHM

The global network topology has a hierarchical routing strategy with two levels. The lowest level is the local distributed routing within the scope of one single PR-subnetwork. The highest level is the global routing algorithm which is necessary to perform communication between subnetworks.

The routing strategy presented in this paper will only discuss the routing algorithm which handles the intra network communication (the communication within a subnet-work).

Figure 8 shows 7 nodes and their connectivity. Each node has an local address which is unique within the subnetwork. The network communication is based on packet switching which means that all messages are transmitted as one or several packets depending on the length of the message. All packets must have address information in the PCI (Protocol Control Information) field which specifies the destination address and the address of the next hop on the route. Hence, one of the advantages of packet switching is that all packets are individually routed through the network. Once a packet has been transmitted from a node, the same node is free to be used for relaying by other nodes. This saves a lot of channel capacity and results in a greater flexibility than circuit switching.

To get from the source address A to the destination address G there exist three route alternatives as shown in Figure 8. To determine the best route alternative it is necessary to know the link quality and the number of radio hops between the source and the destination nodes. The establishment of routing information and the selection of the most optimum path between two nodes are two of the important functions in a distributed routing algorithm.

The fact that node A makes all the decisions in the route selection procedure is the main philosophy of the distributed routing strategy. Node A must have all routing information necessary in its own routing tables to be able to make the best route selection.

3.1 Address assignment

All nodes in the network have a unique global address which is preassigned (TADKOM address). This address would use too much PCI space and contains redundant address information for subnetwork (local) communication. This suggests that a mapping from a global to a local subnetwork address is necessary. The length of the local address which is used in the routing tables is important for the dimensions of these tables and the PROP (Packet Radio Organization Packets) packets that distribute the address information.

The global subscriber address consist of a 4 digit TADKOM number (2 bytes long) . The subscriber address is unique within its own division. However, this address is not used directly in the forwarding algorithm when finding the next hop address from the routing table. The forwarding within a subnetwork require only a local address which is unique for that particular subnetwork. The data element used for local addressing is called a node number which is one byte long. The 7 LSB's of the node number is the local address and the MSB makes it possible to distinguish between a management packet and an application packet.

The size of the node number means that there are 127 local addresses available in a subnetwork. Each node must have a table that contains the mapping between the global subscriber address and the local node address. The mapping is performed during the establishment procedure and is valid for a node's lifetime in the network. The mapping of each subscriber address to the local address must be distributed to all nodes in the subnetwork. For further details, see the section on distribution of routing information.

Figure 9 shows how the global and local addresses are organized in the packet header. Both the source and the destination end addresses are global subscriber addresses of two bytes each. This is necessary in the case where the destination node is deployed in an other subnetwork. The RAX must know the global subscriber address to be able to forward the packet to its final destination.

The link source and the link destination fields in Figure 9 are used for local forwarding purposes. These fields contain local addresses which is specified link by link. The link destination address is the next hop on the route towards the final destination. This address as well as the link source address are therefore going to change as the packet traverses the route.

Figure 10 shows how the mapping of the three subscriber end addresses are mapped into the local node addresses. A packet from node D to F will have a destination end address End-C. The source node D must fetch the local node address corresponding to End-C from its mapping table and then find the link destination address in its routing table, which in this case will be node E. The same procedure must be performed once more when the packet reaches node E to establish the correct address fields in the packet.

The signalling in the establishment procedure, which is necessary for the address assignment, is to be determined.

3.2 The management functions of an established subnetwork

The nature of the application traffic in our PR-subnetwork will in general have a burstly characteristics. High priority application traffic requiring the full capacity of the network, will in general only last a few minutes. This means that in between the heavy traffic loads there are long time intervals which are available for maintaining the network.

3.2.1 Routing table structure

The general routing updating procedure shall ideally develop a complete routing table for each node in the network. This table will only hold addresses which are local to the subnetwork. When a

node transmits a packet with a global destination address, it must request the RAX to forward the packet to the final destination.

One of the important functions in the routing algorithm is to select the most optimum route from the source node to the destination node. This selection is made on the basis of the information contained in the routing table. Each route has its own set of data elements that go into the route selection algorithm. This section will discuss all of these elements in detail. The discussion on the route selection algorithm is included in a later section.

A route with address information and other radio link data constitutes one entry in the routing table. The addresses and the radio link data are the elements that specifies one entry.

3.2.2 Local subnetwork addresses

The section on address assignment discussed the difference of local and global addresses. All addresses in the routing table are local node addresses so that a mapping must take place before these addresses have any meaning.

Each entry in the routing table consists of two local addresses. These addresses are the destination address and the next hop address on the route. A source address is not necessary in the table since it is the same as the owner of the table for all entries.

Figure 11 shows a subnetwork and a routing table representing the node A. The first two elements in each entry are the end destination address and the next hop address. When node A wants to send a packet to node D as the end destination address, the algorithm looks up the entry that has this end address. The next hop address from this entry is node B, which will look in its own tables and get a new next hop address. This will bring the packet closer to its destination.

The source node A does not need to know how the next hop address, node B, forwards the packet to the final destination. When node A receives the PROP packets during the routing updating intervals, it will get the information that node B has a route to node D as the final destination.

3.2.3 Global addresses

Destinations that have global subscriber addresses may only be reached with the assistance of a RAX node. The source node does not have any routing information about a destination node which is deployed in another subnetwork. The routing algorithm must in this case be able to identify that the destination address is global, and send the packet to the RAX for forwarding.

3.2.4 The link factor

From the network topology in Figure 11, we see that some destination addresses are reachable by more than one route alternative. To select the most optimum route alternative it is necessary to collect data about each route between the source and destination nodes. The link factor is one of the elements which is used in the route selection algorithm.

In a general terminology the link factor is a measure of the bit error rate on a radio link. However, the introduction of FEC (Forward Error Correction Codes), will result in only two states of a link. This means that the packet is either received perfectly or the packet may not be retrieved at all.

Even if the packet is received perfectly on more than one radio link, it is possible to give them a different rating. This rating is dependent on the signal to noise ratio on the link as shown in Figure 12. Hence, by this way of rating the link, it is possible to see how resistant each link are to external disturbances.

The link factor may vary among the three values from 10, 20 and 30 dB margin to the noise level which corresponds to the link factors of 1, 2 and 3 respectively. Without any disturbances there is not going to be any significant difference in performance between links of link factors 1 and 3. However, during jamming or other interfering activities, it is clear that a link with factor 3 is the best choice.

3.2.5 Worst Link Factor (WLF)

A multihop route may have link factors that vary from the first to the last hop on the route. It is obvious that the throughput from the source node to the destination node is greatly dependent on the weakest link on that route. The easiest way of avoiding a congestion on a weak link is simply to avoid the route if there are other alternatives. WLF (worst link factor) is therefore an important measure of telling how likely a route is to get congested at some point.

3.2.6 Average Link Factor (ALF)

WLF does not give any information about other links on the route than the worst link. To be able to distinguish between two routes that have the same WLF it is necessary to include an ALF (average link factor). This element is just the average of all link factors on one route from the source node to the destination node.

3.2.7 Radio Hop Count

The number of radio hops is a parameter that goes into the route selection algorithm. The section on route selection will discuss this algorithm in more detail.

3.2.8 Next hop address in voice/data mode

In general we have a homogeneous set of nodes in the PR-subnetwork which are all capable of relaying packets to its destination addresses. However, in our application the nodes must be able to handle both voice and data traffic. Since the nodes that wish to use the voice channel must change the operating frequency, they make themselves unavailable as relay nodes for data traffic.

It is possible for a node to detect if one of its neighbors has switched over to voice mode by listening to the signalling, which is necessary when establishing a voice channel. This signalling must be performed on the data channel. Once a node has detected a neighbor in voice mode, it must be marked as such in the routing tables.

The routing algorithm will always check the voice/data element in

the table, to see if the next hop address is busy on a different operating frequency (voice mode).

Figure 11 shows that node F has switched to a voice channel to talk with node G. Node F will therefore not function as a relay node on the route to the destination address H from the source address A.

3.2.9 Silent nodes

There are a few nodes, that are only allowed to transmit application traffic under certain circumstances. These nodes are not permitted to broadcast PROP packets to maintain routing tables.

During the establishment procedure the silent node must notify the assisting node about its type. The silent node address is then marked as such in the routing table. An entry which has a next hop address marked as a silent node must not be used under normal circumstances.

3.2.1 Missing the link Response (MLR)

The link layer will retransmit the packet several times to try to reach its receiving end on a link. The network layer then gets notified when a packet does not succeed in reaching the other end of a link. Each time the link between the source node and the next hop node malfunction, a MLR count is incremented.

A maximum count is preliminary set to 3 MLR's within a time window (the length of the time window is to be determined). When an entry reaches a maximum count it will be removed from the routing table. This procedure is included to prevent unnecessary deletions of entries from the table. In a network with a changing topology there may be nodes that only temporarily will loose their link connectivity.

3.2.11 Alternative routes listed in the table

The routing table may contain several, up to three, different routes from source to destination address. The route selection algorithm will, based on the route elements discussed above, make a prioritized list of the available routes. How the preferred route is selected is discussed in the chapter on route selection algorithms.

3.3 Distribution of routing information

The general routing algorithm is based on distributing routing information through the network. Each node will build up a table with all local addresses in the network based on the information received in the PROP packets.

3.3.1 The PROP packet layout

Each PROP packet contains all the primary routes from the routing table. Any second and third choice route alternatives are not included to limit the length of the PROP packet. The next hop address field in each entry is redundant, since this address is equal to the TSA (terminal source address) of the PROP packet. Figure 13 shows how the neighbors to node A updates the next hop address by receiving PROP packets.

Node X is new in the network and receives four new entries to include in its routing table. We note that the next hop address is updated from the TSA field in the PROP packet. (Only the address elements are considered in this example).

Each entry (primary route) in the PROP packet need to include the link elements, ALF, WLF and RH, that specifies the quality of the route from source to destination. The receiver of the PROP packet must add the values for the new link to each route. As in Figure 13, node X must include the link factor between itself and node A, when calculating WLF and ALF for the route from X to D.

The voice/data channel information bit is not necessary in the PROP packets since the receiver of the PROP packet will be two hops away from the node that this information concerns. Every node must determine its own voice/data information bit by listening to the signalling procedure which is required to establish a voice channel. The default is that all nodes are in the data mode.

The element that specifies the MLR, is not included in the PROP packet for the same reasons as for the voice/data element. Each node must establish its own MLR statistics on all adjacent links.

The PROP packet must include the silent node element for each entry. This element always corresponds to the next hop address on the route. Any node transmitting a PROP packet therefore writes its own operating mode into the silent node element.

Each PROP packet must include the mapping between the global subscriber address and the local node address. Since a PROP packet is distributed by semi-broadcast the receiver knows that the packet has only travelled one radio hop. This means that the subscriber source address will always correspond to the local link source address. Hence, it is possible to fetch the mapping from the address field in the header of the PROP packet.

When more than one terminal is connected to the same physical node it is necessary with extended mapping. In this case there will be several subscriber addresses to one local node address. The extended mapping must also be distributed in the PROP packets. Since only the mapping between the subscriber address of the source terminal and the local link source address is included in the header, there must be additional extended mapping in the information field of the PROP packet. A separate subscriber address field is included in the PROP packet to hold the additional addresses which are mapped to the local node address. The first part of Figure 14 illustrates the elements included in the PROP packet for one entry. The second part shows how the different entries are packed into the PROP packet. Note the inclusion of the subscriber address field for extended mapping. This field is empty if there is only one terminal connected to the node. The length of the information field in such a packet depends on the number of primary routes established in the network.

It is desirable to keep the length of a PROP packet as short as possible to reduce the demand on the channel capacity when distributing the routing information. The preliminary studies shows that each entry or route requires two bytes to hold the information as discussed above. The maximum number of nodes in such a subnetwork is specified to be 50 nodes which means a maximum PROP packet length of 100 bytes plus the PCI information

field.

3.3.2 PROP distribution

The PROP packets are distributed using semi-broadcast which means that the packets are only transmitted to the neighboring nodes. These packets are not acknowledged by the neighbors upon reception, and hence they may not be retransmitted from the source. This means that it is possible to loose a PROP packet in the routing updating procedure.

3.3.3 Periodic distribution of PROP packets

The periodic distribution of PROP packets is significant for the general routing strategy to conserve bandwidth. All the changes in the routing table are not distributed until the next PROP interval and will propagate one hop further through the network for each new PROP interval. This prevents that any single change in the routing table triggers off a transmission of a PROP packet. (Event driven routing traffic is distributed in that way).

The PROP intervals are periodic with respect to a single node, but asynchronous with respect to all the other nodes in the network. The overall routing traffic for the whole network is thus spread out in time to avoid congestion of PROP packets.

The time between each PROP interval is to be determined by simulating the PROP traffic pattern with varying interval lengths. The demand on the data channel must then be adjusted to be within the available channel capacity.

3.3.4 Varying the PROP time interval

The available channel capacity may vary greatly depending on the current application. The establishment phase will in general be performed some time before there is any demand for application traffic in the network. This fact suggest that it is possible to speed up the propagation of routing information through the network by making the PROP time interval shorter.

It is therefore advisable to have two PROP time intervals. A short PROP time interval is used during (or immediately after) the establishment phase of the network. Then, after 5 to 10 minutes the network should be updated, and the normal PROP interval for maintaining the network is used. It is important to note that if any conflicts should occur, the general PROP traffic has a lower priority than most application traffic.

3.3.5 Loosing a PROP interval

As mentioned earlier, it is possible to loose a PROP interval from a neighbor because the semi-broadcast function does not retransmit if there is any errors on the link. However, it is predicted that there is not going to be any unacceptable inconsistencies in the routing tables when loosing an update interval.

When this happens during the first 5 to 10 minutes of the network history (establishment phase) the updating will take an interval time longer for that particular node. If it happens during regular maintenance of the network, the entries lost is contained in the PROP packet which is transmitted in the next PROP interval as well.

Hence loosing a PROP packet from one of the neighboring nodes will only lead to out-of-date-routes which have that particular neighbor as the next hop address. The route to the end address E in Figure 15 may be inconsistent for only one PROP interval.

3.4 Jamming

One of the advantages with a distributed routing strategy is the robustness against jamming and other external disturbances. However, there are several ways the electronic warfare may affect the network topology.

In the case where the enemy uses a stand off jammer, which will be at some distance from the communication activity, only parts off the network topology is going to be affected. Here it is possible to use one of the alternative routes if the primary route is blocked because of jamming. Because of the distributed routing strategy the source node of any route is not dependent on routing information from a master node in the network which may be temporarily blocked.

3.5 Forwarding algorithms

The distribution of routing information through the network results in developing tables that contains several route alternatives to the same destination end address. The same routing tables also contains data elements that makes it possible to evaluate each route separately and to select the most optimum route at all times.

All radio links are evaluated by link factors as discussed earlier in the paper. These link factors are in general obtained under stable conditions during the establishment phase of the network. The route selection algorithm is then going to make a list of routes with 1st, 2nd and 3rd priority routes. This prioritized list of routes is used as is if the conditions for transmission are kept unchanged since the list was made.

However, one or more nodes in the network may experience a temporary change in the signal to noise ratio which will lead to different link factors for these nodes. Under the new conditions the most optimum route might be the one of the previously rated 2nd or 3rd route choices.

3.5.1 Determination of the 1st priority route alternative

Given stable network conditions for transmission there is not going to be any difference in performance between routes with varying link factors as long as the value is equal to one or greater (see section on link factor). Hence, the route selection algorithm determines the 1st priority route on the basis on other throughput and delay considerations. Having the requirement of minimum link factor fulfilled, it is the route with the lowest number of radio hops which is selected as the 1st priority route.

Figure 16 shows two alternative routes from node A to node B. The route with only two radio hops has a lower link factor than the other, but the radio links are good enough for transmission under normal conditions. Hence, since the route with 2 radio hops is going to introduce smaller packet transmission delays and requires a smaller channel capacity, it will be the 1st priority route.

In the case where all the three route alternatives have the same number of radio hops, the selection has to be based on the link factors. When still assuming that the radio links on all routes fulfill the minimum requirement of link factors it is apparently that all three routes is going to perform equally well.

The selection is now made on the basis on how well the routes is going to perform if any external disturbances are introduced into the transmission environment. Since the link factor gives a direct value describing how robust each link is to external noise, it is quite easy to distinguish between the three routes.

The first element to examine in the table, is the WLF on each route. The route with the highest WLF must be selected as the 1st priority route. This is because the WLF element gives a value of the weakest link on any route. In general, it is assumed that the quality of a route is not to be rated higher than its worst link.

Figure 17 shows 3 alternative routes and their respective link factors. When examining the routing table it is clear that the last entry in the table has the highest WLF value and must be selected as the 1st priority route.

In the last case where all 3 routes have the same WLF value, the route selection must be determined by the value ALF. The route with the highest ALF is selected as the 1st priority route.

3.5.2 Determination of 2nd and 3rd route alternative

In the case where all 3 route alternatives have different number of radio hops it is just to rate the route with the next lowest number of radio hops as the 2nd priority route and so on.

In general, the same route selection algorithm is used to determine the 2nd priority route as for the 1st priority route as described above. The 3rd priority route is defined to be the most resistant route and must therefore be selected on the basis on the link factor rating. See the section on saving the most resistant route alternative.

Figure 17 gives an example on how the three routes are given their respective priorities based on the algorithm described above.

3.5.3 Route selection when experiencing external noise

The radio unit may detect the noise level at all times in the network. A sudden change in the noise level may lead to poor link factor ratings on various routes. Any route to be used for packet forwarding must fulfill the requirement of minimum link factor value.

Lets look at Figure 16 to see what happens if node A experiences a 10 dB rise in the noise level. This means that the first hop on the 1st priority route is going to be marginal with the noise level and will probably not perform as required. In this case the route selection algorithm must examine the detected signal-to-noise-ratio and select the route with a higher link factor rating.

Before the route selection algorithm can fetch the most optimum entry from the routing table, it must first check with the radio unit for any detection of external noise. If normal conditions are

present, it is just to fetch the predetermined optimum route. Otherwise the temporary change in signal to noise ratio has to be examined and included in the route selection algorithm to give the most optimum route.

3.5.4 Saving the most resistant route alternative

The discussion in the previous sections points out the importance of having a very resistant route that can be used during severe conditions. The entries in the routing table are selected with a special emphasis on a low number of radio hops. Hence, some of the routes with the highest priority may have a very poor resistance to external noise. Even worse is the case when all the three selected routes to a specific destination have poor link factors.

This situation is prevented since the third priority route is always selected on the criteria that it must be the most resistant route, i.e. the route with the highest link factors.

4 MEDIUM ACCESS PROTOCOL

In a subnetwork there are a number of communicating radio-nodes sharing a common (radio) channel, see Figure 8. The Radio-Access-Protocol is the mechanism that controls how the channel-capacity is shared between the nodes.

The system being developed must cover a wide range of applications. This means that the number of nodes and the traffic parameters will vary with each different subnet. The system must be flexible and robust. It is also required to be autonomous, i.e. not being dependent on a central node.

4.1 The CSMA-protocol

Based on these requirements , a carrier-sense-multiple-access (CSMA) protocol has been chosen. The CSMA-technique can be described as: A node has a packet to send, it first listens to the channel to see if anyone else is transmitting. If the channel is busy, the node waits until it becomes idle. When the station detects an idle channel, it transmits the packet.

There are various versions of the CSMA-protocol and the particular version we have chosen, is illustrated in Figure 18 and in Figure 19 (flowchart). Consider a node having a packet ready for transmission. It first wait a period of time called the "propagation delay", then a "random delay". During the time, the node is waiting, it is (concurrently) also listening to the channel. Should the node, during this waiting period, detect another node transmitting, it resets the waiting time and waits until the channel again becomes idle.

The priority delay is dependent on the priority of the packet to be sent. The packet with highest priority have no priority delay while packets with low priority have long priority delay. In this way, if the traffic load is heavy, it is possible to give important packets priority accessing the channel.

The "random delay" is a time delay drawn from a uniform distribution. This time is introduced to decrease the probability of having two nodes transmitting simultaneously.

When a node has waited a time equal to both the priority delay and

the random delay, and the channel is still idle, the node turn it's radio from receiving mode to transmitting mode. This turn-operation requires a certain amount of time. (The turn-time is at the moment 10 ms or less for the radio used).

In transmitting mode the radio may now start to transmit a packet. First the radio transmits a special pattern called "preamble". This preamble informs the receiving radio(s) that a data-packet will now arrive. The data packet consists of the protocol control information (PCI) and user-data. Figure 18 also show the packet received by another node.

The propagation delay, i.e. the time from the moment the signal leaves the transmitting antenna to it reaches the receiving node, is assumed to be zero compared to the turn time and the duration of the preamble.

The period from the time the node starts to turn it's radio from receiving to transmitting mode, to the time when the other nodes detects that it is transmitting, is called the "response delay":

Response Delay = Turn Time + Propagation Delay + Preamble

Within this period of time it is hence possible for other nodes to start a transmission, thus there is a finite probability that two or more nodes start to transmit simultaneously. Should this happen, the packets involved will collide, and hence they will be lost. To make sure that the packet being transmitted is correctly received by the other node(s), an acknowledge mechanism is used. A node that receives a packet correctly, reply to the transmitting node by sending an acknowledgement. If the transmitting node does not receive an acknowledgement within a certain period of time, it retransmits the packet.

However, to prevent a deadlock situation and to reduce the probability of collisions, each node applies a random delay interval before each transmission. E.g. consider the situation where one node is transmitting and two or more nodes are listening and waiting for the channel to become idle. The channel becomes idle and the listening nodes fight for their access to the channel. Each node then draw a random time within the "random delay" interval and hence wait this amount of time. This random waiting time reduce the probability for collisions.

The Response Delay divided by the Packet length, is called the factor "a". It is important to get this factor as small as possible for CSMA-protocols.

4.2 The capture effect

The particular radio used in our system is called CORA. (CORA is described in full in a separate paper by Terje Thorvaldsen). CORA is a direct sequence spread spectrum radio and one of its important properties, when considering access protocols, is the Capture Effect.

In our system, the Capture Effect can simply be described as the ability for a node, to receive one out of two or more packets that are transmitted simultaneously .

Looking at Figure 20 we can see two nodes A and B, both transmitting a packet to node C within the response delay interval. Assume that the packet from A arrives C just before the packet from B (a few milliseconds). Because of the Capture Effect, node C receives the packet from A without any interference from the packet from B. I.e. node C "captures" the first packet that arrives.

However, there are certain criteria that must be considered. The CORA radio is designed in such a way that the first signal is captured only if the strength of the first signal divided by the strength of the second signal is larger than -12dB. If the quotient is less than -12dB, both packets are lost.

This means that if node A and B use the same transmission power, the distance from A to C, using an R^4 path loss approximation, may be approximately twice the distance of B to C and still C will be able to capture (receive) the packet from A, if it reach C just before the packet from B.

4.3 Simulation results

There has previously been done a lot of research on access protocols based on the CSMA technique. At NDRE there has been a particular interest concerning the role the Capture Effect has on the CSMA-protocol.

We have modeled a scenario with 16 nodes placed in a 4x4 matrix. The distance between all neighbour nodes is 2 units. The scenario is simulated using 3 sets of radio-ranges, 3, 5 and 10 units. (See Figure 21).

Some system parameters:

Channel bit rate	2400 bits/s
Packet length	100 bytes
Acknowledge length	8 bytes
Preamble	2 bytes
Turn time	3 bytes
Priority delay	5 bytes
Random delay	random, within a sample-space of 118 bytes

The time taken from a node starts to send a packet, to the time it receives the acknowledge packet, assuming everything goes normal, is called one "roundtrip delay". It is found natural to use the round trip delay as a measure for the time-delay in a subnet. (Figure 22).

The data packets have a priority delay of 5 bytes and a random delay of about 1 roundtrip delay. The acknowledgements have first priority and no random delay, thus giving them prior access to the channel. This means that an acknowledgement is sent immediately after the reception of a data packet, and without any competion from any other node. The transmitting node will always allow enough time for the acknowledgement to be sent, before it eventually retransmits the packet.

4.3.1 Complete subnetwork

Figure 22 shows some results obtained after simulating a complete network, i.e. no hidden nodes, where the radio range is 10 units

and the distance between the outer nodes is 6 units. The top graph shows the channel throughput (S) versus the offered channel traffic (G). There are two throughput curves, one representing the case when using the capture effect and one with no capture.

The lower graph shows the avarage packet delay versus the offered channel traffic. The channel bit rate is 2400 bit/s and the outermost left axis show the round trip delay converted to seconds.

If we assume a perfect transmission, i.e. no collisions and no waiting delay for the channel to become idle, the delay will be one round trip delay. For comparisons, we need a reference value. Two round trip delays corresponds to a reasonable network-delay, and is hence chosen. Going from this point on the lower curve to the corresponding two points on the curves of the upper graph, we are able to read the given throughput of the net for this particular delay. It can be seen that with the capture effect the throughput is about 1000 bit/s, and without capture, the throughput is approximately 900 bit/s.

4.3.2 Subnetwork with hidden nodes

However, the normal situation for a subnet is that one or more nodes can not hear all the other nodes in the net. If we consider the same node-scenario, but with the radio-range reduced to 5 units, there will be a new situation where we get hidden nodes. Figure 24 shows the results obtained when simulating this situation. Using the same reference value, we only get a throughput of 600 bit/s using the capture effect, and with no capture it can be seen that the net quickly reaches congestion. This net-configureuration is regarded to be close to the worst case situation. If we decrease the radio-range to 3 units, the throughput will increase, since there may be independent packet transmissions between two outer nodes on one side and between two nodes on the other side. See Figure 25.

4.3.3 Varying the packet length

The length of the packets are also of great importance to optimize the throughput. A number of simulations have been carried out for a complete network, but with varying packet lengths. The curve in Figure 26 shows the throughput as a function of the packet length for a complete network. It can be seen that the capacity of the network reaches an asymptotic value, about 1300 bit/s, for large packet lengths. For short packet lengths the throughput falls to about 400-500 bit/s.

It is important to look a the more realistic case, where hidden nodes are present. Figure 27 shows this situation, and it can be seen that choosing a reasonable packet lenght and avoiding a too big delay, we may get a throughput of 600 bit/s. This may seem like a poor channel utilization. However there are many points to be borne in mind.

1) We want a very flexible system, the number of nodes are changing and the traffic parameters varies for each subscriber.

2) The net topology also varies with each subnet.

3) There is a demand for autonomy and resistivity. I.e., we want to avoid centralized solutions.

Taking these requirements into account, the CSMA-protocol is found to be very suitable.

5 CONCLUSION

The topics discussed in this paper have one major obstacle to circumvent. It is obvious that a data transmission rate of 2.4 kbit/sec. puts a large constraint on the management traffic needed to maintain the network.

In order to reduce the overhead on the radio channel and to fulfill military requirements, a few enhancements to the CCITT/X.25 subnetwork access protocol have been introduced. These enhancements resulted in a minor deviation from the CCITT/X.25 specification.

The general routing strategy has been specified to deal with the operational nature of the network. Because of the unpredictable transmission environment, it is decided to distribute the routing function to each node in the network. This means that each node makes its own decisions when selecting the route for packet forwarding.

A periodic distribution of routing information throughout the networks are carried out to control the information flow of management traffic.

The CSMA-protocol is used to meet the requirements of flexibility when unpredictable network topology and traffic demands are present.

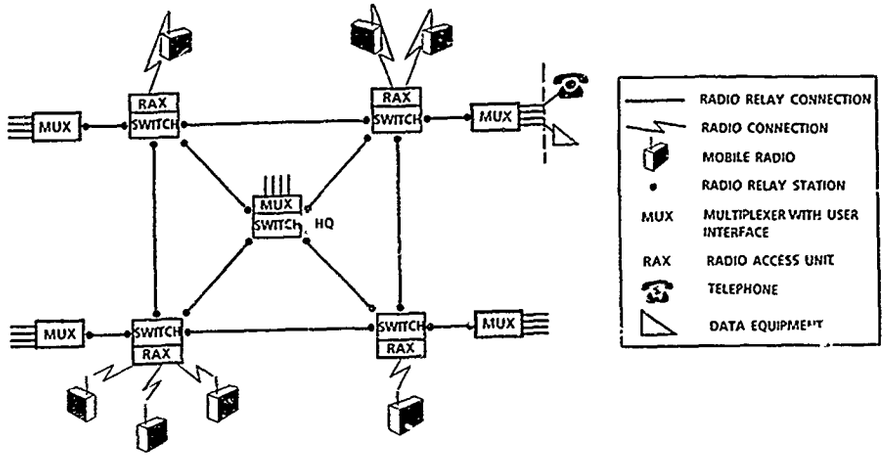

Fig. 1. TADKOM system overview.

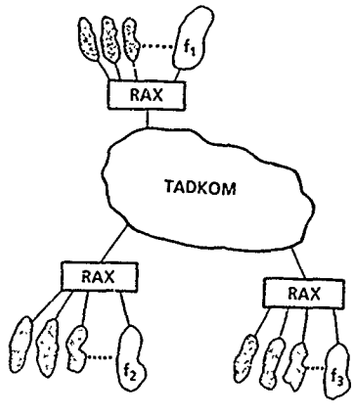

Fig. 2. The global network topology with TADKOM.

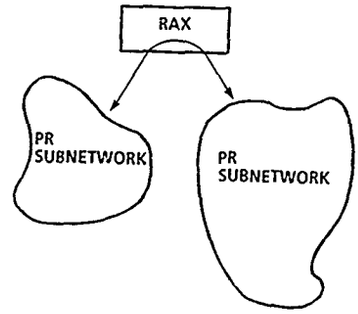

Fig. 3. RAX performs relaying between subnetworks.

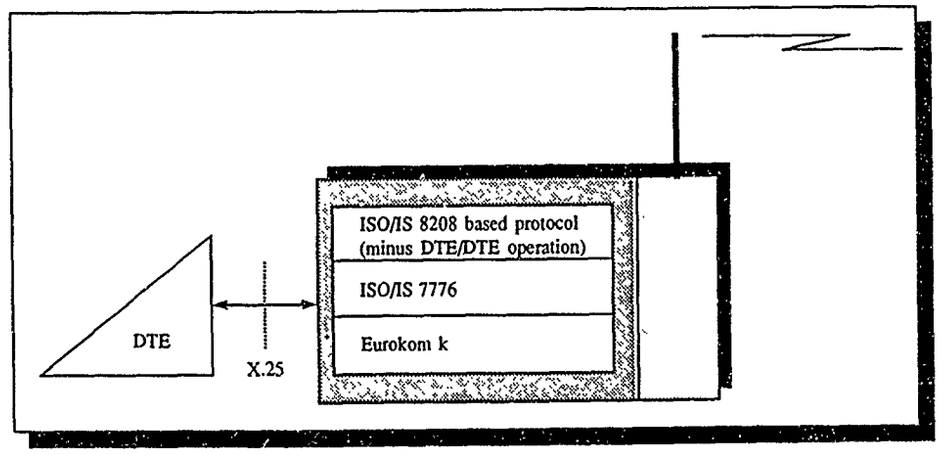

Fig. 4. DCE protocol profile.

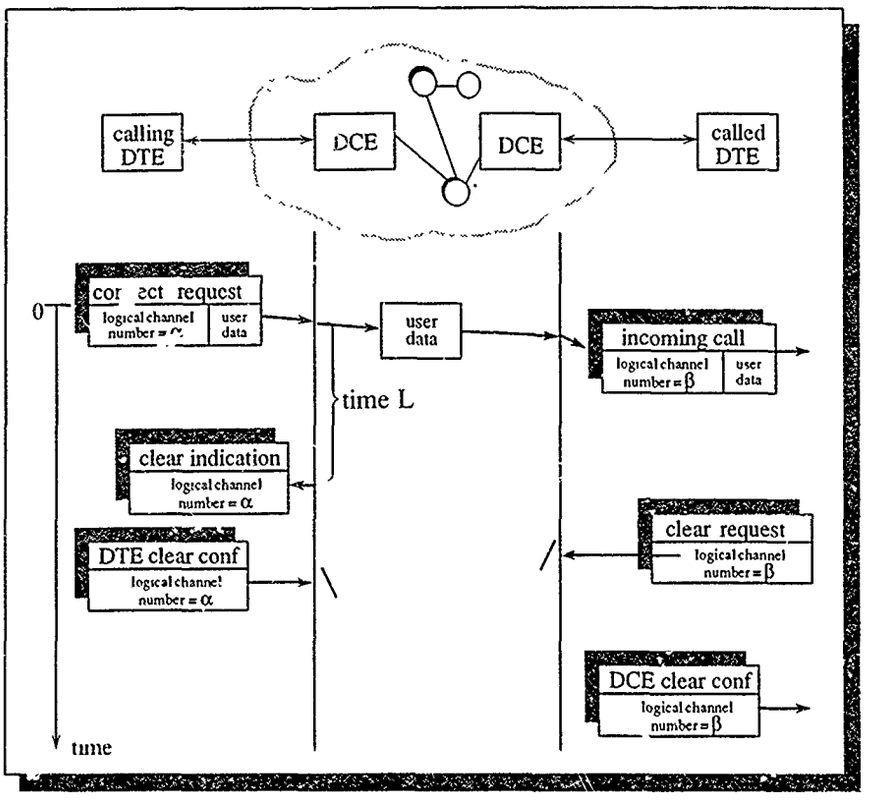

Fig 5 X.25 FS w/RR: successful delivery

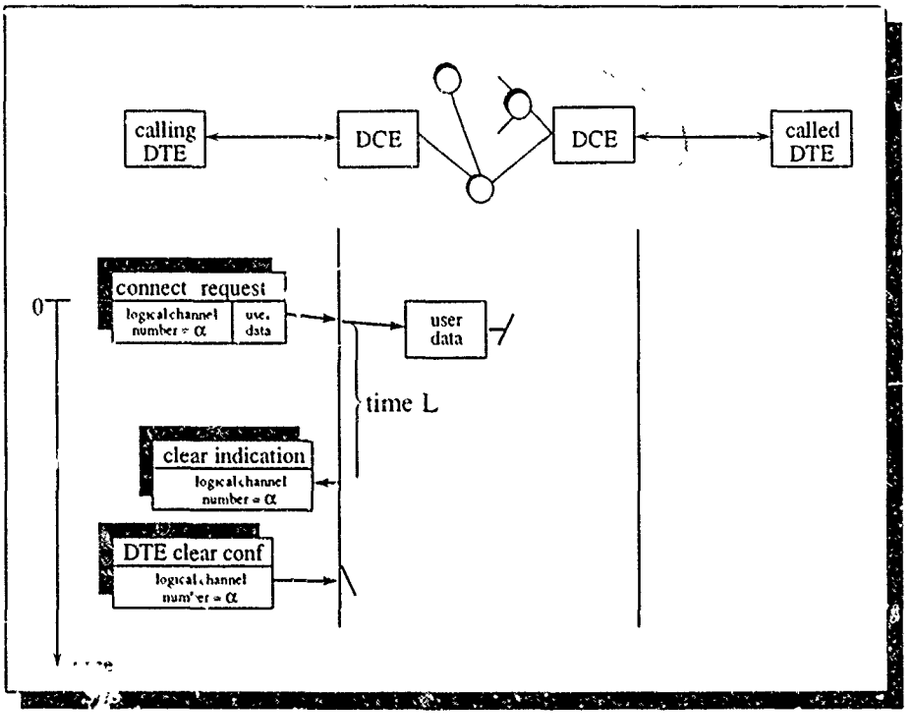

Fig 6 Reduced X.25 FS w/RR: successful delivery

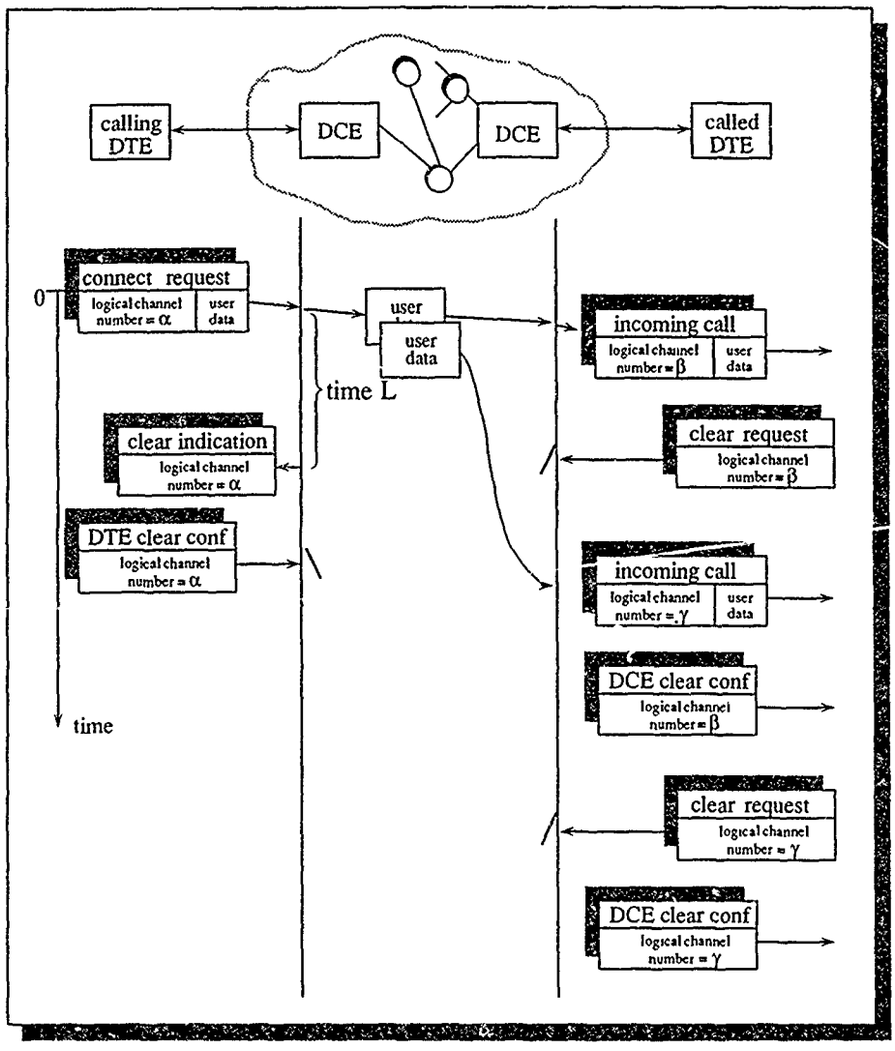

Figure 7 Reduced X.25 FS w/RR: unsuccessful delivery

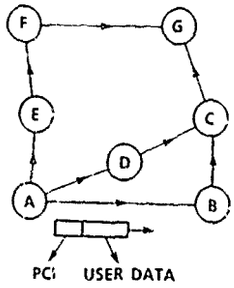

Fig. 8. Routing function within a single subnetwork.

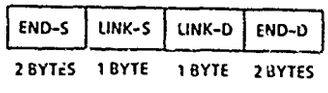

Fig. 9. Address layout in the packet header.

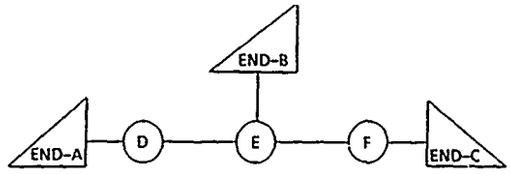

MAPPING TABLE

SUB SCRIBER ADD	LOCAL ADD
END-A	D
END-B	E
END-C	F

Fig. 10. Address mapping in a simple network.

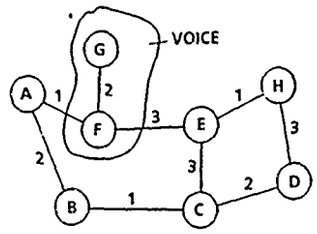

ROUTING TABLE NODE A

END	NEXT	WLF	ALF	RH	V/D	SILENT	MLR	ALT
H	F	1	1,7	3	V	NO	0	1
H	B	1	2	4	D	NO	1	2
E	F	1	2	2	V	NO	0	1
E	B	1	2	3	D	NO	2	2
D	F	1	2,3	4	V	NO	0	2
D	B	1	1,7	3	D	NO	0	1

Fig. 11. Routing table structure.

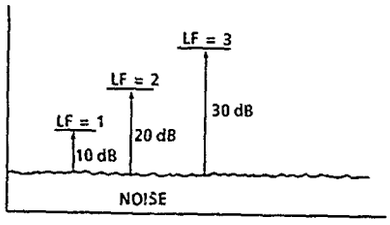

Fig. 12. Link factor.

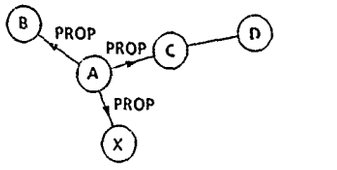

ROUTING TABLE A

END	NEXT	WLF	ALF
B	B	-	-
C	C	-	-
D	C	-	-

ROUTING TABLE X

END	NEXT	WLF	ALF
A	A	-	-
B	A	-	-
C	A	-	-
D	A	-	-

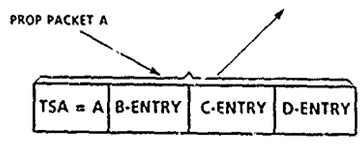

Fig. 13. Distribution of the next node address.

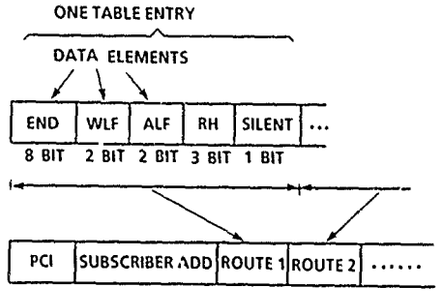

Fig. 14. PROP packet layout.

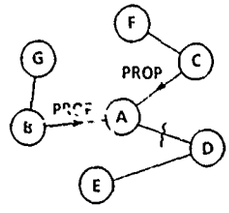

ROUTING TABLE NODE A

END	NEXT	WLF	ALF	
B	B	-	-	
C	C	-	-	
D	D	-	-	
G	B	-	-	
F	C	-	-	
E	D	-	-	OUT OF DATE

Fig. 15. Missing a PROP packet from a neighbor.

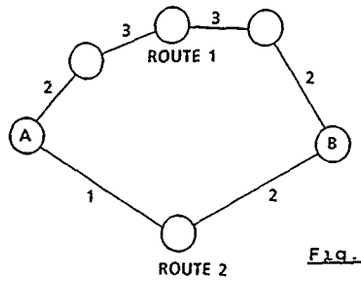

Fig. 16. Selection of 1st priority route.

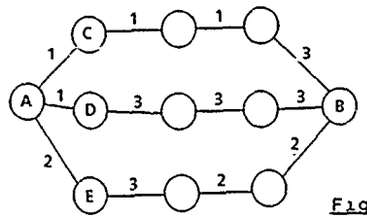

END	NEXT	WLF	ALF	RH	ALT
B	C	1	1,25	4	3
B	C	1	2,5	4	2
G	E	2	2,25	4	1

Fig. 17. Alternative routes with the same number of radio hops.

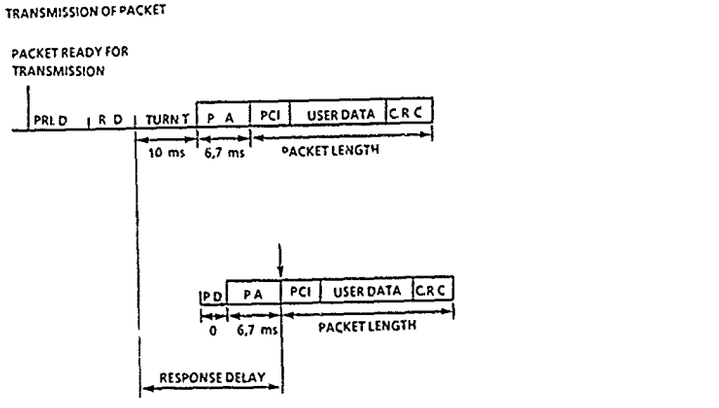

Fig. 18. Time sequence of packet transmission.

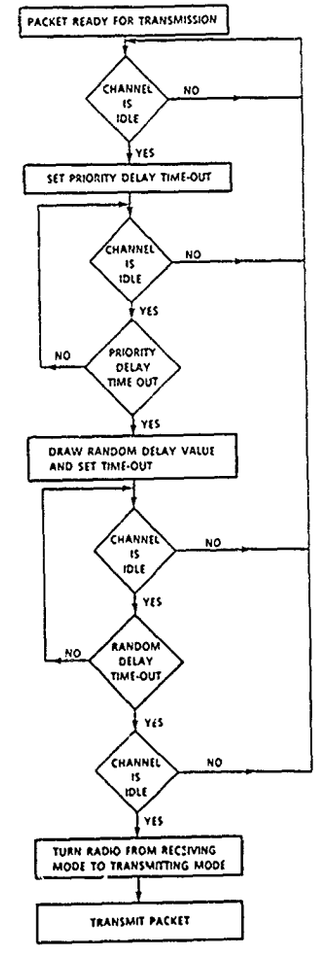

Fig. 19. Flowchart of the CSMA-protocol.

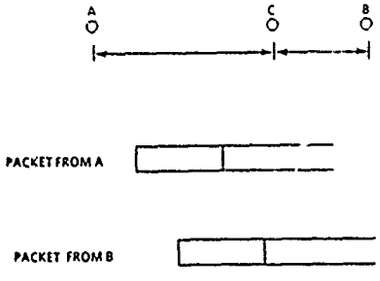

Fig. 20. The capture effect.

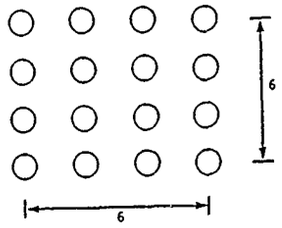

Fig. 21. The subnetwork topology.

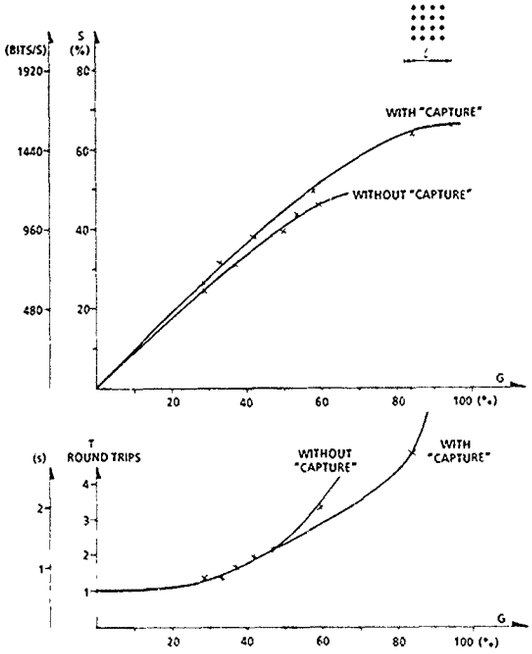

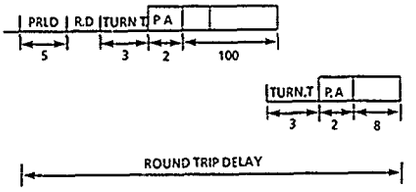

RANDOM TIME DRAWN FROM A UNIFORM DISTRIBUTION WITH SAMPLE-SPACE EQUAL TO 118

Fig. 22. The "roundtrip delay".

Fig. 23. Throughput and delay results for a complete network.

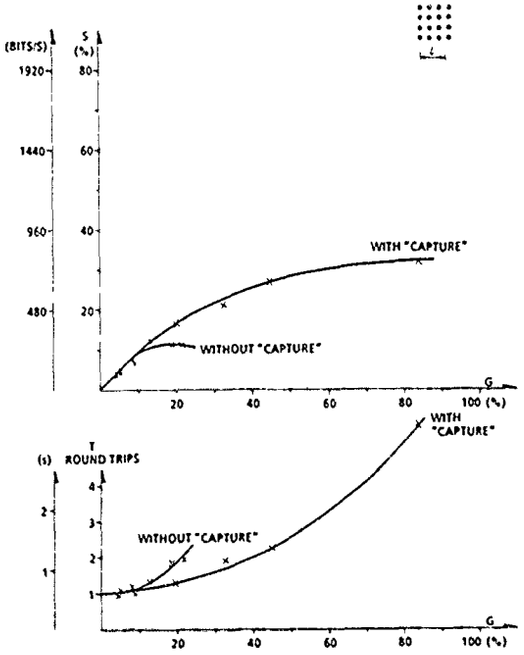

Fig. 24. Throughput and delay results for a network with hidden nodes. Range is 5 units.

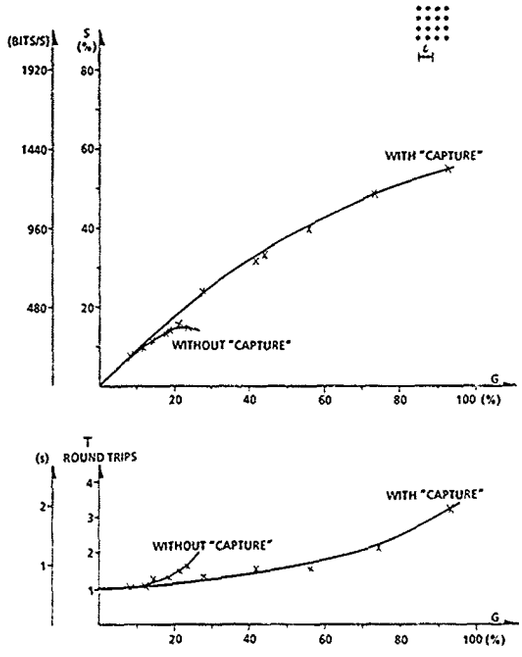

Fig. 25. Throughput and delay results for a network with hidden nodes. Range is 3 units.

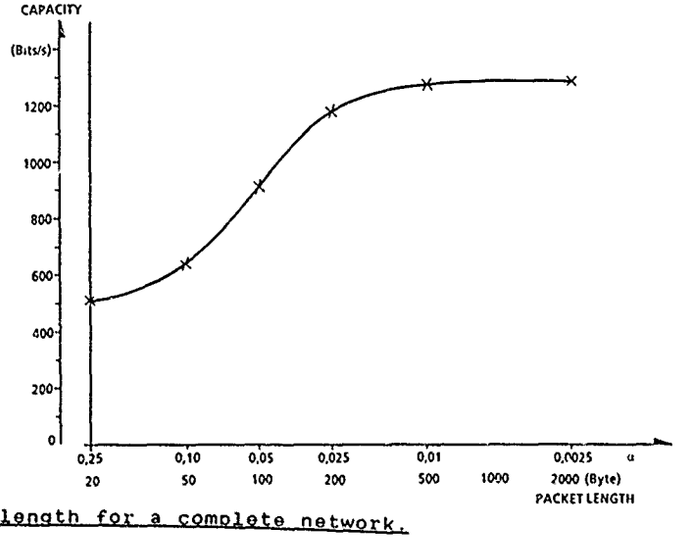

Fig. 26. Varying the packet length for a complete network.

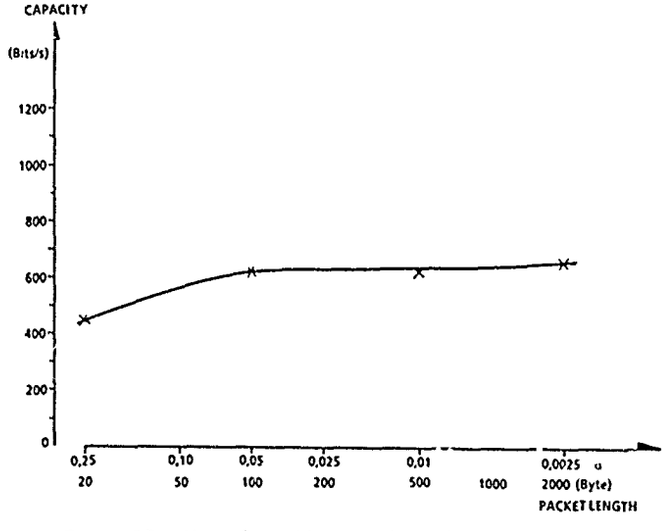

Fig. 27. Varying the packet length for a network with hidden nodes. Range is 5 units.

EXPERIMENTATION D'UN SYSTEME DE TRANSMISSION DE DONNEES PAR CANAL METORIQUE:

THEOREME

par:

Mr P. Sicila
Mr D. Sorais
Mr F. Barrier

THOMSON-CSF
66 rue de Fossé Blanc
92231 GENNEVILLIERS
FRANCE

1 - RESUME

La division Télécommunication de THOMSON-CSF a réalisé un système de transmission de données par canal météorique THEOREME, dont les études ont débuté en février 87. Le projet THEOREME-FF est décomposé en trois phases. La phase 1 est une liaison point à point à l'alternat entre deux stations distantes de 350 km, les phases 2 et 3 sont des liaisons par diffusion respectivement vers un véhicule et vers un avion.

Les expérimentations ont été réalisées pour plusieurs puissances (1 kW, 200W, 100W et 50W) en VHF et en fréquence fixe dans la gamme 40-43 MHz. La maquette a permis d'effectuer des tests mesurant l'ouverture et la fermeture du canal et les taux d'erreurs ainsi que des transmissions de messages.

Les débits moyens mesurés sont d'environ 100 à 185 caractères utiles/seconde avec des maxima pouvant atteindre 300 à 400 car/s.

2 - INTRODUCTION

Les études de système de transmission par rafales sur les météores (T.R.M.) ont commencé au début des années 50, lorsque plusieurs organismes officiels Américains et Canadiens (Central Radio Propagation Laboratory, Canadians. Défense Research Board,...) ont entrepris une série d'études et d'expérimentations en vue de déterminer le contexte d'emploi de ce mode de communication pour une distance moyenne ($\tilde{}$ 1000 km).

Des liaisons expérimentales ont été effectués par le Central Radio Laboratory sur une distance de 1200 km pour une fréquence de 50 MHz et une puissance de 30 kW sur une antenne losange de 20 dB/iso de gain.

Le Canadian Défence Research Board mit en place le premier réseau expérimental (Système JANET) au cours de l'année 1955 sur la liaison Toronto (Ontario) - Port Arhur (Ontario) -Edmenton (Alberta) - Yellow knife (Territoire du Nord Ouest) pour une fréquence de 40 et 50 MHz et une puissance de 500W sur un groupement de 4 antennes YAGI.

Le centre technique du SHAPE a réalisé en Europe pour le compte de l'OTAN des expérimentations sur le circuit LA CRAU (France) - LA HAYE (Hollande) avec le système COMET sur une distance de 1000 km environ dans les années 60 -70.

Par la suite, d'autres systèmes plus opérationnels tel que SNOTEL (à l'ouest des Etats-Unis) et AMBCS en Alaska pour le civil et FEBA pour les applications militaires ont été réalisés.

A la demande de l'Administration militaire Française, THOMSON-CSF a étudié et réalisé THEOREME-FF (Transmission HErtzienne par Ondes REfléchies sur trainées MEtéoriques en Fréquence-Fixe) dans le but principal de démonstration des possibilités d'utilisation en France de ce moyen de communication.

3 - PHYSIQUE DU CANAL

Le nombre de particules de masse supérieure au microgramme qui interceptent journellement l'orbite terrestre est en moyenne de 10^{11}. Ces météores créent, vers 80 à 120 km d'altitude, des cylindres ionisés de 10 à 20 km de longueur capables de diffracter une onde incidente. Les météores radioélectriquement utiles étant nécessairement tangents à des ellipsoïdes dont les foyers sont l'émetteur et le récepteur, les performances du canal sont fonction de la masse, de la vitesse et de la direction des météores. (Figures 1, 2).

Pour une période d'observation T, le canal météorique est partiellement décrit par les paramètres suivants :

- d_0 (en %) : durée d'ouverture du canal (pourcentage de temps pendant lequel le canal est ouvert).
- τ_m : durée de vie moyenne d'une traînée ionisée.
- δ_m : intervalle de temps moyen entre deux météores utiles.

Par définition, ces trois paramètres sont liés par la relation (1) :

$$(1) \qquad d_0 = \frac{\tau_m}{\tau_m + \delta_m}$$

4 - SIMULATION DU CANAL METEORIQUE

Une simulation du canal météorique permettant d'estimer ses performances a été réalisé afin de comparer les résultats de la simulation aux résultats des expérimentations.

4.1 - CALCUL DES PARAMETRES DU CANAL

Dans un premier temps on souhaite estimer le nombre moyen N de météores radio-électriquement exploitables durant la période d'observation T. Les mesures effectuées depuis trente ans tendent à montrer que le flux $\mathfrak{D}$ de météores de masses comprises entre m et m + dm suit une loi du type (2) . ([1], [2])

$$(2) \qquad \mathfrak{D}(m) \propto 1/m^{2\alpha} \qquad \alpha \simeq 1.2$$

La densité électronique q, définie comme étant le nombre d'électrons contenus dans un mètre de traînée ionisée, est proportionnelle à la masse du météore incident. ([2], [3]). A partir de ces données on peut exprimer le flux de météores de densité électronique supérieure à q_{min} :

$$(3) \qquad \Phi(q > q_{min}) \propto \frac{1}{q_{min}^{\alpha}}$$

Pour les traînées de météores dont la densité electronique q est inférieure 10^{14} el/m (météores dits "underdenses") l'expression du bilan de liaison peut se mettre sous la forme (4) (voir [1]) où Pro est la puissance maximale reçue et P_E la puissance fournie à l'antenne d'émission :

$$(4) \qquad \frac{P_{r_0}}{P_E} = \frac{W(P)\,\lambda^2\,q^2\,L^2\,G_E\,G_R}{R_E^2\,R_R^2}$$

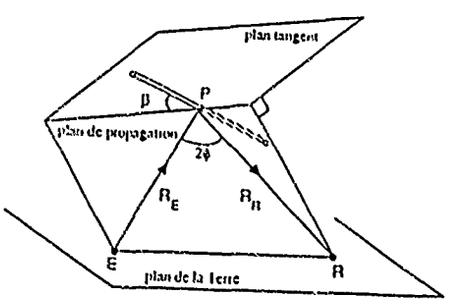

Figure 1

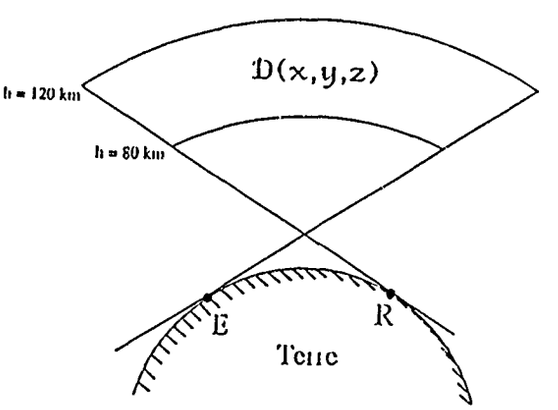

Figure 2

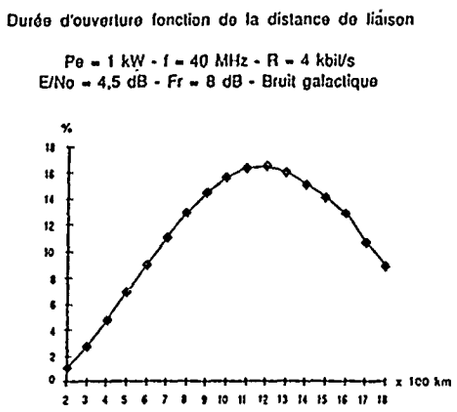

Figure 3

Avec :

G_E, G_R : Gains des antennes d'émission et de réception dans la direction du point brillant P.

L : Longueur de la zone de Fresnel.

λ : Longueur d'onde.

W (P) : Fonction dépendant de l'altitude du point P, de la position relative des points E, R, P ainsi que de la direction de la traînée.

La valeur q_{min} de la densité électronique minimale nécessaire pour que le signal transmis soit détecté est fonction de la puissance rayonnée dans la direction du point P et de la puissance Prmin minimale nécessaire à l'entrée de la chaîne de réception. D'après (4) on obtient :

$$(5) \qquad P_{rmin} = P_E \, q_{min}^2 \, \frac{\lambda^2 L^2 G_E G_R}{R_E^2 R_R^2} \, W(P)$$

A partir de (3) et (5) on peut donc écrire le flux de météores utiles sous la forme :

$$(6) \qquad \Phi (q > q_{min}) \propto \left[\frac{P_E G_E G_R \lambda^2 L^2 W(P)}{R_E^2 R_R^2 P_{rmin}} \right]^{\frac{\alpha}{2}}$$

Pour une période d'observation suffisamment longue, on cherche le nombre de météores radio-électriquement exploitables dans la totalité du domaine D (x, y, z). (voir Fig. 2). La contribution N(P). dV du volume élémentaire dV à l'activité météorique totale est obtenue en prenant en compte le nombre moyen de longueurs de la zone de Fresnel (proportionnel à 1/L) contenues dans le volume dV. L'intégration dans le domaine D (x, y, z) est réduite à une

intégration sur une surface située à l'altitude moyenne h_m d'occurence des météores. Compte tenu de ces éléments on peut calculer la valeur moyenne $\overline{N}$ du nombre de météores exploités durant la période T ($\overline{N}$ est égal à $1/\delta m$) :

$$(7)\quad \overline{N} \propto \left(\frac{P_E}{P_{rmin}}\right)^{\frac{\alpha}{2}} \lambda^{\alpha} \int_{\mathcal{D}(x,y,h_m)} \left[\frac{G_E(P)\, G_R(P)\, W(P)}{R_E^2 R_R^2}\right]^{\frac{\alpha}{2}} dx\, dy$$

L'intégration est effectuée en supposant que la distribution des météores est uniforme en position et en direction. Il résulte de cette hypothèse que la probabilité de présence d'un météore est la même, d'une part, quelque soit l'emplacement du point brillant P dans le volume D (x, y, z) (voir Fig. 2), et d'autre part, quelque soit l'angle entre la traînée et le plan de propagation. On ne prend donc pas en compte la distribution fine des météores qui, pour une liaison donnée, est liée aux mouvements relatifs des météores et de la terre dans le système solaire. Par ailleurs la modification de la polarisation de l'onde transmise (rotation Faraday et diffusion sur la traînée ionisée) n'est pas traitée dans cette simulation.

En prenant en compte la durée moyenne pendant laquelle une traînée est radio-électriquement exploitable le calcul de la durée d'ouverture du canal do est obtenue par la même méthode de calcul. La durée de vie moyenne m est ensuite obtenue par l'expression (1).

4.2 - RESULTATS NUMERIQUES OBTENUS

La simulation précédemment décrite permet d'obtenir des grandeurs relatives proportionnelles aux résultats réels. Les constantes de proportionnalité ont été déterminées en corrèlant les résultats de notre simulation à ceux de l'expérimentation COMET ([3], [4], [5]) de façon à obtenir des moyennes annuelles.

La variation avec la distance de la durée d'ouverture moyenne du canal do (cf figure 3) a été calculée pour des liaisons réalisées avec deux antennes Yagi de cinq éléments (G_E = G_R = 10 dBi) placées à des hauteurs optimales au-dessus du sol. Les résultats obtenus pour P_E = 1 KW et f = 40 MHz, sont semblables à ceux fournis par Brown [6], qui a réalisé une simulation qui prend en compte la distribution des météores en fonction du temps et du lieu géographique.

On a également calculé la durée d'ouverture du canal pour les liaisons entre points fixes effectuées entre PARIS et CHOLET. Les résultats présentés dans les tableaux sont associés aux configurations décrites (figure 4).

5 - PROGRAMME THEOREME

Le programme financé principalement par l'Administration a débuté par l'expérimentation du système THEOREME-FF qui se décompose en trois phases :

- Phase 1 : liaison point à point à l'alternat entre deux stations fixes.

- Phase 2 : liaison par diffusion entre un site fixe et un véhicule se déplaçant sur deux axes.

- Phase 3 : liaison par diffusion entre un site fixe et un avion survolant l'Atlantique (en cours d'expérimentation).

La phase 1 a débuté fin novembre 87 et s'est terminée fin février 88. Les aériens utilisés étaient des antennes du type YAGI à 5 éléments (gain de 9,5 dB/iso) montées à 17m. La puissance émise à la station de CHOLET (près de Nantes) et à la station de Cormeilles-en-Vexin (près de Paris) était de 1kW. La distance de la liaison est d'environ 350 km. La liaison a été réalisée a une fréquence proche de 42 MHz.

RESULTATS SIMULATION THEOREME Phase 1

Paramètres :
- Fréquence 42 MHz
- Distance de liaison 320 km
- Facteur de bruit du récepteur 8 dB
- E / N_0 6 dB
- Rythme binaire 16 kbit/s
- Bruit galactique

Liaisons Yagi - Yagi

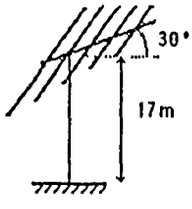

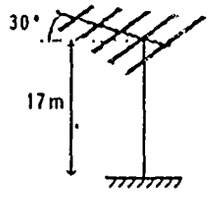

Puissance (W)	1000	500	200	100
d_0 (%)	0,6	0,4	0,23	0,15
τ_m (ms)	97	97	97	97
δ_m (s)	20	30	50	80

Liaisons Dipôles croisés - Yagi

Puissance (W)	h (m)	1,3	3	3,9
2000	d_0 (%)	0,42	0,56	0,66
2000	τ_m (ms)	87	83	80
2000	δ_m (s)	26,5	19	15,5
1000	d_0 (%)	0,28	0,37	0,44
1000	τ_m (ms)	87	83	80
1000	δ_m (s)	40	29	23,5

Figure 4

L'objectif de la phase 1 était d'estimer les potentialités du système de communication via les météores et de caractériser partiellement le canal pour des distances courtes.

La phase 2 a débuté en mars 88 et s'est terminée fin mai 88. Les antennes utilisées à l'émission (site de CHOLET) étaient des dipôles croisés horizontaux ou des antennes de type YAGI 5 éléments en polarisation horizontale ou verticale. La puissance émise était de 2 kW. En réception le véhicule était équipé d'antennes de types cadres croisés sous un radôme et d'un fouet.

Le véhicule s'est déplacé sur deux axes :

- axe 1 : CHOLET-TOULON
- axe 2 : CHOLET-STRASBOURG

Les liaisons ont été réalisées à des fréquences proches de 42 MHz et de 70 MHz.

L'objectif de la phase 2 était de déterminer la zone de couverture d'un système de diffusion omnidirectionnel et d'étudier les variations de performances en fonction de la distance.

6 - DESCRIPTION DE LA MAQUETTE THEOREME-FF

Les synoptiques du système THEOREME phase 1 et 2 sont donnés à la figure 5.

L'antenne de type YAGI est connectée à un amplificateur VHF de 1kW et à un dispositif de commutation de puissance permettant de réaliser l'alternat Emission/Réception en moins de 3ms. Cet amplificateur est excité par un Emetteur/Récepteur TRC 950 utilisé en Fréquence-Fixe entre 40 et 43 MHz. La sensibilité du poste est de -113 dBm pour un facteur de bruit de 8 dB. La modulation est de type FSK et le rythme de modulation de 16 kbits/s.

Un logiciel d'application "MODEM 950" implémenté dans l'Emettreur/Récepteur, permet de détecter une trainée météorique, de réaliser les synchronisations et la gestion des conflits d'accès. Ce logiciel réalise le niveau 1 de la liaison (couche ISO).

L'Emetteur/Récepteur est en liaison avec un Terminal Tactique TRC 747 équipé d'un microprocesseur 8088 16 bits, comprenant un logiciel "MET" réalisant le codage et le décodage des informations, la procédure de transmission par acquittement. Ce logiciel réalise le niveau 2 de la liaison.

Le Terminal Tactique est en liaison avec un calculateur compatible PC équipé d'un logiciel réalisant la gestion des messages émis ou reçus, le dépouillement en temps réel permettant d'afficher des indicateurs de mesures de qualité sur le canal, la synchronisation des stations pour la réalisation automatique d'expérimentation 24h/24.

Pour la phase 2 la station fixe est émettrice et la station mobile est simplement réceptrice.

La station fixe est équipé d'une antenne dipôle croisé fonctionnant à 40 et 70 MHz. Cette antenne a un gain de 6 dB/iso. L'antenne YAGI a aussi été utilisée. L'antenne est connectée à deux amplificateurs 1 kW couplés. La structure des stations à bas niveau est identique a celle de la phase 1. Seuls les logiciels sont différents et permettent la diffusion.

La station mobile est équipée d'une antenne constituée de deux cadres croisés (gain de -6 dB/iso), d'un fouet (gain de -1 dB/iso). De plus un préamplificateur 15 dB de gain et 3 dB de facteur de bruit a été utilisé.

Le système permet de réaliser 3 types de mesures :

- Test canal : Ce test effectue la mesure de l'ouverture et de la fermeture du canal ce qui permet d'en déduire la durée du service.

- Test taux d'erreur : Ce test effectue la mesure des taux d'erreurs moyens sur les traînées et l'évolution de ce taux sur la durée de vie de la traînée.

- Test système : Ce test réalise des mesures de débits, de temps d'acheminement, de taux d'erreurs caractères, d'efficacité de la procédure, etc...

La procédure point à point de la phase 1 fonctionne de la manière suivante (cf figure 6).

La station A veut émettre un message vers la station B. Après l'introduction du message dans le calculateur A, celui-ci est tranmis au Terminal Tactique. Le TRC 747 découpe le message en blocs, et les code par l'intermédiaire d'un module Reed Solomon RS (23,13). La station A émet ensuite, un symbole DPE (demande Pour Emettre). Quand le canal est ouvert la station B reçoit le symbole DPE. Le TRC 950 B émet alors un symbole PIL (Pilote) permettant d'indiquer au TRC 950 A que le canal est ouvert.

A la réception du PIL, l'Emetteur/Récepteur de la station A émet un symbole MESS (Message) de synchronisation et le message.

Si le canal est toujours ouvert le TRC 950 B reçoit le symbole de synchronisation MESS qui lui permet d'identifier les données. Le Terminal Tactique B identifie les blocs par l'entête, les décode et garde en mémoire les blocs corrects. Pour les blocs incorrects, le TRC 747 B réalise un message d'acquittement. Cet acquittement est envoyé de la même manière qu'un message. L'opération est répété jusquà ce que le message soit entièrement transmis et reçu. Durant tout le déroulement de la procédure, les évenements DPE-Emis Station A, DPE-Reçu station B, ACK [B_1, B_2,... B_N], etc... sont enregistrés avec leurs dates à 3 ms près.

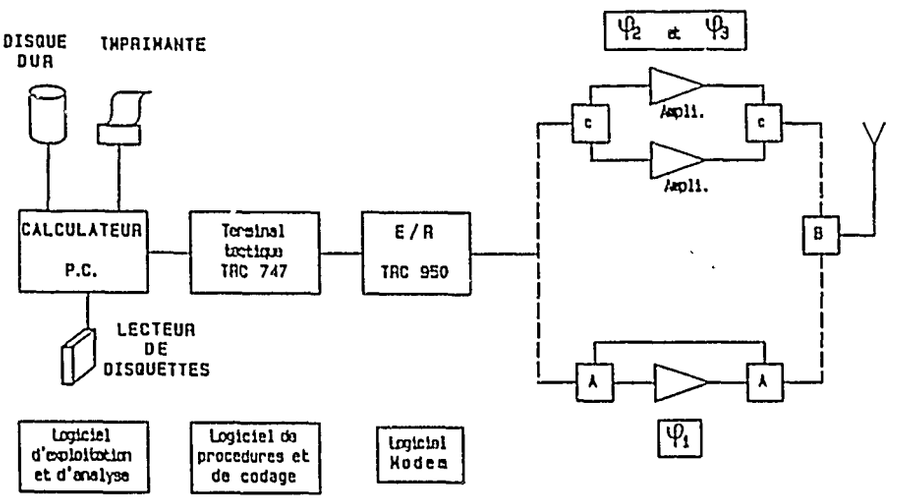

Figure 5

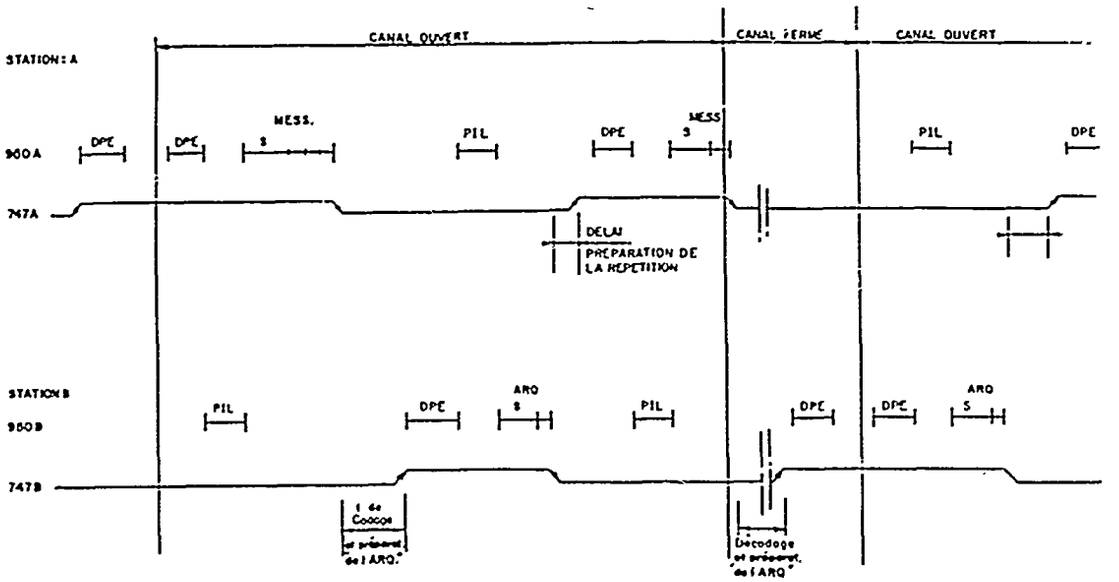

PROCEDURE AVEC SYNCHRONISATION PAR DPE

Figure 6

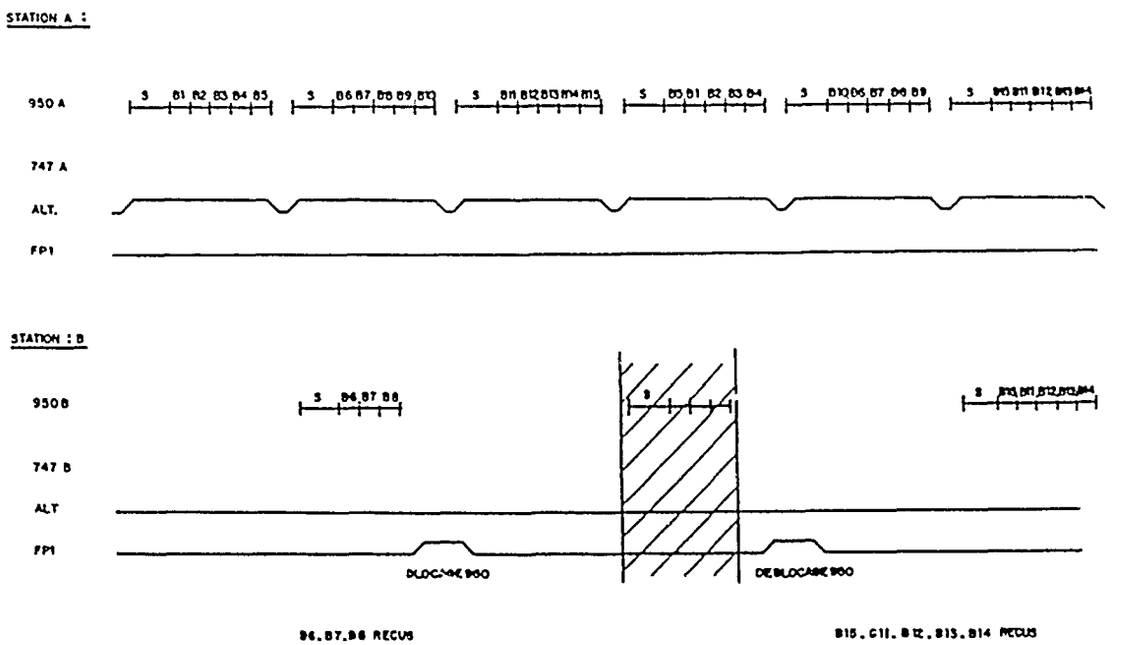

B6, B7, B8 REÇUS

B15, C11, B12, B13, B14 REÇUS

CHRONOGRAMME DE LA PROCEDURE DE DIFFUSION

Figure 7

```
Expe : 2004 Seq : 4 Rep : 1

FICHIERS 747 ET 950 SYNCHRONISES

1                    Alt_B          DataE_B
2                DPE_A
                      78 ms
5                    Pil_B
                       270 ms
8                    FAlt_B
                   33 ms
11  DataR_A       Mess_A
                   855 ms
14  AckE_A        Alt_A
                      627 ms
17                   DPE_B
                   42 ms
20                 Pil_A
                   30 ms
23                 Falt_A
                      33 ms
26                   Mess_B        QUIDR_B
                      78 ms
29                   Alt_B         NAckE_B
                      126 ms
32                   DPE_A
                        78 ms
35                    Pil_B
                        30 ms
38                    FAlt_B
                   33 ms
41  NAckR_A       Mess_A
                   129 ms
44  AckE_A        Alt_A
                      132 ms
47                   DPE_B
                   33 ms
50                 Pil_A
                   30 ms
53                 FAlt_A
                      33 ms
56                   Mess_B        AckR_B
```

Fichiers TRC 950 et TRC 747 synchronisés et datés.

Figure 8

```
                    EXPERIMENTATION N°0012

SEQUENCE N°   1
TYPE DE TEST :TRANSMISSION
ACTION DE LA STATION A: EMISSION
N° DE MESSAGE: 001
NOMBRE DE TEST:   5
**********

SEQUENCE N°   2
TYPE DE TEST :TRANSMISSION
ACTION DE LA STATION A: EMISSION
N° DE MESSAGE: 005
NOMBRE DE TEST:   5
**********

SEQUENCE N°   3
TYPE DE TEST :TRANSMISSION
ACTION DE LA STATION A: EMISSION
N° DE MESSAGE: 010
NOMBRE DE TEST:   5
**********

SEQUENCE N°   4
TYPE DE TEST :TRANSMISSION
ACTION DE LA STATION A: EMISSION
N° DE MESSAGE: 020
NOMBRE DE TEST:   5
**********

SEQUENCE N°   5
TYPE DE TEST :TRANSMISSION
ACTION DE LA STATION A: EMISSION
N° DE MESSAGE: 050
NOMBRE DE TEST:   5
**********

SEQUENCE N°   6
TYPE DE TEST :DUREE D'OUVERTURE CANAL
ACTION DE LA STATION A: EMISSION
NOMBRE DE TEST:   5
**********

SEQUENCE N°   7
TYPE DE TEST :TAUX D'ERREUR
ACTION DE LA STATION A: EMISSION
N° DE MESSAGE: 092
NOMBRE DE TEST:   5
**********
```

Figure 9

La procédure de diffusion phase 2 fonctionne de la manière suivante (cf figure 7).

La station A veut diffuser un message vers la station B. L'opérateur entre le message dans le calculateur qui le transmet au Terminal Tactique. Le TRC 747 A découpe le message en paquet et les paquets en blocs. Chaque paquet contient un groupe de blocs et une entête.

Les paquets sont émis cycliquement avec une synchronisation MESS fournie par le TRC 950 A. Lorsque le canal est ouvert la station B reçoit le symbole MESS et l'entête du paquet donnant les blocs le constituant est décodé.

Lorsque tous les paquets sont reconstitués et sont remis dans l'ordre, le message est alors affiché sur la console du calculateur de la station B.

Les procédures décrites ci-dessus correspondent à la transmission manuelle de message utilisées pour les démonstrations.

Le test canal est réalisé par l'envoi d'une entête sans bloc message. Le test taux d'erreur bit est réalisé par l'envoie d'une entête et d'un message de 900 caractères ne passant pas par les modules de codage et de décodage. Le test système utilise la transmission de message, par l'intermédiaire d'un séquenceur automatique.

Un exemple de fichier d'expérimentation de TRC 950, de TRC 747 et de TRC 950/TRC 747 synchronisé est donné à la figure 8.

La précision des mesures de temps d'ouverture et de fermeture est de ± 10% et celle sur le temps d'acheminement du message est de ± 100 ms.

Des études théoriques sont et ont été menées parallèlement aux différentes expérimentations. Ces études sont de nature à caractériser le canal météorique et à déterminer les performances de systèmes de communication militaires ou civils en étudiant et optimisant les procédures de transmission.

7 - DEROULEMENT DES EXPERIMENTATIONS REALISEES

Le projet THEOREME-FF a permis de réaliser la couverture représentée sur la carte de France de la figure 10.

Dans cet article, il est surtout décrit les résultats de la phase 1 et quelques résultats de la phase 2.

La phase 1 a été décomposée en deux sous-phases :

- sous-phase 1.1 : essais à 1kW et 200W
- sous-phase 1.2 : essais à 100W, 50W et 30W

Plus de 500 heures d'enregistrements ont été effectuées en 3 mois, représentant 40 MO de données brutes.

Des séquences de tests ont été réalisées à toutes les heures du jour et de la nuit comprenant environ 10 à 20 mn de test canal, 10 à 20 mn de test taux d'erreur, et 20 à 40 mn de test système (cf figure 11).

La phase 2 a été réalisée sur deux axes représentant la couverture suivante :

- axe 1 : CHOLET-TOULON. Les distances entre la station fixe et la station mobile étaient de 105, 210, 355, 580 et 680 km.

- axe 2 : CHOLET-STRASBOURG. Les distances entre la station fixe et la station mobile étaient de 225, 520 et 650 km.

Les puissances d'émissions expérimentées ont été 2 kW, 1 kW, 500W et 200W.

Des exemples de séquences d'expérimentation sont données à la figure 9.

Sur une trenche de durée moyenne de 1h00, les tests sont effectués de la manière représentée par la figure ci-après :

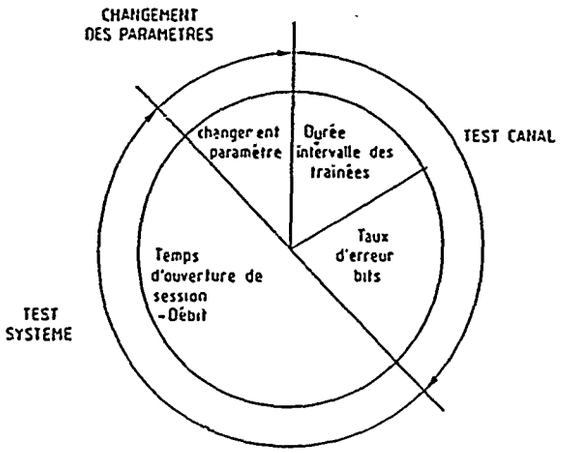

Figure 11

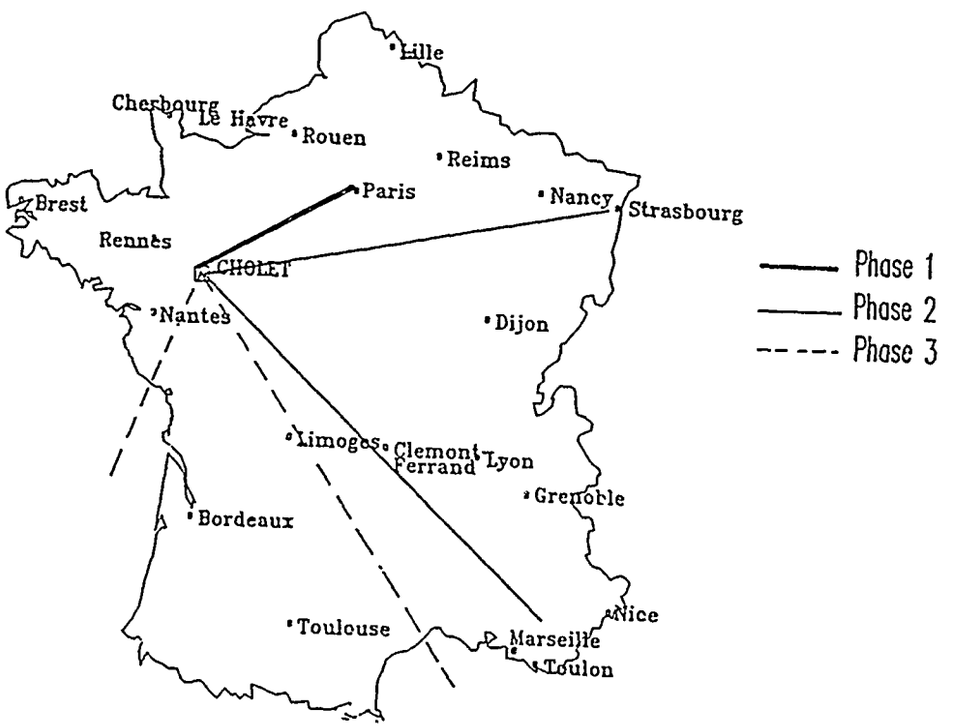

Figure 10

8 - RESULTATS OBTENUS ET INTERPRETATION

Une synthèse des résultats de la phase 1 est présenté ci-après, les courbes et les tableaux de références sont les figures 12 et 13.

La durée moyenne d'ouverture du canal est de 400ms pour 1kW, de 330ms pour 200W et de 350ms pour 100W. Cette valeur moyenne ne dépend pas de la puissance d'émission.

La durée moyenne de fermeture du canal est de 700ms pour 1kW, de 800ms pour 200W, et de 43s pour 100W.

La durée de service varie donc de 36% pour 1kW à 29% pour 200W et à 0,8% pour 100W.

Les écarts types sur les durées d'ouverture et de fermeture du canal sont très importants, la stabilité du canal est obtenue sur 1 heure environ, et l'écart type est alors du même ordre de grandeur que la valeur moyenne (cf Figure 16).

L'activité est à peu près stable sur 24 heures ; on n'observe pas d'heures défavorables vers 18h et favorables vers 6 heures (Figure 15 et Figure 16) (cf résultats des expérimentations COMET).

La procédure point à point adoptée est bien adaptée au puissances de 1kW à 100W. A 50W de nombreux échanges sont effectués, dégradant ainsi les performances du système (cf Figure 17).

Les débits obtenus pour des messages de 250 caractères sont de 158 caractères utiles/seconde pour 1kW, 116 car/s pour 200W, 13 car/s pour 100W et de 1 car/s pour 50W. Ce débit est maximal pour le message de 500 caractères (185 car/s pour 1kW). Les valeurs obtenues deviennent stables en moyennant les résultats relevés sur une durée supérieure à 15mn.

La marge en puissance du système par rapport à 1kW pour un fonctionnement fiable est d'environ 10 dB.
Les expérimentations de la phase 2 ont permis de réaliser des liaisons sur des distances de 100 à 700 km (cf Figure 18).

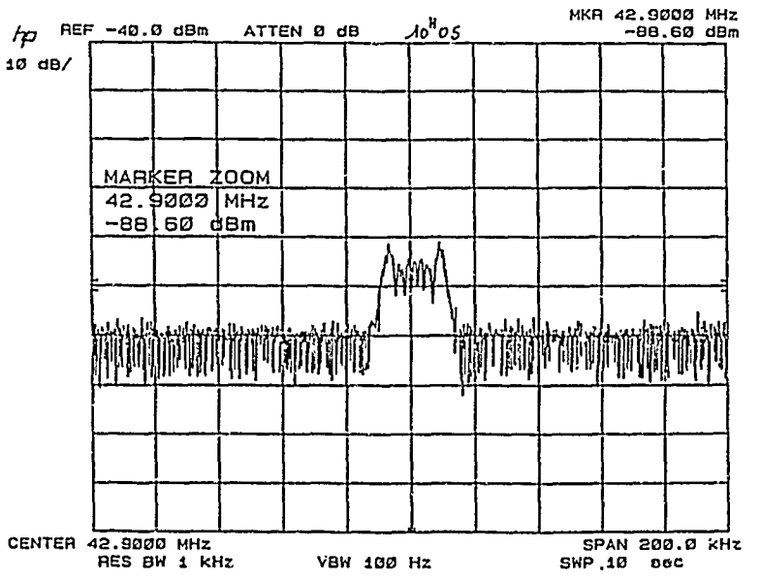

Figure 12

PHASE 1

PUISSANCE EMISSION	DUREE OUVERTURE (ms)	DUREE FERMETURE (ms)	TAUX D'ERREURS BIT MOYEN	DUREE DE SERVICE (%)	DEBIT MOYEN MESSAGE 250 (CAR.)
1000 W	400	710	1.7	36	160
200 W	330	790	2.5	29	110
100 W	350	43000	7.4	0.8	13
50 W	-	-	-	-	1

Figure 13

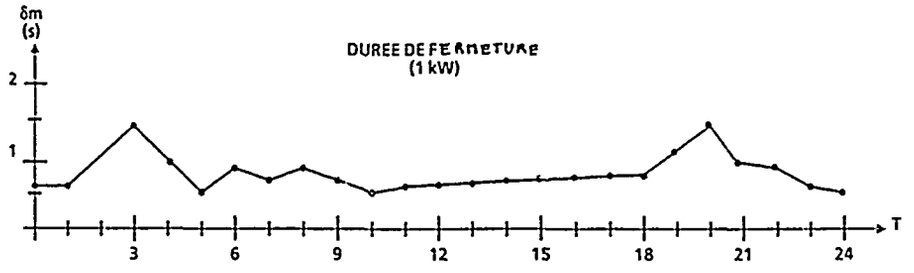

Figure 14

OUVERTURES	$\bar{M}$ (ms)	σ (ms)
1000 W	403	546
200 W	332	550
FERMETURE	$\bar{M}$ (ms)	σ (ms)
1000 W	708	218
200 W	790	1424

Figure 16

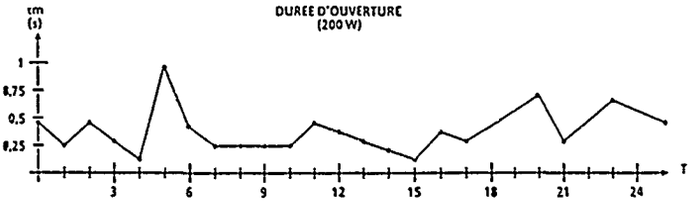

FIgure 15

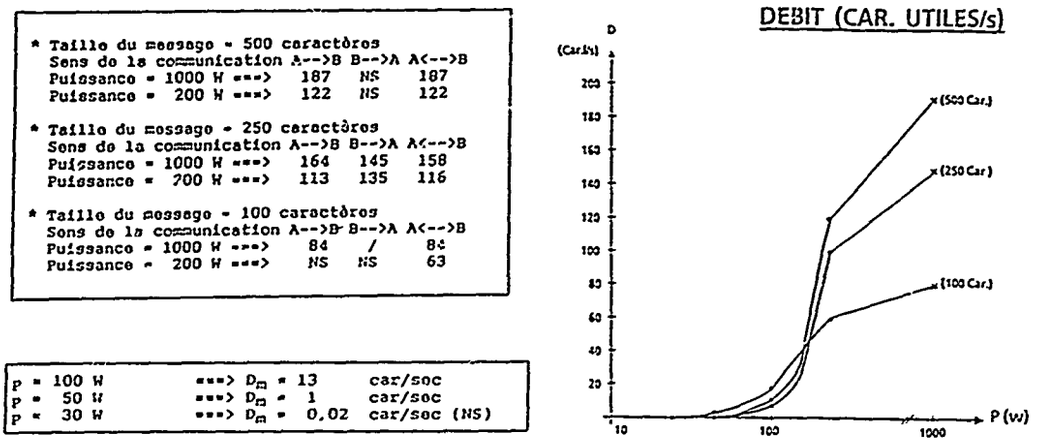

Figure 17

L'activité et le débit moyen sont maxima pour les courtes distances (100 à 250km), puis diminuent pour les distances moyennes (250 à 600km) et réaugmentent pour les longues distances (à partir de 600km).

Aucune différence sensible n'a pu être constatée entre les deux axes CHOLET-TOULON et CHOLET-STRASBOURG.

Les essais en fonction de la fréquence permettent de montrer que la durée des traînées météoriques diminue alors que le temps entre deux traînées augmente, lorsque la fréquence passe de 42 à 69 MHz.

Ces expérimentations montrent une certaine incompatibilité entre les résultats de THEOREME d'une part et les simulations réalisées et les résultats COMET d'autre part. En effet les résultats obtenus en phase 1 et dans une moindre mesure en phase 2 sont très supérieur à ceux attendus. Les différences identifiées, sont les suivantes :

- durées de fermeture expérimentales très inférieures aux durées estimées par les simulations pour des liaisons de 100 à 350 km,
- durée d'ouverture du canal dépendant très peu de la distance (100 à 700km),

- variations journalière non représentatives des fluctuations diurnes de l'activité météorique.

D'autre part des essais préliminaires à la phase 2 ont été réalisés entre les sites de CHOLET et de CORMEILLES en remplaçant l'antenne émettrice de type YAGI par des dipôles croisés alimentés par 2 kW. Les performances alors obtenues sont fortement dégradées, phénomène non expliqué par la simulation réalisée.

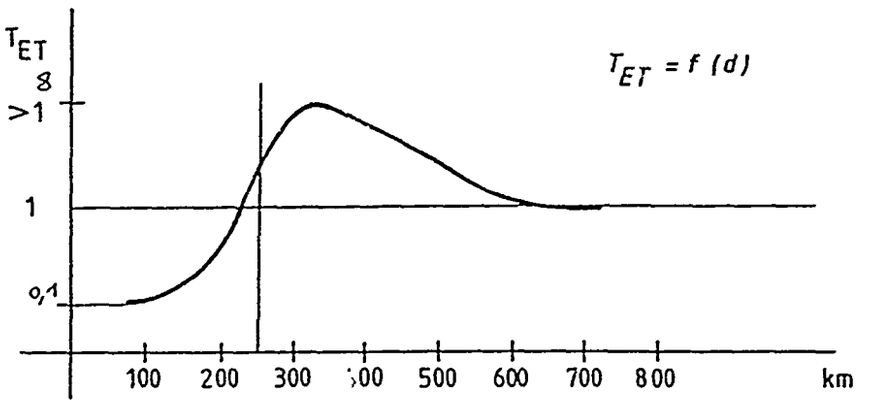

COURBE 1

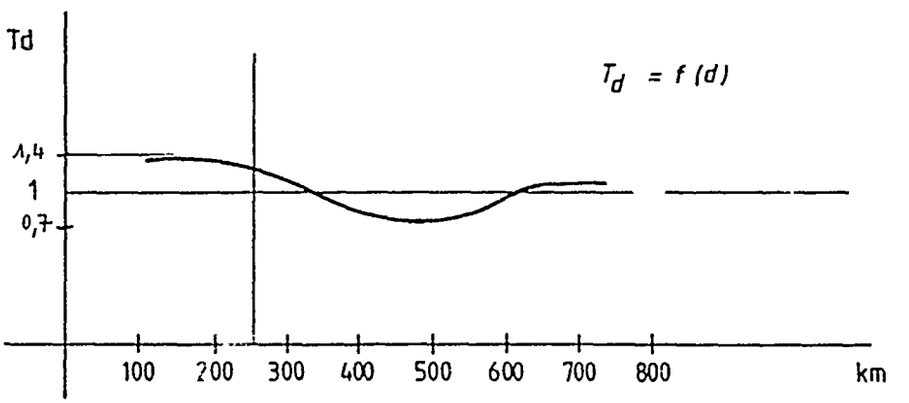

COURBE 2

Courbe 1 : temps entre deux traînées
Courbe 2 : durée de la traînée

Figure 18

9 - CONCLUSION

Les différences entre les résultats expérimentaux et les simulations réalisées ne sont pas à ce jour expliquées. Les grands écarts obtenus avec la configuration de la phase 1 entre les expérimentations et la simulation ne peuvent a priori être compris que par la présence simultanée d'un autre mécanisme de propagation. La hauteur des antennes au-dessus du sol, choisie de manière à pouvoir réaliser des liaisons jusqu'à 1000 km, permet d'obtenir des gains notables aux angles de tir faibles. Cet élément favorise les liaisons les liaisons par diffusion troposphérique,

théoriquement possibles pour les distances étudiées avec une faible durée de service satisfaisant, et dont l'exploitation est possible avec des procédures spécifiques utilisées pour le canal météorique. Cette hypothèse reste cependant à confirmer et un travail important devra donc être effectué afin de discerner les contributions respectives du canal météorique et d'autres mécanismes de propagation aux paramètres physiques mesurés.

En particulier, la variation de la durée moyenne d'ouverture du canal avec la distance de liaison devra être étudiée spécifiquement car elle déterminera le choix des procédures (temps de synchronisation, ...).

L'Administration française et THOMSON-CSF à la suite des démonstrations effectuées et des résultats obtenus ont décidé de poursuivre les études et les expérimentations sur ce canal, qui apparaît d'ors et déjà comme intéressant pour la transmission de données en VHF aux courtes et moyennes distances (100 à 1000 km), dans le but de définir des systèmes opérationnels.

[1] G.R. SUGAR : "Radio Propagation from Meteor Trails" Proceedings of IEEE vol 52, p 116-136, Fév. 1964

[2] J.A. WEITZEN : "Communicating Via Meteor Burst at Short Ranges" IEEE Trans. on communications, vol COM-35, n°11, p 1217, 1221, Novembre 1987

[3] P.J. BARTHOLOME-I.M.VOGT : "COMET- A New Meteor-Burst System Incorporating ARQ and Diversity Reception" IEEE Trans.on Communication Technology, vol COM-16, p 268-278, Avril 1968

[4] D.W. BROWN "The potential of meteor-burst communications with particular to the COMET system" NATO Advanced Strudy Institue on communication systems and random process theory, Août 1977

[5] D.W. BROW-HP. WILLIAMS :
"The performance of meteor-burst communications at different frequencies" AGARD CP 244, Octobre 1977

[6] D.W. BROWN "A Physical Meteor-Burst Propagation Model and Some

[7] E.J. MORGAN Meteor Burst communication :
An Update

[8] S. CANIVENC Propagation des ondes, télécommunications Propagation UHF ionospherique TOME 2, CH3.

System Factors to be considered in Assessing Propagation Effects on Modern Digital Satellite Communications Systems

D J Fang
MTL-Washington Division
Massachusetts Technological Laboratory
4300 Montgomery Ave., Suite 203A, Bethesda, MD 20814, USA

and

H. Soicher
US Army Communications-Electronics Command
AMSEL-COM-TA-1, Fort Monmouth, NJ 07703-5202, USA

ABSTRACT

In the traditional approach of assessing system impact due to propagation anomalies, the primarily effort is on the characterization of a propagation channel to the maximum extent possible. In such an approach, environmental parameters (which affect the channel transfer function) and the system parameters (which dictate the system performance) are largely uncoupled. For instance, the transfer function for an ionospheric scintillation channel is characterized by ionospheric irregularity parameters, irrespect of whether the communications system is digital or analog, with or without inter-leave/coding, in the presence or absence of diversity. From assessing the system impact's viewpoint, the lack of coupling is acceptable to the conventional analog system (an 8dB propagation degradation implies an 8dB reduction of S/N irrespect of whether the system is AM or FM, single side band or double side band), but is not acceptable to the modern digital system (an 8dB propagation degradation can imply 10^{-3} BER for a QPSK system without coding but can also imply 10^{-6} BER for the same system with coding and interleave).

In this paper, system factors to be considered in the assessment of propagation effects are outlined. The essence is to point out, for modern digital satellite communications systems, propagation assessment has to have proper system reference in order to provide readily useful conclusions for system engineers.

I. Introduction

The ultimate objective of communications system engineering is on the efficiency and reliability of message delivery via a realizable means of transmission mode. The basic nature of message can be divided into two categories: Continuous and discrete. Examples of continuous message include voice, temperature, movie, etc. Examples of discrete message include alphabetical symbols in language, population counts, sport scores, etc. The message, irrespect of whether it is continuous or discrete, can be transmitted in two ways, either by the conventional analog communication or by the modern digital communication.

In either way of communications, one can talk about efficiency and reliability according to it unique engineering criteria. An apple-to-apple comparison of efficiency and reliability between analog and digital communications is not always appropriate. Generally speaking, digital communications offer much better control of signal transmission and detection, thus provide superior signal quality, link stability and network versatility in multi-layer hierarchical structures. These advantages are known for many years. The fact that conventional communication systems, up to most recently, have primarily been analog systems is largely due to technology limitations, particularly in A/D and D/A conversion, high speed circuits,

precision timing and synchronization devices, memory capacity, software engineering methodology, etc. With the drastic advancement of electronics and microprocessors, technology limitations are being overcome rapidly in recent years. The modern trend is definitely toward digital communications.

The categorization of a communications system into either a digital or an analog system is largely based on configurations at baseband or IF level. The two types of systems remain basically the same at RF carrier level. Since propagation degradations affect the RF carrier of the signal as a whole, with no prejudice whatsoever on the specific content of the signal, the traditional view is that propagation is propagation, regardless of its baseband or IF composition.

This traditional view is correct for the conventional analog communications system. Under this view, electromagnetic wave propagationists and communications system engineers are largely decoupled in the sense that one group can go on with its business without paying much attention to the other. Even to this date, the majority of propagationists in studying propagation degradations, concern idealistic TEM plane wave only, and rarely address the signal-to-noise-ratio (S/N), a fundamental parameter of analog system engineering. On the other side, system engineers in overwhelming cases treat propagation degradations the same way as noise, quoting applicable dB values and statistics (such as Rayleigh fading statistics) from the propagation papers without paying much attention to propagation physics, such as Brewster angle for low angle transmission, scintillation (S_4) index for ionospheric scintillation, etc.

In this paper, we intent to show that the above view is no longer applicable for digital communications system engineering. In order to make their studies relevant to real world communications system applications, propagationists must realize that their work is not an isolated topic, but a part of the integrated study in system engineering. This is particularly true in the aspect of system optimization. Since propagation anomalies represent the ultimate limiting factors of system performance, and new adaptive schemes to exploit propagation characteristics and to combat propagation effects are being postulated alone the line of technology advances, the system optimization can only be performed by a trade-off process involving both propagation and system considerations.

II. Analog Communications

II.1 Basic Nature - Fidelity in Terms of S/N

Knowing that received signal can never be precisely the same as the transmitted signal, analog communications system engineering concerns the fidelity of reproduction of the original message. Since message is always distorted by the noise in the process of transmission, the fidelity means the ability for a listener to interpret the message, or for a detector to derive the message, in the presence of noise. The interpretability, and/or detectability are inversely proportional to the existence of amount of noise relative to the signal. Hence, signal-to-noise ratio (S/N) is the figure of merit of the communications system.

A typical block diagram is shown in figure 1, where m(t) is the original

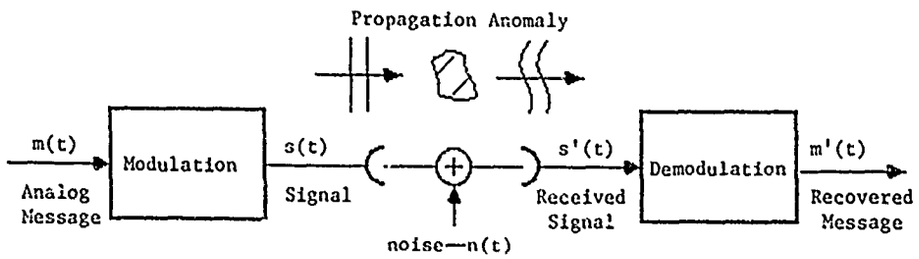

Figure 1 Analog transmission through a medium - Propagationists take a parametric approach that a plane wave penetrating a single, well-defined anomaly. System engineers treat the effect of the medoium as additive noise which downgrades S/N.

signal, m'(t) is the reproduced signal, and noise is represented by n(t). The S/N is represented by

$$S/N = \frac{E[m^2(t)]}{E[m(t) - m'(t)]^2} \qquad (1)$$

where E[.] stands for ensemble averaged value. In analog communications, the message is modulated continuously in either amplitude (AM), frequency (FM) or phase (PM) of the carrier prior to transmission. The S/N can be improved in two ways, either by an increase of transmitted signal power or by a increase of bandwidth. In either way, there are practical limits. Power can not be increased beyond the level of system saturation, intermodulation and interference. On the other hand, bandwidth can not be expanded without limit because of the undesirable effect of noise increase, as noise is generally assumed to be white in nature. To maintain a required performance, the system engineer must trade between power and bandwidth. For the case of angle-modulation (FM or PM), where the modulated RF signal bandwidth is significantly enhanced from the baseband message bandwidth, the reduction in transmitted power can be offset by an increase in the (mean-square) bandwidth by the same factor, or vice versa. The S/N at the receiver improves at least as the square of the modulated bandwidth.

One of the basic property of system engineering is that noise produced from different sources in an RF transmission channel is additive. That is, if one single noise source in the channel results an S/N of 40 dB at the receiver, two identical but independent noise source simultaneously in presence in the channel would result an S/N of 37 dB. As an extension of the additive nature, noises in multiple hops produce cascade effects. For example, the noise generated in a two-hop LOS (line of sight) microwave link of 80 km would yield a 3-dB worsening of S/N at the last receiver than that of the single hop link of 40 km. Therefore, in order to maintain the overall S/N of an n-hop LOS system, the required S/N per each single hop has to increase in proportional to n.

II.2 Propagation Effects - Indiscriminative to System Configuration

Propagation anomalies manifest themselves in a number of ways, including absorption, reflection, diffraction and scattering of waves, resulting attenuation, depolarization, angle of arrival change, phase and group delay, scintillation, etc. of the original signal. It is true that propagation anomalies impact on different types of analog modulations differently. For instance the multipath selective fading effect is much more disastrous on AM than SSB-SC (AM-Single Sideband Suppress Carrier), due to the fact that the carrier and sidebands undergo different amount of random phase fluctuation. But in terms of S/N, these discriminative effects are not most critical. The reason is that as a matter of practical consideration, the modulated bandwidth of signal transmission through the medium is always relatively smaller than the coherent bandwidth of the propagation medium. As such, the signal will remain coherent, the first order propagation effect is the attenuation of the RF carrier. Consequently, propagation degradation is no more than the reduction of S/N, similar to the effect of noise temperature increase. The additive and/or the cascade nature of S/N mentioned earlier still apply. Thus, a 3 dB propagation attenuation would result a 3 dB reduction of S/N at the receiver. If, there is an additional 2 dB attenuation, caused either by the same type or different type of propagation anomalies in the channel, this would result a total of 5 dB reduction of S/N. For a multi-hop system, attenuation add up linearly toward the reduction of S/N at the final receiver. All these are indiscriminative to the system configuration.

II.3 Decoupling Between Propagation and System Engineering

The above discussion suggests that the linkage between EM wave propagationists and system engineers is at most a weak one. An illustration is provided in Figure 2. In the figure, the line separating propagationist and communication engineer is clear. A propagationist does not have to know the system. He provides propagation effect statement as an independent piece of work without being constrained by a

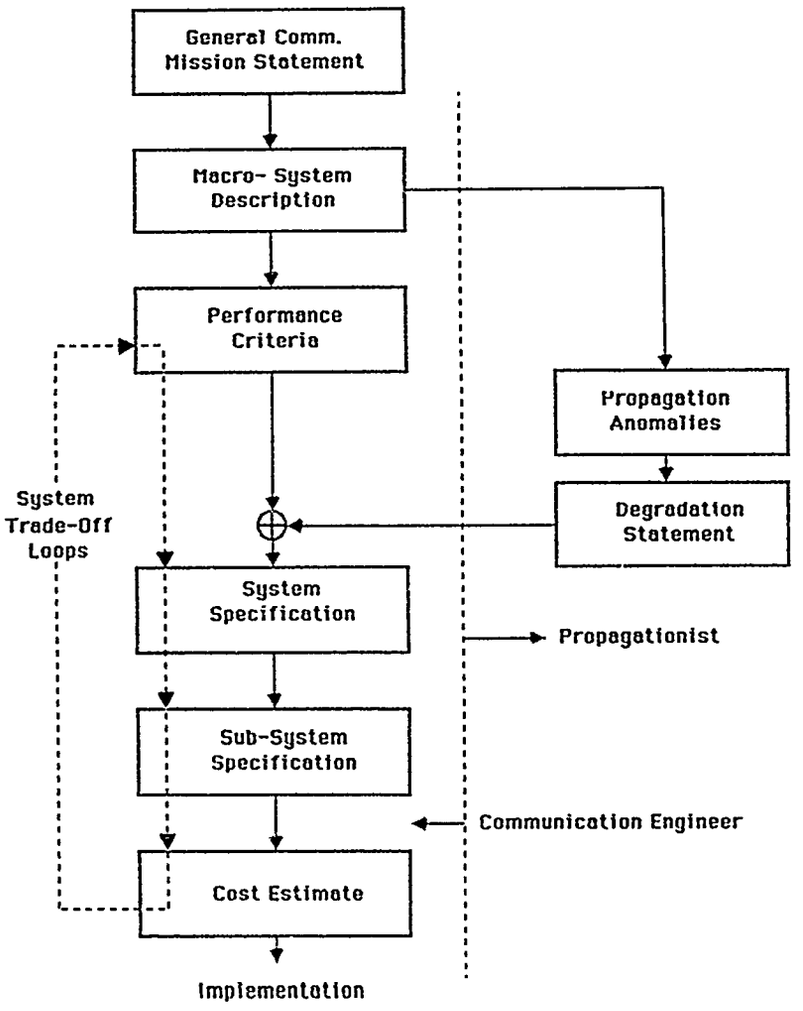

Figure 2 Analog system design block diagram - The separation of propagation study and communications system engineering is a clear one.

specific system configuration. The system engineer, in turn, takes the degradation statement and performs the entire system trade-off without ever having to go back to the propagationist.

III. Digital Communications

III.1 Basic Nature - Bit Rate and Bit Error Rate

In contrast to the case of analog communications where the signal waveforms S(t) can be infinite in spatial and temporal variations, waveforms in digital communications are finite. In the most fundamental case, the waveform is a well known form of a simple square wave (either RZ, NRZ or Manchester form) representing a bit, either 1 or 0. As such, the objective of the receiver is not to reproduce the waveform with fidelity because the waveform is known a priori and the detail shape of waveforms do not carry any useful message any way. Rather, the receiver's objective is to determine the correct bit, either 1 or 0, that was transmitted. Since the presence of bits conveys the information, more information can be conveyed by transmitting more bits per unit time. Thus the essence of digital communication is to transmit and recover maximal amount of bits with least number of bit errors at the receiver. The two important parameters therefore are bit rate R and bit error rate BER.

A general representation of digital communications is given in Figure 3, where we consider M-ary signal waveforms. That is, there are M digital symbols messages m_1, m_2, ...m_M to be transmitted. Each of the symbol is well known by their respective waveform representation $S_1(t)$, $S_2(t)$,... $S_M(t)$ at RF. Just as the case for analog communications, these bits or waveform are corrupted by propagation effects, the received signal at the front end of the receiver is s'(t).

At this point, we may face an argument that digital communication is no more different from analog communication in the sense that both R and BER are functions

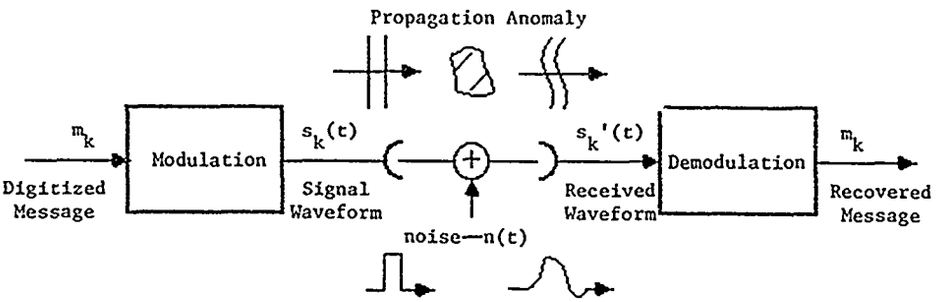

Figure 3 Digital transmission - Signal waveforms are finite and known a priori. Receiver concerns primarily the determination of the kind of waveform being sent. Propagation effects which deforms the waveform is not significant as long as the correct determination can still be made.

of transmission power and bandwidth, and hence the essence of system design is again a trade-off between power and bandwidth using S/N as the figure of merit. In deed, this is precisely the point of Shannon's theorem which stated that the channel capacity C, i.e., the maximum allowable R at a desirably low BER, is given by

$$C = B \log_2 (1 + S/N) \qquad (2)$$

According to the theorem, the throughput of the channel, P, defined by R/B, is given by

$$P = \log_2 (1 + S/N) \qquad (3)$$

Unfortunately, Shannon's theorem and hence equation (3) remain to be the unattainable ideal case. To illustrate this, we present figure 4 [1] where R versus CNR

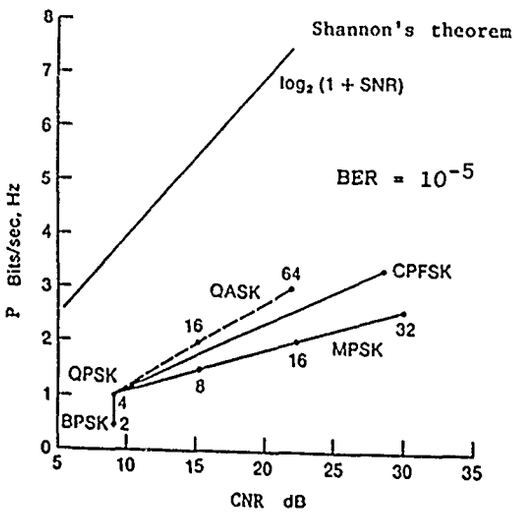

Figure 4 Throughput P versus Carrier to Noise Ratio - The $\log_2(1+SNR)$ curve is the Shannan limit which is unattainable by the current technology.

(Carrier-to-noise ratio, a quantity proportional to S/N) is plotted for a given BER value of 10^{-5}. The point is that, there is a significant gap between the R of the

Shannon's theorem and the R that is technologically attainable, as represented by the curve of (QASK, 64), in figure 4.

It suffices to say, the real-world digital communications system is more than a two-way trade-orf between power and bandwidth. First of all, for given CNR, the throughput R varies for different modulation techniques. Secondly, high throughput is not meaningful unless the BER is under control. If error-correction coding is used for the purpose of reducing BER, the additional redundancy bits require a wider bandwidth to carry throuth, this is directly contrary to desired throughput improvement. Throughput of course can be drastically improved if the conventional constant envelop condition is not required. If we use M levels of amplitude, then $\log_2 M$ bits can be coded onto each carrier burst, as we shown in MASK shown in Figure 4. Further enhancement can be made by incorporating phase divisions. This is in deed the case of modern codulation (modulation plus coding) techniques [2]. The necessary condition for such techniques is that carrier power must be sufficiently high to allow adequate separation of amplitude and phase levels. All these are vulnerable to propagation anomalies.

III.2 Propagation Effects - Discriminative to System Configuration

The digital communications concept is very different from that of the analog communications in the sense that while the RF transmission channel always suffers propagation degradations except in the ideal case of clear sky with no obstructions, as long as the transmitted bits can be eventually detected at the receiving end correctly, the propagation effects are no effects, just as if they are in clear sky with no obstructions. In other words, the severity of propagation degradations is not purely a propagation statement as in the case for analog communication, but is a relative statement depends on the system configuration.

Referring to Figure 3, the transmitted waveforms generally have the following orthogonal property:

$$\int_0^T S_i(t)\, S_j(t)\, dt = \begin{cases} 0 & \text{if } i = j \\ 1 & \text{if } i = j \end{cases} \qquad (4)$$

where T is the period of a waveform. At the receiving end, signal detection is by a correlation principle,

$$\int_\tau^{\tau+T} Sr(t) S_r(t) dt = q \qquad (5)$$

where τ is the propagation delay, $S_r(t)$ is locally generated waveform representing either $S_1(t)$, $S_2(t)$, ... or $S_M(t)$, and q is the correlation value. The decision process is basically to compare q with a preset threshold value at a comparator for determining the correct waveform among m_1, m_2, ... and m_M. The concept is illustrated in Figure 5.

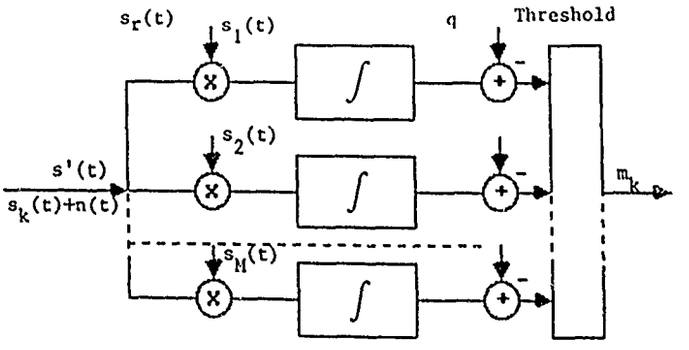

Figure 5 Digital signal detection - Using the orthogonality property among digital waveforms, the detection is done based on correlation of the incoming waveform with the locally generated waveform.

Based on equations (4) and (5), we have the glimpse of propagation impact on digital communications systems. First, the quantity τ can not possibly be a precise constant due to atmospheric/ionospheric propagation delays, surface multipath transmissions, ductings, etc. This group delay effect can create a problem for bit synchronization, intersymbol interference and PLL (Phase Lock Loop)tracking. Random phase dispersion and interference will damage the orthogonality condition of equation (4) which will result errors in (5) for phase shift-key system. To say the least, the additive and cascade nature of propagation attenuation as being the domi-

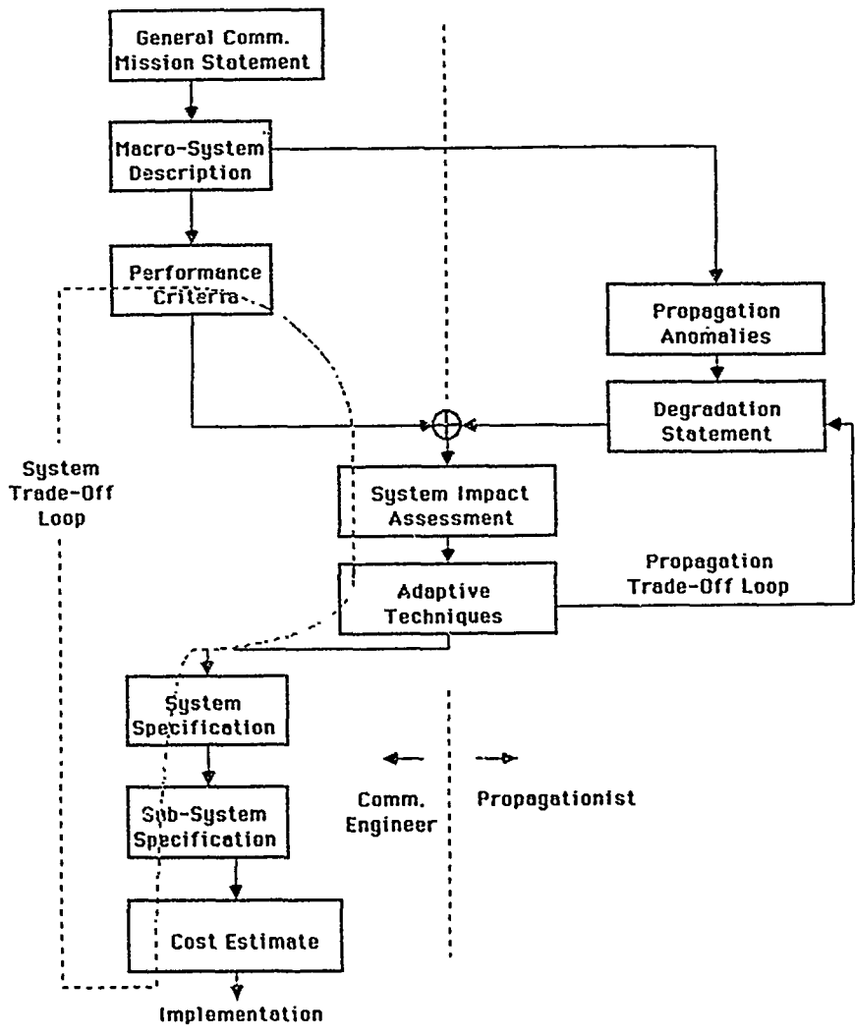

Figure 6 Digital system design block diagram - The systems impact assessment includes a propagation trade-off loop. As such, the separation between the propagation study and system engineering is no longer obvious.

nant effect is no longer true. For a LOS digital communications link, an n-hop system simply has its outage time increase to a factor of n. During the period of non-outage, the link performance (in term of BER) of the n-hop system does not have any noticeable degradation as compared to that of a single-hop link.

III.3 Coupling between Propagation and System Engineering

While propagation effects on an RF signal are non-discriminative, the impact of propagation effects in terms of BER is discriminative to system configurations. Because of this, propagation studies and system engineering are no longer decoupled. Shown in Figure 6, the coupling of propagation study and system engineering is illustrated. In the figure, we see that in actual digital communications system

design, there is a propagation trade-off loop to be dealt with. This is particularly true if we intend to exploit and/or mitigate the propagation environment for optimization of the system performance.

IV. Major Aspect of Propagation Impact Trade-Off Loop

Since the trade-off loop as shown in Figure 6 is system specific, it is difficult to make general statement regarding to its actual procedure. We nevertheless can provide an outline of major aspects to be considered in the loop, which we believe is a useful guideline for propagation research in the future.

IV.1 Threshold Cut Off

Figure 7 compares fade effects on AM, FM and digital radio [3]. The figure shows the threshold effect of received signal level (RSL) beyond which a communication channel is not useful. There is no threshold effect for AM. But the threshold effect for FM and digital radio is obvious. The important point is that for RSL higher than the threshold value, both AM and FM, the channel performance improvement is a gradual one; while for the digital system, the performance jumps to its optimum condition and stays flat. Therefore, during normal propagation conditions, the digital system will operate at a BER as low as to be inconsequential. Such BER condition will prevail for a long while as propagation condition deteriorates until at a threshold level the burst of BER and/or synchronization problem make the link break down.

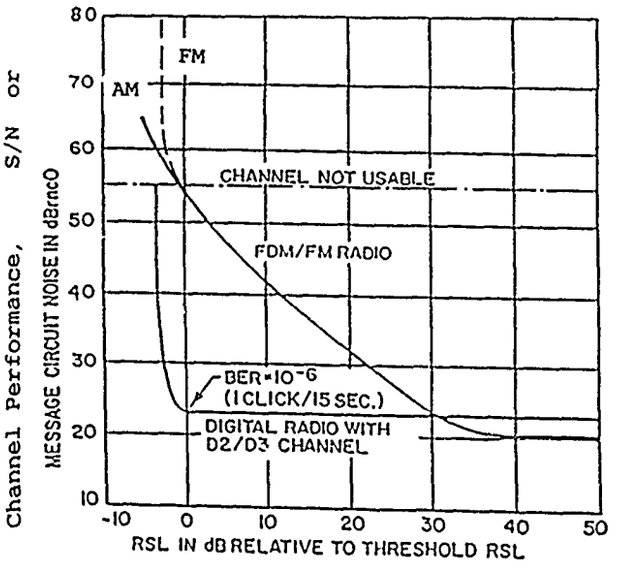

Figure 7 Fade effects on AM, FM and digital radio - The digital system displays a sudden cutoff when the received signal level (RSL) drops below a threshold value.

The system design objective is obviously of pushing the threshold value as low as possible within the power and bandwidth at disposal. Increasing the antenna size and accurate tracking would be among the first objectives to be implemented; diversity arrangement will also come into consideration. As a result, atmospheric effects that cause ducting, angle of arrival changes and multipath fading become critical issues in the propagation trade-off loop. These effects differ as antenna size, height, diversity distance, etc., vary.

IV.2 Maximum Limit of Bit Rate

As high-speed switching electronics and computer software technology advance, system engineers will continue their push of higher bit rate transmission. While the 140 Mbit/s rate is the fastest for practical digital communications for the present radio and microwave systems, there is no reason to assume a rate that is 10 time higher can not be achieved in 5 years. As such, the coherent bandwidth of the medium, which has never been a concern in propagation studies, become an issue.

In designing future high-speed digital communications systems for trunk applications, it is expected that propagation studies will involve a trade-off between atmospheric/ionospheric coherent bandwidth and the transmission bit rate. For UHF to C band satellite communications system, Faraday rotation and its variations will be key factors to be quantized. For higher frequencies, bandwidth dispersion during precipitation and clear air turbulence events due to refractive-index irregularities with scale sizes comparable to Fresnel size become critical.

IV.3 Link Availability

Prior to the satellite communications era, Global HF communications at an availability of 50% of time is considered as typical. Current link availability for international commercial trunk satellite communications at 99.99% is considered as standard. And as computer-to-computer communications become increasingly important, higher availability beyond 99.999% is required. As such, simultaneous occurrence of propagation degradations of different physical origins, which has rarely been addressed by the propagationists, become significant for high availability communications link assessment.

As an example, we cite a recent paper by Fang and Allnutt [1987] studying the simultaneous occurrence of ionospheric scintillation and rain fading. Ionospheric scintillation and rain fading are two impairments of completely different physical origin. For C-band earth stations in equatorial regions at years of high sunspot number, the simultaneous occurrence may have an annual percentage time that is significant to system design. Based on the analysis of 17-month, 4 GHz satellite signal data starting from October 1980 at Djutiluhar earth station in Indonesia, the cumulative simultaneous occurrence time was about 0.06% annually.

Furthermore, Fang and Allnutt reported that the simultaneous events have signatures that are often vastly different from that when only a single impairment, either scintillation or rain alone, is present. While ionospheric scintillation alone is not a depolarization phenomenon, and rain fading alone is not a signal fluctuation phenomenon, the simultaneous events produce a significant amount of signal fluctuations in cross-polarization channel.

In anticipation of the coming era of Integrated Services Digital Network (ISDN), no communications engineers would doubt that satellite systems shall have a role to play in ISDN, particularly in areas of international/domestic connections. The question is, rather, on how significant the role shall be, which is solely dependent on the performance capability of the satellite system. Under the current ISDN concept as defined by CCITT study group XVIII[5], the bit-error-rate (BER) allocation for a Fixed Satellited Service (FSS) transmitting 64 kb/s digital messages over a Hypothetical Reference Digital Path (HRDP) can be summarized as

(1) BER $\leq 10^{-6}$ for more than 98% of any month in one minute interval,

(2) BER $\leq 10^{-3}$ for more than 99.97% of any mouth in one second interval, and

(3) Error Free time exceeding 98.4% of any month in one second interval.

These allocations are extremely stringent a from satellite communications viewpoint. Because of the random behavior of the atmospheric propagations channels, satellite systems may have difficulty in meeting these allocation requirements at a number of earth stations.

To assess the ISDN implications on satellite systems, one has obviously to take account of all foreseeable error-inducing propagation mechanisms, not being limited by a singularly designated propagation anomaly. This "taking account of all foreseeable error-producing propagation mechanisms" is important. It is a concept in contrast to that of conventional approaches of being "parametric" in the sense of isolating propagation mechanisms as separate non-overlapping mechanisms.

IV.4 Small Terminal Considerations

The statement of high bit rate transmission beyond 140 Mbit/s given in Section IV.2 and high availability beyond 99.99% given in Section IV.3 only provides one side for modern digital communications system. The other side is the low bit rate-small antenna-low power-infrequent transmission digital system, which is also on the rise. Two typical examples are the VSAT (Very Small Aperture Terminal) system and the MSAT system, i.e., ultra small aperture terminal mobile communications system.

For the VSAT system [6], the typical antenna size is below 2 meter with an SSPA of smaller than 2 watt transmitting BPSK signals of less than 2400 bit/s among a burst rate of 56 Kbit/s to satellite. One may think such a system is extremely prune to propagation degradations. While this is true, propagation degradation does not become the limiting factor of system design. Rather, the degradation trade-off involve interference, traffic collision, access techniques, etc., in addition to propagations.

Needless to say, coding will play an important role in extenting the system performance under propagation degradations. This is particularly true for land and maritime mobile communications system where the surface and atmospheric multipath effects are severe and highly random. Generally speaking, the degradation consists of frequent shallow fadings of 2 to 3 dB and an occasional, sometimes periodic, deep fadings of 6 to 10 dB [7]. Several parameters are of primary importance: the number of bits in deep fade duration, n_1, and the number of bits in shallow fade duration, n_2, both of which are related to channel data rate and the dynamics of propagation anomalies. The fundamental coding approach is to use FEC (Forward Error Correction) coding with interleave. The purpose of interleaving and de-interleaving is to alter the channel statistics such that the channel appears random to the decoder.

Depending upon whether block coding or convolutional coding is used, the interleaving technique may differ. The block coding case is discussed first. Assuming that the deep fade and the shallow fade durations are constant and periodic, a total of $n_1 + n_2$ bits should be interleaved so that the n_1 bits transmitted during the deep fade duration are totally scrambled throughout the entire period before entering the decoder. The period consists of $(n_1 + n_2)/n$ blocks, with n being the block size. there will be about $n_1 n/(n_1 + n_2)$ bits from the deep fade region. If $n_1 n/(n_1 + n_2) < 1$, some blocks will have no bits which are transmitted during the deep fade duration. The buffer required is approximately $n_1 + n_2$, and can be reduced to approximately $n_1 n$ if $n_1 n < (n_1 + n_2)$. A reasonable, but not optimal, performance can be achieved without total scrambling by allowing certain blocks to have more than $n_1 n(n_1 + n_2)$ bits from the deep fade interval, while some other blocks have zero bits. This can effectively reduce the buffer size. If the maximum number of bits from the interval in block is still less than the minimum distance of the code, the error correcting capability of the code should be able to correct the errors from the deep fade interval. Therefore, the minimum buffer requirement in this case is $n_1 n/d$, where d is the minimum distance of the code.

For the convolutional codes, optimal performance can be achieved if one bit from the deep fade interval is observed each time a decoder makes a bit decision. For convolutional code with convolutional interleaving and threshold decoding, the constraint length of the code, k, is analogous to the block size, n, in block code; therefore, the buffer size for optimal performance is $n_1 k$.

In order to combat the infrequent deep fade scenario more effectively, a concatenated coding scheme may appear attractive. The scheme uses a good random error correcting code as the inner code to ensure that bits transmitted during the shallow fade can be received extremely reliably. The inner code is concatenated with a Reed-Solomon code whose block length is about the same as $n_1 + n_2$, with more parity check bits than n_1. An energy detector may be used to determine the beginning and end of deep fade. Bits received in the interval are deleted. If the data transmitted during nondeep fade intervals are decoded reliably, the cyclic property of the Reed-Solomon code may be used to reconstruct the data lost in the deep fade interval by reencoding the data received during the nondeep fade interval. Since Reed-Solomon codes are maximum distance separable, the effective throughput of the channel is

$n_2/(n_1 + n_2)$ of the nominal channel throughput. This is equivalent to transmit data only during the nondeep fade intervals. Since the transmit side cannot determine a priori when the receive side may experience deep fade and bursts its transmission accordingly, the Reed-Solomon outer code provides a simple solution.

V. Conclusion

In order to make the results useful to digital communications applications, we believe the approach of propagation research has to incorporate system specific considerations. This of course does not mean that a propagationist has to have a complete system description every time he or she undertakes a scattering or diffraction calculations. Rather, it is suggested that the propagation calculation has to be such that the results are part of a module for system impact assessment for various system. Our view is that the propagation trade-off loop as described in Figure 6 will involve at least the following four modules:

* Basic System Module - Which describes antenna, G/T, pointing, power, location, elevation angle, and other basic transmitter/receiver parameters. The module will specify the fundamental service requirement and the basic definition of the link of concern.

* Propagation Module - Which describes the propagation effects. This module will include static descriptions as well as stochastic descriptions at spatial and temporal scales that are critical to the link. The description shall provide parameters that are readily useful for system impact assessment.

* Modulation and Coding Module - Which provides R, BER, throughput conditions that are required for system specific evaluation under known propagation anomalies.

* Optimization Module - Which provides options of adaptive measures for mitigation in a propagation environment. Examples include automatic power control, diversity equalization, polarization compensation, antenna side-lobe nulling, pilot monitoring, and switching, etc.

We believe in the coming ISDN era, propagation research must be aimed for the establishment of the Propagation Module, which is part of the other modules for propagation trade-off evaluations. Such a new approach in propagation study is an important one in the striving for excellence of radio/microwave communications systems in facing the ever-increasing intrusion of optical fiber communications systems.

Acknowledgements - This work is a part of an on-going effort under contract DAAB07-88-C-A007, sponsored by the US Army CECOM at Fort Monmouth, NJ. The views expressed in this paper are not necessarily those of the sponsor.

REFERENCE

[1] Gagliardi, R.M. "Satellite Communications," Van Nostrand Reinhold Company, NY, 1983. ISBN 0-534-02976-0.

[2] Berlekamp, E.R., Peile, R.E. and Pope, S.P. "The Application of Error Control to Communications," IEEE Communications Magazine, Vol. 25, pp 44-57, 1987.

[3] Gill, W.J. "Transmission Engineering Considerations for Digital Microwave Telephony," Telephony, Oct.11, 1976.

[4] Fang, D.J. and Allnutt, J.E. "Simultaneous rain depolarization and ionospheric scintillation impairments at 4 GHz." IEEE Conference Publication No. 274, Part 2, Proceedings of the Fifth International Conference on Antennas and Propagation, pp. 281-284., 1987.

[5] CCITT Study Group XVIII document, Recommendation G. 821, 8th Plenary Assembly, Geneva, June 1985.

[6] Chakraborty, D., "VSAT Communications Network-An Overview," IEEE Communications Magazine, Vol. 26, pp.10-24, 1988.

[7] Fang, D.J., F.T. Tseng and T.O. Calvit. "A Measurement of the MARISAT L-Band Signals at Low Elevation Angles on Board MOBILE AERO," IEEE Trans. Communications, Vol. COM-30, 1982, pp. 359-365.

[8] Fang., and C.H. Liu, "Statistical Characterizations of 4-GHz Equatiorial Scintillation in the Asian Region", Radio Science, Vol. 19, 1984, pp. 345-358.

[9] Sandrin, W.A., and D.J. Fang, "Multipath Fading Characterization of L-Band Maritime Mobile SAtellite Links", COMSAT Technical Review, Vol. 16, pp. 319-338, 1986.

Round Table Discussion
Propagation Effects and Circuit Performance of Military Radio Systems with particular emphasis on those employing Band Spreading

J.S. Belrose (CA) opened the discussion by introducing those at the Table, **C. Goutelard (FR)**, Co-Chairman, with himself, of the Technical Programme Committee, and **M. Darnell (UK)**, who was author/co author of several papers presented during the meeting. He called attention to the fact that a **Round Table Discussion** was a part of AGARD Symposia/Specialists' Meetings. The procedure was that those around the table began the discussion, by commenting briefly on the session they chaired, or on the topic area in which they had a special interest. Their remarks were expected to, in particular, to high-light areas where additional work, a better understanding or more detailed measurements were required. The comments should be somewhat controversial or pose questions so as to stimulate discussion from the Floor. The objective was to give some direction as to where we are going, and to suggest new avenues for propagation research. He noted that he had said **propagation research**, because that was the mandate of the **Electromagnetic Propagation Panel**. However, an emphasis in recent years was on circuit performance in the radio propagation environment, which included radio noise, radio interference, and the performance of antennas in their operational environments. With these few remarks he gave the Floor to Prof. Goutelard.

C. Goutelard (FR) noted that he had followed with a great deal of interest the various subjects dealt with during the session he chaired. The session began by two introductory papers. One by **Col. F.H. Evangelist, USAF** who addressed the general problem of the military requirement for voice and data communications. The overview paper by **J.S. Belrose** reviewed very completely work done in Canada relevant to the theme of the symposium, in the field of radio propagation and communications technologies research. These kick-off papers were followed by a series of more specific presentations. Three were concerned with the high frequency ionospheric channel. **M. Darnell (UK)** spoke first, and then **J.E. Hoffmeyer (US)**. **Y. Le Roux (FR)** was the third speaker on the subject. This was followed by a series of presentations on VHF/UHF propagation, particularly concerned with mobile propagation. More specifically **R.W. Lorenz (GE)** and **J. Citerne (FR)** talked about measurements in the rural/urban area at 900 MHz, and **H. Lakey (US)** dealt with the special problem of propagation through forests. **M. Silvain (FR)** talked about propagation at a much higher frequency 11 GHz. He noted that it was clear that mobile radio communications is an area of strong current interest.

The next paper by **K. Watson (UK)** was concerned with meteor burst communications (MBC), specifically with modelling the characteristics of the channel (by simulation). The last paper by **K.S. Ko (NE)** addressed measurements of radio noise made in a battlefield environment.

By way of additional comment on the presentations C. Goutelard noted that the HF channel (an area in which he has a specific interest) is a dynamically varying channel. It has all the defects that are encountered with other channels, e.g. the mobile radio channel, as well as other defects. It is a is a non stationary anisotropic channel. He noted again the emphasis on mobile radio propagation, particularly in the urban environment, where modelling is very complicated. He commented that there had been no papers on noise, which is a very complex problem, since the signal-to-noise ratio is a fundamental parameter relevant to the performance of a communications system (editor's note: the Effects of Electromagnetic Noise and Interference on the performance of Military Radio Communication Systems was a subject that had been addressed at a recent AGARD/EPP symposium, held in Lisbon, in 1987, ref. AGARD CP 420).

In conclusion C. Goutelard noted that in thinking about the subject area three themes, or three types of questions came to mind: 1) concerning characterization of the channel one needed measurements, measured data; and some new data were presented during the symposium. Are present measurements sufficient? For example in the land mobile band, in the urban environment, where previously we had only a few measurements, we now have some data. Do we

have enough data to characterize the channel? If not what kind of measurements do we need? And, what are we going to do with the results that have been measured? We can question some of the results, we can ask questions to specify or to clarify the presentations given, and we can ask what sort of work is needed in that area? Once we have done with measurement we have to construct models, or design models, and there again we are faced with a number of questions Several models have been presented, very sophisticated models in some cases. In this regard he noted that he was rather astonished by the apparent agreement between calculation, simulation and experiment that **J.E. Hoffmeyer (US)** had found. Why was there such a good agreement? Models are useful, yes, but their use could be dangerous. Models are built on a basis of measurement, and if measurements are incomplete the model will remain incomplete. The same is true for simulators. If the simulator was designed to take into account pertinent characteristics for channels of interest, the simulation can give very good results. If it has not been designed for the objective or purpose the results obtained may not be of sufficient detail to be useful.

M. Darnell (UK) spoke next. He noted that what he did not propose to do was to go through the papers in the session one by one and comment on them. Instead he would try and pick out major themes, and then he would address briefly four areas which particularly struck him as areas requiring more attention, or perhaps in some cases a rethink of our attitudes in terms of system design. The main topics covered in Session Two, which was concerned with New Approaches to Communications System Design, were. system design and control methodologies, the integration of real time channel evaluation information, voice processing, spectrum spreading techniques (both frequency hopping and direct sequence), multiple access techniques; error control both in terms of basic algorithms and also implementation practice; synchronization; and the problems of countering interference practically. He noted that one of the things that struck him as being very important was a remark made by **Colonel Evangelist** in his key note talk the first day, when he said that he thought that the emphasis now in terms of NATO communications requirements ought to be on the reduction of data to be transmitted. Clearly this is a remarkable change in philosophy. In earlier years the emphasis in the Military had been on the provision of facilities to transfer **more-and-more data more-and-more efficiently**. Now we are told by an operational officer that in fact the emphasis ought to be on the reduction of data to be transmitted, or at least heavy filtering of the data to be transmitted over radio communications channels. This represents quite a radical change in attitude which if implemented would certainly impact communications system design. The remark made makes sense, since the more-and-more data one transmits, the more-and-more vulnerable the communication systems become, in very general terms. In this context, M. Darnell noted, it is perhaps significant that only one paper addressed the subject of data compression, or information compression, and that paper by **L. Boucher (CA)** was concerned with frequency compression of the voice signal, that is bandwidth reduction, rather than minimization of the input data rate to the communications system.

A second point was concerned with the area of the complexity of modern communications system design. There is still in the communications community a general resistance to complexity, because of the concern that complexity may lead to unreliability, or to systems that are difficult to control. However, it is complexity that opens the door to the realization of performance improvement. A good illustration of this was the Thompson CSF paper on the Reed Sullivan BCH coding system. The integrated circuits, the chips required for that system are rather complex devices, yet they can be fabricated and implemented in a reasonably economical manner. Digital signal processing is opening up new frontiers in the design of communication systems.

The third area was that of synchronizatic which has become a topic on its own as communication systems change from analogue to dig We need to think/look at all possible methods of abstracting synchronization data from the elements of the communications system, demodulators, decoders, and etc., and put these together to improve the overall synchronization characteristics of the communications system.

In conclusion, M. Darnell continued, that the fourth area related to some of the comments that Professor Goutelard has just made, and that was the whole area of characterization of channels, both off-line and on-line channels. Here we are always requiring better data bases for off-line models, and better techniques for channel evaluation for on line characterization. The objective is to improve the performance of real communication systems in their operational environments.

There is too much attention given to operation in the **ideal channel**, that is thinking of performance in terms of the Shannon limit and gaussian white noise. **D. Fang (US)** pointed out some of the problems with that approach in his paper. The Shannon limit makers certain assumptions about the nature of the communication channel, it makes certain assumption about the channel bandwidth profile, about the distribution of signal and noise energy within the channel, and so on. Also one tends to think of modulation and coding schemes in terms of a ranking in a gaussian white noise environment. That ranking order may well not be applicable, in fact it may be that a quite different ranking order is needed when we have non-gaussian noise. We need to characterize both radio propagation and radio noise and interference, with particular emphasis on interference in order to make sensible decisions about the type of communication system we should adopt for use in particular signal environments. So the final area then is the whole business of better characterization of the channel, including propagation, noise and interference.

J.S. Belrose (CA) commented on the session he chaired, System Performance. In that session various authors had briefly addressed a variety of subjects ranging from HF to EHF, terrestrial as well as satellite systems. He noted that the paper on packet radio had attracted quite a lot of attention. Clearly if packet radio in a military environment is going to be looked at in the detail it deserves, model studies should be more realistic. For example the propagation model should be based on a digital terrain profile. Interference which is a major concern for frequency hop radio needs to be realistically studied, and noise models should better relate to real battlefield scenarios.

Concerning meteor burst communications, he wondered whether new approachs were needed. A basic problem particularly at the higher frequencies was through-put. **P. Cannon (UK)** had remarked that while overdense trails were n very frequent, they were an important consideration. Fading and multi-path was a problem for the longer duration trails. Perhaps what was needed was an adaptable variable rate communications system, employing spread spectrum to overcome the multi-path problem. Multi-path was a particular problem for MBC systems operating in the high latitude region, for transauroral paths, since off path reflections from field aligned irregularities (he noted that he was referring to early Canadian work) frequently severely limits the data rate that could be used.

He noted that the text for the theme of the meeting stated: "the importance of understanding radio wave propagation increases as communications systems become more complex;" and that "the flexibility offered by software implementation makes them ideal vehicles to realize and optimize new approaches. But these realizations can only be achieved by the communications engineer if those conducting propagation research keep pace with the increasing more detailed knowledge needed to specify, and quantify the channel characteristics." These are good motherhood statements, made by those doing propagation research, but what new knowledge on the characteristics of the channel is needed by those designing new sophisticated communications systems? Certainly we heard at this meeting papers by communications engineers on the design of new modems, that employed sophisticated signal processing to combat errors introduced by the propagation environment, but except for acknowledging that multi-path was a problem, channel modelling or the use of channel models was not a part of the design. In fact the trend seemed to be to design systems that would work in-spite-of the limitations of the channel. This subject will be specifically addressed at our meeting next spring, in San Diego, CA. Perhaps in the mobile radio area we have the closest ties between those conducting propagation research and those designing communications systems, but even here we need to improve these ties.

Finally J.S. Belrose noted that he would comment on one topic which he felt needed to be better addressed. This topic related to an emphasis of the meeting which was supposed to specifically address systems employing frequency spreading. There are two kinds of systems employing frequency spreading: frequency hoppers and direct sequence spread spectrum. Both are used for secure communications. For frequency hoppers there is a problem with collisions, that is two signals trying to occupy the same channel at the same time. Spread spectrum systems, particularly in-band spread spectrums, have seen some application for overcoming multi-path. Wide band spread spectrum systems provide not only this immunity, but can enhance the low probability of intercept; i.e. when the transmitter power is spread out over a very wide band the signal effectively disappears into the noise and interference background. In this case we need to know how many signals can in effect be piled on top of each other before the multiplicity of

systems start to degrade themselves. This topic was raised at our Lisbon meeting, about a year ago, but no clear picture has so far emerged. He noted that some people seem to consider that these two types of systems are synonymous, but that in his view there are clear differences.

Concerning the performance of radio communication systems, he noted that in his overview paper he had specifically addressed the use of channel simulators for such studies of performance evaluation, and that sitting with him at the round table **Prof. Goutelard** had specifically commented on HF channel simulators. He noted that one type of simulator that did not depend on having a detailed knowledge of the channel was a recorder type simulator. One could envisage having a library of such recordings to characterize a wide range of ionospheric propagation conditions; for example, recordings made over equatorial paths; mid-latitude paths; high latitude paths, particularly trans-auroral zone paths; short paths, and long paths; and recordings made at times of severe doppler shift, doppler broadining and signal fading. The recorder type channel simulator could then be used to optimize system performance for the propagation conditions characteristic of paths where it would be used.

With these concluding remarks he asked for discussion from the floor.

R. Bultitude (CA): Each one of you has asked the question whether we need to collect more data and what do we do with it, if we get it? This is a very important topic. I have not seen very many propagation reports where the authors have actually explained in their paper how propagation information should be used to predict system performance, and indeed except for channels that do not severely distort the signal I don't think anybody knows exactly how to make such predictions. There should be much more effort in this direction, and when predictions are made there is great deal of work to be done to verify the predictions. As Dr. Fang has mentioned we should be able to work with the systems engineer and tell him if for example we give him five parameters he can expect to be able to predict the performance of his digital communications system when transmitted through a certain type of propagation channel.

P. Mundy (UK): Concerning the subject of how much propagation research do we need and how do we use the results, this is a very big topic. Perhaps I can give one example, during the course of the recent development of a particular system, where a large number of organizations decided to get involved. What basically happened was perhaps summed up by Dr. Fang's last graph, where he showed the interaction between the system designers and the propagation researchers. Each organization did their own propagation research and their own system design, simultaneously with often the same team of engineers. While there was a fair degree of duplication of effort, and a large expenditure of resources on research, the end result was I think worth the effort, although only time will tell. The interaction between the system designer and the propagation researcher was the key to a successful system development.

C. Goutelard (FR): I would like to say that I fully agree with what you have just said, and also with what Dr. Bultitude said. However, there is clearly a problem with the co-ordination of research and development effort. In my own personal experience I am often called upon to give my opinion, on for example coding. But the engineers come to see me only after they have already developed the communications system and field trialed it. During the field trial they have observed that under certain circumstances the system did not work very well; there were too many errors. But they came to see me as one would see a doctor, with the hope that by using an error correcting code, for example, one can cure the problem. But it is too late to see the doctor at the time the patient is about to die. You must go to the doctor before. We can extend this notion. There are three types of people that have to interact: First, there are the radio physics specialists. They have the wide expertise concerning electromagnetic propagation phenomena. Next, there are the theoreticians. They are given data and they try to fit the data to formula, very clever formula that summarize and quantify everything. And then there are the design engineers, who have to design, develop and put together a system which must have a minimum of complexity for a given requirement. This is what Prof. Darnell was saying. But for a given operational complexity the technology complexity should be a minimum. These three types of physicists/engineers have to work together. But this is difficult, because within a company this type of co-ordination does not always happen, even within the same department of a company.

Finally I would like to ask a question about meteor burst communications. Have any studies been made to measure the reciprocity of the channel, because this is a very important factor for the development of such systems?

P. Cannon (UK): No, I do not know of any studies that have been made to specifically measure channel reciprocity. There are however a few comments that can be made, based on current knowledge. First, of course, the noise levels at the two sites may be different. Secondly, the transmission path is generally assumed to be a coherent path of wide bandwidth. But for the meteor trails of longer duration, longer than say 1/2-second, Raleigh fading sets in; and so one can say that reciprocity will not exist, and that perhaps diversity would provide a means of increasing through put.

I would like to come back to an earlier comment made by Dr. Belrose concerning the need for high data rates, and the development of adaptive data rate systems. One problem with developing higher data rate systems is that the channel model has to be good for the development of better algorithms. The use of simple models that, for example, assume simply overdense trails, or underdense trails is inadequate. This is where off-air simulators are very useful for control simulators. It is very difficult to produce a deterministic meteor burst model.

J. S. Belrose (CA): I was referring more to the need for a real time channel evaluation in association with meteor burst systems, rather than to an improvement of models.

P. Cannon (UK): Yes, but I thought you made both comments. With regard to real time channel evaluation, that sort of idea is being pursued both in the UK and in the USA. One problem of course with high data rates is the need for wider bandwidths, and I think that scientists/engineers are well aware of the problems of frequency allocations. This is a problem with the present low power MBC systems, and it will be more of a problem if high power MBC systems come into operational use.

S. Ganguly (US): Have frequencies greater than 100 MHz been used for MBC? And if we increase the power can we increase the range of MBC systems?

J.S. Belrose (CA): In answer to your first question, yes, in experimental systems operated (in earlier years) in Canada. But the through put falls off very rapidly for frequencies > 100 MHz. There are two problems. one is that the burst durations are very short, and secondly there are few such dense trails.

P. Cannon (UK): The USAF Geophysics Laboratory are operating a research MBC system in Greenland, and they do use frequencies slightly greater than 100 MHz. Radio amateurs have reported on meteor burst communications using the 2M band radio amateur band (the 144 MHz band). So there are some measurements/some observations at frequencies above 100 MHz.

S. Ganguly (US): My next comment concerns modelling. The MBC channel has I believe been fairly adequately modelled. For the ionospheric channel one is able to develop physical models based on physical parameters. For urban land mobile, why can't one model a city, put it in a computer and predict the characteristics of the channel?

J. Hoffmeyer (US): I have several comments in response to various remarks made by the chairmen concerning channel modelling. Firstly, a pertinent question to ask is what additional information is needed? One area we are looking into that has not been addressed at this meeting is the need for multipath measurements on land mobile satellite channels. The commonly used technique to use a channel probe using a PN sequence is not very easily done on a satellite channel. We have a program at my Institute to make such measurements, using a global positioning satellite signal; which is using a PN sequence that results in a multi-path delay spread typical of mobile satellite communications channels. This is in support of the engineers who need such data for the development of mobile satellite receiving systems, which of course employ very small aperture antennas.

A second comment concerns the concept of design for the worst case. While this is something we want to do ideaiy, it may not be the optimum design. For example, if one is designing an HF modem that will never be employed for trans-auroral type of paths, there is no use in using a sophisticated modem when a simpler design will do.

Concerning channel simulation, the channel simulator is another area where the propagation researchers can interact with the systems design engineers. I have a figure in my paper, that I did not present during my talk, that shows the interaction between the modeler and the communication system designer. For example one could develop a software model of a channel, say an HF channel for example, and at the same time develop a hypothetical communication system, and so synthesize performance. This approach could be compared with the use of a hardware channel simulator and a physical real communications system. There are clearly advantages and disadvantages to both approaches.

AEG (FRG): A comment was made by a scientist/engineer from AEG, a company that is presently concerned with the development of a packet switched VHF radio system. He noted that comments made by Drs. Belrose and Darnell were most appropriate. An important problem for circuit design is to specify the amount of data that should be transmitted. Clearly the less data the better the network. He noted that he would like to comment on remarks made by Prof. Goutelard concerning data reduction and data compression. There is a significant difference between these two operations. Data compression does not degrade the information content, it only degrades the quality of the reception. Whereas data reduction changes the information resolution. For a battlefield commander it is very difficult for him to reduce data because of the resolution that is needed. The degree to which data can be reduced can only be determined by field trial.

A second point, which also affects the definition of a packet switched network, concerns the error bounds. What error rate can one tolerate? There are at least three levels. The lowest level is the speech error that one can tolerate, because speech is inherently redundant. The next level is the error you can tolerate in transmission of digital data, for the situation where the transmission can be repeated by means of ARQ protocol. The third level concerns the transmission of data over a link where the requirement is such that you cannot ask for a repeat transmission, like for instance in the Norwegian network, the PROP packets are not acknowledged, or only indirectly acknowledged. Clearly for this latter requirement the error rate must be small. What bounds do we have? He noted that he was clearly struck by a view graph presented by den Brinker which tried to set such bounds. For speech, he recalled, the acceptable error rate was something like 10^{-2}; for computer communication 10^{-6}. Clearly this is an area that requires further work. What bounds can one set for realistic communications requirements?

His third comment concerned realistic simulation. He noted that if you ask the user to give some parameters his response is "I do not know because it is a new system." One of the most important parameters is the amount of erlangs that has to be transmitted, because if you know the erlangs you can define the system If you have a new system no one can define the erlangs you need. So either you under estimate or over estimate. It is very difficult.

J.S. Belrose (CA): Your points are well taken. At Thompson CSF yesterday we saw a graph that showed how data rates have dramatically increased with time. If we project this curve into the future we rapidly project the curve off the top of the graph. At some point in time we are going too fast, for radio communications.

P. Cannon (UK): I would like to make comment on what has been said. I agree. I tried in my remarks to make the distinction between compression that occurs at the input to the system by virtue of operational procedures, and compression which the system designer has at his control, for example if the input signal is a voice signal the designer can try and compress that by so much, to narrow the transmission bandwidth.

What I would advocate, however, is that as operational procedures develop, suppose that one does develop operational procedures, that result in less data input to the system, by use of message coding more efficiently, or whatever it may be; clearly the communications system designers

aught to be in constant dialogue with the users because as we reduce the load to the input of the system we make our communications systems more effective.

J.S. Belrose (CA): On that note, and looking at the time which is past the allotted time for this round table discussion, we should conclude. Let me end the discussion in a somewhat humorous vane, perhaps somewhat facetious, I am no expert on the subject. We have been told during this meeting, if we say that our technical visit was a part of the meeting, about two methods to compress the bandwidth of a voice signal. **L. Boucher** spoke about dynamic windowing in the frequency domain; and yesterday during our visit to **Thompson CSF** we were told about, and had the opportunity to test an 800 Hz LPC (linear predictive code) system. I am biased toward the former, which is a Canadian developed technology. However my Laboratory has done a great deal of work on LPC, but wider bandwidth systems (2400 b/s and 4800 b/s data rates). Let me comment on the Thompson CFS 800 Hz LPC system. I spoke with my colleague Luc Boucher using this system. Luc was speaking to me in English, but with a French accent, because I do not speak French. When we switched to the 800 b/s system Luc said "I cannot understand a thing you are saying." In spite of the fact that he was speaking in English I could understand what he was saying, so it must have been his accent. Perhaps the code-book was optimized for the French language. If this is a correct conclusion than this a problem with LPC when pushed to the limit, especially for NATO, since we will have to have a code-book optimized for each language used by the NATO nations!! An alternative explanation (note added in proof) is that English speaking people more or less understand what is said no matter how badly the speaker speaks English or with whatever accent.

The Chairman thanked all those who had contributed to the discussion.

LIST OF PARTICIPANTS

Dr Ing H.J.ALBRECHT	FGAN, Neuenahrer Straße 20, D-5307 Wachtberg-Werthhoven, Germany
Maj. T.ALTAY	3 NCU Hava Ikmal ve Bakım, Merkezi K. Lığı, Etimesgut, Ankara, Turkey
Mr F.ALTMAN	Cybercom Corp., 4105 Fairfax Drive, Arlington, VA 2203, United States
Mr P.ANGLADE	ETCA/CTME, 116, Av. Prieur de la Côte d'Or, 94114 Arcueil, France
Lt. G.ARPAIA	DASRS—RSV, Aeroporto "M. de Bernardi", Pratica di Mare, Rome, Italy
Mr F.BARRIER	Thomson CSF, Div. Telecom., 66, rue du Fosse Blanc BP 156, 92231 Gennevilliers, France
Mr J.C.BAYETTO	SETICS, 194, rue de Tolbiac, 75013 Paris, France
Dr J.S.BELROSE	Communications Research Centre, Station H, PO Box 11490, Ottawa, ON, K2H 8S2, Canada
Mr A.BERTHON	Ste AERO, 3, Av. de l'Opéra, 75000 Paris, France
Mr J.C.BIC	CNET/PAB/RPE, 38—40 rue du Général leclerc, 92131 Issy les Moulineaux, France
Mr A.BISSET	Marconi Secure Radio, Browns Lane, The Airport, Portsmouth PO3 5PH, United Kingdom
Mr E-Y.BLANCHARD	ELECMA, 15 rue Pages, BP 305, 92156 Suresnes, France
Prof. L.BOSSY	174, Av. W. Churchill, UCL, 1180 Bruxelles, Belgium
Mr L.BOUCHER	Communications Research Centre, Station H, PO Box 11490, 3701 Carling Avenue, Ottawa, ON, K2H 8S2, Canada
Mr A.N.BRYDON	Dept. of Electrical Engineering & Electronics, UMIST, PO Box 88, Manchester M6O 1QD, United Kingdom
Dr R.J.BULTITUDE	Communications Research Centre, Station H, PO Box 11490, 3701 Carling Avenue, Ottawa, ON, K2H 8S2, Canada
Mr M.BURLAS	CERTEL/PIPADY, DCAN, BP 77, 83800 Toulon Naval, France
Dr P.S.CANNON	Flight Management Dept., Royal Aerospace Establishment, Farnborough, Hants GU14 6TD, United Kingdom
Dr J.CARATORI	L.E.T.T.I., BP 16, 94230 Cachan, France
LTC. A.CASSARA'	Aeronautica Militaire, DASRS—Rep. Armamento, I-00040 Pratica di Mare, Rome, Italy
Mr Y.CHAMINADAS	EMA, 14, rue Saint Dominique, 75997 Paris Armées, France
Ing.Gen. P.CHEVALIER	Inspecteur Général, ONERA, 29, Av. de la Division Leclerc, 92320 Châtillon-Sous-Bagneux, France
Mr F. CHRISTOPHE	Dept. Micro-Ondes, ONERA-CERT, BP 4025, 31055 Toulouse Cedex, France
Prof. J.CITERNE	INSA/LCST, 20 Av. des Buttes de Coesmes, 35043 Rennes Cedex, France
Mr J.L.COATANHAY	ENSIETA, Pontanezen, 29240 Brest Naval, France
Capt. A.COIMBRA DOS SANTOS	CLAFA/DE, Base de Alfragide, 2700 Amadora, Portugal
Mr C.COLLIN	ATFH/ALCATEL, 55, rue Greffulhe, 92301 Levallois Perret, France
Mr J.C.COUDERC	ETCA/CTME S2, 116, Av. Prieur de la Côte d'Or, 94114 Arcueil, France
Mr G.COURIAULT	La Vallée du Parc, Zone Industrielle, BP 249, 37602 Loches Cedex, France
Mr V.J.COYNE	Riverside Research Institute, 200 Liberty Plaza, Rome, NY 13440, United States
Dr T.A.CROFT	SRI International, 333, Ravenswood Avenue, Menlo Park, CA 94025, United States
Mme A.DANIEL	INSA/LCST, 20, Av. des Buttes de Coesmes, 35043 Rennes Cedex, France
Prof. M.DARNELL	Dept. of Electronic Engineering, University of Hull, Hull HU6 7RX, United Kingdom
Mr G.O.DEUBACH	FGAN, Neuenahrer Straße 20, D-5307 Wachtberg-Werthhoven, Germany
Mr B.DURAND	Thomson CSF/DTC, SNI/LHN, 66, rue du Fosse Blanc, 92231 Gennevilliers, France
Lt. G.B.DURANDO	MARITELERADAR, Viale Italia 72, Livorno, Italy
Mr C.S.Den BRINKER	Technology Director, Rediffusion Radio Systems Ltd, Newton Road, Crawley, W Sussex RH10 2TU, United Kingdom

Col. F.H.EVANGELIST Jr.	Chief, Cz Requirements Sec. Operation Division, SHAPE, OPS DIV/ORX, B-7010 Mons, Belgium
Mr D.FANG	4300 Montgomery Ave, Suite 203 A, Bethesda, MD 20817-4402, United States
Mr R.FLEURY	CNET, Route de Trégastel, BP 40, 22300 Lannion, France
Mr M.FOURNIER	LCTAR, 6, rue Nieuport, 78140 Vélizy Villacoublay, France
ICA. P.FUERXER	DRET, Chef Groupe 2, Télécom. et Détéction, 26, Bd Victor, 75015 Paris, France
Mr S.GANGULY	Center for Remote Sensing, 503-8200 Greensboro Drive, Mclean, VA 22102, United States
Mr B.GOBERT	AEG, A124 E6, Sedanstraße 10, D-7900 Ulm, Germany
Dr GOLE	CNET/PAB/RPE/ETP, 38—40 rue du Général Leclerc, 92131 Issy les Moulineaux, France
Mr C.A.GONCALVES	Instituto Nac. de Meteo. e Geofis., Rua C do Aeroporto. 1700 Lisboa, Portugal
Mr P.Y.GONZALES	55, rue Greffulhe, 92301 Levallois Perret, France
Mr L.GOSSELIN	National Defence HQs, CRAD/DIRD-3, 101 Colonel By Drive, Ottawa, ON, K1A OK2, Canada
Dr G.F.GOTT	Dept. Electrical Eng. & Electronics, UMIST, PO Box 88, Manchester, M6O 1QD, United Kingdom
Prof. C.GOUTELARD	Directeur L.E.T.T.I., Université Paris-Sud, 9, Av de la Division Leclerc, 94230 Cachan, France
Mr E.GUERDENLI	British Telecom Research Labs, Martlesham Heath, Ipswich IP5 7RE, United Kingdom
Mr J.HAGUE	Dept. of Electronic Engineering, University of Hull, Hull HU6 7RX, United Kingdom
Dr R.HANBABA	CNET/LAB/MER/SPI, 22301 Lannion Cedex, France
Mr R.M.HARRIS	Room 6C, P161, FM Dept., Royal Aerospace Establishment, Farnborough, Hants GU14 6TD, United Kingdom
Mr J.HOFFMEYER	Institute for Telecom. Sciences, NTIA/ITS N2, 325 Broadway, Boulder, CO 80303, United States
Mr A.JOISEL	ONERA, BP 72, 92322 Châtillon Cedex, France
Mr J.P.JOLIVET	CNET/LAB/MER/GER, Route de Trégastel, 22301 Lannion, France
Mr G.KANTOROWICZ	Thomson CSF, 31 rue Camille Desmoulins, 92132 Issy les Moulineaux, France
Mr R.KAPAMADJIAN	SEFT Fort d'Issy, 18, rue du Dr. Zamenhoff, 92131 Issy les Moulineaux, France
Mr R.J.KEEFE	GEC Sensors Ltd, Airadio Products Div., Christopher Martin Road, Basildon, Essex SS14 3EL, United Kingdom
Mr K.S.KHO	Physics and Electronics Lab TNO, PO Box 96864, 2509 JG The Hague, Netherlands
Dr E.KRIEZIS	Dept. of Electrical Engineering, Faculty of Technology, Aristotle Univ. of Thessaloniki, GR 54006 Thessaloniki, Greece
Mr L.LADOUX	Thomson CSF/DTC, 66 rue du Fosse Blanc, 92231 Gennevilliers Cedex, France
IETA. L.LANGOT	DRET, Groupe 2, Telecom. et Detection, 26, Bd Victor, 75015 Paris, France
Mr LAURENT	Thomson CSF, Division Télécommunications, 26, rue du Fosse Blanc, 92231 Gennevilliers Cedex, France
Mr. J.C.LE JANNIC	CELAR, 35170 Bruz, France
Dr Y.LEROUX	CNET/LAB/MER/GER, Route de Trégastel, BP 40, 22301 Lannion, France
Dr A.LEVY	CNET/PAB/RPE, 38—40 Av du Général Leclerc, 92131 Issy les Moulineaux, France
Mr J.LILLETROEN	R. No. Material Command, PO Box 10, N-2007 Kjeller, Norway
CDR D.M.LING	OPS DIV., SHAPE, B-7010 Mons, Belgium
Dr Ing. R.W.LORENZ	FTZ, FI 32, Postfach 5000, D-6100 Darmstadt, Germany
Mr R.MAKARUSCHKA	FGAN/FHP-GA, Neuenahrer Straße 20, D-5307 Wachtberg-Werthhoven, Germany

Mr M.MALAQUIN	CERTEL/DCAN, BP 77, 83800 Toulon Naval, France
Mme C.MARTEAU	CERTEL/PIPADY, DCAM, BP 77, 83800 Toulon Naval, France
Dr J.L.MASSON	TRT, DAAC/AES, 5, Av de Réaumur, 92350 Le Plessis Robinson, France
Mr R.MAUGIS	NARDEUX, Av. d'Islande, Z.A. de Courtaboeuf, 91940 Les Ulis, France
Mr J.F.MISSANA	L.E.T.T.I., 9, Av de la Division Leclerc, 94230 Cachan, France
Mr R.MOCAER	Thomson CSF/AVG, 31, rue Camille Desmoulins, 92132 Issy les Moulineaux, France
Mr P.J.MUNDAY	Racal Research Ltd, Worton Drive, Worton Grange Industrial Estate, Reading, United Kingdom
Mr J.NICLOT	CIREM, 18, rue du Dr. Zamenhoff, 92131 Issy les Moulineaux, France
Mr G.OSSEWAARDE	Physics and Electronics Lab. TNO, Oude Waaldorperweg 63, 2509 JG The Hague, Netherlands
Dr J. PAPET-LEPINE	Adj. Dir. CNET, Centre LAB, BP 40, 22301 Lannion, France
Mr J.F.PATRICIO	D.G. Telecomminicaçoes dos CTT, Av. Fontes Pereira de Melo, 40, 1089 Lisboa Codex, Portugal
Mr J.E.RASMUSSEN	AFGL/LID, Hanscom Air Force Base, MA 01731, United States
Dr P.REITBERGER	Rohde und Schwarz GmbH & Co KG, Dep. 6E, Mühldorfstraße 15, D-8000 München 80, Germany
Dr J.H.RICHTER	Head, Ocean & Atmospheric Sciences Division, NOSC, Code 54, San Diego, CA 92152-5000, United States
Mr B.ROBERT	ONERA, BP 72, 92322 Châtillon Cedex, France
Mr H.ROMANET	ETCA/CTME S2, 116, Av. Prieur de la Cote d'Or, 94114 Arcuil, France
Dr Ing. D.K.ROTHER	SEL Pforzheim, Ostendstraße 3, D-7530 Pforzheim, Germany
Mr N.E.RUELLE	CNET/LAB/MER/GER, Route de Trégastel, 22301 Lannion, France
Mr J.E.RUSTAD	NDRE, PO Box 25, N-2007 Kjeller, Norway
Mr D.SCHOLZ	Direktor NARFA, Fernmeldeamt BW — NARFA GE —, Münstereifeler Str. 75, D-5308 Rheinbach, Germany
Mr B.SEBILET	ELECMA, 15, Av. Pages, BP 305, 92156 Suresnes Cedex, France
Mr P.SEHIER	55, rue Greffulhe, 92131 Levallois Perret, France
Mr U.SEIER	ANT Nachrichtentechnik GmbH, Gerberstraße 33, E 325, D-7150 Backnang, Germany
Mr P.SICILIA	Thomson CSF Div. Telecom., 66, rue du Fosse Blanc, BP 156, 92231 Gennevilliers Cedex, France
Mr H.SIZUN	CNET Lannion, route de Trégastel, 22000 Lannion, France
Dr H.SOICHER	US Army, CECOM, AMSEL-RD-C3-TR-4, Fort Monmouth, NJ 07703, United States
Mr D.SORAIS	Thomson CSF Div. Telecom., 66, rue du Fosse Blanc, BP 156, 92231 Gennevilliers Cedex, France
Col. C.R.SPRENKELS	Etat-Major de la Force Aérienne, Section Comm. et Electronique (VDM), Quartier Reine Elisabeth, B-1140 Bruxelles, Belgium
Mr R.D.STEWART	Dept. of Electronics and Computer Science, The University, Southampton SO9 5NH, United Kingdom
Mr K.N.STOKKE	Statens Teleforvaltning, Parkveien 57, Postboks 2592 SOLLI, 0203 Oslo 2, Norway
Mr O.H.STOREN	NDRE, PO Box 25, N-2007 Kjeller, Norway
Mr O.STROEMSNES	Norwegian Navy Material Command, N-5078 Haakonsvern, Norway
Dr M.SYLVAIN	CNET/PAB/RPE, 38—40 rue du Général Leclerc, 92132 Issy les Moulineaux, France
Mr J.C.TEIGLAND	Royal Norwegian Air Force, Material Command, PO Box 10, N-2007 Kjeller, Norway
Mr T.THORVALDSEN	Norwegian Defense Research Establishment, PO Box 25, N-2007 Kjeller, Norway
Dr C.TOKER	Dept. of Electrical Engineering, Elektrik Muh. Bolumu, ODTU, Ankara, Turkey

Mr J.P.TORCHUT	GERPI Informatique, 16, rue des Chênes, 35830 Betton, France
Mr J.A.VAN DER BLIEK	Director, AGARD, 7, rue Ancelle, 92200 Neuilly sur Seine, France
Mr P.A.VAN DER VIS	FEL-TNO, PO Box 96864, 2509 JG The Hague, Netherlands
Mr J.P.VAN UFFELEN	TRT, BP 21, 92350 Le Plessis Robinson, France
Mr G.VENIER	Communications Research Centre, Station H, PO Box 11490, Ottawa, ON, K2H 8S2, Canada
Ir. H.VISSINGA	Physics and Electronics Lab. TNO, PO Box 96864, 2509 JG The Hague, Netherlands
Prof C.VLOEBERGHS	Ecole Royale Militaire, Av de la Renaissance, 30, B-1040 Bruxelles, Belgium
Mr K.WATSON	c/o Department of Electronic Engineering, University of Hull, Hull HU6 7RX, United Kingdom
Prof K.C.YEH	EL, University of Illinois, 1406 W Green Street, Urbana, IL 61801, United States

REPORT DOCUMENTATION PAGE			
1. Recipient's Reference	2. Originator's Reference AGARD-CP-442	3. Further Reference ISBN 92-835-0511-5	4. Security Classification of Document UNCLASSIFIED

5. Originator	Advisory Group for Aerospace Research and Development North Atlantic Treaty Organization 7 rue Ancelle, 92200 Neuilly sur Seine, France
6. Title	PROPAGATION EFFECTS AND CIRCUIT PERFORMANCE OF MODERN MILITARY RADIO SYSTEMS WITH PARTICULAR EMPHASIS ON THOSE EMPLOYING BANDSPREADING
7. Presented at	the Electromagnetic Wave Propagation Panel Symposium held in Arcueil (Paris), France, 17—21 October 1988.

8. Author(s)/Editor(s)	9. Date
Various	December 1989
10. Author's/Editor's Address	**11. Pages**
Various	436

12. Distribution Statement	This document is distributed in accordance with AGARD policies and regulations, which are outlined on the Outside Back Covers of all AGARD publications.

13. Keywords/Descriptors

Propagation	Man-made noise
Radio systems	Synchronization techniques
Bandspreading	Communication systems design

14. Abstract

The importance of understanding radio wave propagation increases as radar and communication systems become more complex, i.e. digital systems, frequency adaptive systems, spread spectrum systems, etc. Increasingly wider frequency bandwidths are used in modern military systems.

Signal processing for modern systems can be realized in software, employing digital signal processing chips to perform the required modulation and demodulation processes. The recent development of such signal processors is radically changing the engineering approach to designing communications equipment.

Advanced realizations for tactical communications in modern armies, now include digital transmission, voice and data capability and ECM resistant systems. Various techniques such as coding encryption, spread spectrum, are needed to enhance security of communications and to improve resistance to jamming. The adaptability to the varying channels conditions, such as mobile radio communications or real time channel evaluation, requires a better knowledge of the propagation medium.

The meeting examined the state-of-the-art in development of present day radio communication systems, the role and the need for radio propagation research; assessed the effects of propagation on existing systems and proposed how new systems can be improved to meet operational requirements.

AGARD Conference Proceedings No.442 Advisory Group for Aerospace Research and Development, NATO PROPAGATION EFFECTS AND CIRCUIT PERFORMANCE OF MODERN MILITARY RADIO SYSTEMS WITH PARTICULAR EMPHASIS ON THOSE EMPLOYING BANDSPREADING Published December 1989 436 pages The importance of understanding radio wave propagation increases as radar and communication systems become more complex, i.e. digital systems, frequency adaptive systems, spread spectrum systems, etc. Increasingly wider frequency bandwidths are used in modern military systems. Signal processing for modern systems can be realized in P.T.O	AGARD-CP-442 Propagation Radio systems Bandspreading Man-made noise Sychronization techniques Communications systems design	AGARD Conference Proceedings No.442 Advisory Group for Aerospace Research and Development, NATO PROPAGATION EFFECTS AND CIRCUIT PERFORMANCE OF MODERN MILITARY RADIO SYSTEMS WITH PARTICULAR EMPHASIS ON THOSE EMPLOYING BANDSPREADING Published December 1989 436 pages The importance of understanding radio wave propagation increases as radar and communication systems become more complex, i.e. digital systems, frequency adaptive systems, spread spectrum systems, etc. Increasingly wider frequency bandwidths are used in modern military systems. Signal processing for modern systems can be realized in P.T.O	AGARD-CP-442 Propagation Radio systems Bandspreading Man-made noise Sychronization techniques Communications systems design
AGARD Conference Proceedings No.442 Advisory Group for Aerospace Research and Development, NATO PROPAGATION EFFECTS AND CIRCUIT PERFORMANCE OF MODERN MILITARY RADIO SYSTEMS WITH PARTICULAR EMPHASIS ON THOSE EMPLOYING BANDSPREADING Published December 1989 436 pages The importance of understanding radio wave propagation increases as radar and communication systems become more complex, i.e. digital systems, frequency adaptive systems, spread spectrum systems, etc. Increasingly wider frequency bandwidths are used in modern military systems. Signal processing for modern systems can be realized in P.T.O	AGARD-CP-442 Propagation Radio systems Bandspreading Man-made noise Sychronization techniques Communications systems design	AGARD Conference Proceedings No.442 Advisory Group for Aerospace Research and Development, NATO PROPAGATION EFFECTS AND CIRCUIT PERFORMANCE OF MODERN MILITARY RADIO SYSTEMS WITH PARTICULAR EMPHASIS ON THOSE EMPLOYING BANDSPREADING Published December 1989 436 pages The importance of understanding radio wave propagation increases as radar and communication systems become more complex, i.e. digital systems, frequency adaptive systems, spread spectrum systems, etc. Increasingly wider frequency bandwidths are used in modern military systems. Signal processing for modern systems can be realized in P.T.O	AGARD-CP-442 Propagation Radio systems Bandspreading Man-made noise Sychronization techniques Communications systems design

software, employing digital signal processing chips to perform the required modulation and demodulation processes. The recent development of such signal processors is radically changing the engineering approach to designing communications equipment. Advanced realizations for tactical communications in modern armies, now include digital transmission, voice and data capability and ECM resistant systems. Various techniques such as coding encryption, spread spectrum, are needed to enhance security of communications and to improve resistance to jamming. The adaptability to the varying channels conditions, such as mobile radio communications or real time channel evaluation, requires a better knowledge of the propagation medium. The meeting examined the state-of-the-art in development of present day radio communication systems; the role and the need for radio propagation research; assessed the effects of propagation on existing systems and proposed how new systems can be improved to meet operational requirements. ISBN 92-835-0511-5	software, employing digital signal processing chips to perform the required modulation and demodulation processes. The recent development of such signal processors is radicany changing the engineering approach to designing communications equipment. Advanced realizations for tactical communications in modern armies, now include digital transmission, voice and data capability and ECM resistant systems. Various techniques such as coding encryption, spread spectrum, are needed to enhance security of communications and to improve resistance to jamming. The adaptability to the varying channels conditions, such as mobile radio communications or real time channel evaluation, requires a better knowledge of the propagation medium. The meeting examined the state-of-the-art in development of present day radio communication systems; the role and the need for radio propagation research; assessed the effects of propagation on existing systems and proposed how new systems can be improved to meet operational requirements. ISBN 92-835-0511-5
software, employing digital signal processing chips to perform the required modulation and demodulation processes. The recent development of such signal processors is radically changing the engineering approach to designing communications equipment. Advanced realizations for tactical communications in modern armies, now include digital transmission, voice and data capability and ECM resistant systems. Various techniques such as coding encryption, spread spectrum, are needed to enhance security of communications and to improve resistance to jamming. The adaptability to the varying channels conditions, such as mobile radio communications or real time channel evaluation, requires a better knowledge of the propagation medium. The meeting examined the state-of-the-art in development of present day radio communication systems; the role and the need for radio propagation research; assessed the effects of propagation on existing systems and proposed how new systems can be improved to meet operational requirements. ISBN 92-835-0511-5	software, employing digital signal processing chips to perform the required modulation and demodulation processes. The recent development of such signal processors is radically changing the engineering approach to designing communications equipment. Advanced realizations for tactical communications in modern armies, now include digital transmission, voice and data capability and ECM resistant systems. Various techniques such as coding encryption, spread spectrum, are needed to enhance security of communications and to improve resistance to jamming. The adaptability to the varying channels conditions, such as mobile radio communications or real time channel evaluation, requires a better knowledge of the propagation medium. The meeting examined the state-of-the-art in development of present day radio communication systems; the role and the need for radio propagation research; assessed the effects of propagation on existing systems and proposed how new systems can be improved to meet operational requirements. ISBN 92-835-0511-5